frontiers | Research Topics

Plant parasitic nematode–host interactions: mechanisms and exploitative management strategies

Edited by
Andressa Machado and Mario Massayuki Inomoto

Coordinated by
Victor Hugo Moura De Souza and James Price

Published in
Frontiers in Plant Science

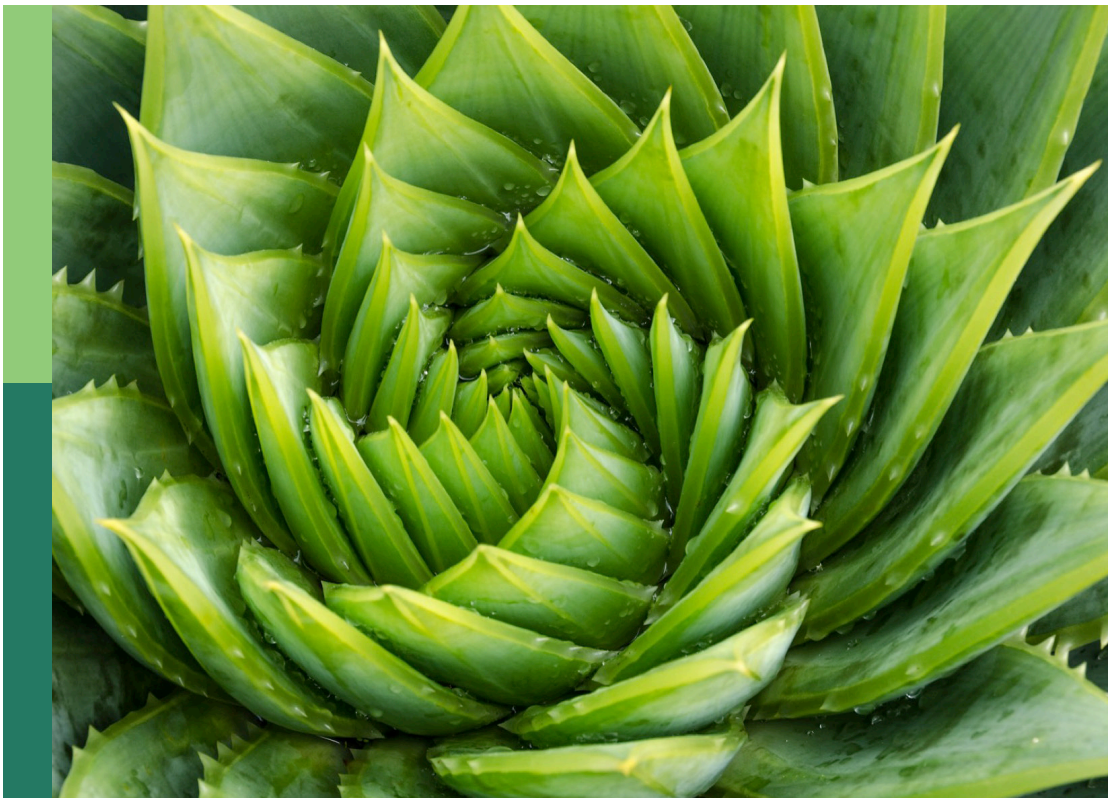

ISSN 1664-8714
ISBN 978-2-8325-5926-0
DOI 10.3389/978-2-8325-5926-0

About Frontiers

Frontiers is more than just an open access publisher of scholarly articles: it is a pioneering approach to the world of academia, radically improving the way scholarly research is managed. The grand vision of Frontiers is a world where all people have an equal opportunity to seek, share and generate knowledge. Frontiers provides immediate and permanent online open access to all its publications, but this alone is not enough to realize our grand goals.

Frontiers journal series

The Frontiers journal series is a multi-tier and interdisciplinary set of open-access, online journals, promising a paradigm shift from the current review, selection and dissemination processes in academic publishing. All Frontiers journals are driven by researchers for researchers; therefore, they constitute a service to the scholarly community. At the same time, the *Frontiers journal series* operates on a revolutionary invention, the tiered publishing system, initially addressing specific communities of scholars, and gradually climbing up to broader public understanding, thus serving the interests of the lay society, too.

Dedication to quality

Each Frontiers article is a landmark of the highest quality, thanks to genuinely collaborative interactions between authors and review editors, who include some of the world's best academicians. Research must be certified by peers before entering a stream of knowledge that may eventually reach the public - and shape society; therefore, Frontiers only applies the most rigorous and unbiased reviews. Frontiers revolutionizes research publishing by freely delivering the most outstanding research, evaluated with no bias from both the academic and social point of view. By applying the most advanced information technologies, Frontiers is catapulting scholarly publishing into a new generation.

What are Frontiers Research Topics?

Frontiers Research Topics are very popular trademarks of the *Frontiers journals series*: they are collections of at least ten articles, all centered on a particular subject. With their unique mix of varied contributions from Original Research to Review Articles, Frontiers Research Topics unify the most influential researchers, the latest key findings and historical advances in a hot research area.

Find out more on how to host your own Frontiers Research Topic or contribute to one as an author by contacting the Frontiers editorial office: frontiersin.org/about/contact

Plant parasitic nematode–host interactions: mechanisms and exploitative management strategies

Topic editors
Andressa Machado — Agronema, Brazil
Mario Massayuki Inomoto — University of São Paulo, Brazil

Topic coordinators
Victor Hugo Moura De Souza — University of Cambridge, United Kingdom
James Price — The James Hutton Institute, United Kingdom

Citation
Machado, A., Inomoto, M. M., De Souza, V. H. M., Price, J., eds. (2025). *Plant parasitic nematode–host interactions: mechanisms and exploitative management strategies*. Lausanne: Frontiers Media SA. doi: 10.3389/978-2-8325-5926-0

Table of contents

frontiers | Frontiers in Plant Science

TYPE Editorial
PUBLISHED 09 January 2025
DOI 10.3389/fpls.2024.1539529

OPEN ACCESS

EDITED AND REVIEWED BY
Choong-Min Ryu,
Korea Research Institute of Bioscience and Biotechnology (KRIBB), Republic of Korea

*CORRESPONDENCE
James Price
james.price@hutton.ac.uk
Victor Hugo Moura de Souza
vhm24@cam.ac.uk

†These authors share first authorship

RECEIVED 04 December 2024
ACCEPTED 20 December 2024
PUBLISHED 09 January 2025

CITATION
Price J, de Souza VHM, Machado ACZ and Inomoto MM (2025) Editorial: Plant parasitic nematode–host interactions: mechanisms and exploitative management strategies.
Front. Plant Sci. 15:1539529.
doi: 10.3389/fpls.2024.1539529

Editorial: Plant parasitic nematode–host interactions: mechanisms and exploitative management strategies

James Price[1*†], Victor Hugo Moura de Souza[2*†], Andressa Cristina Zamboni Machado[3] and Mário Massayuki Inomoto[4]

[1]Cellular & Molecular Sciences, The James Hutton Institute, Dundee, United Kingdom, [2]Crop Science Centre – Department of Plant Sciences, University of Cambridge, Cambridge, United Kingdom, [3]Department of Nematology, Agronema, Londrina, Brazil, [4]Department of Plant Pathology and Nematology – University of São Paulo, Piracicaba, Brazil

KEYWORDS

biological control, resistance to pathogens, alternative control of nematodes, effectors, induced resistance

Editorial on the Research Topic
Plant parasitic nematode–host interactions: mechanisms and exploitative management strategies

By 2060, the human population on Earth is expected to reach 10 billion people and food production to sustain this population is of great concern. Food security is not only pressurised by abiotic factors associated with a rapidly changing climate but also by biotic, pathogenic threats. In many areas of the world, plant-parasitic nematodes (PPN) are the greatest stress on sustainable crop production. However, PPN parasitise all aspects of plant life and, where left unmanaged, could lead to major ecological collapse. Historically, management of PPN relied on incorporation of harmful, non-specific chemicals into infested soils. Generally, PPN control has moved towards integrated pest management (IPM) approaches. This Research Topic addresses how a better understanding of nematode-host interactions can help further develop management strategies.

Although reliance on nematicidal chemicals should be reduced under an IPM approach, they remain an important part of pest management. Many manufactured products are being removed from international markets due to harmful off-target effects. Consequently, there is urgent need for new nematicidal products which are often being developed with naturally occurring ingredients in agreement with green deals. Having plant origin means that these products can be interpreted by the crop boosting defence pathways for defence against any pathogen, not just PPN, in addition to direct nematicidal effects. This is demonstrated by Degroote et al. in their use of the bio-based 'Product X' which was shown to considerably reduce *Meloidogyne incognita* gall formation in tomato plants.

The ongoing boon in availability of -omics data may help shift towards novel bio-based nematode controls such as exogenous application of microRNAs. These technologies offer the opportunity of incredibly targeted control identified through bioinformatics pipelines. Leonetti et al. established the use of a pipeline for identification and creation of cross-

kingdom miRNAs, in this case originating from tomatoes and capable of reducing expression of two key *M. incognita* target genes. The use of miRNAs for nematode control is still a developing area and further research will be required on construct delivery in an applied setting.

This Research Topic has shown that PPN-host interactions do not have to be directly coupled and instead understanding host-associated microorganisms could offer fresh management strategies. The impact of plant growth-promoting bacteria (PGPB) on pathogen suppression was reviewed by Habteweld et al.. This review investigates the three-way interactions shared between PPN-host-PGPB and how influencing PGPB communities can assist root-knot nematode management. One demonstrated example of the use of PGPB to promote pathogen resistance is illustrated by Hu et al. who used *Bacillus velezensis* to promote host resistance against *Heterodera glycines*. Here, bacterial stimulation of the jasmonic acid (JA) biosynthesis pathway resulted in increased JA in root tissues supplying a systemic resistance effect. Jia et al. further develop the idea of both influencing plant-associated microorganisms coupled with novel plant-originating product development for nematode suppression. *Aspergillus* sp. promotes coexistence of *Bursaphelenchus xylophilus* and their vector insect in pine trees. However, inhibiting *Aspergillus* populations with chiricanine A decreased nematode populations, increasing host plant survival.

Plant-parasitic nematode population increases due to host availability drive changes in soil microbial communities. Clavero-Camacho et al. explored this further by observing soil and rhizospheric microbiome changes in *Meloidogyne* spp. infected almonds. Under high infection pressures, fungal saprotrophism is altered and there is reduced impact of predatory nematodes and biological control agents. A significant portion of plant-nematology research focusses on the tight evolutionary relationship and interactions between PPN and host, however, PPN have also adapted for life before host invasion. Better understanding these adaptations could help develop biological controls through use of antagonistic microorganisms.

Natural host resistance is playing an increasing role in IPM of plant-parasitic nematodes. Modern breeding of resistant varieties relies on molecular markers for resistance allowing genotyping to reduce populations before often time-consuming phenotyping. Obata et al. utilised a genome-wide association study (GWAS) and next-generation sequencing to develop markers for sweet potato resistance against *M. incognita*. In complex polyploid crop species, e.g., sweetpotato, tools like these rapidly enable the pre-screening of breeding progeny. Understanding how host resistance genes enable a physical response upon detection of PPN can assist knowledge in further resistance gene discovery, pathogen virulence and developing plant protection products. Histopathology techniques used by Gabriel et al. demonstrate that the *Mi-1.2* gene induces both biochemical protection, reducing root invasion, and a hypersensitive response, causing cell death following *M. javanica* infection. However, virulent populations were unimpaired, avoiding host detection in tomatoes bearing resistance gene.

Effector proteins help virulent populations of PPN infect their hosts. Learning about effectors can help identify routes for control by targeting parts of the host-parasite essential for parasitism. Li et al. characterised a novel effector expressed in the oesophageal gland of *Bursaphelenchus. xylophilus* that induces plant cell death and aids migration. Targeting this effector for reduced expression through RNA interference reduced both disease severity and seedling death.

PPN-host exchanges go beyond effector-mediated interactions and as reviewed by Dominguez-Figueroa et al. there are often infection-associated host transcriptomic changes. Although many differentially expressed genes encoding transcription factors (TF) have been identified, relatively few of these TFs have been functionally characterised. However, these TFs can be segregated into two main groups whether they are defence or development-related. Understanding how these TFs are being abused during pathogen attack could help develop innate TF regulatory controls at the detriment of the nematode.

Author contributions

JP: Writing – original draft, Writing – review & editing. VHMS: Writing – original draft, Writing – review & editing. ACZM: Writing – review & editing. MMI: Writing – review & editing.

Funding

The author(s) declare that financial support was received for the research, authorship, and/or publication of this article. VHMS would like to thank the European Union's Horizon 2020 Research and Innovation Programme under Marie Sklodowska-Curie grant agreement 101025218 and Leverhulme grant RPG-2023-001 for the funding. JP had his work funded by the Rural and Environmental Science and Analytical Service (RESAS) division of the Scottish Government. The funders had no role in the decision to publish or manuscript preparation. ACZM would like to thank the Conselho Nacional de Desenvolvimento Científico e Tecnológico (CNPq) for the granted fellowship. MMI would like to thank both CNPq and Coordenação de Aperfeiçoamento de Pessoal de Nível Superior (CAPES) for the funding.

Acknowledgments

We extend our sincere gratitude to all authors who contributed their valuable work to this Research Topic, as well as to the reviewers who dedicated their time and expertise to evaluating the submissions.

Conflict of interest

The authors declare that the research was conducted in the absence of any commercial or financial relationships that could be construed as a potential conflict of interest.

Publisher's note

frontiers in Plant Science

ORIGINAL RESEARCH
published: 18 March 2022
doi: 10.3389/fpls.2022.858747

Mapping of Nematode Resistance in Hexaploid Sweetpotato Using a Next-Generation Sequencing-Based Association Study

*Nozomi Obata[1], Hiroaki Tabuchi[2], Miyu Kurihara[3], Eiji Yamamoto[4], Kenta Shirasawa[5] and Yuki Monden[1]**

[1] Graduate School of Environmental and Life Science, Okayama University, Okayama, Japan, [2] Kyusyu Okinawa Agricultural Research Center, National Agriculture and Food Research Organization, Miyakonojo, Japan, [3] Faculty of Agriculture, Okayama University, Okayama, Japan, [4] Graduate School of Agriculture, Meiji University, Kawasaki, Japan, [5] Department of Frontier Research and Development, Kazusa DNA Research Institute, Kisarazu, Japan

The southern root-knot nematode (SRKN; *Meloidogyne incognita*) is a typical parasitic nematode that affects sweetpotato [*Ipomoea batatas* (L.) Lam.], causing a significant decrease in crop yield and commercial value. In Japan, the SRKN is classified into 10 races: SP1–SP5, SP6-1, SP6-2, and SP7–SP9, with the dominant race differing according to the cultivation area. Soil insecticides have previously been used to reduce the soil density of SRKNs; however, this practice is both costly and labor intensive. Therefore, the development of SRKN-resistant sweetpotato lines and cultivars is necessary. However, due to the complexity of polyploid inheritance and the highly heterogeneous genomic composition of sweetpotato, genetic information and research for this species are significantly lacking compared to those for other major diploid crop species. In this study, we utilized the recently developed genome-wide association approach, which uses multiple-dose markers to assess autopolyploid species. We performed an association analysis to investigate resistance toward SRKN-SP2, which is the major race in areas with high sweetpotato production in Japan. The segregation ratio of resistant and susceptible lines in the F_1 mapping population derived from the resistant "J-Red" and susceptible "Choshu" cultivars was fitted to 1: 3, suggesting that resistance to SP2 may be regulated by two loci present in the simplex. By aligning the double digest restriction-site associated DNA sequencing reads to the published *Ipomoea trifida* reference sequence, 46,982 single nucleotide polymorphisms (SNPs) were identified (sequencing depth $>$ 200). The association study yielded its highest peak on chromosome 7 (Chr07) and second highest peak on chromosome 3 (Chr03), presenting as a single-dose in both loci. Selective DNA markers were developed to screen for resistant plants using the SNPs identified on Chr03 and Chr07. Our results showed that SRKN-SP2-resistant plants were selected with a probability of approximately 70% when combining the two selective DNA markers. This study serves as a model for the identification of genomic regions that control agricultural traits and the elucidation of their effects, and is expected to greatly advance marker-assisted breeding and association studies in polyploid crop species.

Keywords: polyploidy, nematode, sweetpotato, resistant cultivar, breeding, association study

OPEN ACCESS

Edited by:
Rodomiro Ortiz, Swedish University of Agricultural Sciences, Sweden

Reviewed by:
Carolina Ballen-Taborda, Clemson University, United States
Phatu William Mashela, University of Limpopo, South Africa
G. Craig Yencho, North Carolina State University, United States

***Correspondence:**
Yuki Monden
y_monden@okayama-u.ac.jp

Specialty section:
This article was submitted to Plant Breeding, a section of the journal Frontiers in Plant Science

Received: *20 January 2022*
Accepted: *11 February 2022*
Published: *18 March 2022*

Citation:
Obata N, Tabuchi H, Kurihara M, Yamamoto E, Shirasawa K and Monden Y (2022) Mapping of Nematode Resistance in Hexaploid Sweetpotato Using a Next-Generation Sequencing-Based Association Study. Front. Plant Sci. 13:858747. doi: 10.3389/fpls.2022.858747

INTRODUCTION

Sweetpotato [*Ipomoea batatas* (L.) Lam.], belonging to the Convolvulaceae family, is widely cultivated in both tropic and temperate zones. With an annual worldwide production of 91.8 million tons (FAOSTAT, 2019), it is regarded as the seventh most important crop species. Sweetpotato is rich in carbohydrates, vitamins (A, C, B1, B2, B3, B6, and E), biotin, dietary fiber, potassium, and other nutrients; thus, it plays an important role in food security, especially in developing countries. China is the world's major producer of sweetpotato, followed by Sub-Saharan Africa. Approximately 52.0 million tons of sweetpotato are produced annually in China, accounting for approximately 56.6% of the total global production. Japan produces approximately 748,700 tons of sweetpotato annually and is the 17th largest producer in the world. In Japan, the Kagoshima and Miyazaki prefectures in the Kyushu region, and Ibaraki and Chiba prefectures in the Kanto region are the predominant production areas (Ministry of Agriculture, Forestry and Fisheries, 2020). In addition to being consumed as a raw food, sweetpotato is widely used in animal feed, processed foods, and the preparation of starch and alcohol. Thus, sweetpotato is a commercially important crop, and the development of cultivars with disease, pest, and nematode resistance is required to avoid commercial yield losses and expand the cultivation area.

The southern root-knot nematode (SRKN) (*Meloidogyne incognita*) is a typical nematode of sweetpotato, causing serious damage to the appearance, quality, and yield of the crop (Lawrence et al., 1986). Krusberg and Nielson (1958) reported that the yield of sweetpotato on farms with soil containing root-knot nematodes was 61% less than that on farms with pesticide-treated soil. These nematodes live in warm regions and have an optimum temperature of 25–30°C; furthermore, they have been detected in most areas where sweetpotato is cultivated (Yoshida, 1965; Iwahori et al., 2000; Iwahori and Sano, 2003). The host range of the SRKN is very wide, including thousands of agronomically important plants (Overstreet, 2009). When infested with the SRKN, host roots form humps (galls) with a diameter of 1–2 mm. This destroys and deforms the roots, inhibiting the absorption of nutrients and water, and leads to poor growth and death. In the roots of sweetpotato, dents occur when they are infested with SRKN. As the symptoms progress, constriction and dehiscence occur, resulting in a significant decrease in yield quality, and commercial value. The SRKN is classified into 10 races (SP1– SP5, SP6-1, SP6-2, SP7–SP9) in Japan (Sano and Iwahori, 2005; Tabuchi et al., 2017). Each race has a different geographical distribution. SP1 is mainly distributed in Saga, Kumamoto, and Nagasaki prefectures, and SP4 and SP6 races are predominantly distributed in Okinawa and also detected in Ibaraki and Chiba prefectures (Sano et al., 2002; Sano and Iwahori, 2005; Kuranouchi et al., 2018). SP2 is found mainly in the Kagoshima and Miyazaki prefectures, which have the highest levels of sweetpotato production in Japan. Treatment with insecticides such as D-D agents, although effective in controlling SRKN in the soil, is costly and labor-intensive (Krusberg and Nielson, 1958). Therefore, the development of sweetpotato cultivars with SRKN resistance is required.

Genetic studies in sweetpotato lag considerably behind those in other major diploid crop species owing to its complex mode of polyploid inheritance. Sweetpotato has a large genome (2.2–3 Gb) and is a hexaploid species with 90 chromosomes (2n = 6x = 90) (Isobe et al., 2017; Monden and Tahara, 2017). Although a few cultivars can reproduce among themselves, most show self-incompatibility or cross-incompatibility and are, therefore, genetically heterogeneous (Gurmu et al., 2013; Hirakawa et al., 2015). There is an ongoing debate as to whether sweetpotato is an autohexaploid or allohexaploid (Gao et al., 2020). Several early studies suggested that sweetpotato is allohexaploid (Ting and Kehr, 1953; Jones, 1967; Magoon et al., 1970; Sinha and Sharma, 1992). In contrast, more recent genetic analyses using molecular markers have suggested that it is autohexaploid, with some preferential pairing (Ukoskit and Thompson, 1997; Kriegner et al., 2003; Cervantes-Flores et al., 2008; Zhao et al., 2013; Monden et al., 2015). A recent study using ultra-dense multilocus genetic mapping also suggested that sweetpotato inheritance is highly autohexaploid-like, with random chromosome pairing enabling recombination between all homologous chromosomes during meiosis (Mollinari et al., 2020). Genetic studies have been successful in allopolyploid species due to their similarity to diploids in terms of segregation patterns and chromosomal pairing (Bourke et al., 2018; Mollinari and Garcia, 2019; da Silva Pereira et al., 2020; Yamamoto et al., 2020). However, these genetic approaches are unsuitable in autopolyploids, as they exhibit multiple heterozygous genotypes (Bourke et al., 2018; Yamamoto et al., 2020). Precise genetic mapping in autopolyploids is performed using multiple-dose markers wherein, the allele dosage for each marker needs to be determined (Mollinari et al., 2020; Yamamoto et al., 2020). However, the development of analytical tools for multiple-dose markers requires elaborate analytical algorithms, and this process has been challenging.

Genetic analyses using classical molecular markers such as random amplified polymorphic DNA (RAPD) and amplified fragment length polymorphism (AFLP) markers have identified DNA markers linked to SRKN resistance in sweetpotato (Ukoskit et al., 1997; Mcharo et al., 2005; Cervantes-Flores et al., 2008; Nakayama et al., 2012). Genetic analysis of SP1 and SP2 was performed using 92 lines from an F_1 population derived from a cross between the resistant cultivar "Hi-Starch" and the susceptible cultivar "Koganesengan" (Nakayama et al., 2012). Bulked segregant analysis was performed to screen AFLP markers associated with SP1 and SP2 resistance, and interval mapping was conducted using the selected AFLP markers. As a result of interval mapping, a major quantitative trait locus (QTL) [here, named *qRmi (t)*] associated with resistance to SP1 and SP2 was detected. Furthermore, based on the AFLP markers in the QTL, a sequence characterized amplified region (SCAR) marker was developed to screen for resistant plants. Sasai et al. (2019) analyzed single nucleotide polymorphisms (SNPs) and retrotransposon insertion polymorphisms using next-generation sequencing (NGS) to construct a high-density genetic linkage map integrated with simple sequence repeat (SSR) markers. As a result of the QTL and genome-wide association study (GWAS) analyses, a major QTL common to SP1, SP4, and SP6-1 was

identified, and a selective DNA marker that can easily and efficiently select resistant plants was developed. Additionally, Yamamoto et al. (2020) have developed a novel GWAS method for polyploid species that utilizes multiple-dose markers. With this method, the allele dosage of each marker can be determined using allele dosage probabilities calculated from the read counts of the NGS data. This technique has been shown as effective in the genetic analysis of autohexaploid sweetpotato.

In this study, we performed genetic mapping to identify the genomic regions controlling SRKN-SP2 resistance in sweetpotato. The aims of this study were as follows: (1) to identify a large number of genome-wide SNPs using double-digest restriction site-associated DNA sequencing (ddRAD-seq) analysis; (2) to conduct genetic mapping using the novel GWAS method and estimate the allele dosage probability for each SNP marker calculated on the basis of read depth information from the ddRAD-seq data; and (3) to develop highly selective DNA markers for SRKN resistance based on the DNA sequence of the identified genomic regions. This study presents an effective method to identify genomic regions that control agronomically important traits in sweetpotato and will help to guide future genetic mapping in autohexaploid crop species.

MATERIALS AND METHODS

Plant Materials

The sweetpotato cultivars "J-Red" and "Choshu," and an F_1 mapping population consisting of 107 lines obtained by crossing these two cultivars were used in this study. "J-Red" was developed by crossing a high-starch, disease-resistant "Shiroyutaka" cultivar as the female parent, and a high carotene "86J-6" cultivar introduced from the United States, as the male parent. J-Red is resistant to all SRKN races except SP8 (Sano and Iwahori, 2005; Tabuchi et al., 2017). "Choshu" is a domestic cultivar that is susceptible to the SRKN races, SP1, SP2, SP3, SP4 SP6-1, and SP6-2 (Tabuchi et al., 2017). Genomic DNA was extracted from all plants using the DNeasy Plant Mini Kit according to the manufacturer's instructions (QIAGEN, Hilden, Germany). The yield and quality of the extracted DNA was confirmed using a NanoDrop 2000 instrument (Thermo Fisher Scientific, Wilmington, DE, United States).

Resistance Evaluation

Southern root-knot nematode resistance was evaluated at the National Agriculture and Food Research Organization, Kyusyu Okinawa Agricultural Research Center (Miyakonojo City, Miyazaki Prefecture). The resistance evaluation test was performed using second-stage juveniles (J2) of *M. incognita* according to the method developed by Tabuchi et al. (2017), which is originally described by Sano and Iwahori (2005). The juveniles of *M. incognita* were freshly prepared for each test as follows: A 19-day-old seedling of a susceptible tomato cultivar (Plitz) was inoculated in a 15 cm diameter pot containing approximately 600 g of a seeding culture soil (Kenbyo, Yaenogei, Japan) with approximately 6,000 J2 *M. incognita*, which remained from the former resistance test. Plitz plants were cultivated in a greenhouse at an average temperature of 25.5°C for 41–48 days. The egg masses, formed by the nematodes on the tomato root systems during cultivation, were picked up and placed on a cotton filter partially submerged in water in a beaker at 24°C. In this system, the J2 emerged from the egg masses, migrated through the filter, and accumulated at the bottom of the beaker. The cotton filter was transferred to a new beaker every 2–3 days, and the previous beaker was kept at 13°C, which is close to the developmental zero point for *M. incognita* (Gotoh et al., 1973). J2 individuals were collected from three to five beakers and used for a new resistance test.

Seedlings from each of the 107 lines of the F_1 sweetpotato population and their parental cultivars were rooted in a greenhouse at an average temperature of 25.5°C, and after 7–10 days, a single node was collected by cutting approximately 1.5 cm of the vine. Two to six 9 cm pots containing approximately 200 g of mixed soil (Kenbyo:steam-sterilized andosol, 1:1) were prepared for each line, and a single node cutting was planted. After 3–4 days, 500 J2 (SP2) nematodes were inoculated into each pot. Each pot was covered with a newspaper for the first 3 days after inoculation. After 35 days, the roots were washed, egg masses were stained with a 0.02% erioglausin solution, and the number of egg masses were counted. As described previously (Sasai et al., 2019), we carried out resistance tests for at least four plans in two replications (two plants per replication). When the results of resistance or susceptibility were consistent among plants, the resistance test of the F_1 line was considered complete. When the results were different, we continued resistance tests to obtain more accuracy. Finally, the resistance of F_1 progeny was tested on 2–9 replications (4–18 plants for each line), and the calculated average number of egg masses was used to determine resistance. We used the number of egg masses per plant instead of eggs masses per gram of root for the following reasons: (1) In farmer's fields, the number of egg masses per plant seems to be more important than egg masses per gram of root. (2) The number of egg masses per plant is more stable than that per gram of root because the coefficient of variation of the former is less than that of the latter in over 1,000 times resistance tests (unpublished data). (3) Both values show high correlation (>0.92 unpublished data). Following previous studies (Nakayama et al., 2012; Tabuchi et al., 2017; Sasai et al., 2019), we determined that plants with fewer than 10 egg masses per plant were resistant, and those with more than 10 egg masses were susceptible. The number of resistant and susceptible plants were analyzed, and a Chi-square goodness-of-fit test was performed with the calculated and expected segregation ratios using Microsoft excel.

Genotyping With Double-Digest Restriction Site-Associated DNA Sequencing and Single Nucleotide Polymorphisms Calling

Genotyping was performed using ddRAD-seq according to previously described methods (Shirasawa et al., 2017; Sasai et al., 2019). Genomic DNA was digested with *Msp*I and *Pst*I restriction enzymes (FastDigest Enzymes, Thermo Fisher Scientific, Waltham, MA, United States), and adaptor ligation

and purification were performed to prepare the ddRAD-seq library (Shirasawa et al., 2017). The ddRAD-seq library was sequenced using HiSeq4000 and NextSeq500 systems (Illumina, San Diego, CA, United States) and DNBSEQ-G400 (MGI, Shenzhen, China). The paired-end short reads with a read length of 150 bp were analyzed using the following procedure: first, they were trimmed based on the quality score (QV > 30) and the adapter sequence (5'-AGATCGGAAGAGC-3') was removed using Cutadapt (version 2.8) (Martin, 2011). During this process, the minimum read length was set to 30 bases to obtain high-quality reads. Due to the absence of a pseudomolecule-level reference genome sequence for cultivated hexaploid sweetpotato (*I. batatas*), reads were then aligned to the whole genome sequence of *I. trifida* (Wu et al., 2018) using Bowtie2 (version 2.3.0) software (Langmead and Salzberg, 2012). The parameters were set to "–very-sensitive-local" mode for alignment. SNP calling was performed using the "mpileup" option in SAMtools v. 0.1.19 (Li et al., 2009) and the mpileup2snp option of VarScan 2 v.2.3 (Koboldt et al., 2012). The ddRAD-seq reads were under the accession number DDBJ: DRA013144.

Allele Dosage Estimation and Association Analyses

The allele dosage estimation and association analyses were performed in accordance with an analytical method detailed in Yamamoto et al. (2020). Briefly, this method estimates allele dosage of polyploids by calculating the allele dosage probability using read count information in the NGS data. Here, allele dosage refers to the dosage of the reference genome-type allele for each SNP locus. For hexaploid species, the possible allele dosage states were 0/6 (aaaaaa), 1/6 (Aaaaaa), 2/6 (AAaaaa), 3/6 (AAAaaa), 4/6 (AAAAaa), 5/6 (AAAAAa), and 6/6 (AAAAAA). For the allele dosage estimation, the produced VCF file was loaded into the R platform *via* "read.vcfR" in vcfR (version 1.12.0) (Knaus and Grünwald, 2017). Information on the depths of the total (DP) and reference type (RD) reads were extracted from the VCF file using "extract.gt" in vcfR. High read depth is required for the accurate genotyping of polyploid species when compared with diploids. For example, a DP of 60–80 was recommended to distinguish between the genotypes for tetraploid species (AAAA, AAAa, AAaa, Aaaa, aaaa) (Uitdewilligen et al., 2013; Endelman et al., 2018). In this study, the minimum DP was set to 200 for accurate genotyping in the hexaploid sweetpotato; thus, individual genotypes with DP < 200 and DP > 1,000 were filtered out from further analyses. In addition, markers with missing values > 0.5 and major genotype frequency (MGF) > 0.95 were filtered out.

For the allele dosage estimation, we used the naïve method. The probability (Pr) of dosage for a given DP and RD was calculated using the binomial distribution function, as follows:

$$\Pr\left(\text{Dosage} = d_i\right) = {}_{DP}\mathrm{C}_{RD} \times r_i^{RD} \times (1 - r_i)^{DP-RD}$$

where r_i is the theoretical value of the allele dosage d (i.e., 0/6–6/6) in the individual i. The relative probability (RPr) of the reference type allele dosage for each SNP marker was calculated using the following formula:

$$\mathrm{RPr}\left(\text{Dosage} = d_i\right) = \Pr\left(\text{Dosage} = d_i\right) / \sum_i \Pr\left(\text{Dosage} = d_i\right)$$

The calculation was performed using the R script "alleleDosageEstimation.R." In the actual data, the theoretical probabilities r may deviate owing to errors caused in the experimental procedure. Therefore, the probability of allele dosage in the real data was calculated by including an unknown error probability of 0.001 using the option "read.err.prob" in "alleleDosageEstimation.R." A matrix was obtained for each SNP marker, with individuals and the relative probabilities of the reference allele dosage calculated by the above equation as row and column elements, respectively.

The association study was performed in R (version 3.6.2) using the R script "alleleDosageGLM.R." The number of egg masses was standardized by logarithmic transformation. After adding 1 to the average number of egg masses in each line, the resistance score was calculated by taking the common logarithm and used for GWAS. The four F_1 lines JC5, JC22, JC57, and JC119 were excluded from further analyses because their resistance scores were not stable. In addition, JC2 was also excluded from further analyses because its genomic DNA was not available for genotyping with ddRAD-seq. Therefore, the F_1 population used for the GWAS included 102 lines. The association between marker genotypes and phenotypes was investigated using a generalized linear model (GLM). GLM fitting was performed using "glm" in R (R Core Team, 2020). The augmented family functions "binomial" and "gaussian" were used for binary and continuous traits, respectively. The likelihood-ratio test for the SNP effect was performed using "pchisq" in R (R Core Team, 2020) with deviance and degrees of freedom from each GLM as arguments. The R package used in the analysis in this study is available at https://github.com/yame-repos/ngsAssocPoly. Statistical testing was performed using a Wilcoxon rank sum test. The "Wilcox.exact" function was used in the R package "exactRankTests."

Development of Selective Markers

Selective markers were developed to distinguish between J-Red and Choshu types based on the target SNPs identified by the GWAS. We obtained the chromosomal positions of target SNPs in the diploid reference genome of *I. trifida* (Wu et al., 2018). PCR primers were designed according to a previously described method (Hayashi et al., 2004). In this method, the target SNP was used as the base at the 3' end of the primer, and an artificial mismatch was inserted three bases upstream. When designing the primers, the bam files obtained by aligning the short reads of the parents with the reference sequence of *I. trifida* were visualized using an Integrative Genomics Viewer (IGV) (Robinson et al., 2011), and the sequence information around the target SNP was extracted. If the sequence around the target SNP was not sufficiently covered by the short reads of the ddRAD-seq, the sequence around the SNP was determined by Sanger sequencing after TA cloning of the amplicon with the TOPO TA cloning kit according to the manufacturer's instructions (Invitrogen,

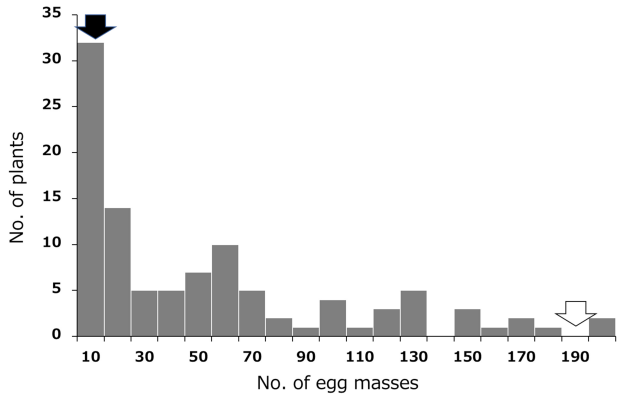

FIGURE 1 | Frequency distribution for the mean number of SP2 *Meloidogyne incognita* egg masses in the F_1 population derived from a cross between resistant "J-Red" and susceptible "Choshu" sweetpotato cultivars. Black and white arrows indicate the values of J-Red and Choshu, respectively.

Carlsbad, CA, United States). Genotyping was performed using primers designed based on the target SNPs. The primers for the positive control were designed based on the *SSII* gene. The PCR solution contained 10 ng of DNA, 1.0 μL of 10 × PCR Buffer, 0.8 μL of dNTPs (2.5 mM each), 0.25 units of TAKARA Taq Hot Start Version, and 0.2 μL each of the forward and reverse primers (50 μM), adjusted to a total volume of 10 μL. The reaction conditions were as follows: initial denaturation at 94°C for 2 min, followed by 30 cycles of denaturation at 94°C for 10 s, annealing at 60°C for 10 s, and extension at 72°C for 30 s. Amplified products were visualized using electrophoresis on a 1.5% agarose gel (BioRAD, Hercules, CA, United States).

RESULTS

Phenotyping for Nematode Resistance

Resistance to SRKN was evaluated by measuring the number of egg masses formed in the sweetpotato roots 35 days after inoculation with 500 nematodes. The results for the SRKN resistance tests in the F_1 population and their parents are shown in **Figure 1** and **Supplementary Table 1**. The average number of egg masses was 1.3 and 192.0 in the resistant parent "J-Red" and the susceptible parent "Choshu," respectively, which indicated that there was a large difference in the resistance between the parental cultivars. The results of the frequency distribution of resistance in the F_1 population showed a few lines with fewer egg masses than "J-Red" and a few lines with more egg masses than "Choshu," and transgressive segregation was observed. The threshold for the number of egg masses that distinguishes resistance and susceptibility was set to 10 with previous studies (Nakayama et al., 2012; Tabuchi et al., 2017; Sasai et al., 2019), and the number of resistant and susceptible lines in the F_1 population was determined to be 32 and 71, respectively. The ratio of the number of resistant and susceptible F_1 lines corroborated with the expected 1:3 segregation ratio ($\chi^2 = 2.023$, $P = 0.155$). In hexaploid species, if one parent has a genotype with two dominant loci of the simplex allele (AaaaaaBbbbbb) and the other parent has a nullplex (aaaaaabbbbbb) genotype, "AaaaaaBbbbbb," "Aaaaaabbbbbb/aaaaaaBbbbbb" and "aaaaaabbbbbb" genotypes were expected to segregate at a ratio of 1:2:1 in the F_1 progeny. Therefore, the genotypes with both dominant loci (AaaaaaBbbbbb) and other genotypes (Aaaaaabbbbbb or aaaaaaBbbbbb or aaaaaabbbbbb) were expected to segregate at a ratio of 1:3 in the F_1 progeny. Here, since the segregation ratios of resistant and susceptible F_1 lines were fitted to 1:3, resistance to SP2 should be regulated by two loci present in a simplex allele.

Association Analyses

Genome-wide SNPs were identified using the ddRAD-seq library, which generated a total of 1,887 million reads. After preprocessing, 1,771 million high-quality reads were obtained. The number of reads obtained from the parental cultivars and F_1 lines is shown in **Supplementary Table 2**. The high-quality reads were aligned to the whole genome sequence of *I. trifida* using Bowtie 2 software and produced an average alignment rate of 94.6% for all plants. The alignment rates in the parental cultivars and F_1 lines are shown in **Supplementary Table 3**. A total of 406,720 SNPs was detected using Varscan. The average read depth at this point was 53.9. In the present study, the minimum DP was set to 200 for the accurate genotyping of hexaploid sweetpotato. The allele dosage probability for each marker was calculated based on the read depth information from the ddRAD-seq genotyping data. After filtering the SNPs with the minimum DP set to 200, the average DP of the SNPs was 224.4. GWAS was performed using the remaining 46,788 SNPs. As a result, the highest peak was detected on chromosome 07 (Chr07), and the second highest peak was detected on chromosome 03 (Chr03) (**Figure 2**).

Investigating the Effects of the Identified Loci

The effects of the two identified loci (on Chr03 and Chr07) on SRKN resistance were examined. The SNP marker for Chr07_1778460 was most associated with resistance on chromosome 7 ($P = 4.671E-06$). In the Chr07_1778460 marker, the resistant parent "J-Red" and the susceptible parent "'Choshu" showed the genotypes of Aaaaaa (simplex) and aaaaaa (nullplex), respectively (**Figure 3**). Here, "A" represents a nucleotide that is identical with that of the reference sequence, while "a" represents a nucleotide that is different from that of the reference sequence. The total number of F_1 lines used to investigate the effects of the identified loci was 102 since five lines were not available (see section "Materials and Methods"). Among the F_1 population, the genotypes of eight lines with DP values < 200 were not determined. As a result, the F_1 mapping population was classified into 43 and 51 lines for the J-Red (Aaaaaa) and Choshu (aaaaaa) types, respectively (**Supplementary Table 4**). In the F_1 mapping population, the lines with the J-Red genotypes were distributed on the resistance side (**Figure 3**), and 20 of these 43 lines (46.5%) showed resistance (<10 egg masses in the resistance test). The average number of egg masses was 30.8 and 69.3 in the J-Red and Choshu types, respectively,

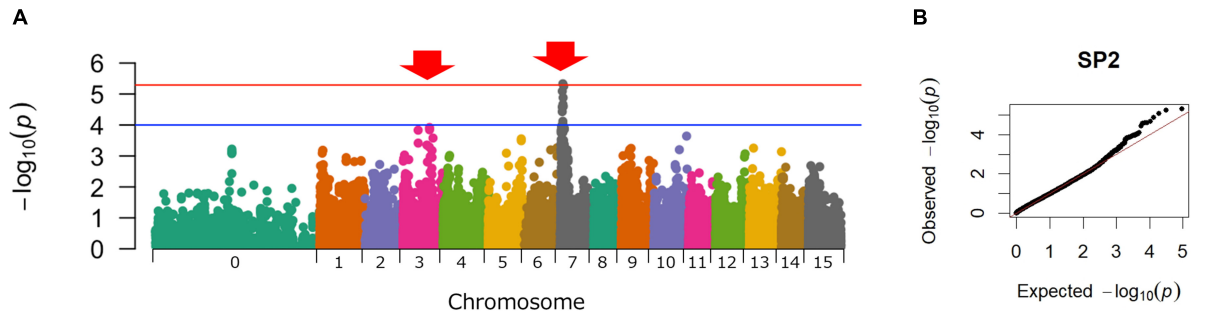

FIGURE 2 | Manhattan and Q-Q plots for sweet potato resistance to SP2 *Meloidogyne incognita.* **(A)** Manhattan plot. *X*-axis: the chromosomal number; *Y*-Axis: -$\log_{10}$(P). The red line represents the significance threshold from the false Discovery rate (FDR) based on the Benjamini–Hochberg procedure (BH) (Benjamini and Hochber, 1995). The blue line represents the significance threshold $-\log_{10}(1 \times 10^{-4})$. **(B)** Q-Q plot.

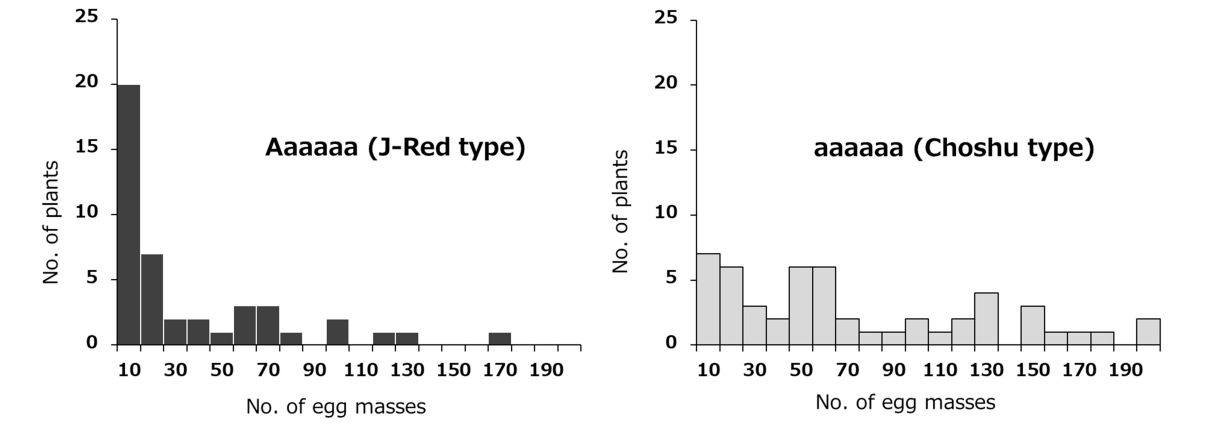

FIGURE 3 | Frequency distribution of the mean number of egg masses on F_1 lines grouped by genotype, based on the Chr07_1778460 SNP. Histograms with black and light gray indicate J-Red and Choshu genotype plants, respectively.

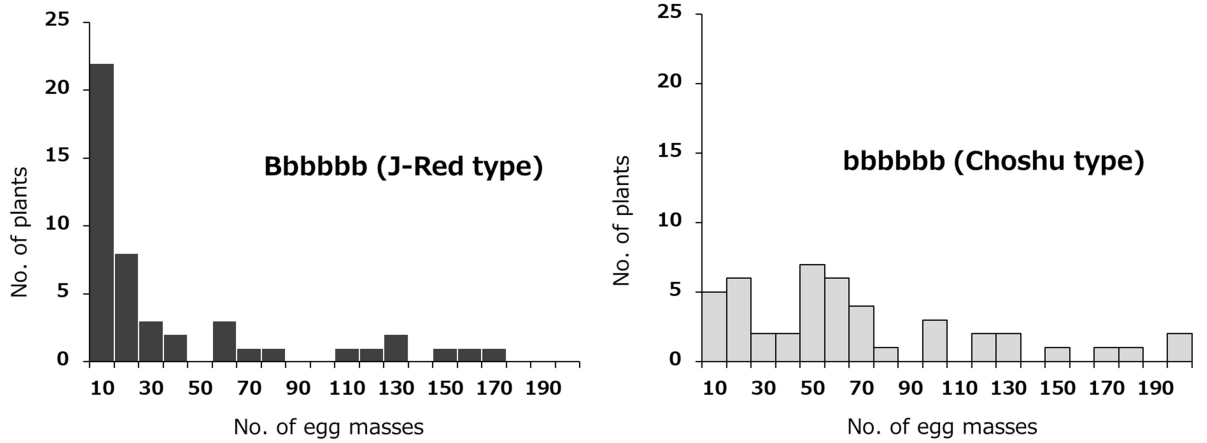

FIGURE 4 | Frequency distribution of the mean number of egg masses on F_1 lines grouped by genotype, based on the Chr03_18847788 SNP. Histograms with black and light gray indicate J-Red and Choshu genotype plants, respectively.

showing a significant difference at the 0.1% level between the two genotypes (P = 3.763E-05, Wilcoxon rank sum test; **Supplementary Figure 1**). Subsequently, the SNP marker for Chr03_18847788 was strongly associated with resistance on chromosome 3 (P = 1.209E-04). In the Chr03_18847788 marker, J-Red and Choshu showed the genotypes of Bbbbbb (simplex)

and bbbbbb (nullplex), respectively. Here, "B" represents a nucleotide that is identical with that of the reference sequence, while "b" represents a nucleotide that is different from that of the reference sequence. In the F_1 population, the genotypes of nine lines with DP values < 200 were not determined. As a result, the F_1 mapping population was classified into 46 and 45 lines for the J-Red (Bbbbbb) and Choshu (bbbbbb) types, respectively (**Supplementary Table 5**). Only two lines (JC159 and JC132) showed genotypes that were unlikely to emerge from their parents. Similar to the marker on Chr07_1778460, the lines with the J-Red genotypes (Bbbbbb) were unevenly distributed on the resistance side (**Figure 4**). Among the 46 lines with the J-Red genotype, 22 lines (47.8%) showed resistance. The average number of egg masses was 33.5 and 64.3 for the J-Red and Choshu genotypes, respectively, showing a significant difference at the 0.1% level between the two genotypes (P = 1.530E-04, Wilcoxon rank sum test; **Supplementary Figure 1**).

The combined effects of the two loci, Chr07_1778460 (Aaaaaa) and Chr03_18847788 (Bbbbbb) on resistance were then investigated. The F_1 mapping population was divided into four groups: 23 lines with the genotype combination of Aaaaaa (J-Red type) and Bbbbbb (J-Red type), 18 lines with the genotype combination of Aaaaaa (J-Red type) and bbbbbb (Choshu type), 20 lines with the genotype combination of aaaaaa (Choshu type) and Bbbbbb (J-Red type), and 25 lines with the genotype combination of aaaaaa (Choshu type) and bbbbbb (Choshu type) (**Figure 5** and **Supplementary Table 6**). The average number of egg masses for the lines in each genotype combination was 8.7, 62.1, 63.6, and 70.4, respectively (**Figure 5**). The number of egg masses on lines showing the J-Red type with both SNP markers was significantly lower than that of lines showing other genotype combinations (significant difference at the 0.1% level on Bonferroni-corrected Wilcoxon rank sum test; **Figure 5**). In addition, the average number of egg masses for Aaaaaa (J-Red type) and Bbbbbb (J-Red type) was 8.7, which was below the resistance threshold of 10. Among the 23 lines with the Aaaaaa (J-Red type) and Bbbbbb (J-Red type) genotype, 16 (69.6%) showed resistance. The rate of resistance was 46.5 and 47.8% for the J-Red type of Chr07_1778460 and Chr03_18847788 SNP markers, respectively. These results suggest that the lines with resistance against SP2 could be selected with a higher probability by combining two loci than by using a single locus.

Development of Selective Markers

J-Red derived (Chr07_1778460 and Chr03_18847788) SNPs were used to design genotyping PCR primers to assess SRKN-SP2 resistance. For designing PCR primers, we extracted the sequence information around the target SNPs based on the ddRAD-seq reads aligned to the *I. trifida* reference sequence. Since the sequence around the Chr07_1778460 SNP was not sufficiently covered by the short reads of the ddRAD-seq, the sequence around the SNP was determined by Sanger sequencing. The primer sequences are shown in **Supplementary Table 7**. A clear single band was observed in J-Red, but not in Choshu, for both Chr03 and Chr07 SNPs (**Figure 6**). Consequently, we used these primers to genotype the parental cultivars and 103 F_1 lines (**Figure 6** and **Supplementary Figure 2**). The total number of F_1 lines used for genotyping with SNP-derived PCR primers was 103 because JC2 was available for this experiment. Using a marker designed to target the Chr03-derived SNP, the PCR product obtained was 749 bp. The presence or absence of the PCR band was 100% consistent with the genotype information. Of the 55 lines identified as J-Red type on the Chr03 SNP, 25 exhibited resistance (45.5%). Using a marker designed to target the Chr07-derived SNP, the PCR product obtained was 311 bp. As for Chr03, the presence or absence of the PCR band was 100% consistent with the genotype information. Of the 48 cultivars identified as J-Red type on the Chr07 SNP, 23 exhibited resistance (47.9%). Of the 27 cultivars that showed the J-red type at both Chr03 and Chr07 loci, 19 showed resistance (70.4%). Thus, it was shown that resistant plants could be selected with a high probability using two selective markers.

DISCUSSION

In this study, we assessed SRKN-SP2 resistance in sweetpotato using a novel GWAS method for polyploids based on allele dosage probability. Because the SRKN causes serious damage to the appearance, quality, and yield of sweetpotato, the development of SRKN-resistant cultivars/lines has been required. However, owing to the complexity of polyploid inheritance and the highly heterogeneous genomic composition of sweetpotato, genetic studies of this crop lag far behind those of major diploid crop species. The segregation ratio of resistant and susceptible lines in the F_1 population suggested that resistance to SP2 is regulated by two loci in a single dose. GWAS analysis identified the two loci on Chr07 and Chr03, and selective DNA markers were developed based on the identified SNPs. Our results demonstrated that when two selective SNP-derived markers were used, resistant plants could be selected with a high probability (∼70%).

Since J-red shows resistance to the SRKN races SP1–9 (except SP8), it can be used as a resistant parental cultivar to identify the genetic regions associated with resistance for most SRKN races. In our previous study, we performed genetic analysis on SP1, SP4, and SP6-1 to identify the genetic regions controlling resistance and develop selective DNA markers (Sasai et al., 2019). For these three races, resistant and susceptible lines in the F_1 population segregated in a 1:1 ratio. Therefore, it was suggested that one major QTL in simplex determined the resistance. As expected, one major QTL common to the three races present in the simplex was detected (Sasai et al., 2019). In contrast, for the SP2 race targeted in this study, the segregation ratio of resistance and susceptible lines in the F_1 population was 1:3. This suggests that resistance to this race is regulated by two loci present in simplex. However, because the segregation ratio is close to 1:4, there is a possibility of regulation by one locus present in a duplex manner. Since the population size used in this study is relatively small for hexaploids (∼ 100 lines), it was difficult to clearly predict whether resistance to SP2 is controlled by two loci present in simplex or one locus present in duplex based on the segregation ratio. The association analysis showed that resistance to the SP2 race was controlled by two loci in

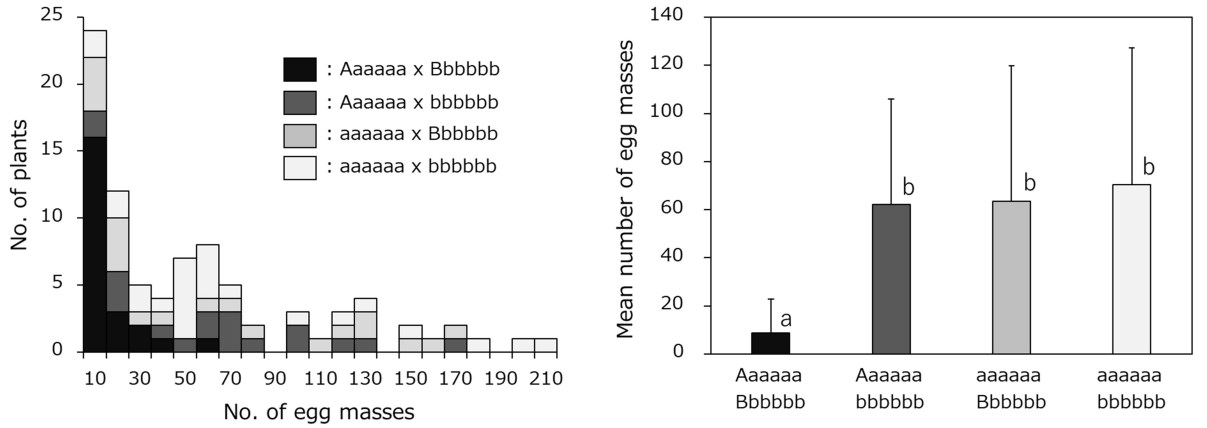

FIGURE 5 | Frequency distribution of the mean number of egg masses on F_1 lines grouped by genotype, based on the Chr07_1778460 (Aaaaaa or aaaaaa) and Chr03_18847788 (Bbbbbb or bbbbbb) SNPs. The F1 mapping population was divided into four groups: Aaaaaa × Bbbbbb, Aaaaaa × bbbbbb, aaaaaa × Bbbbbb, and aaaaaa × bbbbbb.

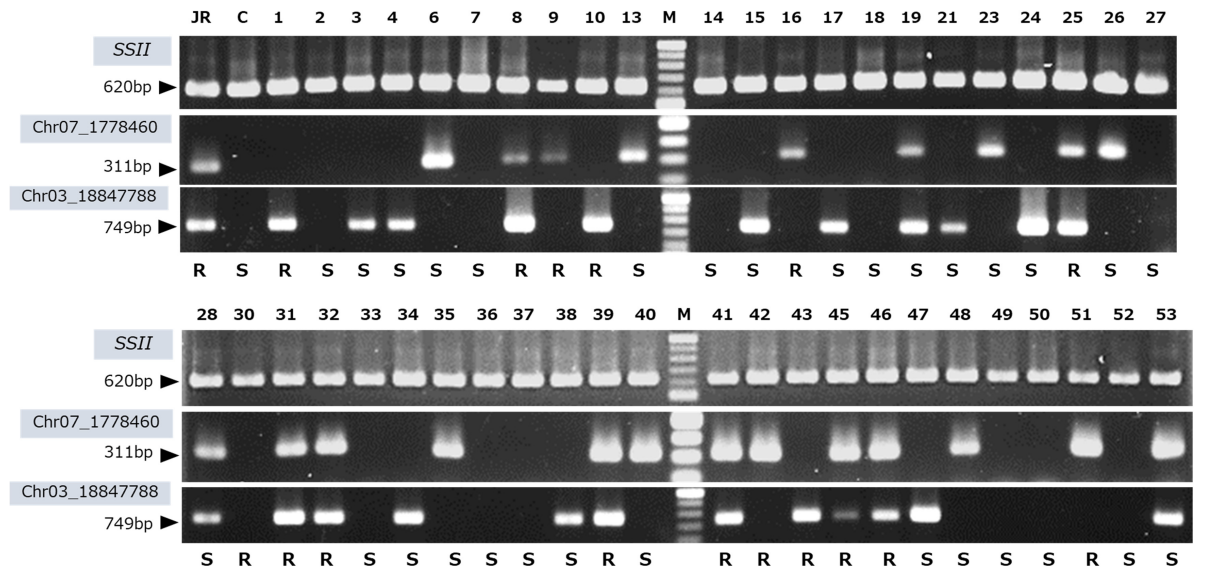

FIGURE 6 | PCR genotyping using the developed DNA markers derived from the Chr07_1778460 and Chr03_18847788 SNPs. *SSII*, positive control; JR, J-Red; C, Choshu, 1-53, F_1 lines; and M, 100 bp DNA ladder. The evaluation of the resistance to the SP2 race is shown on bottom of each lane. R and S indicates resistance and susceptibility, respectively.

simplex. For further confirmation, GWAS was performed using only simplex SNPs showing a simplex segregation ratio according to a previous method (Sasai et al., 2019). The segregation ratio of the SNPs in the F_1 population was calculated, and SNPs fitted to the expected segregation ratio of the single dose were extracted based on a Chi-square goodness-of-fit test ($P \geq 0.01$). Simplex markers that are present in one parent and are absent in the other parent segregate at a 1:1 ratio, and double simplex markers that are present in both parents segregate at a 1:3 ratio (**Supplementary Table 8**). GWAS was performed using the selected simplex SNPs with Tassel version 5.0 (Bradbury et al., 2007). The total number of SNPs selected to be present in simplex for both parents (double simplex) or simplex for one parent was 33,886 (**Supplementary Table 8**). GWAS using these SNPs generated peaks in Chr07 and Chr03 (**Supplementary Figure 3**). Because GWAS peaks were detected at the same loci using two completely independent analytical methods, the results of this study were considered reliable.

Several studies have presented genetic analyses on nematode resistance in sweetpotato. Nakayama et al. (2012) conducted genetic analysis of SP2 race using AFLP markers and developed SCAR markers associated with resistance. A major QTL [*qRmi(t)*] associated with resistance to SP1 and SP2 was detected. At that time, the reference genome for *I. trifida* had not been deciphered, and the chromosomal position of this QTL was unknown. However, we have determined that it is unlikely to

be one of the QTLs identified in our study. The reasons for this are as follows: First, in the 2012 study, resistant and susceptible lines segregated in a 1:1 ratio in the F_1 population of "Hi-starch" and "Koganesengan," and one locus was identified. In contrast, in the present study, resistant and susceptible lines segregated in a 1:3 ratio, and two loci were identified. Second, according to Nakayama et al. (2012), the resistance to SP1 and SP2 in F_1 was highly correlated (r = 0.8199), and a QTL common to SP1 and SP2 was detected, as expected. In contrast, the F_1 population used in our study had a low correlation of resistance to SP1 and SP2 (r = 0.5681), and a single QTL was detected for SP1, whereas two QTLs were detected for SP2. When the primer sequences designed based on the QTL identified by Nakayama et al. (2012) were BLASTed to the reference sequence (*I. trifida*) used in our study, most of them showed no hits or hits on chromosome 12 (E-value < 1e-2). Hence, the genomic regions controlling resistance to SP2 race in the "Hi-Starch" and "J-Red" varieties are probably different.

The analytical method used in our study has the advantage of being relatively easy to use (Yamamoto et al., 2020). Currently, various analytical tools such as MAPpoly and QTLpoly have been developed for polyploid species, which use Mendelian inheritance simplex markers as well as multiplex markers (Mollinari and Garcia, 2019; da Silva Pereira et al., 2020; Mollinari et al., 2020). Recently, Oloka et al. (2021) performed QTL mapping for nematode resistance by constructing a high-density linkage map with single- and multiple-dose SNPs and indels. The authors utilized new bioinformatic tools developed for sweetpotato improvement, such as GBSpoly, a genotyping platform that modifies GBS to polyploid species; MAPpoly, an R package for building linkage maps; and QTLpoly, an R package for QTL mapping. A high-density integrated linkage map was developed using a mapping population derived from a cross between "Tanzania," an African landrace cultivar, and "Beauregard," a major United States cultivar. A major QTL for SRKN race 3 resistance was identified on linkage group 7 (LG7), and the genotypes of the most significant markers associated with resistance were duplex (AAaaaa) for the resistant "Tanzania" cultivar, and nulliplex (aaaaaa) for "Beauregard." Oloka et al. (2021) used the same reference sequence of *I. trifida* (Wu et al., 2018) used in our study, and interestingly, one major peak was commonly detected on chromosome 7 (LG7) in both studies. However, it is unclear whether SRKN race 3 from Oloka et al. (2021) and SP3 used in this study are the same. In addition, the genetic distance between resistance cultivars "Tanzania" and "J-Red" is unknown. From these reasons, it cannot be determined whether the QTLs identified in these studies are consistent and/or derived from the same resistance gene. On the other hand, the analytical methods used in their study were useful for the identification of QTLs and investigation of their effects in hexaploid sweetpotato. However, the analytical tool used in our study is easy to use and can detect target regions without constructing linkage maps, and the obtained results are highly reliable. In general, linkage map construction for polyploid species requires considerable time and computational resources. In addition, when the size of the mapping population is relatively small, it is extremely difficult to accurately calculate the recombination values and marker distances. In contrast, the GWAS method used in this study can identify the genomic regions controlling agronomical traits in a short time (several minutes), even with limited computer resources. Although the loci identified in this study were in a single dose, this technique can also be used to identify loci in multiplexes. Therefore, it was determined that the method used in our analysis can effectively detect QTLs and be used to develop DNA markers in polyploid crop species.

The purpose of plant breeding is to produce excellent cultivars, which requires continuous discovery of desirable genes and pyramiding into breeding lines. Molecular markers linked to a gene or loci of target traits have been effectively utilized in breeding programs for cultivar development. In particular, the importance of molecular markers associated with pest and disease resistance is widely recognized, and such markers facilitate the development of resistant cultivars/lines by marker-assisted selection, which contributes to expanded cultivation areas and increased yields. In this study, the selective DNA markers were developed using the SNPs derived from J-Red resistant cultivar. Using the two selective markers, we could screen resistant lines to SRKN SP2 race with high efficiency (∼70%). However, the utility and effectiveness of these selective markers in other mapping populations and cross combinations have not been validated. In the near future, we aim to perform marker genotyping and resistance evaluation using other mapping populations and various sweetpotato cultivars/lines to validate the effectiveness and utility of these selective markers. In addition, we plan to perform comparative analysis with other tools, such as MAPpoly and QTLpoly, and identify candidate genes using RNA-sequencing analysis and transgenic experiments. Overall, this study provides a model for identifying genomic regions controlling agronomical traits and their effects in polyploid crop species. Our study also serves as a resource describing useful molecular tools for marker-assisted selection in sweetpotato breeding programs.

DATA AVAILABILITY STATEMENT

The datasets presented in this study can be found in online repositories. The names of the repository/repositories and accession number(s) can be found in the article/**Supplementary Material**.

AUTHOR CONTRIBUTIONS

YM and HT conceived and designed the experiments. NO, MK, HT, EY, KS, and YM contributed to the experiments and data analyses. NO, HT, and YM drafted the manuscript. All authors read and approved the final manuscript.

FUNDING

This work was supported by the Japanese Society for the Promotion of Science (JSPS) KAKENHI, Grant Number

20K05984 (to YM) and by a grant from the Ministry of Agriculture, Forestry, and Fisheries of Japan (Genomics-based Technology for Agricultural Improvement, SFC-3003).

ACKNOWLEDGMENTS

We would like to express our appreciation for Kyushu Operation Unit 3 of the Technical Support Center of Kyushu-Okinawa Region, Sanae Nagahashi, Mizuki Maniwa, and Ai Tokiwa at KARC/NARO for their excellent technical assistance, and for Masaru Tanaka for helpful discussion and encouragement. This work could not have been accomplished without F_1 progeny derived from "J-Red" and "Choshu" and SRKN races maintained by Hiroki Nakayama (KARC/NARO), who passed away in 2012. We also thank Editage (www.editage.com) for English language editing.

SUPPLEMENTARY MATERIAL

The Supplementary Material for this article can be found online at: https://www.frontiersin.org/articles/10.3389/fpls.2022.858747/full#supplementary-material

REFERENCES

Benjamini, Y., and Hochberg, Y. (1995). Controlling the false discovery rate: a practical and powerful approach to multiple testing. *J. R. Stat. Soc. Ser. B. Methodol.* 57, 289–300. doi: 10.1111/j.2517-6161.1995.tb02031.x

Bourke, P. M., Voorrips, R. E., Visser, R. G. F., and Maliepaard, C. (2018). Tools for Genetic Studies in Experimental Populations of Polyploids. *Front. Plant Sci.* 9:513. doi: 10.3389/fpls.2018.00513

Bradbury, P. J., Zhang, Z., Kroon, D. E., Casstevens, T. M., Ramdoss, Y., and Buckler, E. S. (2007). TASSEL: software for association mapping of complex traits in diverse samples. *Bioinformatics* 23, 2633–2635. doi: 10.1093/bioinformatics/btm308

Cervantes-Flores, J. C., Yencho, G. C., Pecota, K. V., Sosinski, B., and Mwanga, R. O. M. (2008). Detection of quantitative trait loci and inheritance of root-knot nematode resistance in sweetpotato. *J. Am. Soc. Hortic. Sci.* 133, 844–851. doi: 10.21273/JASHS.133.6.844

da Silva Pereira, G., Gemenet, D. C., Mollinari, M., Olukolu, B. A., Wood, J. C., Diaz, F., et al. (2020). Multiple QTL mapping in autopolyploids: a random-effect model approach with application in a hexaploid sweetpotato full-sib population. *Genetics* 215, 579–595. doi: 10.1534/genetics.120.303080

Endelman, J. B., Carley, C. A. S., Bethke, P. C., Coombs, J. J., Clough, M. E., da Silva, W. L., et al. (2018). Genetic variance partitioning and genome-wide prediction with allele dosage information in autotetraploid potato. *Genetics* 209, 77–87. doi: 10.1534/genetics.118.300685

FAOSTAT (2019). *Food and Agriculture Organization of the United Nations (FAO).* Available online at: https://www.fao.org/faostat/en/#home (accessed August 4, 2021).

Gao, M., Soriano, S. F., Cao, Q., Yang, X., and Lu, G. (2020). Hexaploid sweetpotato (Ipomoea batatas (L.) Lam.) may not be a true type to either auto- or allopolyploid. *PLoS One* 15:e0229624. doi: 10.1371/journal.pone.0229624

Gotoh, A., Sano, Z., and Minagawa, N. (1973). Prediction of the time of emergence of the next generation of the southern root-knot nematode, Meloidogyne incognita, with thermal contents for development from infection populations. *Kyushu Plant Prot. Res.* 19, 124–127.

Gurmu, F., Hussein, S., and Laing, M. (2013). Self-and cross-incompatibilities in sweetpotato and their implications on breeding. *Aust. J. Crop Sci.* 7:2074.

Hayashi, K., Hashimoto, N., Daigen, M., and Ashikawa, I. (2004). Development of PCR-based SNP markers for rice blast resistance genes at the Piz locus. *Theor. Appl. Genet.* 108, 1212–1220. doi: 10.1007/s00122-003-1553-0

Hirakawa, H., Okada, Y., Tabuchi, H., Shirasawa, K., Watanabe, A., Tsuruoka, H., et al. (2015). Survey ofgenome sequences in a wild sweet potato, Ipomoea trifida (H. B. K.) G. Don. *DNA Res.* 22, 171–179. doi: 10.1093/dnares/dsv002

Isobe, S., Shirasawa, K., and Hirakawa, H. (2017). Challenges to genome sequence dissection in sweetpotato. *Breed. Sci.* 67, 35–40. doi: 10.1270/jsbbs.16186

Iwahori, H., and Sano, Z. (2003). Distribution of main plant-parasitic nematodes in sweet potato and taro fields in Kyushu and Okinawa, Japan. 3. Survey in the northern part in Kyushu Island (Fukuoka, Saga, Nagasaki and Ohita Prefs.). *Kyushu Plant Prot. Res.* 49, 83–87. doi: 10.4241/kyubyochu.49.83

Iwahori, H., Sano, Z., and Ogawa, T. (2000). Distribution of main plant-parasitic nematodes in sweet potato and taro fields in Kyushu and Okinawa, Japan. 1. Survey in the central and southern parts in Kyushu Island (Kumamoto, Miyazaki and Kagoshima Prefs.) and development of an effective DNA analysis method for species identification. *Kyushu Plant Prot. Res.* 46, 112–117. doi: 10.4241/kyubyochu.46.112

Jones, A. (1967). *Theoretical Segregation Ratios of Qualitatively Inherited Characters for Hexaploid Sweet Potato (Ipomoea batatas L.). Technical Bulletin No. 1368*. Washington: US Department of Agriculture, Economic Research Service, 1–6.

Knaus, B. J., and Grünwald, N. J. (2017). VCFR: a package to manipulate and visualize variant call format data in R. *Mol. Ecol. Resour.* 17, 44–53. doi: 10.1111/1755-0998.12549

Koboldt, D. C., Zhang, Q., Larson, D. E., Shen, D., McLellan, M. D., Lin, L., et al. (2012). VarScan 2: somatic mutation and copy number alteration discovery in cancer by exome sequencing. *Genom. Res.* 22, 568–576. doi: 10.1101/gr.129684.111

Kriegner, A., Cervantes, J. C., Burg, K., Mwanga, R. O. M., and Zhang, D. (2003). A genetic linkage map of sweet potato [Ipomoea batatas (L.) Lam.] based on AFLP markers. *Mol. Breed.* 11, 169–185. doi: 10.1023/A:1022870917230

Krusberg, L. R., and Nielson, L. W. (1958). Pathogenesis of root-knot nematodes to the Port Rico variety of sweetpotsto. *Phytopathology* 48, 30–39.

Kuranouchi, T., Momota, Y., Takada, A., and Katayama, K. (2018). The composition of southern root-knot nematode (Meloidogyne incognita) race in the resistance test field used for sweetpotato breeding. *Nematol. Res.* 48, 31–34. doi: 10.3725/jjn.48.31

Langmead, B., and Salzberg, S. L. (2012). Fast gapped-read alignment with Bowtie 2. *Nat. Meth.* 9, 357–359. doi: 10.1038/nmeth.1923

Lawrence, G. W., Clark, C. A., and Wright, V. L. (1986). Influence of Meloidogyne incognita on resistant and susceptible sweet potato cultivars. *J. Nematol.* 18, 59–65.

Li, H., Handsaker, B., Wysoker, A., Fennell, T., Ruan, J., Homer, N., et al. (2009). The sequence alignment/map format and SAMtools. *Bioinformatics* 25, 2078–2079. doi: 10.1093/bioinformatics/btp352

Magoon, M. L., Krishnan, R., and Vijaya Bai, K. (1970). Cytological evidence on the origin of sweet potato. *Theor. Appl. Genet.* 40, 360–366. doi: 10.1007/BF00285415

Martin, M. (2011). Cutadapt removes adapter sequences from high-throughput sequencing reads. *EMBnet J.* 17:10. doi: 10.14806/ej.17.1.200

Mcharo, M., LaBonte, D. R., Clark, C., Hoy, M., and Oard, J. H. (2005). Molecular marker variability for southern root-knot nematode resistance in sweetpotato. *Euphytica* 144, 125–132. doi: 10.1007/s10681-005-5271-3

Ministry of Agriculture, Forestry and Fisheries (2020). *The 94th Statistical Yearbook of Ministry of Agriculture, Forestry and Fisheries*. Available online at: https://www.maff.go.jp/e/data/stat/94th/ (accessed February 5, 2022).

Mollinari, M., and Garcia, A. A. F. (2019). Linkage analysis and haplotype phasing in experimental autopolyploid populations with high ploidy level using hidden markov models. *G3* 9, 3297–3314. doi: 10.1534/g3.119.400378

Mollinari, M., Olukolu, B. A., Pereira, G. D. S., Khan, A., Gemenet, D., Yencho, G. C., et al. (2020). Unraveling the hexaploid sweet-potato inheritance using ultra-dense multilocus mapping. *G3* 10, 281–292. doi: 10.1534/g3.119.400620

Monden, Y., Hara, T., Okada, Y., Jahana, O., Kobayashi, A., Tabuchi, H., et al. (2015). Construction of a linkage map based on retrotransposon insertion polymorphisms in sweetpotato via high-throughput sequencing. *Breed. Sci.* 65, 145–153. doi: 10.1270/jsbbs.65.145

Monden, Y., and Tahara, M. (2017). Genetic linkage analysis using DNA markers in sweetpotato. *Breed. Sci.* 67, 41–51. doi: 10.1270/jsbbs.16142

Nakayama, H., Tanaka, M., Takahata, Y., Matsui, K., Iwahori, H., Sano, Z., et al. (2012). Development of AFLP-derived SCAR markers associated with resistance to two races of southern root-knot nematode in sweetpotato. *Euphytica* 188, 175–185. doi: 10.1007/s10681-012-0678-0

Oloka, B. M., da Silva Pereira, G., Amankwaah, V. A., Mollinari, M., Pecota, K. V., Yada, B., et al. (2021). Discovery of a major QTL for root-knot nematode (Meloidogyne incognita) resistance in cultivated sweetpotato (Ipomoea batatas). *Theor. Appl. Genet.* 134, 1945–1955. doi: 10.1007/s00122-021-03797-z

Overstreet, C. (2009). "Chapter 9, Nematoses," in *The Sweetpotato*, eds G. Loebenstein and G. Thottappilly (Berlin: Springer).

R Core Team (2020). *R: A Language and Environment for Statistical Computing*. Vienna: R Foundation for Statistical Computing.

Robinson, J. T., Thorvaldsdóttir, H., Winckler, W., Guttman, M., Lander, E. S., Getz, G., et al. (2011). Integrative genomics viewer. *Nat. Biotechnol.* 29, 24–26. doi: 10.1038/nbt.1754

Sano, Z., and Iwahori, H. (2005). Regional variation in pathogenicity of Meloidogyne incognita populations on sweet potato in Kyushu Okinawa, Japan. *JPN. J. Nematol.* 35, 1–12. doi: 10.3725/jjn1993.35.1_1

Sano, Z., Iwahori, H., Tateishi, Y., and Kai, Y. (2002). Differences in the resistance of sweet potato cultivars and lines to Melodogyne incognita populations. *JPN. J. Nematol.* 32, 77–86. doi: 10.3725/jjn1993.32.2_77

Sasai, R., Tabuchi, H., Shirasawa, K., Kishimoto, K., Sato, S., Okada, Y., et al. (2019). Development of molecular markers associated with resistance to Meloidogyne incognita by performing quantitative trait locus analysis and genome-wide association study in sweetpotato. *DNA Res.* 26, 399–409. doi: 10.1093/dnares/dsz018

Shirasawa, K., Tanaka, M., Takahata, Y., Ma, D., Cao, Q., Liu, Q., et al. (2017). A high-density SNP genetic map consisting of a complete set of homologous groups in autohexaploid sweetpotato (Ipomoea batatas). *Sci. Rep.* 7:44207. doi: 10.1038/srep44207

Sinha, S., and Sharma, S. N. (1992). Taxonomic significance of karyo- morphology in Ipomoea spp. *Cytologia* 57, 289–293. doi: 10.1508/cytologia.57.289

Tabuchi, H., Kuranouchi, T., Kobayashi, A., Monden, Y., Kishimoto, K., Tahara, M., et al. (2017). Southern root-knot nematode race SP6 is divided into two races. *Nematol. Res.* 47, 29–33. doi: 10.3725/jjn.47.29

Ting, Y. C., and Kehr, A. E. (1953). Meiotic studies in the sweet potato (Ipomoea batatas Lam.). *J. Hered.* 44, 207–211. doi: 10.1093/oxfordjournals.jhered.a106395

Uitdewilligen, J. G. A. M. L., Wolters, A. M., D'Hoop, B. B., Borm, T. J., Visser, R. G., and van Eck, H. J. (2013). A next-generation sequencing method for genotyping-by-sequencing of highly heterozygous autotetraploid potato. *PLoS One* 8:e62355. doi: 10.1371/journal.pone.0062355

Ukoskit, K., and Thompson, P. G. (1997). Autopolyploidy versus allo-polyploidy and low-density randomly amplified polymorphic DNA linkage maps of sweet potato. *J. Am. Soc. Hortic. Sci.* 122, 822–828. doi: 10.21273/JASHS.122.6.822

Ukoskit, K., Thompson, P. G., Watson, C. E., and Lawrence, G. W. (1997). Identifying a randomly amplified polymorphic DNA (RAPD) marker linked to a gene for root-knot nematode resistance in sweet potato. *J. Am. Soc. Hortic. Sci.* 122, 818–821. doi: 10.21273/JASHS.122.6.818

Wu, S., Lau, K. H., Cao, Q., Hamilton, J. P., Sun, H., Zhou, C., et al. (2018). Genome sequences of two diploid wild relatives of cultivated sweetpotato reveal targets for genetic improvement. *Nat. Commun.* 9:4580. doi: 10.1038/s41467-018-06983-8

Yamamoto, E., Shirasawa, K., Kimura, T., Monden, Y., Tanaka, M., and Isobe, S. (2020). Genetic mapping in autohexaploid sweet potato with low-coverage NGS-based genotyping Data. *G3* 10, 2661–2670. doi: 10.1534/g3.120.401433

Yoshida, T. (1965). On the geographical distribution of soil nematodes in Chiba Prefecture. *Boll. Chiba Agric. Exp. Stn.* 6, 69–78.

Zhao, N., Yu, X., Jie, Q., Li, H., Li, H., Hu, J., et al. (2013). A genetic linkage map based on AFLP and SSR markers and mapping of QTL for dry-matter content in sweetpotato. *Mol. Breed.* 32, 807–820. doi: 10.1007/s11032-013-9908-y

Conflict of Interest: The authors declare that the research was conducted in the absence of any commercial or financial relationships that could be construed as a potential conflict of interest.

Publisher's Note: All claims expressed in this article are solely those of the authors and do not necessarily represent those of their affiliated organizations, or those of the publisher, the editors and the reviewers. Any product that may be evaluated in this article, or claim that may be made by its manufacturer, is not guaranteed or endorsed by the publisher.

frontiers | Frontiers in Plant Science

TYPE Original Research
PUBLISHED 08 November 2023
DOI 10.3389/fpls.2023.1257744

OPEN ACCESS

EDITED BY
Mohamed Mannaa,
Cairo University, Egypt

REVIEWED BY
Sara Fareed Mohamed Wahdan,
Suez Canal University, Egypt
Tuyong Yi,
Hunan Agricultural University, China

*CORRESPONDENCE
Yunpeng Huang
hyp1234888@126.com
Jun Su
junsu@fafu.edu.cn

†These authors have contributed equally to this work

RECEIVED 12 July 2023
ACCEPTED 24 October 2023
PUBLISHED 08 November 2023

CITATION
Jia J, Chen L, Yu W, Cai S, Su S, Xiao X, Tang X, Jiang X, Chen D, Fang Y, Wang J, Luo X, Li J, Huang Y and Su J (2023) The novel nematicide chiricanine A suppresses *Bursaphelenchus xylophilus* pathogenicity in *Pinus massoniana* by inhibiting *Aspergillus* and its secondary metabolite, sterigmatocystin. *Front. Plant Sci.* 14:1257744. doi: 10.3389/fpls.2023.1257744

The novel nematicide chiricanine A suppresses *Bursaphelenchus xylophilus* pathogenicity in *Pinus massoniana* by inhibiting *Aspergillus* and its secondary metabolite, sterigmatocystin

Jiayu Jia[1†], Long Chen[1†], Wenjing Yu[1†], Shouping Cai[2], Shunde Su[2], Xiangxi Xiao[2], Xinghao Tang[2], Xiangqing Jiang[3], Daoshun Chen[3], Yu Fang[4], Jinjin Wang[1], Xiaohua Luo[5], Jian Li[1], Yunpeng Huang[2*] and Jun Su[1*]

[1]Basic Forestry and Proteomics Research Center, College of Forestry, Fujian Provincial Key Laboratory of Haixia Applied Plant Systems Biology, Fujian Agriculture and Forestry University, Fuzhou, China, [2]Fujian Academy of Forestry, Key Laboratory of National Forestry and Grassland Administration on Timber Forest Breeding and Cultivation for Mountainous Areas in Southern China, Fuzhou, China, [3]Silviculture Department, Shaxian Guanzhuang State-Owned Forest Farm, Sanming, China, [4]Institute of Soil Fertilizer, Fujian Academy of Agricultural Sciences, Fuzhou, China, [5]Forest Fire Prevention Office, Forestry Bureau of Yuoxi County, Sanming, China

Introduction: Pine wilt disease (PWD) is responsible for extensive economic and ecological damage to Pinus spp. forests and plantations worldwide. PWD is caused by the pine wood nematode (PWN, *Bursaphelenchus xylophilus*) and transmitted into pine trees by a vector insect, the Japanese pine sawyer (JPS, *Monochamus alternatus*). Host infection by PWN will attract JPS to spawn, which leads to the co-existence of PWN and JPS within the host tree, an essential precondition for PWD outbreaks. Through the action of their metabolites, microbes can manipulate the co-existence of PWN and JPS, but our understanding on how key microorganisms engage in this process remains limited, which severely hinders the exploration and utilization of promising microbial resources in the prevention and control of PWD.

Methods: In this study we investigated how the PWN-associated fungus *Aspergillus* promotes the co-existence of PWN and JPS in the host trees (*Pinus massoniana*) via its secondary metabolite, sterigmatocystin (ST), by taking a multi-omics approach (phenomics, transcriptomics, microbiome, and metabolomics).

Results: We found that *Aspergillus* was able to promote PWN invasion and pathogenicity by increasing ST biosynthesis in the host plant, mainly by suppressing the accumulation of ROS (reactive oxygen species) in plant tissues that could counter PWN. Further, ST accumulation triggered the biosynthesis of VOC (volatile organic compounds) that attracts JPS and drives the coexistence of PWN and JPS in the host plant, thereby encouraging the local transmission of PWD. Meanwhile, we show that application of an *Aspergillus* inhibitor (chiricanine A

treatment) results in the absence of *Aspergillus* and decreases the *in vivo* ST amount, thereby sharply restricting the PWN development in host. This further proved that *Aspergillus* is vital and sufficient for promoting PWD transmission.

Discussion: Altogether, these results document, for the first time, how the function of *Aspergillus* and its metabolite ST is involved in the entire PWD transmission chain, in addition to providing a novel and long-term effective nematicide for better PWD control in the field.

KEYWORDS

aspergillus, host performance, *Monochamus alternatus*, nematicide, pine wilt disease, pinewood nematode (*Bursaphelenchus xylophilus*), sterigmatocystin

1 Introduction

Pine wilt disease (PWD) has brought great economic and ecological damage to *Pinus* spp. forests and plantations worldwide (Zhao et al., 2014). PWD is caused by the pine wood nematode (PWN) *Bursaphelenchus xylophilus*, which itself is transmitted by vector insects, namely the Japanese pine sawyer (JPS) *Monochamus alternatus* (Hu et al., 2013; Hirata et al., 2017; Carnegie et al., 2018; Wu et al., 2021). Infection with PWN will turn the host into a lure that attracts JPS to spawn, this leading to the PWN and JPS co-existing within the host pine tree, an essential precondition for PWD transmission (Li et al., 2022). In the last decade, tremendous effort has been expended towards developing effective strategies to impair the co-existence of PWN and JPS and thereby suppress the transmission PWD and potential outbreaks in stand. Microbes have proven substantial advantages for long-term pest control (Wang et al., 2017; Ponpandian et al., 2019; Cai et al., 2022; Pires et al., 2022; Tian et al., 2022); however, their efficacy is strongly affected by local environments and a highly structured microbial community, as well as microbe-specific biochemical metabolites. Accordingly, the high-efficiency use of microbes varies with different conditions, being context-dependent (Chaudhary et al., 2023; Poppeliers et al., 2023). Thus, exploring the biochemical basis enabling microbes to interfere with PWN and JPS co-existence is crucial for their use in effective long-term control of PWD.

Microbes are associated with PWN and play a crucial role in its invasion and pathogenicity (Zhao et al., 2014; Feng et al., 2022). The biological function of these PWN-associated microbes (PAMs) has been widely explored. Research has shown these PWN–PAM interactions can be beneficial (a mutualistic relationship), harmful (a parasitic/pathogenic relationship), or neutral (Zhao et al., 2014; Proenca et al., 2017a; Proenca et al., 2017b; Feng et al., 2022). These PAMs can also inactivate the PWN-induced resistance (mainly through the accumulation of reactive oxygen species [ROS]) in host pine trees, thus promoting the invasion and pathogenicity of PWN through adjustments to the microbial community or its members' metabolites, including pathogenic factors, exoenzymes, and toxic secondary metabolites (Zhao et al., 2014; Li, 2018; Liu et al., 2019; Xue et al., 2019; Zhang, 2021; Feng et al., 2022; Li et al., 2022). Yet, because of the complex structure and function of microbial communities, our understanding of the key microorganisms and their functions that affect the invasion and pathogenicity of PWN is still limited. This greatly restricts the exploration and utilization of potent microbial resources in the prevention and control of PWD.

After infection by PWN, the biosynthesis of volatile organic compounds (VOCs) is strongly augmented in host pine trees, which lures JPS for feeding and spawning (Cheng et al., 2005). Several such VOC have been identified that are clearly capable of attracting JPS, including α-pinene, β-pinene, β-phellandrene, myrcene, and other terpene and sterols; some of them were successfully used to bait and trap JPS in the field (Teale et al., 2011). Previous studies have shown that PAM and host plant-associated microbes are directly or indirectly involved in the biosynthesis of the above VOCs via exoenzymes or metabolites (Alicandri et al., 2020). Hence, this hints that these PWN- and host-associated microbes might also affect the host preference of JPS, but this prospect warrants further exploration.

Based on above-mentioned lines of evidence, we hypothesized that a microbe can manipulate the co-existence of PWN and JPS through its metabolites, to influence PWD transmission. In our previous studies(Cai et al., 2022), by using metagenomic sequencing, we identified the key microorganism in host pine trees to be *Aspergillus*, whose abundance and activity are highly enriched during a PWN invasion and positively correlated with the amount and pathogenicity of PWN. Further, from correlations with metabolic data, it is evident that the pivotal metabolite of *Aspergillus* species, sterigmatocystin (ST), is highly induced by a PWN invasion, which might be the biochemical basis enabling *Aspergillus* to facilitate PWN invasion and pathogenicity. Given the above findings, the present study employed phenotypic, genetic, metabolic, and microbiological techniques to comprehensively clarify whether and how ST in the host plant *Pinus massoniana* enhances PWN invasion and pathogenicity; that is, by promoting host synthesis of VOC to attract JPS adults and ultimately sustaining the coexistence of PWN and JPS in their host, thus bolstering the transmission of PWD. Meanwhile, we speculated and tested whether the application of *Aspergillus* inhibitor (chiricanine A) could reduce the ST level in the host, to thus suppress PWN invasion and pathogenicity (Cai et al.,

2022). The successful implementation of this project convincingly demonstrates the intrinsic biochemical mechanism of how key microorganisms, such as *Aspergillus* spp., are able to promote the transmission of PWD, which should encourage exploration of its application prospects in field settings.

2 Materials and methods

2.1 Plants and growth conditions

For the laboratory experiments, 2-year-old seedlings of *P. massoniana* were harvested from a nursery garden in a Shaxian Guanzhuang state-owned forest farm in Sanming, Fujian, China (26.5603°N, 117.7455°E). They were placed in growth chambers (light: dark = 16 h: 8 h, 70% humidity, 28°C in light and 24°C in dark) for 2 months before the experimental treatments began.

The field experiments were carried out in the same state-owned farm. This study area consisted of a 76-ha, 16-year-old pure *P. massoniana* plantation, where the annual average temperature and precipitation is 19.9°C and 1375.2 mm, respectively.

2.2 Inoculation of pine wood nematode

Adults of PWN were cultured as previously described (Cai et al., 2022). 1 mL of a PWN inoculation solution (5000 individuals/mL) was inoculated into *P. massoniana* seedlings as previously described, with 15 replicates (individual plants) used in each treatment. Double-distilled water served as the negative control.

2.3 Seedling injection with sterigmatocystin, *A. arachidicola*, *A. sclerotioniger*, and chiricanine A

Sterigmatocystin (cat no. 10048-13-2, Shanghai Yuanye Bio-Technology Co., Ltd, Shanghai, China) was first dissolved in methanol, to prepare a stock solution (1mg/mL), then diluted to 1/10, 1/100, and 1/1000 with methanol as the working solution. These working solutions were separately injected into *P. massoniana* seedlings (1 mL per individual), as previously described (Xiang et al., 2015). There was n = 15 per treatment, and a methanol solution served as the negative control.

Aspergillus arachidicola (CBS117610) and *A. sclerotioniger* (CBS115572) were ordered from the Westerdijk Fungal Biodiversity Institute (https://wi.knaw.nl/). Each was inoculated separately into *P. massoniana* seedlings (1 mL per individual), with n = 15 for each treatment and double-distilled water used as the negative control.

Under laboratory conditions, 2-year-old *P. massoniana* seedling were inoculated with PWN, then injected with a solution of 4 ppm chiricanine A (cat no. B35217-5mg, Shanghai Yuanye Bio-Technology Co., Ltd, Shanghai, China) and emamectin benzoate (cat no. 155569-91-8, Merck, Shanghai, China). These solutions were injected into *P. massoniana* seedlings (1 mL per individual) as previously described (Xiang et al., 2015); n = 10 for each treatment, for which a 4 ppm methanol solution served as the negative control. Plant samples were harvested at 14 dpi, then stored at –80°C for subsequent experiments. In the field testing chiricanine A and 2% emamectin benzoate (EB) solution (PD20110688, Syngenta, Shanghai, China) were used for the trunk injections. The injection dose was based on the DBH of each tree (1 mL/cm). High-pressure trunk drilling and injection equipment (cat no. ZYJ15B, Greenman, Beijing, China) was used to apply the injections, by following a standard protocol (dose injected into stem at 1 m above the ground at a 45° angle).

2.4 Quantification of ROS accumulation in the host plant *P. massoniana*

The ST-infected and negative control *P. massoniana* seedling samples in the laboratory experiments were harvested at 14 dpi. Their collected pine needles were immediately placed in liquid nitrogen and stored in a –80°C refrigerator. Then the amounts of ROS (cat no. ROS-1-Y, Comin Biology, Suzhou, China) and H_2O_2 (cat no. G0112W, Gris Biology, Suzhou, China) in these samples were measured by following the standard protocols of the above two kits. To ascertain differences among the means of the treatment groups, a one-way analysis of variance (ANOVA) along with Tukey's test was employed.

2.5 Quantification of the relative PWN level

The amount of PWN in live plants was quantified by RT-qPCR (real-time quantitative polymerase chain reaction). Whole 2-year-old seedlings in the laboratory were used for the PWN quantification. The total genomic DNA of each plant sample was extracted using the MoBio PowerSoil DNA isolation kit (cat no.12855-50, MoBio, USA), according to the manufacturer's protocol. The quantity and quality of DNA were measured on a NanoDrop 2000 photometer (Thermo Fisher Scientific, USA), with DNA integrity determined by 1% agarose gel electrophoresis. The extracted DNA was then stored at –80°C until further use. Quantitative PCR were conducted using PWN-specific primers and a host-specific primer (one transcript from *P. massoniana* as the internal control) (Table S32), by using the Hieff^{TM} qPCR SYBR Green Master Mix (Low Rox Plus, cat no. 11202ES08, Yeasen, Shanghai, China) on a QuantStudio 6 Flex PCR (ABI). The qPCR signals were normalized to those of the reference gene *PST* in pine trees, by applying the $2^{-\Delta\Delta CT}$ method (Fang et al., 2023). Biological triplicates with technical triplicates were used. One-way analysis of variance (ANOVA; Tukey's test) was performed to determine the differences among groups.

2.6 Quantification of plant defense genes and *aflR* of *Aspergillus* spp.

Total RNAs were isolated from *P. massoniana* seedlings at 14 dpi by using the Trizol reagent (cat no. 15596026, Invitrogen, CA,

USA). Each sample of total RNA (1 mg) was reverse transcribed by the PrimeScript™ RT reagent Kit with gDNA Eraser (cat no. RR047A, Takara, Japan). The resistance genes examined were the same as those investigated in our previous study (Cai et al., 2022).

The *aflR* gene was extracted and searched by BLAST in the available genomes of the *Aspergillus* series at Genome/NCBI (https://www.ncbi.nlm.nih.gov/genome). The sequences extracted from these genomes were aligned and consensus sequence used to design the primers online in Primer3 Plus (https://www.primer3plus.com). All the gene-specific primers used in this assay are listed in Table S32. RT-qPCR was carried out to quantify the gene expression level (as described in section 2.5). One-way analysis of variance (ANOVA; Tukey's test) was implemented to determine the differences among the means of treatment groups.

2.7 Metabolome sequencing and analysis in the host plant *P. massoniana*

Sample preparation went as described in section 2.3, with three technical replications used. The metabolites were then extracted from each sample by following a previously described protocol (De Vos et al., 2007). The Ultra High Performance Liquid Chromatography (UHPLC) separation was carried out using an A Dionex Ultimate 3000 RS UHPLC (Thermo Fisher Scientific, Waltham, MA, USA) equipped with an ACQUITY UPLC HSS T3 column (1.8 µm, 2.1×100 mm, 186009468, Waters, Milford, USA) by the Oebiotech Company (Shanghai, China). Set to a flow rate of 0.35 mL/min, the mobile phases were 0.1% formic acid in water (A) (A117-50, Thermo Fisher Scientific, Waltham, MA, USA) and 0.1% formic acid in acetonitrile (B) (A998-4, Thermo Fisher Scientific, Waltham, MA, USA). The column temperature was set to 45°C, while the auto-sampler temperature was set to 4°C, and the injection volume was 5 µL (Chen et al., 2007; Theodoridis et al., 2008). Ensuing data were trimmed from different samples to distinguish the insect-induced metabolites. Next, commercial databases, including the Kyoto Encyclopedia of Genes and Genomes (KEGG; http://www.kegg.jp) and MetaboAnalyst (https://www.kegg.jp/) were utilized to search for 'metabolitepathways' (https://www.genome.jp/kegg/pathway.html).

2.8 Metagenome sequencing and analysis

For the microbiota within host pine tree, whole seedlings of *P. massoniana* (n = 5, containing PWN) after 14 dpi under the ST treatments were crushed in liquid nitrogen for their respective total DNA extraction, followed by metagenomic sequencing and analysis, as previously described (Bolger et al., 2014; Cai et al., 2022). Total genomic DNA was extracted from each sample by using the MoBio PowerSoil DNA Isolation Kit (12855-50, MoBio, United States) as per the manufacturer's protocol. The DNA quantity and quality were measured on a NanoDrop 2000 spectrophotometer (Thermo Fisher Scientific, United States). This DNA was then sheared to 300-bp fragments by a Covaris ultrasonic crusher. To prepare each sequencing library, those fragments were treated by end repair, A tailing, and ligation of Illumina compatible adapters. Next all DNA sequencing libraries were deep-sequenced on an Illumina HiSeq platform at the Allwegene Company (Beijing, China). After every run, the image analysis, base calling, and error estimation were carried out using Illumina Analysis Pipeline v2.6. Quality control of the raw data, including the removal of adapter sequence and low-quality reads, was performed using Trimmomatic. High-quality sequences were compared with NR database and classified into different taxonomic groups, using the DIAMOND tool (Buchfink et al., 2015). Then MEGAHIT (Li et al., 2015) was used to assemble the sequencing data, and the contigs were annotated with Prodigal software (Hyatt et al., 2012) to predict the open reading frames (ORFs). After that, CD-HIT software (Li et al., 2001) constructed the non-redundant gene set. To compare the sequencing data with the non-redundant gene set, Bowtie (Langmead et al., 2009) was used, after which the abundance information of genes in the different samples was counted.

2.9 Volatile organic compound sequencing and analysis

For the VOC within the host pine tree, whole seedlings of *P. massoniana* (n = 5, with PWN) at 14 dpi under the ST treatments were examined, as previously described (Fang et al., 2023). First, 500 mg (1 mL) of sample powder was transferred immediately into a 20-mL headspace vial (Agilent, Palo Alto, CA, USA) that contained an NaCl-saturated solution, to inhibit any enzyme reactions. These vials were sealed using crimp-top caps with TFE-silicone headspace septa (Agilent). During the Solid Phase Microextraction (SPME) analysis, each vial was placed accordingly at 60°C for 5 min, then a 120 µm DVB/CWR/PDMS fibre (Agilent) was exposed to the headspace of a given sample for 15 min (also at 60°C).

After completing that sampling procedure, desorption of VOCs from the fiber coating was performed in the injection port of the GC apparatus (Model 8890; Agilent), at 250°C for 5 min, in the splitless mode. The identification and quantification of VOCs was carried out using an Agilent Model 8890 GC and a 7000D mass spectrometer (Agilent). The selected ion monitoring (SIM) mode was used for the identification and quantification of analytes by MS. The ensuing identified metabolites were annotated using KEGG Compound database (http://www.kegg.jp/kegg/compound/); annotated metabolites were then mapped to the KEGG Pathway database (http://www.kegg.jp/kegg/pathway.html). Pathways with significantly regulated metabolites mapped to them were then fed into MSEA (metabolite sets enrichment analysis), whose significance was determined by hypergeometric test's *P*-values.

2.10 Insect host preference and diet quantification assay

Adults of JPS were collected from an experimental population reared at the Fujian Agriculture and Forestry University, Fuzhou, China. All experiments using them, as described below, were

conducted in a growth chamber (light: dark = 12 h: 12 h, 70% humidity, 25°C).

The host performance assay was done as described in a previous study(Geneau et al., 2013), albeit with some minor changes. Healthy and vigorous JPS were collected and starved for 24 h before starting the treatments, using a total 18 JPS adults per treatment (9 males, 9 females). Entire *P. massoniana* seedlings that had been inoculated with ST or 4 ppm methanol solution were the experimental odor source or negative control, respectively. Biological triplicates with technical triplicates were used. The performance of JPS on the host pine plants was expressed as an attraction ratio: [no. of choices by JPS/total no. Of JPS adults] * 100%. To determine statistical differences between treatment groups, first a Kruskal–Wallis test was applied, and then pairwise comparisons were made using multiple Mann-Whitney tests.

The diet of JPS adults was quantified as the consumed area of *P. massoniana* bark by these insects. Healthy and vigorous JPS individuals were collected and starved for 24 h before starting the treatments. A total of 12 JPS adults (6 males, 6 females) were used per treatment. Fresh 2-year-old *P. massoniana* seedlings from the various treatments were fed to the JPS for 3 days; then, the feeding area of the JPS was rubbed with transparent sulfuric acid paper, and this measured on grid coordinate paper. One-way analysis of variance (ANOVA; followed by Tukey's test) was performed to determine the differences among the means of treatment groups.

All the JPS adults from the same treatment of each diet quantification assay were pooled into a single sample, crushed in liquid nitrogen, and divided into three equal aliquots for further analysis. The activities of exo-β-1,4-glucanase/cellobiose hydrolase (cat no. G0533W, Gris Biology, Suzhou, China), endo-β-1,4-glucanase (cat no. G0534W, Gris Biology, Suzhou, China), and β-glucosidase (cat no. G0535W, Gris Biology, Suzhou, China) in each sample were measured by following the standard protocols of corresponding kits. One-way analysis of variance (ANOVA; Tukey's test) was implemented to determine the differences among the means of treatment groups.

3 Results

3.1 Sterigmatocystin increases PWN pathogenicity by suppressing ROS accumulation in *P. massoniana*

Previous results shown that sterigmatocystin (ST) is highly positively associated with the pathogenicity of PWN. Here, we speculated that ST functions during the PWN invasion and pathogenic process (Figure 1A). First, after PWN invasion, the ST level was highly induced (5.2 times, $P < 0.01$). Different concentrations (0.1 mg/mL, 0.01 mg/mL, 0.001 mg/mL) of the exogenous ST treatment applied to PWN-carrying *P. massoniana* (PCP) could significantly ($P < 0.05$) increase the PWN amount in the host, by 9.6, 6.6, and 4.6 times, respectively (Figure 1B). Further, the death rate of host plants was measured at 2 months post-treatment with respect to different concentrations of ST (Figure 1C). Evidently, the death ratio was positively correlated with the exogenous ST amounts; hence, ST could enhance the pathogenicity of PWN. We also measured the ROS level in PCP under the three ST treatments, finding that the rate of ROS (Figure 1D) as well as H_2O_2 (Figure 1E) production in PCP was significantly reduced by ST ($P < 0.05$) and negatively correlated ($P < 0.01$) with the exogenous ST concentration; this weakened resistance in PCP, thus benefiting the PWN invasion and pathogenic process. Further multi-omics (transcriptomics, microbiomes, and metabolic) data revealed that ST was capable of suppressing ROS accumulation through the regulation of a vast array of related genes (*c60547.graph_c0*, *c82953.graph_c0*, *c64867.graph_c0*, *c68789.graph_c0*, *c81022.graph_c0*), microbes (*Cladophialophora*, *Penicillium*, *Trichoderma*, *Achromobacter*, *Chitinophaga*, and *Flavobacterium*), and metabolites (maltotriose, 1-hexadecanoyl-2-(9Z-octadecenoyl)-sn-glycero-3-phosphoethanolamine and myo-inositol) (Figure 1F). We also explored the ST-regulated metabolites from metabolic data. They were mostly enriched in arachidonic acid metabolism, flavonoid biosynthesis, phenylpropanoid biosynthesis, nucleotide metabolism, and *Cyprinus carpio* (common carp) pathways; this suggested secondary metabolites, ST inhibitors (stilbenoid), and VOCs (phenylpropanoids) were highly negatively ($P = 0.021$, $r = -0.979$), positively ($P = 0.006$, $r = 0.994$), and positively ($P = 0.012$, $r = 0.989$) correlated with the ST concentration, respectively (Figure 1G). Also, the richness of several genera of microbes (*Enterobacter*, *Klebsiella*, *Pelagivirga*, *Herbaspirilum*, *Staphylococcus*, *Pseudovibrio*, *Rhizophagus*, *Cronobacter*, *Acinetobacter*, *Achromobacter*) was correlated with the ST concentration, and most of them were predicted to regulate the VOC and flavonoid biosynthesis (Supplementary Figure S1).

3.2 Sterigmatocystin increases VOC accumulation in *P. massoniana* to attract *Monochamus alternatus*

VOCs have been proven to determine the host preference of JPS (Yan et al., 2008; Wang et al., 2016). Accordingly, here we first quantified the VOC amount of *P. massoniana* under each exogenous ST treatment. The latter significantly increased the total VOC amount within *P. massoniana* by 212, 182, and 105 times when compared to the negative control, respectively ($P < 0.001$; Figure 2A). Also, for 10 VOCs (trans-anethole; acetophenone, 4'-hydroxy-; humulene; niacinamide; 4a(2H)-naphthalenol, octahydro-4,8a-dimethyl-,(4.alpha.,4a.alpha.,8a.beta.)-; 6-octen-1-ol,3,7-dimethyl-, (R)-; alpha-pinene; butanoic acid,3-hydroxy-3-methyl-; phenol; beta-myrcene), their amounts were positively correlated with the ST concentration, including three reported JPS-attracting VOCs (acetophenone, alpha-pinene, beta-myrcene) (Li et al., 2015; Zhang, 2016) (Figure 2B). These results led us to speculate whether the exogenous ST treatment can lure JPS adults. So we conducted an olfactory experiment, which showed that exogenous ST treatment can significantly ($P < 0.05$) promote the selective ratio of JPS adults to the host pine tree, and that ratio increased with a higher ST concentration (Figure 2C). Host performance of insects were based on that this behavior is benefit to themselves (Li et al., 2007; Zhu et al.,

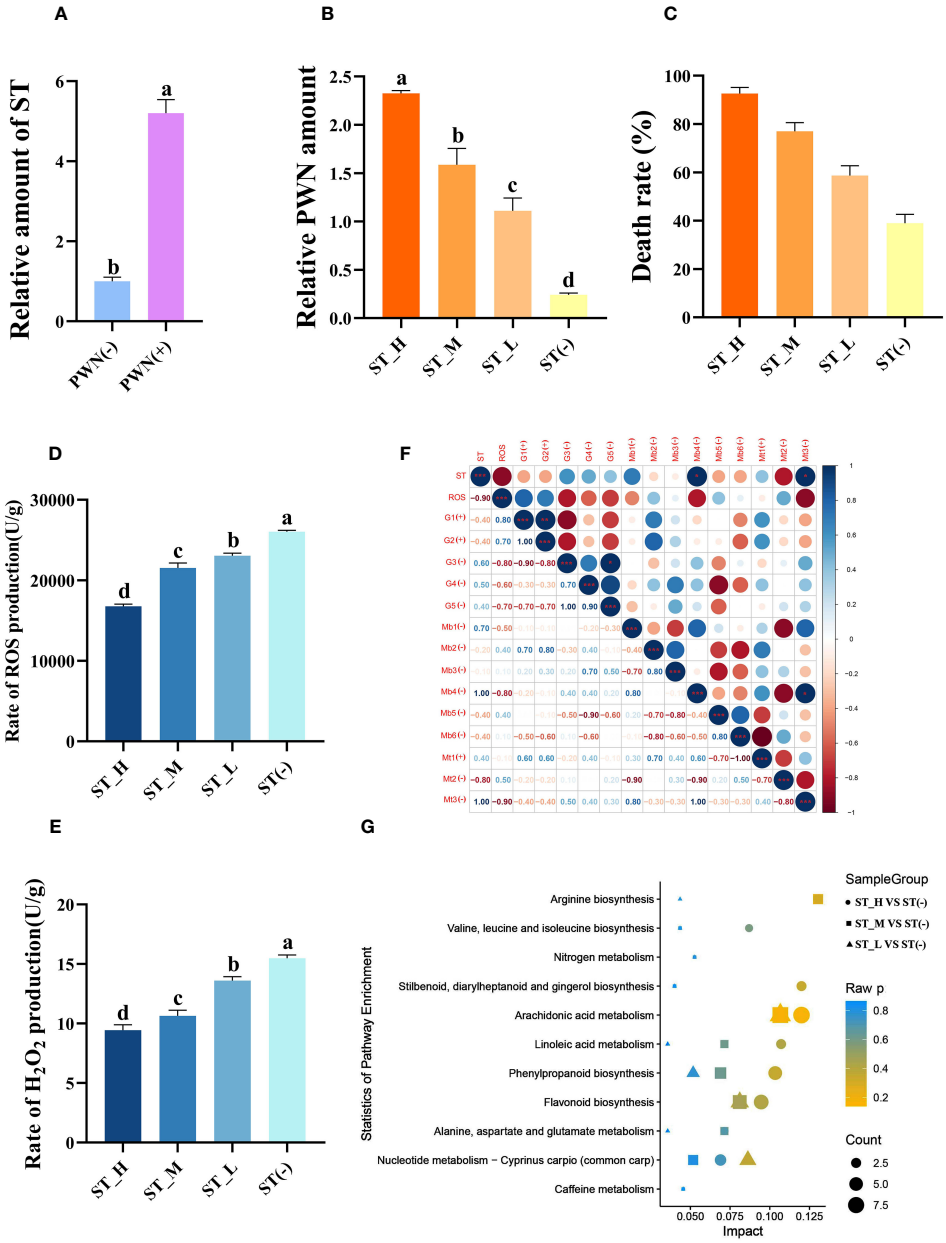

FIGURE 1
Sterigmatocystin (ST) increases Pinewood nematode (PWN) pathogenicity by suppressing ROS accumulation in *Pinus massoniana*. **(A)** Relative ST concentrations in the host plant *P. massoniana* quantified before (PWN(-)) and after (PWN(+)) invasion by PWN. The seedlings were inoculated with an equal amount of PWN (5000 individuals), followed by 0.1 mg/mL (ST_H), 0.01 mg/mL (ST_M), 0.001 mg/mL (ST_L) or a 0 mg/mL (ST(-)) of ST as the treatment, after which the **(B)** relative PWN amount, **(C)** death rate, **(D)** rate of ROS production, and **(E)** rate of H_2O_2 production were quantified at 14 days post-infection. Data shown is the mean ± standard deviation (SD). **(F)** Correlations between ST and their correlated ROS, transcripts, microbes, and metabolites. Metabolite pathways of *P. massoniana* as induced by ST with a highly correlated concentration. Different lowercase letters above bar columns show significant differences between treatments at $P < 0.05$, based on a one-way ANOVA, with multiple comparisons made using Tukey's test. G1–G5 denote different transcripts (c60547.graph_c0, c82953.graph_c0, c64867.graph_c0, c68789.graph_c0, c81022.graph_c0); Mb1–Mb6 correspond to different microbial genera (*Cladophialophora*, *Penicillium*, *Trichoderma*, *Achromobacter*, *Chitinophaga*, and *Flavobacterium*); Mt1–Mt3 indicate different metabolites [maltotriose, 1-hexadecanoyl-2-(9Z-octadecenoyl)-sn-glycero-3-phosphoethanolamine, and myo-inositol]. **(G)** KEGG enrichment map of metabolic pathways of metabolites found significantly related to ST. The abscissa represents the impact of each pathway and the ordinate represents the pathways' name. Impact is expressed as the ratio of the number of differential metabolites to the number of metabolites annotated in a given pathway. The circle represents ST_H vs. ST(-), the square represents ST_M vs. ST(-), and the triangle represents ST_L vs. ST(-), whose sizes indicate the number of differentially expressed metabolites contained in that metabolic pathway. Coloring represents the *P*-values for the enrichment analysis.

2019; Togashi et al., 2022). Furthermore, we also observed whether feeding on ST-treated *P. massoniana* could benefit the development of JPS The consumption area of JPS larvae feeding upon ST-treated *P. massoniana* increased significantly ($P < 0.05$) over time, and the body weight of the 3rd instar along with the spawning ratio of JPS eggs were both significantly increased by 1.67 and 4.7 times vis-à-vis the negative control, respectively (Figures 2D–F). The EG (endo-1,4-β-D-glucanase), CBH (exo-β-1,4-D-glucanase) and β-GC (β-

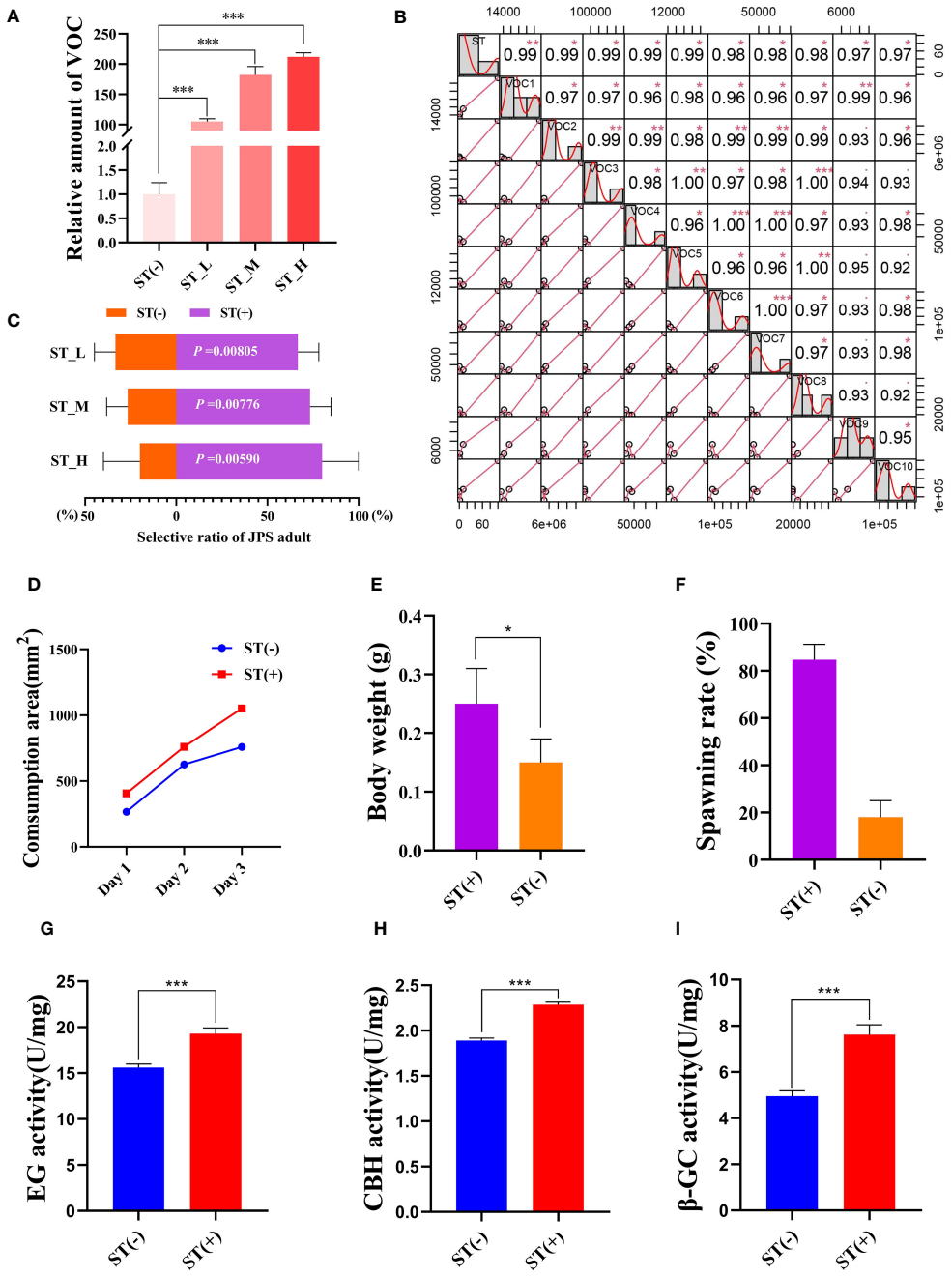

FIGURE 2
Sterigmatocystin (ST) increases VOC accumulation in *Pinus* Massoniana to attract *Monochamus alternatus* (JPS). **(A)** VOC amounts in host plant *P. massoniana* quantified 14 days after treatment with 0.1 mg/mL (ST_H), 0.01 mg/ml (ST_M), 0.001 mg/mL (ST_L), or 0 mg/mL (ST(-)) of ST. **(B)** VOC compounds of *P. massoniana* induced by ST with a high concentration correlation. **(C)** Selective ratio of JPS to different plant samples were plotted, with the *P*-value for the *t* test between samples treated with (ST (+)) and without ST(ST(-)) presented in white. The **(D)** consumption area and **(E)** body weight of 3rd instar JPS larvae, and the **(F)** spawning rate, **(G)** EG (endo-1,4-β-D-glucanase) activity, **(H)** CBH (exo-β-1,4-D-glucanase) activity, and **(I)** β-GC (β-glucosidase) activity in the gut of the JPS adults that fed upon plant samples treated with (ST (+)) and without ST(ST(-)); data shown are the mean ± standard error (SE). The * and *** represents significant differences between treatments at $P < 0.05$ and $P < 0.001$, respectively, based on a one-way ANOVA, with multiple comparisons made using Tukey's test. VOC1–VOC10 indicate different volatile organic compound (trans-anethole; acetophenone, 4'-hydroxy-; humulene; niacinamide; 4a(2H)-naphthalenol, octahydro-4,8a-dimethyl-, (4.alpha.,4a.alpha.,8a.beta.)-; 6-octen-1-ol,3,7-dimethyl-, (R)-; alpha-pinene; butanoic acid, 3-hydroxy-3-methyl-; phenol; beta-myrcene). The ** represents significant differences between treatments at $P < 0.01$.

glucosidase) activity in the gut of the JPS adults that fed upon *P. massoniana* treated with ST were quantified as well, these increasing by 1.24, 1.21, and 1.54 times relative to the negative control, respectively (Figures 2G–I). Altogether, these results suggested ST is able to increase the VOC accumulation in *P. massoniana*, thus attracting the JPS, whose feeding and development obviously improves when eating ST-treated *P. massoniana*, which can therefore manipulate the host preference of JPS.

3.3 An associated microbe *A. arachidicola*, promotes PWN pathogenicity by increasing the sterigmatocystin accumulation in *P. massoniana*

Identify the vital effective microbe is crucial to achieving PWD control in the field. As an important metabolite in *Aspergillus*, ST is positively regulated by *alfR*. Although total species richness of *Aspergillus* harbored by the host plant was negligible influenced by PWN invasion and perhaps even slightly reduced (Figure 3A), evidently the *alfR* expression level was significantly induced (14.06 times, $P < 0.001$) by PWN (Figure 3B). We also found that only a few *Aspergillus* species (*A. arachidicola*, *A. fischeri*, *A. taichungensis*) were strongly ($P < 0.001$) increased or decreased (*A. sclerotioniger*, *A. awamori*, *A. aculeatus*) by PWN (Supplementary Figure S2). This prompted us to compare the functional differences between PWN-increased (*A. sarachidicola*) and -decreased (*A. sclerotioniger*) species and their associated microbes (Figure 3C). After introducing it into *P. massoniana* via PWN, it was found that *A. arachidicola* significantly induced the accumulation of ST in the host (2.61 times, $P < 0.001$) whereas *A. sclerotioniger* did not (Figure 3D). Further, the amount of PWN was respectively quantified in *A. arachidicola*- and *A. sclerotioniger*-infected PCP, which demonstrated the former can increase the PWN population size, whereas the latter cannot (Figure 3E). Comparing the survival ratio of PCP infected by different microbes showed that it was sharply reduced after 2 weeks of infection by *A. arachidicola* but not *A. sclerotioniger* (Figure 3F). Collectively, these results suggested that PWN-induced *Aspergillus* are sufficient to trigger ST accumulation that assists PWN invasion and pathogenicity.

3.4 The fungal inhibitor chiricanine A can suppress the species richness of *Aspergillus* fungi in *P. massoniana* host, thus curtailing *in vivo* PWN population size or pathogenicity in both laboratory and field tests

The *Aspergillus*-inhibitor chiricanine A has long been used to suppress ST accumulation in numerous crops(Arias et al., 2014). Accordingly, we wondered whether chiricanine A could decrease the accumulation of ST by reducing the richness of PWN-induced *Aspergillu* species. We found that the application of chiricanine A significantly decreased ($P < 0.001$) the richness of PWN-induced *Aspergillu* spp. as well as the *aflR* expression level by 4 times and 1.77 times, respectively (Figures 4A, B). When compared with emamectin benzoate, currently the most efficacious nematicide,

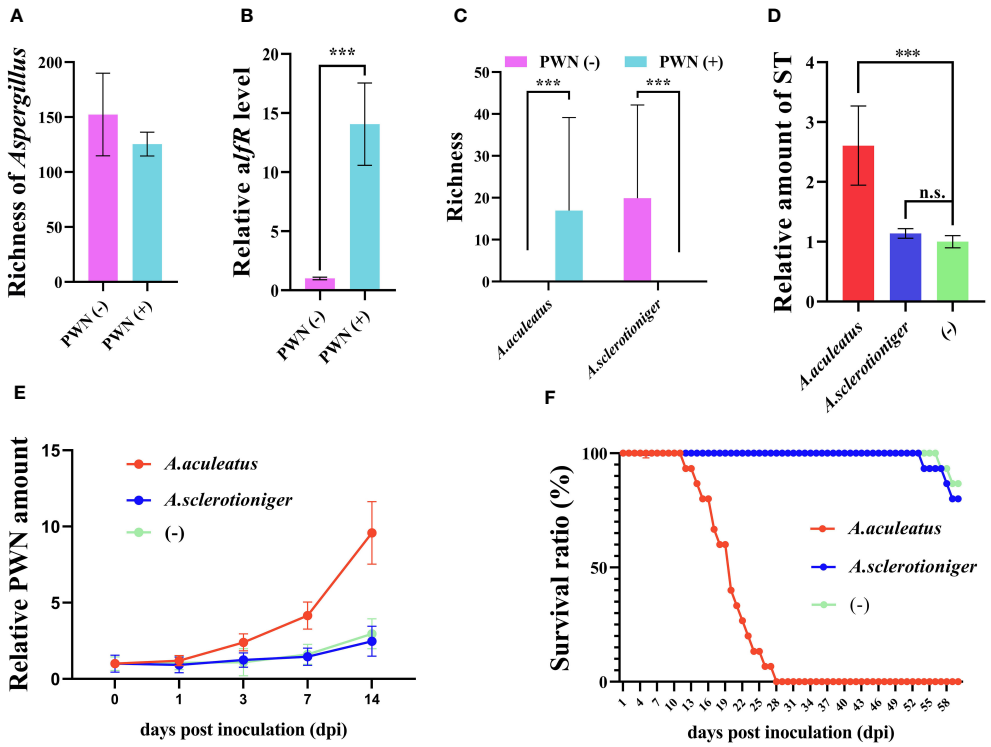

FIGURE 3
Associated microbe *Aspergillus arachidicola* promotes PWN pathogenicity by increasing the sterigmatocystin (ST) accumulation in *Pinus massoniana*. **(A)** Richness of microbes belonging to the *Aspergillus* genus, **(B)** expression level of ST synthesis promoting gene *aflR*, **(C)** richness of *A arachidicola* and *A* sclerotioniger in plant samples before (PWN(-)) and after (PWN(+)), invasion by PWN invasion are plotted. *Aspergillus arachidicola*, *A sclerotioniger*, and inactivated *A arachidicola* (-) were co-incubated with sterilized PWN, then inoculated into *P. massoniana* and the **(D)** ST amount, **(E)** relative PWN amount, and **(F)** survival ratio of different host plants were measured. Data shown are the mean ± standard deviation (SD). The *** represents significant differences between treatments at $P < 0.001$, based on a one-way ANOVA, with multiple comparisons made using Tukey's test; 'n.s.' denotes no significant differences found.

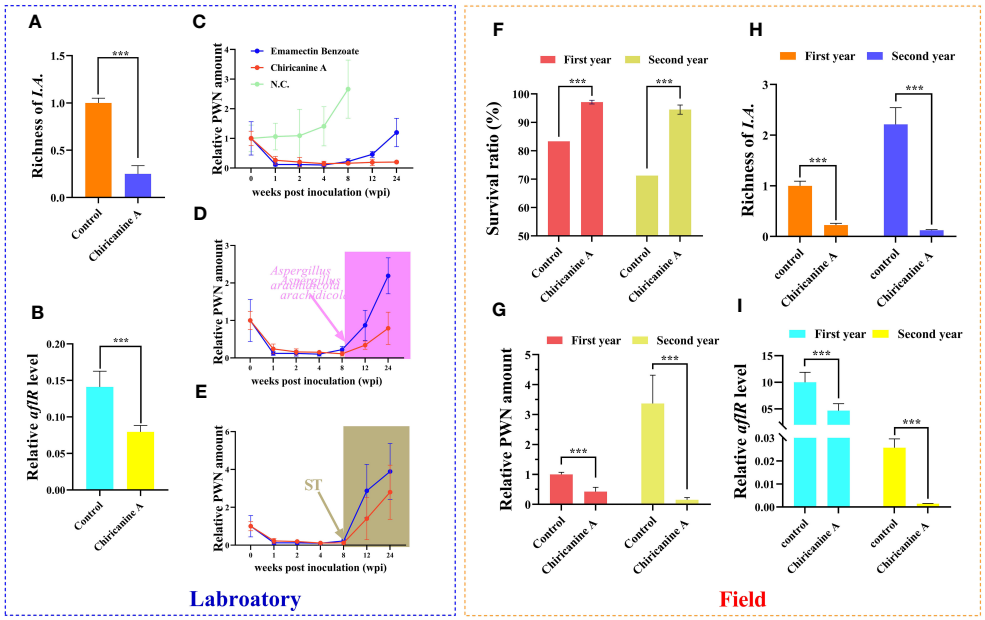

FIGURE 4
The fungal inhibitor chiricanine A can suppress the richness of *Aspergillus* fungi in *Pinus massoniana* to limit *in vivo* PWN population or pathogenicity, in both laboratory and field testing. Under laboratory conditions, 2-year-old *P. massoniana* seedlings were inoculated with PWN, and then inoculated with chiricanine A solution or methanol (control). For these samples, the **(A)** richness of *Aspergillus* fungi highly induced and **(B)** *aflR* expression level in response to PWN invasion were quantified. Relative PWN amount in PWN-carrying *P. massoniana* treated with **(C)** emamectin benzoate and chiricanine A, as well as those **(D)** injected with *A arachidicola* or **(E)** ST at 8 weeks post-inoculation. In the field trial, a solution of chiricanine A or methanol (control) was injected into PWN-carrying *P. massoniana*, and its **(F)** survival ratio, **(G)** relative PWN amount, and the **(H)** richness of *Aspergillus* fungi highly induced and **(I)** *aflR* expression level in response to PWN invasion were quantified after the 1st and 2nd year post-injection. Data shown are the mean ± standard deviation (SD). The *** represents significant differences between treatments at $P < 0.001$, based on a one-way ANOVA, with multiple comparisons made using Tukey's test.

chiricanine A was able to inhibit PWN for much longer (Figure 4C). But when the host is inoculated with *A. arachidicola* or ST, either was clearly able to suppress that long-term effect of chiricanine A (Figures 4D, E).

We also tested the PWN-control functioning of chiricanine A in a 2-year field trial. The application of chiricanine A significantly increased the survival rate of PCP in both years vis-à-vis the control (1.17 and 1.33 times, $P < 0.001$) (Figure 4F). Yet, significant reductions in the amount of PWN (2.36 and 22.05 times, $P < 0.001$), richness of PWN-induced *Aspergillus* spp. (4.44 and 18.07 times, $P < 0.001$), and the *aflR* expression level (2.15 and 18.07 times, $P < 0.001$) of PCP occurred in both years relative to the control (Figures 4G–I). These results indicated that chiricanine A could serve as more efficient nematicide in the field by suppressing ST accumulation thereby performed a long-term control of PWD.

4 Discussion

A paramount prerequisite to manipulating functional microorganisms is identifying those vital effective microbes that drive ecological phenomena, and elucidating their underlying biochemical mechanisms (Ayilara et al., 2023). Associated microbes enable linkages between PWN, host pine, and JPS (Feng et al., 2022); however, our understanding of how microbes directly affect the "PWN- host-JPS" complex through their produced metabolites are largely unknown (Zhao et al., 2014; Santini and Battisti, 2019; Feng et al., 2022). Here, we demonstrated that PWN-associated fungi, *Aspergillus* spp., are able to promote PWN invasion and pathogenicity by increasing biosynthesis of a secondary metabolite, sterigmatocystin (ST), in the host plant *P. massoniana*, mainly via suppressed ROS accumulation in hosts against PWN. Further, ST accumulation triggers VOC biosynthesis for attracting JPS to spawn and this drives the coexistence of PWN and JPS in host trees, thereby encouraging transmission of PWD (Figure 5). Meanwhile, through the application of an *Aspergillus* inhibitor (Chiricanine A), we also showed that the absence of *Aspergillus* sharply restricts the development of PWN in *P. massoniana* (Figure 4), further proving that *Aspergillus* is vital and sufficient to promote PWD transmission.

Ophiostomatoids and molds are two major fungal families well known for being highly correlated with the propagation and distribution of the PWN (Feng et al., 2022). Although molds do play crucial roles in multiple processes of PWD epidemics (Guo et al., 2020), in a way unlike the known contributions of ophiostomatoids to PWN (important food resources) (An et al., 2022; Cai et al., 2022; Li et al., 2022), how molds are involved in PWD epidemics remains unclear. The present work, for the first time, clarifies how an important genus of molds, *Aspergillus*, contributes to the PWD epidemic via its secondary metabolite. The ST biosynthesis is conserved in *Aspergillus* (Sobolev et al., 2018) and promoted by *aflR*, and a pronounced positive correlation

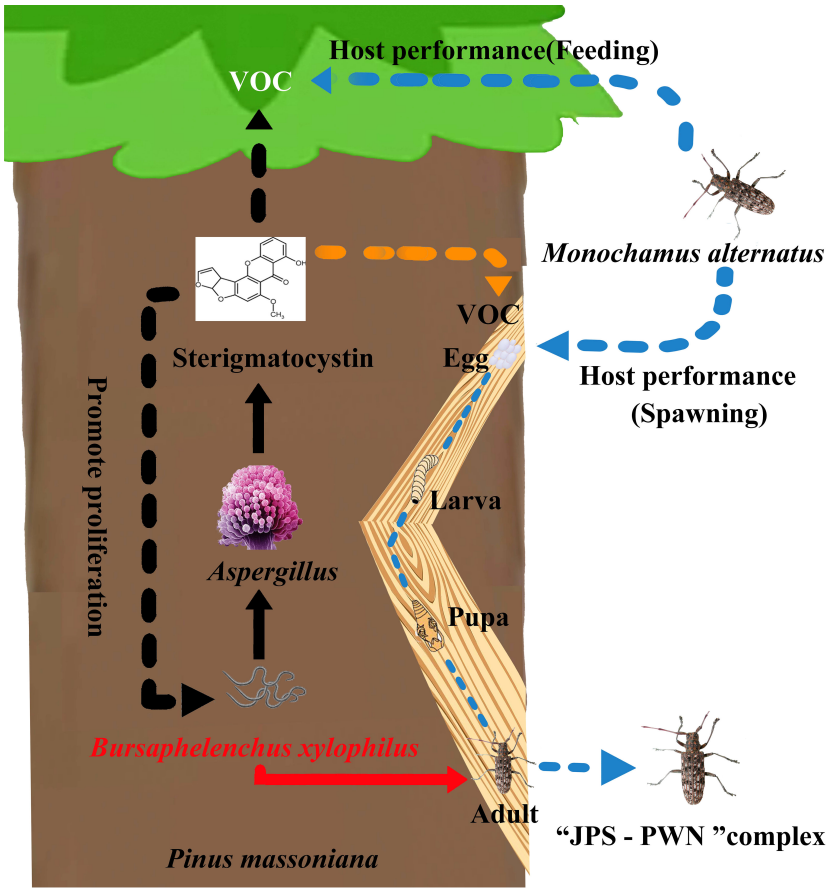

FIGURE 5
Schematic diagram of the pine wood nematode-*Monochamus alternatus* symbiosis promoted by *Aspergillus* fungi in *Pinus massoniana* host trees via sterigmatocystin (ST).

between ST and *aflR* expression was indeed observed in this study, but no correlation of ST with richness of *Aspergillus* spp. Although the absence of *Aspergillus* substantially restricts the PWN's development in its host, among these identified *Aspergillus* species in the PWN-carrying *P. massoniana*, only three of them—*A. fischeri*, *A. arachidicola*, *A. taichungensis*—increased markedly in response to PWN invasion and were very likely transferred by PWN into host plants, in contrast to most of them (like *A. sclerotioniger*) decreasing considerably. These lines of evidence suggest PWN-associated *Aspergillus* fungi are able to reconstruct the host plant-associated microbial community to promote PWN development. This point is also supported by the diversity of the host plant-associated microbial community being severely reduced by the application of a low ST concentration yet increasing with higher ST concentrations. The above point can also explained by the various functions of *Aspergillus* species; most of the plant-associated *Aspergillus* are mutualists (El-Desoky et al., 2021; Cheng et al., 2022; Toth et al., 2022), one of the PWN-associated *Aspergillus* fungi, *A. arachidicola*, has been reported as being harmful to plant and beneficial for insect feeding (El-Desoky et al., 2021; Cheng et al., 2022).

Despite ST being detectable in various of crops and foods (Versilovskis and De Saeger, 2010), its functioning in plants has yet to be resolved. In this work, we demonstrated that ST was able to suppress ROS accumulation in the host pine tree via genetic, metabolic, and microbial level regulation processes. The richness of several genera of microbes—*Enterobacter*, *Klebsiella*, *Pelagivirga*, *Herbaspirilum*, *Staphylococcus*, *Pseudovibrio*, *Rhizophagus*, *Cronobacter*, *Acinetobacter*, and *Achromobacter*—was correlated with the ST concentration, and most of them were predicted to regulate the biosynthesis of VOCs and flavonoids. Further, these functional predictions were supported by the metabolic data. By quantifying the VOC amounts in host pine trees, we find that the total VOC amount is highly induced by ST (more than 100 times), yet only a few of them (mostly terpenes) are induced in a ST-dependent manner; this finding hints that ST might be a potential signal acting to regulate the host performance of insects. Although, some reported JPS-attracting VOCs (acetophenone, pinene, and myrcene) were among the above ST-induced metabolites, it was not clear whether these are all JPS-specific VOC, an aspect worth exploring further. Meanwhile, the amount of flavonoids was significantly increased by ST treatment, indicating that ST may serve as a signal to initiate the later stages of plant defense (Hedrich et al., 2016). Plant flavonoids have been widely demonstrated to be toxic to pests, including the Pine Wood Nematode (PWN) (Shen et al., 2022; Xie et al., 2022). However, over a long period of co-evolution, pests have developed efficient detoxification systems to

counteract the toxic effects of secondary metabolites, including flavonoids (Souto et al., 2021). This suggests that the PWN may possess a highly effective detoxification system to survive the presence of flavonoids in the host plant. Further investigation into the detoxification system of the PWN against plant secondary metabolites would provide a valuable opportunity to shed light on the outbreak of PWD. Interestingly, we also found that synthesis of an ST inhibitor, stilbenoid (Sobolev et al., 2018), was promoted by ST, suggesting that plants may have a conserved system to respond to ST as a signal. Together, we hypothesize that ST can suppress the early stage of PWN resistance and reconstructs the microbial community in the host plant; it may also strongly activate the later stage of pest resistance (flavonoid accumulation) to limits competitors in the same niche, thereby promoting outbreaks of PWD in pine stands.

Emamectin benzoate (EB) is widely regarded as the most useful nematicide against the PWN, largely because it is environmentally friendly and has longer field residence time (i.e., at least 3 years) (Takai et al., 2004; Lu et al., 2020). However, continuous injection is required to maintain an effective dose of EB in a pine tree or whole stand (Rajasekharan et al., 2017; Lu et al., 2020; Chen et al., 2021; Hao et al., 2021). Although neither EB nor chiricanine A can completely eradicate the PWN population in host pines, we propose that chiricanine A has a PWN control efficiency on par with EB, but is able to suppress the PWN population for a longer time. As a plant metabolite, chiricanine A can also be synthesized manually (Park et al., 2011), which greatly reduces the cost of its application. Chiricanine A is plant-originating metabolic that has multiple biological functions: it can be utilized and metabolized by the recipient plant itself (Wang et al., 2018), which may affect its residence time within the host, an aspect that requires future research attention. As an *Aspergillus* inhibitor, chiricanine A is already widely used for eliminating *Aspergillus* spp. in the crops (Sobolev, 2008; Sobolev et al., 2011; Sobolev et al., 2016; Sobolev et al., 2018; Souto et al., 2021), but whether *Aspergillus* spp are the unique target of chiricanine A remains unknown. We know that ST is produced by various species of *Aspergillus* (Versilovskis and De Saeger, 2010), but it can also be produced by other mold species, including some members of *Penicillium*, *Emiricella*, *Chaetomium*, and *Bipolaris* genera, and most of them are pertinent to plant growth (Barnes et al., 1994; Rank et al., 2011). Plenty of above ST-producing microbes could be induced by PWN invasion, though in this study only *Aspergillus* was investigated. Although we show that applying chiricanine A could drastcially reduce the *Aspergillus* and ST levels in host pine trees, it is uncertain whether such chiricanine A applications can limit or benefit other microbes of host plants. In conclusion, we found a new plant-originating nematicide, chiricanine A, that has obvious advantages in terms of residence time to aid in the long-term control of PWN in pine stands, but the side effects of its and underline mechanistic action both require further attention.

Data availability statement

The original contributions presented in the study are included in the article/Supplementary Files, further inquiries can be directed to the corresponding author/s.

Author contributions

JJ: Writing – original draft. LC: Writing – original draft. WY: Writing – original draft. SC: Conceptualization, Writing – original draft. SS: Investigation, Writing – original draft. XX: Software, Writing – original draft. XT: Data curation, Writing – original draft. XJ: Methodology, Writing – review & editing. DC: Supervision, Writing – review & editing. YF: Formal Analysis, Writing – review & editing. JW: Writing – review & editing. XL: Project administration, Writing – review & editing. JL: Funding acquisition, Validation, Writing – review & editing. YH: Resources, Visualization, Writing – original draft. JS: Writing – original draft, Writing – review & editing.

Funding

The author(s) declare financial support was received for the research, authorship, and/or publication of this article. This work was supported by the Fujian Forestry Science and Technology Project (2021FKJ01, LZKG-202205) and the Forestry Peak Discipline Construction Project of Fujian Agriculture and Forestry University (72202200205).

Acknowledgments

We are very grateful to the Fujian Key Laboratory of Forest Cultivation and Forest Products Processing and Utilization, Fujian Forestry Bureau, for help in providing detailed information of the sampling areas in this study, and to Syngenta (China) Investment Co. Ltd. for technical support.

Conflict of interest

The authors declare that the research was conducted in the absence of any commercial or financial relationships that could be construed as a potential conflict of interest.

Publisher's note

Supplementary material

The Supplementary Material for this article can be found online at: https://www.frontiersin.org/articles/10.3389/fpls.2023.1257744/full#supplementary-material

References

Alicandri, E., Paolacci, A. R., Osadolor, S., Sorgona, A., Badiani, M., and Ciaffi, M. (2020). On the evolution and functional diversity of terpene synthases in the *pinus* species: A review. *J. Mol. Evol.* 88 (3), 253–283. doi: 10.1007/s00239-020-09930-8

An, Y. B., Li, Y. X., Ma, L., Li, D. Z., Zhang, W., Feng, Y. Q., et al. (2022). The Changes of Microbial Communities and Key Metabolites after Early *Bursaphelenchus xylophilus* Invasion of *Pinus massoniana*. *Plants-Basel* 11 (21), 2849. doi: 10.3390/plants11212849

Arias, R. S., Sobolev, V. S., Orner, V. A., Dang, P. M., and Lamb, M. C. (2014). Potential involvement of *Aspergillus flavus* laccases in peanut invasion at low water potential. *Plant Pathol.* 63 (2), 354–364. doi: 10.1111/ppa.12088

Ayilara, M. S., Adeleke, B. S., Akinola, S. A., Fayose, C. A., Adeyemi, U. T., Gbadegesin, L. A., et al. (2023). Biopesticides as a promising alternative to synthetic pesticides: A case for microbial pesticides, phytopesticides, and nanobiopesticides. *Front. Microbiol.* 14. doi: 10.3389/fmicb.2023.1040901

Barnes, S. E., Dola, T. P., Bennett, J. W., and Bhatnagar, D. (1994). Synthesis of sterigmatocystin on a chemically defined medium by species of *Aspergillus* and *Chaetomium*. *Mycopathologia* 125 (3), 173–178. doi: 10.1007/BF01146523

Bolger, A. M., Lohse, M., and Usadel, B. (2014). Trimmomatic: a flexible trimmer for Illumina sequence data. *Bioinformatics* 30 (15), 2114–2120. doi: 10.1093/bioinformatics/btu170

Buchfink, B., Xie, C., and Huson, D. H. (2015). Fast and sensitive protein alignment using DIAMOND. *Nat. Methods* 12 (1), 59–60. doi: 10.1038/nmeth.3176

Cai, S. P., Jia, J. Y., He, C. Y., Zeng, L. Q., Fang, Y., Qiu, G. W., et al. (2022). Multi-omics of pine wood nematode pathogenicity associated with culturable associated microbiota through an artificial assembly approach. *Front. Plant Sci.* 12. doi: 10.3389/fpls.2021.798539

Carnegie, A. J., Venn, T., Lawson, S., Nagel, M., Wardlaw, T., Cameron, N., et al. (2018). An analysis of pest risk and potential economic impact of pine wilt disease to *Pinus* plantations in Australia. *Aust. Forest.* 81 (1), 24–36. doi: 10.1080/00049158.2018.1440467

Chaudhary, S., Sindhu, S. S., Dhanker, R., and Kumari, A. (2023). Microbes-mediated sulphur cycling in soil: Impact on soil fertility, crop production and environmental sustainability. *Microbiol. Res.* 271, 127340. doi: 10.1016/j.micres.2023.127340

Chen, C., Gonzalez, F. J., and Idle, J. R. (2007). LC-MS-based metabolomics in drug metabolism. *Drug Metab. Rev.* 39 (2-3), 581–597. doi: 10.1080/03602530701497804

Chen, Y., Zhou, X., Guo, K., Chen, S. N., and Su, X. (2021). Transcriptomic insights into the effects of CytCo, a novel nematotoxic protein, on the pine wood nematode *Bursaphelenchus xylophilus*. *BMC Genomics* 22 (1), 394. doi: 10.1186/s12864-021-07714-y

Cheng, X., Ma, F. P., Yan, Y. M., Zhao, W. L., Shi, J., Xiao, W., et al. (2022). Aspertaichunol A, an immunomodulatory polyketide with an uncommon scaffold from the insect-derived endophytic *aspergillus taichungensis* SMU01. *Organ. Lett.* 24 (40), 7405–7409. doi: 10.1021/acs.orglett.2c02978

Cheng, X. Y., Xu, R. M., and Xie, B. Y. (2005). The role of chemical communication in the infection and spread of pine wood nematodes (*Bursaphelenchus xylophilus*). *Acta Ecol. Sin.* 25 (2), 339–345.

De Vos, R. C., Moco, S., Lommen, A., Keurentjes, J. J., Bino, R. J., and Hall, R. D. J. (2007). Untargeted large-scale plant metabolomics using liquid chromatography coupled to mass spectrometry. *Nat. Protoc.* 2 (4), 778–791. doi: 10.1038/nprot.2007.95

El-Desoky, A. H. H., Inada, N., Maeyama, Y., Kato, H., Hitora, Y., Sebe, M., et al. (2021). Taichunins E-T, isopimarane diterpenes and a 20-nor-isopimarane, from *aspergillus taichungensis* (IBT 19404): structures and inhibitory effects on RANKL-induced formation of multinuclear osteoclasts. *J. Natural Prod.* 84 (9), 2475–2485. doi: 10.1021/ACS.JNATPROD.1C00486

Fang, X., Liu, Y., Xiao, J., Ma, C., and Huang, Y. (2023). GC-MS and LC-MS/MS metabolomics revealed dynamic changes of volatile and non-volatile compounds during withering process of black tea. *Food Chem.* 410, 135396. doi: 10.1016/J.FOODCHEM.2023.135396

Feng, X. H., Zhang, B., and Sun, J. H. (2022). Research progress on the interaction between associated microbes and pine wood nematode-vector beetle complex. *For. Pest Dis.* 41 (03), 30–37. doi: 10.19688/j.cnki.issn1671-0886.20220029

Geneau, C. E., Waeckers, F. L., Luka, H., and Balmer, O. (2013). Effects of extrafloral and floral nectar of Centaurea cyanus on the parasitoid wasp Microplitis mediator: Olfactory attractiveness and parasitization rates. *Biol. Control* 66 (1), 16–20. doi: 10.1016/j.biocontrol.2013.02.007

Guo, Y. J., Lin, Q. N., Chen, L. Y., Carballar-Lejarazu, R., Zhang, A. S., Shao, E. S., et al. (2020). Characterization of bacterial communities associated with the pinewood nematode insect vector *Monochamus alternatus* Hope and the host tree *Pinus* massoniana. *BMC Genomics* 21 (1), 337. doi: 10.1186/s12864-020-6718-6

Hao, X., Wang, B. W., Chen, J., Wang, B. Y., Xu, J. Y., Pan, J. L., et al. (2021). Molecular characterization and functional analysis of multidrug resistance-associated genes of Pinewood nematode (*Bursaphelenchus xylophilus*) for nematicides. *Pesticide Biochem. Physiol.* 177, 104902. doi: 10.1016/j.pestbp.2021.104902

Hedrich, R., Salvador-Recatala, V., and Dreyer, I. (2016). Electrical wiring and long-distance plant communication. *Trends Plant Sci.* 21 (5), 376–387. doi: 10.1016/j.tplants.2016.01.016

Hirata, A., Nakamura, K., Nakao, K., Kominami, Y., Tanaka, N., Ohashi, H., et al. (2017). Potential distribution of pine wilt disease under future climate change scenarios. *PloS One* 12 (8), e0182837. doi: 10.1371/journal.pone.0182837

Hu, S. J., Ning, T., Fu, D. Y., Haack, R. A., Zhang, Z., Chen, D. D., et al. (2013). Dispersal of the Japanese pine sawyer, *monochamus alternatus* (Coleoptera: cerambycidae), in mainland China as inferred from molecular data and associations to indices of human activity. *PloS One* 8 (2), e57568. doi: 10.1371/journal.pone.0057568

Hyatt, D., Locascio, P. F., Hauser, L. J., and Uberbacher, E. C. (2012). Gene and translation initiation site prediction in metagenomic sequences. *Bioinformatics* 28 (17), 2223–2230. doi: 10.1093/bioinformatics/bts429

Langmead, B., Trapnell, C., Pop, M., and Salzberg, S. L. (2009). Ultrafast and memory-efficient alignment of short DNA sequences to the human genome. *Genome Biol.* 10 (3), R25. doi: 10.1186/gb-2009-10-3-r25

Li, Y. (2018). Response of pine endophytic bacteria flora to *Bursaphelenchus xylophilus* infection and Construction of insecticidal gene engineering bacteria with JK-SH007. Doctoral degree thesis (Jiangsu, China: Nanjing Forestry University, Nanjing).

Li, W., Jaroszewski, L., and Godzik, A. (2001). Clustering of highly homologous sequences to reduce the size of large protein databases. *Bioinf. (Oxford England)* 17 (3), 282–283. doi: 10.1093/bioinformatics/17.3.282

Li, Z., Li, B. S., Hu, Z. J., Michaud, J. P., Dong, J., Zhang, Q. W., et al. (2015). The ectoparasitoid *Scleroderma guani* (Hymenoptera: Bethylidae) uses innate and learned chemical cues to locate its host, larvae of the pine sawyer *Monochamus alternatus* (Coleoptera: Cerambycidae). *Florida Entomol.* 98 (4), 1182–1187. doi: 10.1653/024.098.0425

Li, H. M., Shen, P. Y., Fu, P., Lin, M. S., and Moens, M. (2007). Characteristics of the emergence of *Monochamus alternatus*, the vector of *Bursaphelenchus xylophilus* (Nematoda : Aphelenchoididae), from *Pinus thunbergii* logs in Nanjing, China, and of the transmission of the nematodes through feeding wounds. *Nematology* 9 (6), 807–816. doi: 10.1163/156854107782331234

Li, Y. X., Wang, X., Liu, Z. K., and Zhang, X. Y. (2022). Research advance of pathogenic mechanism of pine wood nematode. *For. Pest Dis.* 41 (03), 11–20. doi: 10.19688/j.cnki.issn1671-0886.20220015

Liu, Y., Ponpandian, L. N., Kim, H., Jeon, J., Hwang, B. S., Lee, S. K., et al. (2019). Distribution and diversity of bacterial endophytes from four *Pinus* species and their efficacy as biocontrol agents for devastating pine wood nematodes. *Sci. Rep.* 9 (1), 12461. doi: 10.1038/s41598-019-48739-4

Lu, F., Guo, K., Chen, A. L., Chen, S. N., Lin, H. P., and Zhou, X. (2020). Transcriptomic profiling of effects of emamectin benzoate on the pine wood nematode *Bursaphelenchus xylophilus*. *Pest Manage. Sci.* 76 (2), 747–757. doi: 10.1002/ps.5575

Park, B. H., Lee, H. J., and Lee, Y. R. (2011). Total Synthesis of Chiricanine A, Arahypin-1, trans-Arachidin-2, trans-Arachidin-3, and Arahypin-5 from Peanut Seeds. *J. Natural Prod.* 74 (4), 644–649. doi: 10.1021/np100696f

Pires, D., Vicente, C. S. L., Menendez, E., Faria, J. M. S., Rusinque, L., Camacho, M. J., et al. (2022). The fight against plant-parasitic nematodes: current status of bacterial and fungal biocontrol agents. *Pathogens* 11 (10), 1178. doi: 10.3390/pathogens11101178

Ponpandian, L. N., Rim, S. O., Shanmugam, G., Jeon, J., Park, Y.-H., Lee, S.-K., et al. (2019). Phylogenetic characterization of bacterial endophytes from four *Pinus* species and their nematicidal activity against the pine wood nematode. *Sci. Rep.* 9 (1), 12457. doi: 10.1038/s41598-019-48745-6

Poppeliers, S. W., Sanchez-Gil, J. J., and De Jonge, R. (2023). Microbes to support plant health: understanding bioinoculant success in complex conditions. *Curr. Opin. Microbiol.* 73, 102286–102286. doi: 10.1016/j.mib.2023.102286

Proenca, D. N., Francisco, R., Kublik, S., Schoeler, A., Vestergaard, G., Schloter, M., et al. (2017a). The microbiome of endophytic, wood colonizing bacteria from pine trees as affected by pine wilt disease. *Sci. Rep.* 7 (1), 4205. doi: 10.1038/s41598-017-04141-6

Proenca, D. N., Grass, G., and Morais, P. V. (2017b). Understanding pine wilt disease: roles of the pine endophytic bacteria and of the bacteria carried by the disease-causing pinewood nematode. *Microbiologyopen* 6 (2), e00415. doi: 10.1002/mbo3.415

Rajasekharan, S. K., Lee, J. H., Ravichandran, V., and Lee, J. (2017). Assessments of iodoindoles and abamectin as inducers of methuosis in pinewood nematode, *Bursaphelenchus xylophilus*. *Sci. Rep.* 7 (1), 6803. doi: 10.1038/s41598-017-07074-2

Rank, C., Nielsen, K. F., Larsen, T. O., Varga, J., Samson, R. A., and Frisvad, J. C. (2011). Distribution of sterigmatocystin in filamentous fungi. *Fungal Biol.* 115 (4-5), 406–420. doi: 10.1016/j.funbio.2011.02.013

Santini, A., and Battisti, A. (2019). Complex insect-pathogen interactions in tree pandemics. *Front. Physiol.* 10. doi: 10.3389/fphys.2019.00550

Shen, N., Wang, T. F., Gan, Q., Liu, S., Wang, L., and Jin, B. (2022). Plant flavonoids: Classification, distribution, biosynthesis, and antioxidant activity. *Food Chem.* 383, 132531. doi: 10.1016/j.foodchem.2022.132531

Sobolev, V. S. (2008). Localized production of phytoalexins by peanut (*Arachis hypogaea*) kernels in response to invasion by *Aspergillus* species. *J. Agric. Food Chem.* 56 (6), 1949–1954. doi: 10.1021/jf703595w

Sobolev, V. S., Arias, R., Goodman, K., Walk, T., Orner, V., Faustinelli, P., et al. (2018). Suppression of aflatoxin production in *aspergillus* species by selected peanut (*Arachis hypogaea*) stilbenoids. *J. Agric. Food Chem.* 66 (1), 118–126. doi: 10.1021/acs.jafc.7b04542

Sobolev, V. S., Khan, S. I., Tabanca, N., Wedge, D. E., Manly, S. P., Cutler, S. J., et al. (2011). Biological activity of peanut (*Arachis hypogaea*) phytoalexins and selected natural and synthetic stilbenoids. *J. Agric. Food Chem.* 59 (5), 1673–1682. doi: 10.1021/jf104742n

Sobolev, V. S., Krausert, N. M., and Gloer, J. B. (2016). New Monomeric Stilbenoids from Peanut (Arachis hypogaea) Seeds Challenged by an *Aspergillus* flavus Strain. *J. Agric. Food Chem.* 64 (3), 579–584. doi: 10.1021/acs.jafc.5b04753

Souto, A. L., Sylvestre, M., Tolke, E. D., Tavares, J. F., Barbosa-Filho, J. M., and Cebrian-Torrejon, G. (2021). Plant-derived pesticides as an alternative to pest management and sustainable agricultural production: prospects, applications and challenges. *Molecules* 26 (16), 4835. doi: 10.3390/molecules26164835

Takai, K., Suzuki, T., and Kawazu, K. (2004). Distribution and persistence of emamectin benzoate at efficacious concentrations in pine tissues after injection of a liquid formulation. *Pest Manage. Sci.* 60 (1), 42–48. doi: 10.1002/ps.777

Teale, S. A., Wickham, J. D., Zhang, F., Su, J., Chen, Y., Xiao, W., et al. (2011). A male-produced aggregation pheromone of *monochamus alternatus* (Coleoptera: cerambycidae), a major vector of pine wood nematode. *J. Econ. Entomol.* 104 (5), 1592–1598. doi: 10.1603/ec11076

Theodoridis, G., Gika, H. G., and Wilson, I. D. (2008). LC-MS-based methodology for global metabolite profiling in metabonomics/metabolomics. *Trac-Trends Anal. Chem.* 27 (3), 251–260. doi: 10.4155/bio.12.212

Tian, H. K., Koski, T. M., Zhao, L. L., Liu, Z. Y., and Sun, J. H. (2022). Invasion History of the Pinewood Nematode *Bursaphelenchus xylophilus* Influences the Abundance of *Serratia* sp. in Pupal Chambers and Tracheae of Insect-Vector *Monochamus alternatus*. *Front. Plant Sci.* 13. doi: 10.3389/fpls.2022.856841

Togashi, K., Appleby, J. E., Oloumi-Sadeghi, H., and Malek, R. B. (2022). Relationship between the initial number of carried *Bursaphelenchus xylophilus* and its transmission by *Monochamus carolinensis* with reference to virulence. *Nematology* 24 (6), 679–694. doi: 10.1163/15685411-bja10160

Toth, L., Poor, P., Ordog, A., Varadi, G., Farkas, A., Papp, C., et al. (2022). The combination of *Neosartorya* (*Aspergillus*) *fischeri* antifungal proteins with rationally designed γ-core peptide derivatives is effective for plant and crop protection. *Biocontrol (Dordr)* 67 (2), 249–262. doi: 10.1007/s10526-022-10132-y

Versilovskis, A., and De Saeger, S. (2010). Sterigmatocystin: Occurrence in foodstuffs and analytical methods – An overview. *Mol. Nutr. Food Res.* 54 (1), 136–147. doi: 10.1002/mnfr.200900345

Wang, H. X., Qan, J., and Ding, F. Y. (2018). Emerging chitosan-based films for food packaging applications. *J. Agric. Food Chem.* 66 (2), 395–413. doi: 10.1021/acs.jafc.7b04528

Wang, Z. W., Xu, H. C., Zhang, W. W., and Wang, P. X. (2016). Anoplophora glabripennis host-plant selection with main host-plant volatile chemical component analysis. *J. Zhejiang A&F Univ.* 33 (04), 558–563.

Wang, Z., Zhang, Y., Wang, C., Wang, Y., and Sung, C. (2017). *Esteya vermicola* Controls the Pinewood Nematode, *Bursaphelenchus xylophilus*, in Pine Seedlings. *J. Nematol.* 49 (1), 86–91. doi: 10.21307/jofnem-2017-048

Wu, B., Liang, A., Zhang, H., Zhu, T., Zou, Z., Yang, D., et al. (2021). Application of conventional UAV-based high-throughput object detection to the early diagnosis of pine wilt disease by deep learning. *For. Ecol. Manage.* 486, 118986. doi: 10.1016/j.foreco.2021.118986

Xiang, Y., Wu, X. Q., and Zhou, A. D. (2015). Bacterial Diversity and Community Structure in the Pine Wood Nematode *Bursaphelenchus xylophilus* and *B.mucronatus* with Different Virulence by High-Throughput Sequencing of the 16S rDNA. *PloS One* 10 (9), e0137386. doi: 10.1371/journal.pone.0137386

Xie, W. F., Xu, X. M., Qiu, W. J., Lai, X. L., Liu, M. X., and Zhang, F. P. (2022). Expression of PmACRE1 in *Arabidopsis thaliana* enables host defence against *Bursaphelenchus xylophilus* infection. *BMC Plant Biol.* 22 (1), 541. doi: 10.1186/s12870-022-03929-7

Xue, Q., Xiang, Y., Wu, X. Q., and Li, M. J. (2019). Bacterial Communities and Virulence Associated with Pine Wood Nematode *Bursaphelenchus xylophilus* from Different *Pinus* spp. *Int. J. Mol. Sci.* 20 (13), 3342. doi: 10.3390/ijms20133342

Yan, X. F., Li, X. J., Luo, Y. Q., Xu, Z. C., Tian, G. F., and Zhang, T. L. (2008). Taxis response of *Anoplophora glabripennis* adults to volatiles emanating from their larval host twigs. *J. Beijing Forest. Univ.* 03), 80–84.

Zhang, Q. X. (2016). Application Technical Research of *Monochamus alternatus* High-efficiency Attractant. Master degree thesis (Guangdong, China: South China Agricultural University, Guangzhou).

Zhang, H. T. (2021). Preliminary study on the screening and function ofgenes related to *Bursaphelenchus xylophilus* by *Enterobacter Ludwigii* AA4. Master degree thesis (Heilongjiang, China: Northeast Forestry University, Harbin). doi: 10.27009/d.cnki.gdblu.2021.000270

Zhao, L., Mota, M., Vieira, P., Butcher, R. A., and Sun, J. (2014). Interspecific communication between pinewood nematode, its insect vector, and associated microbes. *Trends Parasitol.* 30 (6), 299–308. doi: 10.1016/j.pt.2014.04.007

Zhu, L. H., Duan, H. J., Fang, X. Y., Yang, Z. D., Guo, C. H., and Wu, G. (2019). Preliminary study on host selection for feeding and oviposition of adult batocera horsfieldi on walnut. *Agric. Res. Appl.* 32 (04), 1–4.

frontiers | Frontiers in Plant Science

TYPE Original Research
PUBLISHED 28 February 2024
DOI 10.3389/fpls.2024.1357141

OPEN ACCESS

EDITED BY
Andressa Machado,
Agronema, Brazil

REVIEWED BY
Jun Su,
Fujian Agriculture and Forestry University, China
Huan Peng,
Chinese Academy of Agricultural Sciences, China

*CORRESPONDENCE
Borong Lin
Boronglin@scau.edu.cn
Jinling Liao
jlliao@scau.edu.cn

RECEIVED 17 December 2023
ACCEPTED 16 February 2024
PUBLISHED 28 February 2024

CITATION
Li Z, Wang H, Cao Y, Shan X, He X, Huang Q, Zhuo K, Liao J and Lin B (2024) A *Bursaphelenchus xylophilus* effector BxICD1 inducing plant cell death, concurrently contributes to nematode virulence and migration.
Front. Plant Sci. 15:1357141.
doi: 10.3389/fpls.2024.1357141

A *Bursaphelenchus xylophilus* effector BxICD1 inducing plant cell death, concurrently contributes to nematode virulence and migration

Zhiwen Li[1], Honghong Wang[2], Yuqing Cao[1], Xiaoling Shan[1], Xiaoxian He[1], Qiuling Huang[1], Kan Zhuo[1,3], Jinling Liao[1,2]* and Borong Lin[1,3]*

[1]College of Plant Protection, South China Agricultural University, Guangzhou, China, [2]Collaborative Innovation Center of Plant Pest Management and Bioenvironmental Health Application Technology, Guangdong Eco-Engineering Polytechnic, Guangzhou, China, [3]Guangdong Province Key Laboratory of Microbial Signals and Disease Control, South China Agricultural University, Guangzhou, China

The migratory endoparasitic phytonematodes *Bursaphelenchus xylophilus* is the causal agent of pine wilt disease and causes significant economic damage to pine forests in China. Effectors play a key role in the successful parasitism of plants by phytonematodes. In this study, 210 genes obtained by transcriptomics analyses were found to be upregulated in *B. xylophilus* infecting *Pinus massoniana* that were not functionally annotated nor reported previously in *B. xylophilus* infecting *P. thunbergii.* Among these differentially expressed genes, a novel effector, BxICD1, that could induce cell death in the extracellular space of *Nicotiana benthamiana* was identified. *BxICD1* was upregulated in the early stages of infection, as shown by RT-qPCR analyses. *In situ* hybridization analysis showed that *BxICD1* was expressed in the esophageal gland of nematodes. The yeast signal sequence trap system indicated that BxICD1 possessed an N-terminal signal peptide with secretion functionality. Using an *Agrobacterium*-mediated transient expression system, it was demonstrated that the cell death-inducing activity of BxICD1 was dependent on *N. benthamiana* brassinosteroid-insensitive 1-associated kinase 1 (NbBAK1). Finally, BxICD1 contributed to *B. xylophilus* virulence and migration in host pine trees, as demonstrated by RNAi silencing assays. These findings indicate that BxICD1 both induces plant cell death and also contributes to nematode virulence and migration in *P. massonian*.

KEYWORDS

***Bursaphelenchus xylophilus*, transcriptome, *Pinus massoniana*, effector, plant cell death activation**

1 Introduction

The pine wood nematode (PWN), *Bursaphelenchus xylophilus*, is a migratory endoparasitic nematode. The nematodes enter the trees through the wounds formed by *Monochamus* beetles feeding (Edwards and Linit, 1992), then colonize the tree's xylem and cortex resin canals, obstructing water and nutrient flow. This ultimately leads to tree wilting and death (Futai, 2013), termed pine wilt disease (PWD). PWD has significant economic and ecological impacts on pine forests in Asia and Europe (Kikuchi et al., 2011). Currently, the methods for preventing and controlling PWD primarily involve directly cutting and incinerating infested trees, fumigating logs with pesticides, applying pesticides to manage *Monochamus* beetles, or injecting nematicides against *B. xylophilus* (Cui et al., 2014). However, these strategies possess certain drawbacks, including environmental pollution and significant costs. To formulate novel and eco-friendly strategies for PWD management, it is necessary to understand the mechanisms of PWN parasitism.

When plant-parasitic nematodes (PPNs) infect host plants, they secrete numerous proteins into the host. These proteins, termed effectors, play crucial roles in successful nematode parasitism, and understanding their functions is crucial to uncovering the molecular mechanisms underlying parasitism (Haegeman et al., 2012; Vieira and Gleason, 2019). Many previous studies have shown that PPN effectors mainly function in plant cell wall degradation, feeding site formation, and the suppression of host immunity (Popeijus et al., 2000; Kikuchi et al., 2006; Kudla et al., 2007; Vanholme et al., 2007; Chen et al., 2017; Verma et al., 2018; Chen et al., 2021; Song et al., 2021). Most studies have focused on sedentary endoparasitic nematodes, such as root-knot nematodes and cyst nematodes. Recently, some effectors from *B. xylophilus* have been characterized, and effectors with plant cell wall-degradation or host immunity suppression functions have been discovered (Kikuchi et al., 2006; Wen et al., 2021, Wen et al., 2022; Hu et al., 2022a; Qiu et al., 2023). Intriguingly, a number of effectors from *B. xylophilus* were found to induce host cell death. Of these, BxCDP1 can trigger plant cell death (PCD) to induce *Pinus thunbergii* resistance against nematodes (Hu et al., 2020; Hu et al., 2022b). Several other effectors, such as BxSapB1, BxSapB2, and BxSapB3, while capable of inducing plant cell death, also function as a virulence factor, during *B. xylophilus* infection (Huang et al., 2019; Hu et al., 2019; Zhao et al., 2020). This phenomenon is relatively common in effectors from fungi and oomycetes, such as the *Fusarium graminearum* effector Fg62 (Wang et al., 2023), the *Phytophthora infestans* effector Pi23226 (Lee et al., 2023), etc., which can induce host cell death and promote pathogen parasitism.

Masson pine (*Pinus massoniana*) is a pioneer species for afforestation timber and oleoresin production, widely distributed in South China. However, it is highly sensitive to *B. xylophilus* (Xue et al., 2013; Liu et al., 2022a). Despite this, the roles of effectors during *B. xylophilus* parasitism in *P. massoniana* are poorly understood. In this study, transcriptomes of *B. xylophilus* feeding on *Pestalotiopsis* sp. and infecting *P. massoniana* were analyzed by RNA sequencing (RNA-seq). Differentially expressed genes of *B. xylophilus* were identified in these two conditions, which were analyzed to identify candidate effectors involved in *B. xylophilus* parasitism in *P. massoniana* parasitism. Among the candidate effectors, a novel effector (named BxICD1) that was expressed in the esophageal gland of *B. xylophilus* and upregulated during nematode parasitism in *P. massoniana* was identified. Here, we showed that the effector BxICD1 not only induces PCD, but also promotes nematode virulence and migration in *P. massoniana*.

2 Materials and methods

2.1 Nematode and plant materials

B. xylophilus was isolated from a wilted Masson pine in Guangdong province, China, purified using a single fertilized adult female, and cultured in the fungus *Pestalotiopsis* sp. grown on potato dextrose agar (PDA) medium at 25°C under 16 h light/8 h dark (16/8 LD) conditions for 6 days.

Approximately 3-year-old *P. massoniana* seedlings were obtained from Yangshan County (24°17′1.6″N, 112°33′42.4″E), Qingyuan City, Guangdong province, China, and grown at temperatures ranging from 25°C to 30°C. *Nicotiana benthamiana* LAB were grown in a glasshouse at 25°C with a relative humidity of 60% under 16/8 LD conditions.

2.2 RNA extraction and cDNA synthesis

B. xylophilus was inoculated into a small, approximately 1 cm, wound in *P. massoniana* stems. After 12 h, mixed-life-stage nematodes were isolated from the pine stems using a Baermann funnel technique (Hu et al., 2019), and approximately 20,000 nematodes were used for RNA extraction. The same number of *B. xylophilus* nematodes were also isolated from *Pestalotiopsis* sp. grown on PDA plates for RNA extraction. Each treatment consisted of two replicates. Total RNA was extracted using the RNAprep Pure Micro Kit (DP420, TianGen Biotech), and first-strand cDNA was synthesized from 1 μg of total RNA using a TransScript One-Step gDNA Removal and the cDNA Synthesis SuperMix kits (AT311, TransGen Biotech, Beijing, China) according to the manufacturer's instruction.

2.3 RNA-seq analysis

Sequencing libraries were constructed using the NEBNext Ultra RNA Library Prep Kit (E7530, NEB, USA) according to the manufacturer's instructions. RNA integrity was determined by the RNA Nano 6000 Assay Kit of the Bioanalyzer 5400 system (Agilent Technologies, CA, USA). Total RNA was used as input material for the RNA library preparations. The library preparations were sequenced on an Illumina Novaseq platform, generating 6.49-6.82 GB of data of 150-base long paired reads per sample (Modi et al., 2021). The raw RNA-Seq data in this study are available through the National Center for Biotechnology Information under the accession number PRJNA1027064.

Paired-end reads were aligned to the reference genome (https://parasite.wormbase.org/Bursaphelenchus_xylophilus_prjea64437/Info/Index) using Hisat2 v2.0.5 (Kim et al., 2019). The reads mapped to each gene were measured using FeatureCounts v1.5.0-p3 (Liao et al., 2014). The FPKM values of each gene were calculated based on the length of the gene and the reads count mapped to this gene (Trapnell et al., 2010).

Differential expression analysis was performed using the DESeq2 R package (1.20.0). The resulting *P*-values were adjusted using the Benjamini and Hochberg's approach for controlling the false discovery rate (Benjamini and Hochberg, 1995). Genes identified by DESeq with an adjusted *P*-value<0.05 and $|Log_2$(fold change)|>1 were considered differentially expressed genes.

2.4 Real-time quantitative PCR assays and data analysis

Real-time quantitative PCR (RT-qPCR) was performed using Green qPCR SuperMix (AQ101, TransGen Biotech, Beijing, China) on a Thermal Cycler Dice Real Time System (Takara, Beijing, China). The RT-qPCR reaction mixture consisted of 1.0 µL cDNA, 0.4 µL of each of the 10 pM primers, 10 µL 2 × Green qPCR SuperMix, and 8.2 µL RNase-free ddH_2O. The ubiquitin-conjugating enzyme gene *BxUBI2* (GenBank accession number CAD5208953.1) and *NbEF1α* (Heese et al., 2007) were used as endogenous controls for gene expression normalization in the different species. All the gene-specific primers used in this study are listed in Supplementary Table 1. The RT-qPCR cycling conditions were as follows: 94°C for 30 sec, followed by 40 cycles of 94°C for 10 s, 55°C annealing for 15 s, 72°C elongation for 10 s. The relative changes in gene expression were determined using the $2^{-\Delta\Delta CT}$ method (Livak and Schmittgen, 2001). Three independent experiments were conducted.

2.5 Screening of putative secreted proteins

Putative secreted proteins encoded by differentially expressed genes (DEGs) were predicted using both SignalP 5.0 (https://services.healthtech.dtu.dk/service.-php?SignalP-5.0) and TMHMM-2.0 (https://services.healthtech.dtu.dk/service.php?TMHMM-2.0) for the presence of an N-terminal signal peptide (SP) and for the absence of a transmembrane domain, respectively. These steps were implemented as a 'secreted protein prediction' workflow (Petitot et al., 2016). Protein functional domains were predicted by EGGNOG-MAPPER (http://eggnog-mapper.embl.de/). The phylogenetic tree was constructed using the NJ method and visualized using MEGA-X (Kumar et al., 2018).

2.6 Gene amplification

The full-length cDNA sequences of 10 candidate genes were amplified by using the corresponding gene-specific primers. The PCR reaction was performed in a total volume of 50 µL containing 1.0 U KOD-FX (KFX-101, Toyobo, Osaka, Japan), 25 µL 2 × PCR Buffer, 10 µL 2 mM dNTPs, 1.5 µL of each of the 10 pM primers, 200 ng cDNA, and sterilized distilled water up to 50 µL. The PCR cycling conditions were as follows: 95°C for 5 min, followed by 30 cycles of 98°C for 10 s, annealing at 55°C for 30 s, elongation at 68°C for 30 s, and final elongation at 68°C for 5 min.

2.7 Plasmid construction

The CaMV35S driven *β-glucuronidase* (*GUS*) gene of the pCAMBIA1305.1 vector was removed and replaced with the *eGFP* gene to generate the binary vector pCambia1305.1$^{\Delta GUS}$ and pCambia1305.1:eGFP. To construct the overexpression vector, the 10 candidate genes mentioned above, with or without the native SP sequence, were amplified and ligated to the linearized pCambia1305.1:eGFP digested by *Nco*I and *Pml*I (FD0574 and FD0364, Thermo Fisher Scientific, MA, USA) to generate pCambia1305.1:gene:eGFP, following the instructions of the ClonExpress II One Step Cloning Kit (C112-01, Vazyme, Nanjing, China). *BxICD1:Flag* was amplified and ligated to the linearized pCambia1305.1$^{\Delta GUS}$ to generate pCambia1305.1:BxICD1:Flag. For pSUC2, vectors were digested by *Eco*RI and *Xho*I (FD0274 and FD0694, Thermo Fisher Scientific, MA, USA) in the appropriate conditions. The SP sequences of *BxICD1* and *Avr1b* were linked to linearized pSUC2 to generate pSUC2:SP^{BxICD1} and pSUC2:SP^{Avr1b} following the instructions of the ClonExpress II One Step Cloning Kit.

2.8 *In situ* hybridization experiments

Approximately 10,000 mixed-life-stage nematodes were collected from pine stems. The primer pairs ISH-BxICD1-F/ISH-BxICD1-R were employed to synthesize digoxygenin (DIG)-labeled sense and antisense DNA probes based on the *BxICD1* fragments of 96–281 bp using a PCR DIG Probe Synthesis Kit (1636090910, Roche Applied Science, Rotkreuz, Switzerland). The primer pair ISH-BxICD2-F/ISH-BxICD2-R was employed to synthesize sense and antisense DNA probes based on the *BxICD2* fragments of 103-311 bp in size. The *in situ* hybridization and staining of the nematodes was performed as described previously (De Boer et al., 1998). Nematodes were then examined using a Nikon ECLIPSE Ni microscope (Nikon, Tokyo, Japan).

2.9 Cell death assay

The cell death assay was performed as described previously (Chen et al., 2017). Briefly, the pCambia1305.1:gene:eGFP constructs mentioned above were individually introduced into *Agrobacterium tumefaciens* GV3101. Then the transformed bacteria were suspended in a buffer containing 10 mM 2-(N-morpholino) ethanesulfonic acid (MES) (pH 5.5) and 200 µM acetosyringone until a 600 nm absorbance (OD_{600}) of 0.6 was reached. Then, the *A. tumefaciens* cell suspensions were infiltrated into 4-week-old

N. benthamiana leaves. After 3 days, the cell-death phenotype was observed and photographed. *eGFP* and the *P. infestans* elicitor gene *INF1*, cloned individually into the pCambia1305.1 vector, were used as the negative and positive control, respectively. The infiltration assay was performed three times, and five different plants with two inoculated leaves were used in each assay.

2.10 Yeast signal sequence trap system

The secretion function of the *BxICD1* SP was verified using the yeast signal sequence trap system described previously (Yin et al., 2018). Briefly, the SP sequence of *BxICD1* was cloned into the pSUC2 vector containing the invertase gene but lacking Methionine (Met) and SP sequence to generate pSUC2:SP^{BxICD1}-Invertase. Additionally, the SP of *Phytophthora sojae* RXLR effector Avr1b has been demonstrated to have secretion function in yeast (Dou et al., 2008) and was also cloned into pSUC2 to generate pSUC2:SP^{Avr1b}-Invertase as a positive control. pSUC2:SP^{BxICD1}-Invertase and pSUC2:SP^{Avr1b}-Invertase were transformed into the yeast strain YTK12 by the lithium acetate method (Gietz and Schiestl, 2007; Yin et al., 2018). The yeast strains YTK12 and YTK12 carrying the pSUC2 empty vector were used as negative controls. YTK12 and YTK12 containing pSUC2-derived plasmids were grown on a CMD-W medium (0.67% yeast N base without amino acids, 0.075% W dropout supplement, 2% sucrose, 0.1% glucose, and 2% agar) to detect the expression of pSUC2-derived plasmids. The enzymatic activity of invertase was confirmed by the reduction of the dye 2,3,5-triphenyltetrazolium chloride (TTC) to the insoluble red-colored 1,3,5-triphenylformazan (TPF).

2.11 Subcellular localization

The subcellular localization assays were performed as described previously (Chen et al., 2017). Briefly, *BxICD1* sequences with or without the native SP were cloned into the pCambia1305.1 vector to generate BxICD1:eGFP and BxICD1$^{\Delta sp}$:eGFP, respectively. *eGFP* alone was used as the control. The constructs were used for the transformation of 4-week-old *N. benthamiana* leaves by agroinfiltration. Then the *N. benthamiana* plants were cultured for 3 days at 25°C under 16/8 LD. *N. benthamiana* leaves expressing the constructs were infiltrated with 30% glycerol for 20 min to induce plasmolysis for the observation of extracellular localization (Chen et al., 2021). The fluorescence was observed using an SP5 Leica confocal microscope (Nikon, Tokyo, Japan).

Western blotting was performed to verify the production of intact BxICD1:eGFP and BxICD1$^{\Delta sp}$:eGFP fusion proteins in *N. benthamiana*, as described previously (Chen et al., 2021). Briefly, the total proteins from *N. benthamiana* leaves were extracted using RIPA lysis buffer. The proteins were denatured, separated on an SDS-PAGE gel, and transferred to a nitrocellulose membrane (PALL, Washington, NY, United States). After blocking with 5% (w/v) non-fat milk for 2 h at room temperature, the membranes were incubated with a primary mouse anti-GFP antibody (1:5000 dilution) (HT801, TransGen Biotech, Beijing, China) in a blocking solution for 2 h. Then membranes were incubated with an anti-mouse horseradish peroxidase-conjugated secondary antibody at a 1:5000 dilution (HS201, TransGen Biotech, Beijing, China). Proteins were visualized using the Immobilon Western Chemiluminescent system with Pierce ECL Western Blotting Substrate (Thermo Fisher Scientific, MA, USA). Ponceau S staining was used to assess equal loading (Goldman et al., 2016).

2.12 Electrolyte leakage assay

Electrolyte leakage assays were performed in *N. benthamiana*, as described previously (Yu et al., 2012). The *A. tumefaciens* harboring BxICD1:eGFP, BxICD1$^{\Delta sp}$:eGFP, eGFP and INF1 were infiltrated into *N. benthamiana* leaves as described above. 36 h after agroinfiltration, five leaf discs (9 mm diameter) were floated on 5 mL distilled water for each sample and shaken at 25°C for 3 h. Then the conductivity of the solution was measured with a conductivity meter (DDS-307A, Shanghai INESA Scientific Instrument) to obtain the value A. In addition, the conductivity of the solution containing the leaf discs was measured after boiling for 30 min to obtain the value B. Ion leakage was calculated according to the formula (value A/value B) × 100%. The experiment was performed three times. Western blotting was performed to detect protein expression as described above.

2.13 In planta RNAi

Virus-induced gene silencing targeting *NbBAK1* and *NbSOBIR1* in *N. benthamiana* was performed as described previously (Lin et al., 2016). Briefly, the vectors pTRV1, pTRV2:*NbBAK1*, pTRV2:*NbSOBIR1*, and pTRV2:*eGFP* were individually transformed into *A. tumefaciens* GV3101. *A. tumefaciens* GV3101 harboring pTRV1 was mixed in a 1:1 ratio with those harboring pTRV2:NbBAK1, pTRV2:*NbSOBIR1* or pTRV2:*eGFP*, respectively, and infiltrated into *N. benthamiana* leaves. The silencing efficiency of *NbBAK1* and *NbSOBIR1* was validated by RT-qPCR. RT-qPCR was performed as described above. The infiltration experiment was performed thrice and three different plants, with three inoculated leaves in each, were used in each assay.

2.14 *In vitro* RNAi

The *BxICD1* gene was silenced using *in vitro* RNAi, as described previously (Liu et al., 2022b). Briefly, the T7-promoter sequence was introduced in the sense and antisense direction of a 186-bp *BxICD1* fragment using the primer pairs RNAi-T7BxICD1-F/RNAi-BxICD1-R and RNAi-BxICD1-F/RNAi-T7BxICD1-R. The PCR was performed as described above. The obtained PCR products were used to synthesize double-stranded RNA (dsRNA) using the Thermo T7 Transcription Kit (TSK-101, Toyobo, Shanghai, China) according to the manufacturer's instructions. The same approach was used to synthesize dsRNA for *eGFP* using the primer pairs RNAi-T7eGFP-F/RNAi-eGFP-R and RNAi-eGFP-F/RNAi-T7eGFP-R. Nematodes were then inoculated in a dsRNA and a

non-dsRNA solution at 25°C for 24 h. The treated nematodes were washed with ddH_2O three times to remove external dsRNA. Subsequently, approximately 5,000 nematodes were collected for RNA extraction. The remaining nematodes were used for nematode virulence, migration, and reproduction analysis. The extent of *BxICD1* silencing was assessed using RT-qPCR. RNA extraction and RT-qPCR were performed as described above, except for the different primer pairs that were used in the RT-qPCR.

2.15 Infection assay

Each 3-year-old *P. massoniana* seedling was inoculated with 1,000 *B. xylophilus* treated with a *BxICD1* dsRNA, *eGFP* dsRNA, and non-dsRNA solution. Nine to ten pine trees were inoculated with each treatment. The experiment was repeated 3 times. Following the classification by Hu et al. (2022a), the morbidity degree of the *P. massoniana* seedlings was categorized into five different grades: 0, all needles were green; I, a few needles have turned yellow; II, approximately half of the needles have turned yellow or brown; III, most of the needles turned brown; and IV, the entire seedling was withered. The following formulas were used to calculate morbidity and the disease severity index.

$$\text{morbidity}(\%) = \frac{\text{Total number of diseased seedlings}}{\text{Total number of seedlings inoculated}} \times 100$$

Disease severity index(DSI)

$$= \frac{\sum \text{Total number of diseased seedlings} \times \text{morbidity degree}}{\text{Total number of seedlings} \times \text{the highest morbidity degree}} \times 100$$

2.16 Migration assay

The migration ability of *B. xylophilus* in *P. massoniana* was determined as described previously (Kusumoto et al., 2014). Briefly, approximately 800 nematodes treated with *BxICD1* dsRNA, *eGFP* dsRNA, and non-dsRNA solutions were used to inoculate 3-year-old *P. massoniana* seedlings. 12 h after inoculation, the pine stem segments 1-2, 2-3, 3-4 and 4-5 cm below the inoculation point were used for nematode extraction using the Baermann funnel method. Nematodes isolated from these stem segments were counted. The experiment was repeated twice with four biological replicates each time. Statistically significant differences between treatments and controls were determined by Duncan's multiple-range test.

2.17 Reproduction and feeding rate analysis

The reproduction and feeding rate of *B. xylophilus* in fungi was assessed as described previously (Hu et al., 2022a). Approximately 100 nematodes treated with *BxICD1* dsRNA, *eGFP* dsRNA, and non-dsRNA solutions were inoculated to PDA plates covered with *Pestalotiopsis* sp. After culturing at 25°C for 8 d, the nematodes were collected from each PDA plate using the Baermann funnel method and counted to calculate their reproduction. The amount of *Pestalotiopsis* sp. remaining on PDA plates was measured to determine the feeding rate of *B. xylophilus*. Six PDA plates were used for each treatment, and the experiment was repeated three times. Statistically significant differences between treatments and controls were determined by Duncan's multiple-range test.

3 Results

3.1 RNA-seq data of *B. xylophilus*

RNA was extracted from *B. xylophilus* during the mycetophagous and phytophagous stages to construct respective RNA-Seq libraries. In total, 181,144,358 raw reads were obtained from all samples. After filtering out low-quality sequences, 177,125,722 clean reads were retained. The GC content of individual libraries was between 48%-49%. On average, 92% of the clean reads mapped to the *B. xylophilus* reference genome (Supplementary Table 2). The high genome coverage of our RNA-Seq data indicated that the transcriptome data were reliable for the further bioinformatics analyses.

3.2 Identification of PCD-inducing effectors

Differential expression analysis showed that 1,233 genes were differentially expressed between the mycetophagous and phytophagous stages of *B. xylophilus*. Compared with the mycetophagous stage, 765 genes were significantly up-regulated, and 468 genes were significantly down-regulated in the phytophagous stage (Figure 1A). To validate the identified DEGs based on the RNA-seq data, seven genes were selected and validated by RT-qPCR. Similar expression levels were observed for all seven genes in both RNA-seq and RT-qPCR datasets, further confirming the reliability of the RNA-seq transcriptome data (Figure 1B).

Among the 765 up-regulated genes, 394 encoded proteins contained an SP and lacked transmembrane domains, as predicted by SignalP 5.0 and TMHMM-2.0. Of these, 210 genes had no functional annotations and were not identified in the transcriptome analysis of *B. xylophilus* infecting *Pinus thunbergii*. 31 of these 210 genes were further considered to be candidate genes encoding for effectors (Supplementary Table 3) based on the following criteria: Log_2(fold change) > 3 and FPKM > 10 with regards to their differential expression, and a gene open reading frame (ORF) is smaller than 600 bp. From this set, 10 genes were randomly selected and were transiently expressed in *N. benthamiana*. The results showed that the genes BXY_0304900 and BXY_1398900 can induce cell death (ICD) in the presence of the native SP. They were named BxICD1 and BxICD2, respectively (Figure 2).

The nematode tissue localization of *BxICD1* and *BxICD2* in the nematodes was further determined by *in situ* hybridization. Hybridization signals were detected in the esophageal gland cells

10.3389/fpls.2024.1357141

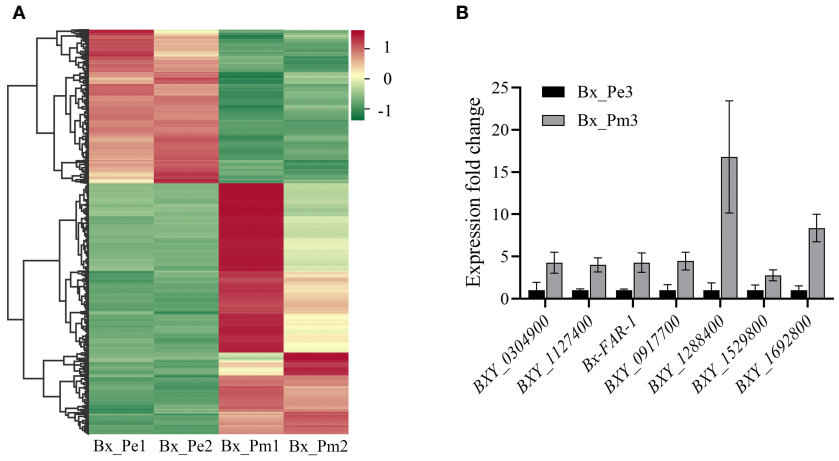

FIGURE 1
Differentially expressed genes at the mycetophagous and phytophagous stages of *Bursaphelenchus xylophilus*. **(A)** Heatmap of differentially expressed genes at the mycetophagous and phytophagous stages. **(B)** Validation of differentially expressed genes (DEGs). Validation of seven DEGs identified in the RNA-seq dataset by quantitative reverse transcription PCR. The relative expression levels were calculated using the $2^{-\Delta\Delta Ct}$ method; data represent shown as the mean ± standard deviation (SD) of three replicated; the experiments were performed twice with similar results. Bx_Pe1, Bx_Pe2, and Bx_Pe3 correspond to the three *B. xylophilus* samples from the mycetophagous stage; Bx_Pm1, Bx_Pm2, and Bx_Pm3 correspond to the three *B. xylophilus* samples from the phytophagous stage.

with the DIG-labeled antisense cDNA probe of *BxICD1* and in the intestinal terminus with the antisense cDNA probe of *BxICD2*. No hybridization signals were detected in *B. xylophilus* tissues with the sense cDNA probe of *BxICD1* and *BxICD2* (Figure 3A, Supplementary Figure 1). The results indicated that *BxICD1* should be a nematode effector because it was expressed in the typical secretory organs of nematodes. Therefore, we selected the effector BxICD1 for further analysis.

3.3 BxICD1 contains a SP with a secretion function

The *BxICD1* gene has a 396-bp ORF, which encodes a 131-amino acid protein. The protein possesses a 19-amino acid SP, as predicted by the SignalP program, and has no putative transmembrane domain according to TMHMM. It also shows similarities to the proteins of *B. xylophilus* by a protein BLAST search, including CAD5219553 (62.3% identity), CAD5219557 (44.6% identity), CAD5219551 (40.2% identity) etc., while no sequences were matched to other organisms. A neighbor-joining (NJ) tree was constructed to examine the phylogenetic relationships among these proteins, with *Bx*ICD1 and CAD5219553 being located in the same branch (Supplementary Figure 2B).

To determine whether the SP of BxICD1 is functional, the predicted SP was cloned into the yeast vector pSUC2. The growth of yeast YTK12 yeast carrying pSUC2, pSUC2:SP^{BxICD1} and pSUC2:SP^{Avr1b} constructs on CMD-W demonstrated the successful transformation with the plasmids. The yeast strain YTK12 carrying pSUC2:SP^{BxICD1}-Invertase or the positive control pSUC2:SP^{Avr1b}-Invertase could reduce TTC to the red-colored TPF. By contrast, no color change was observed in the YTK12 strain used as a negative control, and YTK12 carried the empty pSUC2 vector (Figure 3B). These results suggested that BxICD1 carries a functional secretory SP.

3.4 Apoplastic localization of BxICD1 is required for cell death induction in *N. benthamiana*

Based on the above results, BxICD1 could induce PCD in the presence of the native SP, therefore the subcellular localization of BxICD1 was determined. Three constructs, BxICD1:eGFP, $BxICD1^{\Delta sp}$:eGFP and eGFP were generated and transiently expressed in *N. benthamiana* leaves. Based on the results, the BxICD1:eGFP fusion protein was accumulated in the edges of the tobacco cell, while $BxICD1^{\Delta sp}$:eGFP and eGFP were localized in the cytoplasm (Figure 4A). Plasmolysis was further performed to distinguish the plasma membrane from the apoplast. After the plasmolysis treatment, BxICD1:eGFP fusion proteins were observed in the extracellular space, while $BxICD1^{\Delta sp}$:eGFP and eGFP were still localized in the intracellular space (Figure 4B). Western blot analysis using a GFP antibody revealed bands at approximately 42, 40 and 27 kDa, corresponding to BxICD1:eGFP, $BxICD1^{\Delta sp}$:eGFP, and eGFP, respectively (Figure 4C), indicating that BxICD1:eGFP and $BxICD1^{\Delta sp}$:eGFP fusion proteins were expressed intact. At the same time, BxICD1:eGFP could induce tobacco cell death, while $BxICD1^{\Delta sp}$:eGFP and eGFP could not (Figure 4D). In addition, the electrolyte leakage induced by INF1 or BxICD1:eGFP was significantly greater than that induced by $BxICD1^{\Delta sp}$:eGFP or eGFP (Figure 4E). These results suggested that the presence of BxICD1 in *N. benthamiana* apoplasts triggers cell death.

10.3389/fpls.2024.1357141

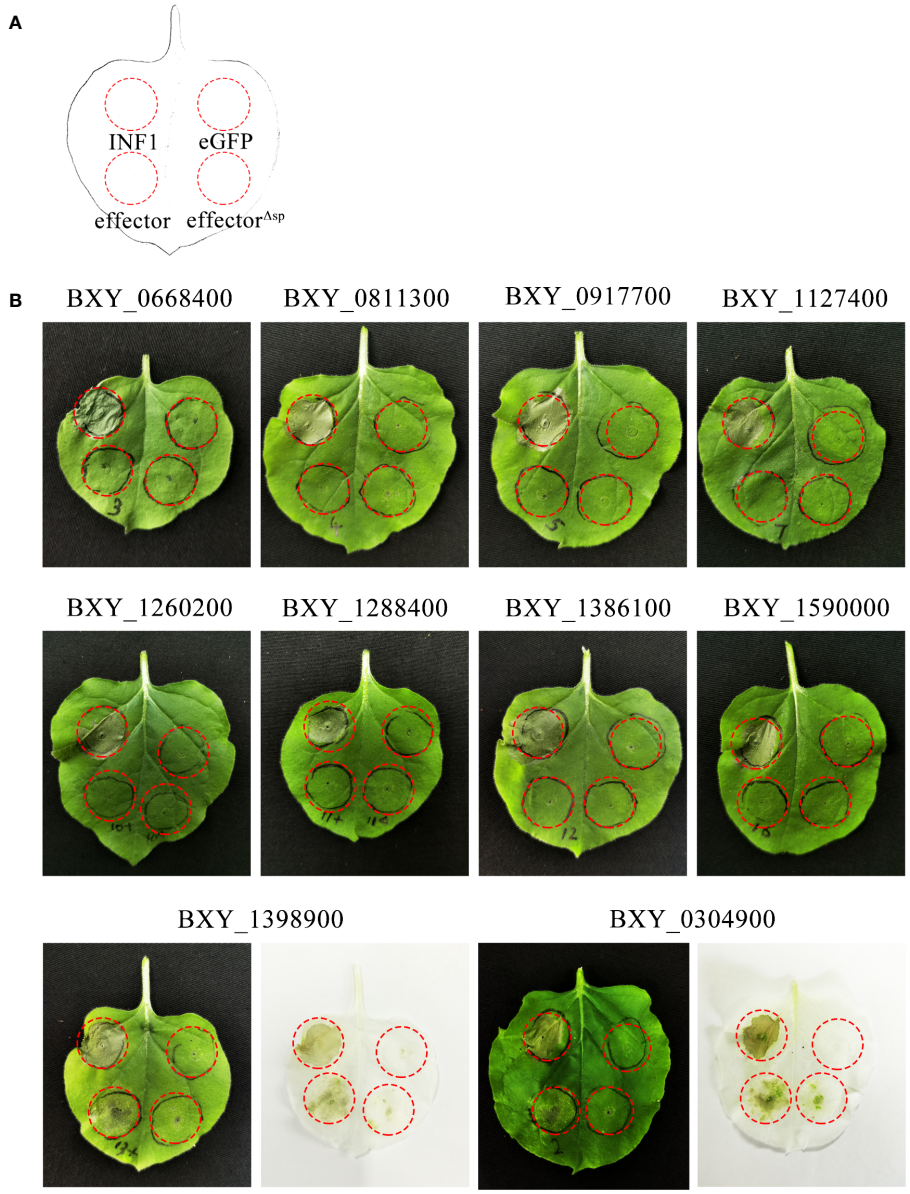

FIGURE 2
Screening of candidate effectors from *Bursaphelenchus xylophilus* capable of inducing plant cell death. **(A)** Schematic diagram of the location of *Agrobacterium tumefaciens*-injected tobacco leaves. INF1 is *Phytophthora infestans* elicitin, a known apoplastic protein that induces cell death in *Nicotiana benthamiana*, used as a positive control. eGFP, an enhanced green fluorescent protein that cannot induce cell death, was used as a negative control. "Effector" represents candidate effectors with the native signal peptide; "effector$^{\Delta sp}$" represents candidate effectors without the native signal peptide. **(B)** Ten candidate effectors were expressed in *N. benthamiana* leaves. The infiltration assay was performed thrice, and five different plants with two inoculated leaves were used in each assay. Similar results were obtained from all experiments.

3.5 BxICD1-triggered PCD depends on NbBAK1

Many studies have demonstrated that BAK1 and SOBIR1 are indispensable for cell death triggered by many apoplastic effectors (Liebrand et al., 2014). To determine whether NbBAK1 and NbSOBIR1 are involved in BxICD1-triggered cell death, they were knocked down using virus-induced gene silencing (VIGS) in *N. benthamiana*. Two weeks after viral inoculation, *N. benthamiana* plants were agroinfiltrated with the pCAMBIA1305.1:BxICD1:Flag, pCAMBIA1305.1:INF1, and pCAMBIA1305.1:eGFP : Flag-expressing constructs, respectively. Based on the results, INF1 failed to induce cell death in *NbBAK1*- or *NbSOBIR1*-silenced plants. Notably, although BxICD1 was unable to induce cell death in *NbBAK1*-silenced plants, it retained the capacity to induce cell death in *NbSOBIR1*-silenced plants (Figure 5A). Neither eGFP nor the EV, used as negative controls, triggered cell death in pTRV2:*NbBAK1*-, pTRV2:*NbSOBIR1*- and pTRV2:*eGFP*- infiltrated plants (Figure 5A). Western blot analysis was used to confirm BxICD1 protein expression in *NbBAK1*-, *NbSOBIR1*- and *eGFP*-silenced

10.3389/fpls.2024.1357141

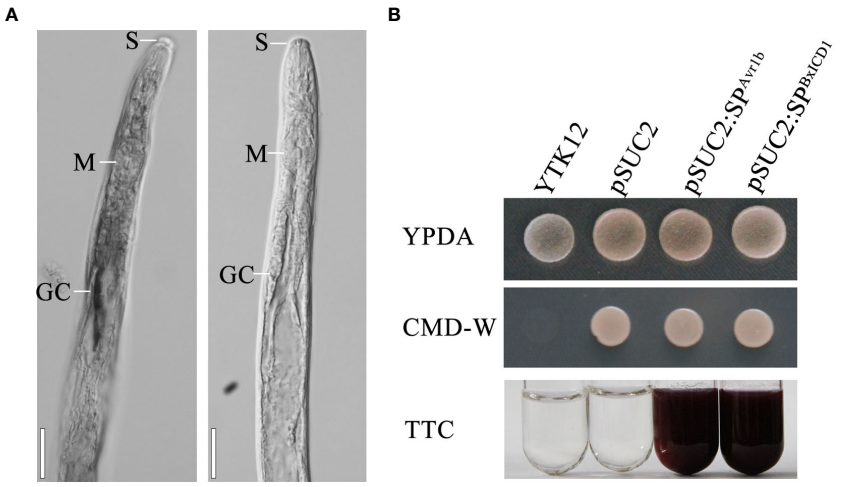

FIGURE 3
Localization of *BxICD1* mRNA and secretion function analysis of BxICD1 signal peptide. **(A)** Localization of *BxICD1* mRNA in esophageal gland cells of *Bursaphelenchus xylophilus* by *in-situ* hybridization. Fixed nematodes were hybridized with digoxigenin-labeled antisense (left) and sense (right) cDNA probes from *BxICD1*. S, stylet; M, median bulb; GC, esophageal gland. Scale bars = 50 μm **(B)** Secretion function analysis of the BxICD1 signal peptide. The predicted signal peptide of BxICD1 was cloned into the yeast vector pSUC2 to generate pSUC2:SP^{BxICD1}-invertase constructs, and pSUC2: SP^{Avr1b}-Invertase was used as a positive control. YTK12 can grow on YPDA plates. CMD-W media was used to ensure the expression of pSUC2-derived plasmids. Invertase can reduce 2,3,5-Triphenyltetrazolium Chloride (TTC) to insoluble red-colored 1,3,5-Triphenylformazan (TPF).

plants (Figure 5B), and RT-qPCR confirmed the successful silencing of *NbBAK1* and *NbSOBIR1* in plants (Figures 5C, D). Taken together, these results indicated that BxICD1-triggered cell death is dependent on NbBAK1.

3.6 *BxICD1* affects *B. xylophilus* virulence and migration in *P. massoniana*

To assess the role of *BxICD1* in nematode parasitism, an RNAi assay was performed by soaking *B. xylophilus* in *BxICD1* dsRNA. The transcript levels of *BxICD1* were significantly decreased after incubation with the *BxICD1* dsRNA, compared to the treatments with eGFP dsRNA and non-dsRNA solution (Figure 6A), demonstrating that RNAi was successful.

Subsequently, inoculation experiments were performed using *B. xylophilus* that underwent different pre-treatment. Compared with the *eGFP* dsRNA-treated and H_2O-treated nematodes at 12 dpi, *BxICD1* dsRNA-treated nematodes caused to a significantly lower morbidity and disease severity index (DSI) in *P. massoniana*. The morbidity was calculated at 36.7%, 34.4%, and 13.7% after inoculation with *eGFP* dsRNA-, H_2O- and *BxICD1* dsRNA-treated nematodes, respectively (Figure 6B), while corresponding DSI was 11.7, 9.5, and 3.4 (Figure 6C). At 20 dpi, the DSI of *P. massoniana* inoculated with *BxICD1* dsRNA-treated nematodes was still significantly lower compared with *P. massoniana* inoculated with *eGFP* dsRNA and non-dsRNA solution-treated nematodes. However, no significant differences in morbidity were observed (Figures 6C, D). Moreover, at 12 h post-inoculation, *B. xylophilus* was isolated from pine stem segments at different distances from the inoculation site. No significant differences were observed in the number of *BxICD1* dsRNA, *eGFP* dsRNA, and the non-dsRNA solution-treated nematodes at pine stem segments 1-2 and 2-3 cm below the inoculation site. However, the number of *BxICD1* dsRNA-treated nematodes was significantly lower compared with *eGFP* dsRNA and non-dsRNA solution-treated nematodes isolated from pine stem segments 3-4 cm below the inoculation site. No nematodes were isolated from pine stem segments 4-5 cm below the inoculation point in all treatments (Figures 6E, F).

In addition, *BxICD1* dsRNA, *eGFP* dsRNA, and the non-dsRNA solution-treated nematodes were cultured on a PDA medium covered with *Pestalotiopsis* sp. After eight days, no significant differences were observed in the amount of nematodes and fungi mycelium in different treatments (Supplementary Figure 3). The above results showed that *BxICD1* affected *B. xylophilus* parasitism and migration in *P. massoniana*, but did not affect the feeding rate and reproduction of *B. xylophilus* in fungi.

4 Discussion

Effectors are the key factors affecting PPNs virulence and parasitism against hosts (Goverse and Smant, 2014). In recent years, a growing number of PPN candidate effectors have been identified by transcriptome sequencing. More than 100 candidate effectors from *B. xylophilus* infecting *P. thunbergii* have been obtained, while a few have been functionally characterized (Tsai et al., 2016; Hu et al., 2019). Interestingly, it was reported that different proteins were detected in the secretomes of *B. xylophilus* during the infection of different pine hosts (Silva et al., 2021). Accordingly, we screened effectors from *B. xylophilus* infecting *P. massoniana* for the first time. As result, 394 candidate effectors were identified through transcriptome data and

10.3389/fpls.2024.1357141

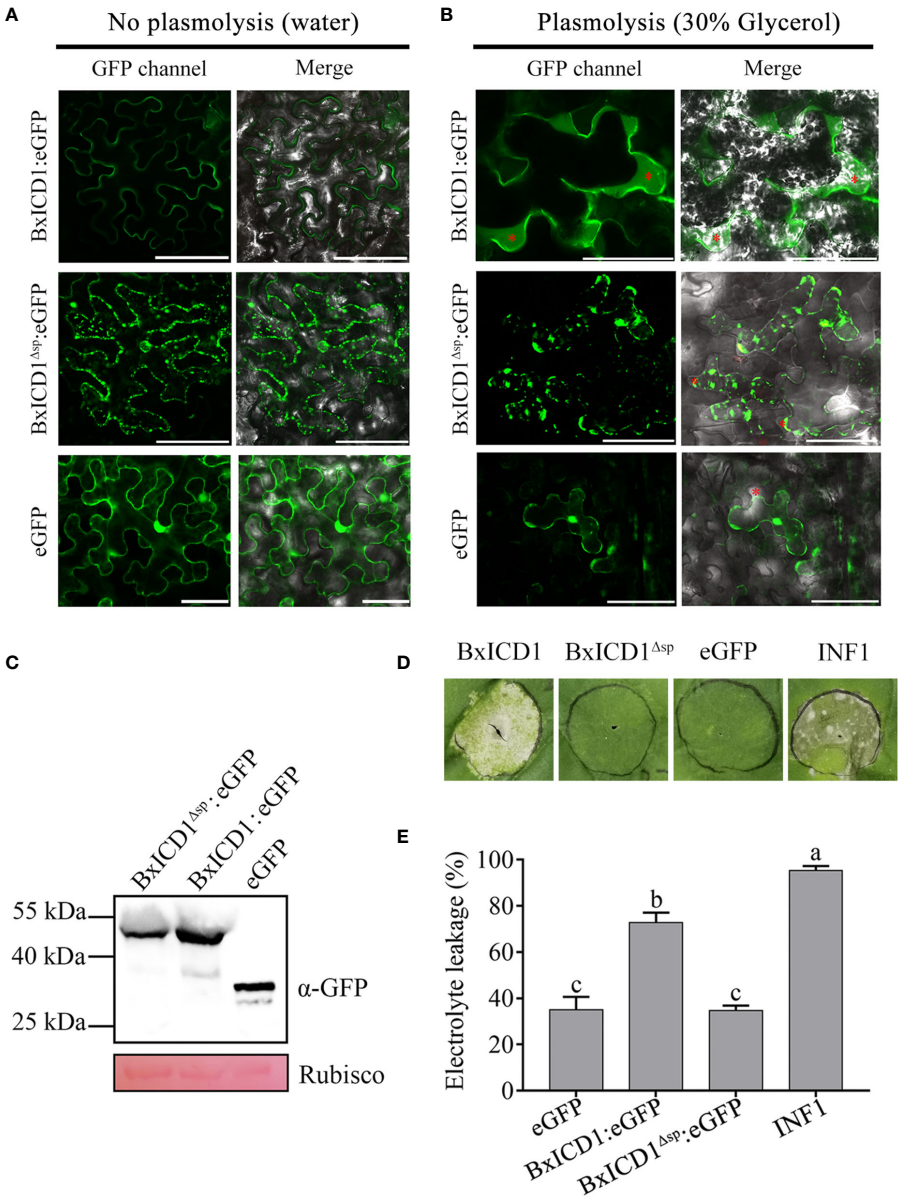

FIGURE 4
Apoplastic localization of BxICD1 is required for the induction of cell death in *Nicotiana benthamiana*. **(A)** *Agrobacterium* strain GV3101 carrying the fusion constructs BxICD1:eGFP, BxICD1$^{\Delta sp}$:eGFP and the eGFP control were infiltrated in *Nicotiana benthamiana* leaves for transient expression analysis. **(B)** *N. benthamiana* leaves expressing BxICD1:eGFP, BxICD1:eGFP$^{\Delta sp}$ and eGFP were treated with 30% glycerol for plasmolysis. GFP signals were observed at 3 days after infiltration. The red asterisks indicate the apoplast region. Scale bars=50 μm. **(C)** BxICD1-triggered cell death in *N. benthamiana*. *Agrobacterium* strain GV3101 carrying the constructs BxICD1:eGFP, BxICD1$^{\Delta sp}$:eGFP, eGFP, and INF1 were infiltrated in *N. benthamiana* leaves for transient expression analysis. The leaf phenotypes were observed after 3 days. **(D)** Quantification of cell death by measuring electrolyte leakage in *N. benthamiana* leaves at 3 days post-infiltration with constructs encoding the indicated proteins. Data represent the mean of three repeats ± SD. Three independent experiments were performed with similar results, with three technical replicates for each reaction. **(E)** Western blot analysis was performed to confirmed the expression of proteins in *N. benthamiana*. Ponceau S staining of RuBisCO was used as indicate the protein loading control.

bioinformatics analysis. Among them, 210 were different from the candidate effectors of *B. xylophilus* infesting *P. thunbergii* and were not annotated in the HMMER homology database, which might be pioneers effectors against *P. massoniana*. One of them, named BxICD1, was found to be significantly upregulated in the early parasitic stages of *B. xylophilus* and specifically present in the esophageal gland cell, a classical effector secretion organ of nematodes (Mitchum et al., 2013). Furthermore, the signal peptide of BxICD1 was confirmed to be functional based on yeast system assays. These data suggest that BxICD1 is a novel effector of *B. xylophilus*.

In this study, we found that BxICD1 could induce PCD in the extracellular space of *N. benthamiana*, which was dependent on NbBAK1. As is known, PCD has different effects on different

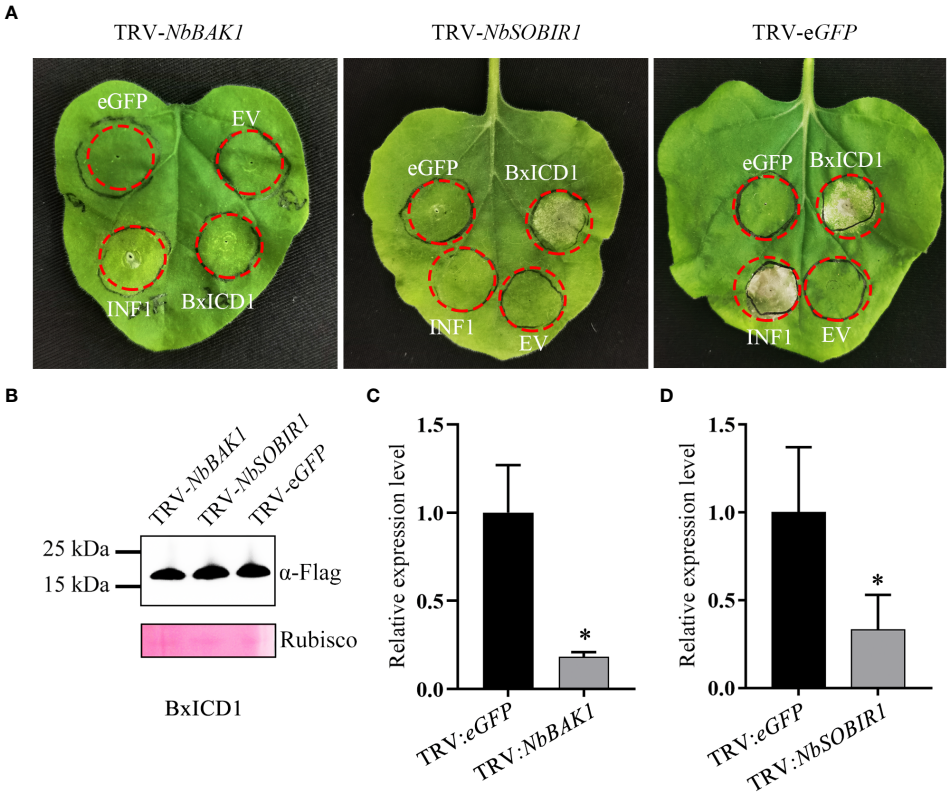

FIGURE 5
BxICD1-triggered cell death depends on NbBAK1. **(A)** NbBAK1, but not NbSOBIR1, is required for BxICD1-triggered cell death in *Nicotiana benthamiana*. *N. benthamiana* plants were subjected to VIGS by inoculation with TRV constructs (TRV:*eGFP*, TRV : *NbBAK1, or* TRV : *NbSOBIR1*). Three weeks after inoculation, BxICD1, INF1, the empty vector (EV), and eGFP were transiently expressed in the gene-silenced leaves and photographed after 3 d. The infiltration experiment was performed thrice, with three different plants with three inoculated leaves were used in each assay. All experiments were performed with similar results. **(B)** Western blot analysis confirmed the expression of BxICD1 protein in gene-silenced plants. Ponceau S staining of RuBisCO was used as indicate the protein loading control. **(C, D)** The relative expression levels of *NbBAK1* and *NbSOBIR1* in gene-silenced plant were determined by RT-qPCR. Data represent the mean of three replicates ± SD. Three independent experiments were performed with similar results. Asterisks indicate significant differences ($P<0.05$).

nutritional pathogens with different lifestyles and feeding strategies. Necrotrophic pathogens need to kill cells and tissues of host plants, and then absorb nutrients. Therefore, PCD facilitates the parasitism of necrotrophic pathogens (Laluk and Mengiste, 2010). However, biotrophic pathogens must acquire nutrients directly from living plant cells and tissues without immediately killing host cells or tissues. Thus, PCD is often detrimental to biotrophic pathogens (Gebrie, 2016). Additionally, hemibiotrophs are biotrophic in the early stage and necrotrophic in the late stage of parasitism. Therefore, PCD inhibits the infection by hemibiotrophs in the early parasitism stage, while it promotes hemibiotroph colonization and facilitates pathogen transition from a biotrophic to a necrotrophic state in the late parasitism stage (Jia et al., 2000; Orbach et al., 2000; Qutob et al., 2002). PPNs are biotrophic pathogens, and it is generally considered that PCD negatively affects nematode parasitism. For example, the potato protein Gpa2 recognizes the *Globodera pallida* effector Gp-Rbp-1 and triggers PCD, which inhibits nematode parasitism (Sacco et al., 2009). A hypersensitive response-like reaction was observed in the *Meloidogyne graminicola*-resistant rice plants but not in the *M. graminicola*-susceptible rice plants under nematode infection (Cabasan et al., 2014). To survive, PPNs secrete effectors to suppress PCD. In recent years, many PPN effectors with PCD-inhibiting properties have been identified, especially from sedentary endoparasitic phytonematodes, e.g., root-knot nematodes and cyst nematodes (Postma et al., 2012; Chen et al., 2017; Song et al., 2021; Chen et al., 2022). In the migratory endoparasitic phytonematode *B. xylophilus*, six effectors were also found to inhibit PCD (Hu et al., 2021; Wen et al., 2021, Wen et al., 2022; Zhang et al., 2022; Hu et al., 2022a; Qiu et al., 2023). Interestingly, five effectors from *B. xylophilus* were confirmed to have the ability to activate PCD. One of them not only induced PCD but also inhibited nematode parasitism. However, BxSapB1, BxSapB2, and BxSapB3, induced PCD but at the same time also enhanced nematode virulence (Huang et al., 2019; Hu et al., 2019, Hu et al., 2020; Zhao et al., 2020; Shinya et al., 2021). In the present study, we found that BxICD1 also promots parasitism of *B. xylophilus* based on RNAi gene silencing assays. This seemingly paradoxical phenomenon was also observed in effectors from oomycetes and fungi, such as PsXEG1 (Ma et al., 2015) from *Phytophthora sojae*, Avh238 (Yang et al., 2017) from *P. essential*, PlAvh142 (Situ et al., 2020) from *Peronophythora litchi* and Fg12 (Yang et al., 2020) from *F.*

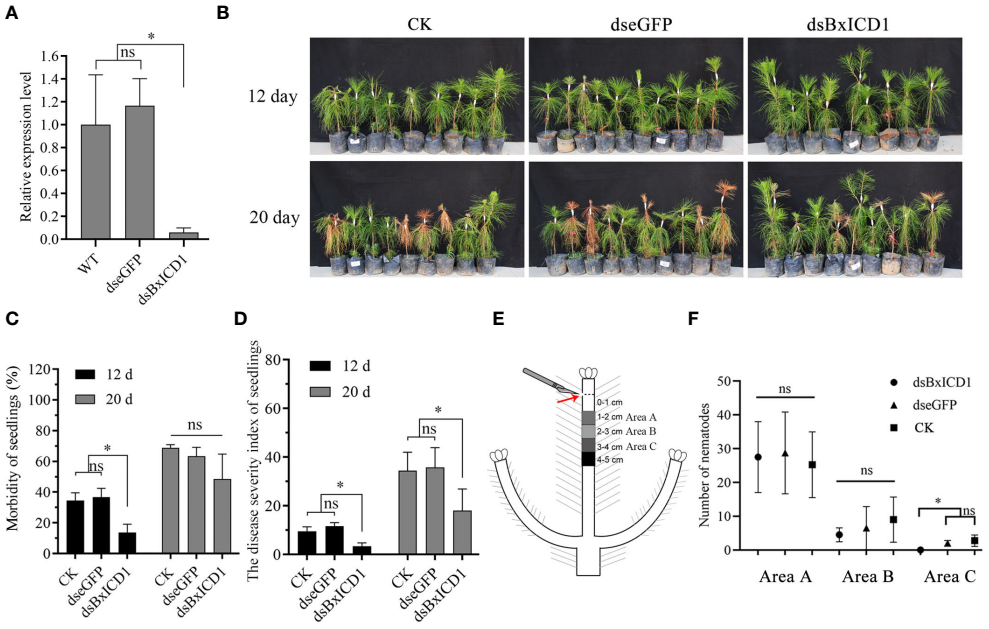

FIGURE 6
BxICD1 contributes to the virulence and migration of *Bursaphelenchus xylophilus*. **(A)** *BxICD1* silencing efficiency after treatment with *BxICD1* dsRNA in *B. xylophilus*. Asterisks indicate significant differences ($P<0.05$). ns indicates no significant differences ($P\geq0.05$). **(B)** Representative photographs of *Pinus massoniana* seedlings at 12 days and 20 days post-inoculation. dseGFP, dsBxICD1 and CK correspond to nematodes inoculated in *eGFP*-, *BxICD1*- and non-dsRNA solution, respectively. **(C)** The morbidity of *Pinus massoniana* seedlings inoculated with dseGFP-, dsBxICD1-, and non-dsRNA solution -treated nematodes. **(D)** The disease severity index of *P. massoniana* seedlings inoculated with dseGFP-, dsBxICD1-, and non-dsRNA solution-treated nematodes. **(E)** Schematic depiction of nematode inoculation and sampling. **(F)** The number of nematodes in Area A, Area B, and Area C wood sections under three different treatments. "ns" indicates no sigificant difference ($p\geq0.05$).

graminearum. Two hypotheses have been proposed to explain this phenomenon. First, the accumulation of effectors is insufficient to induce PCD under natural conditions. Second, other interacting effectors or proteins could suppress PCD activated by effectors during the successful parasitism of pathogens (Ma et al., 2015; Yang et al., 2017; Situ et al., 2020).

This study demonstrated that BxICD1 contributed to nematode migration in *P. massoniana*, but was not involved and did not affect nematode feeding and reproduction in fungi based on the RNAi assays results. It has been reported that pine trees develop resistance by inducing pine resin secretion and lignification in the resin canals. Lignin biosynthesis in cell walls can effectively inhibits the migration of *B. xylophilus* (Kusumoto et al., 2014). In pine trees, highly virulent *B. xylophilus* strains can rapidly destroy the resin-secreting parenchyma cells of cortical and xylem resin canals before cell wall lignification (Jin and Ye, 2007), while weakly virulent strains do not have such capacity. Taken together, the effector BxICD1 has the capacity to induce PCD, resulting in the destruction of parenchyma cells in resin canals, which is beneficial for *B. xylophilus* virulence and migration.

Data availability statement

The datasets presented in this study can be found in online repositories. The names of the repository/repositories and accession number(s) can be found below: BioProject, PRJNA1027064.

Ethics statement

The manuscript presents research on animals that do not require ethical approval for their study.

Author contributions

ZL: Writing – original draft, Writing – review & editing, Data curation, Formal analysis, Investigation, Methodology, Software. HW: Writing – original draft, Methodology, Writing – review & editing, Formal analysis, Investigation. YC: Writing – original draft, Formal analysis, Investigation. XS: Writing – original draft, Formal analysis, Investigation. XH: Writing – original draft, Formal analysis, Investigation. QH: Investigation, Writing – original draft, Formal analysis. KZ: Methodology, Writing – review & editing, Writing – original draft. JL: Writing – original draft, Writing – review & editing, Methodology. BL: Writing – review & editing, Formal analysis, Investigation, Methodology.

Funding

The author(s) declare financial support was received for the research, authorship, and/or publication of this article. This work was supported by the 2023 Special Fund for Affairs of Natural Resources—Project of Ecological Construction of Forestry,

(Guangdong Forestry Finance [2022] No.8) and Dynamic Monitoring of Forest Nematode Diversity in Guangdong Province (Guangdong Resources and Environment Financial [2020] No.28).

Acknowledgments

We acknowledge Guanghui Kong (South China Agricultural University, China) for providing the plasmid pSUC2 and yeast strain YTK12, and Lili Hu (Guangdong Academy of Forestry) for providing *Pinus massoniana* seedlings.

Conflict of interest

The authors declare that the research was conducted in the absence of any commercial or financial relationships that could be construed as a potential conflict of interest.

Publisher's note

All claims expressed in this article are solely those of the authors and do not necessarily represent those of their affiliated organizations, or those of the publisher, the editors and the reviewers. Any product that may be evaluated in this article, or claim that may be made by its manufacturer, is not guaranteed or endorsed by the publisher.

Supplementary material

The Supplementary Material for this article can be found online at: https://www.frontiersin.org/articles/10.3389/fpls.2024.1357141/full#supplementary-material

SUPPLEMENTARY FIGURE 1
Localization of *BxICD2* mRNA in the intestine terminus of *Bursaphelenchus xylophilus* by *in-situ* hybridization. DIG, digoxygenin; Scale bars = 50 μm.

SUPPLEMENTARY FIGURE 2
Multiple sequence alignment and phylogenetic analyses of BxICD1 (BXY_0304900). **(A)** Multiple sequence alignment of the BxICD1 protein with other homologous sequences from *Bursaphelenchus xylophilus*. **(B)** The phylogenetic tree of BxICD1 protein homologs.

SUPPLEMENTARY FIGURE 3
BxICD1 does not affect reproduction or fungal feeding rate in *Bursaphelenchus xylophilus* **(A)** The propagation rate of *B. xylophilus* after culture on *Pestalotiopsis* spp. for 8 days. Data represent the means, and the error bars represent ± standard deviation of six biological replicates. **(B)** The fungal feeding rate of *B. xylophilus* grown on *Pestalotiopsis* spp. Two independent experiments were performed with similar results. dseGFP, dsBxICD1 and CK indicate nematodes inoculated in *eGFP-*, *BxICD1-* and non-dsRNA solution, respectively.

References

Benjamini, Y., and Hochberg, Y. (1995). Controlling the false discovery rate: a practical and powerful approach to multiple testing. *J. R. Stat. Soc Series. B Stat. Methodol.* 57, 289–300. doi: 10.1111/j.2517-6161.1995.tb02031.x

Cabasan, M. T. N., Kumar, A., Bellafiore, S., and De Waele, D. (2014). Histopathology of the rice root-knot nematode, *Meloidogyne graminicola*, on *Oryza sativa* and *O. glaberrima*. *Nematology* 16, 73–81. doi: 10.1163/15685411-00002746

Chen, J., Chen, S., Xu, C., Yang, H., Achom, M., and Wang, X. (2022). A key virulence effector from cyst nematodes targets host autophagy to promote nematode parasitism. *New Phytol.* 237, 1374–1390. doi: 10.1111/nph.18609

Chen, J., Li, Z., Lin, B., Liao, J., and Zhuo, K. (2021). A *Meloidogyne graminicola* pectate lyase is involved in virulence and activation of host defense responses. *Front. Plant Sci.* 12. doi: 10.3389/fpls.2021.651627

Chen, J., Lin, B., Huang, Q., Hu, L., Zhuo, K., and Liao, J. (2017). A novel *Meloidogyne graminicola* effector, MgGPP, is secreted into host cells and undergoes glycosylation in concert with proteolysis to suppress plant defenses and promote parasitism. *PLoS Pathog.* 13, e1006301. doi: 10.1371/journal.ppat.1006301

Cui, H., Jin, H., Liu, Q., Yan, Z., Ding, L., and Qin, B. (2014). Nematicidal metabolites from roots of *Stellera chamaejasme* against *Bursaphelenchus xylophilus* and *Bursaphelenchus mucronatus*. *Pest Manage. Sci.* 70, 827–835. doi: 10.1002/ps.3625

De Boer, J. M., Yan, Y., Smant, G., Davis, E. L., and Baum, T. J. (1998). *In-situ* hybridization to messenger RNA in *Heterodera glycines*. *J. Nematol.* 30, 309–312.

Dou, D., Kale, S. D., Wang, X., Jiang, R. H., Bruce, N. A., Arredondo, F. D., et al. (2008). RXLR-mediated entry of *Phytophthora sojae* effector Avr1b into soybean cells does not require pathogen-encoded machinery. *Plant Cell* 20, 1930–1947. doi: 10.1105/tpc.107.056093

Edwards, O. R., and Linit, M. J. (1992). Transmission of *Bursaphelenchus xylophilus* through oviposition wounds of *Monochamm carolinensis* (Coleoptera: Cerambycidae). *J. Nematol.* 24, 133–139.

Futai, K. (2013). Pine wood nematode, Bursaphelenchus xylophilus. *Annu. Rev. Phytopathol.* 51, 61–83. doi: 10.1146/annurev-phyto-081211-172910

Gebrie, S. A. (2016). Biotrophic fungi infection and plant defense mechanism. *J. Plant Pathol. Microbiol.* 7, 2. doi: 10.4172/2157-7471.1000378

Gietz, R. D., and Schiestl, R. H. (2007). High-efficiency yeast transformation using the LiAc/SS carrier DNA/PEG method. *Nat. Protoc.* 2, 38–41. doi: 10.1038/nprot.2007.15

Goldman, A., Harper, S., and Speicher, D. W. (2016). Detection of proteins on blot membranes. *Curr. Protoc. Protein Sci.* 86, 10.8.1–10.8.11. doi: 10.1002/cpps.15

Goverse, A., and Smant, G. (2014). The activation and suppression of plant innate immunity by parasitic nematodes. *Annu. Rev. Phytopathol.* 52, 243–265. doi: 10.1146/annurev-phyto-102313-050118

Haegeman, A., Mantelin, S., Jones, J. T., and Gheysen, G. (2012). Functional roles of effectors of plant-parasitic nematodes. *Gene* 492, 19–31. doi: 10.1016/j.gene.2011.10.040

Heese, A., Hann, D. R., Gimenez-Ibanez, S., Jones, A. M., He, K., Li, J., et al. (2007). The receptor-like kinase SERK3/BAK1 is a central regulator of innate immunity in plants. *Proc. Natl. Acad. Sci. U.S.A.* 104, 12217–12222. doi: 10.1073/pnas.0705306104

Hu, L. J., Wu, X. Q., Ding, X. L., and Ye, J. R. (2021). Comparative transcriptomic analysis of candidate effectors to explore the infection and survival strategy of *Bursaphelenchus xylophilus* during different interaction stages with pine trees. *BMC Plant Biol.* 21, 224. doi: 10.1186/s12870-021-02993-9

Hu, L. J., Wu, X. Q., Li, H. Y., Wang, Y. C., Huang, X., Wang, Y., et al. (2020). BxCDP1 from the pine wood nematode *Bursaphelenchus xylophilus* is recognized as a novel molecular pattern. *Mol. Plant Pathol.* 21, 923–935. doi: 10.1111/mpp.12939

Hu, L. J., Wu, X. Q., Li, H. Y., Zhao, Q., Wang, Y. C., and Ye, J. R. (2019). An Effector, BxSapB1, induces cell death and contributes to virulence in the pine wood nematode *Bursaphelenchus xylophilus*. *Mol. Plant Microbe Interact.* 32, 452–463. doi: 10.1094/MPMI-10-18-0275-R

Hu, L. J., Wu, X. Q., Wen, T. Y., Qiu, Y. J., Rui, L., Zhang, Y., et al. (2022a). A *Bursaphelenchus xylophilus* effector, BxSCD3, suppresses plant defense and contributes to virulence. *Int. J. Mol. Sci.* 23, 6417. doi: 10.3390/ijms23126417

Hu, L. J., Wu, X. Q., Wen, T. Y., Ye, J. R., Qiu, Y. J., Rui, L., et al. (2022b). The key molecular pattern BxCDP1 of *Bursaphelenchus xylophilus* induces plant immunity and enhances plant defense response via two small peptide regions. *Front. Plant Sci.* 13. doi: 10.3389/fpls.2022.937473

Huang, X., Hu, L. J., and Wu, X. Q. (2019). Identification of a novel effector BxSapB3 that enhances the virulence of pine wood nematode *Bursaphelenchus xylophilus*. *Acta Biochim. Biophys. Sin.* 51, 1071–1078. doi: 10.1093/abbs/gmz100

Jia, Y., McAdams, S. A., Bryan, G. T., Hershey, H. P., and Valent, B. (2000). Direct interaction of resistance gene and avirulence gene products confers rice blast resistance. *EMBO J.* 19, 4004–4014. doi: 10.1093/emboj/19.15.4004

Jin, G., and Ye, J. R. (2007). Histopathological study on the nematode in seedling of *Pinus thunbergii*. *J. Nanjing Forestry Uni.* 50, 115–120. doi: 10.3969/j.jssn.1000-2006.2007.04.026

Kikuchi, T., Cotton, J. A., Dalzell, J. J., Hasegawa, K., Kanzaki, N., McVeigh, P., et al. (2011). Genomic insights into the origin of parasitism in the emerging plant pathogen *Bursaphelenchus xylophilus*. *PLoS Pathog.* 7, e1002219. doi: 10.1371/journal.ppat.1002219

Kikuchi, T., Shibuya, H., Aikawa, T., and Jones, J. T. (2006). Cloning and characterization of pectate lyases expressed in the esophageal gland of the pine wood nematode *Bursaphelenchus xylophilus*. *Mol. Plant Microbe Interact.* 19, 280–287. doi: 10.1094/MPMI-19-0280

Kim, D., Paggi, J. M., Park, C., Bennett, C., and Salzberg, S. L. (2019). Graph-based genome alignment and genotyping with HISAT2 and HISAT-genotype. *Nat. Biotechnol.* 37, 907–915. doi: 10.1038/s41587-019-0201-4

Kudla, U., MILAC, A. L., Qin, L., Overmars, H., Roze, E., Holterman, M., et al. (2007). Structural and functional characterization of a novel, host penetration-related pectate lyase from the potato cyst nematode *Globodera rostochiensis*. *Mol. Plant Pathol.* 8, 293–305. doi: 10.1111/j.1364-3703.2007.00394.x

Kumar, S., Stecher, G., Li, M., Knyaz, C., and Tamura, K. (2018). MEGA X: molecular evolutionary genetics analysis across computing platforms. *Mol. Biol. Evol.* 35, 1547. doi: 10.1093/molbev/msy096

Kusumoto, D., Yonemichi, T., Inoue, H., Hirao, T., Watanabe, A., and Yamada, T. (2014). Comparison of histological responses and tissue damage expansion between resistant and susceptible *Pinus thunbergii* infected with pine wood nematode *Bursaphelenchus xylophilus*. *J. For. Res.* 19, 285–294. doi: 10.1007/s10310-013-0417-y

Laluk, K., and Mengiste, T. (2010). Necrotroph attacks on plants: wanton destruction or covert extortion? *arabidopsis Book* 8, e0136. doi: 10.1199/tab.0136

Lee, S., Kim, J., Kim, M. S., Min, C. W., Kim, S. T., Choi, S. B., et al. (2023). The *Phytophthora* nucleolar effector Pi23226 targets host ribosome biogenesis to induce necrotrophic cell death. *Plant Commun.* 4, 100606. doi: 10.1016/j.xplc.2023.100606

Liao, Y., Smyth, G. K., and Shi, W. (2014). featureCounts: an efficient general purpose program for assigning sequence reads to genomic features. *Bioinformatics* 30, 923–930. doi: 10.1093/bioinformatics/btt656

Liebrand, T. W., van den Burg, H. A., and Joosten, M. H. (2014). Two for all: receptor-associated kinases SOBIR1 and BAK1. *Trends Plant Sci.* 19, 123–132. doi: 10.1016/j.tplants.2013.10.003

Lin, B. R., Zhuo, K., Chen, J. S., Hu, L. L., Sun, L. H., Wang, X. H., et al. (2016). A novel nematode effector suppresses plant immunity by activating host reactive oxygen species-scavenging system. *New Phytol.* 209, 1159–1173. doi: 10.1111/nph.13701

Liu, B., Xie, Y., Yin, H., Zhou, Z., and Liu, Q. (2022a). Identification and defensive characterization of PmCYP720B11v2 from *Pinus massoniana*. *Int. J. Mol. Sci.* 23, 6640. doi: 10.3390/ijms23126640

Liu, X., Zhou, X., Zhou, L., Hu, J., and Guo, K. (2022b). Application of RNA interference in the pinewood nematode, *bursaphelenchus xylophilus*. *J. Vis. Exp.* 181, e63645. doi: 10.3791/63645

Livak, K. J., and Schmittgen, T. D. (2001). Analysis of relative gene expression data using real-time quantitative PCR and the $2^{-\Delta\Delta CT}$ method. *Methods* 25, 402–408. doi: 10.1006/meth.2001.1262

Ma, Z., Song, T., Zhu, L., Ye, W., Wang, Y., Shao, Y., et al. (2015). A *Phytophthora sojae* glycoside hydrolase 12 protein is a major virulence factor during soybean infection and is recognized as a PAMP. *Plant Cell* 27, 2057–2072. doi: 10.1105/tpc.15.00390

Mitchum, M. G., Hussey, R. S., Baum, T. J., Wang, X., Elling, A. A., Wubben, M., et al. (2013). Nematode effector proteins: an emerging paradigm of parasitism. *New Phytol.* 199, 879–894. doi: 10.1111/nph.12323

Modi, A., Vai, S., Caramelli, D., and Lari, M. (2021). The illumina sequencing protocol and the novaSeq 6000 system. *Methods Mol. Biol.* 2242, 15–42. doi: 10.1007/978-1-0716-1099-2_2

Orbach, M. J., Farrall, L., Sweigard, J. A., Chumley, F. G., and Valent, B. (2000). A telomeric avirulence gene determines efficacy for the rice blast resistance gene *Pi-ta*. *Plant Cell* 12, 2019–2032. doi: 10.1105/tpc.12.11.2019

Petitot, A. S., Dereeper, A., Agbessi, M., Silva, C., Guy, J., Ardisson, M., et al. (2016). Dual RNA-seq reveals *Meloidogyne graminicola* transcriptome and candidate effectors during the interaction with rice plants. *Mol. Plant Pathol.* 17, 860–874. doi: 10.1111/mpp.12334

Popeijus, H., Overmars, H., Jones, J., Blok, V., Goverse, A., Helder, J., et al. (2000). Degradation of plant cell walls by a nematode. *Nature* 406, 36–37. doi: 10.1038/35017641

Postma, W. J., Slootweg, E. J., Rehman, S., Finkers-Tomczak, A., Tytgat, T. O., van Gelderen, K., et al. (2012). The effector SPRYSEC-19 of *Globodera rostochiensis* suppresses CC-NB-LRR-mediated disease resistance in plants. *Plant Physiol.* 160, 944–954. doi: 10.1104/pp.112.200188

Qiu, Y. J., Wu, X. Q., Wen, T. Y., Hu, L. J., Rui, L., Zhang, Y., et al. (2023). The *Bursaphelenchus xylophilus* candidate effector BxLip-3 targets the class I chitinases to suppress immunity in pine. *Mol. Plant Pathol.* 24, 1033–1046. doi: 10.1111/mpp.13334

Qutob, D., Kamoun, S., and Gijzen, M. (2002). Expression of a *Phytophthora sojae* necrosis-inducing protein occurs during transition from biotrophy to necrotrophy. *Plant J.* 32, 361–373. doi: 10.1046/j.1365-313X.2002.01439.x

Sacco, M. A., Koropacka, K., Grenier, E., Jaubert, M. J., Blanchard, A., Goverse, A., et al. (2009). The cyst nematode SPRYSEC protein RBP-1 elicits Gpa2-and RanGAP2-dependent plant cell death. *PLoS Pathog.* 5, e1000564. doi: 10.1371/journal.ppat.1000564

Shinya, R., Kirino, H., Morisaka, H., Takeuchi-Kaneko, Y., Futai, K., and Ueda, M. (2021). Comparative secretome and functional analyses reveal glycoside hydrolase family 30 and cysteine peptidase as virulence determinants in the pinewood nematode *Bursaphelenchus xylophilus*. *Front. Plant Sci.* 12. doi: 10.3389/fpls.2021.640459

Silva, H., Anjo, S. I., Manadas, B., Abrantes, I., Fonseca, L., and Cardoso, J. M. (2021). Comparative analysis of *Bursaphelenchus xylophilus* secretome under *Pinus pinaster* and *P. pinea* stimuli. *Front. Plant Sci.* 12. doi: 10.3389/fpls.2021.668064

Situ, J., Jiang, L., Fan, X., Yang, W., Li, W., Xi, P., et al. (2020). An RXLR effector PlAvh142 from *Peronophythora litchii* triggers plant cell death and contributes to virulence. *Mol. Plant Pathol.* 21, 415–428. doi: 10.1111/mpp.12905

Song, H., Lin, B., Huang, Q., Sun, L., Chen, J., Hu, L., et al. (2021). The *Meloidogyne graminicola* effector MgMO289 targets a novel copper metallochaperone to suppress immunity in rice. *J. Exp. Bot.* 72, 5638–5655. doi: 10.1093/jxb/erab208

Trapnell, C., Williams, B. A., Pertea, G., Mortazavi, A., Kwan, G., Van Baren, M. J., et al. (2010). Transcript assembly and quantification by RNA-Seq reveals unannotated transcripts and isoform switching during cell differentiation. *Nat. Biotechnol.* 28, 511–515. doi: 10.1038/nbt.1621

Tsai, I. J., Tanaka, R., Kanzaki, N., Akiba, M., Yokoi, T., Espada, M., et al. (2016). Transcriptional and morphological changes in the transition from mycetophagous to phytophagous phase in the plant-parasitic nematode *Bursaphelenchus xylophilus*. *Mol. Plant Pathol.* 17, 77–83. doi: 10.1111/mpp.12261

Vanholme, B., Van Thuyne, W., Vanhouteghem, K., De Meutter, J. A. N., Cannoot, B., and Gheysen, G. (2007). Molecular characterization and functional importance of pectate lyase secreted by the cyst nematode *Heterodera schachtii*. *Mol. Plant Pathol.* 8, 267–278. doi: 10.1111/j.1364-3703.2007.00392.x

Verma, A., Lee, C., Morriss, S., Odu, F., Kenning, C., Rizzo, N., et al. (2018). The novel cyst nematode effector protein 30D08 targets host nuclear functions to alter gene expression in feeding sites. *New Phytol.* 219, 697–713. doi: 10.1111/nph.15179

Vieira, P., and Gleason, C. (2019). Plant-parasitic nematode effectors—insights into their diversity and new tools for their identification. *Curr. Opin. Plant Biol.* 50, 37–43. doi: 10.1016/j.pbi.2019.02.007

Wang, S., Yang, S., Dai, K., Zheng, W., Zhang, X., Yang, B., et al. (2023). The effector Fg62 contributes to *Fusarium graminearum* virulence and induces plant cell death. *Phytopathol. Res.* 5, 12. doi: 10.1186/s42483-023-00167-z

Wen, T. Y., Wu, X. Q., Hu, L. J., Qiu, Y. J., Rui, L., Zhang, Y., et al. (2021). A novel pine wood nematode effector, BxSCD1, suppresses plant immunity and interacts with an ethylene-forming enzyme in pine. *Mol. Plant Pathol.* 22, 1399–1412. doi: 10.1111/mpp.13121

Wen, T. Y., Wu, X. Q., Ye, J. R., Qiu, Y. J., Rui, L., and Zhang, Y. (2022). A *Bursaphelenchus xylophilus* pathogenic protein Bx-FAR-1, as potential control target, mediates the jasmonic acid pathway in pines. *Pest Manage. Sci.* 78, 1870–1880. doi: 10.1002/ps.6805

Xue, L., Lie, G., Lu, G., and Shao, Y. (2013). Allometric scaling among tree components in *Pinus massoniana* stands with different sites. *Ecol. Res.* 28, 327–333. doi: 10.1007/s11284-012-1021-x

Yang, B., Wang, Q., Jing, M., Guo, B., Wu, J., Wang, H., et al. (2017). Distinct regions of the *Phytophthora essential* effector Avh238 determine its function in cell death activation and plant immunity suppression. *New Phytol.* 214, 361–375. doi: 10.1111/nph.14430

Yang, B., Wang, Y., Tian, M., Dai, K., Zheng, W., Liu, Z., et al. (2020). Fg12 ribonuclease secretion contributes to *Fusarium graminearum* virulence and induces plant cell death. *J. Integr. Plant Biol.* 63, 365–377. doi: 10.1111/jipb.12997

Yin, W., Wang, Y., Chen, T., Lin, Y., and Luo, C. (2018). Functional evaluation of the signal peptides of secreted proteins. *Bio Protoc.* 8, e2839. doi: 10.21769/BioProtoc.2839

Yu, X., Tang, J., Wang, Q., Ye, W., Tao, K., Duan, S., et al. (2012). The RxLR effector Avh241 from *Phytophthora sojae* requires plasma membrane localization to induce plant cell death. *New Phytol.* 196, 247–260. doi: 10.1111/j.1469-8137.2012.04241.x

Zhang, Y., Wen, T. Y., Wu, X. Q., Hu, L. J., Qiu, Y. J., and Rui, L. (2022). The *Bursaphelenchus xylophilus* effector BxML1 targets the cyclophilin protein (CyP) to promote parasitism and virulence in pine. *BMC Plant Biol.* 22, 216. doi: 10.1186/s12870-022-03567-z

Zhao, Q., Hu, L. J., Wu, X. Q., and Wang, Y. C. (2020). A key effector, BxSapB2, plays a role in the pathogenicity of the pine wood nematode *Bursaphelenchus xylophilus*. *For. Pathol.* 50, e12600. doi: 10.1111/efp.12600

frontiers | Frontiers in Plant Science

TYPE Review
PUBLISHED 30 April 2024
DOI 10.3389/fpls.2024.1377453

OPEN ACCESS

EDITED BY
Andressa Machado,
Agronema, Brazil

REVIEWED BY
Abhijeet Shankar Kashyap,
National Bureau of Agriculturally Important Microorganisms (ICAR), India
Emmanuel Tzortzakakis,
Hellenic Agricultural Organization DEMETER, Greece
Rouhallah Sharifi,
Razi University, Iran

*CORRESPONDENCE
Zafar Handoo
Zafar.Handoo@usda.gov

RECEIVED 27 January 2024
ACCEPTED 11 April 2024
PUBLISHED 30 April 2024

CITATION
Habteweld A, Kantor M, Kantor C and Handoo Z (2024) Understanding the dynamic interactions of root-knot nematodes and their host: role of plant growth promoting bacteria and abiotic factors.
Front. Plant Sci. 15:1377453.
doi: 10.3389/fpls.2024.1377453

Understanding the dynamic interactions of root-knot nematodes and their host: role of plant growth promoting bacteria and abiotic factors

Alemayehu Habteweld[1], Mihail Kantor[2], Camelia Kantor[3] and Zafar Handoo[1]*

[1]Mycology and Nematology Genetic Diversity and Biology Laboratory, USDA, ARS, Northeast Area, Beltsville, MD, United States, [2]Plant Pathology and Environmental Microbiology Department, Pennsylvania State University, University Park, PA, United States, [3]Huck Institutes of the Life Sciences, Pennsylvania State University, State College, PA, United States

Root-knot nematodes (*Meloidogyne* spp., RKN) are among the most destructive endoparasitic nematodes worldwide, often leading to a reduction of crop growth and yield. Insights into the dynamics of host-RKN interactions, especially in varied biotic and abiotic environments, could be pivotal in devising novel RKN mitigation measures. Plant growth-promoting bacteria (PGPB) involves different plant growth-enhancing activities such as biofertilization, pathogen suppression, and induction of systemic resistance. We summarized the up-to-date knowledge on the role of PGPB and abiotic factors such as soil pH, texture, structure, moisture, etc. in modulating RKN-host interactions. RKN are directly or indirectly affected by different PGPB, abiotic factors interplay in the interactions, and host responses to RKN infection. We highlighted the tripartite (host-RKN-PGPB) phenomenon with respect to (i) PGPB direct and indirect effect on RKN-host interactions; (ii) host influence in the selection and enrichment of PGPB in the rhizosphere; (iii) how soil microbes enhance RKN parasitism; (iv) influence of host in RKN-PGPB interactions, and (v) the role of abiotic factors in modulating the tripartite interactions. Furthermore, we discussed how different agricultural practices alter the interactions. Finally, we emphasized the importance of incorporating the knowledge of tripartite interactions in the integrated RKN management strategies.

KEYWORDS

root-knot nematodes, root-knot nematode-host interactions, plant growth promoting bacteria, root exudates, volatiles, biotic factors, abiotic factors, agricultural practices

1 Introduction

Plant-parasitic nematodes (PPNs) infect a wide range of food crops and cause severe damage (Nicol et al., 2011; Jones et al., 2013; Kantor et al., 2022). PPNs control costs several billions of dollars annually to the global agriculture industry (Elling, 2013; Gamalero and Glick, 2020; Kantor et al., 2022). Among these, root-knot nematodes (RKN) are the most economically significant plant pathogens due to the high levels of damage and infection they cause, their wide host and geographic ranges, and interaction with other plant pathogens (Rehman et al., 2012; Topalović and Geisen, 2023). The second-stage juvenile (J2) is the only infective stage of RKN. In plant roots, the J2s undergo two developmental stages (J3 and J4) before an adult stage. Adult females establish feeding sites and cause root galls (Eisenback and Triantaphyllou, 1991; Karssen and Moens, 2006; Gheysen and Mitchum, 2011).

The above-ground symptoms of RKN-infected plants include poor plant growth, necrosis on leaves, and rapid wilting under environmental stress caused by water deficiency or other factors (Bernard et al., 2017; Elnahal et al., 2022). The obvious below-ground symptom of RKN infection is the formation of galls on the roots that reduce the absorption and translocation of water and dissolved nutrients. RKN root damage also fosters access to secondary infection of roots by soil pathogens such as fungi and bacteria (Agrios, 2005; Cao et al., 2023). Because of their wide host range and distribution, effective RKN management is becoming a global priority. Effective RKN management may require an integrated application of control strategies such as chemical nematicides, resistant crops, trap crops, organic amendments, and different microbial agents (Desaeger et al., 2020; Forghani and Hajihassani, 2020; Topalović et al., 2020b). Synthetic chemical nematicides are effective in controlling RKN and are widely used around the globe but their use has been restricted due to their negative impact on human health and the environment (Katooli et al., 2010; Desaeger et al., 2020). Thus, there is a critical need for alternative nematode control methods which are both effective in controlling RKN and environmentally sustainable.

RKN management strategies using antagonistic soil microbiota would offer an ecologically sound RKN control (Zhang et al., 2017; Abd-Elgawad, 2021; Aioub et al., 2022). A broad range of soil microbiota reduced nematode infection directly or indirectly in plants (Eberlein et al., 2016; Ashrafi et al., 2017; Hamid et al., 2017; Hussain et al., 2018; Nuaima et al., 2021). These microbes use antibiosis, parasitism, induced systemic resistance (ISR) in plants, or apply a combination of different strategies that can interfere with nematode infection in plants (Chen and Dickson, 1998; Siddiqui et al., 2005; Martínez-Medina et al., 2017; Poveda et al., 2020). One subset of soil microbiota showing RKN suppression is plant growth promoting bacteria (PGPB). Here, we define PGPB as bacterial community inhabiting soil around roots (rhizosphere bacteria) and inside plant roots (endophytic bacteria) and promoting plant growth through a variety of processes such as biofertilization, phytohormone production, antipathogenic activities and ISR (Lugtenburg and Kamilova, 2009; Aioub et al., 2022; Gowda et al., 2022).

PGPB stimulate plant growth by supplying essential plant nutrients such as nitrogen (N), phosphorus (P), potassium (K), and other micronutrients such as iron (Fe), and promote soil bioremediation by secreting a variety of metabolites and hormones (Poria et al., 2022). PGPB have a direct influence on both plant development and metabolism through the production of phytohormones and plant growth regulators (Chandra et al., 2018). Microbial phytohormones and phytostimulators such as auxins, ethylene, cytokines, gibberellin, abscisic acid, salicylic acid and jasmonic acid are important in plant biological processes such as cell division and elongation (Lugtenburg and Kamilova, 2009; Tsukanova et al., 2017; Shaffique et al., 2023). Phytohormones and enzymes such as 1-aminocyclopropane-1-carboxylate (ACC) produced by PGPB also alleviate various forms of stress, including infections by pathogenic bacteria, resistance to stress induced by polyaromatic hydrocarbons, heavy metals such as Ni^{2+} and environmental stresses such as salt and drought (Glick et al., 2007; Lugtenburg and Kamilova, 2009; Zhang et al., 2020; Sharifi et al., 2022). PGPB are also involved in antipathogenic activities through antagonism, signal interference, predation, parasitism, competition, and induced systemic resistance (ISR) (Milner et al., 1996; Bassler, 1999; Ryu et al., 2003; Emmert et al., 2004; Aioub et al., 2022). Thus, the use of PGPB for RKN control is an ecologically sound strategy for suppressing RKN using naturally occurring species, introducing them to the rhizosphere or manipulating the soil through different agricultural practices that enhance their performance (Topalović et al., 2019; Topalović et al., 2020b; Eldeeb et al., 2022).

Despite several promising RKN control results under laboratory and greenhouse settings, transitioning from lab to field has been challenging due to inconsistencies in microbial agent performance in the field conditions (Topalović and Heuer, 2019). Some reasons for that are the weak competitive ability of the microbial agents and the failure to establish a high density in soil ecosystems. In soil ecosystems, host-RKN interactions are complex and can be affected by different soil physicochemical and biological properties (Cao et al., 2023). Soil physicochemical and biological properties modulate host-RKN interactions, and they are in turn affected by different agricultural practices. Therefore, the knowledge of how soil biotic and abiotic factors modulate the host-RKN-PGPB (tripartite, Figure 1) interactions would be critical to develop economically and ecologically sound RKN control strategies. This review emphasizes the tripartite phenomenon with respect to (i) PGPBs' direct and indirect effect on RKN-host interactions; (ii) the host's influence in the selection and enrichment of PGPB in the rhizosphere; (iii) the influence of the host in RKN-PGPB interactions; (iv) the role of soil microbes in enhancing RKN parasitism, and (v) the role of abiotic factors in modulating the tripartite interactions. Furthermore, the paper delves into how different agricultural practices alter the host-RKN-PGPB interactions. Finally, it concludes by emphasizing the importance of incorporating the knowledge of tripartite interactions in the integrated RKN management strategies.

2 Influence of PGPB on host-RKN interactions

PGPB have a direct and indirect effect on RKN and affect the interaction between the host and RKN (Figure 1).

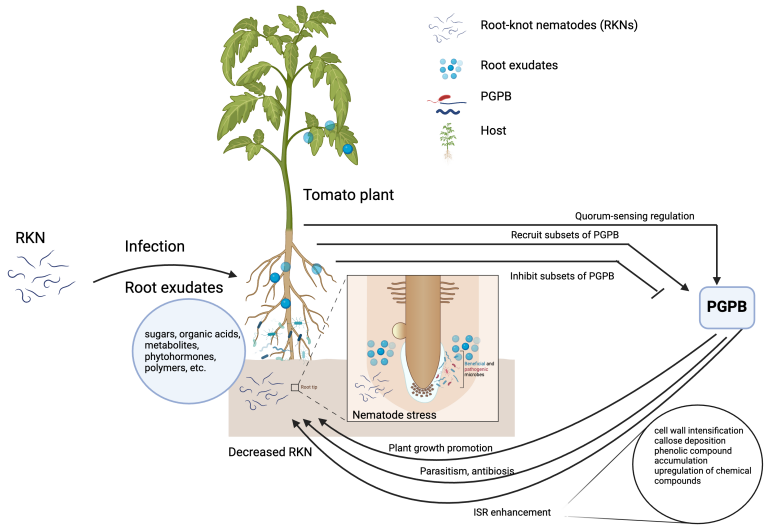

FIGURE 1
Simplified diagrammatic representation of host-RKN-PGPB interactions. Host plants shape the rhizosphere microorganisms by recruiting or inhibiting subsets of plant growth promoting bacteria (PGPB) for its benefits. The PGPB directly attack the root-knot nematodes and/or through plant growth promotion and induced systemic resistance. The figure is created with BioRender.com.

2.1 Direct modulatory mechanisms

Direct modulatory mechanisms refer to the adverse effect of PGPB on RKN through processes such as parasitism and antibiosis. Among these, parasitism stands out as the most effective and direct modulatory mechanism which entails the tropic growth of the PGPB toward RKN, ultimate assault, and disintegration of RKN through enzyme activity (Pal and Gardener, 2006; Singh et al., 2017). For instance, *Pasteuria penetrans* showed strong parasitism to *Meloidogyne graminicola*, *M. incognita*, *M. arenaria*, and *M. hapla* (Ciancio, 2018; Aioub et al., 2022).

Antibiosis involves the release of enzymes, metabolic by-products, and toxins by various PGPB to actively suppress RKNs. The release of these products plays a crucial role in inhibiting nematode hatching, development, and existence (Subedi et al., 2020). Some PGPB such as *Pseudomonas fluorescens*, produce metabolic by-products like 2,4-diacetylphloroglucinol and hydrogen cyanide that suppress RKN density and promote plant growth (Mena et al., 2002; Meyer et al., 2009; El-Rahman et al., 2019). Research on *Corynebacterium paurometabolous* and *Lysobacter capsica* showed that these PGPB expressed chitinase and gelatinase activities which reduced the numbers of galls and egg masses of *M. incognita* in tomatoes (Mena et al., 2002; Lee et al., 2015). *Bacillus cereus* strain (BCM2) released 2,4-2,4-ditert-butylphenol, 3,3 dimethyloctane, chitonase, alkaline serine protease, and neutral protease which resulted in the reduction of *M. incognita* density on tomato (Li et al., 2019a). *B. thuringiensis* is known to produce proteinaceous protoxin crystals that cause lysis of the intestine and the nematode's death (Griffitts et al., 2005; Vachon et al., 2012; Elhady et al., 2017).

Several PGPB strains with antibiosis activity such as *Bacillus aryabhattai* A08, *Paenibacillus alvei* T30, *Bacillus firmus* T11, *Paenibacillus barcinonensis* A10, and *B. cereus* N10w were reported (Viljoen et al., 2019). Application of *P. fluorescens* and *Serratia marcescens* reduced the number of galls and egg masses of RKN species (Ali et al., 2021). *Pseudomonas* spp. and *Bacillus* spp. isolated from RKN suppressive soil exhibited RKN antagonism on tomato (Zhou et al., 2019). Similarly, soils with low- and high-infestations of *M. incognita* demonstrated different microbial communities in the rhizosphere, the low-infested soil contained more of plant beneficial microbes including those with nematocidal activities such as *B. amyloliquefacens* W1 (Zhao et al., 2023).

2.2 Indirect interventional mechanisms

PGPB indirectly suppress RKN by promoting plant growth and development through improved nutrient availability and uptake, producing phytohormones, and activating ISR. Recent studies revealed that N-fixing PGPB strains promote plant growth by providing nitrogen and increase plants' resistance to RKN (Aioub et al., 2022). For instance, *Rhizobium* spp., *Mesorhizobium* spp., *Sinorhizobium* spp., *Bradyrhizobium* spp. and *Frankia* spp. fix N_2, supply it to plants and promote plant growth (Vejan et al., 2016; Dash et al., 2017; Liao et al., 2021). Similarly, *Paenibacillus polymyxa*, a N-fixing PGPB, promoted plant growth and suppressed *Meloidogyne incognita* populations on tomato in a greenhouse experiment (El-Hadad et al., 2011). *Azospirillum* spp., *Azotobacter* spp., and *Rhizobium* spp. decreased root galling caused by *Meloidogyne javanica* in root of chickpea (*Cicer arietinum*) (Siddiqui and Mahmood, 2001). Inoculating tomato plants with *Bacillus firmus*, *B. megaterium* and *B. circulans* also improved plant growth through phosphate acquisition and suppressed *M. incognita* populations (Terefe et al., 2009; El-Hadad et al., 2011). Likewise, phosphate-solubilizing *P. fluorescens* suppressed *M. incognita* population in chickpea field (Rizvi et al., 2012). PGPB with

phytohormone-producing ability promoted plant growth and suppressed PPNs (Backer et al., 2018). For instance, indole acetic acid (IAA) production by the strain *Streptomyces fradiae* NKZ-259 enhanced plant growth (Myo et al., 2019). *Pseudomonas simiae* strain MB751 also produced IAA, improved plant growth, and suppressed *M. incognita* development (Sun et al., 2021).

PGPB decrease the population of RKN by enhancing ISR through eliciting plant innate immunity in plants. This is accomplished through processes like cell wall intensification, callose deposition, phenolic compound accumulation, and upregulation of biochemical compounds such as jasmonic acid, pathogenesis-related proteins, lipopolysaccharides, phytoalexin, siderophores, chitinase, and salicylic acid (Aioub et al., 2022). For instance, *M. javanica* and *M. incognita* population densities were suppressed because of the activation of ISR when *Arabidopsis* roots were treated with PGPB *Bacillus cereus* (Jiang et al., 2020). Similarly, tomato roots inoculated with *P. fluorescens* Pf128 and *B. subtilis* Bbv57 decreased *M. incognita* populations due to increased activity of enzymes involved in ISR (Meena et al., 2012).

3 Plants recruit and shape PGPB communities in the rhizosphere

Different plant species selectively attract different communities of PGPB and influence their composition when grown on the same soil (Berendsen et al., 2012). The PGPB exhibit significantly higher population densities in the rhizosphere compared to the bulk soil, primarily due to plants releasing up to 40% of their photosynthates as root exudates (Bais et al., 2006). However, their diversity is low in the rhizosphere compared to the bulk soil (Berg et al., 2006; Costa et al., 2006; Hein et al., 2008; Berendsen et al., 2012) indicating PGPB community establishment is driven by host plant selection (Li et al., 2019b; Yin et al., 2021). The type and age of the host plant, and biotic and abiotic stresses influence the compositions of root exudates (Lundberg et al., 2012; Chaparro et al., 2014; Bulgarelli et al., 2015; Tkacz et al., 2015; Kantor et al., 2018; Yin et al., 2021). Thus, the composition of root exudates actively secreted by plants shape the PGPB community by stimulating or repressing the subset of the PGPB community in the soil (Doornbos et al., 2012). Components of root exudates such as sugars, organic acids, metabolites, phytohormones, and complex mucus-like polymers play a key role in shaping the composition and structure of PGPB community (Broeckling et al., 2008; Carvalhais et al., 2015; Berendsen et al., 2018; Sasse et al., 2018; Yuan et al., 2018; Wen et al., 2020, 2021; Kong et al., 2021).

For example, long-chain fatty acids and amino acids were identified to play a crucial role in attracting PGPB, including *Pseudomonas* populations (Yuan et al., 2018; Wen et al., 2021). Additionally, a higher release of four short-chain organic acids (citric acid, pyruvate acid, succinic acid, and fumarate) has been linked to the increased presence of PGPB such as *Comamonadaceae* spp (Wen et al., 2020). Root-secreted malic acid has also been linked to the attraction of *Bacillus* spp. to the rhizosphere (Rudrappa et al., 2008). Therefore, the particular ratios and makeup of root exudates significantly influence the PGPB composition (Badri et al., 2009; Zhou and Wu, 2012).

Secondary metabolites secreted by plant roots can also be detrimental for the growth of specific group of microbes in the rhizosphere (Bais et al., 2002; Zhang et al., 2011). Benzoxazinoids are exuded in relatively large quantities from cereal roots and can inhibit rhizosphere microbes (Berendsen et al., 2012). In maize (*Zea mays*), 2,4-dihydroxy- 7-methoxy-2H-1,4-benzoxazin-3(4H)-one (DIMBOA) is the main antimicrobial benzoxazinoid. In contrast, PGPB *P. putida* KT2440 was attracted and tolerant to DIMBOA (Berendsen et al., 2012; Neal et al., 2012). In the absence of DIMBOA, the colonization of roots by KT2440 strain was lower (Berendsen et al., 2012; Neal et al., 2012). Secondary metabolites have shown promising nematocidal activity. Notably, various metabolites synthetized by wild watermelon roots have been documented in literature for their effectiveness in controlling nematodes (Kantor et al., 2018).

Plants also produce compounds that stimulate or repress quorum-sensing (QS)-regulated responses in PGPB. These QS-interfering compounds enable the plant to manipulate gene expression in their PGPB communities (Berendsen et al., 2012). PGPB utilize QS to signal each other and regulate expression of certain genes by using diffusible N-acyl-homoserine lactones (AHLs) (Elasri et al., 2001; Berendsen et al., 2012). AHL-mediated regulation typically makes use of two proteins that resemble the LuxI and LuxR protein families. LuxI-like proteins are AHL synthases, whereas LuxR-like proteins function as receptors of AHL that can form complexes with AHL which in turn can affect gene expression of QS-target genes (Decho et al., 2011; Berendsen et al., 2012). For instance, seedling extracts and exudates of barrel clover (*Medicago truncatula*), pea (*Pisum sativum*), rice (*Oryza sativum*) and green algae (*Chlamydomonas reinhardtii*) had compounds that specifically stimulated or repressed responses in QS-reporter bacteria (Teplitski et al., 2000; Gao et al., 2003; Teplitski et al., 2004; Ferluga and Venturi, 2009). Some plant-associated PGPB have LuxR-like proteins that are stimulated by plant-derived signals, whereas they themselves do not produce AHLs (Ferluga and Venturi, 2009; Berendsen et al., 2012). Thus, plants recruit and shape the rhizosphere microbes through the composition of root exudates and secondary metabolites. These substances selectively attract or repel soil microbiota and play a role in controlling the expression of QS-regulated genes of soil microbiota.

4 Interplay between host and PGPB in RKN suppression

Root exudates are important in nematode attraction to plant roots and directly affect nematode interactions with PGPB by inducing changes in the surface of PPNs. PGPB interact with PPNs through the nematode surface coat (SC). SC is a glycoprotein layer secreted by the hypodermis, or by the excretory and nervous systems (Lin and McClure, 1996; Curtis et al., 2011). Receptors on nematode SC mediate the specific interaction with the lectine-like protein molecules on PGPB surface (Bird, 2004; Davies and Curtis, 2011). Studies showed that nematode SC exposed to different root exudates and secondary metabolites also undergoes modifications which influence PGPB

attachments to RKN surface (Akhkha et al., 2002; Curtis, 2008; Singh et al., 2014; Liu et al., 2017). *Pasteuria penetrans* endospores attachment to J2 of RKN were variable in response to root exudates from different plant species (Singh et al., 2014; Liu et al., 2017). For instance, *M. incognita* J2 exposed to the root exudates showed greater *P. penetrans* endospores attachment (Singh et al., 2014). These results indicated that the influence of specific host root exudates on RKN-PGPB interactions in the soil favors RKN antagonistic microbes attachment (Topalović et al., 2020c).

J2-attached PGPB can also increase hosts' resistance to RKN. PGPB attaching to J2 of *M. hapla* prior to J2 infection enhanced their detection by upregulating several pattern-triggered immunity (PTI)-responsive defense genes (Topalović et al., 2020a). Moreover, chemicals produced by *M. hapla* J2 with attached *Microbacterium* sp. K6 strain activated a greater reactive oxygen species (ROS) response in tomato roots. Such a greater increase in ROS was not detected for nematodes without the K6 strain. Besides, hundred-fold ROS response was observed in the leaves than the roots for J2 with attached *Microbacterium* sp. K6 strain (Topalović et al., 2020a, b, c). Therefore, J2-attached PGPB prior penetrating roots can activate ISR that inhibits RKN establishment.

Recent research findings suggest that the success of RKN root invasion is influenced by the root exudates and PGPB in the rhizosphere which determine whether the RKN surface molecule is recognized by plant roots or not (Topalović et al., 2020c). Thus, host plant root exudates components play a key role for the communications between plants and nematodes, and nematode-PGPB interaction by modulating components of the nematode SC (Topalović et al., 2020c). Based on the host range of the nematode and the PGPB composition, RKN may either bypass plant defense responses to infiltrate the roots or be antagonized within or outside the plant. Thus, plants are utterly dependent on PGPB during nematode invasion, which results in the proliferation of a certain group of PGPB community protecting the host (Hussain et al., 2018; Topalović et al., 2020c). This suggests that the dynamic tripartite phenomenon in soil leads to nematode suppression by microbially induced systemic resistance in plants (Topalović et al., 2020a).

5 Soil microbes could enhance RKNs parasitism

RKN juveniles, while actively searching for roots in the soil, are likely to encounter and attach to a functionally diverse array of soil microbes. This array includes both antagonistic and protective surface microbes (Topalović and Vestergård, 2021). The holobiont concept suggests that each macroorganism has developed a mutually beneficial relationship with specific microbiota that influences its health and survival. Additionally, it infers that the microbial moiety of a holobiont can undergo modifications in response to environmental stress (Bordenstein and Theis, 2015). Soil microbes can protect PPNs in soil by outcompeting nematode antagonists for attachment sites on the nematode's surface, reducing nematode recognition, or by producing compounds that are toxic to nematode antagonists (Topalović and Vestergård, 2021).

RKN J2s may avoid antagonists by recruiting protective soil microbiota to their surface. A recent study revealed that J2-attached microbes' compositions were different on actively moving J2 surface of *Meloidogyne hapla* and *M. incognita* in the presence of *Pseudomonas protegens* strain CHA0, a bacterial antagonist (Topalović et al., 2023). In the absence of *P. protegens* strain CHA0, bacterial genera such as *Delftia*, *Variovorax* and *Pseudomonas* attached on both active and inactive J2s but not on J2 treated with *P. protegens* strain CHA0. *P. protegens* CHA0 also activated proliferation of *Flavobacterium* spp. and *Cutibacterium* spp., and Methylophilaceae family within the Gammaproteobacteria, which might have protective role on active nematodes in *M. hapla* and *M. incognita*, respectively (Tsuru et al., 2021; Topalović et al., 2023). The presence of *P. protegens* CHA0 might also change the surrounding microbial community by reducing the prevalence of nematode antagonistic taxa such as Pseudomonads may be due to a release of secondary metabolites from *P. protegens* CHA0 (Topalović et al., 2023). Such antimicrobial compounds might play a role in reducing the abundance of nematode antagonists in the soil in the presence of RKN protective soil microbiota.

PGPB attachment to nematode surface can reduce the nematode recognition by plants during the infection process by masking the nematode receptors (Curtis, 2008; Mendy et al., 2017; Topalović et al., 2020c). RKN surface-attached microbes may also facilitate RKN establishment by helping in the creation of a feeding site and enhancing nutrition available for the nematodes (Cao et al., 2015). Community analysis of root-associated microbiomes in healthy and RKN-infected tomatoes showed that nematode infections were associated with variation and differentiation of the endophyte and rhizosphere bacterial populations in plant roots (Tian et al., 2015). Bacterial genera with N-fixing (*Sinorhizobium* spp. and *Devosia* spp.) and cellulose-degrading (Sphingomonadaceae) abilities were found associated with different life stages of *M. incognita* on tomato (Cao et al., 2015; Tian et al., 2015). As the plant does not recognize N-fixing bacteria as pathogens, their introduction may deter RKN recognition and immune responses against the RKN. In addition, detecting cellulose-degrading bacterial groups may suggest that the gall-enriched cellulose-degrading bacteria may help nematodes in feeding site formation (Tian et al., 2015; Yergaliyev et al., 2020). Overall, soil type, plant genotype, the specific interaction between soil microbiota and nematode surface, and the movement of J2 influence the composition of J2-attached microbial community (Adam et al., 2014; Elhady et al., 2017; Topalović et al., 2019; Elhady et al., 2021; Topalović et al., 2023).

6 Role of abiotic factors in host-RKN interactions

Soil abiotic factors can affect host-RKN interactions through their impact on plant and RKN growth and development, and/or the activities of PGPB (Figure 2). RKN spend a phase of their life cycle (J2) in soil, the composition, and properties of which affect J2 motility and distribution, as well as their development inside their

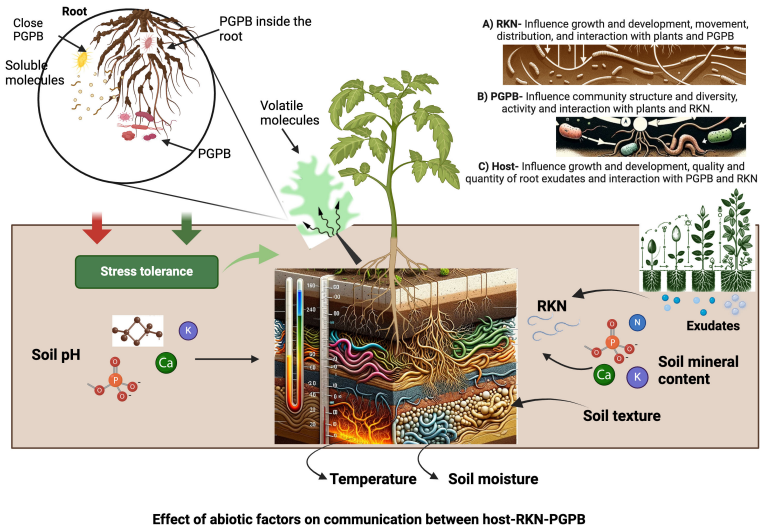

FIGURE 2
Impact of abiotic factors in host-RKN-PGPB interactions and their communications. The figure is created with BioRender.com.

host (Norton, 1989; Mateille et al., 2014). Soil abiotic factors (soil physical properties such as temperature, texture, structure, and moisture content; soil chemical properties such as soil pH and mineral compositions) affect RKN behavior and development and in turn host-RKN interactions (Palomares-Rius et al., 2015). They also affect host growth and development such as root size, numbers, softness and quality and quantity of root exudates, and in turn RKN behavior and development (Castillo et al., 2006; Landa et al., 2014). Soil abiotic factors also affect the movement of volatiles released from roots and PGPB and alter the interactions of host-RKN-PGPB as volatiles play key roles in mediating intra- and inter-kingdom communications (Sharifi and Ryu, 2018; Erktan et al., 2020; Wester-Larsen et al, 2020; Lee and Ryu, 2021). While soil abiotic factors affect soil microbiota which in turn can affect host-RKN interactions as aforementioned, an in-depth analysis of this topic falls beyond the scope of this review as its main theme is to discuss the role of PGPB and abiotic factors on host-RKN interactions. Rather, in the following sections we will mainly discuss the major soil abiotic factors affecting host-RKN interactions by focusing on their impact on plants and RKN.

6.1 Soil temperature

Temperature influences nematode behavior such as egg hatching, nematode movement, root infection, their development and existence in soils (Velloso et al., 2022; Pradhan et al., 2023). Temperature also has a tremendous effect on plant development, reproduction, survival, and resistance to RKN (Hatfield and Prueger, 2015; Pradhan et al., 2023). Different levels of soil temperatures have variable effects on RKN root infection and their metabolism (Verdejo-Lucas et al., 2012, 2013; Khan et al., 2014; Pradhan et al., 2023). The tropical nematodes such as *M. incognita*, *M. javanica* and *M. arenaria* are most active for infection at a temperature of 24–32°C, while other root-knot nematodes such as *M. hapla* and *M. chitwoodi* can remain active in a temperature range of 10°C and 32°C (Davila-Negron and Dickson, 2013; Gine et al., 2021; Pradhan et al., 2023). As temperature increases, the number of RKN generations increase which leads to large increment in nematode population density and greatly reduce plant development (Verdejo-Lucas et al, 2013).

Generally, RKN reproduction increases when the soil temperature is intermittently above 28 °C (Talavera et al., 2009). However, temperatures below 18 °C decreased the J2 motility and subsequent root penetration and development inside roots (Roberts et al., 1981; Prot and Van Gundy, 1981a; Trudgill, 1995). High temperatures are also known to decrease nematode motility and cause lethality (Wallace and Bird, 1965; Wang and McSorley, 2008; Oka, 2019). Similarly, the pace of plant growth and development hinges on the ambient temperature of the plant, with each species having a defined temperature range represented by a minimum, maximum, and optimum temperature (Hatfield and Prueger, 2015). Soil temperature affects physiological processes of host plants such as root growth (Holtzmann, 1965), plant vigor and yield (Abdul-Baki, 1991), and thus, affect host-RKN interactions. For example, heat stress increase heat-shock proteins in plants that may alter the plant defense mechanisms at early stages of nematode infection (Verdejo-Lucas et al., 2013).

High temperature also affects plant resistance to RKN infection (Roberts, 2002). For instance, *Mi-1* gene is responsible for tomato resistance to *M. arenaria*, *M. incognita* and *M. javanica* (Smith, 1944) which greatly reduces the RKN reproduction in tomato (Roberts and Thomason, 1986; Sorribas et al., 2005). However, soil temperature above 28 °C usually negatively affects the resistance traits (Holtzmann, 1965; Dropkin, 1969; Araujo et al., 1982) and lead RKN to break the *Mi*-gene that lead to RKN population increase and affect plant growth and development (Devran and Sögüt, 2010; Verdejo-Lucas et al., 2012, 2013). As plants and RKN, PGPB have minimum, optimum, and maximum temperatures for their physiological activities. Temperature changes lead to

structural and compositional changes in PGPR community which affect their interaction with plants and RKN, and host-RKN interactions (Zhang and Gross, 2021; Omae and Tsuda, 2022). The activity of PGPB enzymes can be influenced by soil temperature. For instance, the effectiveness of enzymes involved in nitrogen fixation varies at different temperatures (Abdul Rahman et al., 2021).

Temperature can influence the tripartite interactions through altering the host and PGPB volatiles concentration and mobility in soil (Kramshøj et al., 2019; Wester-Larsen et al, 2020). Studies showed that temperature increase positively correlated with an increase volatiles concentration by increasing biological activity, and liberating adsorbed and dissolved volatiles (Guenther et al., 1993; Insam and Seewald, 2010; Wester-Larsen et al., 2020). When concentration of volatiles in soil is low, it is not sensed over long distance by host, RKN and PGPB and hence affect the interactions between host-RKN-PGPB.

6.2 Soil texture, structure, and moisture content

Soil texture, structure and moisture are interrelated. Soil texture (proportions of sand, clay, and silt) and structure (soil aggregation) directly influence soil porosity which determines soil aeration, water infiltration and retention, and, indirectly, root growth, nematode movement, nutrient availability, and microbial activity (Saxton and Rawls, 2006; Mateille et al., 2014; Noronha et al., 2021; Garcia et al., 2022). Soil texture impacts the movements of J2 through the water film around soil particles, stimulated by the retention of root exudates that enable RKN to locate the roots (Prot and Van Gundy, 1981b; Garcia et al., 2022). The sandier soils seem to be good habitats for RKN and increase their presence in areas with coarse soil (Prot and Van Gundy, 1981b; Mateille et al., 2014; Kabir et al., 2017; Noronha et al., 2021). More structured soils with higher clay content, greater porosity, and water storage favored RKN because they retained water and created transport films in the soil that facilitated nematode movement (Otobe et al., 2004; Fajardo et al., 2011; Noronha et al., 2021). More structured soil also promotes the abundance, structure, and activity of PGPB which affects host plants, RKN as well as their interactions (Hartmann and Six, 2023).

Conversely, dry soil conditions may inhibit root growth, decrease metabolic activity, and cause electrolyte disturbances. These adverse effects can lead to the death of the plant, which in turn negatively affects the RKN development (Hurd, 1968; Roberts et al., 1981; Chen et al., 2022). Dry soils may not have enough water film for RKNs' movement to locate host roots (Wallace, 1958; Oka, 2019). Dry soil also negatively affects the abundance, structure, and activity of PGPR and as a result of reduced nutrient availability, antipathogenic activities against RKN and the interactions between host and RKN (Bogati and Walczak, 2022; Omae and Tsuda, 2022). For instance, low soil moisture content decreases the movement of nitrogen-fixing bacteria to the rhizosphere, decreases rhizosphere colonization and their plant growth-promoting activity (Islam et al., 2020). Conducive soil physical properties such as water retention, porosity, aeration, and soil temperature enhance plant development, favor RKN and PGPB activity, and increase nematode and PGPB reproduction (Franchine et al., 2018; Notonha et al., 2021).

Soil texture, structure and moisture content affect the diffusion rate of volatiles in soil and as a result modulate the interactions between host, RKN and PGPB (Aochi and Farmer, 2005; Asensio et al., 2008). Soil texture and structure determine the pore sizes (micro or macro) in the soil which in turn influences the movement of soil organisms and soil moisture content (Mateille et al., 2014; Noronha et al., 2021; Garcia et al., 2022). The level of soil moisture content in turn affects the rate of diffusion of volatiles in soil that alters the interactions between host-RKN-PGPB. For instance, the movement of volatiles in wet soil is much slower than in dry soil, influences volatile travel distance and magnitude and impact the sensing ability of soil organisms such as RKN (Moldrup et al., 2000). In contrast, volatiles diffusion in the drier soil is faster and travels longer (Tyc et al., 2015; Erktan et al., 2020). RKN locate and move towards the host root tip by using the concentration gradient of volatiles as cue (Rasmann et al., 2012). Although RKN can better sense roots due to faster diffusion of volatiles, it may not reach to the root due to movement restriction in drier soil condition. Thus, optimal soil pore size and moisture content allows the movement of soil organisms and diffusion of volatiles. Similarly, the movement of PGPB to the root is mediated by the volatiles from the host, and plant roots must sense PGPB volatiles to respond accordingly (Schmidt et al., 2015; Schulz-Bohm et al., 2015; Tyc et al., 2017; Erktan et al., 2020; Sharifi et al. 22).

6.3 Soil pH

Soil pH is one the most important soil abiotic factors influencing soil properties, nutrient availability and solubility, plant growth, and RKN activity (Gentili et al., 2018; Penn and Camberto, 2019; Nisa et al., 2021; Barrow and Hartemink, 2023; Dewangan et al., 2023). Nutrient levels in soil are linked to the concentration of hydrogen ions, reflected in the soil's pH value. Changes in pH level can influence the availability of nutrients, affecting plant growth. The exact influence of pH fluctuations on the soil's microbial populations is not fully understood though it is known that pH is a key factor in determining microbial community structure (Biswas et al., 2007; Msimbira and Smith, 2020). Although the influence of soil pH varies with the host and nematode species (Wallace, 1973; Jones, 1975), soil acidity is a major abiotic stress factor that limits plant and RKN development (Schaller, 1987; Foy et al., 1993; Baligar and Fageria, 1997). In soil pH <5, for instance, aluminum (Al) becomes toxic to root growth while the essential nutrients such as P, K, magnesium (Mg) and calcium (Ca) become less available for uptake and negatively affect plant growth. Prolonged exposure to Al subjects plants to considerable oxidative stress and harms the root systems, impairing their ability to absorb water and nutrients (Kochian et al., 2005; Chai and Schachtman, 2022). Similarly, alkaline soils often have a reduced availability of P, zinc (Zn), Fe, copper (Cu), Boron (B), and manganese (Mn), which results in stunted plant growth

(Melakeberhan et al., 2004; Barrow and Hartemink, 2023). Soil pH higher than 5 was associated with an increase of RKN populations; and pH values of 5.9 and 4.6 favored more pre-adult and adult stages of *M. incognita* than pH 4.3 in soybean roots (Melakeberhan et al., 2004; Kesba and Al-Shalaby, 2008; Nisa et al., 2021). Similarly, soil pH ranging from 5.7-7.9 appears to positively impact the abundance of RKN on sugarcane (Garcia et al., 2022). Based on the plant and RKNs species, specific range of soil pH negatively affects plants and RKN development and their interactions. Although tolerance of PGPB to soil acidity or alkalinity differs, most PGPR prefer pH of 6-7 and a change in range of soil pH alters their composition and activity which also alters their impact on host and RKN. For instance, low soil pH decreased nitrogen-fixing bacteria diversity and the process of N-fixation (Smercina et al., 2019; Abdul Rahman et al., 2021). Microorganisms in soil must have the ability to perceive and adapt to changes in their environment, including shifts in pH, to successfully survive and establish themselves (Biswas et al., 2007).

6.4 Soil organic matter

Increased soil organic matter (SOM) is typically linked to increased water holding capacity, storage of plant nutrients and structure of soil, and heightened microbial activity, and better plant growth, influencing host-RKN interactions (Pimentel et al., 2005; Evanylo et al., 2008; Zasada et al., 2008; Natsheh and Mousa, 2014; Zhang et al., 2014, 2016). One scenario illustrating the influence of SOM on host-RKN interactions involves the promotion of plant growth as indicated by previous studies (Pimentel et al., 2005; Forge and Kempler, 2009). This growth elevates the carrying capacity of plants on which RKN feed (Bongers et al., 1997; Bongers and Bongers, 1998; Bongers and Ferris, 1999; Habteweld et al., 2020a) or enhances microbial activity such as nematode antagonists resulting in RKN suppression (Gine et al., 2016; Silva et al., 2022). SOM also alters the tripartite interactions directly by adsorbing the volatiles released by plants and PGPB directly which decrease their concentration in soil or by involving soil structure and pore formation as aforementioned indirectly (Wester-Larsen et al., 2020).

6.5 Soil nutrient content

The presence of nutrients in the soil has a direct or indirect impact on both plant growth and development as well as RKN densities through the development of host plants (Habteweld et al., 2018). Soil mineral content is an important abiotic factor for nematodes' development as they modify their habitat, metabolism, or movement (Norton, 1989; Mateille et al., 2014; Palomares-Rius et al., 2015). For instance, N is one of the macronutrients essential for plant growth and development and increase nematode reproduction indirectly by enhancing root growth (Santana-Gomes et al., 2013; Lira et al., 2019). Studies showed that high N content in the soil was positively correlated with RKN population densities in sugarcane and tomatoes (Asif et al., 2015; Ngeno et al., 2019).

P promotes root growth which increases nutrients acquisition and overall plant development (Devi et al., 2012). P deficiency induces the exudation of phenolics such as caffeic and protocatechuic acid into the rhizosphere resulting in desorption of P by binding with P-containing minerals in soils to release P for plant uptake (Juszczuk et al., 2004; Hu et al., 2005; Weisskopf et al., 2006; Noronha et al., 2021; Chai and Schachtman, 2022). P also influences RKN through biochemical changes in plants such as the increase in plant oils, phenolics, peroxidases, and ammonia that reduce the reproduction of the nematodes (Noronha et al., 2021). The addition of P fertilizers inhibits hatching and causes J2 mortality of *M. javanica* and *M. incognita* (Habash and Al-Banna, 2011; Hemmati and Saeedizadeh, 2019). K is required for plant development due to its involvement in various metabolic processes such as photosynthesis, protein synthesis, and translocation of sucrose from leaves to the stalk storage tissues (Medina et al., 2013). It is also related to stabilizing cell structure, thickening cell walls, and preventing the expansion of intracellular space (Li et al., 2010). Thus, low K levels in soil contribute to reducing the longevity of plants such as sugarcane (Noronha et al., 2021). K may suppress RKN as the application of K activates various enzymes improving plant resistance against *M. incognita* (Zhao et al., 2016).

While the impact on the development of RKN is not well studied, Ca, Mg, Ca/Mg, Carbon/Nitrogen (C/N) and soil cation exchange capacity (CEC) play important roles in the development of both plants and RKN. Ca is required for plant growth and development due to its involvement in cell wall and cell membrane formation, and N metabolism in plants (Thangavelu and Rao, 2004; Hepler, 2005). Mg is also required for plant growth and development due to its key role in photosynthesis and phosphorus transport (Thangavelu and Rao, 2004; Huber and Jones, 2013). A more recent study showed that increasing Ca/Mg ratio was associated with a decrease in RKNs' densities (Noronha et al., 2021). C/N ratio and CEC improve soil nutrient retention capacity, enabling a steadier release of nutrients, thus having a positive impact on host and RKN populations (Garcia et al., 2022). The presence of heavy metals such as Zn or Cu in the soil suppresses RKN development (Park et al., 2011; Garcia et al., 2022). This effect could be indirect through reduced plant growth and thus lower quality nutritional content for RKN, as these organisms depend on their host plants for nutrition (Garcia et al., 2022). Thus, the imbalance of nutrients in the soil can affect the metabolism of the crop which can indirectly influence RKNs' development (Coyne et al., 2004; Noronha et al., 2021; Garcia et al., 2022). Soil nutrients and their bioavailability influence the abundance, richness, and diversity of PGPB, and the interaction between host and RKN. For instance, addition of Fe and N influences microbial richness in the soil (Lakshmanan et al., 2014; Yang et al., 2015). Soil nutrients also influence the tripartite interaction by reducing the volatiles in soil. Sorption of volatiles to minerals are subject to degradation and catalyzed by mineral surfaces which reduce their diffusion and the sensing by plants, RKN and PGPB (Erktan et al., 2020).

7 Importance of agricultural practices in modulating host-RKN-PGPB interactions

Agricultural practices (APs) modulate the host-RKN-PGPB interactions by affecting plant and RKN development as well as altering soil's physicochemical and biological properties (Habteweld et al., 2022). Common APs in conventional agriculture such as tillage, the use of inorganic fertilizers, and chemical pesticides and herbicides, may increase plant growth but often have harmful effects on the environment and human health (Lal, 2008; Diacono and Montemurro, 2010). For instance, conventional tillage has a negative impact on PPN populations by changing the physicochemical properties of the soil (Dick, 1992; Freckman and Ettema, 1993; Pankaj et al., 2006; Duplay et al., 2014). These changes can modify nematodes' metabolism and reduce their mobility or access to food sources by removing weeds and altering their living habitats (e.g. living depth and soil structure) (McSorley and Dickson, 1990; Ou et al., 2005; Ekschmitt and Korthals, 2006; Mateille et al., 2014; Palomares-Rius et al., 2015; Garcia et al., 2022). The repeated use of synthetic fertilizers causes decline in soil physicochemical and biological properties (Odunze et al., 2012; Eche et al., 2013; Singh et al., 2013) that can in turn affect plant-RKN interactions. Acidic soil pH caused by the repeated application of chemical fertilizers negatively affects soil biological property which favors some pathogens. It also reduces plant growth, nutrient availability, and may affect the tripartite interactions (Singh et al., 2013; Habteweld et al., 2020a). N fertilizers, for example, promote plant growth leading to high carrying capacity for RKNs (Noronha et al., 2021) or decreasing RKN population density due to the release of nitrogenous compounds such as NH_3 (Karajeh and Al-Nasir, 2012; Wei et al., 2012; Patil et al., 2013; 2014). Moreover, the use of insecticides and fungicides and soil disturbances due to tillage could eliminate potential natural enemies of RKN such as nematophagous fungi (Stirling, 2014; Kumar et al., 2017) leading to increased RKN populations and reduced plant growth (Garcia et al., 2022).

In contrast, cultural APs such as organic amendments, mulching, crop rotation, cover cropping and conservation tillage increase the availability of nutrients, improve soil structure leading to better moisture retention and soil microbial activity, reduce fertilizer loses to the environment, and increase plant growth (Oquist et al., 2007; Forge and Kempler, 2009; Glover et al., 2010; Zhang et al., 2014, 2016; Habteweld et al., 2020a, 2020b). Compost stands as one of the most widely employed organic amendments, demonstrating its ability to enhance soil organic matter, augment nutrient content, stimulate microbial activity, suppress pests, and contribute to overall soil health improvement (Bulluck et al., 2002; Forge and Kempler, 2009; Ferris et al., 2012; Habteweld et al., 2018, 2022). Incorporating compost as soil amendment increases soil pH by forming an aluminum complex and increasing base saturation (Shiralipour et al., 1992; Van den Berghe and Hue, 1999). In addition, organic amendments (composts, plant residues, animal manures, and plant derivatives) increase plant growth parameters (shoot fresh weight or dry weight) and decrease RKNs damage attributes, i.e. soil RKNs numbers, number of root galls, and number of eggs/egg masses in roots (Peiris et al., 2020). Organic APs are also known to enhance soil microbial activities including RKN antagonists (Silva et al., 2022). Rhizosphere soil under organic cultivation recruit RKN antagonistic bacteria genera such as *Pseudomonas*, *Serratia*, *Bradyrhizobium*, *Burkholderia* and *Azospirillum* and fungal genera such as *Beauveria*, *Clonostachys*, *Metarhizium*, *Purpureocillium* and *Arthrobotrys* (Silva et al., 2022). Thus, organic APs are potential candidates to modify soil and crop management as part of integrated strategies, thus enhancing the tripartite interactions towards RKN suppression and promoting plant growth and environmental safety.

8 Concluding remarks

RKNs are the most widespread PPNs in agricultural soils, infecting thousands of crops and causing annual losses of billions of dollars around the globe. The currently most effective and widely used RKNs control technique is the use of chemical nematicides. However, due to human health and environmental concerns, the use of many of these nematicides was banned or restricted. Therefore, there is a pressing need for effective and environmentally friendly alternative RKN control strategies. One such alternative is the use of RKN antagonistic microorganisms. However, microbial agents that were found to be effective in controlling RKN in the laboratory and/or in the greenhouse conditions often do not replicate the same level of control in the more complex soil ecosystems. The low efficacy of microbial agents may be attributed to overlooking native microbiota that possesses protective abilities for RKN, as well as to soil abiotic factors that modulate the host-RKN-PGPB interactions. Consequently, a deeper understanding of the dynamics of host-RKN interactions in varied biotic and abiotic environments could be pivotal in devising novel RKN control strategies.

9 Future perspectives of host-RKN-PGPB interactions for RKN mitigation

The utilization of PGPB for controlling RKN and fertilizing plants holds significant importance in agroecosystems, primarily due to their positive environmental impact. The application of PGPB, which facilitates RKNs' control and increases soil fertility, plant growth, and crop safety, is poised to drive sustainable agriculture. However, the use of PGPB as an RKN control strategy requires a comprehensive understanding of the host-RKN-PGPB interactions and of how soil physicochemical and biological properties modulate the interactions. The concept of the holobiont indicates that plants have fostered a symbiotic relationship with specific microorganisms that play a role in their fitness, and that the microbial moiety of a holobiont can experience alterations in response to environmental stress (Bordenstein and Theis, 2015). Soil microbiota can also protect RKN in soil by outcompeting nematode antagonists for attachment sites on

nematode surface, reducing nematode recognition, or by producing compounds that are toxic to nematode antagonists (Topalović and Vestergård, 2021; Topalović et al., 2023). So far, there are very limited studies to understand the role of RKN protective soil microbiota, soil edaphic factors and different agricultural practices in modulating the tripartite interactions. Hence, unraveling the tripartite interactions and understanding their relationship with soil biotic and abiotic factors may provide us with more knowledge on how to enhance PGPB efficiency in controlling RKN in agroecosystems. This knowledge may pave the way for the development of novel PGPB strains capable of competing and establishing themselves in soil ecosystems. It may also aid in selecting appropriate APs that increase PGPB efficiency. Moreover, the incorporation of PGPB into integrated RKN management strategies, particularly through APs such as organic amendments, cover cropping, and crop rotations, can improve soil physicochemical and biological properties. This, in turn, positively influences tripartite interactions, leading to more effective RKN control. However, several pressing questions remain to be addressed. For instance, how do we get deeper insight into the tripartite interactions to weaponize it for sustainable RKN management? How to find the most effective RKN-PGPB species combination that enhances host fitness? How does PGPB and RKN-protective microbiota competition influence the microbial composition in rhizosphere? What are the mechanisms RKN use to recruit protective soil microbiota in soil? What specific component of root exudates are involved in RKN and protective microbiota interactions? What abiotic factors favor RKN-protective microbes? Is RKN protective microbiota directly involved in infection and feeding site establishment? Which APs may help to enhance the abundance and activities of indigenous PGPB, and their communication through volatiles? Answers for these kinds of questions will lead to effective integration of PGPB in sustainable RKN control and ecologically sound agroecosystems.

Author contributions

AH: Conceptualization, Writing – original draft. MK: Conceptualization, Writing – review & editing. CK: Conceptualization, Writing – review & editing. ZH: Conceptualization, Supervision, Writing – review & editing.

Funding

The author(s) declare that no financial support was received for the research, authorship, and/or publication of this article.

Acknowledgments

Alemayehu Habteweld was supported in part by an appointment to the Research Participation Program at the Mycology and Nematology Genetic Diversity and Biology Laboratory USDA, ARS, Northeast Area, Beltsville, MD, administered by the Oak Ridge Institute for Science and Education through an interagency agreement between the U.S. Department of Energy and USDA-ARS. Mention of trade names or commercial products in this publication is solely for purpose of providing specific information and does not imply recommendation or endorsement by the U.S. Department of Agriculture. USDA is an equal opportunity provider and employer.

Conflict of interest

The authors declare that the research was conducted in the absence of any commercial or financial relationships that could be construed as a potential conflict of interest.

Publisher's note

References

Abd-Elgawad, M. M. (2021). Optimizing safe approaches to manage plant-parasitic nematodes. *Plants* 10, 1911. doi: 10.3390/plants10091911

Abdul-Baki, A. A. (1991). Tolerance of tomato cultivars and selected germplasm to heat stress. *HortScience* 116, 1113–1116. doi: 10.21273/JASHS.116.6.1113

Abdul Rahman, N. S. N., Abdul Hamid, N. W., and Nadarajah, K. (2021). Effects of abiotic stress on soil microbiome. *Int. J. Mol. Sci.* 22, 9036. doi: 10.3390/ijms22169036

Adam, M., Westphal, A., Hallmann, J., and Heuer, H. (2014). Specific microbial attachment to root knot nematodes in suppressive soil. *Appl. Environ. Microbiol.* 80, 2679–2686. doi: 10.1128/AEM.03905-13

Agrios, G. (2005). "Sclerotinia diseases," in *Plant pathology*, *5th ed* (Elsevier Academic Press, New York).

Aioub, A. A. A., Elesawy, A. E., and Ammar, E. E. (2022). Plant growth promoting rhizobacteria (PGPR) and their role in plant–parasitic nematodes control: a fresh look at an old issue. *J. Plant Dis. Prot.* 129, 1305–1321. doi: 10.1007/s41348-022-00642-3

Akhkha, A., Kusel, J., Kennedy, M., and Curtis, R. (2002). Effects of phytohormones on the surfaces of plant-parasitic nematodes. *Parasitology* 125, 165–175. doi: 10.1017/S0031182002001956

Ali, A. A., El-Ashry, R. M., and Aioub, A. A. (2021). Animal manure rhizobacteria co-fertilization suppresses phytonematodes and enhances plant production: evidence from field and greenhouse. *J. Plant Dis. Prot.* 129, 155–169. doi: 10.1007/s41348-021-00529-9

Aochi, Y. O., and Farmer, W. J. (2005). Impact of soil microstructure on the molecular transport dynamics of 1, 2-dichloroethane. *Geoderma* 127, 137–153. doi: 10.1016/j.geoderma.2004.11.024

Araujo, M. T., Bassett, M. J., Augustine, J. J., and Dickson, D. W. (1982). Effects of the temperature and duration of the initial incubation period on resistance to *Meloidogyne incognita* in tomato. *J. Nematol.* 14, 411–413.

Asensio, D., Owen, S. M., Llusia, J., and Penuelas, J. (2008). The distribution of volatile isoprenoids in the soil horizons around *Pinus halepensis* trees. *Soil Biol. Biochem.* 40, 2937–2947. doi: 10.1016/j.soilbio.2008.08.008

Ashrafi, S., Helaly, S., Schroers, H.-J., Stadler, M., Richert-Poeggeler, K., Dababat, A., et al. (2017). *Ijuhya vitellina* sp. Nov., a novel source for chaetoglobosin a, is a destructive parasite of the cereal cyst nematode *Heterodera filipjevi*. *PloS One* 12, e0180032. doi: 10.1 371/journal.pone.0180032

Asif, M., Rehman, B., Parihar, K., Ganai, M. A., and Siddiqui, M. A. (2015). Effect of various physico-chemical factors on the incidence of root knot nematode *Meloidogyne* spp. infesting tomato in district Aligarh (Uttar Pradesh) India. *J. Plant Sci.* 10, 234–243. doi: 10.3923/jps.2015.234.243

Backer, R., Rokem, J. S., Ilangumaran, G., Lamont, J., Praslickova, D., Ricci, E., et al. (2018). Plant growth-promoting rhizobacteria: Context, mechanisms of action, and roadmap to commercialization of biostimulants for sustainable agriculture. *Front. Plant Sci.* 9, 1473. doi: 10.3389/fpls.2018.01473

Badri, D. V., Quintana, N., El Kassis, E. G., Kim, H. K., Choi, Y. H., Sugiyama, A., et al. (2009). An ABC transporter mutation alters root exudation of phytochemicals that provoke an overhaul of natural soil microbiota. *Plant Physiol.* 151, 2006–2017. doi: 10.1104/pp.109.147462

Bais, H. P., Walker, T., Schweizer, H., and Vivanco, J. M. (2002). Root specific elicitation and antimicrobial activity of rosmarinic acid in hairy root cultures of *Ocimum basilicum*. *Plant Physiol. Biochem.* 40, 983–995. doi: 10.1016/S0981-9428(02)01460-2

Bais, H. P., Weir, T., Perry, L. G., Gilory, S., and Vivanco, J. M. (2006). The role of root exudates in rhizosphere interactions with plants and other organisms. *Annu. Rev. Plant Biol.* 57, 233–266. doi: 10.1146/annurev.arplant.57.032905.105159

Baligar, V. C., and Fageria, N. K. (1997). "Nutrient use efficiency in acid soils: nutrient management and plant use efficiency," in *Plant soil interactions at low pH: Sustainable agriculture and forestry production*. Eds. A. C. Moniz, A. M. C. Furlani, R. E. Schaffert, N. K. Fageria, C. A. Rosolem and H. Cantarella (Brazilian Soil Science Society, Campinas, Vicosa), 75–96.

Barrow, N. J., and Hartemink, A. E. (2023). The effects of pH on nutrient availability depend on both soils and plants. *Plant Soil* 487, 21–37. doi: 10.1007/s11104-023-05960-5

Bassler, B. L. (1999). How bacteria talk to each other: regulation of gene expression by quorum sensing. *Curr.Opin. Microbiol.* 2, 582–587. doi: 10.1016/S1369-5274(99)00025-9

Berendsen, R. L., Pieterse, C. M. J., and Bakker, P. A. H. M. (2012). The rhizosphere microbiome and plant health. *Trends Plant Sci.* 17, 478–486. doi: 10.1016/j.tplants.2012.04.001

Berendsen, R. L., Vismans, G., Yu, K., Song, Y., de Jonge, R., Burgman, W. P., et al. (2018). Disease-induced assemblage of a plant-beneficial bacterial consortium. *ISME J.* 12, 1496–1507. doi: 10.1038/s41396-018-0093-1

Berg, G., Opelt, K., Zachow, C., Lottmann, J., GÖtz, M., Costa, R., et al. (2006). The rhizosphere effect on bacteria antagonistic towards the pathogenic fungus *Verticillium* differs depending on plant species and site. *FEMS Microbiol. Ecol.* 56, 250–261. doi: 10.1111/fem.2006.56.issue-2

Bernard, G. C., Egnin, M., and Bonsi, C. (2017). The impact of plant-parasitic nematodes on agriculture and methods of control. *Nematology-concepts diagnosis control* 1, 121–151. doi: 10.5772/intechopen.68958

Bird, A. F. (2004). "Surface adhesion to nematodes and its consequences," in *Nematology: Advances and Perspectives*. Eds. Z. X. Chen, S. Chen and D. W. Dickson (CABI Publishing, Wallingford), 295–392.

Biswas, A., Dasgupta, S., Das, S., and Abraham, A. (2007). A synergy of differential evolution and bacterial foraging optimization for global optimization. *Neural Netw. World* 17, 607.

Bogati, K., and Walczak, M. (2022). The impact of drought stress on soil microbial community, enzyme activities and plants. *Agron.* 12, 189. doi: 10.3390/agronomy12010189

Bongers, T., and Bongers, M. (1998). Functional diversity of nematodes. *App. Soil Ecol.* 10, 239–251. doi: 10.1016/S0929-1393(98)00123-1

Bongers, T., and Ferris, H. (1999). Nematode community structure as a bioindicator in environmental monitoring. *Trends Ecol. Evol.* 14, 224–228. doi: 10.1016/S0169-5347(98)01583-3

Bongers, T., van der Mulen, H., and Kortals, G. (1997). Inverse relationship between nematode maturity indexes and plant-parasitic index under enriched nutrient conditions. *Appl. Soil Ecol.* 6, 195–199. doi: 10.1016/S0929-1393(96)00136-9

Bordenstein, S. R., and Theis, K. R. (2015). Host biology in light of the microbiome: ten principles of holobionts and hologenomes. *PloS Biol.* 13, e1002226. doi: 10.1371/journal.pbio.1002226

Broeckling, C. D., Broz, A. K., Bergelson, J., Manter, D. K., and Vivanco, J. M. (2008). Root exudates regulate soil fungal community composition and diversity. *Appl. Environ. Microbiol.* 74, 738–744. doi: 10.1128/AEM.02188-07

Bulgarelli, D., Garrido-Oter, R., Münch, P. C., Weiman, A., Dröge, J., Pan, Y., et al. (2015). Structure and function of the bacterial root microbiota in wild and domesticated barley. *Cell Host Microbe* 17, 392–403. doi: 10.1016/j.chom.2015.01.011

Bulluck, L. R. III, Barker, K. R., and Ristaino, J. B. (2002). Organic and synthetic fertility amendments influence soil microbial, physical and chemical properties on organic and conventional farms. *Appl. Soil Ecol.* 19, 147–160. doi: 10.1016/S0929-1393(01)00187-1

Cao, Y., Lu, N., Yang, D., Minghe, M., Zhang, K. Q., Li, C., et al. (2023). Root-knot nematode infections and soil characteristics significantly affected microbial community composition and assembly of tobacco soil microbiota by a large-scale comparison in tobacco-growing areas. *Front. Microbiol.* 14, 1282609. doi: 10.3389/fmicb.2023.1282609

Cao, Y., Tian, B., Ji, X., Shang, S., Lu, C., and Zhang, K. (2015). Associated bacteria of different life stages of *Meloidogyne incognita* using pyrosequencing-based analysis. *J. Basic Microb.* 5, 950–960. doi: 10.1002/jobm.201400816

Carvalhais, L. C., Dennis, P. G., Badri, D. V., Kidd, B. N., Vivanco, J. M., and Schenk, P. M. (2015). Linking jasmonic acid signaling, root exudates, and rhizosphere microbiomes. *Mol. Plant Microbe Interact.* 28, 1049–1058. doi: 10.1094/MPMI-01-15-0016-R

Castillo, P., Nico, A. I., Azcón-Aguilar, C., Del Río Rincón, C., Calvet, C., and Jiménez-Diaz, R. M. (2006). Protection of olive planting stocks against parasitism of root-knot nematodes by arbuscular mycorrhizal fungi. *Plant Pathol.* 55, 705–713. doi: 10.1111/j.1365-3059.2006.01400.x

Chai, Y. N., and Schachtman, D. P. (2022). Root exudates impact plant performance under abiotic stress. *Trends Plant Sci.* 27, 80–91. doi: 10.1016/j.tplants.2021.08.003

Chandra, S., Askari, K., and Kumari, M. (2018). Optimization of indole acetic acid production by isolated bacteria from stevia rebaudiana rhizosphere and its effects on plant growth. *J. Genet. Eng. Biotechnol.* 16, 581–586. doi: 10.1016/j.jgeb.2018.09.001

Chaparro, J. M., Badri, D. V., and Vivanco, J. M. (2014). Rhizosphere microbiome assemblage is affected by plant development. *ISME J.* 8, 790–803. doi: 10.1038/ismej.2013.196

Chen, Y., Yao, Z., Sun, Y., Wang, E., Tian, C., Sun, Y., et al. (2022). Current studies of the effects of drought stress on root exudates and Rhizosphere microbiomes of crop plant species. *Int. J. Mol. Sci.* 23, 2374. doi: 10.3390/ijms23042374

Chen, Z. X., and Dickson, D. W. (1998). Review of *Pasteuria penetrans* : biology, ecology, and biological control potential. *J. Nematol.* 30, 313–340.

Ciancio, A. (2018). Biocontrol potential of Pasteuria spp. for the management of plant parasitic nematodes. *CAB Rev.* 13, 1–13. doi: 10.1079/PAVSNNR201813013

Costa, R., Götz, M., Mrotzek, N., Lottmann, J., Berg, G., and Smalla, K. (2006). Effects of site and plant species on rhizosphere community structure as revealed by molecular analysis of microbial guilds. *FEMS Microbiol. Ecol.* 56, 236–249. doi: 10.1111/fem.2006.56.issue-2

Coyne, D. L., Sahrawa, K. L., and Plowright, R. A. (2004). The influence of mineral fertilizer application and plant nutrition on plant-parasitic nematodes in upland and lowland rice in Côte d'Ivoire and its implication in long-term agricultural research trials. *Exp. Agric.* 40, 245–256. doi: 10.1017/S0014479703001595

Curtis, R. H. C. (2008). Plant-nematode interactions: environmental signals detected by the nematode's chemosensory organs control changes in the surface cuticle and behaviour. *Parasite* 15, 310–316. doi: 10.1051/parasite/2008153310

Curtis, R. H. C., Jones, J. T., Davies, K. G., Sharon, E., and Spiegel, Y. (2011). "Plant nematode surfaces," in *Biological Control of Plant-Parasitic Nematodes. Building Coherence Between Microbial Ecology and Molecular Mechanisms*. Eds. K. G. Davies and Y. Spiegel (Springer Science + Business Media, Dordrecht), 115–144. doi: 10.1007/978-1-4020-9648-8_5

Dash, N. P., Kumar, A., Kaushik, M. S., Abraham, G., and Singh, P. K. (2017). Agrochemicals influencing nitrogenase, biomass of N2-fixing cyanobacteria and yield of rice in wetland cultivation. *Biocatal. Agric. Biotechnol.* 9, 28–34. doi: 10.1016/j.bcab.2016.11.001

Davies, K. G., and Curtis, R. H. C. (2011). Cuticle surface coat of plant-parasitic nematodes. *Annu. Rev. Phytopathol.* 49, 135–156. doi: 10.1146/annurev-phyto-121310-111406

Davila-Negron, M., and Dickson, D. W. (2013). Comparative thermal time requirements for development of *Meloidogyne arenaria*, *M. incognita*, and *M. javanica*, at constant temperatures. *Nematropica* 43, 152–163.

Decho, A. W., Frey, R., and Ferry, J. L. (2011). Chemical challenges to bacterial AHL signaling in the environment. *Chem. Rev.* 111, 86–99. doi: 10.1021/cr100311q

Desaeger, J. A., Wram, C., and Zasada., I. (2020). New reduced-risk agricultural nematicides- rationale and review. *J. @ Nematol* 52, e2020-91. doi: 10.21307/jofnem-2020-091

Devi, T. C., Bharathalakshmi, M., Kumari, M. B. G. S., and Naidu, N. V. (2012). Effect of sources and levels of phosphorus with zinc on yield and quality of sugarcane. *Sugar Tech.* 14, 195–198. doi: 10.1007/s12355-012-0144-2

Devran, Z., and Sögüt, M. A. (2010). Occurrence of virulent root-knot nematode populations on tomatoes bearing the Mi-gene in protected vegetable-growing areas of Turkey. *Phytoparasitica* 38, 245–251. doi: 10.1007/s12600-010-0103-y

Dewangan, S. K., Shrivastava, S. ,. K., Kumari, L., Minj, P., and Kumari, J. (2023). The effects of soil pH on soil health and environmental sustainability: a review. *ETIR* 10, 611–616.

Diacono, M., and Montemurro, F. (2010). Long-term effects of organic amendments on soil fertility: a review. *Agron. Sustain. Dev.* 30, 401–422. doi: 10.1051/agro/2009040

Dick, R. P. (19921992). A review: long-term effects of agricultural systems on soil biochemical and microbial parameters. *Agric. Ecosyst.Environ.* 40, 25–36. doi: 10.1016/0167-8809(92)90081-L

Doornbos, R., Van Loon, L. C., and Bakker, A. H. M. (2012). Impact of root exudates and plant defense signaling on bacterial communities in the rhizosphere. A review. *Agron. Sustain. Dev.* 32, 227–243. doi: 10.1007/s13593-011-0028-y

Dropkin, V. H. (1969). The necrotic reaction of tomatoes and other hosts resistant to *Meloidogyne*: reversal by temperature. *Phytopathology* 59, 1632–1637.

Duplay, J., Semhi, K., Errais, E., Imfeld, G., Babcsanyi, I., and Perrone, T. (2014). Copper, zinc, lead and cadmium bioavailability and retention in vineyard soils (Rouffach, France): The impact of cultural practices. *Geoderma* 230–231, 318–328. doi: 10.1016/j.geoderma.2014.04.022

Eberlein, C., Heuer, H., Vidal, S., and Westphal, A. (2016). Microbial communities in *Globodera pallida* females raised in potato monoculture soil. *Phytopathology* 106, 581–590. doi: 10.1094/PHYTO-07-15-0180-R

Eche, N. M., Iwuafor, E. N., Amapui, I. Y., and Burns, M. V. (2013). Effects of application of organic and chemical amendments in a continuous cropping system for 10 years on chemical and physical properties of an Alfisol in Northern Guinea Savanna Zone. *Int. J. Agric. Policy Res.* 1, 116–223.

Eisenback, J. D., and Triantaphyllou, H. H. (1991). "Root-knot Nematodes: *Meloidogyne* species and races," in *Manual of Agricultural Nematology*. Ed. W. R. Nickle (Marcel Dekker, New York), 281–286.

Ekschmitt, K., and Korthals, G. W. (2006). Nematodes as sentinels of heavy metals and organic toxicants in the soil. *J. Nematol.* 38, 13–19.

Elasri, M., Delorme, S., Lemanceau, P., Stewart, G., B Laue, B., E Glickmann, E., et al. (2001). Acyl-homoserine lactone production is more common among plant-associated Pseudomonas spp. than among soilborne *Pseudomonas* spp. *Appl. Environ. Microbiol.* 67, 1198–1209. doi: 10.1128/AEM.67.3.1198-1209.2001

Eldeeb, A. M., Farag, A. A. G., Al-Harbi, M. S., Kesba, H., Sayed, S., Elesawy, A. E., et al. (2022). Controlling of *Meloidogyne incognita* (Tylenchida: Heteroderidae) using nematicides, *Linum usitatissimum* extract and certain organic acids on four peppers cultivars under greenhouse conditions. *Saudi J. Biol. Sci.* 29, 3107–3113. doi: 10.1016/j.sjbs.2022.03.018

El-Hadad, M., Mustafa, M., Selim, S. M., El-Tayeb, T., Mahgoob, A., and Aziz, N. H. A. (2011). The nematicidal effect of some bacterial biofertilizers on *Meloidogyne incognita* in sandy soil. *Braz. J. Microbiol.* 42, 105–113. doi: 10.1590/S1517-83822011000100014

Elhady, A., Giné, A., Topalovic, O., Jacquiod, S., Sørensen, S. J., Sorribas, F. J., et al. (2017). Microbiomes associated with infective stages of root-knot and lesion nematodes in soil. *PloS One* 12, e0177145. doi: 10.1371/journal.pone.0177145

Elhady, A., Topalović, O., and Heuer, H. (2021). Plants specifically modulate the microbiome of root-lesion nematodes in the rhizosphere, affecting their fitness. *Microorganisms* 9, 679. doi: 10.3390/microorganisms9040679

Elling, A. A. (2013). Major emerging problems with minor *Meloidogyne* species. *Phytopathology* 103, 1092–1102. doi: 10.1094/PHYTO-01-13-0019-RVW

Elnahal, A. S., El-Saadony, M. T., Saad, A. M., Desoky, E. S. M., El-Tahan, A. M., Rady, M. M., et al. (2022). The use of microbial inoculants for biological control, plant growth promotion, and sustainable agriculture: a review. *Eur. J. Plant Pathol.* 162, 759–792. doi: 10.1007/s10658-021-02393-7

El-Rahman, A., Shaheen, H. A., Abd El-Aziz, R. M., and Ibrahim, D. S. (2019). Influence of hydrogen cyanide-producing rhizobacteria in controlling the crown gall and root-knot nematode, *Meloidogyne incognita*. *Egypt J. Biol. Pest Control.* 29, 1–11. doi: 10.1186/s41938-019-0143-7

Emmert, E. A., Klimowicz, A. K., Thomas, M. G., and Handelsman, J. (2004). Genetics of zwittermicin A production by *Bacillus cereus*. *Appl. Environ. Microbiol.* 70, 104–113. doi: 10.1128/AEM.70.1.104-113.2004

Erktan, A., Or, D., and Scheu, S. (2020). The physical structure of soil: determinant and consequence of trophic interactions. *Soil Biol. Biochem.* 148, 107876. doi: 10.1016/j.soilbio.2020.107876

Evanylo, G., Shorony, C., Spargo, J., Starner, D., Brosius, M., and Haering, K. (2008). Soil and water environmental effects of fertilizer-, manure-and compost-based fertility practices in an organic vegetable cropping system. *Agric. Ecosys. Environ.* 127, 50–58. doi: 10.1016/j.agee.2008.02.014

Fajardo, P. M., Aballay, E. E., and Casanova, P. M. (2011). Soil properties influencing phytoparasitic nematode population on Chilean vineyards. *Chil. J. Agric. Res.* 71, 240–248. doi: 10.4067/S0718-58392011000200009

Ferluga, S., and Venturi, V. (2009). OryR is a LuxR-family protein involved in interkingdom signaling between pathogenic *Xanthomonas oryzae* pv. oryzae and rice. *J. Bacteriol.* 191, 890–897. doi: 10.1128/JB.01507-08

Ferris, H., Sánchez-Moreno, S., and Brennan, E. B. (2012). Structure, function and interguild relationships of the soil nematode assemblage in organic vegetable production. *Appl. Soil Ecol.* 61, 16–25. doi: 10.1016/j.apsoil.2012.04.006

Forge, T. A., and Kempler, C. (2009). Organic mulches influence population densities of root lesion nematodes, soil health indicators and root growth of red raspberry. *Can. J. Plant Pathol.* 31, 241–249. doi: 10.1080/07060660909507597

Forghani, F., and Hajihassani, A. (2020). Recent advances in the development of environmentally benign treatments to control root-knot nematodes. *Front. Plant Sci.* 11. doi: 10.3389/fpls.2020.01125

Foy, C. D., Carter, T. E.Jr., Duke, J. A., and Devine, T. E. (1993). Correlation of shoot and root growth and its role in selecting for aluminium tolerance in soybean. *J. Plant Nutr.* 16, 305–325. doi: 10.1080/01904169309364533

Franchine, J. C., Debiasi, H., Dias, W. P., Ribas, L. N., Silva, J. F. V., and Balbinot, J. A. B. (2018). Relationship among soil properties, root-lesion nematode population, and soybean growth. *Rev. Ciências Agroveterinárias* 17, 30–35. doi: 10.5965/223811711712018030

Freckman, D. W., and Ettema, C. H. (1993). Assessing nematode communities in agroecosystems of varying human intervention. *Agric.Ecosys. Environ.* 45, 239–261. doi: 10.1016/0167-8809(93)90074-Y

Gamalero, E., and Glick, B. R. (2020). The use of plant growth-promoting bacteria to prevent nematode damage to plants. *Biology* 9, 381. doi: 10.3390/biology9110381

Garcia, N., Grenier, E., Buisson, A., and Folcher, L. (2022). Diversity of plant parasitic nematodes characterized from fields of the french national monitoring programme for the columbia root-knot nematode. *PloS One* 17 (3), e0265070. doi: 10.1371/journal.pone.0265070

Gao, M., Teplitski, M., Robinson, J. B., and Bauer, W. D. (2003). Production of substances by *Medicago truncatula* that affect bacterial quorum sensing. *Mol. Plant Microbe Interact.* 16, 827–834. doi: 10.1094/MPMI.2003.16.9.827

Gentili, R., Ambrosini, R., Montagnani, C., Caronni, S., and Citterio, S. (2018). Effect of soil pH on the growth, reproductive investment, and pollen allergenicity of *Ambrosia artemisiifolia* L. *Front. Plant Sci.* 9. doi: 10.3389/fpls.2018.01335

Gheysen, G., and Mitchum, M. G. (2011). How nematodes manipulate plant development pathways for infection. *Curr. Opin. Plant Biol.* 14, 415–421. doi: 10.1016/j.pbi.2011.03.012

Gine, A., Carrasquilla, M., Martínez-Alonso, M., Gaju, N., and Sorribas, F. J. (2016). Characterization of soil suppressiveness to root-knot nematodes in organic horticulture in plastic greenhouse. *Front. Plant Sci.* 7, 164. doi: 10.3389/fpls.2016.00164

Gine, A., Monfort, P., and Sorribas, F. J. (2021). Creation and validation of a temperature-based phenology model for *Meloidogyne incognita* on common bean. *Plants* 10, 240. doi: 10.3390/plants10020240

Glick, B. R., Cheng, Z., Czarny, J., and Duan, J. (2007). Promotion of plant growth by ACC deaminase-producing soil bacteria. *Eur. J. Plant Pathol.* 119, 329–339. doi: 10.1007/s10658-007-9162-4

Glover, J. D., Culman, S. W., Dupont, S. T., Broussard, W., Young, L., Mangan, M. E., et al. (2010). Harvested perennial grasslands provide ecological benchmarks for agricultural sustainability. *Agric. Ecosys.Environ.* 137, 3–12. doi: 10.1016/j.agee.2009.11.001

Gowda, A. P. A., Pankaj,, Singh, D., Awani Kumar Sing, A. ,. K., and Sowmya, R. (2022). Nematicidal potential of plant growth-promoting rhizobacteria against Meloidogyne incognita infesting tomato under protected cultivation. *Egypt. J. Biol. Pest Control* 32, 145. doi: 10.1186/s41938-022-00643-2

Griffitts, J. S., Haslam, S. M., Yang, T., Garczynski, S. F., Mulloy, B., Morris, H., et al. (2005). Glycolipids as receptors for *Bacillus thuringiensis* crystal toxin. *Science* 307, 922–925. doi: 10.1126/science.1104444

Guenther, A. B., Zimmerman, P. R., Harley, P. C., Monson, R. K., and Fall, R. (1993). Isoprene and monoterpene emission rate variability: Model evaluations and sensitivity analyses. *J. Geophys. Res.* 98, 609–12,617. doi: 10.1029/93JD00527

Habash, S., and Al-Banna, L. (2011). Phosphonate fertilizers suppressed root knot nematodes *Meloidogyne javanica* and *M. incognita*. *J. Nematol.* 43, 95–100.

Habteweld, A., Brainard, D., Kravchencko, A., Grewal, P. S., and Melakeberhan, H. (2020a). Effects of integrated application of plant-based compost and urea on soil food web, soil properties, and yield and quality of a processing carrot cultivar. *J. Nematol.* 52, e2020–e2111. doi: 10.21307/jofnem-2020-111

Habteweld, A. W., Brainard, D. C., Kravchenko, A. N., Grewal, P. S., and Melakeberhan, H. (2018). Effects of plant and animal waste-based compost amendments on soil food web, soil properties, and yield and quality of fresh market and processing carrot cultivars. *Nematology* 20, 147–168. doi: 10.1163/15685411-00003130

Habteweld, A., Brainard, D., Kravchenko, A., Grewal, P. S., and Melakeberhan, H. (2020b). Characterizing nematode communities in carrot fields and their bioindicator role for soil health. *Nematropica* 50, 200–210.

Habteweld, A., Kravchenko, A. N., Grewal, P. S., and Melakeberhan, H. (2022). A nematode community-based integrated productivity efficiency (IPE) model that identifies sustainable soil health outcomes: A case of compost application in carrot production. *Soil Syst.* 6, 35. doi: 10.3390/soilsystems6020035

Hamid, M. I., Hussain, M., Wu, Y., Zhang, X., Xiang, M., and Liu, X. (2017). Successive soybean-monoculture cropping assembles rhizosphere microbial communities for the soil suppression of soybean cyst nematode. *FEMS Microbiol. Ecol.* 93, fiw222. doi: 10.1093/femsec/fiw222

Hartmann, M., and Six, J. (2023). Soil structure and microbiome functions in agroecosystems. *Nat. Rev. Earth Environ.* 4, 4–18. doi: 10.1038/s43017-022-00366-w

Hatfield, J. L., and Prueger, J. H. (2015). Temperature extremes: Effect on plant growth and development. *Weather Clim* 10, 4–10. doi: 10.1016/j.wace.2015.08.001

Hein, J., Wolfe, G. V., and Blee, K. A. (2008). Comparison of rhizosphere bacterial communities in *Arabidopsis thaliana* mutants for systemic acquired resistance. *Microb. Ecol.* 55, 333–343. doi: 10.1007/s00248-007-9279-1

Hemmati, S., and Saeedizadeh, A. (2019). Root-knot nematode, *Meloidogyne javanica*, in response to soil fertilization. *Braz. J. Biol.* 80, 621–630. doi: 10.1590/1519-6984.218195

Hepler, P. K. (2005). Calcium: a central regulator of plant growth and development. *Plant Cell* 17, 2142–2155. doi: 10.1105/tpc.105.032508

Holtzmann, O. V. (1965). Effect of soil temperature on resistance of tomato to root-knot nematode (*Meloidogyne incognita*). *Phytopathol.* 55, 990–992.

Hu, H., Tang, C., and Rengel, Z. (2005). Role of phenolics and organic acids in phosphorus mobilization in calcareous and acidic soils. *J. Plant Nutr.* 28, 1427–1439. doi: 10.1081/PLN-200067506

Huber, D. M., and Jones, J. B. (2013). The role of magnesium in plant disease. *Plant Soil* 368, 73–85. doi: 10.1007/s11104-012-1476-0

Hurd, E. A. (1968). Growth of roots of seven varieties of spring wheat at high and low moisture levels. *Agron. J.* 60, 201–205. doi: 10.2134/agronj1968.00021962006000020018x

Hussain, M., Hamid, M. I., Tian, J., Hu, J., Zhang, X., Chen, J., et al. (2018). Bacterial community assemblages in the rhizosphere soil, root endosphere and cyst of soybean cyst nematode-suppressive soil challenged with nematodes. *FEMS Microbiol. Ecol.* 94, fiy142. doi: 10.1093/femsec/fiy142

Insam, H., and Seewald, M. S. A. (2010). Volatile organic compounds (VOCs) in soils. *Biol. Fert. Soils* 46, 199–213. doi: 10.1007/s00374-010-0442-3

Islam, W., Noman, A., Naveed, H., Huang, Z., and Chen, H. Y. H. (2020). Role of environmental factors in shaping the soil microbiome. *Env. Sci. pollut. Res.* 27, 41225–41247. doi: 10.1007/s11356-020-10471-2

Jiang, C., Fan, Z., Li, Z., Niu, D., Li, Y., Zheng, M., et al. (2020). *Bacillus cereus* AR156 triggers induced systemic resistance against *Pseudomonas syringae* pv. tomato DC3000 by suppressing miR472 and activating CNLs-mediated basal immunity in *Arabidopsis*. *Mol. Plant Pathol.* 21, 854–870. doi: 10.1111/mpp.12935

Jones, F. G. W. (1975). The soil as an environment for plant parasitic nematodes. *Ann. Appl. Biol.* 79, 113–139. doi: 10.1111/j.1744-7348.1975.tb01527.x

Jones, J. T., Haegeneman, A., Danchin, E. G. J., Gaur, H. S., Helder, J., Jones, M. G. K., et al. (2013). Top 10 plant-parasitic nematodes in molecular plant pathology. *Mol. Plant Pathol.* 14, 946–961. doi: 10.1111/mpp.12057

Juszczuk, I. M., Wiktorowska, A., Malusa, E., Anna, M., and Rychter, A. M. (2004). Changes in the concentration of phenolic compounds and exudation induced by phosphate deficiency in bean plants (*Phaseolus vulgaris* L.). *Plant Soil* 267, 41–49. doi: 10.1007/s11104-005-2569-9

Kabir, E. B., Bashari, H., Mosaddeghi, M. R., and Bassiri, M. (2017). Soil aggregate stability and organic matter as affected by land-use change in central Iran. *Arch. Agron. Soil Sci.s* 63, 1823–1837. doi: 10.1080/03650340.2017.1308492

Kantor, M., Handoo, Z., Kantor, C., and Carta, L. (2022). Top ten most important US-regulated and emerging plant-parasitic nematodes. *Horticulturae* 8, 208. doi: 10.3390/horticulturae8030208

Kantor, M., Levi, A., Thies, J., Guner, N., Kantor, C., Parnham, S., et al. (2018). NMR analysis reveals a wealth of metabolites in root-knot nematode resistant roots of watermelon plants. *J. Nematol.* 50, 303–316. doi: 10.21307/jofnem-2018-030

Karajeh, M. R., and Al-Nasir, F. M. (2012). Effects of nitrogen fertilizers on the Javanese root-knot nematode *Meloidogyne javanica* and its interaction with cucumber. *Arch. Phytopathol. Plant Prot.* 45, 2177–2188. doi: 10.1080/03235408.2012.724968

Karajeh, M. R., and Al-Nasir, F. M. (2014). Field assessment of efficacy of nitrogen salts to control the root-knot nematode (*Meloidogyne javanica*) on tomato. *Arch. Phytopathol.* 47, 1912–1920. doi: 10.1080/03235408.2013.861986

Karssen, G., and Moens, M. (2006). "Root-knot nematodes," in *Plant nematology*. Eds. R. N. Perry and M. Moens (CABI, Wallingford, UK), 59–90.

Katooli, N., Moghadam, E., Taheri, A., and Nasrollahnejad, S. (2010). Management of root-knot nematode (*Meloidogyne incognita*) on cucumber with the extract and oil of nematicidal plants. *Int. J. Agric. Res.* 5, 582–586. doi: 10.3923/ijar.2010.582.586

Kesba, H., and Al-Shalaby, M. (2008). Survival and reproduction of *Meloidogyne incognita* on tomato as affected by humic acid. *Nematology* 10, 243–249. doi: 10.1163/156854108783476304

Khan, A., Wesemael, W., and Moens, M. (2014). Influence of temperature on the development of the temperate root-knot nematodes *Meloidogyne chitwoodi* and *M. fallax*. *Russ. J. Nematol.* 22, 1–9.

Kochian, L. V., Pineros, M. A., and Hoekenga, O. A. (2005). The physiology, genetics, and molecular biology of plant aluminum resistance and toxicity. *Plant Soil* 274, 175–195. doi: 10.1007/s11104-004-1158-7

Kong, H. G., Song, G. C., Sim, H.-J., and Ryu, C.-M. (2021). Achieving similar root microbiota composition in neighboring plants through airborne signaling. *ISME J.* 15, 397–408. doi: 10.1038/s41396-020-00759-z

Kramshøj, M., Albers, C. N., Svendsen, S. H., Björkman, M. P., Lindwall, F., Björk, R. G., et al. (2019). Volatile emissions from thawing permafrost soils are influenced by meltwater drainage conditions. *Glob. Change Biol.* 25, 1704–1716. doi: 10.1111/gcb.14582

Kumar, U., Berliner, J., Adak, T., Rath, P. C., Dey, A., Pokhare, S. S., et al. (2017). Non-target effect of continuous application of chlorpyrifos on soil microbes, nematodes and its persistence under sub-humid tropical ricee cropping system. *Ecotoxicol. Environ. Saf.* 135, 225–235. doi: 10.1016/j.ecoenv.2016.10.003

Lakshmanan, V., Selvaraj, G., and Bais, H. P. (2014). Functional soil microbiome: belowground solutions to an aboveground problem. *Plant Physiol.* 166, 689–700. doi: 10.1104/pp.114.245811

Lal, R. (2008). Soils and sustainable agriculture. A review. *Agron. Sustain. Dev.* 28, 57–64. doi: 10.1051/agro:2007025

Landa, B. B., Aranda, S., Montes-Borrego, M., Soriano, M. A., Gómez, J. A., and Navas-Corés, J. A. (2014). Soil factors involved in the diversity and structure of soil bacterial communities in commercial organic olive orchards in Southern Spain. *Environ. Microbiol. Rep.* 6, 196–207. doi: 10.1111/1758-2229.12148

Lee, Y. S., Nguyen, X. H., Naing, K. W., Park, Y. S., and Kim, K. Y. (2015). Role of lytic enzymes secreted by *Lysobacter capsici* YS1215 in the control of root-knot nematode of tomato plants. *Indian J. Microbiol.* 55, 74–80. doi: 10.1007/s12088-014-0499-z

Lee, S. M., and Ryu, C. M. (2021). Algae as new kids in the beneficial plant microbiome. *Front. Plant Sci.* 12. doi: 10.3389/fpls.2021.599742

Li, W., He, P., and Jin, J. (2010). Effect of potassium on ultrastructure of maize stalk pith and young root and their relation to stalk rot resistance. *Agric. Sci. China* 9, 1467–1474. doi: 10.1016/S1671-2927(09)60239-X

Li, X., Hu, H.-J., Li, J.-Y., Wang, C., Chen, S.-L., and Yan, S.-Z. (2019a). Effects of the endophytic bacteria *Bacillus cereus* BCM2 on tomato root exudates and *Meloidogyne incognita* infection. *Plant Dis.* 103, 1551–1558. doi: 10.1094/PDIS-11-18-2016-RE

Li, X., Jousset, A., de Boer, W., Carrión, V. J., Zhang, T., Wang, X., et al. (2019b). Legacy of land use history determines reprogramming of plant physiology by soil microbiome. *ISME J.* 13, 738–751. doi: 10.1038/s41396-018-0300-0

Liao, C., Tian, Q., and Liu, F. (2021). Nitrogen availability regulates deep soil priming effect by changing microbial metabolic efficiency in a subtropical forest. *J. For. Res.* 32, 713–723. doi: 10.1007/s11676-020-01148-0

Lin, H. J., and McClure, M. A. (1996). Surface coat of *Meloidogyne incognita*. *J. Nematol.* 28, 216–224.

Lira, R. M., Silva, E. F. F., Silva, G. F., Souza, D. H. S., Pedrosa, E. M. R., and Gordin, L. C. (2019). Content, extraction and export of nutrients in sugarcane under salinity and leaching fraction. *Rev. Bras. Engenharia Agrícola e Ambiental* 23, 432–438. doi: 10.1590/1807-1929/agriambi.v23n6p432-438

Liu, C., Timper, P., Ji, P., Mekete, T., and Joseph, S. (2017). Influence of root exudates and soil on attachment of *Pasteuria penetrans* to *Meloidogyne arenaria*. *J. Nematol.* 49, 304–310. doi: 10.21307/jofnem-2017-076

Lugtenburg, B., and Kamilova, F. (2009). Plant-growth-promoting rhizobacteria. *Annu. Rev. Microbiol.* 63, 541–5556. doi: 10.1146/annurev.micro.62.081307.162918

Lundberg, D. S., Lebeis, S. L., Paredes, S. H., Yourstone, S., Gehring, J., Malfatti, S., et al. (2012). Defining the core *Arabidopsis thaliana* root microbiome. *Nature* 488, 86–90. doi: 10.1038/nature11237

Martínez-Medina, A., Fernandez, I., Lok, G. B., Pozo, M. J., Pieterse, C. M., Saskia, C. M., et al. (2017). Shifting from priming of salicylic acid-to jasmonic acid-regulated defences by *Trichoderma* protects tomato against the root knot nematode *Meloidogyne incognita*. *New Phytol.* 213, 1363–1377. doi: 10.1111/nph.14251

Mateille, T., Tavoillot, J., Martiny, B., and Fargette, M. (2014). Importance of soil characteristics for plant-parasitic nematode communities in European coastal foredunes. *Eur. J. Soil Biol.* 64, 53–60. doi: 10.1016/j.ejsobi.2014.08.002

McSorley, R., and Dickson, D. W. (1990). Vertical distribution of plant-parasitic nematodes in sandy soil under maize. *Plant Soil* 123, 95–100. doi: 10.1007/BF00009931

Medina, N. H., Branco, M. L. T., da Silveira, M. A. G., and Santos, R. B. B. (2013). Dynamic distribution of potassium in sugarcane. *J. Environ. Radioact.* 126, 172–175. doi: 10.1016/j.jenvrad.2013.08.004

Meena, K. S., Jonathan, E., Devrajan, K., and Raguchander, T. (2012). *Pseudomonas fluorescens* induced systemic resistance in tomato against *Meloidogyne incognita*. *Indian J. Nematol.* 42, 5–10.

Melakeberhan, H., Dey, J., Baligar, V. C., and Carter, JR, T. E. (2004). Effect of soil pH on the pathogenesis of *Heterodera glycines* and *Meloidogyne incognita* on *Glycine max* genotypes. *Nematology* 6, 585–592. doi: 10.1163/1568541042665205

Mena, J., Pimentel, E., Hernandez, A., Veloz, L., Vazquez, R., Leon, L., et al. (2002). Mechanism of action of *Corynebacterium pauronetabolum* strain C-924 on nematodes. *Nematology* 4, 287.

Mendy, B., Wang'ombe, M. W., Radakovic, Z. S., Holbein, J., Ilyas, M., Chopra, D., et al. (2017). *Arabidopsis* leucine-rich repeat receptor-like kinase NILR1 is required for induction of innate immunity to parasitic nematodes. *PloS Pathog.* 13, e1006284. doi: 10.1371/journal.ppat.1006284

Meyer, S. L., Halbrendt, J. M., Carta, L. K., Skantar, A. M., Liu, T., Abdelnabby, H. M., et al. (2009). Toxicity of 2, 4-diacetylphloroglucinol (DAPG) to plant-parasitic and bacterial-feeding nematodes. *J. Nematol.* 41, 274–280.

Milner, J., Silo-Suh, L., Lee, J. C., He, H., Clardy, J., and Handelsman, J. (1996). Production of kanosamine by *Bacillus cereus* UW85. *Appl. Environ. Microbiol.* 62, 3061–3065. doi: 10.1128/aem.62.8.3061-3065.1996

Moldrup, P., Olesen, T., Schjønning, P., Yamaguchi, T., and Rolston, D. (2000). Predicting the gas diffusion coefficient in undisturbed soil from soil water characteristics. *Soil Sci. Soc Am. J.* 64, 94–100. doi: 10.2136/sssaj2000.64194x

Msimbira, L. A., and Smith, D. L. (2020). The roles of plant growth promoting microbes in enhancing plant tolerance to acidity and alkalinity stresses. *Front. Sustain. Food Systems. Sec. Crop Biol. Sustainability* 4. doi: 10.3389/fsufs.2020.00106

Myo, E. M., Ge, B., Ma, J., Cui, H., Liu, B., Shi, L., et al. (2019). Indole-3-acetic acid production by *Streptomyces fradiae* NKZ-259 and its formulation to enhance plant growth. *BMC Microbiol.* 19, 1–14. doi: 10.1186/s12866-019-1528-1

Natsheh, B., and Mousa, S. (2014). Effect of organic and inorganic fertilizers application on soil and cucumber (*Cucumis sativa* L.) plant productivity. *Int. J. @ Agric.* 4, 166–170. doi: 10.5923/j.ijaf.20140403.03

Neal, A. L., Ahmad, S., Gordon-Weeks, R., and Ton, J. (2012). Benzoxazinoids in root exudates of maize attract *Pseudomonas putida* to the rhizosphere. *PloS One* 7, e35498. doi: 10.1371/journal.pone.0035498

Ngeno, D. C., Murungi, L. K., Fundi, D. I., Wekesa, V., Haukeland, S., and Mbaka, J. (2019). Soil chemical properties influence abundance of nematode trophic groups and *Ralstonia solanacearum* in high tunnel tomato production. *AAS Open Res.* 2, 3. doi: 10.12688/aasopenres.12932.1

Nicol, J., Turner, S., Coyne, D., den Nijs, L., Hockland, S., and Maafi, Z. T. (2011). "Current nematode threats to world agriculture," in *Genomics and molecular genetics of plant-nematode interactions*. Eds. J. Jones, G. Gheysen and C. Fenoll (Springer, Dordrecht), 21–43.

Nisa, R., Tantray, A. Y., Kouser, N., Allie, K. A., Wani, S. M., Alamri, S. A., et al. (2021). Influence of ecological and edaphic factors on biodiversity of soil nematodes. *Saudi J. Biol. Sci.* 28, 3049–3059. doi: 10.1016/j.sjbs.2021.02.046

Noronha, M. A., Fernandes, M. F., Muniz, M. F. S., Pedrosa, E. M. R., Assunção, M. C., and Calheiros, L. D. S. (2021). Soil abiotic factors associated with meloidogyne spp. and pratylenchus spp. populations in sugarcane. *Nematology* 23, 125–137. doi: 10.1163/15685411-bja10033

Norton, D. C. (1989). Abiotic soil factors and plant-parasitic nematode communities. *J. Nematol.* 21, 299e307.

Nuaima, R. H., Ashrafi, S., Maier, W., and Heuer, H. (2021). Fungi isolated from cysts of the beet cyst nematode parasitized its eggs and counterbalanced root damages. *J. Pest Sci.* 94, 563–572. doi: 10.1007/s10340-020-01254-2

Odunze, A. C., Jinshui, W., Shoulong, L., Hanhua, Z., Tida, G., Yi, W., et al. (2012). Soil quality changes and quality status: a case study of the subtropical China Region Ultisol. *Br. J. Environ. Climate Change* 2, 37–57. doi: 10.9734/BJECC/2012/1148

Oka, Y. (2019). Survival of meloidogyne javanica during the summer season under semiarid conditions. *Eur. J. Plant Pathol.* 155, 917–926. doi: 10.1007/s10658-019-01823-x

Omae, N., and Tsuda, K. (2022). Plant-microbiota interactions in abiotic stress environments. *MPMI* 35, 511–526. doi: 10.1094/MPMI-11-21-0281-FI

Oquist, K. A., Strock, J. S., and Mulla, D. J. (2007). Influence of alternative and conventional farming practices on subsurface drainage and water quality. *J. Environ. Qual.* 36, 1194–1204. doi: 10.2134/jeq2006.0274

Otobe, K., Itou, K., and Mizukubo, T. (2004). Micro-moulded substrates for the analysis of structure-dependent behavior of nematodes. *Nematology* 6, 73–77. doi: 10.1163/156854104323072946

Ou, W., Liang, W., Jiang, Y., Li, Q., and Wen, D. (2005). Vertical distribution of soil nematodes under different land use types in an aquic brown soil. *Pedobiologia* 49, 139–148. doi: 10.1016/j.pedobi.2004.10.001

Pal, K. K., and Gardener, B. M. (2006). Biological control of plant pathogens. *Plant Health Instr*. doi: 10.1094/PHI-A-2006-1117-02

Palomares-Rius, J. E., Castillo, P., Montes-Borrego, M., Juan A. Navas-Cortés, J. A., Blanca, B., and Landa, B. B. (2015). Soil properties and olive cultivar determine the structure and diversity of plant-parasitic nematode communities infesting olive orchards soils in southern Spain. *PloS One* 10, e0116890. doi: 10.1371/journal.pone.0116890

Pankaj, S. H., Gaur, H. S., and Singh, A. K. (2006). Effect of zero tillage on the nematode fauna in a rice-wheat cropping system. *Nematol. Medit.* 34, 175–178.

Park, B.-Y., Lee, J.-K., Ro, H.-M., and Ho Kim, Y. H. (2011). Effects of heavy metal contamination from an abandoned mine on tomato growth and root-knot nematode development. *Plant Pathol. J.* 27, 266–271. doi: 10.5423/PPJ.2011.27.3.266

Patil, J., Miller, A. J., and Gaur, H. S. (2013). Effect of nitrogen supply form on the invasion of rice roots by the root-knot nematode, *Meloidogyne graminicola*. *Nematology* 15, 483–492. doi: 10.1163/15685411-00002694

Peiris, P. U. S., Li, Y., Brown, P., and Xu, C. (2020). Efficacy of organic amendments to control Meloidogyne spp. in crops: a systematic review and meta-analysis. *J. Soils Sediments* 20, 1584–1598. doi: 10.1007/s11368-019-02498-x

Penn, C. J., and Camberto, J. J. (2019). A critical review on soil chemical processes that control how soil pH affects phosphorus availability to plants. *Agriculture* 9, 120–138. doi: 10.3390/agriculture9060120

Pimentel, D., Hepperly, P., Hanson, J., Douds, D., and Seidel, R. (2005). Environmental, energetic, and economic comparisons of organic and conventional farming systems. *BioScience* 55, 573–582. doi: 10.1641/0006-3568(2005)055[0573:EEAECO]2.0.CO;2

Poria, V., Dębiec-Andrzejewska, K., Fiodor, A., Lyzohub, M., Ajijah, N., Singh, S., et al. (2022). Plant Growth-Promoting Bacteria (PGPB) integrated phytotechnology: A sustainable approach for remediation of marginal lands. *Front. Plant Sci.* 13. doi: 10.3389/fpls.2022.999866

Poveda, J., Abril-Urias, P., and Escobar, C. (2020). Biological control of plant-parasitic nematodes by filamentous fungi inducers of resistance: *Trichoderma*, mycorrhizal and endophytic fungi. *Front. Microbiol.* 11. doi: 10.3389/fmicb.2020.00992

Pradhan, P., Naresh, P., Barik, S., Acharya, G. C., Bastia, R., Adamala, A. K., et al. (2023). Breeding for root–knot nematode resistance in fruiting Solanaceous vegetable crops: a review. *Euphytica* 219, 71. doi: 10.1007/s10681-023-03204-2

Prot, J. C., and Van Gundy, S. D. (1981a). Influence of photoperiod and temperature on migrations of Meloidogyne juveniles. *J. Nematol.* 13, 217–220.

Prot, J. C., and Van Gundy, S. D. (1981b). Effect of soil texture and the clay component on migration of *Meloidogyne incognita* second-stage juveniles. *J. Nematol.* 13, 213–217.

Rasmann, S., Ali, J. G., Helder, J., and van der Putten, W. H. (2012). Ecology and evolution of soil nematode chemotaxis. *J. Chem. Ecol.* 38, 615–628. doi: 10.1007/s10886-012-0118-6

Rehman, B., Ganai, M. A., Parihar, K., Siddiqui, M. A., and Usman, A. (2012). Management of root knot nematode, *Meloidogyne incognita* affecting chickpea, *Cicer arietinum* for sustainable production. *Biosci. Int.* 1, 1–5.

Rizvi, R., Mahmood, I., Tiyagi, S. A., and Khan, Z. (2012). Conjoint effect of oil-seed cakes and *Pseudomonas fluorescens* on the growth of chickpea in relation to the management of plant-parasitic nematodes. *Braz. Arch. Biol. Technol.* 55, 801–808. doi: 10.1590/S1516-89132012000600001

Roberts, P. A. (2002). "Concepts and consequences of resistance," in *Plant Resistance to Parasitic Nematodes*. Eds. J. L. Starr, R. Cook and J. Bridge (CABI Publishing, Oxon, UK), 23e41.

Roberts, P. A., and Thomason, I. J. (1986). Variability in reproduction of isolates of *M. incognita* and *M. javanica* on resistant tomato genotypes. *Plant Dis.* 70, 547e551. doi: 10.1094/PD-70-547

Roberts, P. A., Van Gundy, S. D., and McKinney, H. E. (1981). Effects of soil temperature and planting date of wheat on *Meloidogyne incognita* reproduction, soil populations, and grain yield. *J. Nematol.* 13, 345–352.

Rudrappa, T., Czymmek, K. J., Paré, P. W., and Bais, H. P. (2008). Root-secreted Malic acid recruits beneficial soil bacteria. *Plant Physiol.* 148, 1547–1556. doi: 10.1104/pp.108.127613

Ryu, C.-M., Farag, M. A., Hu, C.-H., Reddy, M. S., Wie, H.-X., Paré, P. W., et al. (2003). Bacterial volatiles promote growth of *Arabidopsis*. *Proc. Natl. Acad. Sci. U.S.A.* 100, 4927–4932. doi: 10.1073/pnas.0730845100

Santana-Gomes, S. M., Dias-Arieira, C. R., Roldi, M., Dadazio, T. S., Marini, P. M., and Barizao, D. A. O. (2013). Mineral nutrition in the control of nematodes. *Afr. J. Agric. Res.* 8, 2413–2420. doi: 10.5897/AJARx12.008

Sasse, J., Martinoia, E., and Northen, T. (2018). Feed your friends: do plant exudates shape the root microbiome? *Trends Plant Sci.* 23, 25–41. doi: 10.1016/j.tplants.2017.09.003

Saxton, K. E., and Rawls, W. J. (2006). Soil water characteristic estimates by texture and organic matter for hydrologic solutions. *Soil Sci. Soc Am. J.* 70, 1569–1578. doi: 10.2136/sssaj2005.0117

Schaller, G. (1987). pH changes in the rhizosphere in relation to the pH-buffering of soils. *Plant Soil* 97, 439–444. doi: 10.1007/BF02383234

Schmidt, R., Cordovez, V., De Boer, W., Raaijmakers, J., and Garbeva, P. (2015). Volatile affairs in microbial interactions. *ISME J.* 9, 2329. doi: 10.1038/ismej.2015.42

Schulz-Bohm, K., Zweers, H., de Boer, W., and Garbeva, P. (2015). A fragrant neighborhood: volatile mediated bacterial interactions in soil. *Front. Microbiol.* 6. doi: 10.3389/fmicb.2015.01212

Shaffique, S., khan, M. A., Alomrani, S. O., Injamum-Ul-Hoque, M., Odongkara Peter, O., Muhammad Imran, M., et al. (2023). Unlocking the potential of newly isolated phytohormone-producing bacterial strains for enhanced plant growth and stress tolerance. *Plant Stress* 10, 100260. doi: 10.1016/j.stress.2023.100260

Sharifi, R., Jeon, J.-S., and Ryu, C.-M. (2022). Belowground plant–microbe communications via volatile compounds. *J. Exp. Bot.* 73, 463–486. doi: 10.1093/jxb/erab465

Sharifi, R., and Ryu, C. M. (2018). Sniffing bacterial volatile compounds for healthier plants. Curr. Opin. *Plant Biol.* 44, 88–97. doi: 10.1016/j.pbi.2018.03.004

Shiralipour, A., McConnel, D. B., and Smith, W. H. (1992). *Uses and benefits of municipal solid waste compost* (Tarrytown, NY: Biomass and Bioenergy Pergamon Press).

Siddiqui, I. A., Haas, D., and Heeb, S. (2005). Extracellular protease of *Pseudomonas fluorescens* CHA0, a biocontrol factor with activity against the root-knot nematode *Meloidogyne incognita*. *Appl. Environ. Microbiol.* 71, 5646–5649. doi: 10.1128/AEM.71.9.5646-5649.2005

Siddiqui, Z. A., and Mahmood, I. (2001). Effects of rhizobacteria and root symbionts on the reproduction of *Meloidogyne javanica* and growth of chickpea. *Biores. Technol.* 79, 41–45. doi: 10.1016/S0960-8524(01)00036-0

Silva, J. C. P., Nunes, T. C. S., Guimarães, R. A., Pylro, V. S., Lilian, S. A. S., Costa, L. S. A. S., et al. (2022). Organic practices intensify the microbiome assembly and suppress root–knot nematodes. *J. Pest Sci.* 95, 709–721. doi: 10.1007/s10340-021-01417-9

Singh, D., Jain, P., Gupta, A., and Nemal, R. (2013). Soil diversity: a key for natural management of biological and chemical constitute to maintain soil health and fertility. *Int. J. Bio-Science Bio-Technology* 5, 41–49.

Singh, J., Kumar, M. U., and Walia, R. K. (2014). Influence of plant root exudates on the adherence of *Pasteuria penetrans* endospores. *Nematology* 16, 121–124. doi: 10.1163/15685411-00002768

Singh, H. B., Sarma, B. K., and Keswani, C. (2017). *Advances in PGPR research* (UK: CABI). doi: 10.1079/9781786390325.0000

Smercina, D. N., Evans, S. E., Friesen, M. L., and Tiemann, L. K. (2019). To fix or not to Fix: controls on free-living nitrogen fixation in the rhizosphere. *Appl. Environ. Microbiol.* 85, e02546–e02518. doi: 10.1128/AEM.02546-18

Smith, P. G. (1944). Embryo culture of a tomato species hybrid. *Proc. Amer. Soc Horticult. Sci.* 44, 413e416.

Sorribas, F. J., Ornat, C., Verdejo-Lucas, S., Galeano, M., and Valero, J. (2005). Effectiveness and profitability of the *Mi*-resistant tomatoes to control root-knot nematodes. *Eur. J. Plant Pathol.* 111, 29–38. doi: 10.1007/s10658-004-1982-x

Stirling, G. R. (2014). *Biological control of plant-parasitic nematodes: soil ecosystem management in sustainable agriculture* (UK: CABI). doi: 10.1079/9781780644158.0000

Subedi, P., Gattoni, K., Liu, W., Lawrence, K. S., and Park, S.-W. (2020). Current utility of plant growth-promoting rhizobacteria as biological control agents towards plant-parasitic nematodes. *Plants* 9, 1167. doi: 10.3390/plants9091167

Sun, X., Zhang, R., Ding, M., Liu, Y., and Li, L. (2021). Biocontrol of the root-knot nematode *Meloidogyne incognita* by a nematicidal bacterium *Pseudomonas simiae* MB751 with cyclic dipeptide. *Pest Manage. Sci.* 77, 4365–4374. doi: 10.1002/ps.6470

Talavera, M., Verdejo-Lucas, S., Ornat, C., Torres, J., Vela, M. D., Macias, F. J., et al. (2009). Crop rotations with *Mi*-gene resistant and susceptible tomato cultivars for management of root-knot nematodes in plastic houses. *Crop Prot.* 28, 662–667. doi: 10.1016/j.cropro.2009.03.015

Teplitski, M., Chen, H., Rajamani, S., Goa, M., Merighi, M., Sayre, R. T., et al. (2004). *Chlamydomonas reinhardtii* secretes compounds that mimic bacterial signals and interfere with quorum sensing regulation in bacteria. *Plant Physiol.* 134, 137–146. doi: 10.1104/pp.103.029918

Teplitski, M., Robinson, J. B., and Bauer, W. D. (2000). Plants secrete substances that mimic bacterial N-acyl homoserine lactone signal activities and affect population density-dependent behaviors in associated bacteria. *Mol. Plant Microbe Interact.* 13, 637–648. doi: 10.1094/MPMI.2000.13.6.637

Terefe, M., Tefera, T., and Sakhuja, P. (2009). Effect of a formulation of Bacillus firmus on root-knot nematode Meloidogyne incognita infestation and the growth of tomato plants in the greenhouse and nursery. *J. Invertebr. Pathol.* 100, 94–99. doi: 10.1016/j.jip.2008.11.004

Thangavelu, S., and Rao, K. C. (2004). Calcium, magnesium and sulphur uptake by above ground parts in intergeneric hybrids. *Sugar Tech.* 6, 25–33. doi: 10.1007/BF02942614

Tkacz, A., Cheema, J., Chandra, G., Grant, A., and Poole, P. S. (2015). Stability and succession of the rhizosphere microbiota depends upon plant type and soil composition. *ISME J.* 9, 2349–2359. doi: 10.1038/ismej.2015.41

Topalović, O., Bredenbruch, S., Schleker, A. S. S., and Heuer, H. (2020a). Microbes attaching to endoparasitic phytonematodes in soil trigger plant defense upon root penetration by the nematode. *Front. Plant Sci.* 11. doi: 10.3389/fpls.2020.00138

Topalović, O., Bak, F., Santos, S., Sikder, M. M., Sapkota, R., Ekelund, F., et al. (2023). Activity of root-knot nematodes associated with composition of a nematode-attached microbiome and the surrounding soil microbiota. *FEMS Microbiol. Ecol.* 99, 1–11. doi: 10.1093/femsec/fiad091

Topalović, O., Elhady, A., Hallmann, J., Richert-Pöggeler, K. R., and Heuer, H. (2019). Bacteria isolated from the cuticle of plant-parasitic nematodes attached to and antagonized the root-knot nematode *Meloidogyne hapla*. *Sci. Rep.* 9, 11477. doi: 10.1038/s41598-019-47942-7

Topalović, O., and Geisen, S. (2023). Nematodes as suppressors and facilitators of plant performance. *New Phytol.* 238, 2305–2312. doi: 10.1111/nph.18925

Topalović, O., and Heuer, H. (2019). Plant-nematode interactions assisted by microbes in the Rhizosphere. *Curr. Issues Mol. Biol.* 30, 75–88. doi: 10.21775/cimb.030.075

Topalović, O., Heuer, H., Reineke, A., Zinkernagel, J., and Hallmann, J. (2020b). Antagonistic role of the microbiome from a *Meloidogyne hapla* suppressive soil against species of plant-parasitic nematodes with different life strategies. *Nematol.* 22, 75–86. doi: 10.1163/15685411-00003285

Topalović, O., and Vestergård, M. (2021). Can microorganisms assist the survival and parasitism of plant-parasitic nematodes? *Trends Parasitol.* 37, 947–958. doi: 10.1016/j.pt.2021.05.007

Topalović, O., Hussain, M., and Heuer, H. (2020c). Plants and associated soil microbiota cooperatively suppress plant-parasitic nematodes. *Front. Microbiol.* 11. doi: 10.3389/fmicb.2020.00313

Trudgill, D. L. (1995). An assessment of the relevance of thermal time relationships to nematology. *Fundam. Appl. Nematol.* 18, 407–417.

Tsukanova, K., Meyer, J., and Bibikova, T. (2017). Effect of plant growth promoting Rhizobacteria on plant hormone homeostasis. *S. Afr. J. Bot.* 113, 91–102. doi: 10.1016/j.sajb.2017.07.007

Tsuru, A., Hamazaki, Y., Tomida, S., Ali, M. S., Komura, T., Nishikawa, Y., et al. (2021). Nonpathogenic *Cutibacterium acnes* confers host resistance against *Staphylococcus aureus*. *Microbiol. Spec.* 9, e0056221. doi: 10.1128/Spectrum.00562-21

Tyc, O., Song, C., Dickschat, J. S., Vos, M., and Garbeva, P. (2017). The ecological role of volatile and soluble secondary metabolites produced by soil bacteria. *Trends Microbiol.* 25, 280–292. doi: 10.1016/j.tim.2016.12.002

Tyc, O., Zweers, H., de Boer, W., and Garbeva, P. (2015). Volatiles in inter-specific bacterial interactions. *Front. Microbiol.* 6. doi: 10.3389/fmicb.2015.01412

Vachon, V., Laprade, R., and Schwartz, J.-L. (2012). Current models of the mode of action of Bacillus thuringiensis insecticidal crystal proteins: a critical review. *J. Invertebr. Pathol.* 111, 1–12. doi: 10.1016/j.jip.2012.05.001

Van den Berghe, C. H., and Hue, N. V. (1999). Limiting potential of composts applied to an acid Oxisol in Burundi. *Compost Sci. Util.* 7, 40–46. doi: 10.1080/1065657X.1999.10701962

Vejan, P., Abdullah, R., Khadiran, T., Ismail, S., Nasrulhaq,, and Boyce, A. (2016). Role of plant growth promoting rhizobacteria in agricultural sustainability-a review. *Molecules* 21, 573. doi: 10.3390/molecules21050573

Velloso, J. A., Maquilan, M. A., Campos, V. P., Brito, J. A., and Dickson, D. W. (2022). Temperature Effects on Development of *Meloidogyne enterolobii* and *M. floridensis*. *J. Nematol.* 54, e2022–e2021. doi: 10.2478/jofnem-2022-0013

Verdejo-Lucas, S., Blanco, M., Cortada, L., and Sorribas, E. J. (2013). Resistance of tomato rootstocks to *Meloidogyne arenaria* and *Meloidogyne javanica* under intermittent elevated soil temperatures above 28 °C. *Crop Prot.* 46, 57e62. doi: 10.1016/j.cropro.2012.12.013

Verdejo-Lucas, S., Talavera, M., and Andrés, M. F. (2012). Virulence response to the *Mi-1* gene of *Meloidogyne* populations from tomato in greenhouses. *Crop Prot.* 39, 97–105. doi: 10.1016/j.cropro.2012.03.025

Viljoen, J. J., Labuschagne, N., Fourie, H., and Sikora, R. A. (2019). Biological control of the root-knot nematode *Meloidogyne incognita* on tomatoes and carrots by plant growth-promoting rhizobacteria. *Trop. Plant Pathol.* 44, 284–291. doi: 10.1007/s40858-019-00283-2

Wallace, H. R. (1958). Movement of eelworm I. @ the influence of pore size and moisture content of the soil on the migration of larvae of the beet eelworm, *Heterodera schachtii*. *Ann. Appl. Biol.* 46, 74–85. doi: 10.1111/j.1744-7348.1958.tb02179.x

Wallace, H. R. (1973). *Nematode ecology and plant disease* (London: Edward Arnold).

Wallace, H. R., and Bird, A. F. (1965). The influence of temperature on *Meloidogyne hapla* and *M. javanica*. *Nematologica* 11, 581–589. doi: 10.1163/187529265X00726

Wang, K.-H., and McSorley, R. J. (2008). Exposure time to lethal temperatures for *Meloidogyne incognita* suppression and its implication for soil solarization. *J. Nematol.* 40, 7–12.

Wei, C., Zheng, H., Li, Q., Lü, X., Yu, Q., Zhang, H., et al. (2012). Nitrogen addition regulates soil nematode community composition through ammonium suppression. *PloS One* 7, e43384. doi: 10.1371/journal.pone.0043384

Weisskopf, L., Abou-Mansour, E., Fromin, N., Tomasi, N., Santelia, D., Edelkott, I., et al. (2006). White lupin has developed a complex strategy to limit microbial degradation of secreted citrate required for phosphate acquisition. *Plant Cell Environ.* 29, 919–927. doi: 10.1111/j.1365-3040.2005.01473.x

Wen, T., Yuan, J., He, X., Lin, Y., Huang, Q., and Shen, Q. (2020). Enrichment of beneficial cucumber rhizosphere microbes mediated by organic acid secretion. *Hortic. Res.* 7, 154. doi: 10.1038/s41438-020-00380-3

Wen, T., Zhao, M., Yuan, J., Kowalchuk, G. A., and Shen, Q. (2021). Root exudates mediate plant defense against foliar pathogens by recruiting beneficial microbes. *Soil Ecol. Lett.* 3, 42–51. doi: 10.1007/s42832-020-0057-z.\

Wester-Larsen, L., Kramshøj, M., Albers, C. N., and Rinnan, R. (2020). Biogenic volatile organic compounds in Arctic soil: a field study of concentrations and variability with vegetation cover. *J. Geophys. Res. Biogeosci.* 125, e2019JG005551. doi: 10.1029/2019JG005551

Yang, Z., Hautier, Y., Borer, E., Zhang, C., and Du, G. (2015). Abundance- and functional based mechanisms of plant diversity loss with fertilization in the presence and absence of herbivores. *Oecologia* 179, 261–270. doi: 10.1007/s00442-015-3313-7

Yergaliyev, T. M., Alexander-Shani,, Dimerets, H., Pivonia, S., McK Bird, D., Rachmilevitch, S., et al. (2020). Bacterial community structure dynamics in Meloidogyne incognita-infected roots and its role in worm-microbiome interactions. *mSphere* 5, e00306–e00320. doi: 10.1128/mSphere.00306-20

Yin, C., Casa Vargas, J. M., Schlatter, D. C., Hagerty, C. H., Hulbert, S. H., and Paulitz, T. C. (2021). Rhizosphere community selection reveals bacteria associated with reduced root disease. *Microbiome* 9, 86. doi: 10.1186/s40168-020-00997-5

Yuan, J., Zhao, J., Wen, T., Zhao, M., Li, R., Goossens, P., et al. (2018). Root exudates drive the soil-borne legacy of aboveground pathogen infection. *Microbiome* 6, 156. doi: 10.1186/s40168-018-0537-x

Zasada, I. A., Avendaño, F., Li, Y. C., Logan, T., Melakeberhan, H., and Koenning, S. R. (2008). Potential of an alkaline stabilized biosolid to manage nematodes: case studies on soybean cyst and root-knot nematodes. *Plant Dis.* 92, 4–13. doi: 10.1094/PDIS-92-1-0004

Zhang, S., Gan, Y., Ji, W., Xu, B., Hou, B., and Liu, J. (2017). Mechanisms and characterization of *Trichoderma longibrachiatum* T6 in suppressing nematodes (*Heterodera avenae*) in wheat. *Front. Plant Sci.* 8. doi: 10.3389/fpls.2017.01491

Zhang, Y., and Gross, C. A. (2021). Cold shock response in bacteria. *Annu. Rev. Genet.* 55, 377–400. doi: 10.1146/annurev-genet-071819-031654

Zhang, H., Kaushal, R., Singh, S. K., Paul, W., and Paré, P. W. (2020). "Bacterial volatile-mediated plant abiotic stress tolerance," in *Bacterial volatile compounds as mediators of airborne interactions*. Eds. C.-M. Ryu, L. Weisskopf and B. Piechulla (Springer, Singapore), 87–200. doi: 10.1007/978-981-15-7293-7

Zhang, P., Wei, T., Jia, Z., Han, Q., Ren, X., and Li, Y. (2014). Effects of straw incorporation on soil organic matter and soil water-stable aggregates content in semiarid regions of northwest China. *PloS One* 9, e92839. doi: 10.1371/journal.pone.0092839

Zhang, Z., Zhang, X., Mahammood, M., Zhang, S., Huang, S., and Liang, W. (2016). Effect of long-term combined application of organic and inorganic fertilizers on soil nematode communities within aggregates. *Sci. Rep.* 6, 31118. doi: 10.1038/srep31118

Zhang, S. S., Zhu, W., Wang, B., Tang, J., and Chen, X. (2011). Secondary metabolites from the invasive *Solidago canadensis* L. accumulation in soil and contribution to inhibition of soil pathogen *Phytium ultimum*. *Appl. Soil Ecol.* 48, 280–286. doi: 10.1016/j.apsoil.2011.04.011

Zhao, X., Hu, W., Zhang, S., Zhao, Q., and Wang, Q. (2016). Effect of potassium levels on suppressing root-knot nematode (*Meloidogyne incognita*) and resistance enzymes and compounds activities for tomato (*Solanum lycopersicum* L.). *Academia J. Agric. Res.* 4, 306–314.

Zhao, X., Lin, C., Tan, J., Yang, P., Wang, R., and Qi, G. (2023). Changes of rhizosphere microbiome and metabolites in *Meloidogyne incognita* infested soil. *Plant Soil* 483, 331–353. doi: 10.1007/s11104-022-05742-5

Zhou, D., Feng, H., Schuelke, T., De Santiago, A., Zhang, Q., Zhang, J., et al. (2019). Rhizosphere microbiomes from root knot nematode non-infested plants suppress nematode infection. *Microb. Ecol.* 78, 470–481. doi: 10.1007/s00248-019-01319-5

Zhou, X., and Wu, F. (2012). *p-Coumaric* acid influenced cucumber rhizosphere soil microbial communities and the growth of *Fusarium oxysporum* f.sp. *cucumerinum* Owen. *PLoS One* 7, e48288. doi: 10.1371/journal.pone.0048288

frontiers | Frontiers in Plant Science

TYPE Original Research
PUBLISHED 08 May 2024
DOI 10.3389/fpls.2024.1383986

OPEN ACCESS

EDITED BY
Andressa Machado,
Agronema, Brazil

REVIEWED BY
Raghavendra Aminedi,
Indian Council of Agricultural Research (ICAR), India
Abdelfattah A. Dababat,
International Maize and Wheat Improvement Center, Mexico

*CORRESPONDENCE
Paola Leonetti
paola.leonetti@cnr.it
Lorenzo Pasotti
lorenzo.pasotti@unipv.it
Anca Macovei
anca.macovei@unipv.it

RECEIVED 08 February 2024
ACCEPTED 22 April 2024
PUBLISHED 08 May 2024

CITATION
Leonetti P, Dallera D, De Marchi D, Candito P, Pasotti L and Macovei A (2024) Exploring the putative microRNAs cross-kingdom transfer in *Solanum lycopersicum-Meloidogyne incognita* interactions.
Front. Plant Sci. 15:1383986.
doi: 10.3389/fpls.2024.1383986

Exploring the putative microRNAs cross-kingdom transfer in *Solanum lycopersicum-Meloidogyne incognita* interactions

Paola Leonetti[1]*, Debora Dallera[2], Davide De Marchi[2], Pamela Candito[2], Lorenzo Pasotti[2]* and Anca Macovei[3]*

[1]Institute for Sustainable Plant Protection of the National Research Council, Unit of Bari, Bari, Italy, [2]Laboratory of Bioinformatics, Mathematical Modelling, and Synthetic Biology, Department of Electrical, Computer and Biomedical Engineering - Centre for Health Technology, University of Pavia, Pavia, Italy, [3]Plant Biotechnology Laboratory, Department of Biology and Biotechnology "L. Spallanzani", University of Pavia, Pavia, Italy

Introduction: Plant-pathogen interaction is an inexhaustible source of information on how to sustainably control diseases that negatively affect agricultural production. *Meloidogyne incognita* is a root-knot nematode (RKN), representing a pest for many crops, including tomato (*Solanum lycopersicum*). RKNs are a global threat to agriculture, especially under climate change, and RNA technologies offer a potential alternative to chemical nematicides. While endogenous microRNAs have been identified in both *S. lycopersicum* and *M. incognita*, and their roles have been related to the regulation of developmental changes, no study has investigated the miRNAs cross-kingdom transfer during this interaction.

Methods: Here, we propose a bioinformatics pipeline to highlight potential miRNA-dependent cross-kingdom interactions between tomato and *M. incognita*.

Results: The obtained data show that nematode miRNAs putatively targeting tomato genes are mostly related to detrimental effects on plant development and defense. Similarly, tomato miRNAs putatively targeting *M. incognita* biological processes have negative effects on digestion, mobility, and reproduction. To experimentally test this hypothesis, an *in vitro* feeding assay was carried out using sly-miRNAs selected from the bioinformatics approach. The results show that two tomato miRNAs (sly-miRNA156a, sly-miR169f) soaked by juvenile larvae (J2s) affected their ability to infect plant roots and form galls. This was also coupled with a significant downregulation of predicted target genes (*Minc11367, Minc00111*), as revealed by a qRT-PCR analysis.

10.3389/fpls.2024.1383986

Discussions: Therefore, the current study expands the knowledge related to the cross-kingdom miRNAs involvement in host-parasite interactions and could pave the way for the application of exogenous plant miRNAs as tools to control nematode infection.

KEYWORDS

bioinformatics pipeline, miRNAs, cross-species target prediction, plant-pathogen interaction, tomato, root-knot nematode

1 Introduction

Root-knot nematodes (RKNs) are pathogens that attack many economically important crops, negatively impacting crop yield, quality, and subsequently food security (Kaloshian and Teixeira, 2019). Damage caused by RKNs has been estimated to range between 80 - 157 billion $US per year, although this evaluation may be largely underestimated (Palomares-Rius et al., 2021). Among the RKNs, members of the *Meloidogyne* genus are the most widespread and have a broad range of hosts. These parasites can penetrate host roots and induce the formation of specialized feeding structures (root galls), which supply the resources required for nematode development. The formation of root galls is highly damaging because they affect the plants' ability to uptake water and nutrients (Singh et al., 2015). Tomato (*Solanum lycopersicum* L.), one of the most important and extensively grown horticultural crops in the Mediterranean region (EUROSTAT, 2021), is the preferential host for many *Meloidogyne* species. Yield losses due to *M. incognita* RKNs can range between 25-100% (Seid et al., 2015). Control methods generally include the use of chemical fumigants or nematicides, but since the ban of chemicals with a broad action on non-target organisms, emerging RKN populations continue to bypass plant host defenses. Therefore, alternative approaches (e.g., eco-friendly fumigants, bio-control agents) that can stimulate plant defense mechanisms, are needed to control their spread (Leonetti and Molinari, 2020). Currently, much focus is given to the use of RNA interference (RNAi) as an eco-friendly strategy (Banerjee et al., 2018; Banakar et al., 2020; Iqbal et al., 2020), as demonstrated for fungal small RNAs that suppress plant immunity by hijacking host RNAi pathways (Weiberg et al., 2013; Hua et al., 2018). Examples of cross-kingdom RNAi during plant-pathogen interactions are also available. For instance, the *Botrytis cinerea* sRNA produced by Dicer-like (DCL) proteins can target and silence *DCL* genes in Arabidopsis with subsequent effects on fungal pathogenicity and growth (Wang et al., 2016). Other examples include the transfer of ds-siRNA and miRNAs from plants to Coleoptera species, with consequences on gene transcription and insect growth (Zhang L. L. et al., 2019; Kleaveland, 2023). Additionally, miRNAs are being investigated as important regulatory actors in the plant-nematode interaction (Jaubert-Possamai et al., 2019), supporting the development of novel tools to advance modern agriculture.

As small, evolutionary conserved, and generally non-coding RNA molecules, microRNAs finely regulate gene expression being involved in developmental and stress responses. In plants, miRNAs achieve their function through perfect or near-perfect complementarity to target mRNAs, while in animals three types of miRNA-target interactions are recognized: (1) partial binding, mainly to the seed region; (2) complete or near-complete binding that enables AGO-mediated endonucleolytic cleavage of the target; and (3) extended/bulged binding to the seed region which specifies target-directed miRNA degradation (Kleaveland, 2023). When addressing host-parasite interactions, the involvement of miRNAs and long non-coding RNAs in the relation between *S. lycopersicum* and *M. incognita*, has been investigated (Kaur et al., 2017; Yang et al., 2020, 2022). While Zhang Y. et al. (2016) focused mainly on the high-throughput identification and annotation of miRNAs in *M. incognita*, Kaur et al. (2017) directed their attention to the identification of tomato miRNAs in susceptible plants during nematode infection. However, no study has investigated the miRNAs cross-species potential during this interaction. Several works have studied miRNAs transfer to other organisms along with possible regulatory functions (LaMonte et al., 2012; Zhang et al., 2012; Cheng et al., 2013; Zhu et al., 2017; Avsar et al., 2020; Cai et al., 2021), making it reasonable to hypothesize that this exchange may be well-represented during plant-parasite interactions, and that this can be exploited as an alternative tool to sustainably fight pathogens (Gualtieri et al., 2020; Rabuma et al., 2022). So far, the miRNA cross-kingdom transfer ability has been demonstrated in several plant-pathogen interactions, like *Gossypium hirsutum–Verticillum dahliae* (Zhang H. et al., 2016), *Triticum aestivum–Puccinia striiformis* (Wang et al., 2017), and *Arabidopsis thaliana–Plutella xylostella* (Zhang L. L. et al., 2019).

In the current study, we propose a bioinformatics pipeline to investigate the putative effects of cross-species miRNAs transfer during the interaction between *S. lycopersicum* - *M. incognita*. Specific miRNAs and transcripts from the two species have been retrieved from public databases and used to predict candidate targets in a cross-kingdom manner, based on different miRNA-mRNA hybridization rules. Biological processes of Gene Ontology significantly affected by the target genes were identified and examples of bidirectional cross-targeting predictive miRNAs, with potentially interesting applications to fight disease development, are provided. Additionally, three tomato miRNAs (sly-miRNA 156a, sly-miRNA166b, sly-miRNA169f) were selected for *in vitro*

validation studies on juvenile *M. incognita* larvae (J2s) infecting the roots of susceptible tomato plants.

2 Materials and methods

The bioinformatics workflow adopted in this work includes the following steps: (1) miRNA and transcript sequence collection from public data, (2) cross-kingdom miRNA target prediction by two different procedures, and (3) analysis of target genes and enriched biological processes resulting from the predicted miRNA-target pairs. Subsequently, experimental methods for the *in vitro* evaluation of the effect of selected *S. lycopersicum* miRNAs on *M. incognita* larvae are provided.

2.1 Datasets

A collection of *S. lycopersicum* miRNAs (sly-miRNAs) was obtained by merging the entries found in public databases and literature. The miRbase repository (Kozomara et al., 2019) included 147 sly-miRNAs, of which 137 were unique. The sly-miRNA list reported by Kaur et al. (2017) was added, including 136 sequences (56 miRNAs classified as conserved or variants, and 60 as novel miRNAs), which account for 70 unique miRNAs after duplicate removal. Thus, a total of 207 sly-miRNAs (obtained from the two merged lists), with 185 unique sequences, represent the final collection used for tomato miRNAs. The *S. lycopersicum* transcript dataset (ITAG 2.4.v) was retrieved from psRNATarget (Dai et al., 2018) and included 34,725 transcripts, covering a large part of the tomato annotated genome (37,872 genes) available on NCBI.

Since *M. incognita* miRNAs (min-miRNAs) are not included in public databases, only literature works were used to define this collection. The list of Zhang Y. et al. (2016) included 144 min-miRNAs (38 classified as conserved and 106 as novel miRNAs), which accounts for 63 unique miRNAs after duplicate removal. The list of Wang et al. (2015) included 102 min-miRNAs, corresponding to 70 unique sequences, of which about 40% is composed of conserved miRNAs. From the 133 min-miRNAs obtained by merging the two lists, 126 were unique and represented the final collection of RKN miRNAs. The *M. incognita* transcript and CDS datasets were retrieved from the V2 genome assembly (Blanc-Mathieu et al., 2017), available at the INRAE *Meloidogyne* Genomic Resources website (https://*meloidogyne*.inrae.fr), which includes 43,718 transcript and CDS sequences. The *M. incognita* 3'UTRome was obtained by processing the transcripts and CDS lists above with a custom Python (v3.8) script, resulting in 20,201 sequences because not all the full transcripts have an annotated 3'UTR.

2.2 miRNA target prediction

The cross-kingdom search of miRNA targets in *S. lycopersicum* and *M. incognita* transcriptome was performed using the psRNATarget (https://www.zhaolab.org/psRNATarget/) and RNAhybrid (https://bibiserv.cebitec.uni-bielefeld.de/rnahybrid/) tools, respectively, previously proposed for miRNA target prediction in plants (Dai et al., 2018) and animals (Kruger and Rehmsmeier, 2006). The collections of *M. incognita* and *S. lycopersicum* miRNAs were used as input for both tools, together with the transcriptome of the target organism (tomato and nematode, respectively). The two tools have been validated on intra-kingdom miRNA-target data in their original publications. However, it is worth mentioning that no large-scale validation is available for cross-kingdom predictions because of the very low number of validated miRNA-target pairs. Even though no gold standard tool or set of rules has been defined for cross-kingdom miRNA interactions, we assumed that such regulations follow the rules of the host organism, as it was assumed in other works (Shu et al., 2015; Chin et al., 2016; Zhang H. et al., 2016; Hou et al., 2018; Zhao et al., 2018; Bellato et al., 2019), thus motivating the use of plant- and animal-specific prediction tools. Consistent with previous in silico and *in vivo* studies (Liu et al., 2017; Li Z. et al., 2018; Lukasik et al., 2018; Mal et al., 2018; Wang et al., 2018), instead of restricting the search to the 3'UTRome, reported to be the preferential target of endogenous miRNA regulation in animals (Bartel, 2004), the full transcript sequences were used to search for targets in the RKN transcriptome. For the reasons above, the miRNA-target pairs found by the two tools represent putative regulations that may occur in nature, even though other herein neglected biological factors could play important roles.

RNAhybrid and psRNATarget were both run by setting a maximum of 50 targets per miRNA as previously done (Zhang H. et al., 2016; Bellato et al., 2019), to obtain a balanced set of miRNA-target pairs to be analyzed downstream. RNAhybrid was run using a Minimum Free Energy (MFE) threshold of -25 kcal/mol, corresponding to the upper bound of many experimentally found miRNA-target pairs (Zhang H. et al., 2016). Putative targets were ranked based on their MFE value (lowest to highest) for further selection of a subset of these genes, as required in the downstream steps (see 2.3). psRNATarget was run with an Expectation value of 3, corresponding to a slightly relaxed threshold in terms of prediction results stringency, as reported by Dai and Zhao (2011). Default values were used for the other psRNATarget parameters, as previously done in other studies (Bellato et al., 2019): Penalty for G:U pair = 0.5, Penalty for other mismatches = 1, Extra weight in seed region = 1.5, Seed region = 2-13 nucleotides, Mismatches allowed in seed region = 0, HSP size = 19.

In addition to the procedure described above (indicated as *cross-kingdom hybridization*), we followed a second search method that does not assume any hybridization rule in cross-kingdom interaction. This alternative method (indicated as *seed region-based search*) was carried out to find sly-miRNA targets in *M. incognita* transcriptome and included the following steps: (1) intra-kingdom hybridization (i.e., min-miRNAs *vs.* RKN transcriptome via RNA hybrid); (2) selection of all the sly-miRNAs that share a seed region (nucleotides 2-7 of the miRNA) with the collection of min-miRNAs; (3) association of the selected sly-miRNAs to the targets of the min-miRNAs with the same seed region. Location (CDS or UTRs) of the predicted miRNA binding and sequence similarity

outside the seed region were also recorded to support further selection steps.

2.3 Biological process analysis

Statistically over-represented Gene Ontology (GO) terms in the Biological Process (BP) category were computed via enrichment analysis using the predicted miRNA targets obtained above. Duplicate genes in the target list were removed before analysis. The ClueGO application (v2.5.6) (Bindea et al., 2009) of Cytoscape (v3.7.3) (Shannon et al., 2003) was used as a GO analysis tool. A right-sided hypergeometric test with the Benjamini-Hochberg correction for multiple hypothesis testing and a P-value cutoff of 0.05 was used.

For *M. incognita* enrichment analysis, an *ad hoc* construction of the GO library was necessary for ClueGO analyses, as this organism was not previously included in this tool. To this aim, the GO biological processes list reported by Somvanshi et al. (2018) was used as a source, converted into a ClueGO-compatible format using a custom Python script, and integrated into ClueGO. In total, 5,508 and 6,098 unique GO terms in the BP category were present for *S. lycopersicum* and *M. incognita*, respectively. The BPs presented in this work after enrichment analysis refer to the most relevant term of the functionally grouped term networks provided by ClueGO. The number of input genes in enrichment analysis was set to obtain a comparable number of relevant terms between plant and RKN.

To further analyze the obtained biological processes, individual genes in the miRNA target list associated with the process were considered, and their function was searched in the literature. For *S. lycopersicum*, gene information was retrieved from the ITAG 2.4 annotations available in Phytozome v.12 (DOE JGI, https://jgi.doe.gov/more-intuitive-phytozome-interface/). For *M. incognita*, orthologous genes from other nematodes (mainly *C. elegans*) were obtained using WormBase ParaSite (https://parasite.wormbase.org/index.html) (Howe et al., 2017). This approach was considered because specific information on RKN genes is not directly available in public online resources. Finally, a subset of BP terms from Somvanshi et al. (2018) related to nematode development was selected and used to filter the sly-miRNA targets in the RKN transcriptome.

2.4 *In vitro* interaction assays of sly-miRNAs soaked by *M. incognita* juvenile larvae

For the *in vitro* interaction assay, sly-miR166b, sly-miR169f, and sly-miR156a were selected taking into account the bioinformatics data obtained from the cross-kingdom hybridization and the seed region-based search approach. These microRNAs were obtained from Invitrogen™ Custom Primer Service (BMR Genomics, Padova, Italy) and the relative sequences are given: sly-miR166b (5'-UCGGACCAGGCUUCAUUCCCC-3', STAR strand GGAAUGUUGUCUGGCUCGAGG), sly-miR156a (5'-UUGACAGAAGAUAGAGAGCAC-3', STAR strand GCUCUCUAUGCUUCUGUCAU) sly-miR169f (5'-UAGGCGUUGUCUGAGGCUAAC-3', STAR strand AUCCGUUACUGAGGAACCGAUAG).

Susceptible tomato seedlings (Roma cv.) and axenic cultures of phytoparasitic nematodes were prepared as described by Molinari and Miacola (1997). Freshly hatched *M. incognita* J2s (infective second-stage juveniles) larvae were used for soaking experiments, following a modified protocol (Danchin et al., 2013; Tan et al., 2013). About 8,000 J2s were soaked for 24 hours in a 40µl final volume of mineral water containing different solutions: (1) a siRNA designed to have no similarity in the *M. incognita* genome (Dalzell et al., 2010) defined as negative control solution (C-J2); and (2) three different solutions of 0.05 mg/ml sly-miRNAs corresponding to each tested tomato miRNA. J2s from each soaking experiment were washed twice with water by centrifugation at 10,000 g for 3 min, and re-suspended in 100 µl of water. Subsequently, the miRNA-soaked J2s were observed using a Leica M125 stereomicroscope (Leica Microsystem S.r.l, Buccinasco, Milano, Italy) to confirm their vitality and split in two Eppendorf tubes: one used for infection assay and another used for RNA extraction (frozen at -80°C).

For the interaction assay, the sly-miRNAs soaked J2 larvae (approx. 50 J2s/root apex) were loaded in wells placed on agar plates at 0.1 mm from the tomato root. Each plate contained three susceptible tomato seedlings, growth in axenic conditions. The infection was observed for six weeks, during which the penetration in the roots was evaluated in terms of gradual enlargements of the root tip caused by rapid cell division and proliferation. The giant cell induction and galls formation was monitored using a modified LEICA Software image analysis (unpublished), and the following scoring system was used: "+" ranging between 0-30%, "++" ranging between 31-60%, and "+++" ranging between 61-90% (Melillo et al., 2006; Cabrera et al., 2015). The parameters referring to both root enlargements and formation of galls (91-100%), were counted and scored as the number of symptoms normalized to the number of roots in which the phenomena were observed. All experiments were conducted in triplicates coming from two independent trials.

2.5 RNA extraction and qRT-PCR analysis

RNA was extracted using the TRIzol Reagent (Invitrogen, CA, USA) method, as indicated by the manufacturer. For this, 500 J2s soaked for 24 h in the control solution (C-J2) or the respective sly-miRNAs (miR156a-J2, miR169f-J2) solutions, were used. For the reverse transcription, 1 µg of total RNA was used along with the QuantiTect Reverse Transcription Kit (QIAGEN S.r.l, Milano) following the manufacturer's instructions.

The qRT-PCR reactions were carried out using the StepOnePlus (Applied Biosystems, Life Technologies, Zurich, Switzerland) system and assembled in a reaction with 1.5 µl cDNA, 10 µl SYBR® Select Master Mix (Applied Biosystem, Life Technologies, Zurich, Switzerland), 0.2 µl each of 100 µM of forward and reverse primers, and RNAse free water to 20 µl (total volume). Thermocycling was carried out with one cycle at 95°C for 5 min, followed by 40 cycles of 95°C for 45 s and 58°C for 1 min and 72°C

for 45 s. The dissociation curve of the final products was checked to ascertain the presence of a single amplification product. The relative quantification was carried out using the 18S ribosomal RNA gene (NCBI accession HE667742.1, WormBase accession Minc3s09153g42974) as a reference gene. The *Minc11367* (WormBase Accession Minc3s00025g01614) gene, was selected and tested as a putative target for sly-miR156a, while *Minc00111* (WormBase Accession Minc3s00001g00015) was selected as a putative target of sly-miR169f. Oligonucleotide sequences to amplify the genes of interest were designed with Primer3Plus (https://primer3plus.com) and further validated through the online software Oligo Analyzer (https://eu.idtdna.com/calc/analyzer). All the oligonucleotide sequences are provided in Supplementary Table 1. The ΔΔCt method was used to quantify gene expression. The reactions were performed in triplicate samples of each cDNA and using two independent replicates.

2.6 Statistical analysis

Results of experimental data are shown as mean ± standard deviation (SD) obtained from two independent experiments each with three replicates. Statistical analyses were conducted using the two-way analysis of variance (ANOVA), along with the heteroscedastic Student's *t*-test (where *, $P \leq 0.05$; **, $P \leq 0.01$), available within the Microsoft Excel package.

3 Results and discussion

3.1 Overview of the bioinformatics pipeline

In this work, a bidirectional bioinformatics workflow was carried out to predict miRNAs cross-kingdom potential in the host-parasite interaction between tomato and RKNs. These predictions are based on sequence complementarity between miRNAs and cross-species targets, as well as sequence similarity between tomato and nematode miRNAs. A total of 523 miRNA-target pairs were found in the cross-kingdom hybridization between *S. lycopersicum* transcripts and min-miRNAs, corresponding to 469 unique genes and 105 unique min-miRNAs (Supplementary Dataset 1). The majority of genes were targeted by a single miRNA, but putative targeting by two miRNAs occurred as well (Figure 1A). All the target genes were adopted for subsequent enrichment analysis that yielded 43 biological processes (BPs), divided into 10 functional groups, as described below in Section 3.2. Conversely, 8,926 transcripts corresponding to 6,428 unique genes were found in *M. incognita* by cross-kingdom hybridization with the sly-miRNAs (Supplementary Dataset 2). Each gene was putatively targeted by one or more miRNAs (Figure 1B). Based on the MFE of the targets, the 290 top-ranked genes were used for the enrichment analysis that resulted in 86 BPs in the 10 functional groups, described further in Section 3.3.

The seed region-based search resulted in the identification of 7 sly-miRNAs having homologies with 9 min-miRNAs; using these sly-miRNAs, a total of 450 putative target genes were identified in *M. incognita* (Supplementary Dataset 3).

3.2 *M. incognita* miRNAs predicted to target tomato genes may inhibit plant development

To analyze the obtained datasets, we first looked at the potential effects that min-miRNAs would have on the development of tomato plants providing discussions based on the function of putatively targeted genes. The biological processes found to be enriched among the putative cross-species targets of RKN miRNAs against *S. lycopersicum* transcripts are reported in Supplementary Dataset 4 and graphically represented in Figure 2. These processes clustered in several major GO terms and the most abundant networks included brassinosteroid-mediated signaling pathway, response to herbivores, and positive regulation of protein catabolic process. Other processes like inositol-lipid mediated signaling, co-translational protein targeting to membrane, non-recombinant repair, rRNA methyl transferase, and cellular response to starvation, were less abundant. Considering the min-miRNAs putatively targeting genes in the

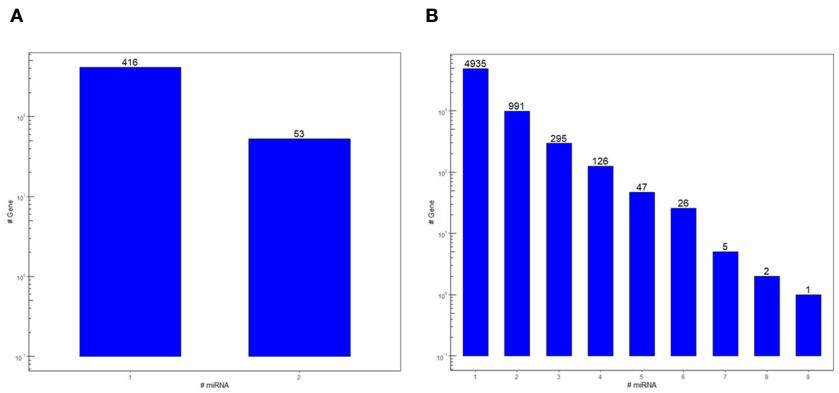

FIGURE 1
Count of the *S. lycopersicum* **(A)** and *M. incognita* **(B)** miRNA targets in the cross-kingdom hybridization bioinformatic pipeline run on the two species. Bars represent the number of genes that are putatively targeted by one or more miRNA.

10.3389/fpls.2024.1383986

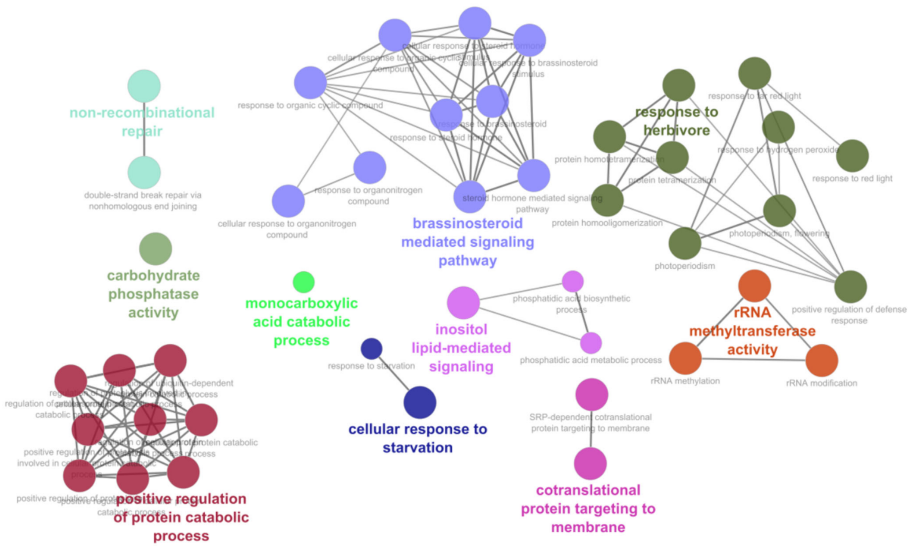

FIGURE 2
Biological processes and functional network clusters resulting from enrichment analysis carried out using the *M. incognita* miRNA putatively targeting *S. lycopersicum* mRNAs. The most relevant terms of the functional groups are highlighted.

tomato dataset, the enriched terms list includes 26 miRNAs and 46 unique targets, with the most interesting ones being summarized in Table 1. Within the brassinosteroid-mediated signaling pathway, different phosphatases, phosphodiesterase, and proteases were predicted to be targeted by NOVEL-18-1, min_miRNA6, and min_miRNA98. Many protease gene families are well-known to be involved in plant immune responses (Balakireva and Zamyatnin, 2018). For instance, aspartyl proteases are specifically linked to systemic acquired resistance (SAR) induced in response to local infections (Breitenbach et al., 2014; Molinari et al., 2014; Molinari

TABLE 1 List of representative *M. incognita* miRNAs putatively targeting genes in *S. lycopersicum*, based on bioinformatics cross-kingdom predictions.

GO_ID	GO Term	*M. incognita* miRNA	*S. lycopersicum* Gene Accession	Gene Name
GO:0009742	Brassinosteroid mediated signaling pathway	NOVEL-18-1	Solyc06g073960	Calcineurin-like phosphoesterase domain, apaH type
		min_miRNA6	Solyc06g074000	Aspartyl protease
		min_miRNA98	Solyc09g074320	Serine/threonine-protein phosphatase BSL1-related
GO:0080027	Response to herbivore	NOVEL-8	Solyc09g008790	serine/threonine-protein kinase SRPK3
		miR-50, miR-50_1	Solyc09g009010	Glucomannan 4-beta-mannosyltransferase
		min_miRNA29	Solyc09g009040	Delta(14)-sterol reductase/Sterol C14-reductase
GO:0045732	Positive regulation of protein catabolic process	NOVEL-22-1	Solyc02g069230	RBR family ring finger and IBR domain-containing
		min_miRNA206	Solyc06g073340	E3 ubiquitin-protein ligase ARI10-related
		NOVEL-18-1	Solyc08g005150	E3 ubiquitin-protein ligase RNF14
GO:0008649	rRNA methyltransferase activity	NOVEL-44	Solyc01g100430	18S rRNA (adenine(1779)-N(6)/adenine (1780)-N(6))-dimethyltransferase
		NOVEL-6-1	Solyc11g005580	16S rRNA (cytosine(1402)-N (4))-methyltransferase
		miR-76, miR-76_1	Solyc11g020870	Metal dependent hydrolase-related

(Continued)

TABLE 1 Continued

GO_ID	GO Term	*M. incognita* miRNA	*S. lycopersicum* Gene Accession	Gene Name
GO:0048017	Inositol lipid-mediated signaling	miR-87	Solyc01g065740	F-box domain
		NOVEL-10-1	Solyc01g066050	RNA polymerase II-associated protein 3
		min_miRNA37	Solyc01g100020	Phospholipase D P2
		min_miRNA206	Solyc06g051720	GDSL esterase/lipase CPRD49
GO:0006613	Cotranslational protein targeting to membrane	NOVEL-35	Solyc03g093970	Signal recognition particle subunit SRP68
		miR-76, miR-76_1	Solyc03g116810	Signal recognition particle subunit SRP54
GO:0072329	Monocarboxylic acid catabolic process	miR-34_1	Solyc08g005610	Abscisic acid 8'-hydroxylase 1-related
		min_miRNA112 NOVEL-28	Solyc10g008110	Acyl-coenzyme A oxidase-like protein
GO:0000726	Non-recombinational repair	NOVEL-12	Solyc01g091350	ATP-dependent DNA helicase 2 subunit 2 (XRCC5, KU80, G22P2)
		miR-87	Solyc01g091370	AT hook motif DNA-binding family protein-related
		let-7	Solyc02g093330	nuclear pore complex protein Nup98-Nup96
		NOVEL-16-1	Solyc02g093690	ATP synthase mitochondrial F1 complex assembly factor 2 (ATPeAF2, ATPAF2, ATP12)
GO:0009267	Cellular response to starvation	min_miRNA109	Solyc01g090890	Xenotropic and polytropic retrovirus receptor 1-related, SPX domain-containing protein
		min_miRNA151	Solyc02g037510	Solute carrier family 7 (SLC7A2, ATRC2)
		NOVEL-37	Solyc09g014790	VHS domain containing protein family
GO:0019203	Carbohydrate phosphatase activity	miR-81 min_miRNA112	Solyc07g062140 Solyc07g062410	Trehalose-p6-phosphate synthase (TPS)
		min_miRNA206	Solyc01g006740 Solyc10g081660	Sucrose-phosphate phosphatase (SPP)

Gene Ontology (GO) ID and terminology are provided along with gene names and corresponding accessions.

and Leonetti, 2019). Other miRNAs, like NOVEL-8, miR-50, and min_miRNA29, are predicted to target genes playing important roles in the response to herbivores. The S-receptor kinase-like genes, aside from being involved in stress responses and host-pathogen defense, have also important functions in cell signaling and development (Takasaki et al., 2000; Becraft, 2002; Pastuglia et al., 2002). Similarly, genes involved in the cuticle and cell wall development and composition (e.g., sterols, mannans) represent important defense lines against many types of pathogens (Wang et al., 2013; Kazan and Gardiner, 2017). Other min-miRNAs (min_miRNA206, NOVEL-18-1) were predicted to target different E3 ubiquitin-protein ligases in tomatoes; these proteins play important roles in the regulation of cell homeostasis and thus they are key regulators of plant growth and stress responses (Liu et al., 2021). Importantly, they are involved in the regulation of plant innate immunity (Duplan and Rivas, 2014).

Similarly, miRNAs (e.g., NOVEL-44, NOVEL-6-1, miR-76) affecting translational regulation can play critical roles in the plant defense against pathogen infection. In addition to the essential role of DNA repair in maintaining genome stability, recent works are discussing the involvement of DNA repair proteins in plant-pathogen interactions and SAR (Fu and Dong, 2013; Camborde et al., 2019). Moreover, the miRNA-mediated control over DNA damage responses is starting to gain more interest from both an endogenous (Gualtieri et al., 2021; Macovei et al., 2021) and cross-kingdom fashion (Bellato et al., 2019). An interesting finding in this sense is the case of let-7, one of the most abundant miRNAs found in nematodes, putatively targeting the nuclear pore complex protein Nup98-Nup96 in tomatoes. This complex plays a role in nuclear-cytoplasmic trafficking and mRNA export, being involved in several important biological events such as mitotic checkpoints. Nup98-deficient mutants share pleiotropic phenotypes (decreased root elongation, accelerated floral transition, reduced fertility, and robustness), indicating that it has a critical role in plant development (Parry, 2013).

Other miRNAs worth mentioning are miR-81, min_miRNA112, and min_miRNA206 predicted to putatively target genes involved in sugar metabolism, like sucrose-phosphate phosphatase (SPP) and trehalose-p6-phosphate synthase (TPS). SSP is an important regulator of carbon partitioning and loss-of-function of this gene leads to altered carbohydrate distribution resulting in a reduced

growth rate (Chen et al., 2005, 2008). TPS leads to the formation of the trehalose-6-phosphate (T6P), a metabolic intermediate acting as a signaling molecule that regulates sugar metabolism (Paul, 2008), and its silencing in the tomato caused dysfunction in ROS accumulation and decreased expression of genes responsible for defense against pathogenic infections (Suárez et al., 2008).

To conclude, the prediction analyses show that the tomato genes putatively targeted by *M. incognita* miRNAs have essential roles in plant development and stress response, and their silencing can have negative repercussions for the plant. This is in agreement with the parasitic relation between the two organisms, where *M. incognita* tries to hijack the plant systems to promote its development.

3.3 sly-miRNAs predicted to target *M. incognita* genes may have detrimental effects on nematode development

When tomato miRNAs were evaluated against the nematode, the enrichment analysis of target genes resulted in BPs related to regulation of Wnt protein secretion, striate muscle contraction, sterol transported activity, ubiquinol-cytochrome-c reductase activity, [2Fe-2S] cluster assembly, glycogen biosynthetic process, defense response to fungus, serine-type exopeptidase, and apoptotic mitochondrial changes (Figure 3; Supplementary Dataset 5).

Among the most interesting examples investigated are sly-miR156, sly-miR166, and sly-miR319, given that they have been previously identified as highly abundant in roots during *M. incognita* infection (Kaur et al., 2017). The abundance of these miRNAs may favor their uptake in high amounts during feeding. Table 2 presents the biological processes and putatively cross-kingdom targeted genes in relation to these three miRNAs. The data shows that sly-miR166(b,c) has the most abundant number of putative targets, distributed in GO terms related to response to stress and developmental processes. Although *M. incognita* genome has been sequenced (Abad et al., 2008), its annotation is not completed. To understand the roles of these putative targets we have looked at orthologues in related species. Among the genes involved in neuromuscular developmental processes, *rGCs* (guanylyl cyclases) plays a role in sensory processing (Maruyama, 2017), *lev-11* (LEVamisole resistant) encodes a conserved CUB-domain containing transmembrane protein (Gally et al., 2004), *snt-1* (SyNapTotagmin) functions as a Ca^{2+} sensor (Li L. et al., 2018), and *nep-2* (NEPrilysin metallopeptidase family) is a homolog of the extracellular peptidase neprilysin whose loss-of-function leads to movement anomalies (Soh et al., 2020). Impaired movement can be also caused by dysfunctions in the genes coding for proteins that are part of the collagen extracellular matrix. This may be the case of *dpy-17* (DumPY: shorter than wild-type), involved in cuticle development (Lang and Lundquist, 2021), and *emb-9* (abnormal EMBroygenesis), an alpha1(IV) collagen gene with embryo lethal effects when mutated (Guo et al., 1991; Li-Leger et al., 2021). Other putative target genes of sly-miR166 are involved in cell cycle regulation, like *cdc48* (Franz et al., 2014), *rpt-2* (Papaevgeniou and Chondrogianni, 2014), and *flub-2* (Haskell and Zinovyeva, 2021), nutrient availability (*rpb-7*, Collins et al., 2016), and gonad development (*gon-1*, Blelloch et al., 1999). Regarding sly-miR156a, this was predicted to target *dhc1*, encoding for the dynein heavy chain protein, and *smrc-1*, belonging to the Swi/snf chromatin remodeling complex. Dynein is an ATP-powered microtubule-based molecular motor, whose function includes the transport of cargo around the cell, while the loss-of-function of this gene inhibits apoptosis (Harders et al., 2018). The *smrc-1* gene is involved in the protection against DNA replication stress and its loss-of-function leads to the accumulation of chronic replication stress (Yang et al., 2019). Finally, sly-miR319a was predicted to target the *dlat-1* gene, encoding an enzyme with acetyltransferase activity; its lack of function leads to an early embryonic arrest (Li-Leger et al., 2021).

In the subsequent analysis, tomato miRNAs that share sequence homology with *M. incognita* miRNAs were analyzed via the seed

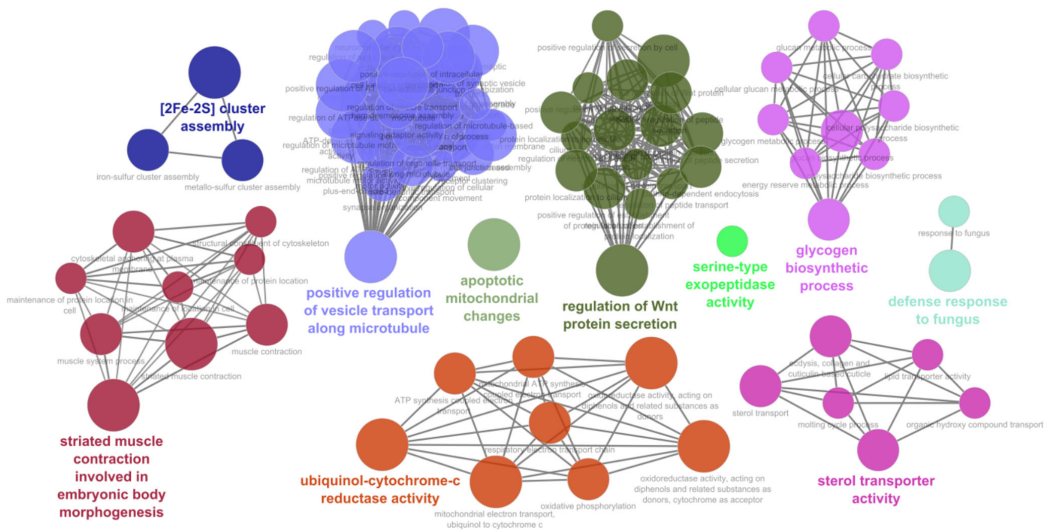

FIGURE 3
Biological processes and functional network clusters resulting from enrichment analysis carried out using the *S. lycopersicum* miRNA putatively targeting *M. incognita* mRNAs. The most relevant terms of the functional groups are highlighted.

10.3389/fpls.2024.1383986

TABLE 2 List of representative *S. lycopersicum* miRNAs putatively targeting genes in *M. incognita* obtained from the cross-kingdom hybridization approach.

GO_ID	GO Term	*S. lycopersicum* miRNA	*M. incognita*Gene Accession	Orthologue Gene Name
GO:0001101	Response to acid chemical	sly-miR166b	Minc3s01925g27230 (Minc10092)	Guanylate cyclase (*M.hapla*, *G. pallida*, *C. elegans*)
			Minc3s03236g33246	F53F4.10 (*C. elegans*)
GO:0002119	Nematode larval development		Minc3s02352g29617	dpy-17, DumPY: shorter than wild-type (*C. elegans*)
			Minc3s02644g31015	dpy-17 (*C. elegans*)
GO:0003006	Developmental process involved in reproduction		Minc3s02193g28780	emb-9, abnormal EMBroygenesis (*C. elegans*)
			Minc3s00798g17488	gon-1,abnormal GONad development (*C. elegans*)
GO:0002119	Nematode larval development	sly-miR166c	Minc3s01495g24259	rpb-7, RNA Polymerase II (B) subunit (*C. elegans*)
GO:0006950	Response to stress		Minc3s01397g23468	cdc-48.1, cdc-48.2 (*C. elegans*)
GO:0007275	Multicellular organism development		Minc3s00400g11662	rpt-2,proteasome Regulatory Particle, ATPase-like (*C. elegans*)
GO:0008219	Cell death		Minc3s00015g00977	lev-10,(LEVamisole resistant) (*C. elegans*)
GO:0009605	Response to external stimulus		Minc3s00180g06927	Y54F10AR.1 (*C. elegans*)
			Minc3s02523g30444	Cre-snt-1 (*C. remanei*)
GO:0032101	Regulation of response to external stimulus		Minc3s00007g00476	Bma-lst-6 (*B. malayi*)
			Minc3s00643g15541	nep-2 NEPrilysin metallopeptidase family (*C. elegans*)
GO:0031047	Gene silencing by RNA		Minc3s00047g02560	fubl-2 FUBp (FUBP) Like (*C. elegans*)
GO:0002119	Nematode larval development	sly-miR156a	Minc3s01128g20986	dhc-1 Dynein Heavy Chain (*C. elegans*)
GO:0000003	Reproduction		Minc3s00513g13571	smrc-1, Swi/snf (SWI/SNF) related (*C. elegans*)
GO:0007275	Multicellular organism development	sly-miR319a	Minc3s00613g15138	dlat1, Dihydro- Lipoyllysine-residue AcetylTransferase (*C. elegans*)

Gene Ontology (GO) ID and terminology are provided along with gene names and corresponding accessions.

region-based approach. Annotated orthologues of some predicted targets are collected in Table 3. Among the targeted biological processes, neurological development is much represented by putative targets such as *tgs-1* (trimethyl guanosine synthase), *gcy-9* (receptor-type guanylate cyclase), *mig-6* (abnormal cell MIGration, papilin), *kal-1* (human KALlmann syndrome homolog), as well as chemosensory genes like *Mi-odr-1* (Minc3s00015g01026, Minc3s00056g02910). A recent study indicated that *Mi-odr-1* is present in two copies in *M. incognita*, and was found to be expressed in the cell bodies of amphidal neurons and phasmids (Shivakumara et al., 2019). Silencing the *Mi-odr* and *Mi-gpa* genes could affect the nematode perception and infestation of the tomato root system (Li et al., 2022). Loss of *tgs-1* function in *C. elegans* leads to neurological phenotypes similar to those caused by the survival motor neuron (SMN) deficiency (Chen et al., 2022) whereas *gcy-9* mutants have different physiology in relation to adaptation and plasticity (Rossillo and Ringstad, 2020). The *C. elegans kal-1* gene affects epidermal morphogenesis by regulating the development of the substrate neuroblasts, and *kal-1* mutants show delayed migration of the ventral neuroblasts (Hudson et al., 2006). Loss-of-function mutants for the extracellular matrix molecule *mig-6* result in defects in dendrite formation (Ramirez-Suarez et al., 2019). Other important genes, like *unc-52* and *cbp*-1,2,3, are involved in larval development (Merz et al., 2003) and embryogenesis (Shi and Mello, 1998). Inhibition of these genes results in defects in myofilament assembly, larval movement deficiencies, or developmental arrest (Rogalski et al., 1995; Shi and Mello, 1998).

Hence, most *M. incognita* genes putatively targeted by sly-miRNAs have important roles in nematode development, leading to adverse effects on digestion, mobility, and reproduction, often with lethal outcomes. This finding is of utmost importance for the agricultural sector in view of developing plant miRNA-based technologies to control nematode diffusion.

When considering the use of different computational methods to predict miRNA targets in a cross-kingdom manner, such as the ones used in this work, it is important to underline that these rely on

TABLE 3 List of some representative *S. lycopersicum* miRNAs putatively targeting genes in *M. incognita* obtained from the *seed region-based search* approach.

GO_ID	GO Term	*S. lycopersicum* miRNA	Min-miRNAs	*M. incognita* Gene Accession	Orthologue Gene Name
GO:0050907	Detection of chemical stimulus involved in sensory perception	sly-miR156a	min_miRNA51	Minc3s00025g01614 (Minc11367)	gcy-9, Receptor-type guanylate cyclase (*C. elegans*)
GO:0007168	Receptor guanylyl cyclase signaling pathway				
GO:0007165	Signal transduction			Minc3s02931g32115	T08G11.4, Trimethyl Guanosine Synthase homolog tgs-1 (*C. elegans*)
GO:0008173	RNA methyltransferase activity				
GO:0031047	Gene silencing by RNA				
GO:0000902	Cell morphogenesis	sly-miR319a	min_miRNA306, NOVEL-5	Minc3s01898g27043 (Minc13237)	mig-6, abnormal cell MIGration (*C. elegans*)
GO:0040002	Collagen and cuticulin-based cuticle development				
GO:0002119	Nematode larval development			Minc3s01574g24825 (Minc12944)	unc-79, UNCoordinated, (*C. elegans*)
GO:0042493	Response to drug				
GO:0007044	Cell-substrate junction assembly	sly-miR169f, sly_miRNA3291	NOVEL-40, min_miRNA37	Minc3s00001g00015 (Minc00111)	unc-52, UNCoordinated (*C. elegans*)
GO:0006941	Striated muscle contraction			Minc3s00053g0281 (Minc11499)	Cbr-unc-52 (*C.briggsae*)
GO:0009792	Embryo development ending in birth or egg hatching	sly-miR169e-3p	miR-72	Minc3s00145g05964 (Minc02858)	kal-1, human KALlmann syndrome homolog (*C. elegans*)
GO:0048730	Epidermis, morphogenesis				
GO:0003724	RNA helicase activity			Minc3s02703g31258	ddx-27, DEAD boX helicase homolog (*C. elegans*)
GO:0016887	ATP hydrolysis activity				
GO:0007275	Multicellular organism development		miR-72_1	Minc3s01556g24691	T09B9.4 (*C. elegans*)
GO:0009790	Embryo development			Minc3s00060g03099	cbp-3, cbp-2, CBP/p300 homolog (*C. elegans*)
GO:0006915	Apoptotic process				
GO:0007018	Microtubule-based movement	sly_miRNA4126	min_miRNA32	Minc3s01128g20986 (Minc02896)	dhc-1, Dynein Heavy Chain (*C. elegans*)
GO:0005524	ATP binding				

Gene Ontology (GO) ID and terminology are provided along with sly-miRNAs, min-miRNAs, M. incognita accessions and orthologous from related species (e.g., Caenorhabditis elegans, Caenorhabditis briggsae).

different assumptions on targeting rules and are still necessary to face our currently limited knowledge in miRNA trans-species interactions. Experimental confirmations are therefore needed to understand the actual targeting roles of the illustrated miRNAs. The availability of these computational methods is however useful to guide researchers in the selection of miRNA candidates for further investigation, despite the target prediction algorithm outcomes could be different due to the different underlying assumptions.

3.4 *In vitro* experimental validation of tomato miRNAs influencing *M. incognita* infection

To investigate the hypothesized cross-kingdom miRNAs transfer along with its potential to control the RKN infection, an *in vitro* experimental system was designed based on soaking assay, nematode larvae phenotyping, and gene expression profiling. To this purpose, J2 larvae were fed with solutions containing tomato miRNAs (sly-miR166b, sly-miR156a, sly-miR169f) selected from the bioinformatics data. The sly-miR166b - *Minc3s01925g27230* (formerly named *Minc10092*) pair was chosen from the cross-kingdom hybridization approach (Table 2). No *C. elegans* homolog was found for this gene but a protein orthologue was identified as guanylate cyclase (UniProtKB/TrEMBL accession A0A1I8B0V8_MELHA) in *M. hapla*. The sly-miRNA156a - *Minc3s00025g01614* (formerly named *Minc11367*) pair was selected from the seed-based approach (Table 3). This miRNA has a complete seed-region homology with min_miRNA51 targeting the *Minc11367* gene, as shown in Supplementary Figure 1. In plants, it is well known that miR156 targets the SQUAMOSA PROMOTER BINDING PROTEIN-LIKE (SPL) transcription factor, controlling genes involved in the regulation of reactive oxygen species (ROS) (Yin et al., 2019). In the RKN trans-kingdom approach, this sly-miRNA putative target was predicted as the *C. elegans* homologous *gcy-9* (guanylyl cyclase,

WBGene00001536). A homologue of this gene was also identified in the parasitic nematode *Haemonchus contortus*, a close relative of *M. incognita* (Winter et al., 2012). Lastly, sly-miR169f was predicted to target *Minc3s00001g00015* (formerly named *Minc00111*, Supplementary Figure 2), an orthologue of the *C. elegans unc-52* (WBGene00006787) gene. In the GO analysis, this accession was related to functions connected to cell junction organization or muscle system.

Following the selection of tomato miRNAs to be tested in the nematode system, an *in vitro* soaking assay was performed as described in Section 2.4. The motility and vitality of the J2 larvae were observed and compared with those of larvae kept in the control solution. Subsequently, these larvae were used to infect tomato seedlings. Figure 4 shows the effects of the infection symptoms classified as "+", "++", "+++", along with galls formation on the roots. The values represent the percentage of symptoms normalized to the number of roots where the phenomena were observed. When the effects of the control solution and sly-miRNA156a soaked J2 larvae were compared, the best statistically significant reduction was detected in terms of gall formation. The amount of "+/roots", "++/roots" and "+++/roots" was also reduced up to 1/3, while the number of "galls/roots" was reduced up to 1/4. A significant reduction of the same parameters was observed also for the J2s soaked with sly-miR169f, where root enlargements ("+/roots", "++/roots", "+++/roots") were reduced up to 60% compared to control, and the number of "galls/roots" was halved. In the case of sly-miR166b, the observed reduction was less prominent, ranging from 15% ("+/roots") to 25% ("galls/roots").

Because the most prominent reduction of the galling process was observed for the sly-miRNA156a and sly-miRNA169f soaked larvae, these were selected for further molecular analysis. Quantitative RealTime-PCR was employed to measure the relative expression of the *Minc11367* (Minc3s00025g01614) and *Minc00111* (Minc3s00001g00015) genes, putatively targeted by these miRNAs. The obtained data show a downregulation of 54% in the miR156a-J2 and 29% in the miR169f-J2 treated larvae compared to the control (Figure 5). This result indirectly indicates that, in the *in vitro* experimental setup applied in this study, sly-miRNA156a and sly-miRNA169f have a cross-kingdom influence on the expression of *Minc11367* and *Minc00111* nematode genes.

To summarize these findings, Figure 6 shows a schematic representation of how the *in vitro* sly-miRNAs soaking experiments performed on J2 larvae led to a decrease in the *M. incognita* infection symptoms along with the downregulation of putative cross-kingdom

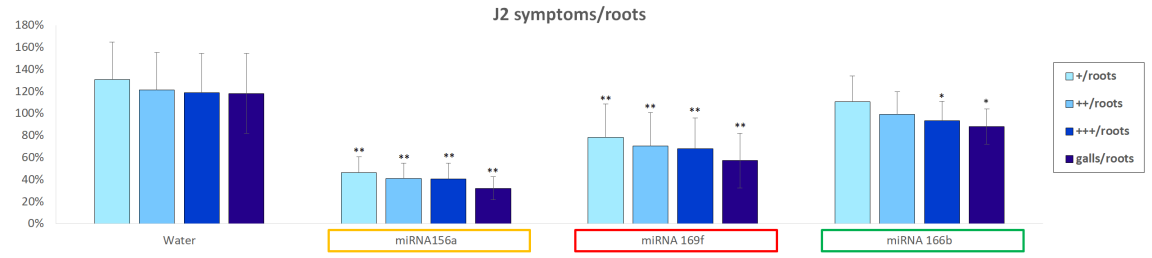

FIGURE 4
In vitro assay regarding soaked sly-miRNAs J2 larvae and susceptibility of the tomato root infections. The symptoms of infection (normalized with respect to the number of roots) with increasing apex enlargement, are categorized as "+", "++", "+++" and "galls". Data represents percentages expressed compared to the soaked J2s control solution, expressed as mean ± SD of three independent experiments for each plant/miRNA. Statistical differences, in terms of Student's *t*-test, are given (*$P \leq 0.05$; **$P \leq 0.01$). FDR, False Discovery Rate.

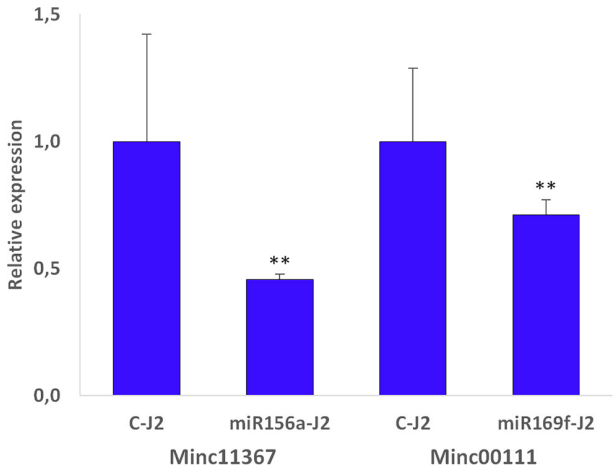

FIGURE 5
Relative expression data in miRNA156a and miRNA169f soaked J2s relative to control (C-J2). Transcript levels for *Minc11367* (Minc3s00025g01614) and *Minc00111* (Minc3s00001g00015) were measured by qRT-PCR after soaking treatment and compared to their transcript level in control samples. Data are shown as mean ± SD from two independent replicates. Statistical differences, in terms of Student's *t*-test, are given (**$P \leq 0.01$).

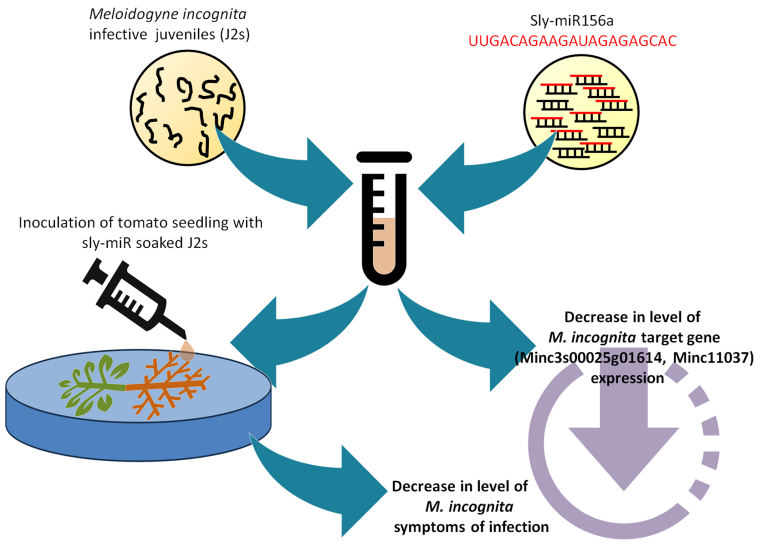

FIGURE 6
Schematic representation of the *in vitro* feeding assay showing the Sly-miRNAs soaking experiments performed on J2 larvae. The inoculation of tomato seedlings with sly-miR caused a decrease in the *M. incognita* infection symptoms and downregulation of putative cross-kingdom targets.

targets. To our knowledge, this is the first evidence showing that tomato miRNAs can be used to alter the infection ability of *M. incognita* larvae. Other studies related to the trans-kingdom transfer of tomato miRNAs to pathogens focused mainly on the *Botrytis cinerea* fungal infection. For instance, sly-miR1001 was shown to inhibit fungal virulence and conidiospore germination by targeting genes encoding for an ATP-dependent metallopeptidase and a cysteine-type endopeptidase (Meng et al., 2020). More recently, a genome-wide study identified multiple sRNAs and miRNAs with antifungal properties (Wu et al., 2023). The same study demonstrated that exogenous application of sly-miR396a was able to suppress the virulence of *B. cinerea*. Therefore, the data provided in our study together with other experimental evidence form the literature, evidence that tomato miRNAs can be effectively used to limit plant pathogen infection. However, given that most studies provide *in vitro* evidence to support this fact, in the future it would be required to further investigate how this transfer occurs and how is it conditioned by concentration and bioavailability in an *in vivo* system.

4 Conclusions

Following the increasing availability of omics data, bioinformatic studies are providing powerful tools to aid in setting up pertinent experimental designs based on preliminary predictions. This applies to miRNA-target interactions (both intra- and inter-specific) since different tools are available for target predictability based on sequence complementarity or hybridization energy. In this work, bidirectional bioinformatics analyses were conducted to uncover the potential miRNA-dependent cross-kingdom interactions between tomato and the phytoparasitic nematode *M. incognita* in terms of putative repressed genes and related biological processes. The obtained results are compatible with the host-parasite interactions between tomato and RKNs, suggesting that exogenous miRNAs may play a role in such processes. Although bioinformatics provides solid grounds to formulate hypotheses, some limitations are present considering the use of different computational methods, target prediction algorithms, and the lack of general guidelines applicable specifically for cross-kingdom predictions. Therefore, an *in vitro* experimental system was developed to support the potential cross-kingdom miRNAs effect during the *S. lycopersicum* - *M. incognita* interaction. The presented data evidence that the administration of sly-miR156a and sly-miR169f to J2s larvae was able to significantly lower root infection. This was also coupled with the downregulation of predicted cross-kingdom targets, *Minc11367* and *Minc00111*. Thus, the current study expands the knowledge on the host-parasite interactions between tomato and RKNs paving the way for future application of exogenous miRNAs as tools to control *M. incognita* infection. However, this is still preliminary work and further analyses should be taken into account to understand the highly complex *in vivo* mechanism of plant miRNA-mediated gene control in the context of nematode research.

Data availability statement

The original contributions presented in the study are included in the article/Supplementary Material. Further inquiries can be directed to the corresponding authors.

Ethics statement

The manuscript presents research on animals that do not require ethical approval for their study.

Author contributions

PL: Writing – original draft, Writing – review & editing, Conceptualization, Funding acquisition, Data curation. DD: Writing

– review & editing, Software. DM: Writing – review & editing, Software. PC: Writing – review & editing, Software. LP: Writing – original draft, Writing – review & editing, Conceptualization, Data curation. AM: Writing – original draft, Writing – review & editing, Conceptualization, Data curation.

Funding

The author(s) declare financial support was received for the research, authorship, and/or publication of this article. PL acknowledges the support from the Project NUTR-AGE (FOE-2021) DSBAD005.225.

Acknowledgments

PL would like to thank Campanale Antonia for the technical assistance during the *in vitro* experiments and Vitantonio Pantaleo for critical reading and discussions of the study. LP kindly thanks Gabriela Bindea (INSERM, Laboratory of Integrative Cancer Immunology, Université Paris Descartes, France) for the help provided for the ClueGO analysis on RKNs.

Conflict of interest

The authors declare that the research was conducted in the absence of any commercial or financial relationships that could be construed as a potential conflict of interest.

Publisher's note

Supplementary material

The Supplementary Material for this article can be found online at: https://www.frontiersin.org/articles/10.3389/fpls.2024.1383986/full#supplementary-material

SUPPLEMENTARY DATA SHEET 1
Complete dataset regarding cross-kingdom prediction based on *M. incognita* miRNAs putatively targeting genes in *S. lycopersicum*. Information regarding miRNA and target sequence, perfect seed complementarity (no GU), seed complementarity (with GU), percentage (%) of the match without seed and GU, % match without seed but with GU, and multiplicity, are provided.

SUPPLEMENTARY DATA SHEET 2
Complete dataset generated using the *cross-kingdom hybridization* approach regarding *S. lycopersicum* miRNAs putatively targeting genes in *M. incognita*. Information regarding Minimum Free Energy (MFE), miRNA and target sequence, perfect seed complementarity (no GU), seed complementarity (with GU), percentage (%) of the match without seed and GU, % match without seed but with GU, multiplicity, and 3′ÚTR targeting, are provided.

SUPPLEMENTARY DATA SHEET 3
Complete dataset using the *seed region-based search* approach regarding *S. lycopersicum* miRNAs putatively targeting genes in *M. incognita*. Information regarding Minimum Free Energy (MFE), miRNA and target sequence, perfect seed complementarity (no GU), seed complementarity (with GU), percentage (%) of the match without seed and GU, % match without seed but with GU, multiplicity, and 3′ÚTR targeting, are provided.

SUPPLEMENTARY DATA SHEET 4
List of enriched *S. lycopersicum* Biological Process GO terms, with the relevant terms of the functionally grouped term networks provided by ClueGO shown in bold. Genes relative to each term and the miRNAs targeting each gene are shown.

SUPPLEMENTARY DATA SHEET 5
List of enriched *M. incognita* Biological Process GO terms, with the relevant terms of the functionally grouped term networks provided by ClueGO shown in bold. Genes relative to each term and the miRNAs targeting each gene are given.

References

Abad, P., Gouzy, J., Aury, J.-M., Castagnone-Sereno, P., Danchin, E. G. J., Deleury, E., et al. (2008). Genome sequence of the metazoan plant-parasitic nematode *Meloidogyne incognita*. *Nat. Biotechnol.* 26, 909–915. doi: 10.1038/nbt.1482

Avsar, B., Zhao, Y., Li, W., and Lukiw, W. J. (2020). *Atropa belladonna* expresses a microRNA (aba-miRNA-9497) highly homologous to *Homo sapiens* miRNA-378 (hsa-miRNA-378); both miRNAs target the 3'-untranslated region (3'-UTR) of the mRNA encoding the neurologically relevant, zinc-finger transcription factor ZNF-691. *Cell Mol. Neurobiol.* 40, 179–188. doi: 10.1007/s10571-019-00729-w

Balakireva, A. V., and Zamyatnin, A. A. (2018). Indispensable role of proteases in plant innate immunity. *Int. J. Mol. Sci.* 19, 629. doi: 10.3390/ijms19020629

Banakar, P., Hada, A., Papolu, P. K., and Rao, U. (2020). Simultaneous RNAi knockdown of three FMRFamide-like peptide genes, *Mi-flp1*, *Mi-flp12*, and *Mi-flp18* provides resistance to root-knot nematode, *Meloidogyne incognita*. *Front. Microbiol.* 11. doi: 10.3389/fmicb.2020.573916

Banerjee, S., Gill, S. S., Gawade, B. H., Jain, P. K., Subramaniam, K., and Sirohi, A. (2018). Host delivered RNAi of two cuticle collagen genes, *Mi-col-1* and *Lemmi-5* hampers structure and fecundity in *Meloidogyne incognita*. *Front. Plant Sci.* 8. doi: 10.3389/fpls.2017.02266

Bartel, D. P. (2004). MicroRNAs: genomics, biogenesis, mechanism, and function. *Cell* 116, 281–297. doi: 10.1016/S0092-8674(04)00045-5

Becraft, P. W. (2002). Receptor kinase signaling in plant development. *Annu. Rev. Cell Dev. Biol.* 18, 163–192. doi: 10.1146/annurev.cellbio.18.012502.083431

Bellato, M., De Marchi, D., Gualtieri, C., Sauta, E., Magni, P., Macovei, A., et al. (2019). A bioinformatics approach to explore microRNAs as tools to bridge pathways between plants and animals. Is DNA Damage Response (DDR) a potential target process? *Front. Plant Sci.* 10. doi: 10.3389/fpls.2019.01535

Bindea, G., Mlecnik, B., Hackl, H., Charoentong, P., Tosolini, M., Kirilovsky, A., et al. (2009). ClueGO: a Cytoscape plug-in to decipher functionally groupedgene ontology and pathway annotation networks. *Bioinformatics* 25, 1091–1093. doi: 10.1093/bioinformatics/btp101

Blanc-Mathieu, R., Perfus-Barbeoch, L., Aury, J. M., Da Rocha, M., Gouzy, J., Sallet, E., et al. (2017). Hybridization and polyploidy enable genomic plasticity without sex in the most devastating plant-parasitic nematodes. *PloS Genet.* 13, e1006777. doi: 10.1371/journal.pgen.1006777

Blelloch, R., Anna-Arriola, S. S., Gao, D., Li, Y., Hodgkin, J., and Kimble, J. (1999). The *gon-1* gene is required for gonadal morphogenesis in *Caenorhabditis elegans*. *Dev. Biol.* 216, 382–393. doi: 10.1006/dbio.1999.9491

Breitenbach, H. H., Wenig, M., Wittek, F., Jordá, L., Maldonado-Alconada, A. M., Sarioglu, H., et al. (2014). Contrasting roles of the apoplastic aspartyl protease APOPLASTIC, ENHANCED DISEASE SUSCEPTIBILITY1-DEPENDENT1 and

LEGUME LECTIN-LIKE PROTEIN1 in Arabidopsis systemic acquired resistance. *Plant Physiol.* 165, 791–809. doi: 10.1104/pp.114.239665

Cabrera, J., Diaz-Manzano, F. E., Barcala, M., Arganda-Carreras, I., de Almeida-Engler, J., Engler, G., et al. (2015). Phenotyping nematode feeding sites: Three-dimensional reconstruction and volumetric measurements of giant cells induced by root-knot nematodes in Arabidopsis. *New Phytol.* 206, 868–880. doi: 10.1111/nph.13249

Cai, C., Li, C., Sun, R., Zhang, B., Nichols, R. L., Hake, K. D., et al. (2021). Small RNA and degradome deep sequencing reveals important roles of microRNAs in cotton (*Gossypium hirsutum* L.) response to root-knot nematode *Meloidogyne incognita* infection. *Genomics* 113, 1146–1156. doi: 10.1016/j.ygeno.2021.02.018

Camborde, L., Raynaud, C., Dumas, B., and Gaulin, E. (2019). DNA-damaging effectors: New players in the effector arena. *Trends Plant Sci.* 24, 1094–1101. doi: 10.1016/j.tplants.2019.09.012

Chen, L., Roake, C. M., Maccallini, P., Bavasso, F., Dehghannasiri, R., Santonicola, P., et al. (2022). TGS1 controls snRNA 3' end processing, prevents neurodegeneration and ameliorates SMN-dependent neurological phenotypes in *vivo*. *Nucleic Acids Res.* 28, 12400-12424. doi: 10.1101/2020.10.27.356782

Chen, S., Hajirezaei, M., Peisker, M., Tschiersch, H., Sonnewald, U., and Börnke., F. (2005). Decreased sucrose-6-phosphate phosphatase level in transgenic tobacco inhibits photosynthesis, alters carbohydrate partitioning, and reduces growth. *Planta* 221, 479–492. doi: 10.1007/s00425-004-1458-4

Chen, S., Hajirezaei, M. R., Zanor, M.-I., Hornyik, C., Debast, S., Lacomme, C., et al. (2008). RNA interference-mediated repression of sucrose-phosphatase in transgenic potato tubers (*Solanum tuberosum*) strongly affects the hexose-to-sucrose ratio upon cold storage with only minor effects on total soluble carbohydrate accumulation. *Plant Cell Environ.* 31, 165–176. doi: 10.1111/j.1365-3040.2007.01747.x

Cheng, G., Luo, R., Hu, C., Cao, J., and Jin, Y. (2013). Deep sequencing-based identification of pathogen-specific microRNAs in the plasma of rabbits infected with *Schistosoma japonicum*. *Parasitology* 140, 1751–1761. doi: 10.1017/S0031182013000917

Chin, A. R., Fong, M. Y., Somlo, G., Wu, J., Swiderski, P., Wu, X., et al. (2016). Cross-kingdom inhibition of breast cancer growth by plant miR159. *Cell Res.* 26, 217–228. doi: 10.1038/cr.2016.13

Collins, K. M., Bode, A. R., Fernandez, R. W., Tanis, J. E., Brewer, J. C., Creamer, M. S., et al. (2016). Activity of the C. elegans egg-laying behavior circuit is controlled by competing activation and feedback inhibition. *eLife* 5, e21126. doi: 10.7554/eLife.21126

Dai, X., and Zhao, P. X. (2011). psRNATarget: a plant small RNA target analysis server. *Nucleic Acids Res.* 39, W155–W159. doi: 10.1093/nar/gkr319

Dai, X., Zhuang, Z., and Zhao, P. X. (2018). psRNATarget: a plant small RNA target analysis server, (2017 release). *Nucleic Acids Res.* 46, W49–W54. doi: 10.1093/nar/gky316

Dalzell, J. J., McMaster, S., Fleming, C. C., and Maule, A. G. (2010). Short interfering RNA-mediated gene silencing in Globodera pallida and *Meloidogyne incognita* infective stage juveniles. *Int. J. Parasitol.* 40, 91–100. doi: 10.1016/j.ijpara.2009.07.003

Danchin, E., Arguel, M., Campan-Fournier, A., Perfus-Barbeoch, L., Magliano, M., Rosso, M., et al. (2013). Identification of novel target genes for safer and more specific control of root-knot nematodes from a pan-genome mining. *PloS Pathog.*, e1003745. doi: 10.1371/journal.ppat.1003745

Duplan, V., and Rivas, S. (2014). E3 ubiquitin-ligases and their target proteins during the regulation of plant innate immunity. *Front. Plant Sci.* 5. doi: 10.3389/fpls.2014.00042

EUROSTAT (2021). Available online at: https://ec.europa.eu/info/sites/default/files/food-farming-fisheries/farming/documents/tomatoes-production_en.pdf.

Franz, A., Ackermann, L., and Hoppe, T. (2014). Create and preserve: proteostasis in development and aging is governed by Cdc48/p97/VCP. *Biochim. Biophys. Acta* 1843, 205–215. doi: 10.1016/j.bbamcr.2013.03.031

Fu, Z. Q., and Dong, X. (2013). Systemic acquired resistance: turning local infection into global defense. *Annu. Rev. Plant Biol.* 64, 839–863. doi: 10.1146/annurev-arplant-042811-105606

Gally, C., Eimer, S., Richmond, J. E., and Bessereau, J. L. (2004). A transmembrane protein required for acetylcholine receptor clustering in *Caenorhabditis elegans*. *Nature* 431, 578–582. doi: 10.1038/nature02893

Gualtieri, C., Gianella, M., Pagano, A., Cadeddu, T., Araújo, S., Balestrazzi, A., et al. (2021). Exploring microRNA signatures of DNA Damage Response using an innovative system of genotoxic stress in *Medicago truncatula* seedlings. *Front. Plant Sci.* 12. doi: 10.3389/fpls.2021.645323

Gualtieri, C., Leonetti, P., and Macovei, A. (2020). Plant miRNA cross-kingdom transfer targeting parasitic and mutualistic organisms as a tool to advance modern agriculture. *Front. Plant Sci.* 11. doi: 10.3389/fpls.2020.00930

Guo, X. D., Johnson, J. J., and Kramer, J. M. (1991). Embryonic lethality caused by mutations in basement membrane collagen of *C. elegans*. *Nature* 349, 707–709. doi: 10.1038/349707a0

Harders, R. H., Morthorst, T. H., Lande, A. D., Hesselager, M. O., Mandrup, O. A., Bendixen, E., et al. (2018). Dynein links engulfment and execution of apoptosis via CED-4/Apaf1 in *C. elegans*. *Cell Death Dis.* 9, 1012. doi: 10.1038/s41419-018-1067-y

Haskell, D., and Zinovyeva, A. (2021). KH domain containing RNA-binding proteins coordinate with microRNAs to regulate *Caenorhabditis elegans* development. *G3 (Bethesda)* 11, jkab013. doi: 10.1093/g3journal/jkab013

Hou, D., He, F., Ma, L., Cao, M., Zhou, Z., Wei, Z., et al. (2018). The potential atheroprotective role of plant MIR156a as a repressor of monocyte recruitment on inflamed human endothelial cells. *J. Nutr. Biochem.* 57, 197–205. doi: 10.1016/j.jnutbio.2018.03.026

Howe, K. L., Bolt, B. J., Shafie, M., Kersey, P., and Berriman, M. (2017). WormBase ParaSite - a comprehensive resource for helminth genomics. *Mol. Biochem. Parasitol.* 215, 2–10. doi: 10.1016/j.molbiopara.2016.11.005

Hua, C., Zhao, J. H., and Guo, H. S. (2018). Trans-kingdom RNA silencing in plant-fungal pathogen interactions. *Mol. Plant* 11, 235–244. doi: 10.1016/j.molp.2017.12.001

Hudson, M. L., Kinnunen, T., Cinar, H. N., and Chisholm, A. D. (2006). *C. elegans* Kallmann syndrome protein KAL-1 interacts with syndecan and glypican to regulate neuronal cell migrations. *Dev. Biol.* 294, 352–365. doi: 10.1016/j.ydbio.2006.02.036

Iqbal, S., Fosu-Nyarko, J., and Jones, M. G. K. (2020). Attempt to silence genes of the RNAi pathways of the root-knot nematode, *Meloidogyne incognita* results in diverse responses including increase and no change in expression of some genes. *Front. Plant Sci.* 11. doi: 10.3389/fpls.2020.00328

Jaubert-Possamai, S., Noureddine, Y., and Favery, B. (2019). MicroRNAs, new players in the plant-nematode interaction. *Front. Plant Sci.* 10. doi: 10.3389/fpls.2019.01180

Kaloshian, I., and Teixeira, M. (2019). Advances in plant-nematode interactions with emphasis on the notorious nematode genus *Meloidogyne*. *Phytopathology* 109, 1988–1996. doi: 10.1094/PHYTO-05-19-0163-IA

Kaur, P., Shukla, N., Joshi, G., VijayaKumar, C., Jagannath, A., Agarwal, M., et al. (2017). Genome-wide identification and characterization of miRNAome from tomato (*Solanum lycopersicum*) roots and root-knot nematode (*Meloidogyne incognita*) during susceptible interaction. *PloS One* 12, e0175178. doi: 10.1371/journal.pone.0175178

Kazan, K., and Gardiner, D. M. (2017). Targeting pathogen sterols: Defence and counterdefence? *PloS Pathog.* 13, e1006297. doi: 10.1371/journal.ppat.1006297

Kleaveland, B. (2023). SnapShot: Target-directed miRNA degradation. *Cell* 25, 5674–5674. doi: 10.1016/j.cell.2023.11.020

Kozomara, A., Birgaoanu, M., and Griffiths-Jones, S. (2019). miRBase: from microRNA sequences to function. *Nucleic Acids Res.* 47, D155–D162. doi: 10.1093/nar/gky1141

Kruger, J., and Rehmsmeier, M. (2006). RNAhybrid: microRNA target prediction easy, fast and flexible. *Nucleic Acids Res.* 34, W451–W454. doi: 10.1093/nar/gkl243

LaMonte, G., Philip, N., Reardon, J., Lacsina, J. R., Majoros, W., Chapman, L., et al. (2012). Translocation of sickle cell erythrocyte microRNAs into *Plasmodium falciparum* inhibits parasite translation and contributes to malaria resistance. *Cell Host Microbe* 12, 187–199. doi: 10.1016/j.chom.2012.06.007

Lang, A. E., and Lundquist, E. A. (2021). The collagens DPY-17 and SQT-3 direct anterior-posterior migration of the Q neuroblasts in *C. elegans*. *J. Dev. Biol.* 9, 7. doi: 10.3390/jdb9010007

Leonetti, P., and Molinari, S. (2020). Epigenetic and metabolic changes in root-knot nematode-plant interactions. *Int. J. Mol. Sci.* 21, 7759. doi: 10.3390/ijms21207759

Li, L., Liu, H., Wang, W., Chandra, M., Collins, B. M., and Hu, Z. (2018). SNT-1 functions as the Ca^{2+} sensor for tonic and evoked neurotransmitter release in *Caenorhabditis Elegans*. *J. Neurosci.* 38, 5313–5324. doi: 10.1523/JNEUROSCI.3097-17.2018

Li, Y., Ren, Q., Bo, T., Mo, M., and Liu, Y. (2022). AWA and ASH homologous sensing genes of *Meloidogyne incognita* contribute to the tomato infection process. *Pathogens* 11, 1322. doi: 10.3390/pathogens11111322

Li, Z., Xu, R., and Li, N. (2018). MicroRNAs from plants to animals, do they define a new messenger for communication? *Nutr. Metab. (Lond).* 15, 68. doi: 10.1186/s12986-018-0305-8

Li-Leger, E., Feichtinger, R., Flibotte, S., Holzkamp, H., Schnabel, R., and Moerman, D. G. (2021). Identification of essential genes in *Caenorhabditis elegans* through whole-genome sequencing of legacy mutant collections. *G3 (Bethesda)* 11, jkab328. doi: 10.1093/g3journal/jkab328

Liu, Y. C., Chen, W. L., Kung, W. H., and Huang, H. D. (2017). Plant miRNAs found in human circulating system provide evidences of cross kingdom RNAi. *BMC Genomics* 18, 112. doi: 10.1186/s12864-017-3502-3

Liu, R., Xia, R., Xie, Q., and Wu, Y. (2021). Endoplasmic reticulum-related E3 ubiquitin ligases: Key regulators of plant growth and stress responses. *Plant Commun.* 2, 100186. doi: 10.1016/j.xplc.2021.100186

Lukasik, A., Brzozowska, I., Zielenkiewicz, U., and Zielenkiewicz, P. (2018). Detection of plant miRNAs abundance in human breast milk. *Int. J. Mol. Sci.* 19, E37. doi: 10.3390/ijms19010037

Macovei, A., Rubio-Somoza, I., Paiva, J. A. P., Araújo, S., and Donà, M. (2021). Editorial: MicroRNA signatures in plant genome stability and genotoxic stress. *Front. Plant Sci.* 12. doi: 10.3389/fpls.2021.683302

Mal, C., Aftabuddin, M., and Kundu, S. (2018). IIKmTA: inter and intra kingdom miRNA-target analyzer. *Interdiscip. Sci.* 10, 538–543. doi: 10.1007/s12539-018-0291-6

Maruyama, I. N. (2017). Receptor guanylyl cyclases in sensory processing. *Front. Endocrinol. (Lausanne)* 7. doi: 10.3389/fendo.2016.00173

Melillo, M. T., Leonetti, P., Bongiovanni, M., Castagnone-Sereno, P., and Bleve-Zacheo, T. (2006). Modulation of reactive oxygen species activities and H_2O_2 accumulation during compatible and incompatible tomato-root-knot nematode interactions. *New Phytol.* 170, 501–512. doi: 10.1111/j.1469-8137.2006.01724.x

Meng, X., Jin, W., and Wu, F. (2020). Novel tomato miRNA miR1001 initiates cross-species regulation to suppress the conidiospore germination and infection virulence of *Botrytis cinerea in vitro*. *Gene* 759, 145002. doi: 10.1016/j.gene.2020.145002

Merz, D. C., Alves, G., Kawano, T., Zheng, H., and Culotti, J. G. (2003). UNC-52/perlecan affects gonadal leader cell migrations in *C. elegans* hermaphrodites through alterations in growth factor signaling. *Dev. Biol.* 256, 173–186. doi: 10.1016/S0012-1606(03)00014-9

Molinari, S., and Miacola, C. (1997). Antioxidant enzymes in phytoparasitic nematodes. *J. Nematol.*, 153–159.

Molinari, S., Fanelli, E., and Leonetti, P. (2014). Expression of tomato salicylic acid (SA)-responsive pathogenesis-related genes in Mi-1-mediated and SA-induced resistance to root-knot nematodes. *Mol. Plant Pathol.* 15, 255–264. doi: 10.1111/mpp.12085

Molinari, S., and Leonetti, P. (2019). Bio-control agents activate plant immune response and prime susceptible tomato against root-knot nematodes. *PloS One* 14, e0213230. doi: 10.1371/journal.pone.0213230

Palomares-Rius, J. E., Hasegawa, K., Siddique, S., and Vicente, C. S. L. (2021). Editorial: Protecting our crops - Approaches for plant parasitic nematode control. *Front. Plant Sci.* 12. doi: 10.3389/fpls.2021.726057

Papaevgeniou, N., and Chondrogianni, N. (2014). The ubiquitin proteasome system in *Caenorhabditis elegans* and its regulation. *Redox Biol.* 2, 333–347. doi: 10.1016/j.redox.2014.01.007

Parry, G. (2013). Assessing the function of the plant nuclear pore complex and the search for specificity. *J. Exp. Bot.* 64, 833–845. doi: 10.1093/jxb/ers289

Pastuglia, M., Swarup, R., Rocher, A., Saindrenan, P., Roby, D., Dumas, C., et al. (2002). Comparison of the expression patterns of two small gene families of S gene family receptor kinase genes during the defence response in *Brassica oleracea* and *Arabidopsis thaliana*. *Gene* 282, 215–225. doi: 10.1016/S0378-1119(01)00821-6

Paul, M. J. (2008). Trehalose 6-phosphate: a signal of sucrose status. *Biochem. J.* 412, e1–e2. doi: 10.1042/BJ20080598

Rabuma, T., Gupta, O. P., and Chhokar, V. (2022). Recent advances and potential applications of cross-kingdom movement of miRNAs in modulating plant's disease response. *RNA Biol.* 19, 519–532. doi: 10.1080/15476286.2022.2062172

Ramirez-Suarez, N. J., Belalcazar, H. M., Salazar, C. J., Beyaz, B., Raja, B., Nguyen, K. C. Q., et al. (2019). Axon-dependent patterning and maintenance of somatosensory dendritic arbors. *Dev. Cell.* 48, 229–244.e4. doi: 10.1016/j.devcel.2018.12.015

Rogalski, T. M., Gilchrist, E. J., Mullen, G. P., and Moerman, D. G. (1995). Mutations in the *unc-52* gene responsible for body wall muscle defects in adult *Caenorhabditis elegans* are located in alternatively spliced exons. *Genetics* 139, 159–169. doi: 10.1093/genetics/139.1.159

Rossillo, M., and Ringstad, N. (2020). Development of specialized sensory neurons engages a nuclear receptor required for functional plasticity. *Genes Dev.* 34, 1666–1679. doi: 10.1101/gad.342212.120

Seid, A., Fininsa, C., Mekete, T., Decraemer, W., and Wesemael, W. M. L. (2015). Tomato (*Solanum lycopersicum*) and root-knot nematodes (*Meloidogyne* spp.) – a century-old battle. *Nematology* 17, 995–1009. doi: 10.1163/15685411-00002935

Shannon, P., Markiel, A., Ozier, O., Baliga, N. S., Wang, J. T., Ramage, D., et al. (2003). Cytoscape: a software environment for integrated models of biomolecular interaction networks. *Genome Res.* 13, 2498–2504. doi: 10.1101/gr.1239303

Shi, Y., and Mello, C. (1998). A CBP/p300 homolog specifies multiple differentiation pathways in *Caenorhabditis elegans*. *Genes Dev.* 12, 943–955. doi: 10.1101/gad.12.7.943

Shivakumara, T. N., Dutta, T. K., Chaudhary, S., von Reuss, S. H., Williamson, V. M., and Rao, U. (2019). Homologs of *Caenorhabditis elegans* chemosensory genes have roles in behavior and chemotaxis in the root-knot nematode *Meloidogyne incognita*. *Mol. Plant Microbe Interact.* 32, 876–887. doi: 10.1094/MPMI-08-18-0226-R

Shu, J., Chiang, K., Zempleni, J., and Cui, J. (2015). Computational characterization of exogenous microRNAs that can be transferred into human circulation. *PloS One* 10, e0140587. doi: 10.1371/journal.pone.0140587

Singh, S., Singh, B., and Singh, A. P. (2015). Nematodes: A threat to sustainability of agriculture. *Proc. Environ. Sci.* 29, 215–216. doi: 10.1016/j.proenv.2015.07.270

Soh, M. S., Cheng, X., Vijayaraghavan, T., Vernon, A., Liu, J., and Neumann, B. (2020). Disruption of genes associated with Charcot-Marie-Tooth type 2 lead to common behavioural, cellular and molecular defects in *Caenorhabditis elegans*. *PloS One* 15, e0231600. doi: 10.1371/journal.pone.0231600

Somvanshi, V. S., Ghosh, O., Budhwar, R., Dubay, B., Shukla, R. N., and Rao, U. (2018). A comprehensive annotation for the root-knot nematode *Meloidogyne incognita* proteome data. *Data Brief.* 19, 1073–1079. doi: 10.1016/j.dib.2018.05.131

Suárez, R., Wong, A., Ramírez, M., Barraza, A., Del Carmen Orozco, M., Cevallos, M. A., et al. (2008). Improvement of drought tolerance and grain yield in common bean by overexpressing trehalose-6-phosphate synthase in Rhizobia. *Mol. Plant Microbe Interact. J.* 21, 958–966. doi: 10.1094/MPMI-21-7-0958

Takasaki, T., Hatakeyama, K., Suzuki, G., Watanabe, M., Isogai, A., and Hinata, K. (2000). The S receptor kinase determines self-incompatibility in *Brassica stigma*. *Nature* 403, 913–916. doi: 10.1038/35002628

Tan, J. A., Jones, M. G., and Fosu-Nyarko, J. (2013). Gene silencing in root lesion nematodes (*Pratylenchus* spp.) significantly reduces reproduction in a plant host. *Exp. Parasitol.* 133, 166–178. doi: 10.1016/j.exppara.2012.11.011

Wang, W., Liu, D., Zhang, X., Chen, D., Cheng, Y., and Shen, F. (2018). Plant microRNAs in cross-kingdom regulation of gene expression. *Int. J. Mol. Sci.* 19, E2007. doi: 10.3390/ijms19072007

Wang, Y., Mao, Z., Yan, J., Cheng, X., Liu, F., Xiao, L., et al. (2015). Identification of microRNAs in *Meloidogyne incognita* using deep sequencing. *PloS One* 10, e0133491. doi: 10.1371/journal.pone.0133491

Wang, Y., Mortimer, J. C., Davis, J., Dupree, P., and Keegstra, K. (2013). Identification of an additional protein involved in mannan biosynthesis. *Plant J.* 73, 105–117. doi: 10.1111/tpj.12019

Wang, B., Sun, Y., Song, N., Zhao, M., Liu, R., Feng, H., et al. (2017). *Puccinia striiformis* f. sp. tritici microRNA-like RNA 1 (Pst-milR1), an important pathogenicity factor of Pst, impairs wheat resistance to Pst by suppressing the wheat pathogenesis-related 2 gene. *New Phytol.* 215, 338–350. doi: 10.1111/nph.14577

Wang, M., Weiberg, A., Lin, F. M., Thomma, B. P., Huang, H. D., and Jin, H. (2016). Bidirectional cross-kingdom RNAi and fungal uptake of external RNAs confer plant protection. *Nat. Plants.* 2, 16151. doi: 10.1038/nplants.2016.151

Weiberg, A., Wang, M., Lin, F. M., Zhao, H., Zhang, Z., Kaloshian, I., et al. (2013). Fungal small RNAs suppress plant immunity by hijacking host RNA interference pathways. *Science* 342, 118–123. doi: 10.1126/science.1239705

Winter, A. D., Weir, W., Hunt, M., Berriman, M., Gilleard, J. S., Devaney, E., et al. (2012). Diversity in parasitic nematode genomes: the microRNAs of *Brugia pahangi* and *Haemonchus contortus* are largely novel. *BMC Genomics* 13, 4. doi: 10.1186/1471-2164-13-4

Wu, F., Huang, Y., Jiang, W., and Jin, W. (2023). Genome-wide identification and validation of tomato-encoded sRNA as the cross-species antifungal factors targeting the virulence genes of *Botrytis cinerea*. *Front. Plant Sci.* 14. doi: 10.3389/fpls.2023.1072181

Yang, F., Ding, L., Zhao, D., Fan, H., Zhu, X., Wang, Y., et al. (2022). Identification and functional analysis of tomato microRNAs in the biocontrol *Bacterium pseudomonas putida* induced plant resistance to *Meloidogyne incognita*. *Phytopathology* 112, 2372–2382. doi: 10.1094/PHYTO-03-21-0101-R

Yang, B., Xu, X., Russell, L., Sullenberger, M. T., Yanowitz, J. L., and Maine, E. M. (2019). A DNA repair protein and histone methyltransferase interact to promote genome stability in the *Caenorhabditis elegans* germ line. *PloS Genet.* 15, e1007992. doi: 10.1371/journal.pgen.1007992

Yang, F., Zhao, D., Fan, H., Zhu, X., Wang, Y., Liu, X., et al. (2020). Functional analysis of long non-coding RNAs reveal their novel roles in biocontrol of bacteria-induced tomato resistance to *Meloidogyne incognita*. *Int. J. Mol. Sci.* 21, 911. doi: 10.3390/ijms21030911

Yin, H., Hong, G., Li, L., Zhang, X., Kong, Y., Sun, Z., et al. (2019). miR156/SPL9 regulates reactive oxygen species accumulation and immune response in *Arabidopsis thaliana*. *Phytopathology* 109, 632–642. doi: 10.1094/PHYTO-08-18-0306-R

Zhang, L., Hou, D., Chen, X., Li, D., Zhu, L., Zhang, Y., et al. (2012). Exogenous plant MIR168a specifically targets mammalian LDLRAP1: evidence of cross-kingdom regulation by microRNA. *Cell Res.* 22, 107–126. doi: 10.1038/cr.2011.158

Zhang, L. L., Jing, X. D., Chen, W., Wang, Y., Lin, J., Zheng, L., et al. (2019). Host plant-derived miRNAs potentially modulate the development of a cosmopolitan insect pest, *Plutella xylostella*. *Biomolecules* 9, 602. doi: 10.3390/biom9100602

Zhang, H., Li, Y., Liu, Y., Liu, H., Wang, H., Jin, W., et al. (2016). Role of plant microRNA in cross-species regulatory networks of humans. *BMC Syst. Biol.* 10, 60. doi: 10.1186/s12918-016-0292-1

Zhang, B., Li, W., Zhang, J., Wang, L., and Wu, J. (2019). Roles of small RNAs in virus-plant interactions. *Viruses* 11, 827. doi: 10.3390/v11090827

Zhang, Y., Wang, Y., Xie, F., et al. (2016). Identification and characterization of microRNAs in the plant-parasitic root-knot nematode *Meloidogyne incognita* using deep sequencing. *Funct. Integr. Genomics* 16, 127–142. doi: 10.1007/s10142-015-0472-x

Zhao, Q., Mao, Q., Zhao, Z., Dou, T., Wang, Z., Cui, X., et al. (2018). Prediction of plant-derived xenomiRs from plant miRNA sequences using random forest and one-dimensional convolutional neural network models. *BMC Genomics* 19, 839. doi: 10.1186/s12864-018-5227-3

Zhu, K., Liu, M., Fu, Z., Zhou, Z., Kong, Y., Liang, H., et al. (2017). Plant microRNAs in larval food regulate honeybee caste development. *PloS Genet.* 13, e1006946. doi: 10.1371/journal.pgen.1006946

frontiers | Frontiers in Plant Science

TYPE Review
PUBLISHED 08 May 2024
DOI 10.3389/fpls.2024.1370532

OPEN ACCESS

EDITED BY
Andressa Machado,
Agronema, Brazil

REVIEWED BY
Muhammad Shahzad Anjam,
Swedish University of Agricultural Sciences, Sweden
Robert Malinowski,
Polish Academy of Sciences, Poland

*CORRESPONDENCE
Carolina Escobar
carolina.escobar@uclm.es

†These authors have contributed equally to this work

RECEIVED 14 January 2024
ACCEPTED 10 April 2024
PUBLISHED 08 May 2024

CITATION
Domínguez-Figueroa J, Gómez-Rojas A and Escobar C (2024) Functional studies of plant transcription factors and their relevance in the plant root-knot nematode interaction. *Front. Plant Sci.* 15:1370532. doi: 10.3389/fpls.2024.1370532

Functional studies of plant transcription factors and their relevance in the plant root-knot nematode interaction

Jose Domínguez-Figueroa[1,2†], Almudena Gómez-Rojas[1†] and Carolina Escobar[1*]

[1]Facultad de Ciencias Ambientales y Bioquímica, Universidad de Castilla-La Mancha, Toledo, Spain, [2]Centro de Biotecnologia y Genomica de Plantas (CBGP), Universidad Politecnica de Madrid and Instituto de Investigacion y Tecnologia Agraria y Alimentaria-Consejo Superior de investigaciones Cientificas (UPM-INIA/CSIC), Madrid, Spain

Root-knot nematodes are polyphagous parasitic nematodes that cause severe losses in the agriculture worldwide. They enter the root in the elongation zone and subtly migrate to the root meristem where they reach the vascular cylinder and establish a feeding site called gall. Inside the galls they induce a group of transfer cells that serve to nurture them along their parasitic stage, the giant cells. Galls and giant cells develop through a process of post-embryogenic organogenesis that involves manipulating different genetic regulatory networks within the cells, some of them through hijacking some molecular transducers of established plant developmental processes, such as lateral root formation or root regeneration. Galls/giant cells formation involves different mechanisms orchestrated by the nematode´s effectors that generate diverse plant responses in different plant tissues, some of them include sophisticated mechanisms to overcome plant defenses. Yet, the plant-nematode interaction is normally accompanied to dramatic transcriptomic changes within the galls and giant cells. It is therefore expected a key regulatory role of plant-transcription factors, coordinating both, the new organogenesis process induced by the RKNs and the plant response against the nematode. Knowing the role of plant-transcription factors participating in this process becomes essential for a clear understanding of the plant-RKNs interaction and provides an opportunity for the future development and design of directed control strategies. In this review, we present the existing knowledge of the TFs with a functional role in the plant-RKN interaction through a comprehensive analysis of current scientific literature and available transcriptomic data.

KEYWORDS

plant-RKNs interaction, galls, giant cells, transcription factors, new organogenesis, plant defense, plant-development

Introduction

Plant-parasitic nematodes have the ability to infect a wide range of host plants from which they feed depleting their resources, resulting in significant economic losses in agricultural production worldwide (Singh et al., 2015; Kikuchi et al., 2017). Among these destructive pathogens, the endoparasitic Root-Knot Nematodes (RKNs; *Meloidogyne* spp.) are one of the most economically impactful (Elling, 2013). RKNs, use their stylet and a diverse range of effectors to invade the plant roots and initiate the formation of specialized feeding cells known as giant cells (GCs). These GCs are contained within a novel pseudo-organ called gall that constitutes their feeding site (Escobar et al., 2015). While the significant role of the pericycle in gall formation is well-established from experiments with transgenic lines that induce chemical ablation, the precise origin of the GCs precursor cells remains not fully understood. However, some evidence points to their origin from precursor cells of the pericycle, xylem and/or vascular cambium (Cabrera et al., 2014b; Olmo et al., 2017, Olmo et al., 2020). GCs undergo mitosis accompanied by incomplete cytokinesis and DNA endoreduplication forming a multinucleated cell with greatly increased volume and a dense cytosol. Moreover, GCs also show fragmented vacuoles, undergo cell wall modifications, and ultimately develop membrane invaginations, becoming transfer cells to nourish the nematode (de Almeida Engler and Favery, 2011; Cabrera et al., 2014b; Escobar et al., 2015). RKNs employ sophisticated mechanisms to overcome plant defenses and modulate the host biochemistry and physiology (Kikuchi et al., 2017). They manipulate different genetic regulatory programs of the plant cells, including the cell cycle, various developmental programs, and stress responses, in order to undergo new post-embryogenic organogenesis leading to gall formation. For instance, *Meloidogyne javanica* infection alters pathways involved in *de novo* organogenesis leading to feeding site formation by interfering with auxins signaling cascades (Cabrera et al., 2014b). Consequently, a substantial transcriptional response is triggered (e.g., in *Arabidopsis thaliana*; Jammes et al., 2005; Fuller et al., 2007; Barcala et al., 2010; Silva et al., 2022).

Due to the mentioned dramatic transcriptomic changes described in galls, a pivotal regulatory role of transcription factors (TFs) is therefore expected, coordinating both, the new organogenesis process induced by the RKNs and the plant response against the nematode. Therefore, understanding the role of TFs during RKN infection is essential for a deeper understanding of the plant-nematode interaction and for the development of future control strategies. In this review, we have explored the existing knowledge on TFs involved in the plant-RKN interaction through a comprehensive analysis of current scientific literature and available transcriptomic data, the latter focused on Arabidopsis as considerable transcriptomic data is available and it was shown to be a good model of the plant-RKN interaction (Gheysen and Fenoll, 2011). Our aim is to compile the existing knowledge regarding the crucial role of TFs in the orchestration of the transcriptional response activated within the plant after RKN infection.

Transcriptional profiling of transcription factors families in arabidopsis

Several transcriptomic analyses have been performed to investigate mRNA population changes during RKNs establishment and gall formation in Arabidopsis plants (Jammes et al., 2005; Fuller et al., 2007; Barcala et al., 2010; Silva et al., 2022). These studies have provided valuable insights into the genetic and transcriptional dynamics associated with gall development. Functional classification of differentially expressed genes (DEGs) revealed RNA-related pathways as one of the groups with a high number of DEGs (Barcala et al., 2010), which are mostly involved in biological processes such as transcriptional regulation. Therefore, we analyzed the data contained in the NEMATIC database (NEMatode-Arabidopsis-Transcriptomic-Interaction-Tool; Cabrera et al., 2014a) that includes the most representative transcriptomic experiments of the RKN interaction in Arabidopsis, and the data from a recent RNAseq of galls 3 days post-infection (dpi) in Arabidopsis (Silva et al., 2022). These data show that of the 1717 annotated TF loci in the Arabidopsis genome based on the criteria of the Plant Transcription Factor Data Base (PlantTFDB; Jin et al., 2014), 834 TFs are differentially expressed (DE) in one or more experiments, that correspond to approximately 49% of the total known TFs in Arabidopsis. Among the 58 families classified according to PlantTFDB (Jin et al., 2014), 53 of them have DE members at some stage of gall formation (91%; Figure 1A), 52 TFs families at early stage (3 dpi) and 37 at medium-late stages (7, 14 and 21 dpi), (89% and 64%, respectively; Figure 1A). In GCs at 3 dpi, 29 TF family members were DE (50%; Figure 1B). Only 5 TFs families did not show DE members in either GCs or any of the gall stages. This indicates that most of the TF families are DE at one or more stages of gall and/or GCs formation, which presumably should have a great impact in the dramatic transcriptional changes described in galls (see introduction). Figures 1C–E also shows the percentage of DE TFs within the top 36 TF families with the highest number of DE members in early and mid-late stage galls and GCs. Six of these belong to TF superfamilies in which all TF members were included. The predominant families in all three transcriptomes were MYB, bHLH, ERF, NAC and WRKY. The role of several members of these TF families during the plant-nematode interaction was analysed and is our focus throughout the manuscript.

While all these data indicate a substantial involvement of TFs in regulating the transcriptional responses of plants to RKN infection, it is worth noting that the functional roles of only over 30 Arabidopsis TFs and about a dozen in tomato (*Solanum lycopersicum*) have been investigated (Table 1). Therefore, our

10.3389/fpls.2024.1370532

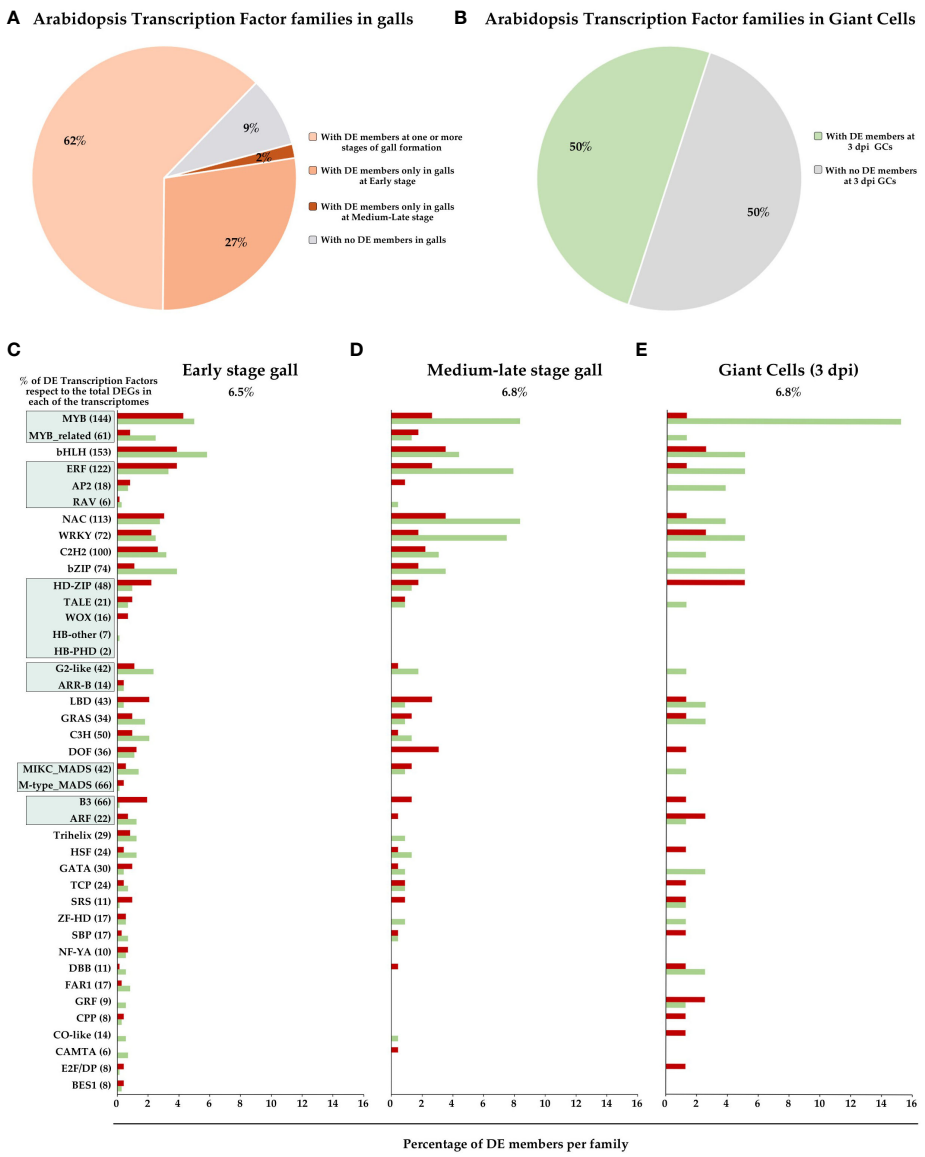

FIGURE 1
Overview of Arabidopsis Transcription Factor (TF) family profiles in gall formation. Percentage of TF families (58 families according to PlantTFDB; Jin et al., 2014) with and without differentially expressed (DE) members in different gall developmental stages as indicated **(A)** and GCs at 3 dpi **(B)**. The top 36 TF families and the top 6 superfamilies with the highest number of DE members in the RKNs transcriptomes, at early-stage galls [3 dpi galls; **(C)**], galls at mid-late stages [7, 14 and 21 dpi; **(D)**] and GCs 3 dpi **(E)** were represented. X axis, percentage of DE genes in each TFs family in Arabidopsis, with respect to the total members identified in PlantTFDB. Y axis, TFs families and superfamilies indicated by green squares [GARP (G2-like and ARR-B), B3 (ARF and B3), AP2/ERF (RAV, AP2 and ERF), MYB (MYB and MYB_related), MADS (M type, and MIKC) and Homeobox (HD-ZIP, HB-other, TALE, WOX and HB-PHD)] of Arabidopsis according to PlantTFDB. Red, induced genes, green, repressed genes, grey, non-differentially expressed.

understanding of the regulatory networks orchestrated by TFs in plant-RKN interaction remains rather limited.

Plant transcription factors with a role in plant-defense during the RKNs interaction

Plants have developed a multitude of defense mechanisms to counter potential pathogen attacks. The two primary plant immune responses are PAMP-triggered immunity (PTI), which is initiated by the recognition of receptors that recognize pathogen-associated molecular patterns (PAMPs), and effector-triggered immunity (ETI), in which pathogen effectors are recognized by plant resistance proteins known as R proteins (Peng et al., 2018). Both signaling pathways trigger similar molecular processes such as MAPK cascades, the production of reactive oxygen species, secondary metabolites and an increase in the biosynthesis of hormones such as salicylic acid (SA), jasmonic acid (JA), abscisic acid (ABA) and ethylene (ETH; Peng et al., 2018; Isah, 2019). However, PTI induces rapid and transient activation of MAPKs to

enhance local immune responses without triggering plant cell death, whereas ETI results in prolonged and sustained MAPK activity, usually leading to hypersensitive response and programmed cell death (Tsuda et al., 2013). However, both PTI and ETI pathways seem to be interconnected as it has recently been described that the activation of either PTI or ETI alone is not sufficient for effective resistance to the bacterial plant-pathogen *Pseudomonas syringae*. Thus, both immune responses mutually potentiate to activate strong defences against pathogens (Ngou et al., 2020). In any case, plant defense involves a complex interconnected signaling network that ensures a precise transcriptional response. Consequently, several TFs have been identified as crucial for fine-tuning the plant's transcriptional immune response (Birkenbihl et al., 2017). In this respect, TFs from different families, such as WRKY, MYB, AP2 and bZIP, typically induced in response to various biotic and abiotic stresses (Ambawat et al., 2013; Jiang et al., 2017) were also differentially expressed during the RKNs interaction (e.g., in *Arabidopsis thaliana;* Jammes et al., 2005; Fuller et al., 2007; Silva et al., 2022) including the GCs (Barcala et al., 2010). However, plant-parasitic nematodes, like other pathogens such as bacteria, fungi, oomycetes and some insects, secrete proteins and small molecules, called effectors, to suppress or evade host defense responses and alter host cell structure and function to their advantage, thereby facilitating nematode establishment (Rutter et al., 2022). This section of the review explores the existing literature on defense-related transcription factors (TFs) and their role in the context of the plant-RKNs interaction.

The WRKY family is one of the largest TF families found exclusively in plants. Its members play critical roles in various plant processes, encompassing growth, development, abiotic and biotic stress responses, and plant innate immunity (Wani et al., 2021). Some of them are key components in pathways responsible for PTI and ETI activation (Ribeiro et al., 2022). In an RNAseq data of tomato roots after *M. javanica* infection (15 dpi; Chinnapandi et al., 2017), several WRKYs were identified as negative regulators of the defence response. Among the up-regulated genes, *SlWRKY45* was further studied using a *promoter::GUS* reporter line. The line showed considerable activation at 5 dpi, which continued through feeding-site development and gall maturation (15 and 28 dpi; Table 1), in line with the RNAseq data. Two independent overexpressing lines of *35S:SlWRKY45* showed an increase in nematode infection and GCs area compared to the control lines, although the number of GCs within the galls was not affected (Chinnapandi et al., 2017, Table 1). Consistently, qRT-PCR revealed a down-regulation of defence-related genes, which are typical markers of JA and SA-mediated pathways, such as those encoding pathogenesis-related (PR-1) and proteinase inhibitor II (Pin2) proteins respectively, which could explain the increased nematode infection in the overexpressing line. In this respect, it has been recently described that SlWRKY45 interact with JA-ZIM domain family proteins that are key repressors of the JA signalling, and it is also able to bind and inhibit the activity of the promoter of the JA biosynthesis gene ALLENE OXIDE CYCLASE (AOC) (Huang et al., 2022). All of this is consistent with the attenuated resistance to *Meloidogyne incognita* of *SlWRKY45* overexpression and confirm its role as a negative regulator fo the defense response (PTI) against *Meloidogyne* spp. Additionally, *SlWRKY45* is upregulated by cytokinins, and its overexpression caused the repression of the cytokinin response factor 1 (*CRF1*) and *CRF6* (Chinnapandi et al., 2017). RKNs and cyst nematodes (CNs) have the ability to synthesize and secrete cytokinins, as noted by De Meutter et al. (2003). Furthermore, it has been demonstrated that the CN *Heterodera shachtii* has a functional cytokinin-synthesizing isopentenyltransferase gene which is essential for virulence and feeding site expansion (Siddique et al., 2015).The secretion of nematode cytokinins could potentially disrupt the balance of plant hormones and cytokinin signalling. Therefore, SlWRK45 may play a crucial role in coordinating hormone signals that promote nematode development within the root tissue. Similarly, recent studies have identified SlWRKY16 and SlWRKY31 as negative regulators of plant immunity and defence (PTI) in tomato. Both genes were induced during nematode infection until late infection stages (28 dpi). Overexpression of these genes in tomato lines using *R. rhizogenes*-mediated transformation under the control of the *CaMV35S* promoter resulted in increased susceptibility to *M. javanica*, as evidenced by enhanced galling and reproduction parameters (Kumar et al., 2023; Table 1).

In contrast to SlWRKY45, 16, and 31, which act as negative regulators of the plant defence response to RKNs, other members of the WRKY family have been described as positive regulators of defence against RKNs. For instance, *WRKY11*, whose expression is induced 24 hours after infection with *M. incognita*, and WRKY17, which can function in partial redundancy with WRKY11, are associated with the activation of basal defence mechanisms (PTI). The Arabidopsis lines *wrky11*, *wrky17*, and *wrky11/wrky17* exhibited increased susceptibility to *M. incognita*. This was evident from the significantly higher number of galls observed 4 weeks after inoculation in both the single and double mutant lines compared to the wild-type plants. However, there were no significant differences between the single mutants and the double mutant, indicating that these two TFs do not function redundantly in this pathogenic interaction (Teixeira et al., 2016; Table 1). Similarly, mutant lines *wrky11* and *wrky17* showed more susceptibility in Arabidopsis infected with the CN *Heterodera schachtii* (Ali et al., 2014), indicating commonalities in the basal resistance mechanisms between both plant-(RKNs and CNs) interactions. Additionally, *WRKY11pro::GUS* lines showed that the *WRKY11* promoter was activated in the root elongation zone and root tip 24 hai with *M. incognita* (Table 1). Furthermore, in assays based on treatments with crude extracts of J2 larvae, GUS activity was also detected in roots, mainly in the elongation zone where RKNs invade roots. The promoter activity was detected in the absence of any mechanical damage produced by RKNs penetration and intercellular migration (Teixeira et al., 2016). This suggests that the gene is an early responder to the presence of the nematode. Similarly, GUS staining was observed restricted to the root elongation zone of *MYB51pro::GUS* plants early after infection with *M. incognita* (Table 1; Figure 2). MYB51 is a member of the MYB Transcription Factor family and, together with MYB34, regulates glucosinolate biosynthesis. Accordingly, the Arabidopsis *myb51 myb34* double mutant, which is completely

TABLE 1 Transcription factors (TFs) analyzed for their functional role in RKNs interaction in different plant species.

TFs family	TF	Plant specie	RKN specie	Promoter activity	Funcional assays	Loss and Gain of function lines	Gall phenotype	Giant cells phenotype	Expression analysis	TFs activity	Reference
WRKY	SlWRKY45	*S. lycopersicum*	*M. javanica*	2, 5, 15, 28 dpi	Yes	Overexpressor lines (*35S:SlWRKY45*)		28 dpi	5, 15, 28 dpi (RNAseq)	Repressor	Chinnapandi et al., 2017
	SlWRKY3			2, 5, 15, 28 dpi	Yes	Overexpressor hairy root lines (*oe:wk-02*; *oe:wk-03*) RNAi silenced lines (*RNAi:wk-03*; *RNAi:wk-04*)			5, 15, 28 dpi (RNAseq)	Activator	Chinnapandi et al., 2019
	SlWRKY35			2, 5, 15, 28 dpi					5, 15, 28 dpi (RNAseq)		
	SlWRKY16	*S. lycopersicum*	*M. javanica*	2, 5, 10, 15, 28 dpi	Yes	Overexpressor hairy root lines (*WRKY16-OE-E2; WRKY16-OE-E5*)			2, 5, and 15 dpi (RNAseq)	Repressor	Kumar et al., 2023
	SlWRKY31					Overexpressor hairy root lines (*WRKY31-OE-E1; WRKY31-OE-E6*)					
	SlWRKY80		*M. incognita*		Yes	VIGS in Motelle and Moneymaker			3, 6 dpi (Motelle versus M82; q-PCR)	Activator	Nie et al., 2023
	SlWRKY72a	*S. lycopersicum*	*Mi-1 virulent M. incognita P77R3*		Yes	VIGS in Motelle and Moneymaker			0, 12, 24, 36 dpi (qRT-PCR)	Activator	Bhattarai et al., 2010
	SlWRKY72b										
	AtWRKY72	*A. thaliana*			Yes	T-DNA insertion lines				Activator	

(Continued)

10.3389/fpls.2024.1370532

TABLE 1 Continued

TFs family	TF	Plant specie	RKN specie	Promoter activity	Funcional assays	Loss and Gain of function lines	Gall phenotype	Giant cells phenotype	Expression analysis	TFs activity	Reference
						(*wrky-72-1; wrky72-2*)					
	SlWRKY70	*S. lycopersicum*	*Mi-1 avirulent M. javanica*		Yes	VIGS in Motelle and Moneymaker			0, 12, 24, 36 hpi (qRT-PCR)	Activator	Atamian et al., 2012
	WRKY11	*A. thaliana*	*M. incognita*	24hpi	Yes	T-DNA insertion lines (*wrky11; wrky11/17*)			24 hpi (qRT-PCR)	Activator	Teixeira et al., 2016
	WRKY17				Yes	T-DNA insertion lines (*wrky11; wrky11/17*)				Activator	
	OsWRKY34	*Oryza sativa*	*M. graminicola*						3, 7 dpi (RNAseq)		Kyndt et al., 2012
	OsWRKY36										
	OsWRKY62										
ERF	ERF109	*A. thaliana*	*M. incognita*	1 dpi, initiation and gall formation	Yes	T-DNA insertion line (*erf109*)				Activator	Zhou et al., 2019; Ribeiro et al., 2024
			M. incognita	(3, 5, 7, 10, 14, 21 dpi)							
	ERF115		*M. incognita*	1 dpi, initiation and gall formation	Yes	Dominant repressor line (*35S:ERF115-SRDX*); T-DNA insertion lines (*erf115*, *erf115/pat1-2*), *ERF115* overexpressing line	7, 14, 21 dpi	30 - 40 dpi		Activator	
			M. incognita	(3, 5, 7, 10, 14, 21 dpi)							
	ERF114		*M. incognita*	3, 5, 7, 10, 14, 21 dpi	Yes	*ERF114* overexpressing line	7, 14, 21 dpi	30 - 40 dpi		Activator	Ribeiro et al., 2024
	ERF6		*M. incognita*		Yes						

(*Continued*)

10.3389/fpls.2024.1370532

TABLE 1 Continued

TFs family	TF	Plant specie	RKN specie	Promoter activity	Funcional assays	Loss and Gain of function lines	Gall phenotype	Giant cells phenotype	Expression analysis	TFs activity	Reference
						T-DNA insertion line (*erf6-1*)			7 dpi (qRT-PCR) 0,7dpi (Microarray)		Warmerdam et al., 2019
	PUCHI		*RKN*	1, 2, 3, 5, 7 dpi	Yes	T-DNA insertion line (*puchi-1*, TILLING line *puchi-2*)	14 dpi	3, 5, 7, 28-42 dpi	1, 2, 3, 5, 7 dpi	Activator	Suzuki et al., 2021b
MYB	MYB3R1	*A. thaliana*	*M. incognita*		Yes	T-DNA insertion lines (*myb3r1; myb3r1/4; myb3r1/3/5)*					Suzuki et al., 2021a
	MYB3R3			7 dpi	Yes	T-DNA insertion lines (*myb3r3; myb3r3/5; myb3r1/3/5*)				Activator	
	MYB3R4			3, 5, 7 dpi	Yes	T-DNA insertion lines (*myb3r4; myb3r1/4*)				Activator	
	MYB3R5			3, 5, 7 dpi	Yes	T-DNA insertion lines (*myb3r5; myb3r3/5; myb3r1/3/5*)					
	MYB51	*A. thaliana*	*M. incognita*	24 hpi	Yes	T-DNA insertion line (*myb34/51*)			24 hpi (qRT-PCR)	Activator	Teixeira et al., 2016

(Continued)

10.3389/fpls.2024.1370532

TABLE 1 Continued

TFs family	TF	Plant specie	RKN specie	Promoter activity	Funcional assays	Loss and Gain of function lines	Gall phenotype	Giant cells phenotype	Expression analysis	TFs activity	Reference
	MYB34				Yes	T-DNA insertion line (*myb34/51*)			3 dpi (Microarray, RNAseq)	Activator	
ARF	ARF3	*A. thaliana*	*M. javanica*	3 dpi							Cabrera et al., 2016
	ARF5	*A. thaliana*	*M. javanica*	1-14 dpi	Yes	Artificial microRNA line (*ARF5-amiR*), hypomorphic mutated line *arf5-2*, Dominant repressor line (ARF5-SRDX)			7 dpi (qRT-PCR)	Activator	Olmo et al., 2020
	ARF7	*A. thaliana*	*M. javanica*	1-14 dpi	Yes	Mutagenized seeds lines and T-DNA lines (*arf7-1/arf19-1; nph4-1/arf19-1; slr-1/arf7-1/ arf19-1*), gain of function mutation (*slr*)			7 dpi (qRT-PCR)		
	ARF19	*A. thaliana*	*M. javanica*	1-14 dpi	Yes	Mutagenized seeds lines and T-DNA lines (*arf7-1/arf19-1; nph4-1/arf19-1; slr-1/arf7-1/ arf19-1*), gain of function mutation (*slr*)			7 dpi (qRT-PCR)		
	SIARF8A	*S. lycopersicum*	*M. incognita*	7, 14 dpi	Yes	CRISPR lines *(slarf8b, slarf8ab)*		21 dpi	7, 14 dpi (RNAseq)	Activator	Noureddine et al., 2023
	SIARF8B	*S. lycopersicum*	*M. incognita*	7, 14 dpi	Yes	CRISPR lines (*slarf8b, slarf8ab*)		21 dpi	7, 14 dpi (RNAseq)	Activator	

(Continued)

10.3389/fpls.2024.1370532

TABLE 1 Continued

TFs family	TF	Plant specie	RKN specie	Promoter activity	Funcional assays	Loss and Gain of function lines	Gall phenotype	Giant cells phenotype	Expression analysis	TFs activity	Reference
WOX	WOX4	*A. thaliana*	*M. javanica/ M. incognita*	3, 5, 7 dpi	Yes	T-DNA insertion line (*wox4-1*)	7 dpi		7 dpi (RT-PCR)		Yamaguchi et al., 2017
	WOX5		*M. javanica*	2, 5, 8 dpi	Yes	T-DNA insertion line (*wox5-1*)				Activator	Olmo et al., 2020
GRAS	SCR	*A. thaliana*	*M. javanica*	2, 5, 7 dpi	Yes	*scr-3*				Activator	Olmo et al., 2020
	SHR			3,4,7 dpi	Yes	*shr-2*				Activator	
	PAT1		*M. incognita*	3, 5, 7, 10, 14, 21 dpi	Yes	*T-DNA insertion lines (pat1-2 and erf115/ pat1-2); PAT1 overexpressing line*	7, 14, 21 dpi	30 - 40 dpi		Activator	Ribeiro et al., 2024
GATA	GATA23	*A. thaliana*	*M. javanica*	1-29 dpi	Yes	RNA intereference line (*GATA23: RNAi*)	15 dpi	15 dpi		Activator	Olmo et al., 2020
G2-LIKE	APL	*A. thaliana*	*M. incognita*	3, 5, 7, 17 dpi						Activator	Suzuki et al., 2021a; Absmanner et al., 2013
HSF	SCZ	*A. thaliana*	*M. javanica*	3, 4, 7dpi 2-40 dpi	Yes	Ac/Ds transposon tagged lines and mutagenized seeds lines (*scz-2; scz1-1; scz-4*)				Activator	Olmo et al., 2020
HD-ZIP	ATHB8	*A. thaliana*	*M. javanica / M. inognita*	3, 5, 7 dpi	Yes	T-DNA insertion line (*athb8-11*)	7 dpi		7 dpi (RT-PCR)		Yamaguchi et al., 2017

(Continued)

10.3389/fpls.2024.1370532

TABLE 1 Continued

TFs family	TF	Plant specie	RKN specie	Promoter activity	Funcional assays	Loss and Gain of function lines	Gall phenotype	Giant cells phenotype	Expression analysis	TFs activity	Reference
DP-E2F-like 1	DEL1	*A. thaliana*	*M. incognita*		Yes	Overexpresor line (*DEL1*^{OE}) *del1-1* mutant		7, 14, 21 dpi	7 dpi (*in situ*)	Repressor	de Almeida Engler et al., 2012; Nakagami et al., 2020
		Prunus Sogdiana	*M. incognita*						0, 3, 7, 14, 21, 28, 35 dpi (RT-PCR) 0, 3, 7, 14, 21 dpi (*in situ*)		Xiao et al., 2020
LBD	LBD16	*A. thaliana*	*M. javanica* / *M. arenaria*	2-29 dpi / 2-45 dpi	Yes	Dominant repressor lines (*35S::LBD16: SDRX; pLBD16: lbd16-SDRX*) T-DNA insertion line (*lbd16-1*)	14 dpi/-	14 dpi/-		Activator	Cabrera et al., 2014b: Olmo et al., 2017
AP2	TOE1	*A. thaliana*	*M. javanica*		Yes	Overexpression line (*35S::TOE1*^{R})	14 dpi	14 dpi	3 dpi (qPCR)	Repressor	Diaz-Manzano et al., 2018
SBP	SPL7	*A. thaliana*	*M. incognita*	3, 7,14 dpi	Yes	T-DNA insertion line (*spl7*)		7 weeks		Activator	Noureddine et al., 2022

Columns indicate the TF family, the TF name, the plant to which a functional role was assessed, the RKN species used, the infection stages at which promoter activity was confirmed, the stage at which infection and/or reproductive parameters were recorded in lines with altered function, the stage at which gall phenotype was recorded in lines with altered function, the stage at which GCs phenotype was recorded in lines with altered function, the role assigned as activator or repressor, the available expression analysis in infected tissues, and references. An empty cell indicates that no information is available. Dpi, days post infection. hpi, hours post infection. Only in a few cases, no information on TFs functional role was available, however they were included in the table, as they were mentioned within the text.

10.3389/fpls.2024.1370532

10.3389/fpls.2024.1370532

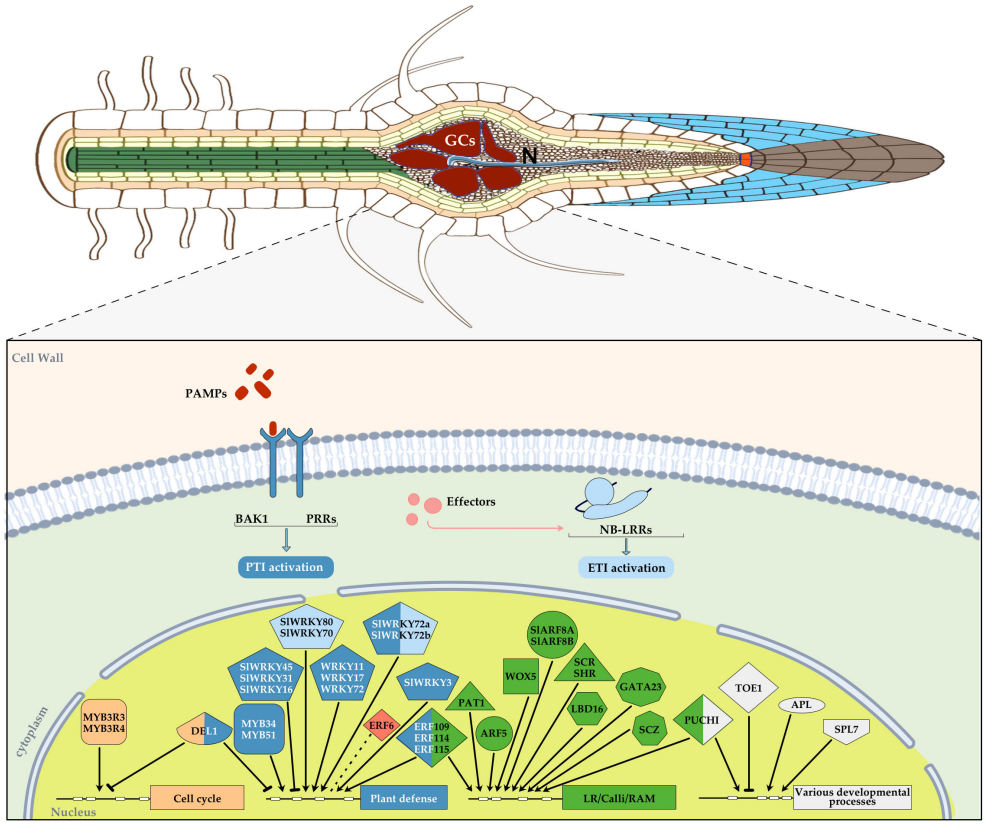

FIGURE 2
Diagram showing an overview of those transcription factors (TFs) with an assigned function during plant-RKNs interaction in different plant species, mainly *Arabidopsis thaliana* and *Solanum licopersicum*, integrated in a basic diagram of a plant cell. TFs were categorized into different groups according to their function and a color was assigned in each geometric figure, i.e. cell cycle, light orange, plant defense, blue, lateral root/calli/Root apical meristem (RAM), green, various developmental processes, white, abiotic stress, red. In some cases, a dual function was demonstrated and therefore, two colors were assigned. A blunt end arrow indicates a TF with a repressor role and an arrowhead indicates its function as an activator. RAM, root apical meristem, each TF family was assigned a different geometric figure. ETI, light blue, PTI, dark blue.

impaired in glucosinolate production (Frerigmann and Gigolashvili, 2014), displayed a higher number of galls compared to wild-type plants in *M. incognita* infection assays. This increased susceptibility of the double mutant point to a positive role of glucosinolates in RKNs defense (Teixeira et al., 2016; Table 1; Figure 2). Importantly, WRKY11 and MYB51 are involved in BRASSINOSTEROID INSENSITIVE-ASSOCIATED KINASE 1 (BAK1)-dependent PTI responses activated by RKN infection, however, another BAK-independent immune signaling pathway was detected probably involved in the camalexin biosynthetic pathway (Teixeira et al., 2016). It is well-established that nematodes can suppress defense-related genes in feeding cells. In this respect, transcriptomic data of Arabidopsis and tomato micro-dissected GCs induced by *M. javanica* at early infection stages (3 dpi) showed a down-regulation of *MYB34* in Arabidopsis and its ortholog in tomato, as reported by Barcala et al. (2010) and Portillo et al. (2013), respectively. In contrast, the RNAseq analysis conducted by Silva et al. (2022) at the same infection stage, showed that *MYB34* is induced in whole galls compared to control non-infected root segments. These findings suggest that RKNs may inhibit glucosinolate production in feeding cells, while a defense response is likely maintained in the remaining gall tissues. Other WRKY members related to the basal defense against RKNs as positive regulators are *AtWRKY72* and its orthologs in *Solanum lycopersicum*, *SlWRKY72a* and *SlWRKY72b* (Bhattarai et al., 2010; Table 1; Figure 2). Arabidopsis WRKY72 mutant lines showed a significant increase in egg masses compared to Col-0. Tomato roots of the susceptible cultivar (cv) Moneymaker (*mi-1/mi-1*), with *SlWRKY72a* and/or *SlWRKY72b* transient silenced or co-silenced showed similar results, confirming the involvement of *SlWRKY72* in basal defense (PTI) in both plant species (Bhattarai et al., 2010; Table 1). In addition, data obtained with the tomato resistant cv. Motelle (*Mi-1/Mi-1*) indicated that *SlWRKY72* is also involved in gene-for-gene resistance (ETI) during RKN infection of tomato roots. Thus, a significant increase of *SlWRKY72a* expression level was observed in response to *M. incognita* 12 and 36 hours after inoculation (hai), as well as of *SlWRKY72b* expression at 12 hai in tomato roots of the resistant cv. Motelle (*Mi-1/Mi-1*), whereas this was not observed in the susceptible cv. Moneymaker (*mi-1/mi-1*, Bhattarai et al., 2010). Functional confirmation of the participation of both TFs in tomato gene-for-gene resistance was obtained by transient silencing or co-silencing *SlWRKY72a* and *SlWRKY72b* in the resistant Motelle

roots. This resulted in an increased susceptibility to RKNs, while no infection was observed in the control Motelle roots. The expression changes of another WRKY family member in tomato, *SlWRKY70*, also suggest a putative role in *Mi-1*-mediated resistance (ETI), as its mRNA was up-regulated in both susceptible and non-susceptible lines and RKNs were able to infect and reproduce in *WRKY70* transiently silenced tomato roots of the resistant cv. Motelle, whereas no infection and reproduction was observed in non-silenced Motelle tomato roots (Atamian et al., 2012; Table 1; Figure 2). In addition, WRKY70 has been described in Arabidopsis to mediate basal and R gene defence in response to aphids (Knoth et al., 2007). Therefore, both WRKY70 and WRKY72 showed a conserved role as activators of defense in different plant species in response to different pests and pathogens (Knoth et al., 2007; Bhattarai et al., 2010; Atamian et al., 2012). However, they appear to mediate defense through different signaling pathways; in Arabidopsis, WRKY70 acts as a mediator between the SA and JA defense pathways during biotic stress (Li et al., 2006); a similar scenario might be happening in tomato as *SlWRKY70* is up-regulated during the first hours after SA treatment, but repressed after Methyl jasmonate (MeJA) application (Atamian et al., 2012; Table 1). On the other hand, WRKY72 seems to be involved in plant defence against pathogens in a SA independent manner as genes deregulated in *Atwrky72* did not respond to SA analogues (Bhattarai et al., 2010).

During the interaction with RKN, other members of the WRKY transcription factor family in tomato, such as *WRKY3* and *35*, were induced and functional, i.e., *SlWRKY3pro::GUS* and *SlWRKY35pro::GUS* lines showed GUS signal at early infection stages with *M. javanica* (2 and 5 dpi). Furthermore, the overexpression of *SlWRKY3* in transgenic hairy root lines led to a decrease in the reproduction of *M. javanica*. This was accompanied by an increase in the accumulation of defence molecules from the shikimate and oxylipin pathways. On the other hand, *SlWRKY3 RNAi* lines promoted reproduction compared to wild-type plants, confirming its role in basal defence (PTI) against RKNs (Chinnapandi et al., 2019; Table 1; Figure 2). Moreover, SlWRKY80 was also recently identified as a positive regulator that affects *Mi-1*-mediated resistance (ETI). In Motelle lines carrying the *Mi-1* resistance gene, *SlWRKY80* transcript levels increased by more than 3.21 and 4.56-fold at 3 and 6 dpi, respectively, compared to the control reference M82 variety. The expression of *SlWRKY80* was also significantly induced by the defence hormones JA and SA in tomato Motelle. Furthermore, virus-induced gene silencing (VIGS) assays demonstrated that silencing *SlWRKY80* in the resistant Motelle tomato resulted in a significant increase in the number of egg masses in the roots of individual plants and a significant decrease in its resistance level. This confirms the role of SlWRKY80 as a positive regulator of *Mi-1*-mediated tomato resistance (Nie et al., 2023; Table 1; Figure 2).

Finally, it is possible that WRKY family members are involved in defence responses induced during the infection by RKNs in monocotyledonous species. This is supported by a transcriptomic study of galls at 3 and 7 dpi of *Oryza sativa* infected with *M. graminicola* that revealed upregulation of *OsWRKY34*, *OsWRKY36* and *OsWRKY62* (Kyndt et al., 2012; Table 1; Figure 2). Yet, further analysis is required to determine the functional implications of these TFs in rice responses against RKNs.

Plant transcription factors with a dual link to stress caused by RKNs and plant developmental programs

Although, the structure of this review makes a sharp separation between those TFs involved in plant defense and those involved in plant development, the boundaries are not always clear. In recent years, a connection between stress signaling and developmental programs, such as root regeneration, has been extensively described (Ikeuchi et al., 2019). One example of the RKNs interaction involves the ERF109 and ERF115 transcription factors, which belong to the Ethylene Responsive Factor (ERF) subfamily within the APETALA2/ETHYLENE RESPONSIVE FACTOR (AP2/ERF) superfamily (Sakuma et al., 2002; Wu et al., 2022). These transcription factors are involved in a core molecular network triggered by wound-induced JA, which induces stem cell activation and regeneration of *Arabidopsis thaliana* roots (Zhou et al., 2019). ERF109 and ERF115 play a crucial role in maintaining the quiescence of the root stem organizer cells, also known as the quiescent center (QC). ERF109 is activated transcriptionally within minutes in response to JA and wounding and operates upstream of ERF115. Conversely, ERF115 operates upstream of the protein complex RBR-SCR, which regulates the asymmetric cell divisions of root stem cells, QC quiescence, and the activation of the QC regulatory protein WOX5. In addition, it is worth noting that ERF115 is activated not only by JA but also by auxin signaling, which is crucial in galls (Cabrera et al., 2014b; Olmo et al., 2020). It is interesting to observe that GUS staining assays revealed the induction of both ERF109 and ERF115 promoters after the infection of the *M. incognita* as early as 1 dpi. Furthermore, time course experiments have shown that *ERF109* is induced during nematode penetration, while *ERF115* is strongly induced in vascular and/or endodermal cells at all stages from penetration and feeding site initiation until gall formation. Interestingly the repressor activity of ERF115 in the dominant-negative *ERF115-SRDX* line resulted in a loss of root growth recovery capacity after infection with *M. incognita* compared to Col-0. Furthermore, the *erf109* mutant and *ERF115-SRDX* line exhibited reduced susceptibility to infection and developed fewer egg masses compared to Col-0 seedlings 7 weeks after inoculation. Consistently, gall formation in *ERF115-SRDX* roots progressed slower than in Col-0, and DNA synthesis at feeding sites was less active compared to Col-0 (Zhou et al., 2019). Therefore, the JA-induced regeneration pathway, with ERF109 and ERF115 acting as regulators, stimulates root growth

following nematode infection and contributes to the reproductive success of *M. incognita* (Zhou et al., 2019; Table 1; Figure 2). In this respect, it is relevant to mention that the damage caused by *H. schachtii* during invasion also activates a jasmonate-dependent ERF109 pathway, promoting secondary root formation (Guarneri et al., 2022). Therefore, new root-growth and/or regeneration in both RKNs and CNs interaction seems to be mediated by common JA responsive transducers as ERF109. Furthermore, ERF115 interacts with PAT1, a transcription factor belonging to the PHYTOCHROME A TRANSDUCTION 1 (PAT1) GRAS subfamily, forming heterodimers, and *erf115*, *pat1-2*, and *erf115/pat1-2* double mutants showed GCs often with less cytoplasm, fewer nuclei, and less ploidy than the wild-type lines, which probably caused a delay in nematode development. Furthermore, overexpression of *ERF115* (*ERF115OE*), *ERF114*, and *PAT1* resulted in accelerated gall induction and downstream activation of key players in the regenerative pathway, possibly related to the high cell division rates observed, particularly in the *ERF115OE* line, following mechanical stress induced by RKNs. In conclusion, the ERF115-PAT1 complex contributes to the regenerative potential of nematode-induced galls by facilitating tissue healing, thereby maintaining the gall's functionality until maturation and nematode reproduction (Ribeiro et al., 2024; Table 1; Figure 2).

ERF6 is another stress-related gene that does not appear to regulate plant defenses. It is a member of the Ethylene Responsive Factors (ERF) family and has a unique AP2/ERF domain (Nakano et al., 2006). It was identified from a quantitative trait loci (QTL) study that investigated the relationship between allelic variation in specific loci (QTLs) and the susceptibility of Arabidopsis to *M. incognita* (Warmerdam et al., 2019). qPCR analysis showed a significant down-regulation of *ERF6* in Arabidopsis wild type seedling roots at 7 dpi in association with nematode infections. Reproduction tests were conducted on the *erf6-1* mutant line infected with *M. incognita* at 7 dpi, which resulted in a significant increase of 28% in egg masses per plant compared to the wild type line. In addition, microarray analysis revealed that there were 489 differentially expressed genes in the roots of *erf6-1* nematode-infected plants compared to infected wild-type plants (Warmerdam et al., 2019). Previous studies have shown that ERF6 is phosphorylated by MPK3/MPK6 during biotic stress, which activates the expression of Jas/ETH defense genes such as *PDF1.2a* and *PDF1.2b*, thereby enhancing Arabidopsis' defense against fungal infections (Meng et al., 2013; Wang et al., 2022). However, in *erf6* RKNs-infected roots, the expression of *PDF1.1* and *PDF1.2* was not significantly altered compared to wild-type infected plants. This is similar to the expression of other pathogenesis-related genes, such as *PR1*, *PR2*, *PR3*, and *PR4*, which are known to be regulated by ERFs. These findings suggest that ERF6 does not suppress plant defenses during the RKNs interaction. Many of the genes that are differentially regulated in the roots of nematode-infected *erf6-1* plants at 7 dpi are putatively involved in responses to abiotic stresses, such as osmotic stress. This suggests that ERF6 regulates abiotic stress responses in the plant-nematode interaction (Warmerdam et al., 2019; Table 1; Figure 2).

Plant transcription factors relevant during RKNs infection with impact in plant-development

The root-knot nematodes induce feeding cells, GCs, with enlarged nuclei within their heterogeneous feeding sites or feeding organs called galls, which indicates increased DNA replication cycles (de Almeida Engler et al., 1999). This process is called endoreduplication and occurs when successive phases of DNA synthesis (S) follow each other without intervening mitosis or cytokinesis. Endopolyploidy is observed in differentiated and enlarged plant cells, such as Arabidopsis trichomes, endosperm, and fruit (Sabelli et al., 2007). Somatic polyploidy is particularly prevalent in higher plants. A high-resolution DNA endoploidy map of the developing Arabidopsis root has revealed the importance of endoreduplication for the expression of genes encoding cell-wall modifying enzymes. These enzymes are crucial during GC development, suggesting that these responses may serve as a buffering system for stress conditions (Wieczorek, 2015; Bhosale et al., 2018). In this respect, the TF E2Fe/DEL1 is an inhibitor of endoreduplication that maintains the mitotic state of proliferating cells by suppressing transcription of genes necessary to enter the endocycle (Dimova and Dyson, 2005; Inzé and De Veylder, 2006). The timing of cell cycle exit and onset of endoreduplication is determined by the levels of E2Fe/DEL1, which control anaphase-promoting activator genes such as CCCS52A2 (Lammens et al., 2008). Arabidopsis has three *DEL* genes (*DEL1*, *DEL2* and *DEL3*). Loss of DEL1 function results in increased ploidy, while ectopic expression of *DEL1* results in decreased endoreduplication levels and cells are prone to rapid expansion (Ramirez-Parra et al., 2004; Vlieghe et al., 2005; Lammens et al., 2008). The role of E2Fe/DEL in GCs formation induced by RKNs was analyzed. Ectopic expression of *DEL1* resulted in morphological changes of the GCs within the galls, as the GCs were smaller with profuse cell wall invaginations and smaller nuclei than in the wild type line at 21 dpi. Furthermore, the *DEL1* overexpressing line exhibited a significant reduction in the number of *M. incognita* egg masses due to an induction of the mitotic state, resulting in severe impairment of reproduction. Conversely, the *del1-1* loss of function line displayed small and malformed GCs with reduced mitotic activity and little cytoplasm, possibly due to a premature initiation of the endocycle (de Almeida Engler et al., 2012; Vieira et al., 2013; Table 1; Figure 2). The results indicate that multiple nuclei resulting from acytokinetic mitotic events are not sufficient to drive GC expansion. Therefore, during the plant-RKNs interaction, there is a reprogramming of the plant cell cycle machinery, inducing mitotic cycles in GCs followed by repeated endoreduplication cycles, both of which are necessary for correct GC development (de Almeida Engler et al., 2012; Table 1; Figure 2). Although only data from the variation of expression levels during RKNs infection and *in situ* localization of its transcripts are available, the orthologue *DEL1* gene from Arabidopsis in woody plants, such as *Prunus sogdiana*, *PsoDEL1*, also appears to be

negatively correlated with endoreduplication and growth of GCs. *PsoDEL1* exhibited weak expression in the feeding sites during the early stages of infection (3 dpi). As the infection progressed, the hybridization signal was barely detected at the feeding site and within the GCs at 7, 14 and 21 dpi (Xiao et al., 2020; Table 1; Figure 2). Therefore, it is highly probable that the role of DEL1 is conserved in distant plant species during feeding site and GCs formation.

Interestingly, E2Fe/DEL1 also plays a role in SA biosynthesis as a transcriptional repressor of a member of the isochorismate pathway, *ENHANCED DISEASE SUSCEPTIBILITY 5 (EDS5)*, that encodes a SA transporter required for elevated SA immunity in Arabidopsis (Chandran et al., 2014). Repression of genes involved in plant defenses is a characteristic of the compatible interaction between RKNs and dicotyledonous or monocotyledonous species, such as Arabidopsis and rice, particularly in GCs (Barcala et al., 2010; Ji et al., 2013). Furthermore, the identification of *M. incognita* effectors, such as Mi-ISC-1, confirms that the nematode actively deploys a functional isochorismatase to suppress SA-mediated plant defences by altering the isochorismate synthase pathway for SA biosynthesis, favoring parasitism (Qin et al., 2022). The *del1-1* mutant showed SA accumulation in 7 dpi Arabidopsis galls, while in uninfected roots, the SA levels did not change significantly compared to the control background Col-0. Therefore, DEL1 seems to repress SA biosynthesis in RKNs-induced galls in Arabidopsis (Nakagami et al., 2020; Table 1; Figure 2). As a result, *del1-1* mutant galls at 5 dpi exhibited more intense lignin staining than wild type galls, and the expression patterns of genes encoding enzymes related to lignin biosynthesis, such as 4-coumarate: CoA ligase 1 (4CL1), 4CL2, alcohol dehydrogenase 5 (CAD5), phenylalanine ammonia-lyase 1 (PAL1), PAL2, and cinnamate 4-hydroxylase (C4H) were significantly up-regulated as compared to wild type galls (Nakagami et al., 2020). The loss of function of DEL1/E2Fe in Arabidopsis galls leads to enhanced resistance and it also causes growth inhibition, likely due to excessive lignification and/or SA accumulation in RKNs-induced galls. Therefore, DEL1 may mediate a balance between growth and defense by limiting the accumulation of SA in the infection sites (Nakagami et al., 2020), similar to what was reported during fungal infection in leaves (Chandran et al., 2014).

Plant MYB3R TFs, which are homologous to Myb oncoproteins, are also involved in controlling mitosis and cytokinesis progression by recognizing Mitotic-specific activator (MSA) elements present in genes expressed during the G2 and M-phase, such as *B-cyclins* (Ito et al., 1998, 2001; Menges et al., 2005). The MYB transcription factor family is a large family found in all eukaryotes and is involved in various processes that control plant development, metabolism, and responses to biotic and abiotic stress (Dubos et al., 2010). In Arabidopsis, five *MYB3R* genes have been identified. Among them, *MYB3R1* and *MYB3R4* function redundantly as activators, with *MYB3R4* contributing more to the activation of G2/M phase-specific genes (Haga et al., 2007; Ito et al., 2001). However, MYB3R1 has a dual function as it can act as a repressor along with MYB3R3 and MYB3R5. *MYB3R4* is only expressed during the G2/M phase, whereas the repressor-type MYB3Rs are active in post-mitotic cells and proliferative cells outside the G2/M phase (Kobayashi et al., 2015a; Kobayashi et al., 2015b). In Arabidopsis, *MYB3R4::GUS* lines showed a GUS signal in the vasculature, where a weak expression of *MYB3R5::GUS* was detected. Following *M. incognita* infection, the *MYB3R4::GUS* line exhibited GUS signal in the centre of 3, 5 and 7 dpi galls, while the *MYB3R5::GUS* line showed two strands of signal surrounding the centre of 3 and 5 dpi galls that decreased and became patchy at 7 dpi. In contrast, no signal was detected in the roots of the *MYB3R3::GUS* line, whether infected or uninfected. The loss of function lines *myb3r1*, *myb3r5* and *myb3r1/3/5* showed no effect on nematode infection. In contrast, *myb3r3*, *myb3r4*, *myb3r1/4* and *myb3r3/5* showed a significant reduction in the number of galls compared to wild type plants (Suzuki et al., 2021a; Table 1; Figure 2). It is known that the *myb3r1/4* mutant presents aberrant cytokinesis and down-regulation of cell cycle genes (Haga et al., 2007, Haga et al., 2011), and MYB3R4 is involved in endoreduplication, acting as an activator or repressor depending on its phosphorylation state (Chandran et al., 2010). In addition, MYB3Rs proteins can form complexes during cell cycle progression. For example, MYB3R4 interacts with RBR1 (Retinoblastoma-related) and E2FB, while MYB3R3 interacts with RBR1 and E2FC, which are necessary for endoreduplication (Del Pozo et al., 2002, 2006). In this respect, as mentioned before, the overexpression of a transcription factor of the DP-E2F-like family (E2Fe/DEL1) that maintains the mitotic state of proliferating cells, caused increased mitotic activity and consequent endocycle inhibition in the galls formed by RKNs. Thus, the feeding cells within the galls showed multiple nuclei and inhibited cell expansion affecting nematode development (de Almeida Engler et al., 2012, de Almeida Engler and Favery, 2011).Therefore, although a direct interaction of MYB3Rs proteins with E2F members has not yet been described in the RKN interaction, the role of MYB3Rs activators in the RKNs-interaction may be related to the regulation of key cellular processes during cell cycle progression in galls/GCs development.

One of the characteristics observed in the transcriptomes of Arabidopsis galls and micro-dissected GCs are the high number of genes included in categories such as development or hormone metabolism, both directly related (Barcala et al., 2010; Silva et al., 2022). Experimental data has confirmed that gall and GCs formation share TFs that are molecular components of transduction pathways involved in lateral root and callus formation, as well as other plant developmental processes such as tuberization, nodulation, fruit development, and flowering time (Cabrera et al., 2014b; Medina et al., 2017; Diaz-Manzano et al., 2018; Olmo et al., 2019, Olmo et al., 2020). One of the initial examples discussed is LBD16, a member of the LATERAL ORGAN BOUNDARIES-DOMAIN TF family. LBD16 is a crucial component of the auxin pathway that leads to cell divisions in the xylem pole pericycle, which are necessary for lateral root formation (Goh et al., 2019) and is also involved in pluripotency acquisition in callus cells (Liu et al., 2018). *LBD16* is activated early during nematode establishment in xylem pole pericycle cells near the nematode head and by nematode secretions in protoplast. Within the forming galls its expression was maintained till medium infection stages (11 dpi) as indicated by a promoter-GUS fusion. It also showed a crucial function during RKNs establishment, but

not during the establishment of CNs as loss of function lines of LBD16 (*lbd16*-1, *35S::LBD16-SRDX*; *pLBD16::LBD16-SRDX*) showed significant less infections by *M. javanica* than the control wild type line. LBD16 is also important for the GCs and galls development, as smaller galls and less expanded GCs were observed than in Col-0 in some of those mentioned loss of function lines. Interestingly, *LBD16* is regulated by auxins in galls as also described during lateral root formation (Cabrera et al., 2014b; Table 1; Figure 2). Unexpectedly, *LBD16* was locally induced in the vascular tissue of leaves after RKNs infection, as it was proven that *M. javanica* is able to establish, induce GCs, and reproduce in *in vitro* cultured Arabidopsis leaves. LBD16 is also essential for feeding site formation in leaves, as evidenced by the inability of RKNs to establish in the *35S::LBD16-SRDX* line, which contains the *LBD16* coding sequence fused to the transcriptional repressor domain SRDX driven by the 35S promoter (Olmo et al., 2017; see Table 1). Thus, LBD16 appears to be a conserved molecular hub connecting developmental signals with those necessary for RKNs feeding site formation in Arabidopsis. A role for LBD16 in feeding site formation induced by CNs has not been described. However, *LBD16* is induced in a WOX11-dependent manner in the primordia of adventitious lateral roots that are promoted after *H. schchatii* infection (Willig et al., 2024). This finding connects the plant-responses to both, RKNs and CNs, to the activation of critical transducers of root developmental programs. *ABERRANT LATERAL ROOT FORMATION 4* (*ALF4*) is another gene relevant to lateral root formation and gall development. It encodes a nuclear-localized protein that is not a transcription factor. However, due to its localization and participation upstream of the auxin signaling pathways leading to lateral root formation, we are mentioning it (DiDonato et al., 2004; Bagchi et al., 2018). It is also involved in developmental processes such as vascular vessels reconnection in grafting, hormone-induced callus formation or *de novo* root organogenesis from leaf explants (Sugimoto et al., 2010; Melnyk et al., 2015). *ALF4* was induced at very early infection stages of infection by *M. javanica* (1dpi), as indicated by the activation of a *pALF4:.GUS* construct. The GUS signal increased at 4 dpi and it was maintained at medium stages of gall development (7–10 dpi), but disappeared at 14 dpi. ALF4 is necessary for the proper development of galls and GCs formed by *Meloidogyne* spp in Arabidopsis, as the mutant *alf4-1* presents aberrant galls and GCs with severe structural abnormalities that cause a dramatic reduction in the nematode's reproduction (Olmo et al., 2019).

PUCHI, a member of the ERF Transcription factor family, is also involved in the formation of new organs such as lateral roots or floral formation (Hirota et al., 2007; Karim et al., 2009). It is activated by auxin through LBD16, controlling lateral root primordium patterning (Hirota et al., 2007; Goh et al., 2019). Interestingly, it is up-regulated in galls at early-mid stages (3, 5 and 7 dpi; Yamaguchi et al., 2017; Table 1; Figure 2) in line with its promoter activity (Suzuki et al., 2021b; Table 1; Figure 2). The expression peaked at 5 dpi, but there was no significant difference in the number of galls at 2 dpi or the number of egg masses in the mutant line *puchi-1* compared to the control wild type line. These results suggest that PUCHI does not play a significant role in nematode invasion, gall formation, or nematode reproduction (Suzuki et al., 2021b; Table 1; Figure 2). However, the function of PUCHI during nematode infection may be related to cell wall morphology. This is suggested by the observation that the *puchi-1* mutant line displayed aberrant giant cells (GCs) with dramatic protrusions and invaginations containing thick cell walls that were not present in galls from the wild type line (Suzuki et al., 2021b). Trinh et al. (2019) reported that PUCHI controls the biosynthesis pathway of very long-chain fatty acid (VLCFA) during lateral root formation. Additionally, Uemura et al. (2023) found that VLCFAs can modify the cell wall through the activation of MYB93, which regulates cell wall genes. RNAseq and promoter::GUS activation assays revealed up-regulation of genes encoding 3-KETOACYL-COA SYNTHASE 1 (KCS1) and KCS20, enzymes implicated in very-long-chain fatty acid (VLCFA) synthesis in galls. Their expression peaked at around 5 dpi, similar to that of PUCHI. Additionally, GCs from the mutants *kcs1-5* and *puchi-1* exhibited a similar phenotype with thicker walls and protuberances compared to wild-type galls. Therefore, the observed phenotype in the *puchi-1* mutant may be attributed to modifications in the VLCFA composition of the cell wall and cell membrane of the GCs (Suzuki et al., 2021b). However, PUCHI does not significantly affect nematode infectivity or reproductive parameters.

The formation of galls by RKNs is a process of post-embryonic new organogenesis as new structures specialized for nematode nourishment are induced by the nematode into the vascular cylinder of the host plant roots. The study of two TFs involved in common signaling pathways for lateral root formation, AUXIN-RESPONSIVE-FACTOR-5/ARF5, a key factor for root stem-cell niche regeneration and lateral root initiation, and GATA-TRANSCRIPTION FACTOR-23/GATA23 that specifies pluripotent founder cells during lateral root formation (De Rybel et al., 2010; De Smet et al., 2010; Efroni et al., 2016) shed light on the plant transduction pathways used or hijacked by the nematode to achieve those dramatic reprogramming events. The impact on nematode infection, galls, and GCs development was significant in the *arf5-2* mutant, as well as in inducible knockout lines for ARF5, and in a knockdown line of *GATA23* as compared to wild type lines. *pGATA23::GUS*, was induced at early infection stages, 3 dpi-7 dpi, but at 14 dpi no signal was detected, whereas *ARF5::GUS* was active in a shorter window, i.e., at 3 dpi a clear signal was detected that faded at 7 dpi, this confirmed their induction at early-mid infection according to their putative roles during galls/GCs formation (Olmo et al., 2020; Table 1; Figure 2). Therefore, the results suggest that transient pluripotency reprogramming, which leads to lateral root founder cell-like specification and root regeneration, is also necessary for gall/GCs organogenesis. In contrast, other TFs that are the main upstream transducers during lateral root development, such as ARF7 and ARF19 (Okushima et al., 2007), did not exhibit a significant role or specific expression pattern during gall/GCs formation (Olmo et al., 2020; Table 1; Figure 2). However, the regulation of another auxin TF in galls, ARF3, was also similar to that of lateral root growth (Marin et al., 2010; Cabrera et al., 2016). ARF3 is a TF that participates in a regulatory module. In this module, miR390a controls the biogenesis of TAS3-derived tasiRNAs that regulate

the auxin responsive factors ARF2, ARF3 and ARF4 by degrading their transcripts and controlling lateral root growth (Marin et al., 2010). Two sensor lines (*pARF3:ARF3-GUS* and a tasiRNA-resistant ARF3 line, *pARF3:ARF3m-GUS*) indicated the binding of TAS3-derived tasiRNAs to the ARF3 sequence in galls. The results strongly suggest that the promoters of miR390 and TAS3 are active, and their products are functional in galls, repressing ARF3 (Cabrera et al., 2016; Table 1). Therefore, silencing of *ARF3* seems to be important during gall development and establishment of RKNs. Recently, other ARFs, such as ARF8A and ARF8B, have been studied in tomato. These were induced during the early to mid-infection stages (7-14 dpi) in galls and GCs of tomato transgenic lines *pARF8A:GUS* and *pARF8B:GUS*. The up-regulation of *ARF8A/B* transcripts in galls compared to uninfected roots in transcriptomic analysis (RNAseq) is due to the high activity of their promoter combined with reduced silencing by miR167. Furthermore, the mutant lines *slarf8a*, *slarf8ab*, and *slarf8ab* showed severely compromised infection and reproduction of *M. incognita*. In addition, expression of *ARF8A* and *ARF8B* is required for correct giant development as the former mutant lines showed giant cells significantly smaller than in the wild type line (Noureddine et al., 2023; Table 1; Figure 2). All these data, support a key role for ARF8s in feeding site formation.

Following the robust hypothesis that gall/GCs formation is a new organogenesis process, and the described similarities with callus formation, it is important to note that callus formation involves the differentiation of pericycle or pericycle-like cells in a process that resembles root tip organization. Thus, crucial root meristem (RAM) TFs marker genes, namely *SHORTROOT/SHR, SCARECROW/SCR, SCHIZORIZA/SCZ, and WUSCHELRELATED-HOMEOBOX-5/WOX5* are expressed (Sugimoto et al., 2010). It also requires the ectopic activation of a lateral root developmental program and consequently the expression of *LBD* genes (Sugimoto et al., 2010). It is noteworthy that these genes were induced very early during gall formation (2-5 dpi), but no signal was detected 7-8 dpi and most of them also played important roles in the establishment of RKNs. Thus, the activation of plant developmental programs that promote transient pluripotency/stemness leads to the generation of quiescent center and meristematic-like cell identities within the vascular cylinder of galls (Olmo et al., 2020; Table 1; Figure 2). Moreover, a process of new organogenesis also involves revascularisation, which is crucial for maintaining GCs growth as they are symplastically isolated specialized transfer cells (Hoth et al., 2008; Rodiuc et al., 2014). Phloem formation is induced during gall development (Bartlem et al., 2014). APL (Altered phloem development), a MYB coiled-coil-type TF involved in phloem identity acquisition, is expressed in protophloem, metaphloem and companion cells (Bonke et al., 2003). It is induced early after infection with *M. incognita* and *M. javanica* in Arabidopsis, as shown by an *APL::GUS* line with a strand signal in 3 dpi galls that increases at 5 dpi (Suzuki et al., 2021a; Table 1; Figure 2). However, functional tests are still needed to confirm its role during gall formation.

It is known that the balance between cell proliferation and cell differentiation in the procambium is regulated downstream of the receptor and kinase cascade by the WOX4 TF. Cyst nematodes have been shown to modulate the procambial cell proliferation of feeding cell formation probably by mimicking the plant B-type CLE TDIF (tracheary element differentiation inhibitory factor) peptide that is encoded by two genes *CLE41* and *CLE44* in Arabidopsis, and by taking control of the (TDIF RECEPTOR/PHLOEM INTERCALATED WITH XYLEM (TDR/PXY)-WOX4 signaling pathway (Guo et al., 2017). In this regard, *WOX4* and *ATHB8*, typical procambium marker genes, were induced in *M. incognita* galls at 3, 5 and 7 dpi. However, the analysis of *athb8-11* and *wox4-1* loss-of-function mutants did not cause any visible effect on the infection parameters or gall diameter. These genes usually function redundantly; therefore, single mutations were probably not sufficient to prevent procambial cell formation (Yamaguchi et al., 2017; Table 1; Figure 2). Nevertheless, the connection between gall formation and different developmental pathways is evident. The riboregulator miRNA172 post-transcriptionally targets a small group of regulatory repressor genes, including *APETALA2* (*AP2*) and AP2-like genes, such as *TARGET OF EARLY ACTIVATION TAGGED 1* (*TOE1*). These miRNA172-targeted AP2-like TFs are involved in controlling several developmental processes, such as plant aging, flowering time, tuber formation, fruit growth, and nodulation (Martin et al., 2009; Zhu and Helliwell, 2010; Yan et al., 2013; Wang et al., 2014; Ripoll et al., 2015). Functional analysis of RKNs infective and reproductive parameters was conducted on Arabidopsis lines with altered activities based on *35S::MIMICRY172 (MIM172)*, *35S::TARGET OF EARLY ACTIVATION TAGGED 1* (*TOE1*)*-miR172-resistant* (*35S::TOE1R*) and mutant (flowering locus T-10 (*ft-10*)) during gall and GCs development. The results indicated that the regulatory module miRNA172/TOE1/FT plays a crucial role during GCs and gall development (Diaz-Manzano et al., 2018; Table 1; Figure 2). Therefore, the repression of *TOE1* by miRNA172 is relevant for the normal establishment of RKNs and the formation of galls/GCs.

Interestingly, the SPL7/MIR408-UCC2/MIR398-CSD1 copper module (Griffiths-Jones et al., 2007) is also functional and active within galls (Noureddine et al., 2022; Table 1; Figure 2). Loss of function lines of miR398b/c and miR408 in Arabidopsis, resulted in fewer galls and smaller infection sites as compared with the control lines. These findings together with the expression data of two microRNA families, *miR398* and *miR408*, upregulated in galls, similarly to that of the TF SLP7, strongly suggest that the expression of *MIR408* and *MIR398B* and *-C* is activated by SPL7 in response to a decrease in copper concentration in galls (Noureddine et al., 2022). The role of this module might be related to its involvement in lignin metabolism (Reyt et al., 2020) as the cell wall suffer dramatic changes during gall and GCs development and numerous cell wall modifying enzymes are activated (Wieczorek, 2015). However, further research will be needed to elucidate it.

Conclusion

Despite the abundance of DEGs encoding plant TFs during the RKNs interaction in several plant species, that for example in the

Arabidopsis transcriptomes cover most of the TFs families identified within the genome (Figure 1), their biological function during RKNs infection is still poorly understood. The functional role of only around 40 TFs have been assessed (Table 1). Most of the data was obtained from plant lines with altered expression for each TF, mainly loss of function lines, that were infected, and significant differences either in the infection rate, gall formation, gall or GCs development compared to their control wild type lines were encountered. As a result, a clear phenotype during RKNs infection was identified. Two main groups of functionalities can be identified: TFs related to plant defenses, whose downstream targets are defense-related genes (see Table 1; Figure 2), and TFs involved in plant developmental programs, such as lateral root and/or callus formation, root apical meristem, or root regeneration. These are presumably hijacked by nematodes for their own benefit, including some TFs with a role in basic cellular functions, such as cell cycle control (Table 1; Figure 2). Interestingly, there is increasing evidence of the involvement of TFs with a dual role in plant development and defense and/or as integrator hubs between stress signals and developmental signals, such as DEL1, ERF109, ERF115, ERF114 and ERF6 (Table 1; Figure 2). However, the signal transduction pathways regulated by those TFs during RKNs infection are mostly unknown or only partially understood. Nevertheless, few regulatory modules involving TFs have been fully or partially proven in the interaction between RKNs and plants. These include the miRNA172/TOE1/FT module (Diaz-Manzano et al., 2018) and the SPL7/MIR408-UCC2/MIR398-CSD1 copper module (Noureddine et al., 2022). Clearly, further studies are needed to increase our knowledge in the regulatory networks driven by plant TFs modified by the nematode and as a plant response during the RKN interactions.

Author contributions

JD-F: Conceptualization, Data curation, Validation, Visualization, Writing – original draft, Writing – review & editing, Formal analysis, Investigation, Methodology, Software. AG-R: Investigation, Methodology, Writing – original draft. CE: Conceptualization, Writing – original draft, Data curation, Funding acquisition, Project administration, Resources, Supervision, Validation, Visualization, Writing – review & editing.

Funding

The author(s) declare financial support was received for the research, authorship, and/or publication of this article. This work was supported by the Spanish Government (PID2019-105924RB-I00 and PID2022-138989OB-I00, Ministerio de Ciencia e Innovacion, MCIN/AEI/10.13039/501100011033 FEDER, UE), CPP2021-008347. 2022-2024. MICIN/AEI/10.13039/501100011033 and by the European Union Next Generation EU/PRTR, by the Castilla-La Mancha Government (SBPLY/17/180501/000287; SBPLY/21/180501/000033), to CE. AG-R was a recipient of a grant from Plan Propio I+D+I of UCLM co-financed by FSE [2019/5964] and JD-F received funding from Ministerio de Universidades-European Union in the frame of NextGenerationEU RD 289/2021 (Universidad Politécnica de Madrid).

Conflict of interest

The authors declare that the research was conducted in the absence of any commercial or financial relationships that could be construed as a potential conflict of interest.

The author(s) declared that they were an editorial board member of Frontiers, at the time of submission. This had no impact on the peer review process and the final decision.

Publisher's note

References

Absmanner, B., Stadler, R., and Hammes, U. Z. (2013). Phloem development in nematode-induced feeding sites: The implications of auxin and cytokinin. *Front. Plant Sci.* 4, 241. doi: 10.3389/fpls.2013.00241

Ali, M. A., Wieczorek, K., Kreil, D. P., and Bohlmann, H. (2014). The beet cyst nematode Heterodera schachtii modulates the expression of WRKY transcription factors in syncytia to favour its development in Arabidopsis roots. *PloS One* 9, e102360. doi: 10.1371/journal.pone.0102360

Ambawat, S., Sharma, P., Yadav, N. R., and Yadav, R. C. (2013). MYB transcription factor genes as regulators for plant responses: an overview. *Physiol. Mol. Biol. Plants* 19, 307–321. doi: 10.1007/s12298-013-0179-1

Atamian, H. S., Eulgem, T., and Kaloshian, I. (2012). SlWRKY70 is required for Mi-1-mediated resistance to aphids and nematodes in tomato. *Planta* 235, 299–309. doi: 10.1007/s00425-011-1509-6

Bagchi, R., Melnyk, C. W., Christ, G., Winkler, M., Kirchsteiner, K., Salehin, M., et al. (2018). The Arabidopsis ALF4 protein is a regulator of SCF E3 ligases. *EMBO J.* 37, 255–268. doi: 10.15252/embj.201797159

Barcala, M., García, A., Cabrera, J., Casson, S., Lindsey, K., Favery, B., et al. (2010). Early transcriptomic events in microdissected Arabidopsis nematode-induced giant cells. *Plant J.* 61, 698–712. doi: 10.1111/tpj.2010.61.issue-4

Bartlem, D. G., Jones, M. G. K., and Hammes, U. Z. (2014). Vascularization and nutrient delivery at root-knot nematode feeding sites in host roots. *In J. Exp. Bot.* 65, 1789–1798. doi: 10.1093/jxb/ert415

Bhattarai, K. K., Atamian, H. S., Kaloshian, I., and Eulgem, T. (2010). WRKY72-type transcription factors contribute to basal immunity in tomato and Arabidopsis as well as gene-for-gene resistance mediated by the tomato R gene Mi-1. *Plant J.* 63, 229–240. doi: 10.1111/j.1365-313X.2010.04232.x

Bhosale, R., Boudolf, V., Cuevas, F., Lu, R., Eekhout, T., Hu, Z., et al. (2018). A spatiotemporal DNA endoploidy map of the arabidopsis root reveals roles for the endocycle in root development and stress adaptation. *Plant Cell* 30, 2330–2351. doi: 10.1105/tpc.17.00983

Birkenbihl, R. P., Liu, S., and Somssich, I. E. (2017). Transcriptional events defining plant immune responses. *Curr. Opin. Plant Biol.* 38, 1–9. doi: 10.1016/j.pbi.2017.04.004

Bonke, M., Thitamadee, S., Mähönen, A. P., Hauser, M.-T., and Helariutta, Y. (2003). APL regulates vascular tissue identity in Arabidopsis. *Nature* 426, 181–186. doi: 10.1038/nature02100

Cabrera, J., Barcala, M., García, A., Rio-Machín, A., Medina, C., Jaubert-Possamai, S., et al. (2016). Differentially expressed small RNAs in Arabidopsis galls formed by Meloidogyne javanica: a functional role for miR390 and its TAS3-derived tasiRNAs. *New Phytol.* 209, 1625–1640. doi: 10.1111/nph.13735

Cabrera, J., Bustos, R., Favery, B., Fenoll, C., and Escobar, C. (2014a). NEMATIC: A simple and versatile tool for the in silico analysis of plant–nematode interactions. *Mol. Plant Pathol.* 15, 627–636. doi: 10.1111/mpp.12114

Cabrera, J., Diaz-Manzano, F. E., Saínchez, M., Rosso, M. N., Melillo, T., Goh, T., et al. (2014b). A role for LATERAL ORGAN BOUNDARIES-DOMAIN 16 during the interaction Arabidopsis-Meloidogyne spp. provides a molecular link between lateral root and root-knot nematode feeding site development. *New Phytol.* 203, 632–645. doi: 10.1111/nph.12826

Chandran, D., Inada, N., Hather, G., Kleindt, C. K., and Wildermuth, M. C. (2010). Laser microdissection of Arabidopsis cells at the powdery mildew infection site reveals site-specific processes and regulators. *Proc. Natl. Acad. Sci. United States America* 107, 460–465. doi: 10.1073/pnas.0912492107

Chandran, D., Rickert, J., Huang, Y., Steinwand, M. A., Marr, S. K., and Wildermuth, M. C. (2014). Atypical E2F transcriptional repressor DEL1 acts at the intersection of plant growth and immunity by controlling the hormone salicylic acid. *Cell Host Microbe* 9;15, 506–513. doi: 10.1016/j.chom.2014.03.007

Chinnapandi, B., Bucki, P., and Braun-Miyara, S. (2017). SlWRKY45, nematode-responsive tomato WRKY gene, enhances susceptibility to the root knot nematode; M. javanica infection. *Plant Signaling Behav.* 2, 12(12). doi: 10.1080/15592324.2017.1356530

Chinnapandi, B., Bucki, P., Fitoussi, N., Kolomiets, M., Borrego, E., and Braun-Miyara, S. (2019). Tomato SlWRKY3 acts as a positive regulator for resistance against the root-knot nematode Meloidogyne javanica by activating lipids and hormone-mediated defense-signaling pathways. *Plant Signaling Behav.* 14, 1601951. doi: 10.1080/15592324.2019.1601951

de Almeida Engler, J., and Favery, B. (2011). "The plant cytoskeleton remodelling in nematode induced feeding sites," in *Genomics and molecular genetics of plant-nematode interactions* (London, UK: Springer Science & Business Media, B.V.), 369–393. doi: 10.1007/978-94-007-0434-3_18

de Almeida Engler, J., De Vleesschauwer, V., Burssens, S., Celenza, J. L. Jr., Inzé, D., Van Montagu, M., et al. (1999). Molecular markers and cell cycle inhibitors show the importance of cell cycle progression in nematode-induced galls and syncytia. *Plant Cell* 11, 793–808. doi: 10.1105/tpc.11.5.793

de Almeida Engler, J., Kyndt, T., Vieira, P., Van Cappelle, E., Boudolf, V., Sanchez, V., et al. (2012). CCS52 and DEL1 genes are key components of the endocycle in nematode-induced feeding sites. *Plant J.* 72, 185–198. doi: 10.1111/j.1365-313X.2012.05054.x

Del Pozo, J. C., Boniotti, M. B., and Gutierrez, C. (2002). Arabidopsis E2Fc functions in cell division and is degraded by the ubiquitin-SCFAtSKP2 pathway in response to light. *Plant Cell* 14, 3057–3071. doi: 10.1105/tpc.006791

Del Pozo, J. C., Diaz-Trivino, S., Cisneros, N., and Gutierrez, C. (2006). The balance between cell division and endoreplication depends on E2FC-DPB, transcription factors regulated by the ubiquitin-SCFSKP2A pathway in Arabidopsis. *Plant Cell* 18, 2224–2235. doi: 10.1105/tpc.105.039651

De Meutter, J., Tytgat, T., Witters, E., Gheysen, G., Van Onckelen, H., and Gheysen, G. (2003). Identification of cytokinins produced by the plant parasitic nematodes Heterodera schachtii and Meloidogyne incognita. *Mol. Plant Pathol.* 4, 271–277. doi: 10.1046/j.1364-3703.2003.00176.x

De Rybel, B., Vassileva, V., Parizot, B., Demeulenaere, M., Grunewald, W., Audenaert, D., et al. (2010). A novel aux/IAA28 signaling cascade activates GATA23-dependent specification of lateral root founder cell identity. *Curr. Biol.* 12;20, 1697–1706. doi: 10.1016/j.cub.2010.09.007

De Smet, I., Lau, S., Voss, U., Vanneste, S., Benjamins, R., Rademacher, E. H., et al. (2010). Bimodular auxin response controls organogenesis in Arabidopsis. *Proc. Natl. Acad. Sci. U.S.A.* 9;107, 2705–2710. doi: 10.1073/pnas.0915001107

Diaz-Manzano, F. E., Cabrera, J., Ripoll, J. J., Del Olmo, I., Andrés, M. F., Silva, A. C., et al. (2018). A role for the gene regulatory module microrna172/TARGET OF EARLY ACTIVATION TAGGED 1/FLOWERING LOCUS T (Mirna172/TOE1/FT) in the feeding sites induced by meloidogyne javanica in arabidopsis thaliana. *New Phytol.* 217, 813–827. doi: 10.1111/nph.14839

DiDonato, R. J., Arbuckle, E., Buker, S., Sheets, J., Tobar, J., Totong, R., et al. (2004). Arabidopsis ALF4 encodes a nuclear-localized protein required for lateral root formation. *Plant J.* 37, 340–353. doi: 10.1046/j.1365-313X.2003.01964.x

Dimova, D. K., and Dyson, N. J. (2005). The E2F transcriptional network: Old acquaintances with new faces. *Oncogene* 24, 2810–2826. doi: 10.1038/sj.onc.1208612

Dubos, C., Stracke, R., Grotewold, E., Weisshaar, B., Martin, C., and Lepiniec, L. (2010). MYB transcription factors in Arabidopsis. *Trends Plant Sci.* 15, 573–581. doi: 10.1016/j.tplants.2010.06.005

Efroni, I., Mello, A., Nawy, T., Ip, P. L., Rahni, R., DelRose, N., et al. (2016). Root regeneration triggers an embryo-like sequence guided by hormonal interactions. *Cell* 16;165, 1721–1733. doi: 10.1016/j.cell.2016.04.046

Elling, A. A. (2013). Major emerging problems with minor Meloidogyne species. *Phytopathology* 103, 1092–1102. doi: 10.1094/PHYTO-01-13-0019-RVW

Escobar, C., Barcala, M., Cabrera, J., and Fenoll, C. (2015). Overview of root-knot nematodes and giant cells. *Adv. Botanical Res.* 73, 1–32. doi: 10.1016/bs.abr.2015.01.001

Frerigmann, H., and Gigolashvili, T. (2014). MYB34, MYB51, and MYB122 distinctly regulate indolic glucosinolate biosynthesis in Arabidopsis thaliana. *Mol. Plant* 7, 814–828. doi: 10.1093/mp/ssu004

Fuller, V. L., Lilley, C. J., Atkinson, H. J., and Urwin, P. E. (2007). Differential gene expression in Arabidopsis following infection by plant-parasitic nematodes Meloidogyne incognita and Heterodera schachtii. *Mol. Plant Pathol.* 8, 595–609. doi: 10.1111/j.1364-3703.2007.00416.x

Gheysen, G., and Fenoll, C. (2011). "Arabidopsis as a tool for the study of plant–nematode interactions," in *Genomics and molecular genetics of plant–nematode interactions*. Eds. J. Jones, G. Gheysen and C. Fenoll (Springer, Dordrecht, the Netherlands), 139–156.

Goh, T., Toyokura, K., Yamaguchi, N., Okamoto, Y., Uehara, T., Kaneko, S., et al. (2019). Lateral root initiation requires the sequential induction of transcription factors LBD16 and PUCHI in Arabidopsis thaliana. *New Phytol.* 224, 749–760. doi: 10.1111/nph.16065

Griffiths-Jones, S., Saini, H. K., Van Dongen, S., and Enright, A. J. (2007). miRBase: tools for microRNA genomics. *Nucleic Acids Res.* 36, D154–D158. doi: 10.1093/nar/gkm952

Guarneri, N., Willig, J. J., Sterken, M. G., Zhou, W., Hasan, M. S., Sharon, L., et al. (2022). Root architecture plasticity in response to endoparasitic cyst nematodes is mediated by damage signaling. *New Phytol.* 237, 807–822. doi: 10.1111/nph.18570

Guo, X., Wang, J., Gardner, M., Fukuda, H., Kondo, Y., Etchells, J. P., et al. (2017). Identification of cyst nematode B-type CLE peptides and modulation of the vascular stem cell pathway for feeding cell formation. *PloS Pathog.* 13, e1006142. doi: 10.1371/journal.ppat.1006142

Haga, N., Kato, K., Murase, M., Araki, S., Kubo, M., Demura, T., et al. (2007). R1R2R3-Myb proteins positively regulate cytokinesis through activation of KNOLLE transcription in Arabidopsis thaliana. *Development* 134, 1101–1110. doi: 10.1242/dev.02801

Haga, N., Kobayashi, K., Suzuki, T., Maeo, K., Kubo, M., Ohtani, M., et al. (2011). Mutations in MYB3R1 and MYB3R4 cause pleiotropic developmental defects and preferential down-regulation of multiple G2/M-specific genes in Arabidopsis. *Plant Physiol.* 157, 706–717. doi: 10.1104/pp.111.180836

Hirota, A., Kato, T., Fukaki, H., Aida, M., and Tasaka, M. (2007). The auxin-regulated AP2/EREBP gene PUCHI is required for morphogenesis in the early lateral root primordium of arabidopsis. *Plant Cell* 19, 2156–2168. doi: 10.1105/tpc.107.050674

Hoth, S., Stadler, R., Sauer, N., Hammes, U. Z., Beachy, R. N., and Danforth, D. (2008). Differential vascularization of nematode-induced feeding sites. *Proc. Natl. Acad. Sci.* 105, 12617–12622. doi: 10.1073/pnas.0803835105

Huang, H., Zhao, W., Qiao, H., Li, C., Sun, L., Yang, R., et al. (2022). SlWRKY45 interacts with jasmonate-ZIM domain proteins to negatively regulate defense against the root-knot nematode Meloidogyne incognita in tomato. *Hortic. Res.* 5;9, uhac197. doi: 10.22541/au.164151237.72268573/v1

Ikeuchi, M., Favero, D. S., Sakamoto, Y., Iwase, A., Coleman, D., Rymen, B., et al. (2019). Molecular mechanisms of plant regeneration. *Annu. Rev. Plant Biol.* 70, 377–406. doi: 10.1146/annurev-arplant-050718-100434

Inzé, D., and De Veylder, L. (2006). Cell cycle regulation in plant development. *Annu. Rev. Genet.* 40, 77–105. doi: 10.1146/annurev.genet.40.110405.090431

Isah, T. (2019). Stress and defense responses in plant secondary metabolites production. *Biol. Res.* 52, 39. doi: 10.1186/s40659-019-0246-3

Ito, M., Araki, S., Matsunaga, S., Itoh, T., Nishihama, R., Machida, Y., et al. (2001). G2/M-Phase-Specific Transcription during the Plant Cell Cycle Is Mediated by c-Myb-Like Transcription Factors. *Plant Cell* 13, 1891–1905. doi: 10.1105/tpc.010102

Ito, M., Iwase, M., Kodama, H., Lavisse, P., Komamine, A., Nishihama, R., et al. (1998). A novel cis-acting element in promoters of plant B-type cyclin genes activates M phase-specific transcription. *Plant Cell* 10, 331–341. doi: 10.1105/tpc.10.3.331

Jammes, F., Lecomte, P., de Almeida-Engler, J., Bitton, F., Martin-Magniette, M. L., Renou, J. P., et al. (2005). Genome-wide expression profiling of the host response to root-knot nematode infection in Arabidopsis. *Plant J.* 44, 447–458. doi: 10.1111/j.1365-313X.2005.02532.x

Ji, H., Gheysen, G., Denil, S., Lindsey, K., Topping, J. F., Nahar, K., et al. (2013). Transcriptional analysis through RNA sequencing of giant cells induced by Meloidogyne graminicola in rice roots. *J. Exp. Bot.* 64, 3885–3898. doi: 10.1093/jxb/ert219

Jiang, J., Ma, S., Ye, N., Jiang, M., Cao, J., and Zhang, J. (2017). WRKY transcription factors in plant responses to stresses. *J. Integr. Plant Biol.* 59, 86–101. doi: 10.1111/jipb.12513

Jin, J. P., Zhang, H., Kong, L., Gao, G., and Luo, J. C. (2014). PlantTFDB 3.0: a portal for the functional and evolutionary study of plant transcription factors. *Nucleic Acids Res.* 42, D1182–D1187. doi: 10.1093/nar/gkt1016

Karim, M. R., Hirota, A., Kwiatkowska, D., Tasaka, M., and Aida, M. (2009). A role for arabidopsis PUCHI in floral meristem identity and bract suppression. *Plant Cell* 21, 1360–1372. doi: 10.1105/tpc.109.067025

Kikuchi, T., Eves-van den Akker, S., and Jones, J. T. (2017). Genome evolution of plant-parasitic nematodes. *Annu. Rev. Phytopathol.* 55, 333–354. doi: 10.1146/annurev-phyto-080516-035434

Knoth, C., Ringler, J., Dangl, J. L., and Eulgem, T. (2007). Arabidopsis WRKY70 is required for full RPP4-mediated disease resistance and basal defense against Hyaloperonospora parasitica. *Mol. Plant Microbe Interact.* 20, 120–128. doi: 10.1094/MPMI-20-2-0120

Kobayashi, K., Suzuki, T., Iwata, E., Magyar, Z., Bögre, L., and Ito, M. (2015a). MYB3Rs, plant homologs of Myb oncoproteins, control cell cycle-regulated transcription and form DREAM-like complexes. *Transcription* 6, 106–111. doi: 10.1080/21541264.2015.1109746

Kobayashi, K., Suzuki, T., Iwata, E., Nakamichi, N., Suzuki, T., Chen, P., et al. (2015b). Transcriptional repression by MYB3R proteins regulates plant organ growth. *EMBO J.* 34, 1992–2007. doi: 10.15252/embj.201490899

Kumar, A., Sichov, N., Bucki, P., and Miyara, S. B. (2023). SlWRKY16 and SlWRKY31 of tomato, negative regulators of plant defense, involved in susceptibility activation following root-knot nematode Meloidogyne javanica infection. *Sci. Rep.* 5;13, 14592. doi: 10.1038/s41598-023-40557-z

Kyndt, T., Denil, S., Haegeman, A., Trooskens, G., Bauters, L., Van Criekinge, W., et al. (2012). Transcriptional reprogramming by root knot and migratory nematode infection in rice. *New Phytol.* 196, 887–900. doi: 10.1111/j.1469-8137.2012.04311.x

Lammens, T., Boudolf, V., Kheibarshekan, L., Zalmas, L. P., Gaamouche, T., Maes, S., et al. (2008). Atypical E2F activity restrains APC/CCCS52A2 function obligatory for endocycle onset. *Proc. Natl. Acad. Sci. U.S.A.* 23;105, 14721–14726. doi: 10.1073/pnas.0806510105

Li, J., Brader, G., Kariola, T., and Tapio Palva, E. (2006). WRKY70 modulates the selection of signaling pathways in plant defense. *Plant J.* 46, 477–491. doi: 10.1111/j.1365-313X.2006.02712.x

Liu, J., Hu, X., Qin, P., Prasad, K., Hu, Y., and Xu, L. (2018). The WOX11-LBD16 pathway promotes pluripotency acquisition in callus cells during *de novo* shoot regeneration in tissue culture. *Plant Cell Physiol.* 59, 734–743. doi: 10.1093/pcp/pcy010

Marin, E., Jouannet, V., Herz, A., Lokerse, A. S., Weijers, D., Vaucheret, H., et al. (2010). miR390, Arabidopsis TAS3 tasiRNAs, and their AUXIN RESPONSE FACTOR targets define an autoregulatory network quantitatively regulating lateral root growth. *Plant Cell* 22, 1104–1117. doi: 10.1105/tpc.109.072553

Martin, A., Adam, H., Diaz-Mendoza, M., Zurczak, M., Gonzalez-Schain, N. D., and Suarez-Lopez, P. (2009). Graft-transmissible induction of potato tuberization by the microRNA miR172. *Development* 136, 2873–2881. doi: 10.1242/dev.031658

Medina, C., da Rocha, M., Magliano, M., Ratpopoulo, A., Revel, B., Marteu, N., et al. (2017). Characterization of microRNAs from Arabidopsis galls highlights a role for miR159 in the plant response to the root-knot nematode Meloidogyne incognita. *New Phytol.* 216, 882–896. doi: 10.1111/nph.14717

Melnyk, C. W., Schuster, C., Leyser, O., and Meyerowitz, E. M. (2015).). A developmental framework for graft formation and vascular reconnection in Arabidopsis thaliana. *Curr. Biol.* 25, 1306–1318. doi: 10.1016/j.cub.2015.03.032

Meng, X., Xu, J., He, Y., Yang, K. Y., Mordorski, B., Liu, Y., et al. (2013). Phosphorylation of an ERF transcription factor by Arabidopsis MPK3/MPK6 regulates plant defense gene induction and fungal resistance. *Plant Cell* 25, 1126–1142. doi: 10.1105/tpc.112.109074

Menges, M., De Jager, S. M., Gruissem, W., and Murray, J. A. H. (2005). Global analysis of the core cell cycle regulators of Arabidopsis identifies novel genes, reveals multiple and highly specific profiles of expression and provides a coherent model for plant cell cycle control. *Plant J.* 41, 546–566. doi: 10.1111/j.1365-313X.2004.02319.x

Nakagami, S., Saeki, K., Toda, K., Ishida, T., and Sawa, S. (2020). The atypical E2F transcription factor DEL1 modulates growth–defense tradeoffs of host plants during root-knot nematode infection. *Sci. Rep.* 1;10, 8836. doi: 10.1038/s41598-020-65733-3

Nakano, T., Suzuki, K., Fujimura, T., and Shinshi, H. (2006). Genome-wide analysis of the ERF gene family in arabidopsis and rice. *Plant Physiol.* 140, 411–432. doi: 10.1104/pp.105.073783

Ngou, B. P. M., Ahn, H. K., Ding, P., and Jones, J. D. G. (2020). Mutual potentiation of plant immunity by cell-surface and intracellular receptors. *Nature* 592, 110–115. doi: 10.1038/s41586-021-03315-7

Nie, W., Liu, L., Chen, Y., Luo, M., Feng, C., Wang, C., et al. (2023). Identification of the Regulatory Role of SlWRKYs in Tomato Defense against Meloidogyne incognita. *Plants (Basel)* 22;12, 2416. doi: 10.3390/plants12132416

Noureddine, Y., da Rocha, M., An, J., Médina, C., Mejias, J., Mulet, K., et al. (2023). AUXIN RESPONSIVE FACTOR8 regulates development of the feeding site induced by root-knot nematodes in tomato. *J. Exp. Bot.* 29;74, 5752–5766. doi: 10.1093/jxb/erad208283-295

Noureddine, Y., Mejias, J., da Rocha, M., Thomine, S., Quentin, M., Abad, P., et al. (2022). Copper microRNAs modulate the formation of giant feeding cells induced by the root knot nematode Meloidogyne incognita in Arabidopsis thaliana. *New Phytol.* 236, 283–297. doi: 10.1111/nph.18362

Okushima, Y., Fukaki, H., Onoda, M., Theologis, A., and Tasaka, M. (2007). ARF7 andARF19 regulate lateral root formation via direct activation of LBD/ASL genes in Arabidopsis. *Plant Cell* 19, 118–130. doi: 10.1105/tpc.106.047761

Olmo, R., Cabrera, J., Diaz-Manzano, F. E., Ruiz-Ferrer, V., Barcala, M., Ishida, T., et al. (2020). Root-knot nematodes induce gall formation by recruiting developmental pathways of post-embryonic organogenesis and regeneration to promote transient pluripotency. *New Phytol.* 227, 200–215. doi: 10.1111/nph.16521

Olmo, R., Cabrera, J., Fenoll, C., and Escobar, C. (2019). A role for ALF4 during gall and giant cell development in the biotic interaction between Arabidopsis and Meloidogyne spp. *Physiol. Plant* 165, 17–28. doi: 10.1111/ppl.12734

Olmo, R., Cabrera, J., Moreno-Risueno, M. A., Fukaki, H., Fenoll, C., and Escobar, C. (2017). Molecular transducers from roots are triggered in arabidopsis leaves by root-knot nematodes for successful feeding site formation: A conserved post-embryogenic *de novo* organogenesis program? *Front. Plant Sci.* 26:8. doi: 10.3389/fpls.2017.00875

Peng, Y., van Wersch, R., and Zhang, Y. (2018). Convergent and divergent signaling in PAMP-triggered immunity and effector-triggered immunity. *Mol. Plant-Microbe Interact.* 31, 403–409. doi: 10.1094/MPMI-06-17-0145-CR

Portillo, M., Cabrera, J., Lindsey, K., Topping, J., Andrés, M. F., Emiliozzi, M., et al. (2013). Distinct and conserved transcriptomic changes during nematode-induced giant cell development in tomato compared with Arabidopsis: a functional role for gene repression. *New Phytol.* 197, 1276–1290. doi: 10.1111/nph.12121

Qin, X., Xue, B., Tian, H., Fang, C., Yu, J., Chen, C., et al. (2022). An unconventionally secreted effector from the root knot nematode Meloidogyne incognita, Mi-ISC-1, promotes parasitism by disrupting salicylic acid biosynthesis in host plants. *Mol. Plant Pathol.* 23, 516–529. doi: 10.1111/mpp.13175

Ramirez-Parra, E., López-Matas, M. A., Fründt, C., and Gutierrez, C. (2004). Role of an atypical E2Ftranscription factor in the control of Arabidopsis cell growth and differentiation. *Plant Cell* 16, 2350–2363. doi: 10.1105/tpc.104.023978

Reyt, G., Chao, Z., Flis, P., Salas-Gonzalez, I., Castrillo, G., Chao, D. Y., et al. (2020). Uclacyanin proteins are required for lignified nanodomain formation within casparian strips. *Curr. Biol.* 19;30, 4103–4111.e6. doi: 10.1016/j.cub.2020.07.095

Ribeiro, D. G., Mota, A. P. Z., Santos, I. R., Arraes, F. B. M., Grynberg, P., Fontes, W., et al. (2022). NBS-LRR-WRKY genes and protease inhibitors (PIs) seem essential for cowpea resistance to root-knot nematode. *J. Proteomics* 15;261, 104575. doi: 10.1016/j.jprot.2022.104575

Ribeiro, C., de Melo, B. P., Lourenço-Tessutti, I. T, Ballesteros, H. F., Ribeiro, K. V. G., Menuet, K., et al. (2024). MicroRNA regulation of fruit growthThe regeneration conferring transcription factor complex ERF115-PAT1 coordinates a wound-induced response in root-knot nematode induced galls. *New Phytol.* 241, 878–895. doi: 10.1111/nph.19399

Ripoll, J. J., Bailey, L. J., Mai, Q. A., Wu, S. L., Hon, C. T., Chapman, E. J., et al. (2015). MicroRNA regulation of fruit growth. *Nat. Plants* 30;1, 15036. doi: 10.1038/nplants.2015.36

Rodiuc, N., Vieira, P., Banora, M. Y., and de Almeida Engler, J. (2014). On the track of transfer cell formation by specialized plant-parasitic nematodes. *Front. Plant Sci.* 5;5. doi: 10.3389/fpls.2014.00160

Rutter, W. B., Franco, J., and Gleason, C. (2022). Rooting out the mechanisms of root-knot nematode-plant interactions. *Annu. Rev. Phytopathol.* 60, 43-76. doi: 10.1146/annurev-phyto-021621-120943

Sabelli, P. A., Nguyen, H., and Larkins, B. A. (2007). "Cell cycle and endosperm development," in *Annual plant reviews, volume 32: cell cycle control and plant development*. Ed. E. ,. D. Inzé (Blackwell Publishing Ltd, Oxford), 294–310.

Sakuma, Y., Liu, Q., Dubouzet, J. G., Abe, H., Shinozaki, K., and Yamaguchi-Shinozaki, K. (2002). DNA-binding specificity of the ERF/AP2 domain of Arabidopsis DREBs, transcription factors involved in dehydration- and cold-inducible gene expression. *Biochem. Biophys. Res. Commun.* 290, 998–1009. doi: 10.1006/bbrc.2001.6299

Siddique, S., Radakovic, Z. S., de la Torre, C. M., Chronis, D., Novák, O., Ramireddy, E., et al. (2015). A parasitic nematode releases cytokinin that controls cell division and orchestrates feeding site formation in host plants. *PNAS,112* 41), 12669–12674. doi: 10.1073/pnas.1503657112

Silva, A. C., Ruiz-Ferrer, V., Müller, S. Y., Pellegrin, C., Abril-Urías, P., Martínez-Gómez, Á., et al. (2022). The DNA methylation landscape of the root-knot nematode-induced pseudo-organ, the gall, in Arabidopsis, is dynamic, contrasting over time, and critically important for successful parasitism. *New Phytol.* 236, 1888–1907. doi: 10.1111/nph.18395

Singh, S., Singh, B., and Singh, A. P. (2015). Nematodes: A threat to sustainability of agriculture. *Proc. Environ. Sci.* 29, 215–216. doi: 10.1016/j.proenv.2015.07.270

Sugimoto, K., Jiao, Y., and Meyerowitz, E. M. (2010). Arabidopsis regeneration from multiple tissues occurs via a root development pathway. *Dev. Cell* 16;18, 463–471. doi: 10.1016/j.devcel.2010.02.004

Suzuki, R., Ueda, T., Wada, T., Ito, M., Ishida, T., and Sawa, S. (2021a). Identification of genes involved in meloidogyne incognita-induced gall formation processes in arabidopsis thaliana. *Plant Biotechnol.* 38, 1–8. doi: 10.5511/plantbiotechnology.20.0716a

Suzuki, R., Yamada, M., Higaki, T., Aida, M., Kubo, M., Tsai, A. Y. L., et al. (2021b). PUCHI regulates giant cell morphology during root-knot nematode infection in arabidopsis thaliana. *Front. Plant Sci.* 12. doi: 10.3389/fpls.2021.755610

Teixeira, M. A., Wei, L., and Kaloshian, I. (2016). Root-knot nematodes induce pattern-triggered immunity in Arabidopsis thaliana roots. *New Phytol.* 211, 276–287. doi: 10.1111/nph.13893

Trinh, D. C., Lavenus, J., Goh, T., Boutté, Y., Drogue, Q., Vaissayre, V., et al. (2019). PUCHI regulates very long chain fatty acid biosynthesis during lateral root and callus formation. *Proc. Natl. Acad. Sci. U.S.A.* 116, 14325–14330. doi: 10.1073/pnas.1906300116

Tsuda, K., Mine, A., Bethke, G., Igarashi, D., Botanga, C. J., Tsuda, Y., et al. (2013). Dual regulation of gene expression mediated by extended MAPK activation and salicylic acid contributes to robust innate immunity in Arabidopsis thaliana. *PloS Genet.* 9, e1004015. doi: 10.1371/journal.pgen.1004015

Uemura, Y., Kimura, S., Ohta, T., Suzuki, T., Mase, K., Kato, H., et al. (2023). A very long chain fatty acid responsive transcription factor, MYB93, regulates lateral root development in Arabidopsis. *Plant J.* 115, 1408–1427. doi: 10.1111/tpj.16330

Vieira, P., Kyndt, T., Gheysen, G., and de Almeida Engler, J. (2013). An insight into critical endocycle genes for plant-parasitic nematode feeding sites establishment. *Plant Signal Behav.* 8, e24223. doi: 10.4161/psb.24223

Vlieghe, K., Boudolf, V., Beemster, G. T., Maes, S., Magyar, Z., Atanassova, A., et al. (2005). The DP-E2F-like gene DEL1 controls the endocycle in Arabidopsis thaliana. *Curr. Biol.* 11;15, 59–63. doi: 10.1016/j.cub.2004.12.038

Wang, X., Meng, H., Tang, Y., Zhang, Y., He, Y., Zhou, J., et al. (2022). Phosphorylation of an ethylene response factor by MPK3/MPK6 mediates negative feedback regulation of pathogen-induced ethylene biosynthesis in Arabidopsis. *J. Genet. Genomics* 49, 810–822. doi: 10.1016/j.jgg.2022.04.012

Wang, Y., Wang, L., Zou, Y., Chen, L., Cai, Z., Zhang, S., et al. (2014). Soybean miR172c targets the repressive AP2 transcription factor NNC1 to activate ENOD40 expression and regulate nodule initiation. *Plant Cell* 26, 4782–4801. doi: 10.1105/tpc.114.131607

Wani, S. H., Anand, S., Singh, B., Bohra, A., and Joshi, R. (2021). WRKY transcription factors and plant defense responses: latest discoveries and future prospects. *Plant Cell Rep.* 40, 1071–1085. doi: 10.1007/s00299-021-02691-8

Warmerdam, S., Sterken, M. G., Van Schaik, C., Oortwijn, M. E. P., Lozano-Torres, J. L., Bakker, J., et al. (2019). Mediator of tolerance to abiotic stress ERF6 regulates susceptibility of Arabidopsis to Meloidogyne incognita. *Mol. Plant Pathol.* 20, 137–152. doi: 10.1111/mpp.12745

Wieczorek, K. (2015). "Chapter three- cell wall alterations in nematode-infected roots," in *Botanical research*, vol. 73, 2015 . Eds. C. Escobar and C. Fenoll. (London: Academic Press), 61–90. doi: 10.1016/bs.abr.2014.12.002

Willig, J. J., Guarneri, N., van Loon, T., Wahyuni, S., Astudillo-Estévez, I. E., Xu, L., et al. (2024). Transcription factor WOX11 modulates tolerance to cyst nematodes via adventitious lateral root formation. *Plant Physiol.* 8, kiae053. doi: 10.1093/plphys/kiae053

Wu, Y., Li, X., Zhang, J., Zhao, H., Tan, S., Xu, W., et al. (2022). ERF subfamily transcription factors and their function in plant responses to abiotic stresses. *Front. Plant Sci.* 13. doi: 10.3389/fpls.2022.1042084

Xiao, K., Chen, W., Chen, X., Zhu, X., Guan, P., and Hu, J. (2020). CCS52 and DEL1 function in root-knot nematode giant cell development in Xinjiang wild myrobalan plum (Prunus sogdiana Vassilcz). *Protoplasma* 257, 1333–1344. doi: 10.1007/s00709-020-01505-0

Yamaguchi, Y. L., Suzuki, R., Cabrera, J., Nakagami, S., Sagara, T., Ejima, C., et al. (2017). Root-knot and cyst nematodes activate procambium-associated genes in arabidopsis roots. *Front. Plant Sci.* 13;8. doi: 10.3389/fpls.2017.01195

Yan, Z., Hossain, M. S., Wang, J., Valdes-Lopez, O., Liang, Y., Libault, M., et al. (2013). MiR172 regulates soybean nodulation. *Mol. Plant–Microbe Interact.* 26, 1371–1377. doi: 10.1094/MPMI-04-13-0111-R

Zhou, W., Lozano-Torres, J. L., Blilou, I., Zhang, X., Zhai, Q., Smant, G., et al. (2019). A jasmonate signaling network activates root stem cells and promotes regeneration. *Cell* 177, 942–956.e14. doi: 10.1016/j.cell.2019.03.006

Zhu, Q. H., and Helliwell, C. A. (2010). Regulation of flowering time and floral patterning by miR172. *J. Exp. Bot.* 62, 487–495. doi: 10.1093/jxb/erq295

frontiers | Frontiers in Plant Science

TYPE Original Research
PUBLISHED 04 July 2024
DOI 10.3389/fpls.2024.1411825

OPEN ACCESS

EDITED BY
Brigitte Mauch-Mani,
Université de Neuchâtel, Switzerland

REVIEWED BY
Phatu William Mashela,
University of Limpopo, South Africa
Paola Leonetti,
National Research Council (CNR), Italy

*CORRESPONDENCE
Tina Kyndt
tina.kyndt@ugent.be
Sven Mangelinckx
sven.mangelinckx@ugent.be

RECEIVED 03 April 2024
ACCEPTED 13 June 2024
PUBLISHED 04 July 2024

CITATION
Degroote E, Schoorens C, Pockelé S, Stojilković B, Demeestere K, Mangelinckx S and Kyndt T (2024) A combination of plant-based compounds and extracts acts nematicidal and induces resistance against *Meloidogyne incognita* in tomato. *Front. Plant Sci.* 15:1411825. doi: 10.3389/fpls.2024.1411825

A combination of plant-based compounds and extracts acts nematicidal and induces resistance against *Meloidogyne incognita* in tomato

Eva Degroote[1,2,3], Chloë Schoorens[1], Stefaan Pockelé[3], Boris Stojilković[1], Kristof Demeestere[4], Sven Mangelinckx[2]* and Tina Kyndt[1]*

[1]Department of Biotechnology, Faculty of Bioscience Engineering, Ghent University, Ghent, Belgium, [2]Synthesis, Bioresources and Bioorganic Chemistry Research Group, Department of Green Chemistry and Technology, Faculty of Bioscience Engineering, Ghent University, Research and Development, Ghent, Belgium, [3]Research and Development, Lima Europe NV, Rumst, Belgium, [4]Research Group Environmental Organic Chemistry and Technology (EnVOC), Department of Green Chemistry and Technology, Faculty of Bioscience Engineering, Ghent University, Ghent, Belgium

Considering the stricter European regulations for chemical pesticides (e.g. abolishment of the use of chemical soil fumigation products, such as methyl bromide), the need for more sustainable plant protection products is strongly increasing. In this research, Product X, an innovative mixture of bio-nematicidal compounds was developed and evaluated for efficacy. Product X showed a direct nematicidal effect against the root-knot nematode *Meloidogyne incognita*. In pot trials with tomato plants infected with *M. incognita*, Product X treatment lead to a significant reduction in nematode-induced gall formation. mRNA-sequencing indicated alterations in phytohormone levels and ROS-metabolism in tomato roots upon treatment with Product X, which was subsequently biochemically validated. Increased levels of abscisic acid and peroxidase activity seem to be the main factors in the response of tomato plants to Product X. Long-term administration of Product X did not yield negative effects on tomato growth or yield. In conclusion, Product X provides a new interesting mix of bio-active compounds in the combat against root-knot nematodes.

KEYWORDS

nematicide, salvia extract, salicylic acid, ascorbic acid, geraniol, garlic extract, *Meloidogyne incognita*, *Solanum lycopersicum*

Abbreviations: AA, Ascorbic acid; ABA, Abscisic acid; DEGs, Differentially expressed genes; dpt, Day(s) post treatment; ET, Ethylene; GO, Gene ontology; IAA, Indole-3-acetic acid; J2, Second stage juveniles; JA, Jasmonic acid; KEGG, Kyoto encyclopedia of genes and genomes; MDA, Malondialdehyde; PCA, Principal component analysis; PPP, Plant protection products; RNA, Ribonucleic acid; ROS, Reactive oxygen species; SA, Salicylic acid; SAR, Systemic acquired resistance.

1 Introduction

Climate change is altering the world at a quick pace, due to global changes such as increased temperatures some plant pathogens are becoming more abundant and more prevalent in different crops and areas around the world (Dutta and Phani, 2023). Additionally, sustainability gains importance throughout society. The European Green Deal is an international initiative to improve sustainability and resource-efficiency in the European Union (European Commission, 2019). Within the European Green Deal, the 'Farm to Fork' strategy aims to make food production systems fair, healthy, and environmentally-friendly (European Commission, 2020). Additionally, ecologically harmful chemical pesticides are progressively banned or put on a substitution list by the European Food Safety Authority (EFSA). Products on the substitution list need to be replaced when adequate alternatives become available. This results in an urgent need for sustainable and innovative pesticides and plant protection products (PPPs).

PPPs remain a valuable part of Integrated Pest Management (IPM) programs to keep populations of e.g. damaging insects, bacteria, fungi or nematodes under economic injury levels. Although often not recognized as the main culprit due to their generic symptoms and subterranean location, nematodes or roundworms cause an annual worldwide average crop loss of 12.3% (Talavera-Rubia et al., 2022). Among the thousands of plant-parasitic nematode species present in agricultural ecosystems, root-knot nematodes (*Meloidogyne* spp.) are most damaging to crop plants. They penetrate the plant root as second-stage juveniles (J2) (Abad et al., 2008) and induce the formation of a feeding site consisting of giant cells inside the vascular tissue. Via the feeding sites, nematodes withdraw nutrients from the host and interfere with water transport (Abad et al., 2008). Root-knot nematode infection results in the formation of so-called root-knots or galls, which are the most visible symptom of the disease (Abad et al., 2008). Plant-parasitic nematodes are often managed with chemical products (nematicides and fumigants), some of which are harmful to the environment and human health. Since many nematicides and fumigants have been banned in the EU, there is a clear need for new nematicidal products (Chen et al., 2020).

Various alternatives to chemical PPPs have been proposed. The first possible alternative is the use of biopesticides, including PPPs from botanical origin (reviewed in Ntalli and Caboni, 2012; Chen and Song, 2021). Another option is to target host resistance instead of directly targeting the PPN. This can be achieved through resistance breeding (Milligan et al., 1998), genetic modification (Dutta et al., 2015), or 'induced resistance'. Induced resistance (IR) involves the activation and priming of the immune system of the plant by an external stimulus (Mauch-Mani et al., 2016; De Kesel et al., 2021). Defense mechanisms will be activated faster and more intensively upon pathogen attack compared to naive plants (Mauch-Mani et al., 2016; De Kesel et al., 2021). For example, Benzothiadiazole (BTH), a salicylic acid-analogue (Melillo et al., 2014) is a successful resistance inducer against *M. incognita* in tomato. IR is a novel way of protecting plants from pathogen attack that has also been proven to be effective in the field (reviewed in Desmedt et al., 2021b).

In this work, we report on a new nematode management product consisting of ingredients of natural origin that combines nematicidal and resistance-inducing activities. A thorough literature study was done to select candidate bio-active compounds. The selected active ingredients include geraniol, rosemary and garlic extract, salicylic acid (SA), ascorbic acid (AA), and chitosan. A vegetable oil mixture consisting of sunflower, olive, and linseed oil was also added, which has both a nematicidal activity and formulation properties. The optimized mixture, together with emulsifiers and stabilizers, will henceforth be called 'Product X'. The aim of this study was to examine how nematodes and plants react to this mixture. We investigated the direct nematicidal effect of Product X on *Meloidogyne incognita in vitro* and *in planta* in tomato (*Solanum lycopersicum)*. Moreover, the response of tomato plants to Product X treatment was examined at a transcriptional and biochemical level. Finally, we investigated the long-term effect of Product X application on tomato growth and development.

2 Material and methods

2.1 Growing tomato plants

Tomato (*Solanum lycopersicum* L. 'Moneymaker') seeds were sterilized before germination. Seeds were incubated for 2 minutes in 70% ethanol (Chemlab) after which they were incubated for 12 minutes in a 5% bleach (Guest Medical) solution with 0.0002 v% Tween20 (Sigma Aldrich) and rinsed 5 times with sterile H_2O. After sterilization, seeds were put in moist potting soil (Structural Universal Type 1, Snebbout) and incubated in a growth room at a temperature of 24.5°C and light/dark regime of 16h/8h respectively. Seeds were incubated for 7 days before transplanting them to a sand:soil (1:1 v/v) mixture.

2.2 Culturing *Meloidogyne incognita*

Seeds of tomato plants were sterilized and germinated as described above. Plants of one month of age were inoculated with approximately 1000 *Meloidogyne incognita* J2 per pot containing three plants. These J2 originate from an in-house culture, initially provided by Shahid Siddique. Watering with a fertilizing solution (1 g/L Soluplant NPK 19–8-16 + 4 MgO + ME (micro-elements), Haifa Chemicals) happened twice per week depending on the age of the plants (200 ml – 750 ml per pot), until their harvest at 4 to 6 months after inoculation. At harvest, the required amount of galled roots (depending on the number of J2 needed per experiment) were separated from the potting soil and put on a sieve (200 µm pore diameter) covered with moist paper tissues (Tork). This sieve was put in a tray with tap water, allowing the nematodes to migrate from the roots through the sieve into the water. After 3 days, nematodes were collected by sieving the collection water over a sieve with pore diameter of 20 µm (Whitehead and Hemming, 1965). The number of nematodes in this solution was counted using a light microscope (Leica S8 APO, Leica microsystems).

2.3 Composition of Product X

Product X contains several components as listed in Table 1. Per compound, a weight percentage and a concentration in mg/L and mM (if possible) is displayed. The oil mixture makes up 20.5 wt% of Product X and consists of 10.3 wt% linseed oil, 67.1 wt% sunflower oil and 22.6 wt% olive oil.

2.4 Direct nematicidal testing

The direct nematicidal effect of Product X was evaluated *in vitro* by incubating 50 *M. incognita* J2 in 500 µL of 0.2 v% Product X for 24 h or 48 h (Supplementary Figure 1A). As a negative control, nematodes were incubated in sterile tap water. As a positive control, 0.2 v% of Vertimec (active ingredient: abamectin) was used (Li et al., 2018). Nematodes were kept at room temperature and were counted at 24 h and 48 h using a stereo microscope. Nematodes were recorded as dead if they did not respond to prodding with a small dissection needle. For every treatment, 6 technical replicates were included. The experiment was repeated twice independently. Mortality was calculated relative to the negative control using the Schneider-Orelli equation (Schneider-Orelli, 1947).

2.5 Infection experiments

Plants were grown as described above. Two weeks after transplant (BBCH 103), tomato roots were treated with 20 mL of 0.2 v% Product X, 20 mL of water (negative control) or 20 mL of 0.2 v% Vertimec (positive control) (Supplementary Figure 1B). Per treatment, 8 plants were included. One or 3 day(s) after treatment, 250 J2 (*M. incognita*) per plant were inoculated on the plant roots. During their growth, plants were supplemented 3 times per week with 30 mL of a 1 g/L tomato fertilizer solution (Soluplant NPK 19–8-16 + 4 MgO + ME, Haifa Chemicals). Plants were harvested 28 days post inoculation: shoots were cut, dried (65°C for four days) and weighed, and roots were cleaned and stored in a 1:1 (v:v) ethanol:glycerol solution before galls were counted for every root system. After counting, roots were cleaned thoroughly, dried (65°C for four days) and weighed to determine root dry weight. The experiment was independently repeated two times.

2.6 mRNA-sequencing

Plants were grown as described above. After growing for two weeks in a soil:sand mixture, roots were treated with 20 mL of a 0.2 v% Product X solution (Supplementary Figure 1C). Control plants (roots) were treated with an equal amount of water. Every treatment consisted of 3 biological replicates that were pools of 4 individual plants. Plants were harvested 24 h after treatment, roots were washed to remove substrate and they were flash frozen in liquid N_2. Samples were ground using a liquid nitrogen-chilled pestle and mortar, after which RNA was extracted from 100 mg of ground root tissue (RNeasy Plant Mini kit - Qiagen) with an extra sonication step after adding the RLT buffer (3 times 10 seconds) (Ghaemi et al., 2020). After extraction, RNA was washed to improve purity using ethanol-sodium acetate precipitation. Briefly, 20 µL extracted RNA, 3 µL 2 M sodium acetate (Sigma Aldrich) and 50 µL of absolute ethanol (Chemlab) were mixed and stored at -20°C overnight. Samples were centrifuged (Eppendorf-Centrifuge 5417R) for 20 min at 4°C at 19930 g. The supernatant was discarded and 200 µL of 75% absolute ethanol in RNAse free water was added. After centrifuging for 5 minutes at 4°C at full speed and removal of the supernatant, the pellet was dried for 15 min at 37°C. The pellet was redissolved in 20 µL RNAse free water. Quantity and purity were re-assessed using NanoDrop 2000 (ThermoFisher Scientific).

Prior to sequencing of complete mRNA of the samples, an RNA library was prepared using QuantSeq 3' mRNA-Seq Library Prep

TABLE 1 Composition of active ingredients of Product X in weight percentage, mg/L and – if possible – mM.

Active ingredient	Weight %	mg/L	mM	Manufacturer
Geraniol	**22.1**	**450.8**	**2.92**	**Sigma Aldrich – Merck group**
Garlic extract	**3.1**	**63.2**	**NA**	**Shaanxi Senlang Biochemical Co., LTD**
Rosemary extract	**1.4**	**28.6**	**NA**	**Sigma Aldrich – Merck group**
Oil mixture	**20.5**	**418.2**	**NA**	
Linseed oil	**10.3**	**43.1**	**NA**	**Vandeputte Group s.a.**
Sunflower oil	**67.1**	**280.6**	**NA**	**Group Vandamme NV**
Olive oil	**22.6**	**94.5**	**NA**	**Bertolli s.a.**
Salicylic acid	**1.0**	**20.4**	**0.15**	**Sigma Aldrich – Merck group**
Ascorbic acid	**3.1**	**63.2**	**0.36**	**Sigma Aldrich – Merck group**
Chitosan	**2.3**	**46.9**	**NA**	**Qingdao BZ oigo Biotech Co., LTD**

For complex mixtures no molecular weight is known, hence the concentration in mM cannot be calculated (indicated with NA – not available). The oil mixture present in Product X consists of linseed, sunflower and olive oil at a wt% of 10.3, 67.1 and 22.6, respectively. Emulgators and stabilizers used in the final formulation of Product X are not mentioned.

Kit (Lexogen). Library quality was assessed using an Agilent Bioanalyzer 2100. RNA was sequenced using an IlluminaNextSeq 500. Library preparation and sequencing was performed by the NXTGNT facility (Ghent University, Belgium) (Ghaemi et al., 2020).

Analysis of RNA sequencing data starts with quality control of raw reads using FastQC (version 0.11.8) and Trimmomatic softwares (version 0.38; Window size = 4:30). Using STAR software (outFilterMultimapNmax = 1; outSAMtype = BAM SortedByCoordinate), trimmed reads were mapped onto the tomato reference genome (ITAG 4.0). Employing the GenomicAlignments (version 1.36.0) and DESeq2 (version 1.40.2) packages implemented in the Microsoft open R software (version 4.3) for quantifying read numbers (SummarizeOverlaps function) and differential expression analysis (DESeq function), respectively, differentially expressed genes (DEGs) were identified (FDR-adjusted p-value < 0.10). Exploratory data visualization was done via principal component analysis (PCA) using the rlog – for log2 transformation – and ggplot – for plotting – functions (DESeq2 and ggplot2 packages respectively). The volcano plot was produced using the R-package EnhancedVolcano (version 1.18.0). Gene ontology analysis was done using PLAZA 5.0 (Ghaemi et al., 2020) and g:Profiler (Raudvere et al., 2019).

2.7 Hormone measurements

Plants were grown as described above. After growing for two weeks in a soil:sand mixture, roots were treated with 20 mL of a 0.2 v% Product X solution (Supplementary Figure 1D). The control plants were water-treated. Every treatment consisted of 5 pools of tomato plants, with every pool containing material of 4 separate plants. Plants were harvested 24 h, 48 h or 72 h after treatment, and shoots and roots were crushed separately in liquid N_2 until a fine grounded powder was obtained. Phytohormone extraction and analysis was performed according to Haeck et al (Haeck et al., 2018). Therefore, 100 mg of homogenized plant material (5 biological replicates per treatment, each biological replicate consists of 4 individual plants) was weighed in a 12 mL polypropylene tube (Greiner Bio-One International B.V.B.A.), and 5 mL of cold extraction buffer (approximately 4°C) was added. This buffer consisted of 75:20:5 (*v*/*v*/*v*) methanol, ultrapure water, and formic acid (Sigma Aldrich). Thereafter, the sample was vortexed (Kisker Biotech GmbH & Co. KG, via BaseClear Labproducts) for 30 s until all plant material was homogenized into the extraction solvent, after which they were shaken on ice for approximately 1 h. Subsequently, the samples were stored at – 80°C overnight. After the cold extraction, 4 mL of supernatant was transferred to a 30 kDa Amicon® Ultra centrifugal filter unit (Merck Millipore), which was centrifuged for 30 min at 3900 rpm and 4°C in a SW9 R centrifuge (Froilabo). Afterwards, 2.5 mL of the purified extract was dried under N_2 at 10°C by means of a Turbovap® LV automated concentration evaporator (Biotage) in a silanized test tube. The extract was then redissolved with 0.5 mL methanol/water (20:80, *v*/*v*) with 0.1% formic acid, establishing a 5-fold concentration. This final extract was vortexed for 1 min and centrifuged for 2 min at 1000 rpm (EBA20, Andreas Hettich GmbH & Co.KG). The sample was then transferred to a HPLC-vial, and analyzed using an ultra-high performance liquid chromatography system, coupled to a Q-Exactive™ bench top MS/HRMS quadrupole-Orbitrap mass spectrometer, equipped with a heated electrospray ionization (HESI) source, and operating in both the positive or negative mode (Haeck et al., 2018). Xcalibur™ and TraceFinder (version 4.1) software (Thermo Scientific) were used for data processing, targeted plant hormone screening and quantification.

2.8 Peroxidase assay

Plants were grown as described above. After treating tomato roots with 20 mL of 0.2 v% Product X or 20 mL water for negative control plants, plants were harvested at 1, 2 and 3 days after treatment (Supplementary Figure 1E). For 1 day post treatment (dpt), every treatment consisted of 5 pools of tomato plants with every pool containing material of 4 separate plants. For 2 and 3 dpt, every treatment consisted of 10 pools of tomato plants with every pool containing material of 3 separate plants. Plant roots were crushed in liquid N_2 and ground into a fine powder. Based on the protocol of MacAdam et al. (1992), using a photospectral method, 50 mg of crushed material was used to determine peroxidase levels per sample. First, an extraction buffer that consisted of 100 mM potassium buffer (K_2HPO_4 and KH_2PO_4; pH = 6, VWR), 0.8 M KCl (Sigma Aldrich) and 80 mg/mL polyvinylpolypyrrolidone (Sigma Aldrich) was made. Second, the assay buffer consisting of 100 mM potassium phosphate buffer (K_2HPO_4 and KH_2PO_4, pH = 6.0, VWR), 0.4 mM hydrogen peroxide (Sigma Aldrich) and 3.3 mM guaiacol (Sigma Aldrich) was prepared. The sample was suspended in 8 µL extraction buffer/mg sample, vortexed and centrifuged at 19930 g for 10 minutes at 4°C (Eppendorf-Centrifuge 5417R). Further steps were performed on ice. Ten µL of extract was transferred to a cuvette (disposable polystyrene cuvette, VWR) and 990 µL of assay buffer was added. After pipetting and measuring baseline absorbance at 436 nm, absorbance was measured at 30 s intervals for 3 minutes (VWR UV1600P).

Next, the total protein concentration in the sample was evaluated using a Bradford assay. In a 96-well plate, a combination of 20 µL extract and 180 µL of 1:5 diluted Bradford (Sigma Aldrich) reagent was measured at 595 nm after a 30 minute period of incubation at room temperature in the dark. Protein concentration can be calculated as the difference between the absorbance of the sample and the absorbance of the blank divided by 0.0014 (MacAdam et al., 1992). The peroxidase activity was then normalized by the total protein concentration per sample.

2.9 Malondialdehyde measurements

Plants were grown as described above. Every treatment consisted of 5 pools of tomato plants with every pool containing material of 4 separate plants (Supplementary Figure 1D). Plant

material was ground in liquid nitrogen and 100 mg was used for executing malondialdehyde measurements. Ten µL/mg material of cold 5% w/v trichloroacetic acid in distilled water was added to each sample. After briefly vortexing, samples were centrifuged for 15 min at 13 000 rpm and 4°C. The supernatant was divided in 2 aliquots of 250 µL. After making a 2% w/v butylated hydroxytoluene in ethanol solution, 0.01% v/v of this solution was added to 20% w/v trichloroacetic acid in distilled water. 250 µL of this solution was added to one of the aliquots of sample supernatant. To the other aliquot, the same solution was added with the addition of 0.65% w/v thiobarbituric acid. Samples were heated in a hot water bath (95°C) for 30 minutes and then placed on ice to halt the reaction. After centrifuging at 4°C for 10 min, 100 µL of each sample was added to a 96 well plate and the malondialdehyde content was determined using a plate reader at 440, 532 and 600 nm and the formulas listed in Hodges et al (Hodges et al., 1999).

2.10 Long-term administration of Product X

The roots of two infected tomato plants (as described above) were cut and mixed with a potting soil and sand mixture (2:1, v/v). This mixture was moistened with tap water and incubated for 2 days at 25°C. The inoculated soil was treated with 500 mL water or with 500 mL 0.2 v% of Product X (Supplementary Figure 1B). After incubating for another 3 days at 25°C, 5 week old tomato plants were planted in the inoculated and treated soil. Per treatment, 8 plants were used. Plants were treated 7 times with 50 mL Product X or water as a control treatment with 2 week intervals. After 4 months, plants were harvested. The amount of tomatoes was counted, the biomass of plants was measured, and the efficacy of Product X treatment was assessed by scoring root galling using the Zeck scale (Zeck, 1971b). This experiment was independently repeated two times.

2.11 Statistical analysis

All data-analyses (statistical testing and graphical visualization) were done using Microsoft Open R software (version 4.3). Statistical tests were selected from the 'stats' package, while graphics were made using the 'ggplot2' package. P-values lower than 0.05 were regarded as statistically significant. Data-analysis of transcriptome data was already described earlier. Other data were first checked for normality with the Shapiro-Wilk test. Homoscedasticity of the data was checked using diagnostic plots. Both conditions were met for short-term infection experiments testing of Product X, student's t-tests were performed between control and Product X-treated plants. Data of nematicidal assays (*in vitro* testing) of Product X were assessed using a generalized linear binomial model (GLM), combined with a Tukey range test. Differences between all treatments (water-treatment, Product X-treatment and Vertimec-treatment) were evaluated.

Data that did not adhere to normality or homoscedasticity were subjected to non-parametric testing. Data of hormone measurements, peroxidase and MDA-assays and long-term effects on yield were checked for significance by applying a Wilcoxon-Mann-Whitney test. Differences in median between values rendered by control-treated plants and Product X-treated plants were assessed.

3 Results

3.1 Product X has a direct nematicidal effect against root-knot nematodes and protects tomato plants from infection

In vitro nematicidal potential of Product X was tested against *Meloidogyne incognita*. Exposure to Product X leads on average to 70.0 or 82.3% mortality of *M. incognita* after 1 day or 2 days, respectively (p-values < 0.001) (Figure 1A).

Next, the product was tested for its potential as nematicidal product in a pot trial with *Solanum lycopersicum* infected by *M. incognita*. Plant roots were treated with water or Product X, and inoculated with *M. incognita* juveniles 1 or 3 days later (Figure 1B and Supplementary Figure 1, respectively). After one growth cycle of the nematodes (28 days), root galls were counted and root and shoot dry weight were assessed. When inoculation was executed 1 dpt (dpt; Figure 1B), the number of galls per mg dried root tissue was significantly lower compared to water-treated plants (p-value = 0.0063). An average increase of 10% in root dry weight was observed compared to water-treated plants (p-value = 0.044), while the shoot dry weight of Product X-treated plants was not significantly affected (p-value = 0.21). When inoculation was done at 3 dpt (Supplementary Figure 1), a significant reduction in galls per mg of dried root was observed (p = 0.011), while no differences in root and shoot dry weight were detected (p-values = 0.60 and 0.76, respectively).

3.2 Product X induces transcriptional changes related to induced resistance in tomato at one dpt

Product X contains ingredients such as salicylic acid that could potentially elicit induced resistance in treated plants. An mRNA-sequencing experiment was performed to evaluate this hypothesis, by monitoring gene expression in roots at 1 dpt. An exploratory principal component analysis (PCA) (Supplementary Figure 3) clearly separated water-treated and Product X-treated samples. A volcano plot (Figure 2A) reveals the general transcriptional response of all detected tomato genes in response to Product X treatment. Genes were considered as differentially expressed in response to Product X if the Log2FC was below 0.25 or above -0.25 and the adjusted p-values was below 0.10. An overview of all

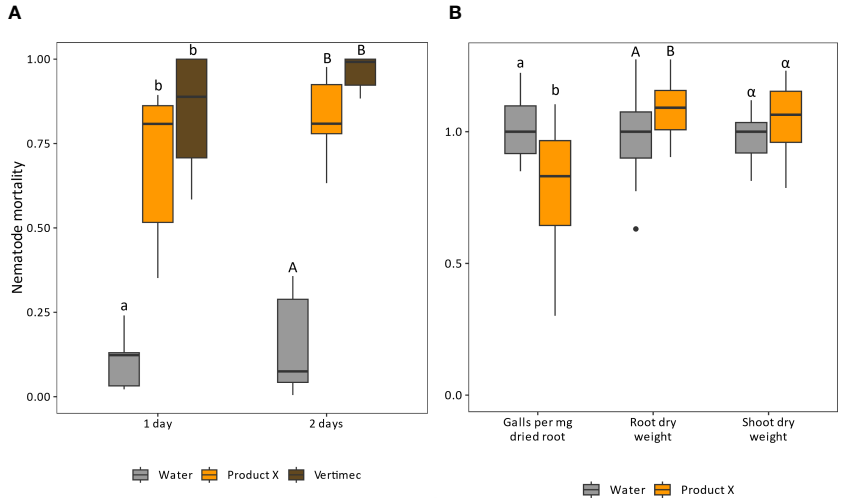

FIGURE 1
(A) Efficacy of Product X as a direct nematicidal agent. Vertimec (commercial formulation of abamectin) was used as a positive control. Product X as well as Vertimec were used at 0.2 v%. Nematode mortality was corrected to the negative control (not shown) using the Schneider-Orelli equation (Schneider-Orelli, 1947). Two independent repeats were performed. (n = 2x6). **(B)** Normalized gall number, root and shoot dry weight of plants inoculated with *M. incognita* at one day post treatment with Product X or water. Two independent repeats were performed. (n=2x8).

DEGs can be found in the Supplementary Information. Gene ontology and KEGG enrichment analyses were performed on up- or downregulated DEGs (significance level of 0.10) using g:Profiler (Figure 2B) (Raudvere et al., 2019). A complete overview of GO-terms in significantly up- and downregulated genes can be found in Supplementary Information (Supplementary Table 1 and Supplementary Figure 4). GO terms such as *Hydrogen peroxide catabolic/metabolic process*, *Response to oxidative stress*, *Reactive oxygen species metabolic process* and *Peroxidase activity* are significantly enriched in the list of highly induced genes,

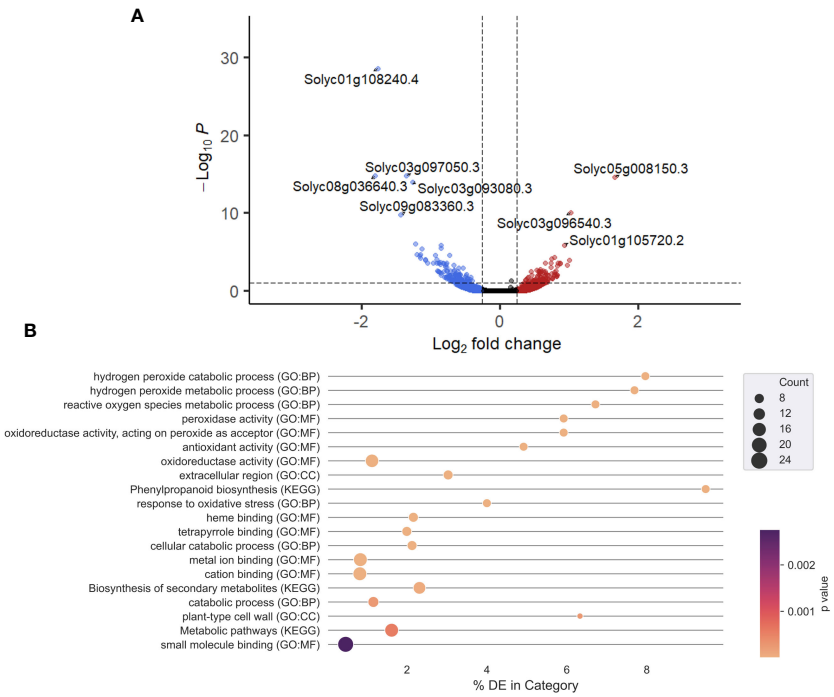

FIGURE 2
(A) Volcano plot of gene expression in roots treated with Product X. Horizontal line indicates threshold of a p-adjusted value higher than 0.10, while vertical lines indicate Log2FC of more than 0.25 (right, red) and lower than -0.25 (left, blue). Every point represents one gene. Upper left quadrant indicates genes with a p-adjusted value < 0.10 and Log2FC < -0.25, while the upper right quadrant indicates genes with a p-adjusted value < 0.10 and Log2FC > 0.25. Genes with the most extreme p-adjusted values are labeled. Their function is described in Table 2. **(B)** GO-analysis of significantly upregulated genes in roots treated with Product X. Top 20 gene ontology terms are displayed. Lighter colors indicate lower p-values, the size of the dots corresponds to the number of genes present in each category.

10.3389/fpls.2024.1411825

indicating that ROS metabolism is significantly altered in roots of Product X-treated tomato plants.

Next, a more in-depth analysis of up- and downregulated genes was performed, focusing on ROS metabolism and phytohormone pathways, well-known hallmarks of induced resistance (De Kesel et al., 2021) (Table 2). Several peroxidase-encoding genes were upregulated, as the GO-analysis already suggested. Most genes associated with phytohormone signaling and/or biosynthesis were downregulated. Interestingly, an abscisic acid 8'-hydroxylase CYP707A2 (*Solyc08g005610.3*) was downregulated, indicating that the abscisic acid (ABA) level in roots treated with Product X might be elevated.

TABLE 2 A selection of differentially expressed genes (DEGs) related to ROS-metabolism and phytohormones.

Gene ID	Function	Log2FC
Solyc08g036640.3	JAZ9	-2.75
Solyc01g108240.4	Ethylene Response Factor D3	-2.05
Solyc09g083360.3	Basic helix-loop-helix protein – DNA binding	-2.02
Solyc04g079730.1	Allene oxide synthase 1	-1.81
Solyc03g097050.3	Cellulose synthase-like protein	-1.59
Solyc03g093080.3	Xyloglucan endotransglucosylase/ hydrolase 9	-1.46
Solyc08g005610.3	Abscisic acid 8'-hydroxylase CYP707A2 (ABA degradation)	-1.33
Solyc03g095770.3	WRKY70	-0.78
Solyc03g122340.3	lipoxygenase D (wound and JA-response)	-0.76
Solyc08g077020.1	Small auxin upregulated RNA 79	-0.69
Solyc05g046010.4	Peroxidase	0.49
Solyc06g051360.3	Gibberellin 2-beta-dioxygenase 1	0.56
Solyc07g047740.3	Peroxidase	0.57
Solyc01g015080.3	Peroxidase	0.58
Solyc02g092580.3	Peroxidase	0.59
Solyc01g108320.3	Peroxidase	0.72
Solyc03g080150.3	Peroxidase	0.76
Solyc02g087070.4	Peroxidase	0.83
Solyc12g005790.2	Peroxidase	1.05
Solyc01g006310.3	Peroxidase	1.06
Solyc01g105720.2	Unknown function	1.12
Solyc03g096540.3	Wound/stress protein	1.17
Solyc05g008150.3	Metallocarboxypeptidase inhibitor	2.27

DEGs were identified by comparing expression in roots of Product X-treated tomato plants versus control plants.
The eight genes with the lowest p-adjusted values were also incorporated based on the Volcano plot (Figure 2A). DEGs were identified based on adjusted p-values < 0.10. Log2FC (Log-2 fold change) value indicates a Log2 transformed change in gene expression of Product X-treated roots versus water-treated roots. Negative values indicate downregulation, while positive values signify upregulation. A complete overview of DEGs can be found in Supplementary Information.

3.3 Phytohormone levels in roots and shoots are altered upon Product X application

Phytohormone measurements were performed at three different timepoints, i.e. at 1, 2 and 3 dpt with Product X or water (negative control) and in both roots and shoots (summarized in Table 3 and in more detail in Supplementary Figures 5–8). For JA a transient decrease over time was observed in roots (p-values = 0.056 and 0.0079, respectively), but not in shoots. Similarly, a strong but transient decrease of SA was observed in root tissue at 1 and 2 dpt with Product X (both p-values = 0.0079), but no differences in shoot tissue. ABA level increased strongly in the roots at 1 and 2 dpt, but decreased after three days (p-values = 0.016, 0.0079 and 0.0079, respectively). In the shoots treated with Product X, an increase in ABA was observed at all three timepoints (p-values = 0.0079, 0.0079 and 0.016, respectively). For IAA, a decrease at 2 and 3 dpt was detected in root tissue (p-values = 0.0079 and 0.016).

3.4 ROS-metabolism is altered by Product X treatment

Based on the sequencing data and the composition of Product X, it was hypothesized that ROS-metabolism could be altered upon Product X treatment. To confirm this hypothesis, peroxidase levels in the roots (Figure 3A) and malondialdehyde (MDA) levels, in the roots (Figure 3B) and shoots (Figure 3C) of treated plants were measured at 1, 2 and 3 day(s) post treatment.

For peroxidase levels in roots, an increase at 1 dpt followed by a decrease at 2 dpt was observed (p-values = 0.055 and 0.0015). However, at 3 dpt, the effect leveled out, and both Product X and water treated plants displayed the same peroxidase activity in the roots (p-value = 0.58).

MDA is a product of lipid peroxidation and is considered as an approximation for endogenous ROS levels and oxidative stress in plants (Morales and Munné-Bosch, 2019). In roots, no significant difference in MDA was detected between Product X-treated and water-treated plants both at 1 and 2 dpt (p-values = 0.28 and 0.34 respectively). However, in shoots, an increase in MDA-levels in Product X-treated plants was observed at 2 dpt (p-value = 0.0079), while this was not the case for 1 dpt (p-value = 1.0). At 3 dpt, no significant changes were observed for both root and shoot MDA content.

3.5 No negative effects on plant growth and yield were observed upon treating plants with Product X throughout their growth season

During prolonged administration (8 times over the course of 4 months) of Product X to tomato plants, no negative but rather positive effects were observed on growth or development (Figure 4). The biomass (shoot weight) and number of tomatoes of treated

10.3389/fpls.2024.1411825

TABLE 3 Summarized overview of fold changes in phytohormone levels in roots and shoots of Product X-treated plants compared to water-treated plants (negative control).

	Root			Shoot		
	1 dpt	2 dpt	3 dpt	1 dpt	2 dpt	3 dpt
JA	0.50	**0.33**	0.67	1.06	0.87	0.92
SA	**0.56**	**0.54**	1.00	0.98	1.30	1.16
ABA	**1.32**	**3.85**	**0.78**	**1.31**	**1.91**	**1.15**
IAA	0.87	**0.78**	**0.70**	NA	NA	1.30

Fold change was calculated as the quotient of medians of phytohormone levels of Product X-treated compared to water-treated material (shoot or root). A fold change > 1 means an increase in phytohormone level in Product X-treated plants versus water-treated plants. Similarly, a fold change < 1 means a decrease. Values in bold indicate a significant difference between medians of phytohormones in Product X-treated and water-treated plants. NA indicates that phytohormone levels were below the limit of detection. Actual hormone levels ($ng.mg^{-1}$ fresh weight) and data visualization in figure format are represented in Supplementary Information (Supplementary Figures 5–8).

plants was significantly increased compared to control plants (p-values of 0.034 and 0.046, respectively). Additionally, Zeck-scale (Zeck, 1971a) evaluation of nematode infestation revealed a decrease of approximately 40% in treated plants compared to untreated plants (p-value = 0.0022). This could possibly explain the increase in biomass and number of tomatoes in treated plants (Figure 4).

4 Discussion and conclusions

4.1 Product X has a direct and indirect effect on *Meloidogyne incognita*

Product X was tested for its direct nematicidal activity against *Meloidogyne incognita*. After 48 h, nematode mortality amounted to over 80% (Figure 1A). Next to that, Product X reduces galling in tomato plants infected by *M. incognita* (Figure 1B and Supplementary Figure 1, Figure 4). Several components included in Product X have previously described *in vitro* and *in vivo* nematicidal properties, namely geraniol, garlic and rosemary extracts, salicylic acid and linseed oil. For every compound, the concentration reported in literature was here converted to the equivalent in mg/L (*between brackets and italics*) to ensure ease of comparison between studies.

First, geraniol was previously reported to be nematicidal against several nematodes and was included in Product X at a concentration of 451 mg/L. Geraniol belongs to the group of monoterpenes, which are produced by plants as secondary metabolites. Monoterpenes contain several well-known compounds such as geraniol, menthol and citral. Geraniol in particular has been attributed antitumor and antidiabetic activities (Lei et al., 2019), as well as broad-spectrum nematicidal activity. Tsao and Yu tested several monoterpenoid compounds against *Pratylenchus penetrans* and found an *in vitro* nematicidal activity of geraniol of 43% at a concentration of 250 µg/mL (*250 mg/L*) (Tsao and Yu, 2000). Antinematode activity against *M. incognita* was evaluated by Echeverrigaray et al. by investigating egg hatching ability and J2 mobility *in vitro*. Both parameters were reduced by more than 90% compared to the control treatment after 48 h, at a concentration of 500 mg/L geraniol (Echeverrigaray et al., 2010). Next to that, geraniol concentrations of 100 and 250 mg/kg substrate (*1996 and 4990 mg/L*, respectively), significantly reduced galling of tomatoes planted in nematode infected and geraniol treated substrate (Echeverrigaray et al., 2010). Similar studies were performed to evaluate the effect on *M. javanica* and *Ditylenchus dipsaci* (Nasiou and Giannakou, 2018; Stavropoulou et al., 2021). After 48 h, no nematode mobility could be observed for *M. javanica* at a geraniol concentration of 500 ppm (*499 mg/L*) (Nasiou and Giannakou, 2018). For *D. dipsaci*, a concentration of 2000 µL/l (*1778 mg/L*) rendered on average 40% nematode immobility after 48 h (Stavropoulou et al., 2021). The concentration of geraniol in Product X is 451 mg/L, which is in the range of other studies reported here. The observed activity is hence in line with other studies.

Second, an extract of garlic is included in Product X at a concentration of 63.2 mg/L. Nematicidal effects of garlic extracts have been reported at different timepoints and concentrations. D'Addabbo et al. found an *in vitro* mortality of 100% for *Xiphinema index* – the California dagger nematode – after 8 h of exposure at a concentration of 0.5 mL/L (*390 mg/L*) Nemguard, a commercially available garlic extract-based nematicide (D'Addabbo et al., 2023). The same concentration leads to 50% reduction of the *X. index* soil population (D'Addabbo et al., 2023). Similarly, a watery extract (10 g FW/100 mL H_2O) of fresh garlic leaves reduces *M. incognita* viability *in vitro* by 22% and in soil by almost 60% (Abo-Elyousr et al., 2009). *M. incognita* galling was reduced by almost 60% under greenhouse conditions when the treatment was applied twice with a 20 day interval (Abo-Elyousr et al., 2009). However, when compared to the results of Abo-Elyousr et al., the *in vitro* effectivity of Product X is higher than that of pure garlic extract (Abo-Elyousr et al., 2009). The nematicidal activity of garlic extract has been attributed to diallyl polysulfide compounds (Block et al., 1993), bio-active molecules that are derived from sulfur-containing amino acids by enzymatic transformation (Block et al., 1993). For example, pure allicin displays 100% mortality against *M. incognita* after 48 h of *in vitro* exposure at a concentration of 12.5 mg/L (Block et al., 1993; Gupta and Sharmaj, 1993). Although similar results have been regularly reported in literature, small differences could be due to differences in concentrations (D'Addabbo et al., 2023), susceptibility of different nematodes (D'Addabbo et al., 2023), application methods (Abo-Elyousr et al., 2009), or the use of a pure active compound versus an extract (Gupta and Sharmaj, 1993).

Third, an essential oil derived from *Salvia rosmarinus* was included in Product X at a concentration of 28.6 mg/L. According to literature, the effect of *S. rosmarinus* is two-fold, i.e. both nematicidal and inducing plant resistance. During a two-year field trial, oil derived from *S. rosmarinus* was observed to protect *Pisum sativum* against *M. javanica* (Mattei et al., 2014), although only in one of the two trials. A concentration of 3% (*27 240 mg/L*) rendered approximately 50% reduction in gall number (Mattei et al., 2014). Essential oil extracted from *S. rosmarinus* at a concentration of 1.5 v

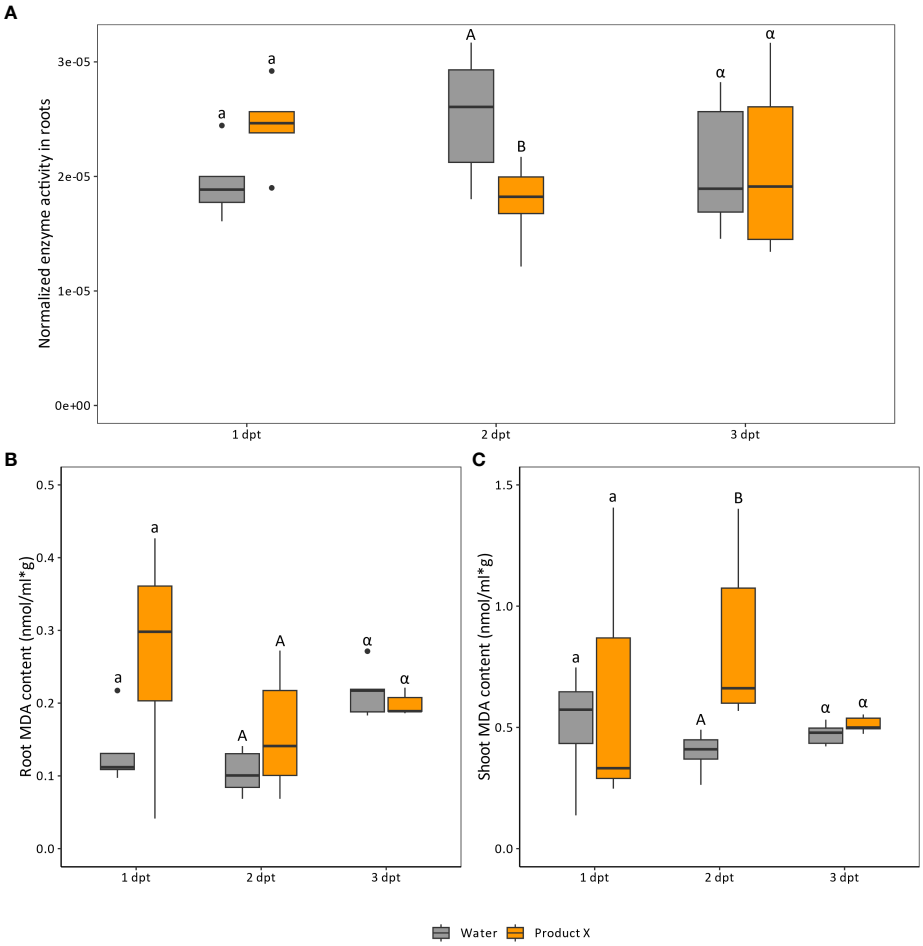

FIGURE 3
(A) Peroxidase levels in root material treated with Product X at one (n=5), two (n=10) and three (n=10) days post treatment. At one dpt 5 pools of 4 plants were used, while at two and three dpt 10 pools of 3 plants were assessed. **(B, C)** MDA content (nmol MDA/(ml*g fresh sample weight) in root **(B)** and shoots **(C)** in water-treated and Product X-treated plants. Water treatment was used as a negative control treatment. Each biological replicate consists of a pool of 4 plants. (n=5). Per timepoint comparisons were made between control and Product X-treated plants. Statistical significance is indicated with a/b for 1 dpt, A/B for 2 dpt and α/β for 3 dpt. Different letters indicate statistical significant comparisons.

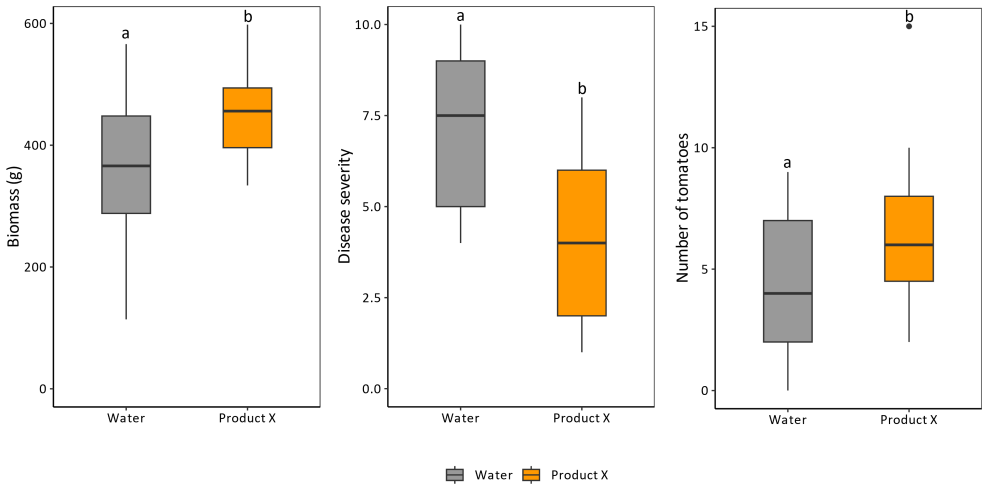

FIGURE 4
Effects of long-term application (8 times over a course of 4 months) of Product X on biomass production, nematode disease severity and number of tomatoes. Disease severity is expressed by the Zeck-scale which is an ordinal scale between 0 and 10, with 0 being no nematode infection (Zeck, 1971a). Two independent repeats were performed. (n = 2x8).

% (*6.81 mg/L*) causes an *in vitro* nematicidal effect of 100% against *Meloidogyne* sp. after 50 h of exposure (Iler-Iler et al., 2017). The first study used a significantly higher amount of *S. rosmarinus* extract than the concentration in Product X, while the latter only tested the *in vitro* effect of the *S. rosmarinus* extract.

A fourth compound present in product X, salicylic acid (SA, 20.4 mg/L), has been reported to have nematicidal properties. *In vitro* SA had an LC50 value of 46 mg/L on *Meloidogyne incognita* (Wuyts et al., 2006). The low pH of this solution (3.0), could partly explain its nematicidal effect. However, the activity of SA as stimulus of induced resistance is well-known (Corina Vlot et al., 2009; Liu et al., 2019; Saleem et al., 2020).

Finally, a concentration of 1 mL/L (*930 mg/L*) linseed oil reduces the nematode population in pepper plants by 36–50% depending on the used cultivar (Eldeeb et al., 2022). Formulated linseed oil was tested against *M. incognita* infecting tomato plants and 26% less galls were observed at a dose of 0.3 mL formulated linseed oil/kg substrate (Radwan et al., 2007). Product X contains 43.1 mg/L linseed oil, which is remarkably lower compared to literature values. The addition of (linseed) oil has a dual function, combining nematicidal activity with positive effects on product stability.

Several components present in Product X have been reported to hold anti-nematode activity *in vitro* and/or *in vivo*. However, all these compounds were tested as standalone treatments in previous studies. This sometimes limits the concentration range in which a product can be used, because of issues of phytotoxicity (Echeverrigaray et al., 2010). Combining different components with similar activities can render an additive effect in the combined mixture, without exceeding phytotoxic concentrations for any individual compound, allowing to work with lower concentrations of active compounds in mixtures versus single molecules. Probably, geraniol, garlic extract, rosemary essential oil and linseed oil contribute to the anti-nematode activity observed in this work (Figure 1A).

4.2 Product X induces transcriptional and biochemical changes in roots and shoots of tomato

To investigate the hypothesis that plant defense mechanisms would be activated upon Product X treatment in tomato, transcriptional analyses linked with biochemical validation were performed.

An mRNA-sequencing experiment was performed on Product X-treated and water-treated plants to assess transcriptional changes. Principal component analysis (PCA) revealed a clear separation between Product X-treated and water-treated tomato plants (Supplementary Figure 3), indicating that transcriptomic changes occur in Product X-treated plants. Gene ontology enrichment analysis revealed significant enrichment of GO-terms related to ROS metabolism among the DEGs (Figure 2B). Appropriately timed and localized ROS bursts play an important role in plant defense (Balmer et al., 2015). Other hallmarks of plant defense activation include altered phytohormone homeostasis, cell wall reinforcement via (often ROS- and peroxidase-dependent) mechanisms such as callose deposition, oxidative cross-linking and lignification (Balmer et al., 2015; Liu et al., 2015, 2018).

Among the DEGs, a large group of genes is related to phytohormone- and ROS-metabolism. Genes related to phytohormones (JA, ethylene (ET), SA and auxin) are generally downregulated. However, an ABA hydroxylase, which is related to ABA degradation, is downregulated (Table 2). This was confirmed by phytohormone measurements in roots, where ABA levels increase at 1 dpt and rise further at 2 dpt with Product X (Table 3). At 3 dpt with Product X, root ABA levels decrease, probably because of a negative feedback mechanism. In shoots, ABA levels increase at all three timepoints (Table 3). Iriti and Faoro showed that ABA plays a role in chitosan-induced resistance against tobacco necrosis virus (Iriti and Faoro, 2008). ABA levels inside the plant increased three-fold upon application of chitosan (Iriti and Faoro, 2008). The observed endogenous ABA increase could be induced by the presence of chitosan in Product X.

ABA is commonly associated with responses to abiotic stress such as drought, salinity and cold (Finkelstein, 2013), but also plays an important but complex role in plant immunity that is highly dependent on concentration, pathosystem and environment (Mauch-Mani and Mauch, 2005). Based on the observed endogenous ABA increases in tomato roots, we hypothesize that Product X can also protect plants from abiotic stresses. Although not studied in this work, this could render new and exciting research opportunities.

Next to that, levels of JA and SA decrease strongly at 1 and 2 dpt in root tissue (Table 3). It has been shown by Nahar et al. that exogenously applied ABA can interfere with JA, SA and ET pathways increasing susceptibility of *Oryza sativa* for *Hirschmanniella oryzae* (Nahar et al., 2012). At 3 dpt, the levels of SA and JA have returned to basal levels in Product X treated roots. In shoots, no differences in JA or SA levels were detected at any time point (Table 3). Similarly, combined foliar application of COS-OGA – chitosan oligomers and pectin-derived oligogalacturonides – has been shown to induce resistance in rice against *Meloidogyne graminicola* independently of JA or SA (Singh et al., 2019). Instead, the phenylpropanoid pathway was a main player in the induced resistance (Singh et al., 2019). This was also the case in tomato where 0.3 mM (*49.8 mg/L*) piperonylic acid induced resistance against *Meloidogyne incognita* via the phenylpropanoid pathway, independent of JA- or SA-levels (Desmedt et al., 2021a). Similarly, the phenylpropanoid pathway may play a role in Product X-treated plants (Figure 2B). *Phenylalanine ammonia-lyase* (PAL) and *Cinnamoyl-COA reductase* encode important enzymes early in the phenylpropanoid pathway and, seeing that these genes are upregulated, this could have downstream effects in the phenylpropanoid pathway.

SA was strongly reduced in roots at 1 and 2 dpt with Product X (Table 3). It is important to note that SA is present in Product X at a concentration of 20.4 mg/L. This hormone has been implicated in several plant physiological processes including but not limited to flowering, disease resistance as well as tolerance to certain abiotic stresses (Corina Vlot et al., 2009; Liu et al., 2019; Rhaman et al., 2021; Barwal et al., 2023). SA plays a major role in Systemic Acquired Resistance (SAR), which is a form of induced resistance (De Kesel et al., 2021). In addition, SA affects the plant antioxidant system by regulating key enzymes such as dehydroascorbate reductase and glutathione reductase (Mustafa et al., 2018; Yan et al., 2018; Saleem et al., 2020). Reduction of SA levels in roots could be caused by a negative feedback loop that is activated because of the presence of SA in Product X.

Indole-3-acetic acid (IAA), the principal auxin, was less abundant in roots at 2 and 3 dpt (Table 3). IAA is elevated locally during nematode infection, and required for successful giant cell development (Oosterbeek et al., 2021). The lower endogenous IAA content in Product X treated roots could hamper nematode infection and/or alter their post-invasion development. Although IAA plays important roles in plant growth and development (Gomes and Scortecci, 2021), tomato plants do not seem to suffer from repeated Product X application, while on the contrary minor positive effects were observed (Figures 1B, 4).

In this work, we observed an upregulation of genes encoding peroxidases in roots treated with Product X (Table 2). The disturbance of ROS homeostasis in treated plants could be linked to the presence of SA and AA, which both act as antioxidants (Cheng et al., 1996). Confirming mRNA-sequencing results, peroxidase levels were increased at 1 dpt in treated roots, while a decrease was observed at 2 dpt. At 3 dpt, levels of treated and untreated roots converged to the same level (Figure 3A). Next to that, MDA content, considered as a proxy for lipid peroxidation and linked to cell wall degradation, was determined in roots and shoots treated with Product X (Figures 3B, C). While no significant difference in MDA levels was observed in roots (Figure 3B), shoots contain significant higher MDA-levels at 2 dpt with Product X (Figure 3C). The lack of strong effect in MDA levels could be due to the presence of both SA and AA as antioxidants. Free ROS could also be used for cell wall modifications by the elevated peroxidase activity. This could explain why even though transcriptional and biochemical changes in peroxidase activity were observed, clear signs of oxidative stress were not observed in the roots of treated plants. Furthermore, it should be taken into account that when MDA levels are measured on complex plant mixtures, interfering agents such as carbohydrates or anthocyanins could be present (Morales and Munné-Bosch, 2019).

4.3 Product X shows no negative effects upon long-term application

Product X influences phytohormone homeostasis – SA and JA – and ROS metabolism which are both considered hallmarks of plant defense (De Kesel et al., 2021). However, influencing and/or activating pathways *in planta* can bring about a certain fitness cost that has a negative effect on plant growth and development (De Kesel et al., 2021). Next to that, geraniol and SA have been reported to cause phytotoxicity when used at high concentrations (>250 mg/kg and 276.24 mg/l respectively) (Echeverrigaray et al., 2010; Tripathi et al., 2019; Koo et al., 2020).

To assess whether this occurs at the concentrations used, Product X was repeatedly applied to infected tomato plants over a prolonged period of time. No negative effect on growth or development could be observed (Figure 4). On the contrary, plant biomass and number of tomatoes increased.

In this research, we demonstrate that Product X has a nematicidal effect on the root-knot nematode *M. incognita*. Next to that, transcriptional and biochemical analyses revealed that Product X influences phytohormone levels and ROS metabolism *in planta*. This suggests that Product X can activate plant defense mechanisms that help protect tomato against *M. incognita*. Furthermore, ABA was strongly induced in Product X-treated plants, with potential benefits for abiotic stress tolerance that should be investigated in future research. This work indicates that there is an additive effect of the compounds in Product X. Finally, no negative long-term effects of repeated product X administration on tomato growth and development were observed. This renders Product X an interesting candidate to be included in IPM strategies to control parasitic nematodes.

Data availability statement

The datasets presented in this study can be found in online repositories. The names of the repository/repositories and accession number(s) can be found below: https://www.ncbi.nlm.nih.gov/, PRJNA1095548.

Author contributions

ED: Conceptualization, Data curation, Formal Analysis, Funding acquisition, Investigation, Methodology, Project administration, Resources, Software, Validation, Visualization, Writing – original draft, Writing – review & editing. CS: Investigation, Writing – review & editing. SP: Conceptualization, Funding acquisition, Investigation, Methodology, Project administration, Resources, Supervision, Writing – review & editing. BS: Software, Writing – review & editing. KD: Investigation, Writing – review & editing. SM: Conceptualization, Funding acquisition, Investigation, Methodology, Project administration, Resources, Supervision, Writing – review & editing. TK: Conceptualization, Funding acquisition, Investigation, Methodology, Project administration, Resources, Supervision, Writing – review & editing.

Funding

The author(s) declare financial support was received for the research, authorship, and/or publication of this article. This project was funded by a VLAIO Baekeland mandate HBC.2020.2877.

Acknowledgments

The authors would like acknowledge Lien Desmet and Patrick De Wispelaere for their technical support during phytohormone analyses.

Conflict of interest

ED is employed by Lima Europe NV. SP, TK, SM, and ED are co-inventors on a European patent DV.A218590 regarding the composition and activity of Product X.

The remaining authors declare that the research was conducted in the absence of any commercial or financial relationships that could be construed as a potential conflict of interest.

The author(s) declared that they were an editorial board member of Frontiers, at the time of submission. This had no impact on the peer review process and the final decision.

Publisher's note

Supplementary material

The Supplementary Material for this article can be found online at: https://www.frontiersin.org/articles/10.3389/fpls.2024.1411825/full#supplementary-material.

References

Abad, P., Gouzy, J., Aury, J. M., Castagnone-Sereno, P., Danchin, E. G. J., Deleury, E., et al. (2008). Genome sequence of the metazoan plant-parasitic nematode Meloidogyne incognita. *Nat. Biotechnol.* 26, 909–915. doi: 10.1038/nbt.1482

Abo-Elyousr, K. A. M., Awad, M. E. M., and Abdel Gaid, M. A. (2009). Management of tomato root-knot nematode meloidogyne incognita by plant extracts and essential oils. *Plant Pathol. J.* 25, 189–192. doi: 10.5423/PPJ.2009.25.2.189

Balmer, A., Pastor, V., Gamir, J., Flors, V., and Mauch-Mani, B. (2015). The "prime-ome": towards a holistic approach to priming. *Trends Plant Sci.* 20, 443–452. doi: 10.1016/J.TPLANTS.2015.04.002

Barwal, S. K., Goutam, C., Chauhan, C., Vimala, Y., AlYemeni, M. N., Ahmad, P., et al. (2023). Salicylic acid alleviates salt-induced phytotoxicity by modulating physiochemical attributes and upregulating the AsA-GSH cycle and glyoxalase system in Capsicum annuum L. seedlings. *South Afr. J. Bot.* 161, 222–237. doi: 10.1016/J.SAJB.2023.07.061

Block, E., Naganathan, S., Putman, D., and Zhao, S. H. (1993). Organosulfur chemistry of garlic and onion: Recent results. *Pure Appl. Chem.* 65, 625–632. doi: 10.1351/PAC199365040625/MACHINEREADABLECITATION/RIS

Chen, J., Li, Q. X., and Song, B. (2020). Chemical nematicides: recent research progress and outlook. *J. Agric. Food Chem.* 68, 12175–12188. doi: 10.1021/acs.jafc.0c02871

Chen, J., and Song, B. (2021). Natural nematicidal active compounds: Recent research progress and outlook. *J. Integr. Agric.* 20, 2015–2031. doi: 10.1016/S2095-3119(21)63617-1

Cheng, I. F., Zhao, C. P., Amolins, A., Galazka, M., and Doneski, L. (1996). A hypothesis for the in *vivo* antioxidant action of salicyclic acid. *BioMetals* 9, 285–290. doi: 10.1007/BF00817929/METRICS

Corina Vlot, A., Dempsey, D. A., and Klessig, D. F. (2009). Salicylic acid, a multifaceted hormone to combat disease. *Ann. Rev. Phytopathol.* 47, 177–206. doi: 10.1146/ANNUREV.PHYTO.050908.135202

D'Addabbo, T., Ladurner, E., and Troccoli, A. (2023). Nematicidal Activity of a Garlic Extract Formulation against the Grapevine Nematode Xiphinema index. *Plants* 12, 1–7. doi: 10.3390/PLANTS12040739

De Kesel, J., Conrath, U., Flors, V., Luna, E., Mageroy, M. H., Mauch-Mani, B., et al. (2021). The induced resistance lexicon: do's and don'ts. *Trends Plant Sci.* 26, 685–691. doi: 10.1016/J.TPLANTS.2021.01.001

Desmedt, W., Jonckheere, W., Nguyen, V. H., Ameye, M., De Zutter, N., De Kock, K., et al. (2021a). The phenylpropanoid pathway inhibitor piperonylic acid induces broad-spectrum pest and disease resistance in plants. *Plant Cell Environ.* 44, 1–18. doi: 10.1111/pce.14119

Desmedt, W., Vanholme, B., and Kyndt, T. (2021b). "Plant defense priming in the field: A review," in *Recent highlights in the discovery and optimization of crop protection products* (Elsevier: Cambridge, Massachusetts, United States), 87–124. doi: 10.1016/B978-0-12-821035-2.00045-0

Dutta, T. K., Papolu, P. K., Banakar, P., Choudhary, D., Sirohi, A., and Rao, U. (2015). Tomato transgenic plants expressing hairpin construct of a nematode protease gene conferred enhanced resistance to root-knot nematodes. *Front. Microbiol.* 6. doi: 10.3389/FMICB.2015.00260/ABSTRACT

Dutta, T. K., and Phani, V. (2023). The pervasive impact of global climate change on plant-nematode interaction continuum. *Front. Plant Sci.* 14. doi: 10.3389/FPLS.2023.1143889/BIBTEX

Echeverrigaray, S., Zacaria, J., and Beltrão, R. (2010). Nematicidal activity of monoterpenoids against the root-knot nematode Meloidogyne incognita. *Phytopathology* 100, 199–203. doi: 10.1094/PHYTO-100-2-0199

Eldeeb, A. M., Farag, A. A. G., Al-Harbi, M. S., Kesba, H., Sayed, S., Elesawy, A. E., et al. (2022). Controlling of Meloidgyne incognita (Tylenchida Heteroderidae) using nematicides, Linum usitatissimum extract and certain organic acids on four peppers cultivars under greenhouse conditions. *Saudi J. Biol. Sci.* 29, 3107–3113. doi: 10.1016/J.SJBS.2022.03.018

European Commission (2019). *What is the european green deal?* doi: 10.2775/97540

European Commission (2020). *A Farm to Fork Strategy for a fair, healthy and environmentally-friendly food system* (Brussels). Available at: https://agridata.ec.europa.eu/Qlik_Downloads/Jobs-Growth-sources.htm.

Finkelstein, R. (2013). Abscisic acid synthesis and response. *Arabidopsis Book* 11, e0166. doi: 10.1199/tab.0166

Ghaemi, R., Pourjam, E., Safaie, N., Verstraeten, B., Mahmoudi, S. B., Mehrabi, R., et al. (2020). Molecular insights into the compatible and incompatible interactions between sugar beet and the beet cyst nematode. *BMC Plant Biol.* 20, 1–16. doi: 10.1186/s12870-020-02706-8

Gomes, G. L. B., and Scortecci, K. C. (2021). Auxin and its role in plant development: structure, signalling, regulation and response mechanisms. *Plant Biol.* 23, 894–904. doi: 10.1111/PLB.13303

Gupta, R., and Sharmaj, N. K. (1993). A study of the nematicidal activity of allicin—an active principle in garlic, Allium sativum L., against root-knot nematode, Meloidogyne incognita (Kofoid and White 1919) chitwood 1949. *Int. J. Pest Manag* 39, 390–392. doi: 10.1080/09670879309371828

Haeck, A., Van Langenhove, H., Harinck, L., Kyndt, T., Gheysen, G., Höfte, M., et al. (2018). Trace analysis of multi-class phytohormones in Oryza sativa using different scan modes in high-resolution Orbitrap mass spectrometry: method validation, concentration levels, and screening in multiple accessions. *Anal. Bioanal Chem.* 410, 4527–4539. doi: 10.1007/s00216-018-1112-9

Hodges, D. M., DeLong, J. M., Forney, C. F., and Prange, R. K. (1999). Improving the thiobarbituric acid-reactive-substances assay for estimating lipid peroxidation in plant

tissues containing anthocyanin and other interfering compounds. *Planta* 207, 604–611. doi: 10.1007/S004250050524/METRICS

Iler-Iler, D., Moreno-Toasa, G., Rodriguez-Maecker, R., and Arancibia, M. (2017). *Thyme and rosemary essential oils as an alternative control of plant-parasitic nematodes* (MDPI AG, Basel, Switzerland). doi: 10.3390/MOL2NET-02-03900

Iriti, M., and Faoro, F. (2008). Abscisic acid is involved in chitosan-induced resistance to tobacco necrosis virus (TNV). *Plant Physiol. Biochem.* 46, 1106–1111. doi: 10.1016/j.plaphy.2008.08.002

Koo, Y. M., Heo, A. Y., and Choi, H. W. (2020). Salicylic acid as a safe plant protector and growth regulator. *Plant Pathol. J.* 36, 1. doi: 10.5423/PPJ.RW.12.2019.0295

Lei, Y., Fu, P., Jun, X., and Cheng, P. (2019). Pharmacological properties of geraniol-A review. *Planta Med.* 85, 48–55. doi: 10.1055/A-0750-6907/BIB

Li, B., Ren, Y., Zhang, D. X., Xu, S., Mu, W., and Liu, F. (2018). Modifying the Formulation of Abamectin to Promote Its Efficacy on Southern Root-Knot Nematode (Meloidogyne incognita) under Blending-of-Soil and Root-Irrigation Conditions. *J. Agric. Food Chem.* 66, 799–805. doi: 10.1021/ACS.JAFC.7B04146/ASSET/IMAGES/LARGE/JF-2017-04146V_0005.JPEG

Liu, J., Li, L., Yuan, F., and Chen, M. (2019). Exogenous salicylic acid improves the germination of Limonium bicolor seeds under salt stress. *Plant Signal Behav.* 14, 1–8. doi: 10.1080/15592324.2019.1644595

Liu, Q., Luo, L., and Zheng, L. (2018). Lignins: biosynthesis and biological functions in plants. *Int. J. Mol. Sci.* 19, 1–16. doi: 10.3390/IJMS19020335

Liu, Q., Zheng, L., He, F., Zhao, F. J., Shen, Z., and Zheng, L. (2015). Transcriptional and physiological analyses identify a regulatory role for hydrogen peroxide in the lignin biosynthesis of copper-stressed rice roots. *Plant Soil* 387, 323–336. doi: 10.1007/S11104-014-2290-7/FIGURES/7

MacAdam, J. W., Nelson, C. J., and Sharp, R. E. (1992). Peroxidase activity in the leaf elongation zone of tall fescue : I. Spatial distribution of ionically bound peroxidase activity in genotypes differing in length of the elongation zone. *Plant Physiol.* 99, 872. doi: 10.1104/PP.99.3.872

Mattei, D., Dias-Arieira, C. R., Biela, F., Roldi, M., Da Silva, T. R. B., Rampim, L., et al. (2014). Essential oil of Rosmarinus officinalis in the control of Meloidogyne javanica and Pratylenchus brachyurus in soybean. *J. Biosci.* 30, 469–476.

Mauch-Mani, B., and Mauch, F. (2005). The role of abscisic acid in plant-pathogen interactions. *Curr. Opin. Plant Biol.* 8, 409–414. doi: 10.1016/j.pbi.2005.05.015

Mauch-Mani, B., Pozo, M. J., Martinez-medina, A., Flors, V., Heil, M., Pieterse, C. M. J., et al. (2016). Recognizing plant defense priming. *Trends Plant Sci.* 21, 818–822. doi: 10.1016/j.tplants.2016.07.009

Melillo, M. T., Leonetti, P., and Veronico, P. (2014). Benzothiadiazole effect in the compatible tomato-Meloidogyne incognita interaction: changes in giant cell development and priming of two root anionic peroxidases. *Planta* 240, 841–854. doi: 10.1007/S00425-014-2138-7/FIGURES/7

Milligan, S. B., Bodeau, J., Yaghoobi, J., Kaloshian, I., Zabel, P., and Williamson, V. M. (1998). The root knot nematode resistance gene Mi from tomato is a member of the leucine zipper, nucleotide binding, leucine-rich repeat family of plant genes. *Plant Cell* 10, 1307–1319. doi: 10.1105/TPC.10.8.1307

Morales, M., and Munné-Bosch, S. (2019). Malondialdehyde: facts and artifacts. *Plant Physiol.* 180, 1246–1250. doi: 10.1104/PP.19.00405

Mustafa, M. A., Ali, A., Seymour, G., and Tucker, G. (2018). Treatment of dragonfruit (Hylocereus polyrhizus) with salicylic acid and methyl jasmonate improves postharvest physico-chemical properties and antioxidant activity during cold storage. *Sci. Hortic.* 231, 89–96. doi: 10.1016/J.SCIENTA.2017.09.041

Nahar, K., Kyndt, T., Nzogela, Y. B., and Gheysen, G. (2012). Abscisic acid interacts antagonistically with classical defense pathways in rice-migratory nematode interaction. *New Phytol.* 196, 901–913. doi: 10.1111/j.1469-8137.2012.04310.x

Nasiou, E., and Giannakou, I. O. (2018). Effect of geraniol, a plant-based alcohol monoterpene oil, against Meloidogyne javanica. *Eur. J. Plant Pathol.* 152, 701–710. doi: 10.1007/s10658-018-1512-x

Ntalli, N. G., and Caboni, P. (2012). Botanical nematicides: A review. *J. Agric. Food Chem.* 60, 9929–9940. doi: 10.1021/JF303107J/ASSET/IMAGES/LARGE/JF-2012-03107J_0001.JPEG

Oosterbeek, M., Lozano-Torres, J. L., Bakker, J., and Goverse, A. (2021). Sedentary plant-parasitic nematodes alter auxin homeostasis via multiple strategies. *Front. Plant Sci.* 12. doi: 10.3389/FPLS.2021.668548/FULL

Radwan, M. A., Kassem, S. M. I., Abu-Elamayem, M. M., and El-Maadawy, E. K. (2007). Use of some emulsified plant seed oils as a safe alternative for the management of Meloidogyne incognita infecting tomato. *Arch. Phytopathol. Plant Prot.* 40, 345–352. doi: 10.1080/03235400600587607

Raudvere, U., Kolberg, L., Kuzmin, I., Arak, T., Adler, P., Peterson, H., et al. (2019). g: Profiler: a web server for functional enrichment analysis and conversions of gene lists, (2019 update). *Nucleic Acids Res.* 47, W191–W198. doi: 10.1093/NAR/GKZ369

Rhaman, M. S., Imran, S., Rauf, F., Khatun, M., Baskin, C. C., Murata, Y., et al. (2021). Seed priming with phytohormones: An effective approach for the mitigation of abiotic stress. *Plants* 10, 1–17. doi: 10.3390/PLANTS10010037

Saleem, M., Fariduddin, Q., and Janda, T. (2020). Multifaceted role of salicylic acid in combating cold stress in plants: A review. *J. Plant Growth Regul.* 40, 464–485. doi: 10.1007/S00344-020-10152-X

Schneider-Orelli, O. (1947). *Entomologisches praktikum. 2nd Edn* (Aarau: Sauerlaünder).

Singh, R. R., Chinnasri, B., De Smet, L., Haeck, A., Demeestere, K., Van Cutsem, P., et al. (2019). Systemic defense activation by COS-OGA in rice against root-knot nematodes depends on stimulation of the phenylpropanoid pathway. *Plant Physiol. Biochem.* 142, 202–210. doi: 10.1016/J.PLAPHY.2019.07.003

Stavropoulou, E., Nasiou, E., Skiada, P., and Giannakou, I. O. (2021). Effects of four terpenes on the mortality of Ditylenchus dipsaci (Kühn) Filipjev. *Eur. J. Plant Pathol.* 160, 137–146. doi: 10.1007/s10658-021-02229-4

Talavera-Rubia, M., Dolores Vela-Delgado, M., and Verdejo-Lucas, S. (2022). A cost-benefit analysis of soil disinfestation methods against root-knot nematodes in mediterranean intensive horticulture. *Plants* 11, 1–11. doi: 10.3390/plants11202774

Tripathi, D., Raikhy, G., and Kumar, D. (2019). Chemical elicitors of systemic acquired resistance—Salicylic acid and its functional analogs. *Curr. Plant Biol.* 17, 48–59. doi: 10.1016/j.cpb.2019.03.002

Tsao, R., and Yu, Q. (2000). Nematicidal activity of monoterpenoid compounds against economically important nematodes in agriculture. *J. Essential Oil Res.* 12, 350–354. doi: 10.1080/10412905.2000.9699533

Whitehead, A. G., and Hemming, J. R. (1965). A comparison of some quantitative methods of extracting small vermiform nematodes from soil. *Ann. Appl. Biol.* 55, 25–38. doi: 10.1111/J.1744-7348.1965.TB07864.X

Wuyts, N., Swennen, R., and De Waele, D. (2006). Effects of plant phenylpropanoid pathway products and selected terpenoids and alkaloids on the behaviour of the plant-parasitic nematodes Radopholus similis, Pratylenchus penetrans and Meloidogyne incognita. *Nematology* 8, 89–101. doi: 10.1163/156854106776179953

Yan, Y., Pan, C., Du, Y., Li, D., and Liu, W. (2018). Exogenous salicylic acid regulates reactive oxygen species metabolism and ascorbate–glutathione cycle in Nitraria tangutorum Bobr. under salinity stress. *Physiol. Mol. Biol. Plants* 24, 577–589. doi: 10.1007/S12298-018-0540-5/FIGURES/5

Zeck, W. M. (1971a). A rating scheme for field evaluation of root-knot nematode infestations. *Pflanzenschutz-Nachrichten Bayer* 24, 141–144.

Zeck, W. M. (1971b). Ein Bonitierungsschema zur Feldauswertung von Wurzelgallenbefall. *Pflanzenschutz - Nachrichten Bayer* 24, 144–147.

frontiers | Frontiers in Plant Science

TYPE Original Research
PUBLISHED 23 August 2024
DOI 10.3389/fpls.2024.1425336

OPEN ACCESS

EDITED BY
Mario Massayuki Inomoto,
University of São Paulo, Brazil

REVIEWED BY
Renê Gonçalves Da Silva Carneiro,
Universidade Federal de Goiás, Brazil
Pedro Confort,
University of São Paulo, Brazil

*CORRESPONDENCE
Sheila F. de Almeida
sheilafreitas92@hotmail.com
Regina M. D. G. Carneiro
regina.carneiro@embrapa.br

RECEIVED 29 April 2024
ACCEPTED 09 July 2024
PUBLISHED 23 August 2024

CITATION
Gabriel M, Santos MFA, Mattos VS, Gomes ACMM, de Almeida SF, Castagnone-Sereno P, Boiteux LS, Cares JE and Carneiro RMDG (2024) Comparative histopathology of virulent and avirulent *Meloidogyne javanica* populations on susceptible and resistant tomato plants. *Front. Plant Sci.* 15:1425336. doi: 10.3389/fpls.2024.1425336

Comparative histopathology of virulent and avirulent *Meloidogyne javanica* populations on susceptible and resistant tomato plants

Márcia Gabriel[1,2], Marcilene F. A. Santos[2], Vanessa S. Mattos[2], Ana Cristina M. M. Gomes[2], Sheila F. de Almeida[2,3]*, Philippe Castagnone-Sereno[4], Leonardo S. Boiteux[5], Juvenil E. Cares[3] and Regina M. D. G. Carneiro[2]*

[1]Universidade Federal de Santa Maria, Santa Maria–RS, Dep. de Agronomia, Brazil, [2]Embrapa Recursos Genéticos e Biotecnologia (Cenargen), Brasília, Brazil, [3]Universidade de Brasília, Dep. de Fitopatologia, Brasília, DF, Brazil, [4]INRAE, Université Côte d'Azur, CNRS, ISA, Sophia Antipolis, France, [5]Embrapa Hortaliças (CNPH), Brasília, Brazil

The *Mi*-1.2 gene confers resistance to a wide range of *Meloidogyne* species, being the most important resistance factor employed in tomato breeding so far. However, many aspects related to the interaction of *Mi*-1.2-carrying tomato cultivars and virulent/avirulent *Meloidogyne* populations have not yet been clarified. Herein, comparative histopathological analyses were carried after inoculation of the homozygous (*Mi*-1.2/*Mi*-1.2) tomato rootstock 'Guardião' and the susceptible cultivar 'Santa Clara' (*mi*-1.2/*mi*-1.2) with virulent and avirulent populations of *M. javanica.* In the susceptible control, it was possible to visualize second stage juveniles (J2) of avirulent population and feeding sites from 2 to 30 days after infection (DAI) with females reaching maturity at 24-34 DAI. In the resistant rootstock, the *Mi*-1.2 gene-mediated resistance was related mainly to early defense responses (pre-infection and hypersensitive reaction), which led to an immunity-like phenotype that completely prevented the reproduction of the avirulent *Meloidogyne* population. On the other hand, J2s of the virulent *M. javanica* population were able to penetrate roots much more than the avirulent population, migrated and developed normally, showing intense and similar pattern of penetration from 4 to 34 DAI in the root tissues of both resistant and susceptible tomato genotypes. The total numbers of J2, J3, J4, and females counted in 'Santa Clara' for the virulent population of *M. javanica* were higher than in 'Guardião'.

KEYWORDS

***Solanum lycopersicum*, *S. peruvianum*, Mi-1.2 gene, hypersensitivity reaction. HR : realce, root-knot nematode**

Introduction

The root-knot nematodes (RKN), genus *Meloidogyne* Göldi, 1887 have a cosmopolitan distribution, inducing severe damages in a wide range of economically important host plants (Maleita et al., 2011). In several crops, including Solanaceae species, the problems induced by *Meloidogyne* species can be controlled through resistance genes (Williamson and Kumar, 2006; Fuller et al., 2008). Resistance to RKNs in tomato is conferred by a single dominant gene, *Mi*-1.2, located on chromosome 6, which originated from the wild tomato species *Solanum peruvianum* L (Smith, 1944). The *Mi*-1.2 gene confers resistance against populations of 13 *Meloidogyne* species occurring in Brazil: *M. javanica* (Treub, 1885) Chitwood, 1949, *M. incognita* (Kofoid & White, 1919) Chitwood, 1949, *M. arenaria* (Neal, 1889) Chitwood, 1949, *M. morocciensis* Rammah & Hirschmann, 1990, *M. ethiopica* Whitehead, 1968, *M. inornata* Lordello, 1956, *M. luci* Maleita, Esteves, Cardoso, Cunha, Carneiro & Abrantes, 2018, *M. konaensis* Eisenback, Bernard & Schmitt, 1994, *M. paranaensis* Carneiro, Carneiro, Abrantes, Santos & Almeida, *M. izalcoensis* Carneiro, Almeida, Gomes & Hernandez, 2005, *M. petuniae* Charchar, Eisenback & Hirschmann, 1999 and *M. exigua* Göldi, 1887 (Gabriel et al., 2020).

RKNs induce substantial modifications of root ultrastructure and morphology, resulting in the formation of giant cells and galls (Huang and Maggenti, 1969). By blocking nematode development in the roots, the *Mi*-1.2 gene prevents these disturbances. However, in a few specific situations, the gene may lose its effectiveness. In particular, at continuous soil temperatures above 28°C (Holzmann, 1965), or when virulent populations are present (Castagnone-Sereno et al., 1994a; Roberts, 1995; Ornat et al., 2001; Devran and Söğüt, 2010). Furthermore, the heterozygous *versus* homozygous allelic state (allelic dosage) of the *Mi*-1.2 gene was shown to reduce the level of resistance expression (Jacquet et al., 2005; Maleita et al., 2011; Iberkleid et al., 2014; Gabriel et al., 2024). The mechanisms of plant resistance to nematodes can occur during pre-penetration or post-penetration. Pre-penetration resistance mechanisms prevent the invasion of plant roots by the nematodes. During this phase, the production of chemical substances in root exudates inhibits nematode attraction, or the reinforcement of physical barriers via the accumulation of cell wall–strengthening compounds such as lignin and callose (Mitsumasu et al., 2015) block nematode entry in root tissues. In the post-penetration resistance mechanisms, the invasion of J2s triggers a cascade of both local and systemic physiological and molecular processes in the host plant, including increased calcium flux, a burst of reactive oxygen species and defence gene expression (Williamson and Kumar, 2006; Sato et al., 2019; Rutter et al., 2022). These mechanisms act to impede or delay the migration or development of the nematode, thereby inhibiting the formation of feeding sites and/or limiting the reproduction of females.

The reproduction of *Meloidogyne* spp. virulent populations in resistant tomato cultivars bearing the *Mi*-1.2 gene has been reported across several countries, leading to a limitation of this strategy of control. Such nematode populations can be naturally virulent, that is, without the selection pressure exerted by previous exposure to a resistant cultivar (Ornat et al., 2001; Silva et al., 2019; Gabriel et al., 2022), or after repeated exposure to resistant cultivars in the field (Devran and Söğüt, 2010; Tzortzakakis et al., 2014; Gabriel et al., 2022) or under controlled conditions (Castagnone-Sereno et al., 1994b; Williamson, 1998).

Some resistance mechanisms have been observed in plants parasitized by RKNs, including the hypersensitive reaction (HR) due to the accumulation of phenolic compounds and the formation of phytoalexins and the activity of phenylalanine ammonia-lyase (PAL) related enzymes, *b*-glucanase, peroxidase, and polyphenol oxidase, among others (Sato et al., 2019). This is the case of tomato plants carrying the *Mi*-1.2 gene, where the primary resistance mechanism takes place in the first days after nematode infection, triggering the HR and working as a biochemical barrier blocking the development of second-stage juveniles (J2s) (Dropkin, 1969; Schaff et al., 2007). To the best of our knowledge, most of the information available on the histological features associated to the breaking of tomato resistance by RKN relate to the species *M. incognita.* The objective of the present study was to provide and analyse comparative data on nematode infection and the plant anatomical responses induced by avirulent and virulent populations using the tomato/*M. javanica* pathosystem. For that purpose, we developed two complementary experimental approaches: (*i*) the quantification of nematode penetration and development of avirulent and virulent *M. javanica* populations inoculated to susceptible and resistant tomato plants; (*ii*) the analysis of the histopathological changes associated with infection by avirulent and virulent populations of *M. javanica* into resistant and susceptible tomato cultivars.

Materials and methods

Nematode populations

Two populations of *M. javanica* sampled on tomatoes in Brazil were used in the study, one virulent to the *Mi*-1.2 gene from Frederico Westphalen, RS (27° 21' 32'' S/53° 23' 38'' O, cv.'Guardião') and the other avirulent from Rodeio Bonito, RS (27° 28' 15'' S/53° 10' 08'' O, cv. Kada). They were previously identified by esterase phenotype Est J3 by Gabriel et al. (2022) and confirmed using the same enzymatic characterization, according to the methodology described by Carneiro and Almeida (2001).

Plant material

The susceptible tomato (*Solanum lycopersicum* L.) cv. 'Santa Clara'(*mi*-1.2/*mi*-1.2) and the resistant rootstock cv. 'Guardião (*Mi*-1.2/*Mi*-1.2), homozygous for the *Mi-1.2* gene were studied previously (Gabriel et al., 2022) and used in the experiments. Seeds were purchased at Vegetal AgroNegócio in Brasília, DF.

Inoculum preparation

The nematode populations were multiplied on cv. 'Santa Clara' and kept in a greenhouse under temperatures ranging from 23 °C to

28 °C. The suspension of eggs from each population was obtained according to the methodology of Hussey and Barker (1973) by grinding the roots in a blender with 0.5% sodium hypochlorite for approximately 30 seconds. The juveniles used as inocula in histopathological studies were obtained by hatching of nematode eggs in modified Baermann funnels collected for one week under 25° C (Flegg, 1967). The inoculum is counted using a Peter's slide and calibrated with dilutions.

Quantification of nematode penetration and development

Experiments were conducted in a greenhouse under temperatures ranging from 24 to 28°C in 2 L pots, using fine sand texture. The substrate was sterilized using autoclave at 120°C for 2 hours. To study the penetration and development of the two nematode populations inside the roots of the susceptible and resistant cv. 'Santa Clara' and 'Guardião', respectively. Tomato plants were cultivated in pots containing sterilized sand and fertilized with Forth Cote (15-09-12). Fifteen days after emergence, the seedlings were inoculated with the two populations separately. For this, 10,000 second-stage juveniles (J2s) were placed in four holes close to the stem of each plant, 2,500 in each hole. Plants of each cultivar (three replicates) were carefully removed from the pots at 2, 4, 7, 9, 11, 13, 16, 21, 27, and 34 days after inoculation (DAI). Their roots were carefully washed with tap water and stained with acid fuchsin, as described by Byrd et al. (1983). Subsequently, 40 stained root segments were cut under a stereomicroscope to observe and quantify the penetration and localization of J2s and to follow the subsequent development of the nematodes inside of the the roots (J3, J4, females and males). Root fragments showing infection by nematodes were mounted on slides for examination under an optical microscope and photographed (AxioPhot; Zeiss). The statistical analyses of the two experiment were performed using the SISVAR system, for each sample, the number of individuals was transformed to $\sqrt{(x+1)}$ to normalize data and, after analysis of variance, the means were compared using Scott–Knott's test at the 5% probability level (Scott and Knott, 1974).

Histopathological studies

In parallel, three other root systems of each combination nematode population/tomato cultivar were sliced in thin sections of 2.5µm using a Leica ultracut UCT. Unstained root fragments, either showing galls or thickening or without symptoms were cut under a stereomicroscope. Approximately 60 root tips per DAI were analyzed at different times per treatment, and then fixed and embedded in Technovit 7100 epoxy resin (Kulzer Friedrichsdorf), as described by Pegard et al. (2005), and following manufacturer's recommendations. Unstained root sections were mounted on glass slides, and fluorescence was observed under ultraviolet (UV) light, using a filter of 365-395 nm. The same sections were stained (1 min. at 60°C) with 0.5% toluidine blue in 0.1 M sodium phosphate buffer, pH 5.5, and observed using alight microscopy (AxioPhot, Zeiss). More than 5,000 sections of each treatment were visualized and documented.

Results

Avirulent *Meloidogyne javanica*

Inoculation with the avirulent *M. javanica* population confirmed the host status of both tomato genotypes: nematodes could massively invade and develop in the roots of the susceptible cv. 'Santa Clara', while their penetration and further development were almost totally impaired in the roots of the resistant cv. 'Guardião' ($P \leq 0.05$; Table 1). Very few J2 were observed in the roots of the resistant cultivar (two and three at 4 and 7 DAI, respectively), and no other developmental stages could be detected, excepted three females without egg-masses at 34 DAI (Table 1). In the susceptible cultivar, the major steps of nematode development kinetics were observed as follows: J2 from 4 to 16 DAI; J3 from 11 to

TABLE 1 Number of second-stage juveniles (J2) penetration and development of third (J3) and fourth (J4) nematode stages, of avirulent *Meloidogyne javanica* population in 40 sections of three tomato roots repetitions of the cultivar 'Santa Clara' and rootstock 'Guardião' inoculated with 10,000 J2.

		4° DAI*	7° DAI	9° DAI	11° DAI	13° DAI	16° DAI	24° DAI	34° DAI	Nema-todes **
J2	Guardião	2	3	0	0	0	0	0	0	5 b
	S. Clara	96	259	274	123	55	31	1	1	840 a
J3	Guardião	0	0	0	0	0	0	0	0	0 b
	S. Clara	0	0	0	229	192	56	50	16	543 a
J4	Guardião	0	0	0	0	0	0	0	0	0 b
	S. Clara	0	0	0	6	154	383	147	156	846 a
Females without egg mass	Guardião	0	0	0	0	0	0	3	0	3 b
	S. Clara	0	0	0	0	0	0	498	445	943 a

(Continued)

10.3389/fpls.2024.1425336

TABLE 1 Continued

		4° DAI*	7° DAI	9° DAI	11° DAI	13° DAI	16° DAI	24° DAI	34° DAI	Nematodes **
Females laying eggs	Guardião	0	0	0	0	0	0	0	0	0 b
	S. Clara	0	0	0	0	0	0	0	63	63 a
Male	Guardião	0	0	0	0	0	0	0	0	0
	S. Clara	0	0	0	0	0	0	0	0	0

* DAI: Days after J2 inoculation; ** Means of total nematodes followed by the same lowercase letter for different RKN stages in the column do not differ statistically from each other according to the Scott-Knott test at 5% probability ($P \leq 0.05$). Cv = 28.1 (virulent population) and Cv = 26.4 (avirulent population).

34 DAI; J4 from 13 to 34 DAI; females without egg-masses from 24 to 34 DAI and females starting to lay eggs at 34 DAI, respectively (Table 1). No males were observed in the roots of either the susceptible or the resistant tomatoes 'Santa Clara' and 'Guardião', respectively.

Observation of the roots of the susceptible cv. 'Santa Clara' stained with acid fuchsin at 4–16 DAI revealed the presence of numerous J2 (Figure 1A) in the cortical region with some of them in the vascular cylinder (a location compatible with the initiation of feeding sites) (Figures 1A, B). Light microscopic observations of

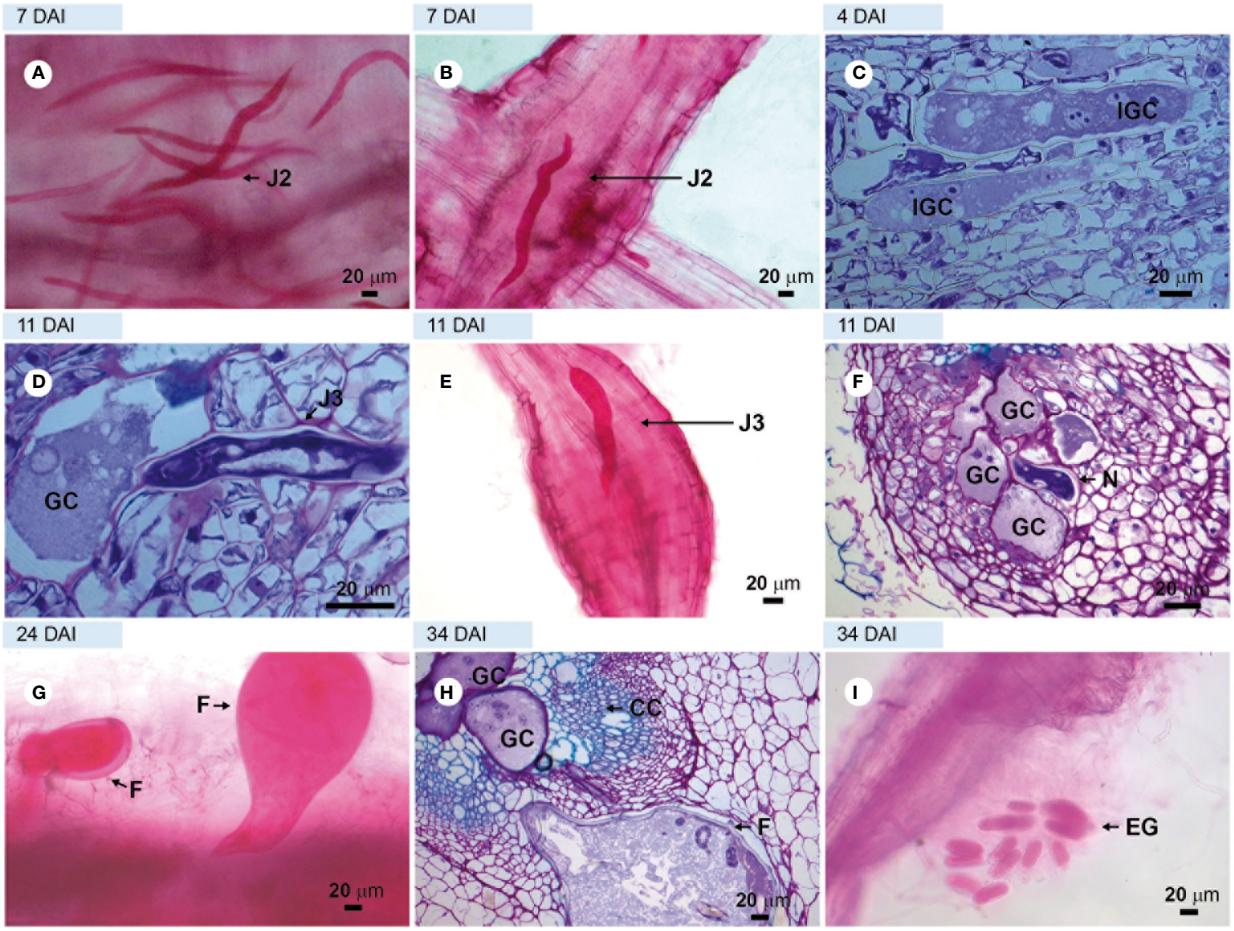

FIGURE 1
Compatible interaction observed in the susceptible tomato plant. Roots of cv. Santa Clara (control) infected with avirulent *Meloidogyne javanica*. **(A, B, E, G, I)** in light microscopy (LM) observations of root fragments stained with acid fuchsin. Sections **(C, D, F)**; and H = roots stained with toluidine blue. **(A)** = second-stage juveniles (J2s) in the cortex and vascular cylinder, and **(B)** = swollen J2s into vascular cylinder. **(C)** = sections showing the beginning of giant cell formation at 4 DAI; **(D)** = third-stage juvenile (J3) next to giant cells; **(E)** = third-stage juvenile (J3) in the vascular cylinder and root enlargement; **(F)** = giant cells formed next to J4; **(G)** = young females; **(H)** = adult female and giant cells with multiple nucleus and thick cell wall and **(I)** = egg mass at 34 DAI. DAI, days after inoculation; N, nematode; GC, giant cell; IGC, initial giant cell; EG, egg mass; YF, young female; CC, vascular cylinder.

root sections stained with toluidine blue at 4 DAI confirmed this time point as the beginning of giant cell formation in the vascular tissue, as observed in longitudinal sections (Figure 1C). At 11 DAI, giant cells were observed next to third-stage juveniles (J3; Figure 1D), along with root enlargement (Figure 1E), and next to fourth-stage juveniles (J4), with cell wall thickening noticed between giant cells (Figure 1F). At 24 DAI, young females were clearly visible in acid fuchsin stained tissues (Figure 1G) and at 34 DAI, adult females were observed next to multinucleate giant cells in the vascular cylinder, together with egg-masses extruded outside the root (Figures 1H, I respectively), thus completing the nematode life cycle.

The roots of the highly resistant rootstock cv. 'Guardião', stained with acid fuchsin, showed that very few avirulent *M. javanica* J2 could penetrate the roots at 4–7 DAI (Figure 2A). Through sections visualized under ultraviolet light (UV), obtained at 7 DAI, it was possible to observe a hypersensitive reaction (HR) at several locations in the cortical region: epidermis, parenchymatous cortex (Figures 2B, C) close to the vascular cylinder. When stained with toluidine blue, these sections appeared strongly stained at the same sites (Figure 2D), a signal characteristic of cell death. Despite numerous observations from 4 to 34 DAI, it was not possible to detect any other nematode stages within the vascular cylinder cells in the root tissues of the resistant rootstock, suggesting an early resistance mechanism closely related to immunity.

Virulent *Meloidogyne javanica*

As expected, the *M. javanica* virulent population was able to infect, develop and reproduce on the resistant rootstock cv. 'Guardião', as well as on the susceptible cv. 'Santa Clara'. After staining the roots with acid fuchsin, monitoring of inoculations revealed identical development kinetics on both cultivars ($P \leq 0.05$; Table 2), and very similar to that previously observed for the avirulent population on the susceptible cultivar (Table 1). In terms of nematodes counted in the roots, significantly higher cumulative numbers of individuals were found in the susceptible cv. 'Santa Clara' compared with the resistant cv. 'Guardião' for the J2, J3 and female with egg mass stages, and equivalent numbers for the other developmental stages ($P \leq 0.05$; Table 2). Some males were observed on both cv. from 21 to 27 DAI.

Examinations of roots and root sections of the susceptible cv. 'Santa Clara' and the resistant cv. 'Guardião' stained with acid fuchsin showed that the virulent nematode population was equally able to penetrate roots and complete its development cycle up to the production of egg-masses by adult females on both cultivars. (Figures 3A, C, D, F, H, I and Figures 4A, C, F, G, respectively). The only notable difference was the presence of numerous males on 'Guardião' at 27 DAI. Males were observed releasing themselves from J4 cuticles inside the roots at 34 DAI (Figures 4H, I).

Histological observations revealed numerous feeding sites in both the susceptible and the resistant cultivars, with the formation

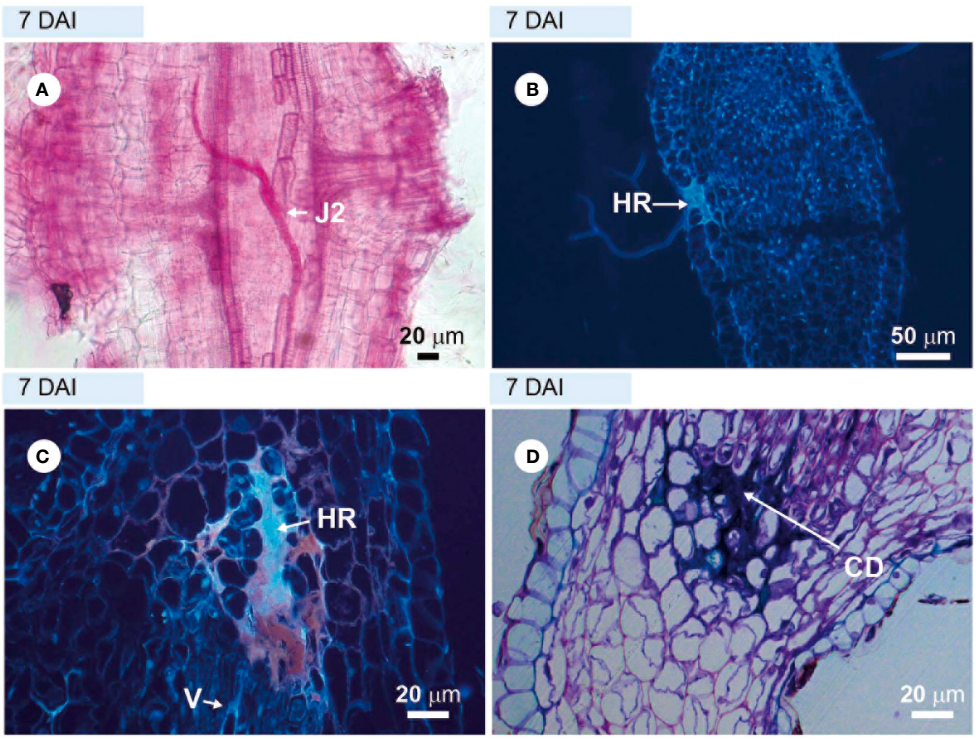

FIGURE 2
Incompatible interaction observed in roots of the resistant hybrid tomato plant 'Guardião' infected with avirulent *Meloidogyne javanica*. **(A)** = light microscopy observations of root fragment stained with acid fuchsin. **(B, C)** = unstained sections visualized under UV light; **(D)** = section stained with toluidine blue, showing cell death (CD). **(A)** = second-stage juvenile (J2) inside the root; **(B)** and **(C)** = hypersensitivity reaction (HR). DAI, days after inoculation; V, vessel.

10.3389/fpls.2024.1425336

TABLE 2 Number of second-stage juveniles (J2) penetration and development of third (J3) and fourth (J4) nematode stages, of virulent *Meloidogyne javanica* population in 40 sections of three tomato roots repetitions of the cultivar 'Santa Clara' and rootstock 'Guardião' inoculated with 10,000 J2.

		2°	4°	7°	9°	11°	13°	16°	21°	27°	34°	Nematodes
		DAI	DAI	DAI	DAI	DAI	DAI	DAI	DAI	DAI	DAI	**
J2	Guardião	2	253	444	322	134	65	21	1	3	10	1255 b
	S. Clara	4	374	540	424	236	110	6	3	8	34	1739 a
J3	Guardião	0	0	0	8	410	379	258	116	21	10	1202 b
	S. Clara	0	0	0	4	463	417	335	149	26	21	1415 a
J4	Guardião	0	0	0	0	4	199	389	187	116	14	909 a
	S. Clara	0	0	0	0	2	230	434	286	52	10	1014 a
Females without egg mass	Guardião	0	0	0	0	0	2	205	317	428	116	1068 a
	S. Clara	0	0	0	0	0	0	305	382	365	56	1108 a
Females laying eggs	Guardião	0	0	0	0	0	0	0	0	481	576	1057 b
	S. Clara	0	0	0	0	0	0	0	0	608	830	1438 a
Male	Guardião	0	0	0	0	0	0	0	0	9	64	73
	S. Clara	0	0	0	0	0	0	0	9	14	8	31

*DAI, Days after J2 inoculation; ** Means of total nematodes followed by the same lowercase letter for different RKN stages in the column do not differ statistically from each other according to the Scott-Knott test at 5% probability ($P \leq 0.05$). Cv = 28.1 (virulent population) and Cv = 26.4 (avirulent population).

of giant cells initiated in the vascular cylinder region at 7 DAI (Figures 3B, 4B) and illustrated further at 13 and 27 DAI in roots of 'Santa Clara' (Figures 3E–G) and at 11 and 13 DAI in 'Guardião' (Figures 4D, E). The histological changes observed in the root cells of both the resistant and susceptible cultivars when parasitized by the virulent population of *M. javanica* exhibited a high degree of similarity. Additionally, these changes closely resembled those observed in roots of the susceptible cv. parasitized by the avirulent population of *M. javanica*.

Discussion

Plant resistance responses to RKN are diverse and can occur either before or after pre-parasitic juveniles have penetrated root tissues (Rutter et al., 2022). The structure of the root itself can act as a physical barrier to J2 penetration, as has been observed in many plant species, e.g., in pepper (Pegard et al., 2005) or rice (Cabasan et al., 2012). However, it is often difficult to separate the early effects of these physical barriers to nematode penetration from the chemical defense responses that the host will initiate following RKN infection, thus leading to plant immunity. In the case of basal immunity, the plant recognizes nematode-derived molecules referred to as pathogen-associated molecular patterns (PAMPs) and activates a series of both local and systemic defense responses that include callose deposition, a burst of reactive oxygen species (ROS), and activation of defense gene expression, all these mechanisms being collectively known as PAMP - detected immunity (PTI) (Goode and Mitchum, 2022; Siddique et al., 2022). When the plant harbours dominant resistance (R) gene(s), nematode effectors are triggered by intracellular receptors, which in turn initiates programmed cell death within the host, a pathway designated as effector-triggered immunity (ETI). In particular, nucleotide-binding and leucine-rich repeat (NB-LRR) genes constitute most of known ETI R genes against RKN in dicotyledones, in both annual and perenial crops, e.g., *Mi-1.2* in tomato (Milligan et al., 1998) or *Ma* in plum (Claverie et al., 2011).

Previous histopathological studies of tomato plants harboring the *Mi-1.2* resistance gene have indicated that it mediates defense responses to *M. incognita* associated with the induction of an hypersensitive reaction (HR), which prevents the development of giant cells by blocking the parasite's penetration in the root and the completion of its life cycle (Melillo et al., 2006). Here, our results showed that two different mechanisms might be involved in the expression of resistance of the tomato rootstock 'Guardião' and an avirulent *M. javanica* population. The first mechanism occurred as a strong pre-infection defense response that prevented the nematodes from penetrating the root epidermis, suggesting a potential association with physical or biochemical barriers. Although we did not observe any anatomical reinforcement of the root epidermis in the resistant plants, additional experiments are needed to specify more precisely which of these two mechanisms acts as a barrier to J2 penetration, or whether they act in combination. This early defense layer proved to be powerful and blocked about 99% of the J2 penetration compared to susceptible plants. Such barriers were previously suggested to occur in various crops, e.g., grape (Anwar and McKenry, 2000) or cotton (Anwar et al., 1994) One of the resistance mechanisms of tomato related to *Mi*-1.2 gene to RKN is inhibiting the penetration of juvenile (J2) during invasion. However, there is variation in numbers of penetrating J2, depending on the nematode population and tomato genotype but the reason is not clear (Wubie and Temesgen, 2019).

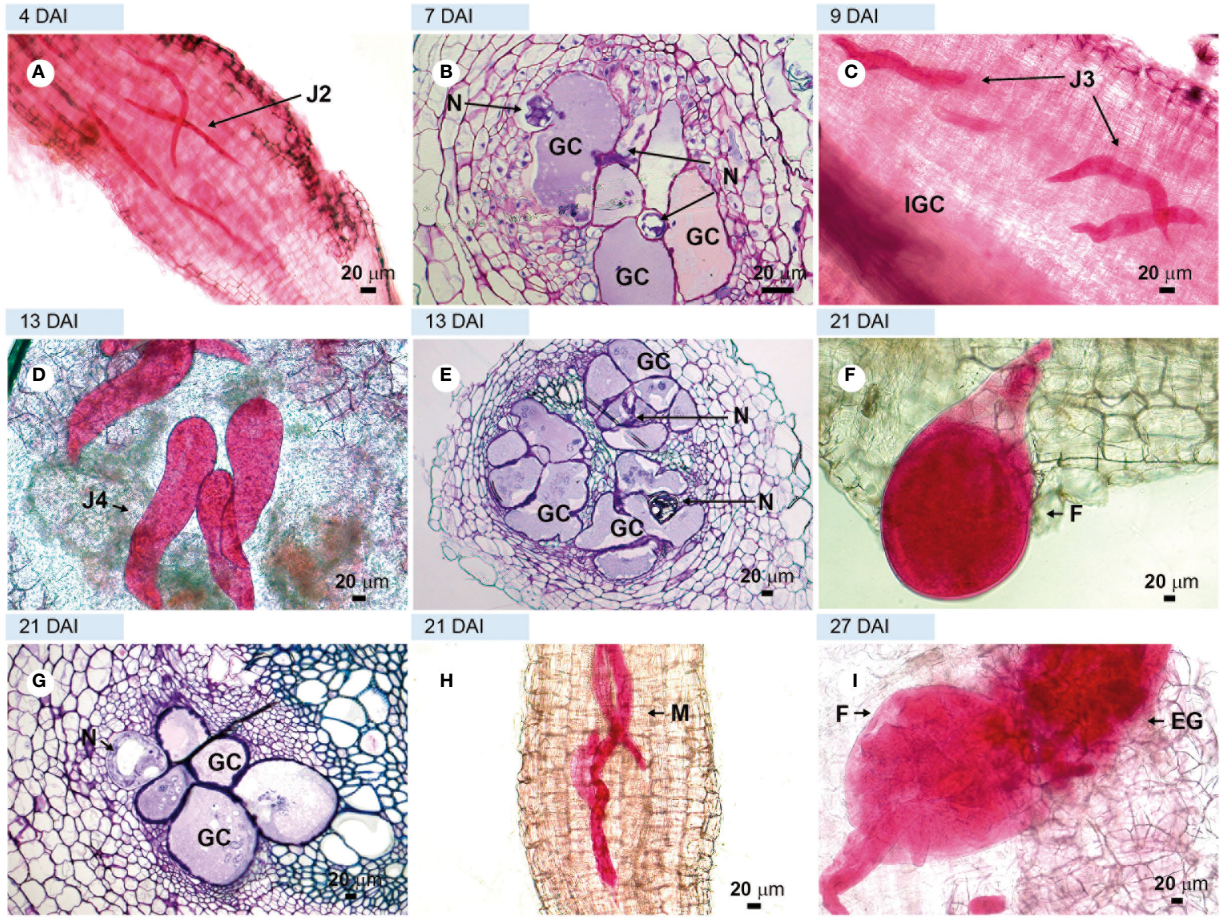

FIGURE 3
Compatible interaction. Roots of tomato plant cv. 'Santa Clara' susceptible, infected with virulent *Meloidogyne javanica*. **(A, C, D, F, H, I)** = light microscopy observations of root fragments stained with acid fuchsin. **(B, E, G)** = sections stained with toluidine blue. **(A)** = second stage juveniles (J2) inside the roots at 4 DAI; **(B)** = initial giant cell formation in the vascular cylinder; **C** = third-stage juvenile (J3); **(D)** = fourth-stage juvenile (J4) in the vascular cylinder. **(E)** = large number of giant cells in the vascular cylinder; **(F)** = young female feeding in the vascular cylinder in a well-thickened root; **(G)** = well-formed giant cells; **(H)** = males in large numbers and **(I)** = adult female with egg-mass. DAI, days after inoculation; GC, giant cell; M, male; F, female; CC, vascular cylinder; N, nematodes.

Complementary, a second resistance mechanism occurred as a post-infection defense response at 4-7 DAI, soon after J2 penetration in the root tissues, with HR-cell death observed in the cortex and vascular cylinder regions of the root, as has been observed in some tomato genotypes resistant to RKN (Dropkin, 1969; Regaieg and Horrigue-Raouani, 2012). This mechanism was described in several plant species hosts for other RKN species, including pepper (Pegard et al., 2005), cotton (Mota et al., 2012; Lopes et al., 2020), coffee (Lima et al., 2015) and rice (Mattos et al., 2019). Overall, very few J2s were able to penetrate the tomato roots, and were further blocked due to the HR. But this phenomenon was much less intense than the non-penetration of J2s into the roots, which may result from various, non-exclusive pathways: either the roots did not attract or even repelled J2s, or J2 penetrated then rapidly left the roots, although we could not get strong anatomical evidence for the latter option. For example, such protection was shown for *Cucumis sativus* L., in which the triterpene cucurbitacin isolated from root exudates repelled J2s (Hayne and Jones, 1976). Similarly, amino acids exuded from *Sesamum indicum* L. roots have a nematostatic effect on *Meloidogyne* J2 (Tanda et al., 1989). In the past decades, much emphasis has been given to the mechanisms linked to HR, but studies related to physical and chemical defense layers have been rather neglected, probably due to the technical difficulties in identifying plant molecules that modulate nematode behavior in soil (Siddique et al., 2022).

As expected, the penetration experiment and the histopathological observations of tomato roots inoculated with the *M. javanica* virulent population agree with the *in vivo* infection test we previously conducted with the same plant genotypes (Gabriel et al., 2024). The nematode established feeding sites and maintained healthy giant cells, containing several nuclei and thickened cell walls in roots of resistant tomato plants, similar to those observed in the susceptible cultivar 'Santa Clara'. The ability of virulent RKN to induce feeding sites and complete their life cycle has been reported previously on tomato cultivars harbouring the *Mi-1.2* resistance gene (e.g., Regaieg and

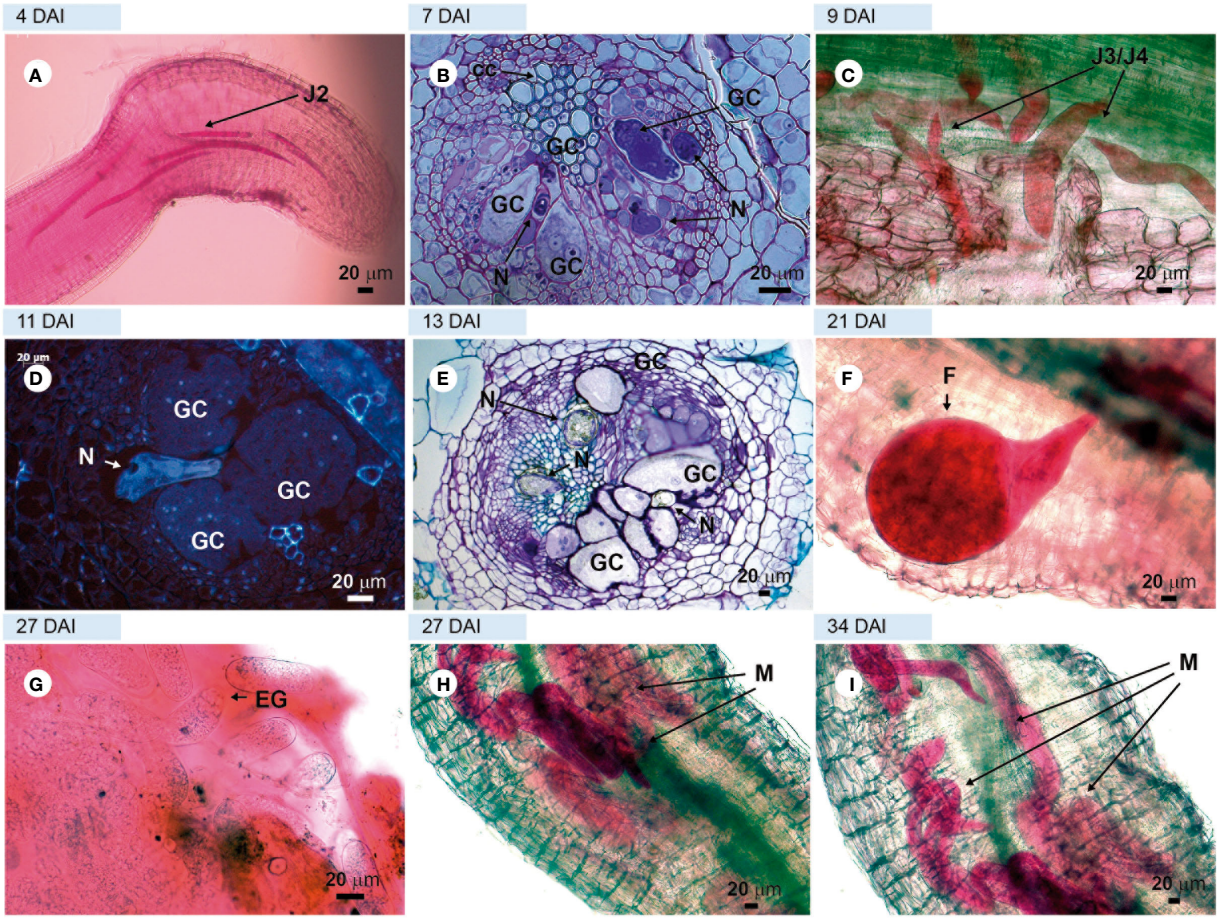

FIGURE 4
Compatible interaction. Tomato roots of 'Guardian' rootstock infected with virulent *Meloidogyne javanica*. **(A, C, F, G, H, I)** = light microscopy observations of a root fragment stained with acid fuchsin. **(B, E)** = sections stained with toluidine blue. D = unstained sections viewed under UV; **(A)** = second-stage juvenile (J2) in the apical region of the root; **(B)** = giant cell in formation; **(C)** = third and fourth-stage juveniles **(J3/J4)** in the vascular cylinder; **(D)** = well-formed feeding site without the presence of HR; **(E)** = thick-walled giant cells; **(F)** = female feeding into the vascular cylinder; **(G)** = eggs; **(H)** = male emerging from the J4 cuticle layers and **(I)** = a large number of males in different regions of the root: cortex and vascular cylinder. GC, giant cell; F, female; EG, eggs inside egg mass; HR, hypersensitivity reaction; N, nematodes.

Horrigue-Raouani, 2012; Iberkleid et al., 2014; Ploeg et al., 2023). Here, we showed that the same observation can be done on a resistant rootstock. Variability in the level of reproduction of virulent RKN on resistant tomato has been documented, and possibly correlated to a dosage effect of the *Mi-1.2* gene when it is present in hetezygous allelic state (Tzortzakakis et al., 1998; Jacquet et al., 2005; Iberkleid et al., 2014). Better results were observed in our previous study where heterozygous tomato rootstocks were classified solely as resistant rather than as highly resistant in homozygous plants (Gabriel et al., 2024).

In summary, our findings indicate that the resistance to *M. javanica* conferred by the tomato *Mi-1.2* gene results in early plant responses involving both pre-infection mechanisms and HR, which ultimately prevent the nematode from completing its development cycle. In addition, we also demonstrated that nematodes virulent to this resistance gene are able to develop normally on both susceptible and resistant plants, and induce in both cases feeding sites identical to those observed in a compatible interaction between a susceptible tomato and an avirulent nematode. To our knowledge, this is the first report of an in-depth histological characterization of a *M. javanica* population able to overcome the resistance conferred by the tomato *Mi-1.2* gene. The broad implication of the present research is that virulent *M. javanica* populations may represent a major agronomic risk if widely dispersed in tomato crops. Since the long-term use of both homozygous and heterozygous resistant crop genotypes can lead to the emergence of virulent nematode populations, management of resistance genes in the field is of utmost importance to promote their durability. In particular, pyramiding of two different resistance genes in one genotype or alternating different resistance genes in rotation are strategies that suppressed or reduced the emergence of virulent RKN isolates, as demonstrated in sweet pepper (Djian-Caporalino et al., 2014). To that respect, combining the use *Mi-1.2* with other natural RKN resistance genes that have been identified in tomato (El-Sappah et al., 2019) is clearly a challenge for the future. In complement, the association of host resistance to other management practices, such

as solarization, organic matter, wet fallow, and biological control, among others, will undoubtedly increase the control of RKN and consequently the long-term sustainability of tomato production.

Data availability statement

The original contributions presented in the study are included in the article/supplementary material. Further inquiries can be directed to the corresponding authors.

Ethics statement

The manuscript presents research on animals that do not require ethical approval for their study.

Author contributions

MG: Methodology, Writing – review & editing. MS: Methodology, Writing – review & editing. VM: Methodology, Writing – review & editing. AG: Methodology, Supervision, Writing – review & editing. SdA: Methodology, Writing – review & editing. PC-S: Writing – original draft, Writing – review & editing. LB: Writing – original draft. JC: Funding acquisition, Writing – original draft. RC: Conceptualization, Formal analysis, Investigation, Project administration, Resources, Supervision, Writing – original draft, Writing – review & editing.

Funding

The author(s) declare financial support was received for the research, authorship, and/or publication of this article. Univesidade de Brasília (UnB). Edital DPI/DPG/BCE nº 01/2024, apoio a projetos de pesquisas científicas, tecnológicas e de inovação.

Conflict of interest

The authors declare that the research was conducted in the absence of any commercial or financial relationships that could be construed as a potential conflict of interest.

Publisher's note

All claims expressed in this article are solely those of the authors and do not necessarily represent those of their affiliated organizations, or those of the publisher, the editors and the reviewers. Any product that may be evaluated in this article, or claim that may be made by its manufacturer, is not guaranteed or endorsed by the publisher.

References

Anwar, S. A., and McKenry, M. V. (2000). Penetration, development and reproduction of *Meloidogyne arenaria* on two new resistant *Vitis* spp. *Nematropica* 30, 9–17.

Anwar, S. A., Trudgill, D. L., and Philipps, M. S. (1994). The contribution of variation in invasion and development rates of *Meloidogyne incognita* to host status differences. *Nematologica* 40, 579–586. doi: 10.1163/003525994X00436

Byrd, D. W. Jr., Kirkpatrick, J., and Barker, K. R. (1983). An improved technique for clearing and staining plant tissues for detection of nematodes. *J. Nematol.* 15, 142–143.

Cabasan, M. T. N., Kumar, A., and De Waele, D. (2012). Comparison of migration, penetration, development and reproduction of Meloidogyne graminicola on susceptible and resistant rice genotypes. *Nematology* 14, 405–415. doi: 10.1163/156854111X602613

Carneiro, R. M. D. G., and Almeida, M. R. A. (2001). Técnica de eletroforese usada no estudo de enzimas dos nematoides de galhas para identificação de espécies. *Nematologia Bras.* 25, 35–44.

Castagnone-Sereno, P., Bongiovanni, M., and Dalmasso, A. (1994a). Reproduction of virulent isolates of *Meloidogyne incognita* on susceptible and *Mi*-resistant tomato. *J. Nematol.* 26, 324–328.

Castagnone-Sereno, P., Wajnberg, E., Bongiovanni, M., Leroy, F., and Dalmasso, A. (1994b). Genetic variation in *Meloidogyne incognita* virulence against the tomato Mi resistance gene: evidence from isofemale line selection studies. *Theor. Appl. Genet.* 88, 749–753. doi: 10.1007/BF01253980

Claverie, M., Dirlewanger, E., Bosselut, N., Van Ghelder, C., Voisin, R., Kleinhentz, M., et al. (2011). The Ma gene for complete-spectrum resistance to *Meloidogyne* species in *Prunus* is a TNL with a huge repeated C-terminal post-LRR region. *Plant Physiol.* 156, 779–792. doi: 10.1104/pp.111.176230

Devran, Z., and Söğüt, M. A. (2010). Occurrence of virulent root-knot nematode populations on tomatoes bearing the *Mi* gene in protected vegetable-growing areas of Turkey. *Phytoparasitica* 38, 245–251. doi: 10.1007/s12600-010-0103-y

Djian-Caporalino, C., Palloix, A., Fazari, A., Marteu, N., Barbary, A., Abad, P., et al. (2014). Pyramiding, alternating or mixing: comparative performances of deployment strategies of nematode resistance genes to promote plant resistance efficiency and durability. *BMC Plant Biol.* 14, 53. doi: 10.1186/1471-2229-14-53

Dropkin, V. H. (1969). The necrotic reaction of tomatoes and other hosts resistant to *Meloidogyne*: reversal by temperature. *Phytopathology* 59, 1632–1637.

El-Sappah, A., Islam, M. M., El-Awady, H. H., Yan, S., Qi, S., Liu, J., et al. (2019). Tomato natural resistance genes in controlling the root-knot nematode. *Genes* 10, 925. doi: 10.3390/genes10110925

Flegg, J. J. M. (1967). Extraction of *Xiphinema* and *Longidorus* species from soil by a modification of CoBB' decanting and sieving technique. *Ann. Appl. Biol.* 60, 429–437. doi: 10.1111/j.1744-7348.1967.tb04497.x

Fuller, V. L., Lilley, C. J., and Urwin, P. E. (2008). Nematode resistance. *New Phytol.* 180, 27–44. doi: 10.1111/j.1469-8137.2008.02508.x

Gabriel, M., Kulczynski, S. M., Muniz, M. F. B., Boiteux, L. S., and Carneiro, R. M. D. G. (2020). Reaction of a heterozygous tomato hybrid bearing the *Mi-1.2* gene to 15 *Meloidogyne* species. *Plant Pathol.* 69, 944–952. doi: 10.1111/ppa.13179

Gabriel, M., Kulczynski, S. M., Santos, M. F. A., Souza, C. F. B., Muniz, M. F. B., Boiteux, L. S., et al. (2022). A novel virulent Brazilian pathotype of *Meloidogyne javanica* towards the tomato *Mi-1.2* gene and pathogenicity to resistant rootstock. *J. Plant Dis. Prot.* 129, 1269–1276. doi: 10.1007/s41348-022-00618-3

Gabriel, M., Santos, M. F. A., Mattos, V. S., Almeida, S. F., Boiteux, L. S., and Carneiro, R. M. D. G. (2024). Assessment of allelic *Mi*-1.2 dosage effects on levels of resistance to virulent and avirulent *Meloidogyne* spp. populations in some tomato rootstocks. *Nematology*. 26, 289-298. doi: 10.1163/15685411-bja10308

Goode, K., and Mitchum, M. G. (2022). Pattern-triggered immunity against root-knot nematode infection: A minireview. *Physiologia Plantarum* 174, e13680. doi: 10.1111/ppl.13680

Hayne, R. L., and Jones, C. M. (1976). Effects of the *Bi* locus in cucumber on reproduction, attraction, and response of the plant to infection by the southern root-knot nematode. *J. Am. Soc. Hortic. Sci.* 101, 422–424. doi: 10.21273/JASHS.101.4.422

Holzmann, O. V. (1965). Effects of soil temperature on resistance of tomato to root-knot nematode (*Meloidogyne incognita*). *Phytopathology* 55, 990–992.

Huang, C. S., and Maggenti, A. R. (1969). Wall modifications in developing giant cells of *Vicia faba* and *Cucumis sativus* induced by root knot nematode. *Meloidogyne javanica*. *Phytopathol.* 59, 931–937.

Hussey, R. S., and Barker, K. R. (1973). Comparison of methods of collecting inocula of *Meloidogyne* spp., including a new technique. *Plant Dis. Rep.* 57, 1025–1028.

Iberkleid, I., Ozalvo, R., Feldman, L., Elbaz, M., Patricia, B., and Brown Horowitz, S. (2014). Responses of tomato genotypes to avirulent and *Mi*-virulent *Meloidogyne javanica* isolates occurring in Israel. *Phytopathology* 104, 484–496. doi: 10.1094/PHYTO-07-13-0181-R

Jacquet, M., Bongiovanni, M., Martinez, M., Verschave, P., Wajnberg, E., and Castagnone-Sereno, P. (2005). Variation in resistance to the root-knot nematode *Meloidogyne incognita* in tomato genotypes bearing the *Mi* gene. *Plant Pathol.* 54, 93–99. doi: 10.1111/j.1365-3059.2005.01143.x

Lima, E. A., Furlanetto, C., Nicole, M., Gomes, A. C. M. M., Almeida, M. R. A., Jorge-Júnior, A., et al. (2015). The multi-resistant reaction of drought-tolerant coffee Conilon clone 14 to *Meloidogyne* spp. and late hypersensitive-like response in *Coffea canephora*. *Phytopathology* 105, 805–814. doi: 10.1094/PHYTO-08-14-0232-R

Lopes, C. M. L., Suassuna, N. D., Cares, J. E., Gomes, A. C. M. M., Perina, F. J., Nascimento, G. F., et al. (2020). Marker-assisted selection in *Gossypium* spp. for *Meloidogyne incognita* resistance and histopathological characterization of a near immune line. *Euphytica* 216, 1–15. doi: 10.1007/s10681-020-2554-7

Maleita, C. M., Santos, M. C. V., Curtis, R. H. C., Powers, S. J., and Abrantes, I. M. O. (2011). Effect of the *Mi* gene on reproduction of *Meloidogyne hispanica* on tomato genotypes. *Nematology* 13, 939–949. doi: 10.1163/138855411X566449

Mattos, V. S., Leite, R. R., Cares, J. E., Gomes, A. C. M. M., Moita, A. W., Lobo, V. L. S., et al. (2019). *Oryza glumaepatula*, a new source of resistance to *Meloidogyne graminicola* and histological characterization of its defense mechanisms. *Phytopathology* 109, 1941–1948. doi: 10.1094/PHYTO-02-19-0044-R

Melillo, M. T., Leonetti, P., Bongiovanni, M., Castagnone-Sereno, P., and Bleve-Zacheo, T. (2006). Modulation of reactive oxygen species activities and H_2O_2 accumulation during compatible and incompatible tomato-root-knot nematode interactions. *New Phytol.* 170, 501–512. doi: 10.1111/j.1469-8137.2006.01724.x

Milligan, S. B., Bodeau, J., Yaghoobi, J., Kaloshian, I., Zabel, P., and Williamson, V. M. (1998). The root-knot nematode resistance gene *Mi* from tomato is a member of the leucine zipper, nucleotide binding, leucine-rich repeat family of plant genes. *Plant Cell* 10, 1307–1319. doi: 10.1105/tpc.10.8.1307

Mitsumasu, K., Seto, Y., and Yoshida, S. (2015). Apoplastic interactions between plants and plant root intruders. *Front. Plant Sci.* 6. doi: 10.3389/fpls.2015.00617

Mota, F. C., Alves, G. C. S., Giband, M., Gomes, A. C. M. M., Sousa, F. R., Mattos, V. S., et al. (2012). New sources of resistance to *Meloidogyne incognita* race 3 in wild cotton accessions and histological characterization of the defense mechanisms. *Plant Pathol.* 62, 1173–1183. doi: 10.1111/ppa.12022

Ornat, C., Verdejo-Lucas, S., and Sorribas, F. J. (2001). A population of *Meloidogyne javanica* in Spain virulent to the resistance gene *Mi* in tomato. *Plant Dis.* 85, 271–276. doi: 10.1094/PDIS.2001.85.3.271

Pegard, A., Brizzard, G., Fazari, A., Soucaze, O., Abad, P., and Djian-Caporalino, C. (2005). Histological characterization of resistance to different root-knot nematode species related to phenolics accumulation in *Capsicum annuum*. *Phytopathology* 95, 158–165. doi: 10.1094/PHYTO-95-0158

Ploeg, A. T., Stoddard, C. S., Turini, T. A., Nunez, J. J., Miyao, E. M., and Subbotin, S. A. (2023). Tomato *Mi*-gene resistance-breaking populations of *Meloidogyne* show variable reproduction on susceptible and resistant crop cultivars. *J. Nematol.* 55, e20230043. doi: 10.2478/jofnem-2023-0043

Regaieg, H., and Horrigue-Raouani, N. (2012). Histological response of resistant tomato cultivars to infection of virulent Tunisian root-knot nematode (*Meloidogyne incognita*) populations. *Arch. Phytopathol. Plant Prot.* 45, 2036–2045. doi: 10.1080/03235408.2012.720470

Roberts, P. A. (1995). Conceptual and practical aspects of variability in *Meloidogyne* related to host plant resistance. *Annu. Rev. Phytopathol.* 33, 199–221. doi: 10.1146/annurev.py.33.090195.001215

Rutter, W. B., Franco, J., and Gleason, C. (2022). Rooting out the mechanisms of root-knot nematode-plant interactions. *Annu. Rev. Phytopathol.* 60, 43–76. doi: 10.1146/annurev-phyto-021621-120943

Sato, K., Kadota, Y., and Shirasu, K. (2019). Plant immune responses to parasitic nematodes. *Front. Plant Sci.* 10. doi: 10.3389/fpls.2019.01165

Schaff, J. E., Nielsen, D. M., Smith, C. P., Scholl, E. H., and McK Bird, D. (2007). Comprehensive transcriptome profiling in tomato reveals a role for glycosyltransferase in *Mi*-mediated nematode resistance. *Plant Physiol.* 144, 1079–1092. doi: 10.1104/pp.106.090241

Scott, A. J., and Knott, M. (1974). A cluster analysis method for grouping means in the analysis of variance. *Biometrics* 30, 507. doi: 10.2307/2529204

Siddique, S., Coomer, A., Baum, T., and Williamson, V. M. (2022). Recognition and response in plant-nematode interactions. *Annu. Rev. Phytopathol.* 60, 143–162. doi: 10.1146/annurev-phyto-020620-102355

Silva, R. V., Lima, B. V., Peixoto, F. R., Gondim, J. P. E., and Miranda, B. E. C. (2019). Supplanting resistance of the *Mi* gene by root-knot nematode in industrial tomato in the Cerrado in Goiás State of Brazil. *Ciec. Rural* 49, e20180784. doi: 10.1590/0103-8478cr20180784

Smith, P. G. (1944). Embryo culture of a tomato species hybrid. *Proc. Am. Soc. Hortic. Sci.* 44, 413–416.

Tanda, A. S., Atwal, A. S., and Bajaj, Y. P. S. (1989). *In vitro* inhibition of root-knot nematode *Meloidogyne incognita* by sesame root-exudate and its amino acids. *Nematologica* 35, 115–124. doi: 10.1163/002825989X00124

Tzortzakakis, E. A., Conceição, I., Dias, A. M., Simoglou, K. B., and Abrantes, I. (2014). Occurrence of a new resistant breaking pathotype of *Meloidogyne incognita* on tomato in Greece. *J. Plant Dis. Prot.* 121, 184–186. doi: 10.1007/BF03356508

Tzortzakakis, E. A., Trudgill, D. L., and Phillips, M. S. (1998). Evidence for a dosage effect of the *Mi* gene on partially virulent isolates of Meloidogyne javanica. *J. Nematol.* 30, 76–80.

Williamson, V. M. (1998). Root-knot nematode resistance genes in tomato and their potential for future use. *Annu. Rev. Phytopathol.* 36, 277–293. doi: 10.1146/annurev.phyto.36.1.277

Williamson, V. M., and Kumar, A. (2006). Nematode resistance in plants: the battle underground. *Trends Genet.* 22, 396–403. doi: 10.1016/j.tig.2006.05.003

Wubie, M., and Temesgen, Z. (2019). Resistance mechanisms of tomato (*Solanum lycopersicum*) to root-knot nematodes (*Meloidogyne* species). *J. Plant Breed. Crop Sci.* 11, 33–40. doi: 10.5897/JPBCS2018.0779

frontiers | Frontiers in Plant Science

TYPE Original Research
PUBLISHED 23 September 2024
DOI 10.3389/fpls.2024.1386535

OPEN ACCESS

EDITED BY
Andressa Machado,
Agronema Brazil

REVIEWED BY
Heriksen Higashi Puerari,
Federal University of Piauí, Brazil
Jeronimo Vieira De Araujo Filho,
Federal University of Pelotas, Brazil

*CORRESPONDENCE
Juan E. Palomares-Rius
palomaresje@ias.csic.es

RECEIVED 15 February 2024
ACCEPTED 02 September 2024
PUBLISHED 23 September 2024

CITATION
Clavero-Camacho I, Ruiz-Cuenca AN, Cantalapiedra-Navarrete C, Castillo P and Palomares-Rius JE (2024) Diversity of microbial, biocontrol agents and nematode abundance on a susceptible *Prunus* rootstock under a *Meloidogyne* root gradient infection. *Front. Plant Sci.* 15:1386535. doi: 10.3389/fpls.2024.1386535

Diversity of microbial, biocontrol agents and nematode abundance on a susceptible *Prunus* rootstock under a *Meloidogyne* root gradient infection

Ilenia Clavero-Camacho[1,2], Alba N. Ruiz-Cuenca[1,3], Carolina Cantalapiedra-Navarrete[1], Pablo Castillo[1] and Juan E. Palomares-Rius[1]*

[1]Institute for Sustainable Agriculture (IAS), Spanish National Research Council (CSIC), Cordoba, Spain, [2]Instituto de Estudios de Postgrado, Departamento de Agronomía, Universidad de Córdoba, Cordoba, Spain, [3]Departament of Animal Plant Biology and Ecology, Universidad de Jaén, Jaén, Spain

Root-knot nematodes (RKNs) of the genus *Meloidogyne* are one of the most damaging genera to cultivated woody plants with a worldwide distribution. The knowledge of the soil and rhizosphere microbiota of almonds infested with *Meloidogyne* could help to establish new sustainable and efficient management strategies. However, the soil microbiota interaction in deciduous woody plants infected with RKNs is scarcely studied. This research was carried out in six commercial almond groves located in southern Spain and infested with different levels of *Meloidogyne* spp. within each grove. Several parameters were measured: nematode assemblages, levels and biocontrol agents in *Meloidogyne*'s eggs, levels of specific biocontrol agents in rhizoplane and soil, levels of bacteria and fungi in rhizoplane and soil, fungal and bacterial communities by high-throughput sequencing of internal transcribed spacer (ITS), and 16S rRNA gene in soil and rhizosphere of the susceptible almond hybrid rootstock GF-677 infested with *Meloidogyne* spp. The studied almond groves showed soil degradation by nematode assemblies and fungi:bacterial ratio. Fungal parasites of *Meloidogyne* eggs were found in 56.25% of the samples. However, the percentage of parasitized eggs by fungi ranged from 1% to 8%. Three fungal species were isolated from *Meloidogyne* eggs, specifically *Pochonia chlamydosporia*, *Purpureocillium lilacinum*, and *Trichoderma asperellum*. The diversity and composition of the microbial communities were more affected by the sample type (soil vs rhizosphere) and by the geographical location of the samples than by the *Meloidogyne* density, which could be explained by the vigorous hybrid rootstock GF-677 and a possible dilution effect. However, the saprotrophic function in the functional guilds of the fungal ASV was increased in the highly infected roots vs the low infected roots. These results indicate that the presence of biocontrol agents in almond fields and the development of new management strategies could increase their populations to control partially RKN infection levels.

KEYWORDS

metabarcoding, *Meloidogyne*, 16S rRNA, ITS, biological control

1 Introduction

Almond (*Prunus dulcis*) is a representative tree of the Mediterranean countryside and Spain. In terms of extension, the area dedicated to almond cultivation in Spain is around 744,000 ha, with more than 30% of this area located in Andalusia, Southern Spain (MAPA, 2022). Behind this crop, there is a whole industry of great economic importance that has led Spain to be the second largest producer of almonds in the world (FAOSTAT, 2021). In the last decades, almond consumption has increased worldwide due to its high nutritional and eating quality. The growing demand for almonds worldwide has promoted the expansion of intensive almond groves characterized by a high density of trees per hectare, irrigation, fertilization, new cultivars and rootstocks from breeding programs, new pruning systems, and pest and disease management (Micke, 1996). The key to success of the establishment of the new intensive almond groves was strongly supported by the selection of new rootstocks with higher tolerance to iron chlorosis and greater resistance/tolerance to pests and diseases, and self-compatible cultivars (Ortega and Dicenta, 2003; Jiménez et al., 2008; Rubio-Cabetas et al., 2017). Rootstocks play an essential role in the successful establishment and maintenance of an almond grove, as tolerance to soil-borne diseases depend upon them. The main soil-borne pathogens that can compromise tree growth and grove yield, even causing the death of young trees, include the fungi *Armillaria mellea* and *Phytophtora* spp. and plant-parasitic nematodes (PPNs) (Nyczepir, 1991; Baumgartner et al., 2011; Browne, 2017). Four nematode genera have been reported as major diseases causing severe losses in yield and quality in *Prunus* spp. grove, specifically root-knot (*Meloidogyne* spp.), root-lesion (*Pratylenchus* spp.), dagger (*Xiphinema* spp.), and ring (*Criconemoides* spp.) nematodes (Nyczepir, 1991). Rootstock breeding programs have focused on three species of *Meloidogyne* (*Meloidogyne arenaria*, *Meloidogyne incognita*, and *Meloidogyne javanica*) and one of *Pratylenchus* (*Pratylenchus vulnus*), which can become important limiting factors for this crop in warm environments (Alcañiz et al., 1996; Pinochet et al., 1996; Esmenjaud et al., 1997).

Focusing on root-knot nematodes (RKNs) (*Meloidogyne* spp.), these are obligate plant parasites with a worldwide distribution and a wide host range (Jones et al., 2013). These nematodes are sedentary endoparasites characterized by inducing the formation of galls on the roots of susceptible plants (Moens et al., 2009). The nematode parasitism causes stunted plant growth, reduced fruit quality, and lower yields. In the Mediterranean region, the most widespread RKNs are *Meloidogyne arenaria*, *M. incognita*, and *M. javanica*, although other species have also been reported affecting *Prunus* groves. Specifically, *Meloidogyne floridensis* (Handoo et al., 2004)), *Meloidogyne hispanica* (Hirschmann, 1986), and *Meloidogyne morocciensis* (Rammah and Hirschmann, 1990) were described parasitizing peach in Florida, Spain, and Morocco, respectively. Recently, *M. floridensis* was reported infecting almond groves in California (Westphal et al., 2019). As for other PPNs, control methods and management strategies against RKNs include prevention measures and methods to reduce nematode population, such as crop rotation, solarization, nematicides, resistant/tolerant rootstocks, and biological control (Verdejo-Lucas and Talavera, 2009). However, some of these methods have limitations due to the wide host range of most PPN affecting almond groves and the fact that woody crops remain for decades in the same field. Moreover, in Spain, there are no authorized nematicides for use on *Prunus* crops (MAPA, 2023). To establish a plantation, resistant rootstocks to RKNs are the most economical, sustainable, and effective method to manage the most harmful *Meloidogyne* spp (Saucet et al., 2016). In Spain, the most commonly used rootstock is the hybrid GF-677 (*Prunus dulcis* x *Prunus persica*), which adapts well to edaphic and climatic conditions, although it is susceptible to *Meloidogyne* spp. Intensive and high-density plantations are gaining ground because of the high yields and cost reduction, as well as organic almond groves, due to growing consumer demand for sustainable agriculture and food safety. Integrated management based on pest identification, progress monitoring, and agronomic practices, such as efficient use of water, cover crops, rootstocks, and biological control, is essential to ensure high yields and economic and environmental sustainability of the crop in the long term.

Plants live in close association with the microorganisms that inhabit the soil, which make up the plant microbiota (Trivedi et al., 2020). The rhizosphere is a natural reservoir of microorganisms, some of which can act as biological control agents (BCAs) by protecting the plant directly or indirectly against pathogens (Köhl et al., 2019). Bacteria, collembola, fungi, predatory nematodes, mites, and protozoans have been reported as BCAs against PPNs, with bacteria and fungi considered to be the most extended and effective nematode antagonists (Stirling, 2014). Some genera of rhizospheric bacteria, such as *Pseudomonas*, *Bacillus*, and *Pasteuria*, have shown efficacy for PPN control (Chen and Dickson, 1998; Abd-El-Khair et al., 2019; Migunova and Sasanelli, 2021). Likewise, nematophagous fungi, such as *Arthrobotrys* spp., *Trichoderma* spp., *Hirsutella rhossiliensis*, *Pochonia chlamydosporia*, and *Purpureocillium lilacinum*, are well-known BCAs against nematodes (Kiewnick and Sikora, 2006; Zhang et al., 2006; Singh et al., 2007; Escudero and Lopez-Llorca, 2012; Pocurull et al., 2020). Additionally, of these specific BCAs against plant-parasitic nematodes, the rhizospheric microbiome plays an important role in plant health. Recent studies have showed that transplanting the rhizospheric microbiome from one plant to another significantly alleviated *M. incognita* and *Pratylenchus penetrans* infections (Elhady et al., 2018; Zhou et al., 2019). However, many of these interactions were difficult to study because the majority of the soil microbiota are difficult or impossible to culture using laboratory methodology. In recent years, massive parallel sequencing has allowed us to increase our knowledge of the soil microbiome. Specifically, several studies have analyzed the occurrence of taxonomic groups of bacteria and fungi, including BCAs, in nematode-infested soils and different crops, such as potato, banana, soybean, and tomato (Castillo et al., 2017; Toju and Tanaka, 2019; Zhou et al., 2019; Ciancio et al., 2022). Since intensive production practices can decrease the occurrence of BCAs, integrated pest management practices and soil microbiota should be considered to increase the efficacy and persistence of beneficial microorganisms (Abd-Elgawad, 2021). Recent studies of the response of soil microbiota in almond crops under different management practices showed changes in the microbial community (Özbolat et al.,

2023; Camacho-Sanchez et al., 2023). However, the knowledge of the microbiota associated with almond crop, as well as the interaction of *Meloidogyne* spp. with the almond rhizosphere microbiota and native BCAs, is still limited. Moreover, the severity of damage caused by *Meloidogyne* spp. depends on several factors, including crop, season, soil type, and initial inoculum density (Jones et al., 2013). Thus, knowledge of soil and rhizosphere microbiota associated with almond crops, as well as their interaction with *Meloidogyne* spp., is essential to establish sustainable pest management strategies. The main hypothesis of this research is to know if the increase in root-knot nematode egg levels (and nodulation-root damage) in roots changes the soil ecology, including potential *Meloidogyne* biocontrol agents, in a susceptible hybrid rootstock in commercial almond plantations. Specifically, we analyzed soil and rhizosphere microbial and nematode communities and BCAs associated with the susceptible *Prunus* rootstock (GF-677) in a *Meloidogyne* gradient infection in almond groves. Therefore, six commercial groves with different *Meloidogyne* population densities were selected in order to (i) characterize fungal and bacterial communities of a hybrid rootstock (GF-677) using a metabarcoding approach; (ii) determine the presence of potential indigenous BCAs; (iii) evaluate the effect of different infection root levels of *Meloidogyne* on soil (soil close to the roots), rhizosphere microbiota (soil attached to the roots), and BCAs; and (iv) compare nematode communities between different levels of *Meloidogyne* spp. root infected in different areas of Southern Spain.

2 Materials and methods

2.1 Study area and sample collection

In a previous survey, the PPN community associated with the rhizosphere of *Prunus* rootstocks was studied in the main stone-production areas in Spain (Clavero-Camacho et al., 2022, 2024). From this study, the groves where selected based on the presence of *Meloidogyne* spp. and with different infection levels throughout the field. Six commercial almond groves in which a *Meloidogyne* root gradient infection was detected in that previous study were considered (all of them in Andalusia, Southern Spain) (Supplementary Figure 1). These commercial groves are managed with similar agronomic practices, specifically irrigation, tilling, herbicide application, and the same rootstock [GF-677, susceptible *Prunus* rootstock to *Meloidogyne* spp (Esmenjaud et al., 1997)]. To study different *Meloidogyne* population levels, two to three samples were collected in each grove resulting in a total of 16 sampling points (Table 1). Soil and root samples were collected from the rhizosphere of GF-677 rootstock using a shovel and considering the upper 5- to 40-cm depth of soil from four to five trees randomly selected and mixed to constitute a sampling point in each sampling site. The samples were put into polythene bags, transported in coolers to the laboratory, and stored at 4°C until processed. Roots were separated from the soil and divided into two subsamples, one for the extraction of root-knot nematodes (*Meloidogyne* spp.) and the other for rhizosphere microbiota extraction. Homogenized soil was divided into three subsamples, one of which was used for the nematode extraction, another for the physicochemical properties analysis, and the other was frozen at −30°C for total DNA extraction directly from soil (soil microbiota).

2.2 Nematode extraction and identification

Total soil nematodes were extracted from 500-cm^3 subsamples of soil by the centrifugal–flotation method (Coolen, 1979) and visualized at ×10–×20 or ×40–×100 magnification. To assess nematode density and prevalence, nematodes extracted from soil were counted and identified at genus level using an integrative taxonomic approach as described by Clavero-Camacho et al. (2024). Then, nematodes were classified into five trophic groups (bacterivores, fungivores, herbivores, omnivores, and predators) according to Yeates et al. (1993). Prevalence was computed by dividing the number of samples in which a nematode genus was detected by the total number of samples and expressed as percentage (Boag, 1993). For each identified genus, nematode density was calculated as the number of individuals of a particular nematode genus per 500 cm^3 of soil (Boag, 1993). Two ecological indices [maturity index (MI) for free-living nematodes and plant-parasitic index (PPI)] and three functional indices [channel index (CI), enrichment index (EI), and structure index (SI)] were calculated using the web application Nematode Join Indicator Analysis (NINJA) (Sieriebriennikov et al., 2014) and analyzed with R software 4.3.1 (R Core Team, 2023). After identification and counting, the nematode suspensions were allowed to settle to reduce the volume and frozen at −80°C prior to total DNA extraction for detection of target nematophagous fungi by real-time qPCR.

Regarding RKN, females were collected directly from galled almond roots, while males, second-stage juveniles (J2), and eggs were extracted from roots by blender maceration in a 1% sodium hypochlorite solution (Hussey and Barker, 1973) followed by centrifugal–flotation method (Coolen, 1979). The molecular identification of *Meloidogyne* species was conducted using a multiplex PCR assay from 10 individuals per sample extracted separately in different nematode stages (females, males, and juveniles), which allows the identification of the three most predominant species, specifically, *M. arenaria*, *M. incognita*, and *M. javanica* (Kiewnick et al., 2013) and allowed us to detect species mixtures in the groves. Specifically, multiplex PCR was performed with species-specific primers as follows: Far (5′-TCGGCGATAGA GGTAAATGAC-3′) and Rar (5′-TCGGCGATAGACACTACAACT-3′) (Zijlstra et al., 2000) for *M. arenaria*, Mi2F4 (5′-ATGAAGCTAAG ACTTTGGGCT-3′) and Mi1R1 (5′-TCCCGCTACACCCTCAA CTTC-3′) (Kiewnick et al., 2013) for *M. incognita*, and Fjav (5′-GGTGCGCGATTGAACTGAGC-3′) and Rjav (5′-CAGGCCCTT CAGTGGAACTATAC-3′) (Zijlstra et al., 2000) for *M. javanica*. The multiplex PCR cycling profile consisted of 15 min 95°C and 40 cycles of 30 s at 94°C, 1 min at 57°C and 2 min at 68°C, with a final extension cycle of 9 min at 68°C. Amplifications were carried out in a final volume of 20 µl using primer concentrations as described by Kiewnick et al. (2013). RKN density in root was calculated as the number of individuals of each *Meloidogyne* species per gram of root. To study the effect of different infection root levels of *Meloidogyne* on soil and rhizosphere microbial communities, RKN density in the roots was

10.3389/fpls.2024.1386535

TABLE 1 Nematode population density (nematodes per gram of root) and prevalence (%) of root-knot nematodes (*Meloidogyne* spp.) found parasitizing roots of almond in Andalusia (southern Spain).

Sample code	Almond groves	Locality			*Meloidogyne* spp./g of root		
			Lat	Lon	*M. arenaria*	*M. incognita*	*M. javanica*
PR13	1	Córdoba	37.82357778	−4.88607530	-[c]	–	1,209
PR15	1	Córdoba	37.82357778	−4.88607530	–	–	465
PR25A	2	Carmona (Sevilla)	37.51301330	−5.74003634	–	508	–
PR25B	2	Carmona (Sevilla)	37.51301330	−5.74003634	–	639	–
PR25C	2	Carmona (Sevilla)	37.51301330	−5.74003634	–	303	–
PR61A	3	Los Palacios (Sevilla)	37.14548089	−5.86129138	–	220	–
PR61C	3	Los Palacios (Sevilla)	37.14548089	−5.86129138	–	446	–
PR74A	4	Marmolejo (Jaén)	38.01327995	−4.19168131	139	139	–
PR77A	4	Marmolejo (Jaén)	38.02284420	−4.20999267	1,113	–	–
PR78B	4	Marmolejo (Jaén)	38.02078401	−4.17746518	–	448	448
PR90A	5	Alcalá del Río (Sevilla)	37.51437691	−5.97160655	–	–	24
PR90B	5	Alcalá del Río (Sevilla)	37.51437691	−5.97160655	–	–	2,052
PR90E	5	Alcalá del Río (Sevilla)	37.51437691	−5.97160655	–	–	265
PR231B	6	Alcolea (Córdoba)	37.93704798	−4.659543894	–	4,127	–
PR233A	6	Alcolea (Córdoba)	37.93704798	−4.659543894	–	3,588	–
PR234	6	Alcolea (Córdoba)	3.793968296	−4.652517177	–	449	–
Global							
Prevalence[a]					12.50	62.50	37.5
Density[b]					626 (139–1,113)	1,087 (139–4,127)	744 (24–2,052)

[a]Prevalence = percentage of samples in which a *Meloidogyne* spp. was detected with respect to the total number of samples processed.
[b]Nematode density = mean of nematodes of each species per gram of root in all sampling points where that genus was detected (mean, minimum, and maximum).
[c]–: Not detected.

categorized into two categories: low (<600 eggs per g of root) and high (>600 egg per g of root). In addition, *Meloidogyne* eggs extracted from roots were used to evaluate fungal egg parasitism.

2.3 Analysis of physicochemical soil properties

Prior to physicochemical analysis, the rhizosphere soil was air dried and sieved (2-mm mesh size). These analyses were conducted by the Agri-food Laboratory from Córdoba (Córdoba, Spain). Cation exchange capacity (CEC) was determined using the ammonium saturation method (Bower et al., 1952). The concentration of calcium (Ca) and magnesium (Mg) was measured using the titration method (Diehl et al., 1950). The concentration of sodium (Na) and potassium (K) were determined using the flame photometer method (Richards, 1954). The relative proportion of sand, silt, and clay particles was determined by the Bouyoucos method (Day, 1965), and these data were used to estimate texture according to the USDA soil texture classification. Available phosphorus (P) was measured using the Olsen method (Olsen, 1954). The carbonate content was determined by volumetric method (Allison and Moodie, 1965). Electrical conductivity (EC) and pH of soil were measured in a 1:5 and 1:2.5 soil/water extract, respectively, using a conductivity/pH meter. The percentage of organic matter (OM) was determined by potassium dichromate oxidation (Jackson, 1958) and organic nitrogen content by the Kjeldahl digestion (Bremner, 1965). With these data, the carbon-to-nitrogen (C:N) ratio was calculated. Differences of physicochemical measurements between the six almond groves were tested with ANOVA, followed by Tukey's honest significant difference (HSD) at $p = 0.05$.

2.4 DNA extraction and quantification

To characterize the fungal and bacterial community associated with *Meloidogyne*-infected almond groves, total genomic DNA was extracted from soil nematodes, soil (soil associated with roots from rhizosphere), and rhizosphere samples (soil and microbes attached to roots and extracted using a specific protocol below). All DNA extractions were performed using DNeasy PowerSoil Pro Kit (Qiagen) according to the manufacturer's instructions, except that soil DNA was extracted from 500 mg instead of 250 mg. Prior to the rhizosphere DNA extraction, we followed the protocol described by Aranda et al. (2011) to obtain from roots a suspension that includes bacteria and fungi from the rhizoplane adhered soil. Subsequently, 3 ml of each rhizosphere suspension was centrifuged at 11,000 rpm for 4 min and the recovered precipitate was used for rhizosphere DNA extraction. Total DNA from nematodes with adhering microorganisms was extracted using DNeasy PowerSoil Pro Kit (Qiagen) and the FastPrep-24 Instrument (MP Biomedicals, Inc. France) for 40 s at high speed to efficiently disrupt bacterial and fungal cells. All DNA samples were quantified using a Qubit dsDNA HS Assay Kit (Thermo Fisher Scientific) and stored at −20°C until metabarcoding and real-time qPCR analysis.

2.5 Fungal egg parasitism

To assess the occurrence and isolate *Meloidogyne* spp. fungal egg parasites, we used the protocol described by Giné et al. (2016) with some modifications. Egg masses could not be handpicked because of the hardness of the woody roots of *Prunus*. In total, 100 µl of eggs' suspension extracted as mentioned above were spread onto Petri dishes (9-cm diameter) that contain a growth-restricted medium (1% agar; Rose Bengal 50 mg L^{-1}; chloramphenicol, 50 mg L^{-1}; chlortetracycline, 50 mg L^{-1}; streptomycin, 50 mg L^{-1}; Triton, 50 mg L^{-1}). For each sample, three replicated Petri dishes were prepared with approximately 1,000 eggs per plate. Petri dishes were incubated at 25°C in darkness, and parasitism was evaluated after 48 h under a Leica DMi1 inverted microscope. In each Petri dish, 100 eggs were randomly selected for parasitism visual classification, and the number of parasitized eggs (with fungal hyphae inside) was counted and expressed as percentage of parasitism. At least 20 parasitized eggs per sampling points were individually transferred to potato dextrose agar (PDA) to establish pure cultures. Plates were incubated at 25°C in darkness for 3 to 5 days. Subsequently, morphological and molecular identification of the isolates were performed. Fungal isolates were identified by PCR amplification and sequencing of the ITS region (ITS1-5.8S-ITS2). Fungal DNA extraction was carried out using i-genomic plant DNA extraction mini kit (Intron Biotechnology). The ITS1-5.8S-ITS2 rDNA was amplified using primers ITS5 (5′-GGAAGTAAAAGTC GTAACAAGG-3′) and ITS4 (5′-TCCTCCGCTTATTAGATATGC-3′) (White et al., 1990). The PCR cycling conditions were as follows: 95°C for 15 min, followed by 35 cycles of 94°C for 30 s, 52°C for 30 s, and 68°C for 1 min, and a final extension cycle of 68°C for 7 min. PCRs were performed in a final volume of 20 µl, containing 3 µl of 5× HOT FIREpol Blend Master Mix (Solis Biodyne, Tartu, Estonia), 0.3 µM of each primer, 2 µl of template DNA, and 13.8 µl of ultrapure water. After amplification, PCR products were purified using ExoSAP-IT (Affimetrix, USB products, Kan-del, Germany) and used for direct sequencing in both directions. The resulting products were purified and run in a DNA multi-capillary sequencer (Model 3130XL Genetic Analyzer; Applied Biosystems, Foster City, CA, USA) using the BigDye Terminator Sequencing Kit v.3.1 (Applied Biosystems) at the Stab Vida sequencing facility (Caparica, Portugal). Species identification was implemented by comparison of DNA sequence data obtained in this study with those available in the GenBank database using the basic local alignment search tool (BLAST) at the National Center for Biotechnology Information (NCBI).

2.6 Identification of target nematophagous fungi by real-time qPCR

DNA extracted from nematode samples were used to study the occurrence of target organisms by real-time qPCR. A total of six nematophagous fungi (NF) belonging to the three main NF groups (Nordbring-Hertz et al., 2011) and with a different way of nematode parasitism were screened: nematode-trapping (*Arthrobotrys dactyloides*, *A. oligospora*, and *Gamsylella gephyropagum*), endoparasitic (*Catenaria* sp. and *Hirsutella rhossilliensis*), and egg-parasitic fungi (*Pupureocillium lilacinum*). qPCR assays were performed with species-specific primers and Taqman probes. All real-time qPCR assays were performed on an CFX Connect Real Time PCR System (Bio-Rad Laboratories, Inc.) in hard-shell PCR plates 96-well, thin well (Bio-Rad Laboratories, Inc.). These target organisms were detected in independent runs with negative (no sample) controls in all plates, with three technical repetitions per sample. Reactions were performed in a final volume of 20 µl and contained 1× iTaq Universal Probes Supermix (Bio-Rad Laboratories, Inc.), 300 nM BSA (New England BioLabs, Inc.), and 2 ng of DNA per reaction. The specific primers and probes used in this study are shown in Table 2. Primer and probe concentrations as well as qPCR conditions were as described by Atkins et al. (2005); Pathak et al. (2012); Campos-Herrera et al. (2019), and Zhang et al. (2006). *Purpureocillium lilacinum* and *Arthrobotrys dactyloides* had been previously isolated and maintained in pure cultures in PDA (Difco Laboratories) at 25°C in darkness. Thus, these fungi could be quantified by real-time qPCR with a standard curve. To do this, DNA was extracted from these pure cultures with i-genomic plant DNA extraction mini kit (Intron Biotechnology) and used to prepare the standard curves. To develop the standard curve, the DNA was diluted in serial 10-fold dilutions from 0.01 to 10^{-6} ng μl^{-1} concentration. For quantification, individual reactions per species were carried out including the standard curve (5 points) and a negative control, each sample per triplicate, following MIQE guidelines (Bustin et al., 2009). For the rest of the target fungi, only their occurrence was studied.

2.7 Bacterial and fungal quantification

Soil and rhizosphere associated with rootstock GF-677 were evaluated for DNA copy number of bacterial/fungi ratio using real-

TABLE 2 Specific primers and Taqman probes used to detect/quantify nematophagous fungi in nematode samples.

Organism	Sequence primers and probe (5′–3′)	References for primers/probe concentration and qPCR conditions
Arthrobotrys dactyloides	F: AGGTCGGTTTTGAGCTGGCTTA	Pathak et al., 2012; Campos-Herrera et al., 2019
	R: CCACCCCACCTAGAACAAGTATGT	
	P: FAM-ACCCAAGCCGGTTTTAAAGT-MGB	
Arthrobotrys oligospora	F: CGGTTTGCTGTTGCAGCTTGTT	Pathak et al., 2012; Campos-Herrera et al., 2019
	R: GGTTCACAAAGGGTTTACCAGG	
	P: FAM-CTGTCTTCCGGTTGGTAAGC-MGB	
Catenaria sp.	F: GCCGTGTAGGCAAAAATTCCGACT	Pathak et al., 2012; Campos-Herrera et al., 2019
	R: GCAGCCTGGATTGTTTGATGGCCT	
	P: FAM-TGCTCAACGTCACGAGTAAACCAACA-MGB	
Hirsutella rhossiliensis	F419: TGCGCAGTAGCTCCCAGAG	Zhang et al., 2006; Campos-Herrera et al., 2019
	R480: TTGTTTTACGGCGTGACCG	
	P442: FAM-TCGCACCGGAAACGCGGAG-TAMRA	
Gamsylella gephyropagum	F: GTCGTAACAAGGTTTCCGTAGG	Pathak et al., 2012
	R: TTGTAAAATGGGTGCCAGCG	
	P: FAM-CCAAAACATAGCTGTCGGGT-MGB	
Purpureocillium lilacinum	PLrtF: GACCCAAAACTCTTTTTGCATTACG	Atkins et al., 2005
	PLrtR: AGATCCGTTGTTGAAAGTTTTGATTCATTTGTTTTG	
	PLrt P: FAM-CCGGCGGAATTTCTTCTCTGAGTTGC-TAMRA	

(F, forward primer; R, reverse primer; P, probe).

time qPCR following the bacterial protocol and primer concentrations of Jorgensen et al. (2012) with the primers 341F (5′-CCTACGGGNGGCWGCAG-3′) (Herlemann et al., 2011) and 519R (5′-GWATTACCGCGGCKGCTG-3′) (Engelbrektson et al., 2010) in the 16S rRNA and the fungal protocol and primer concentrations of Ihrmark et al. (2012) with the primers gITS7 (5′-GTGAATCATCGAATCTTTG-3′) (Ihrmark et al., 2012) and ITS4 (5′-TCCTCCGCTTA TTGATATGC-3′) (White et al., 1990) in the ITS2 region. Real-time qPCR assays were conducted in polypropylene 96-well plates on an CFX Connect Real Time qPCR System (Bio-Rad Laboratories, Inc.). iQ™ SYBR® Green Supermix (Bio-Rad Laboratories, Inc.) with 5 ng of DNA/reaction in a final volume of 20 µl. Each sample was quantified in a triplicate reaction. Control samples without DNA template (NTC) were included in each plate in triplicate. Bovine serum albumin (BSA) (New England BioLabs, Inc.) was added at a final concentration of 300 nM to reduce the potential inhibition of humic acids and other compounds present in soil (Kreader, 1996). Melting curve analysis of the PCR products was conducted following each assay to confirm that the fluorescence signal originated from specific PCR products and not from primer dimers or other artifacts. Standard curves were constructed using purified PCR products from the 16S rRNA of *Escherichia coli* using the primers 8F and 1492R (Turner et al., 1999) and ITS products from *Rosellinia necatrix* using the primers ITS1f (Gardes and Bruns, 1993) and ITS4. PCR products were purified using GeneClean® Turbo Kit (MP Biomedicals), and the molecular weight of each purified DNA fragment was calculated based on the number of bases of the DNA fragment. Estimation of gene-copy number in each representative purified DNA fragment was based on the molecular weight in accordance with DNA Copy Number and Dilution Calculator (ThermoFisher Scientific), with copy number adjusted in a 10-fold dilution series used to generate standard curves for real-time experiments. The calibration curves were linear over eight orders of magnitude ($100–10^6$). Optical data was visualized and analyzed in CFX Maestro™ Software v. 1.1 (Bio-Rad Laboratories, Inc.). Differences of fungal:bacterial ratio, ITS and 16S copy numbers between sample type (rhizosphere, soil) and between *Meloidogyne* density (low, high) were evaluated (Wilcoxon, $p < 0.05$).

2.8 DNA metabarcoding library preparation and sequencing

Rhizosphere and soil samples were analyzed to study the bacterial and fungal diversity using a metabarcoding sequencing approach. DNA metabarcoding analyses were carried out by AllGenetics & Biology S.L. (La Coruña, Spain) (www.allgenetics.eu). The DNA extracted from soil and rhizosphere samples was adjusted to 10 ng μl^{-1} and used to amplify the V3–V4 region of bacterial 16S rRNA gene and the internal transcribed spacer 2 (ITS2) region of fungi. The PCR of the 16S rRNA region was carried out with the primers

341F (5′-CCTACGGGNGGCWGCAG-3′) (Herlemann et al., 2011) and 805R (5′-GACTACHVGGGTATCTAATCC-3′) (Herlemann et al., 2011) to amplify a fragment of approximately 420 bp. The primers ITS86F (5′-GTGAATCATCGAATCT TTGAA-3′) (Turenne et al., 1999) and ITS4 (5′-TCCTCC GCTTATTGATATGC-3′) (White et al., 1990) were used to amplify the complete fungal ITS2 region of approximately 300 bp. All primers were modified to include Illumina adapters to their 5′ ends. To prevent the amplification of the host *Prunus* DNA, a blocking primer was included in the library preparation. The blocking primer BP_Bakt805R_prunus (5′-CTAATCCCA TTTGCTCCCCTAGCTTTCGTCT-3′) was previously designed following the approach of Vestheim and Jarman (2008) with *Prunus* sp. chloroplast 16S sequences deposited in GenBank and using Geneious 11.1.5. Blocking primers were modified with a C3 (3 hydrocarbons) at the 3′ end to prevent elongation of *Prunus* sp.

For bacteria, PCRs were performed in a final volume of 12.5 µl containing 1.25 µl of template DNA, 300 nM of the primers, 6 µM of the blocking primers, 3.25 µl of Supreme NZYTaq 2x Green Master Mix (NZYTech), and ultrapure water up to 12.5 µl. The PCR conditions were as follows: 95°C for 5 min, followed by 20 cycles of 95°C for 30 s, 50°C for 45 s, 72°C for 45 s, and a final extension step at 72°C for 7 min. The oligonucleotide indices that are required for multiplexing different libraries in the same sequencing pool were attached in a second amplification step with identical conditions but only 5 cycles and 60°C as the annealing temperature. A negative control with water instead of DNA template was included in every PCR round.

For fungal library preparation, two amplification steps were also performed. First, amplifications of ITS2 region were carried out in a final volume of 12.5 µl, containing 3.25 µl of template DNA, 0.5 µM of each primer, 10 µM of the blocking primers, 3.25 µl of Supreme NZYTaq 2× Green Master Mix (NZTYech), and ultrapure water up to 12.5 µl. PCR amplifications consisted of a 5-min denaturation at 95°C, followed by 35 cycles of 30 s at 95°C, 45 s at 49°C, 45 s at 72°C, and a final extension of 7 min at 72°C. The oligonucleotide indices that are required for multiplexing different libraries in the same sequencing pool were attached in a second amplification step with identical conditions but only 5 cycles and 60°C as the annealing temperature. Negative control (no template DNA) were included in all PCRs.

To verify the fungal and bacterial libraries size, the PCR products were run on 2% agarose gels stained with GreenSafe (NZYTech). Libraries were purified using the Mag-Bind RXNPure Plus magnetic beads (Omega Biotek) following the manufacturer's instructions. Then, libraries were quantified using a Qubit dsDNA HS Assay (Thermo Fisher Scientific), and equimolar amounts from each individual sample were pooled and sequenced in a fraction of a NovaSeq PE250 flow cell (Illumina) at the AllGenetics and Biology SL facilities (La Coruña, Spain).

2.9 Sequence processing

The quality of the FASTQ files was checked with the software FastQC (Andrews, 2010), and the output was summarized with MultiQC (Ewels et al., 2016). The tool DADA2 (Callahan et al., 2016a), implemented in QIIME2 (Bolyen et al., 2019), was used to trim primers, filter reads according to their quality, denoise using the parametric error model, merge the forward and reverse reads, remove the chimeric reads, and cluster the resulting sequences into amplicon sequence variants (ASVs). In the case of fungi, due to the high length variability of the ITS2 region, together with the fact that the sequencing reads were longer than the amplicons, non-biological DNA (primers or sequencing adapters) could appear at the ends of the reads. Therefore, Cutadapt (Martin, 2011) was used to remove primer and/or adapter sequences. After checking the quality, reads were truncated at position 249 for forward reads, and at position 240 for reverse reads, for bacteria. In the case of fungi, reads were truncated at position 248 for forward reads and at position 249 for reverse reads. After processing the reads with DADA2, a table with the occurrences of each observed ASV in each sample was created. The taxonomic assignment of each ASV was conducted using a pre-trained classifier of the SILVA reference database (Quast et al., 2012) for bacteria, and the UNITE v8.3 reference database (Abarenkov et al., 2020) for fungi, using, in both cases, the *feature-classifier classify-sklearn* approach implemented in QIIME2 (Bokulich et al., 2018). A final OUT table for each combination of target region (ITS2 or 16S) and sample type (soil or rhizosphere) was generated excluding Singletons, eukaryotic sequences of chloroplast and mitochondrial origin, unidentified sequences, ASVs occurring at a frequency below 0.01% in each sample, and sequences assigned only at kingdom level. The final filtered ASV table was converted into a Biological Observation Matrix file (.biom) that was imported into R software 4.3.1 (R Core Team, 2023) using the *phyloseq* package (v1.44.0) (McMurdie and Holmes, 2013) for further analyses.

To construct the ASV-based phylogenetic trees, ASV sequences after the filtering process were aligned using MAFFT (v7.490) (Katoh and Standley, 2013). The alignment was used to generate a maximum likelihood tree in IQ-TREE (v2.2.0) (Minh et al., 2020) with 1,000 ultrafast bootstrap replicates and the SH-like approximate likelihood ratio test (Guindon et al., 2010). The best-fit models were selected by jModelTest (Darriba et al., 2012) according to the Bayesian information criterion (BIC). The model for the bacterial ASVs was GTR+F+I+G4 and for the fungal ASVs was GTR+F+G4, the GTR model with base frequencies empirically computed from the MSA (+F), with invariant sites allowed, with four categories of site-rate heterogeneity under the Gamma mode. Subsequently, phylogenetic trees were rooted at their midpoint using the midpoint.root function in the *phytools* R package (v1.9.16) (Revell, 2012).

Finally, we synthesized all data generated (ASV table, taxonomy table, phylogenetic tree, and sample data) into one phyloseq object for bacterial ASVs and another object for fungal ASVs, in R using the *phyloseq* package. The sample data set included sample information, such as locality, sample type (soil or rhizosphere), fungal:bacterial ratios, soil physicochemical properties, and abundance data of the identified nematode genera.

Data processing was done in AllGenetics & Biology S.L. (La Coruña, Spain) and the supercomputing platform in High Performance Computing Cluster provided by the Centro

Informático Científico de Andalucía, Junta de Andalucía. The original raw sequences have been deposited in the NCBI SRA archive (Bioproject: PRJNA993485).

2.10 Fungal and bacterial diversity

After taxonomic assignment of each ASV, we checked that all ASVs were assigned to phylum level and applied prevalence filtering (Callahan et al., 2016b). First, we determined the prevalence, i.e., the fraction of total samples in which an ASV was observed, and defined a prevalence threshold of 6.25% to retain phyla detected in at least two of the samples analyzed. We also removed ASVs for which no class could be assigned. Subsequently, analyses of the composition, diversity, and functions of the microbial communities were performed using R software version 4.3.1.

To explore the composition of the fungal and bacterial communities in soil and rhizosphere, bar plots were generated using the *microbiome* package (1.22.0) (Lahti and Shetty, 2012-2019) to show all phyla, orders, and families with >1% relative abundances, while phyla, orders, and families with <1% relative abundance were grouped as "other." Alpha diversity measurements, including the number of observed ASVs, Shannon diversity index, and Faith phylogenetic diversity, were calculated using the packages *phyloseq* (1.44.0) and *picante* (1.8.2) (Kembel et al., 2010). Statistical significance of differences in diversity estimates in soil and rhizosphere were tested by Wilcoxon rank-sum tests, and data were not transformed. Principal coordinate analysis of Bray–Curtis and weighted Unifrac distance matrices were used to evaluated differences among microbial communities according to sample type (soil or rhizosphere). To understand the relationship between fungal and bacterial communities in rhizosphere and soil, PCoA plots were generated using the ordinate and plot_ordination functions in *phyloseq*, and data were not transformed. To test the effect of sample type in community composition, Bray–Curtis and weighted Unifrac distance matrices were subject to permutational analysis of variance (PERMANOVA) with 999 random permutations using the adonis2 function within the *vegan* package (2.6.4) (Oksanen et al., 2007). We chose this statistical analysis because it is a powerful statistical technique to detect changes in community structure (Anderson and Walsh, 2013). Analysis of the homogeneity of variance among sample type groups was performed using the betadisper function in the *vegan* package. According to the relative abundance of genera in the fungal and bacterial community compositions, the top ranked 25 genera were selected to construct a clustering heatmap. Heatmaps were performed using the *microbiomeutilities* package (1.0.17) (Shetty and Lahti, 2023).

The linear discriminant analysis effect size (LEfSe) algorithm (Segata et al., 2011) was carried out to identify taxa, at genus level or above, that significantly differed between low and high *Meloidogyne* densities in roots. Rhizosphere and soil samples were analyzed separately. Analyses were performed using the *lefser* package (1.10.1) (Khleborodova, 2023). The threshold for the logarithmic linear discriminant analysis (LDA) score was set at 2.0 and the Wilcoxon p-value at 0.05. Results with $p < 0.05$ between groups were considered statistically significant and represented in bar plots.

The ecological guild information was extracted for each fungal ASV based on their taxonomic assignment using the FUNGuild database (Nguyen et al., 2016) with the *FUNGuildR* package (0.2.0.9) (Furneaux and Song, 2021). The assignments classified as "probable" and "highly probable" in the confidence ranking were selected and grouped into eight categories based on trophic groups and guilds: animal pathogen, arbuscular mycorrhizal, ectomycorrhizal, endophyte, endophyte-plant pathogen, fungal parasite, plant pathogen, and saprotroph. Regarding the functional analysis of bacterial communities, the software PICRUSt2 (Douglas et al., 2020) was used to perform functional predictions based on 16S rRNA gene sequencing data. Predicted Kegg Ortholog (KO) abundance data was imported into R and converted to KEGG pathway abundances using the *ggpicrust2* package (1.7.3) (Yang et al., 2023). Then, a differential abundance analysis was performed using the ALDEx2 method to determine if microbial communities in soil and rhizosphere samples from almond groves with low *Meloidogyne* densities in roots differed functionally from samples with high *Meloidogyne* densities in the roots. The KEGG pathways were also mapped to primary and secondary pathways. The primary pathways were classified into six fundamental metabolic categories: cellular processes, environmental information processing, genetic information processing, human diseases, metabolism, and organismal systems.

3 Results

3.1 Nematode community assessment and ecological analysis

A total of 41 nematode genera belonging to 27 families were identified in the rhizosphere of the six commercial almond groves studied (16 samples). The total prevalence and density of these genera are shown in Supplementary Figure 2 and Supplementary Table 1. Nematodes reported in this study belong to five trophic groups, with bacterivores and herbivores being the most diverse, both with 13 genera, followed by fungivores and predators both with 7 genera, and omnivores with only 1 genus. Bacterivores and herbivores were the most abundant trophic groups, followed by fungivores. Specifically, in four of the six almond groves, herbivores were the most abundant, and in the remaining two groves, bacterivores were the most abundant (Figure 1). Besides *Meloidogyne* spp., 12 other genera of PPNs (herbivores) were found in almond rhizosphere, including *Paratylenchus*, *Pratylenchus*, and *Xiphinema*. From these 12 genera, *Paratylenchus* was the most prevalent, found in 62.5% of the samples, followed by *Helicotylenchus*, *Merlinius* and *Tylenchorhynchus*, all three in 31.25% of the samples. Within bacterivores, *Cephalobus*, *Mesorhabditis*, *Chiloplacus*, *Acrobeles*, and *Stegelletina* were the most widespread genera, detected in 81.25%, 75.00%, 62.50%, and 56.25% of the samples, respectively. Regarding fungivores, *Filenchus*, *Aphelenchoides*, and *Aphelenchus* were the most prevalent, which

were identified in 87.50%, 75.00%, and 56.25% of the samples, respectively. Although *Aporcelaimus*, *Discolaimus*, and *Aporcelaimellus* were present in 56.25%, 31.25%, and 25.00% of the samples, predators, along with omnivores, were the least abundant trophic groups.

The MI and PPI are indicators of the ecological successional status of a soil community. The MI varied from 2.36 to 1.88. No differences ($p > 0.05$) were found between localities (Supplementary Figure 3A). Likewise, PPI did not show significant differences between localities, with values ranging from 3.16 to 2.5 (Supplementary Figure 3B). For the CI, significant differences were observed between the commercial almond groves located in Carmona and Los Palacios. The CI, indicators of organic matter decomposition mediated by fungi, ranged from 100% (in Carmona) to 17.78% (in Los Palacios) (Supplementary Figure 3C). Neither SI, indicator of soil food web complexity, nor the EI, indicator of organic matter decomposition mediated by bacteria, significantly changed between localities. The EI and SI are descriptors of food web condition; a diagram representing these indices classified soils as maturing, disturbed, and degraded. The majority of the soil samples were in the disturbed N-enriched quadrant (n = 6) and degraded–depleted quadrant (n = 6) and the other samples in the maturing N-enriched quadrant (n = 4) (Figure 2A). Only all sampling points were in the quadrant degraded and depleted Carmona field, and all points of Cordoba field were in the disturbed and N-enriched quadrant. Sample distribution in this graph was not associated to *Meloidogyne* density in roots (Figure 2B). Additionally, MI, PPI, and CI were not statistically different among the low and high *Meloidogyne* densities in roots (Supplementary Figure 4).

3.2 Physicochemical soil properties

The commercial almond groves showed statistically significant differences in several of the soil physicochemical properties studied (Supplementary Table 2). Soil pH, cation exchange capacity, as well as concentration of calcium, magnesium, potassium, and sodium, were lower in the samples located in Carmona (PR25A–PR25C) than the other sampling groves. Specifically, the soil pH in Carmona was 5.6, while in the rest of the samples, the pH was approximately 8.6. The percentage of organic matter (OM), phosphorous content (P), and carbon to nitrogen (C:N) ratio were similar in the six groves (Supplementary Table 2).

3.3 Egg-parasitic fungi isolated against *Meloidogyne* spp.

After spreading eggs extracted from almond roots in Petri dishes containing a growth-restricting medium, fungal parasites of *Meloidogyne* eggs were found in 56.25% of the samples (Table 3). The percentage of parasitized eggs by fungi ranged from 1% to 8%. Three fungal species were isolated from *Meloidogyne* eggs, specifically *Pochonia chlamydosporia*, *Purpureocillium lilacinum*, and *Trichoderma asperellum* (Figure 3). All sequences obtained for these species matched well with the accessions from the same species deposited in GenBank, showing 99%–100% similarity. In addition, the morphology of these fungal isolates agreed with that described in literature (Samson, 1974; Samuels, 1996; Evans and Kirk, 2017). The most frequent fungal species isolated was *P. chlamydosporia*, which was found in three of

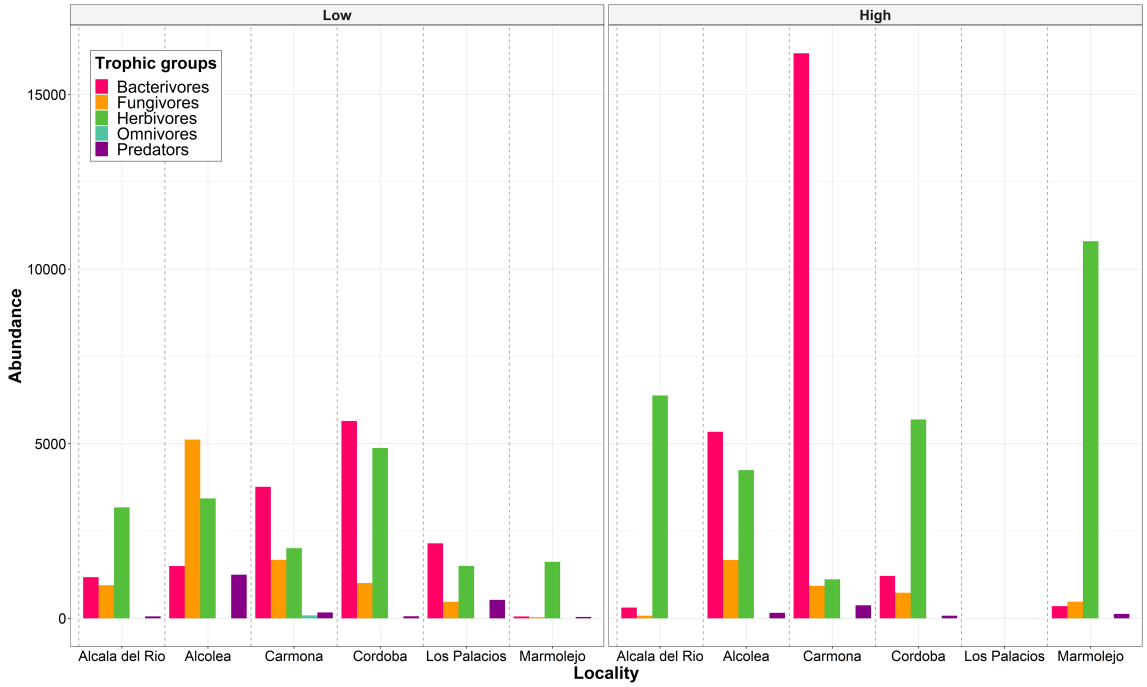

FIGURE 1
Abundance (number of individuals of each trophic group/500 cm^3 of soil) of nematode trophic groups in each locality studied separating the samples according to *Meloidogyne* density categories: low (<600 eggs per g of root) and high (>600 eggs per g of root).

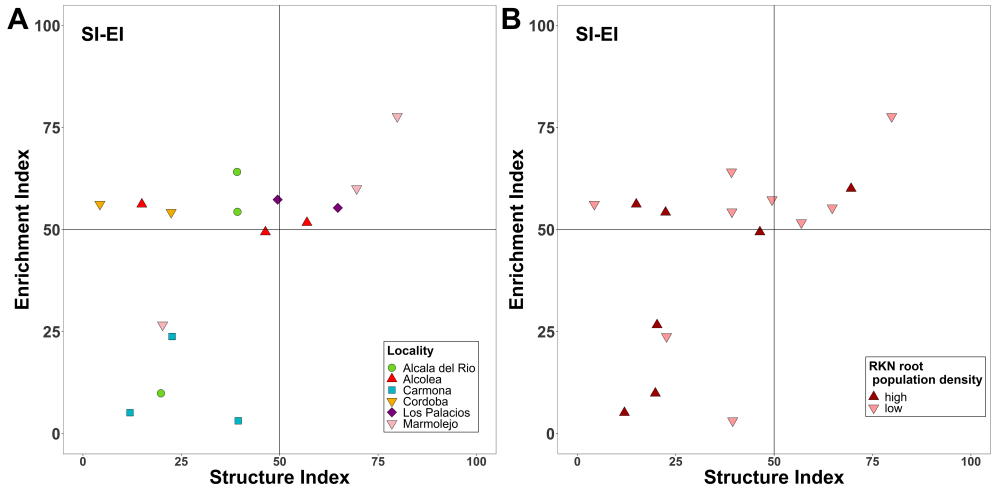

FIGURE 2
Nematode fauna profiles representing the structure and enrichment conditions of the soil food web for the different localities sampled **(A)** and for the two defined categories of *Meloidogyne* population density in roots [low (<600 eggs per g of root) and high (>600 eggs per g of root)] **(B)**.

the six commercial almond groves, specifically in Alcala del Rio, Carmona, and Marmolejo, while *P. lilacinum* and *T. asperellum* were only isolated in one grove, both in Carmona. In this study, five *P. chlamydosporia* sequences, four *P. lilacinum* sequences, and seven *T. asperellum* sequences were deposited in the GenBank database (OR801652–OR801667).

3.4 Fungal and bacterial quantification by real-time qPCR

The microbial communities were quantified by real-time qPCR of the 16S rRNA gene and ITS region. Total bacteria were quantitatively similar between rhizosphere and soil samples, with a mean abundance of 1,153,500 ± 453,021 and 1,306,000 ± 460,084 16S rRNA gene copies per 1 ng of DNA, respectively, while the fungal ITS gene copy numbers were significantly higher in rhizosphere samples (54,213 ± 46,634) than in soil samples (12,266 ± 11,226). Likewise, the fungal:bacterial ratio showed a similar trend; rhizosphere samples had a significantly higher ratio than soil samples (Supplementary Figure 5). No significant differences were found when comparing fungal and bacterial quantification data between low and high *Meloidogyne* densities ($p > 0.05$) (Supplementary Figure 5).

3.5 Detection of nematophagous fungi by real-time qPCR

Four of the six nematophagous fungi screened were detected in the nematode samples by real-time qPCR as follows: *Arthrobotrys dactyloides*, *A. oligospora*, *Catenaria* sp,. and *Purpureocillium lilacinum* (Table 3). *Purpureocillium lilacinum* was the most widespread nematophagous fungi, detected in 15 of the 16 sampling points. *Arthrobotrys dactyloides* was detected in three sampling sites, in three different almond groves, while *A. oligospora* was detected in two sampling points in the same almond grove. *Catenaria* sp. was detected only in one sample.

3.6 Metabarcoding analyses

Rarefaction curves of ITS region and 16S rRNA sequencing for all samples were constructed to assess species richness and

TABLE 3 Percentage of parasitized eggs of *Meloidogyne* spp. and samples in which target nematophagous fungi were detected by real-time qPCR.

Sample	Almond grove	Locality	*Fungal egg parasitism (%)*	*Arthrobotrys oligospora*	*Arthrobotrys dactyloides*	*Catenaria* sp.	*Purpureocillium lilacinum*
PR13	1	Córdoba	7	-[a]	–	–	+
PR15	1	Córdoba	8	–	+[b]	+	+
PR25A	2	Carmona (Sevilla)	3	–	–	–	+
PR25B	2	Carmona (Sevilla)	3	–	–	–	+
PR25C	2	Carmona (Sevilla)	3	–	–	–	+

(Continued)

10.3389/fpls.2024.1386535

TABLE 3 Continued

Sample	Almond grove	Locality	*Fungal egg parasitism (%)*	*Arthrobotrys oligospora*	*Arthrobotrys dactyloides*	*Catenaria* sp.	*Purpureocillium lilacinum*
PR61A	3	Los Palacios (Sevilla)	0	+	–	–	+
PR61C	3	Los Palacios (Sevilla)	0	+	–	–	+
PR74A	4	Marmolejo (Jaén)	0	–	–	–	+
PR77A	4	Marmolejo (Jaén)	2	–	–	–	+
PR78B	4	Marmolejo (Jaén)	0	–	–	–	–
PR90A	5	Alcalá del Río (Sevilla)	1	–	+	–	+
PR90B	5	Alcalá del Río (Sevilla)	1	–	–	–	+
PR90E	5	Alcalá del Río (Sevilla)	1	–	–	–	+
PR231B	6	Alcolea (Córdoba)	0	–	–	–	+
PR233A	6	Alcolea (Córdoba)	0	–	–	–	+
PR234	6	Alcolea (Córdoba)	0	–	+	–	+

[a]–: Not detected.
[b]+: Detected.

estimated the sequencing depth (Supplementary Figure 6). Rarefaction analysis of 16S rRNA sequences showed that two rhizospheric samples, PR74Ar and PR78Br, did not reach the plateau in species richness (Supplementary Figure 6C) and were therefore removed from the ASV table. A total of 1,932,009 and 3,091,470 reads remained for the fungal and bacterial libraries, respectively. For fungal data set, the number of sequences in each sample ranged from 14,709 to 116,075, with an average of 60,375 (standard deviation, *s.d.*: 22,081). After the quality and prevalence filtering steps, a total of 1,194 ASVs for ITS and 8,644 ASVs for 16S were obtained. For the bacterial data set, the number of sequences in each sample ranged from 19,051 to 206,974, with an average of 103,049 (*s.d.*: 28,813).

The 1,194 fungal ASVs were assigned to 13 phyla, 35 classes, 80 orders, 162 families, 301 genera, and 377 species. Ascomycota was the most abundant phylum with a relative abundance of 81.44% and

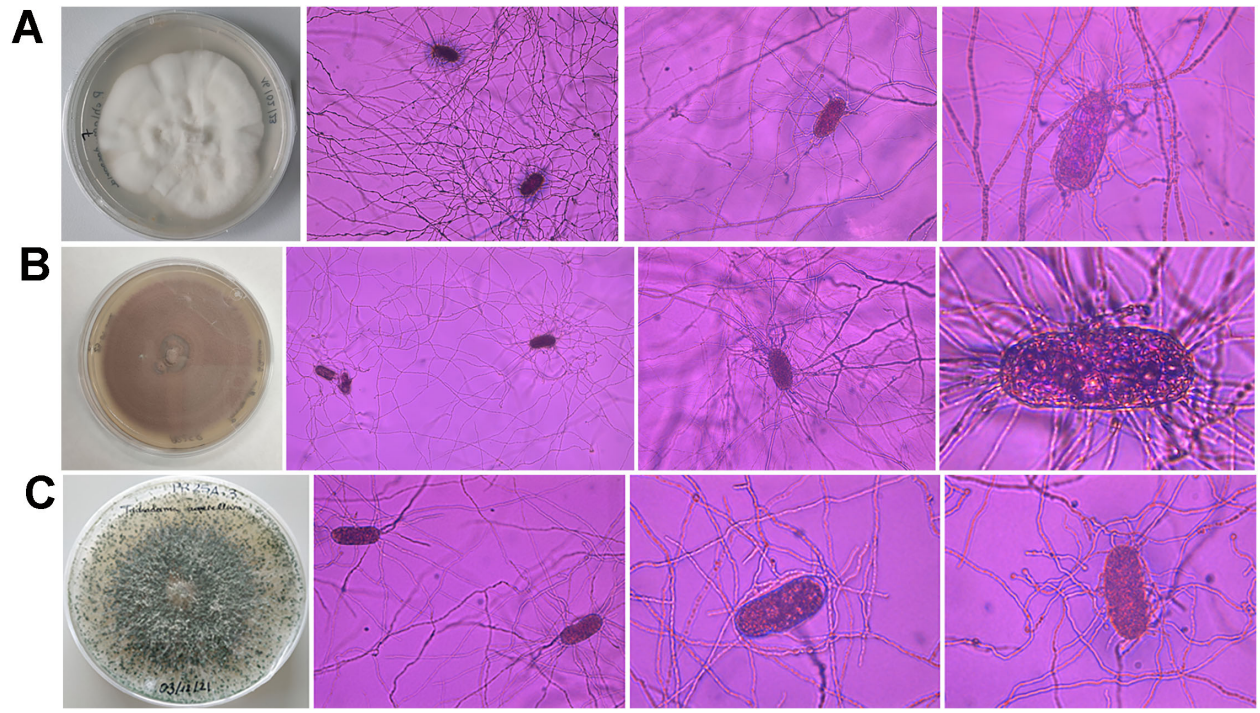

FIGURE 3
Morphological characteristics of *Pochonia chlamydosporia* **(A)**, *Purpureocillium lilacinum* **(B)**, and *Trichoderma asperellum* **(C)** colonies on PDA and *Meloidogyne* eggs parasitized by these fungi.

88.25% in rhizosphere and soil samples, respectively. Basidiomycota was the second phylum most abundant in both rhizosphere (16.31%) and soil (10.06%) samples, while the remaining 11 phyla together accounted for less than 3% of the relative abundance (Figure 4A). At the order level, eight orders accounted for almost 90% of the relative abundance, with Hypocreales being the most abundant in both rhizosphere (54.10%) and soil (51.70%) (Figure 4B). In the rhizosphere, the next seven most abundant orders were as follows: Agaricales (6.72%), Capnodiales (6.63%), Polyporales (4.29%), Sordariales (3.57%), Branch06 (3.43%), Pleosporales (3.34%), and Eurotiales (2.29%), whereas in soil, the next seven most abundant orders were as follows: Sordariales (10.02%), Capnodiales (8.03%), Agaricales (5.60%), Pleosporales (4.96%), Eurotiales (4.16), Glomerellales (3.23%), and Tremellales (1.70%). In both rhizosphere and soil samples, Nectriaceae was the most dominant fungal family with a relative abundance of 36.43% and 37.65%, respectively (Figure 4C). In soil, Chaetomiaceae (8.17%) and Cladosporiaceae (6.56%) were the second and third most abundant families, although the relative abundance of both families decreased in the rhizosphere to 2.31% and 5.04%, respectively. In contrast, the relative abundance of Bionectriaceae increased from 3.30% in the soil to 6.41% in rhizosphere samples (Figure 4C).

Regarding bacterial community composition, the 8,644 ASVs were assigned to 36 phyla, 93 classes, 216 orders, 334 families, 609 genera, and 370 species. In both sample types, Proteobacteria and Actinobacteriota were the most abundant phyla (Figure 4D). However, the relative abundance of Proteobacteria was higher in the rhizosphere (58.04%) than in the soil (27.94%) in contrast with Actinobacteriota, whose relative abundance was lower in rhizosphere samples (12.47%) than in soil samples (21.06%). Both phyla accounted for around 70% of the relative abundance in the rhizosphere. Firmicutes and Acidobacteriota were the third and fourth most abundant phyla in the soil; however, their relative abundance decreased in the rhizosphere from 12.05% to 1.99%, and from 10.17% to 4.50%, respectively (Figure 4D). In the rhizosphere, Sphingomonadales (11.91%), Rhizobiales (11.63%), and Burkholderiales (9.82%) were the most abundant orders. While the three most abundant orders in soil samples were as follows: Bacillales (9.58%), Gemmatimonadales (6.67%), and Rhizobiales (6.61%) (Figure 4E). At the family level, Sphingomonadaceae (11.96%) was the most abundant family in rhizosphere samples, followed by Steroidobacteraceae (5.65%), Rhizobiaceae (4.65%), Chitinophagaceae (4.35%), and Comamonadaceae (4.23%). In contrast, these families showed a relative abundance of less than 2% in the soil (Figure 4F). In the soil, the most abundant families were as follows: Bacillaceae (8.63%), Gemmatimonadaceae (6.71%), Rubrobacteriaceae (2.25%), Nitrosomonadaceae (2.21%), and Microscillaceae (2.17%) (Figure 4F). In both soil and rhizosphere, most orders and families showed a relative abundance of less than 1%, so these were merged into the "other" category for graphical representation of fungal and bacterial community composition.

Fungal and bacterial alpha diversity, including observed ASVs, Shannon diversity, and Faith's phylogenetic diversity (Faith's PD) indices, decreased significantly ($p < 0.05$) in rhizosphere samples compared to soil samples (Figure 5). Rhizosphere samples have significant lower fungal species richness (142 ± 60.64) than soil samples (229 ± 64.17) measured by the observed number of ASVs. Likewise, fungal community diversity, measured by Shannon index and Faith's PD, decreased in the rhizosphere. Shannon diversity index for fungi in rhizosphere samples ranged from 1.19 to 4.27 (average 2.87 ± 0.85), while in soil samples, this index ranged from 2.11 to 4.31 (average 3.43 ± 0.59). Faith's PD ranged from 11.59 to 48.94 (average 30.82 ± 10.49) in rhizosphere samples, and in soil samples, this index ranged from 21.74 to 61.62 (average 42.20 ± 8.94) (Figure 5A). Regarding bacterial community diversity, it was observed that rhizosphere samples have lower bacterial diversity than soil samples (Figure 5B). For the Shannon diversity index, the value of rhizosphere samples (5.88 ± 0.77) was lower than that of soil samples (6.72 ± 0.42). Likewise, Faith's PD was lower in rhizosphere samples (171 ± 42.23) than in soil samples (214 ± 35.26). Additionally, rhizosphere samples (171 ± 72) have lower bacterial species richness than soil samples (1,581 ± 339). Statistical comparison between low and high *Meloidogyne* densities in soil and rhizosphere samples showed no difference in any of the alpha diversity indices studied (Supplementary Figure 7).

The Bray–Curtis and weighted Unifrac distances between rhizosphere and soil samples were visualized with a principal coordinate analysis (PCoA) (Figure 6). Bray–Curtis based on PCoA showed that fungal communities were grouped according to the type of sample (Figure 6A). However, the phylogenetic diversity of the rhizosphere fungal community was not statistically different from that of the soil fungal community. UniFrac-based PCoA showed that the rhizosphere and soil fungal communities overlapped (Figure 6B). Considering weighted UniFrac distance and Bray–Curtis dissimilarity, PCoA analyses showed a separate cluster between rhizosphere bacterial community and soil bacterial community (Figures 6C, D).

The top 25 fungal and bacterial genera with the highest relative abundance were shown in the heatmaps (Figure 7) to identify similarity and differences between microbial communities according to sample type and *Meloidogyne* densities. With respect to fungi, *Fusarium*, *Cladosporium*, and *Neocosmospora* were the most relatively abundant genera. Rhizosphere fungal communities were not observed to form two different clusters between rhizosphere and soil samples (Figure 7A). Regarding bacteria, *Bacillus* and *Steroidobacter* were the most relatively abundant bacterial genera. Hierarchical clustering showed that rhizosphere samples tended to cluster together, separating the rhizosphere bacterial community from the soil community, with the exception of Carmona samples (field PR25) (Figure 7B). Some bacterial genera, such as *Novosphingobium*, *Allorhizobium–Neorhizobium–Pararhizobium–Rhizobium*, and *Sphingomonas*, showed a higher relative abundance in rhizosphere samples than in soil samples, whereas other bacterial genera had a lower relative abundance in rhizosphere samples than in soil samples, including *Skermanella*, *JG30-KF-CM45*, *Rubrobacter*, *MB-A2-108*, *Gaiella*, *Vicinamibacteraceae*, *RB41*, *bacteriap25*, and *MND1*. The genera *Acidocella* and *Burkholderia–Caballeronia–Paraburkholderia* are clearly associated with acidic soil in Carmona (field PR25).

To identify fungal and bacterial taxa associated with *Meloidogyne* densities, LEfSe analyses were conducted. Different fungal and

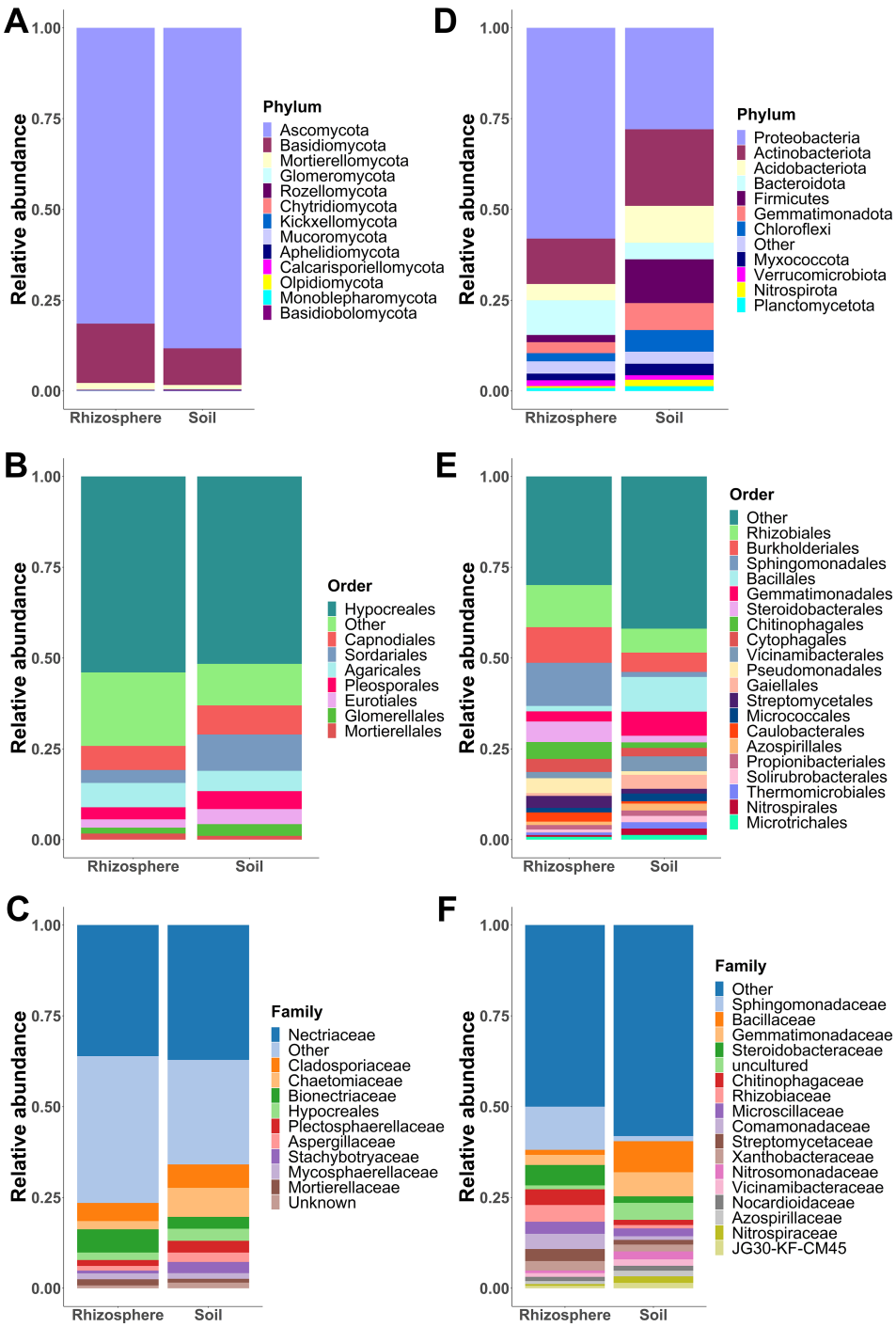

FIGURE 4
Fungal and bacterial community composition. Relative abundances of fungal phyla **(A)**, orders **(B)**, and families **(C)** pooled by sample type (soil and rhizosphere). Relative abundances of bacterial phyla **(D)**, orders **(E)**, and families **(F)** grouped by sample type (soil and rhizosphere). Phyla, orders, and families with a relative abundance greater than 1% are shown, while those with a relative abundance less than 1% are merged as "others.".

bacterial taxa were detected characterizing samples with low and high *Meloidogyne* density depending on the type of sample, rhizosphere, or soil. In the rhizosphere, no fungal taxon was selected as differentially abundant between samples with low and high *Meloidogyne* densities. In soil samples, two fungal genera (*Mycosphaerella* and *Sporobolomyces*) and one class (Sordariomycetes) were enriched in samples with low *Meloidogyne* densities, whereas one genus (*Cephaliophora*) and one order (Tremellales) were significantly more abundant in samples with high *Meloidogyne* densities (Supplementary Figure 8A). The rhizosphere of samples with low *Meloidogyne* densities was characterized by the predominance of five bacterial genera (*Arthrobacter*, *PAUC26f*, *Planctomycetales*, *Tagaea*,

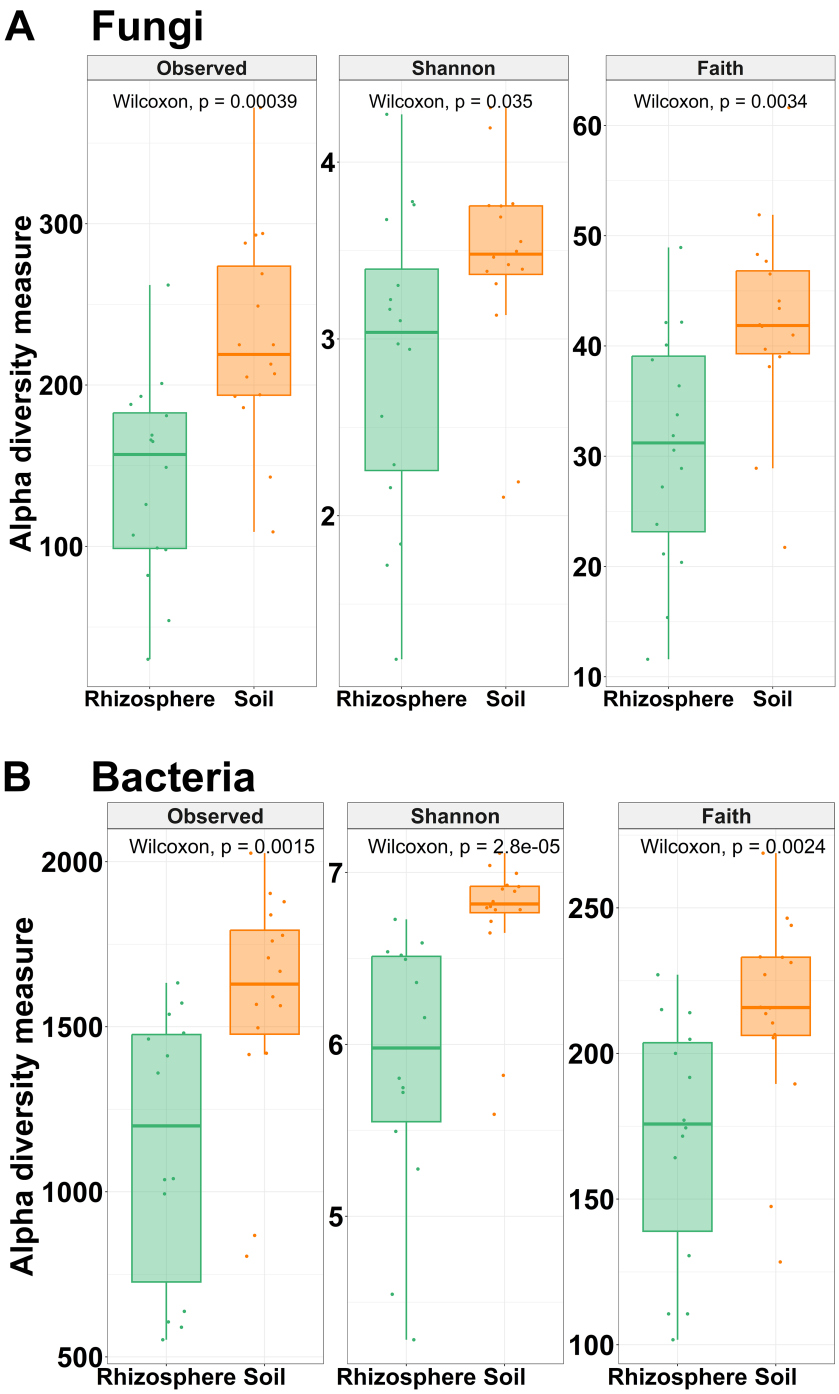

FIGURE 5
Alpha diversity. Box plots illustrating the differences in the three metrics of alpha diversity (observed ASVs, Shannon diversity index, and Faith's phylogenetic diversity index) of the fungal **(A)** and bacterial **(B)** communities between soil and rhizosphere samples. Wilcoxon rank-sum tests between soil and rhizosphere samples are shown. All comparisons were statistically significant by Wilcoxon rank-sum tests ($p < 0.05$).

and *Virgisporangium*) and one family (Xanthomonadaceae), while three bacterial genera (*Aestuariicella*, *Cellvibrio*, and *Prosthecobacter*) were enriched in the rhizosphere of samples with high *Meloidogyne* density (Supplementary Figure 8B). Finally, only two bacterial genera (*Clostridium sensu stricto 8* and *Nitrososphaeraceae*) were identified as predominant in soil samples with low *Meloidogyne* density, whereas the soil of samples with high *Meloidogyne* density was characterized by the abundance of seven bacterial genera (*Dyadobacter*, *Fluviicola*, *Niabella*, *Permianibacter*, *Polyangium brachysporum group*, *Promicromonospora*, and *Pseudogulbenkiania*) (Supplementary Figure 8C).

The nematophagous fungi detected by real-time qPCR and isolated from *Meloidogyne* eggs (Table 3) were compared with those identified by high-throughput sequencing (Supplementary Figure 9). *Arthrobotrys dactyloides*, *A. oligospora*, *Catenaria* sp., and *P. lilacinum* were detected in the same samples by both real-time qPCR and metabarcoding. *Purpureocillium lilacinum* and *Pochonia*

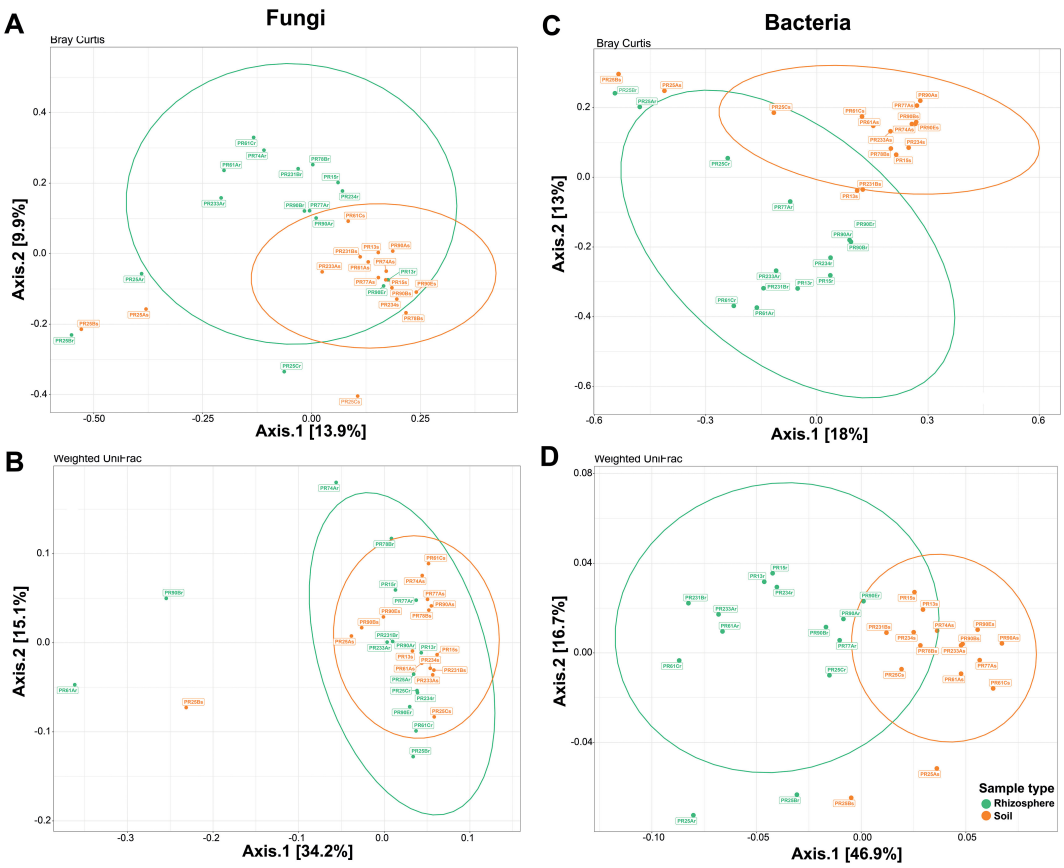

FIGURE 6
Beta diversity ordinations of the fungal and bacterial communities. Principal coordinate analysis (PCoA) ordinations of the fungal community based on Bray–Curtis dissimilarity **(A)** and weighted UniFrac distance **(B)** between soil (orange) and rhizosphere samples (green). PCoA ordinations of the bacterial community based on Bray–Curtis dissimilarity **(C)** and weighted UniFrac distance **(D)** between soil and rhizosphere samples. Bray–Curtis dissimilarity beta diversity measure for fungal communities was statistically significant (p = 0.003 by PERMANOVA), whereas weighted UniFrac distance beta diversity measure for fungal communities was not statistically significant (p = 0.233 by PERMANOVA). Both beta diversity measures for bacterial communities were statistically significant (p = 0.001 by PERMANOVA).

chlamydosporia were isolated from *Meloidogyne* eggs in one and three almond groves, respectively, although both species were detected in all almond groves by metabarcoding, such as *Trichoderma asperellum*, which was identified parasitizing *Meloidogyne* eggs in one almond grove, but it was detected in three groves by metabarcoding. It should be noted that *T. asperellum* was isolated from *Meloidogyne* eggs in the almond grove where a higher abundance of reads assigned to this species was detected, while the other two almond groves where this species was detected by metabarcoding showed a lower abundance of reads (Supplementary Figure 9).

3.7 Functional analyses

A total of 830 fungal ASVs (69.51% of the total filtered ASVs) were assigned to any guild and trophic mode. After excluding assignments with a confidence of "possible," 565 ASVs (47.32% of the total filtered ASVs) were considered. These ASVs were assigned to seven trophic modes and 42 guilds, which were merged into eight fungal functional guilds: animal pathogen, arbuscular mycorrhiza, ectomycorrhiza, endophyte, endophyte-plant pathogen, fungal parasite, plant pathogen, and saprotroph. Among the eight guilds defined here, most fungi were classified into the saprotroph guild, indicating a higher ecosystem function related to decomposition (Figure 8). Saprotrophs were the most abundant guild with a relative abundance from 17.37% to 95.49% (average 55.46%), followed by endophytes (relative abundance from 0% to 48.35%, average 13.87%), plant pathogens (relative abundance from 0.09% to 52.31%, average 10.63%), endophyte-plant pathogens (relative abundance from 0.07% to 25.52%, average 8.27%), and animal pathogens (relative abundance from 0.09% to 30.58%, average 14.51%), while fungal parasites, ectomycorrhizae, and arbuscular mycorrhizae were found in low frequency, with relative abundances of 0%–18.09% (average 3.97%), 0%–10.94% (average 1.07%), and 0%–4.82% (average 0.48%), respectively. Saprotrophs showed an increasing trend with *Meloidogyne* density. The relative abundance of saprotrophs was higher in samples with high *Meloidogyne* densities, whereas plant pathogens and endophyte-plant pathogens showed higher relative abundance in samples with low *Meloidogyne* density (Figure 8).

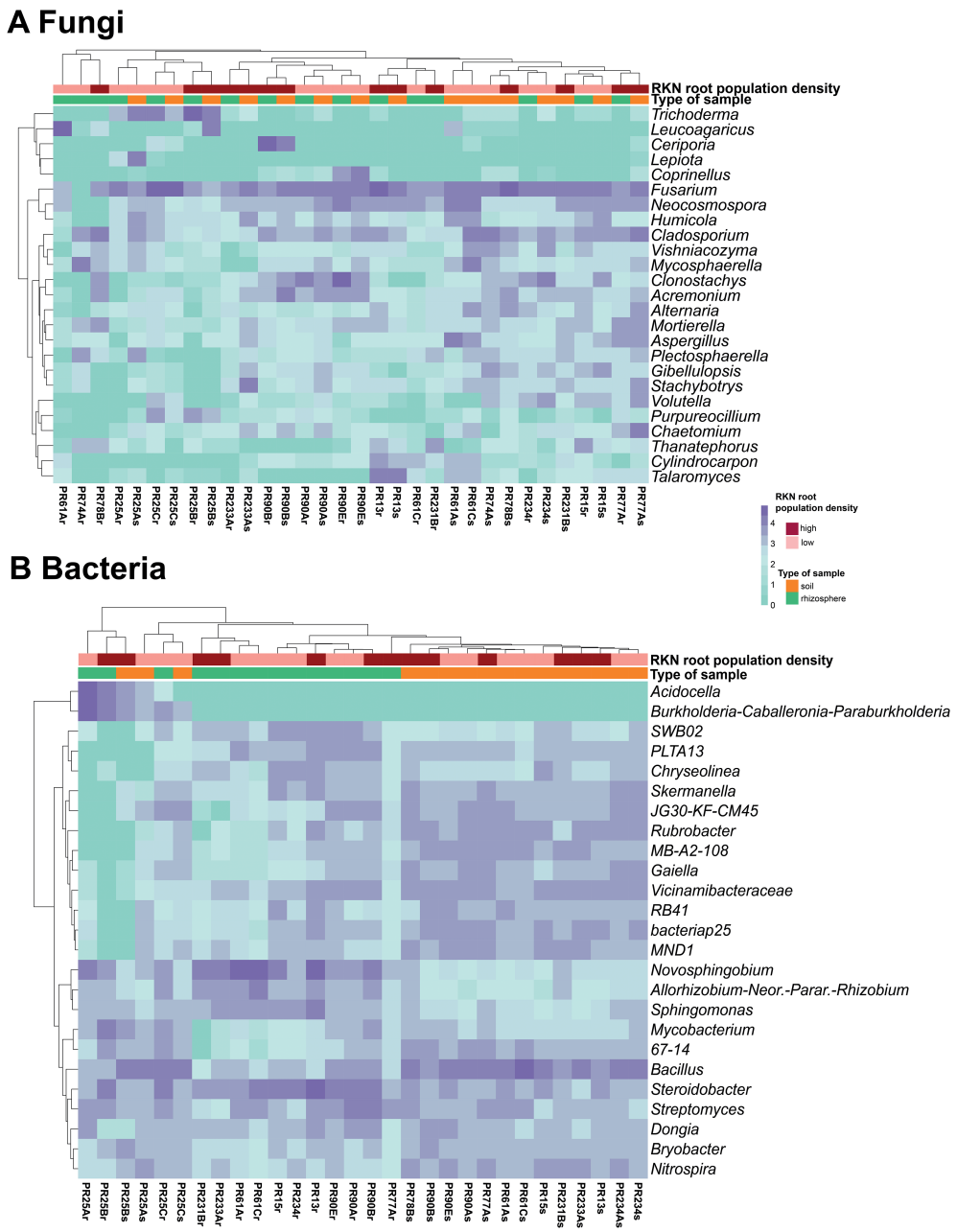

FIGURE 7
Heatmap of relative abundance (log_{10} transformed) of the 25 most abundant taxa at the genus level of fungal **(A)** and bacterial **(B)** microbiota composition. The horizontal clustering indicates the similarity of genus richness in different samples. The color of heatmap displays the relative abundance of each taxon across all samples.

Functional gene annotations predicted by PICRUSt2 identified a total of six primary pathways and 41 secondary pathways. The relative abundance of KEGG primary pathways are shown in Supplementary Figure 10, which illustrates that the predicted functions at all samples were dominated by metabolism-related pathways. Specifically, metabolism-related pathways exhibited a relative abundance from 68.53% to 71.08% (average 70.01%). In particular, within the primary metabolism-related pathway, carbohydrates and amino acid metabolism pathways were the dominant secondary pathways. The second and third most abundant primary pathways were those related to genetic information processing (relative abundance from 11.93% to 14.76%, average 13.43%) and environmental information processing (relative abundance from 8.79% to 10.77%, average 9.82%), while pathways related to cellular processes (relative abundance from 3.45% to 4.63%, average 3.87%), human diseases (relative abundance from 1.30% to 2.25%, average 1.69%), and organismal systems (relative abundance from 1.12% to 1.27%, average 1.18%) accounted less than 10% of relative abundance. No trend was observed in the relative abundance of the bacterial functional predictions with respect to *Meloidogyne* density levels (low–high). The differential abundance analysis performed with

the *ggpicrust2* package revealed no statistically significant differences ($p > 0.05$) in KEGG pathways between low and high *Meloidogyne* densities.

4 Discussion

Control methods and management strategies against RKNs include prevention measures, methods to reduce nematode populations, such as crop rotation, solarization, nematicides, resistant/tolerant rootstocks, and biological control. Knowledge of soil and rhizosphere microbiota associated with almond crops, as well as their interactions with *Meloidogyne* spp., is essential to stablish new sustainable pest management strategies. Only a few researches are trying to understand the relationships of soil and root microorganisms (bacterial and fungi) with *Meloidogyne* plant infection from different point of views, such as temporal (Yergaliyev et al., 2020), nematode density (Zhou et al., 2019; Lu et al., 2023), and microbiomes in the root, soil, and nematode (Cao et al., 2015; Tian et al., 2015; Toju and Tanaka, 2019; Lamelas et al., 2020; Masson et al., 2020; Yergaliyev et al., 2020). Yergaliyev et al. (2020) found that bacterial gall communities differed from root segments lacking the gall in eggplant, and this structure is maintained throughout the crop season. These bacteria were modulated in connection with root structure modifications, polysaccharide metabolism, and chitin metabolism (Yergaliyev et al., 2020). Bacteria in the gall are often found in hypotoxic and anaerobic environments, and this could lead to infective juveniles to select uninfected root regions (Yergaliyev et al., 2020). The diversity of the rhizospheric bacteria gradually changed with the increasing severity of RKN infection in tobacco plants (Lu et al., 2023). However, all of these studies are based on herbaceous plants (many of them using tomato). This research provides some new insights into the *Meloidogyne* and plant relationships in mature deciduous woody trees (almond grafted into the hybrid rootstock GF-677) with different levels of *Meloidogyne* density in roots and their interaction with soil microbiota, which has not been explored to our knowledge. Deciduous woody trees have some different ecological traits vs horticultural crops, such as negligent root growth during a period of time (winter) and pushes of root growth during spring and summer. Additionally, rootstocks are classified by vigor, and the main susceptible hybrid rootstock used in Spain (GF-677) is classified as vigorous. The holistic point of this paper (soil nematode, fungal and bacterial soil and rhizosphere densities, bacterial and fungi diversity, and percentage of different taxa using metabarcoding, specific real-time qPCR to detect and quantify biocontrol agents in soil nematodes and parasitism levels in eggs of our samples) gives data and cues about the processes occurring in the rhizosphere and soil niches among different microorganisms.

Our selected almond groves showed soil degradation in the majority of sampling points based on the data obtained analyzing the nematode communities. Nematodes represent several trophic groups, fulfill important roles in ecosystem processes, and respond rapidly to environmental disturbance with good ecological indices for their analysis (Neher, 2001; Du Preez et al., 2022). In this sense,

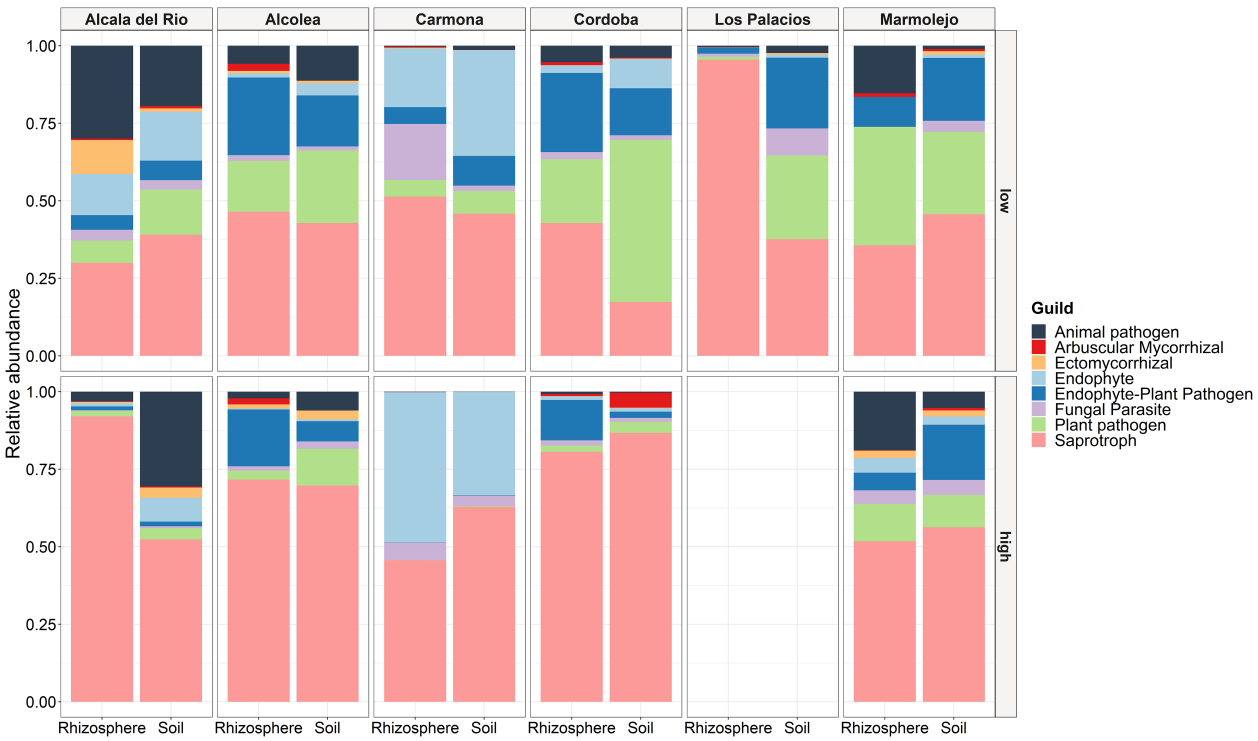

FIGURE 8
Relative abundance of fungal functional guilds between different localities, type of sample (soil and rhizosphere), and *Meloidogyne* population density in roots [low (<600 eggs per g of root) and high (>600 eggs per g of root)].

the densities of predatory nematodes were not related with the levels of *Meloidogyne* in soil or in the roots. This could be related to more susceptibility to these K-strategist nematodes with a longer generation time of months, producing few but large eggs, and they cannot rapidly respond numerically to new food resources (Bongers and Bongers, 1998). In this case, the soil movement in the grove to create flattening and grooves and the intensification of the almond crop with irrigation and high amounts of fertilizers and chemicals through drip irrigation for several years (during the tree life) could change the soil ecosystem for these sensitive microorganisms and other microbes in the soil (i.e., BCAs). Additionally, the biocontrol effects in perennial crops must be maintained during long periods of time, and in some cases, these crops have deeper root distribution than annuals, which means that BCAs need to operate deeper complicating the action of some biocontrol agents (Stirling, 2014). In this sense, the levels of fungal parasites of *Meloidogyne* eggs were found in a good prevalence (56.25% of the samples), but in a low incidence parasitizing eggs in the roots (from 1% to 8%). This low level of egg infections has been related with the size of the gall and the root infection levels, in which bigger galls creates a more protected environment for eggs in the egg mass than in smaller galls with more exposed egg masses to the soil (Kerry, 2000), or the depth at which the *Prunus* rootstock roots are found maybe are not coupled with these biocontrol agent's requirements. Additionally, in all groves, the drip irrigation is the way to irrigate and fertilize plants and where high concentrations of chemicals could be found, which could affect the establishment of these biocontrol agents. In some fewer intensive crops in the area of study, such as olive, the irrigation increased the abundance (not the presence) of *P. lilacinum* and *Hirsutella rhossiliensis* (Campos-Herrera et al., 2022). Stirling et al. (1979) found that *Dactylella oviparasitica* controlled the infection of *Meloidogyne* spp. in the rootstock Lovell in California. In our sampling, the fungal egg parasitism was conducted by *P. chlamydosporia*, *P. lilacinum*, and *Trichoderma asperellum*. The most frequent fungal species isolated was *P. chlamydosporia*, which was found in three of the six (50%) commercial almond groves. Surprisingly, even with the prevalence of *P. lilacinum* in all sampled fields and at different *Meloidogyne* levels detected by real-time qPCR in the extracted soil nematodes, the controlling effect in *Prunus* rootstock-embedded *Meloidogyne* egg masses was low. *Pupureocillium lilacinum* has been effective using 7.5×10^3 or 1×10^4 chlamydospores gram of soil in pot experiments from a strain isolated in peach against an inoculum of second-stage juveniles of *M. javanica* (Saeed et al., 2023). We could suggest that *P. lilacinum* did not colonize the *Prunus* trees, or other consortia of microorganisms reduce the ability to infect egg masses and nematodes. As mentioned before, the position of the egg masses in woody plants could differ and reduce the penetration efficacy. Ratios between fungi and bacteria are also showing a bacterial-dominated environment in *Prunus* groves managed conventionally, with the exception of Carmona grove, which has a very low pH and high levels of sand, which could induce the presence of a more dominating fungi environment.

According to the nematode community analysis, most of the soils sampled were classified as disturbed or degraded soils. Another measure that can be used as indicator of soil status is the fungal:bacterial ratio. The low fungal:bacterial ratio of our samples (ranging from 0.0034 to 0.092) would also indicate the low soil quality of the sampled almond groves. Fungal-dominated ecosystems can sequester more carbon (C) than bacterial-dominated communities and have been associated with a qualitative and quantitative enhancement of organic matter and greater self-regulation (Bardgett and McAlister, 1999; Six et al., 2006). Therefore, these results and those of a previous study (Clavero-Camacho et al., 2024) showed that the intensification of the almond crop in recent years could increase the damage of PPN and reduce the soil quality. To improve the soil quality of almond groves in Spain, practices, such as reduced tillage or no-tillage, reduction of agrochemicals, introduction of organic farming practices, or cover crops, are needed to increase the microbial biomass toward a fungal-dominated community and thus increase C sequestration (Six et al., 2006).

The molecular tools used in this study, including real-time qPCR and metabarcoding by high-throughput sequencing, allowed the identification of nematophagous fungi in the rhizosphere and soil of GF-677 almond rootstocks, and with both techniques, we obtained identical results. Some of these fungi were isolated from *Meloidogyne* eggs, thus confirming that these can act as parasites of root-knot nematodes. The presence in rhizosphere and soil samples of fungi isolated by spreading *Meloidogyne* eggs on a growth-restricting medium was confirmed by molecular tools. However, some nematophagous fungi were identified in some samples by real-time qPCR and metabarcoding, but these were not isolated from *Meloidogyne* eggs. This could be due to the extraction process of *Meloidogyne* eggs, as the egg masses cannot be handpicked because of the hardness of the woody roots of *Prunus*. On the other hand, fungi, such as *P. chlamydosporia* and *P. lilacinus*, are saprophytes, so these can grow on a wide range of organic materials (Stirling, 2014). Therefore, the study of the parasitism of *Meloidogyne* eggs may be useful to confirm that these fungi act as nematophagous fungi.

There are important diversity and composition differences between the rhizoplane and the soil microbiota in the sampled groves. The lower diversity found in the rhizoplane could be associated to a selection of microorganism by the root and the bigger soil amount included in the soil sample (approximately 0.5 g). Additionally, the majority of the ASVs are shared between the rhizoplane and the soil suggesting that additionally, through the selection by the plant, many of the microbial species came from the nearby soil (Berg and Smalla, 2009). The fungal phyla Ascomycota and Basidiomycota and bacterial phyla Proteobacteria, Actinobacteriota, Acidobacteriota, and Bacteroidota were dominant in both soil and rhizosphere. These results are in agreement with those reported in a previous study on the soil microbial community of almond crops under different management strategies (Camacho-Sanchez et al., 2023). The fungal orders Hypocreales, Capnodiales and Sordariales, and fungal families Nectriaceae, Cladosporiaceae, and Chaetomiaceae were also dominant in this previous study (Camacho-Sanchez et al., 2023), while the dominant bacterial orders and families found in our study differ from those reported by Camacho-Sanchez et al. (2023). In our research, the bacterial orders Rhizobiales, Burkholderiales,

Sphingomonadales, and Bacillales, and bacterial families Sphingomonadaceae, Bacillaceae, and Gemmatimonadaceae stood out, whereas the orders Vicinamibacterales, Gemmatimonadales, and Chitinophagales, and the families Gemmatimonadaceae, Vicinamibacteraceae, and Chitinophagaceae were reported as dominant by Camacho-Sanchez et al. (2023). Our sampling is geographically wider than that of Camacho-Sanchez et al. (2023), which could also explain the difference patterns in the levels and prevalence of some microbial interacting with *Prunus* roots. Our results showed a significant variation in fungal and bacterial diversity, both alpha and beta diversity, that could be attributed to the type of sample (rhizosphere or soil). The geographical location of the samples probably affects the diversity and composition of fungal and bacterial communities more than the *Meloidogyne* density. PCoA analyses showed that samples of the same almond groves tended to cluster together. In particular, Carmona samples (PR25) appear separated from the rest of the samples, which could be due to the different soil psychochemical properties. In addition, these samples showed differences in community composition, specifically, some bacterial genera were more abundant (*Acidocella* and *Burkholderia–Caballeronia–Paraburkholderia*) and associated with acidic soils (Kishimoto et al., 1995; Hetz and Horn, 2021), while other genera presented a low abundance (*SWB02*, *PLTA13*, *Chryseolinea*, *Skermanella*, *JG30-KF-CM45*, *Rubrobacter*, *MB-A2-108*, *Gaiella*, *Vicinamibacteraceae*, *RB41*, *bacteriap25*, and *MND1*) in these samples. Additionally, for the vigorous hybrid rootstock GF-677 that could tolerate better the *Meloidogyne* parasitism than other horticultural crops, such as tomato, our sampling is based on natural infected roots in which different infection timings could dilute the response to the plant and, in this sense, affect the plant response, which could conduct different exudates and relationships with the soil microbiota. However, several fungal and bacterial taxa, and different fungal functions could be found as differential in low and high levels of *Meloidogyne* eggs in the root. The increase in saprotrophic function in fungal community in soil and rhizosphere at high levels of nematodes infecting the roots (with the exception of rhizosphere in acidic soils in Carmona samples and similar levels of this function in the soils of Marmolejo samples) indicates that the plant is increasing the levels of nutrients in the roots, and the nematode feeding sites are creating a sink for photoassimilates. Carbon partitioning analysis showed that nematodes are strong metabolic sinks and significantly change the carbon distribution pattern in soybean *Meloidogyne*-infected plants (Carneiro et al., 1999). However, this differential response of different functions is not retained for bacteria in low and high levels of *Meloidogyne* in the roots. Only a few fungi and bacterial differential taxonomic groups were found associated with different levels of *Meloidogyne* in the rhizosphere and the soil. The highly different microbiota found between the sampled groves (Figure 6) could make this analysis difficult to find differential genera between high and low levels of *Meloidogyne*. However, this specific data about taxa differentiation is difficult to explain because we could not find a clear trend in the large diversity of functions found in these fungi and bacteria taxonomic groups. Specifically, ecological constraints or competence among other species in the ecosystem for each species could influence in their selection.

In conclusion, this work explores the effects of soil microbiota, nematodes, and BCAs in several almond fields infected with different gradient of *Meloidogyne* infecting almond roots. The data showed the scarce impact of BCAs and predator nematodes in conventional almond production to the regulation of *Meloidogyne* in the field, even with their presence in the field. The data also showed that *Meloidogyne* infection does not change dramatically the root microbiome in adult trees, probably because of the vigorous growth of the susceptible hybrid rootstock GF-677. However, fungal saprotrophism function in the microbiome is altered by the infection of the nematode at high levels in rhizosphere and soil. This study reveals the soil complexity in field experiments and the need for a better understanding of the underground relationship between plant–fungi–bacteria–nematodes to choose better practices than promote biocontrol of *Meloidogyne* in the field.

Data availability statement

The datasets presented in this study can be found in online repositories. The names of the repository/repositories and accession number(s) can be found below: https://www.ncbi.nlm.nih.gov/, Bioproject: PRJNA993485; https://www.ncbi.nlm.nih.gov/, OR801652-OR801667.

Ethics statement

The manuscript presents research on animals that do not require ethical approval for their study.

Author contributions

IC-C: Writing – original draft, Writing – review & editing. AR-C: Writing – original draft, Writing – review & editing. CC-N: Writing – original draft, Writing – review & editing. PC: Writing – original draft, Writing – review & editing, Conceptualization, Funding acquisition. JP-R: Conceptualization, Funding acquisition, Writing – original draft, Writing – review & editing.

Funding

The author(s) declare financial support was received for the research, authorship, and/or publication of this article. This research was supported by grant RTI2018-095925-A-100, "Interactions among soil microorganisms as a tool for the sustainability of the resistance of rootstocks fruit trees against plant-parasitic nematodes" funded by the Ministry of Science and Innovation (MCIN) and by the European Regional Development Fund (ERDF) "A way of making Europe". This work was also supported by Junta de Andalucia, Qualifica Project (QUAL21_023 IAS).

Acknowledgments

The authors thank J. Martín Barbarroja and G. León Ropero from IAS-CSIC for their excellent technical assistance. IC-C is a recipient of a grant (PRE2019-090206) funded by the European Social Fund (ESF) "Investing in your future." AR-C is a recipient of a postdoctoral grant for the requalification of the Spanish University System 2021–2023 (modality "Margarita Salas") and financed by Next Generation EU (NGEU) funding through the Spanish Ministry of Universities.

Conflict of interest

The authors declare that the research was conducted in the absence of any commercial or financial relationships that could be construed as a potential conflict of interest.

The author(s) declared that they were an editorial board member of Frontiers, at the time of submission. This had no impact on the peer review process and the final decision.

Publisher's note

Supplementary material

The Supplementary Material for this article can be found online at: https://www.frontiersin.org/articles/10.3389/fpls.2024.1386535/full#supplementary-material

References

Abarenkov, K., Zirk, A., Piirmann, T., Pöhönen, R., Ivanov, F., Nilsson, R. H., et al. (2020). *UNITE QIIME release for Fungi. Version 04.02.2020* (UNITE Community). doi: 10.15156/BIO/786385

Abd-Elgawad, M. M. M. (2021). Optimizing safe approaches to manage plant-parasitic nematodes. *Plants* 10, 1911. doi: 10.3390/plants10091911

Abd-El-Khair, H., El-Nagdi, W. M. A., Youssef, M. M. A., Abd-Elgawad, M. M. M., and Dawood, M. G. (2019). Protective effect of *Bacillus subtilis*, *B. pumilus*, and *Pseudomonas fluorescens* isolates against root knot nematode *Meloidogyne incognita* on cowpea. *Bull. Natl. Res. Centre* 43, 64. doi: 10.1186/s42269-019-0108-8

Alcañiz, E., Pinochet, J., Fernández, C., Esmenjaud, D., and Felipe, A. (1996). Evaluation of *Prunus* rootstocks for root-lesion nematode resistance. *HortScience* 31, 1013–1016. doi: 10.21273/HORTSCI.31.6.1013

Allison, L. E., and Moodie, C. D. (1965). "Carbonate," in *Methods of Soil Analysis. Part 2*. Ed. A. G. Norma (American Society of Agronomy, Madison, Wisconsin, USA), 1379–1396.

Anderson, M. J., and Walsh, D. C. I. (2013). PERMANOVA, ANOSIM, and the Mantel test in the face of heterogeneous dispersions: what null hypothesis are you testing? *Ecol. Monogr.* 83, 557–574. doi: 10.1890/12-2010.1

Andrews, S. (2010). *FastQC: a quality control tool for high throughput sequence data*. Available online at: https://www.bioinformatics.babraham.ac.uk/projects/fastqc/ (Accessed April 21, 2024).

Aranda, S., Montes-Borrego, M., Jiménez-Díaz, R. M., and Landa, B. B. (2011). Microbial communities associated with the root system of wild olives (*Olea europaea* L. subsp. *europaea* var. *sylvestris*) are good reservoirs of bacteria with antagonistic potential against *Verticillium dahliae*. *Plant Soil* 343, 329–345. doi: 10.1007/s11104-011-0721-2

Atkins, S. D., Clark, I. M., Pande, S., Hirsch, P. R., and Kerry, B. R. (2005). The use of real-time PCR and species-specific primers for the identification and monitoring of *Paecilomyces lilacinus*. *FEMS Microbiol. Ecol.* 51, 257–264. doi: 10.1016/j.femsec.2004.09.002

Bardgett, R. D., and McAlister, E. (1999). The measurement of soil fungal:bacterial biomass ratios as an indicator of ecosystem self-regulation in temperate meadow grasslands. *Biol. Fertil. Soils* 29, 282–290. doi: 10.1007/s003740050554

Baumgartner, K., Coetzee, M. P. A., and Hoffmeister, D. (2011). Secrets of the subterranean pathosystem of *Armillaria*. *Mol. Plant Pathol.* 12, 515–534. doi: 10.1111/j.1364-3703.2010.00693.x

Berg, G., and Smalla, K. (2009). Plant species and soil type cooperatively shape the structure and function of microbial communities in the rhizosphere. *FEMS Microbiol. Ecol.* 68, 1–13. doi: 10.1111/j.1574-6941.2009.00654.x

Boag, B. (1993). Standardisation of ecological terms in nematology. *Fundam. Appl. Nematol.* 16, 190–191.

Bokulich, N. A., Kaehler, B. D., Rideout, J. R., Dillon, M., Bolyen, E., Knight, R., et al. (2018). Optimizing taxonomic classification of marker-gene amplicon sequences with QIIME 2's q2-feature-classifier plugin. *Microbiome* 6, 90. doi: 10.1186/s40168-018-0470-z

Bolyen, E., Rideout, J. R., Dillon, M. R., Bokulich, N. A., Abnet, C. C., Al-Ghalith, G. A., et al. (2019). Reproducible, interactive, scalable and extensible microbiome data science using QIIME 2. *Nat. Biotechnol.* 37, 852–857. doi: 10.1038/s41587-019-0209-9

Bongers, T., and Bongers, M. (1998). Functional diversity of nematodes. *Appl. Soil Ecol.* 10, 239–251. doi: 10.1016/S0929-1393(98)00123-1

Bower, C. A., Reitemeier, R. F., and Fireman, M. (1952). Exchangeable cation analysis of saline and alkali soils. *Soil Sci.* 73, 251–262. doi: 10.1097/00010694-195204000-00001

Bremner, J. M. (1965). "Total Nitrogen," in *Methods of Soil Analysis: part 2 chemical and microbiological properties*. Ed. A. G. Norma (American Society of Agronomy, Wisconsin), 1149–1178.

Browne, G. T. (2017). Resistance to *Phytophthora* species among rootstocks for cultivated *Prunus* species. *HortScience* 52, 1471–1476. doi: 10.21273/hortsci10391-17

Bustin, S. A., Benes, V., Garson, J. A., Hellemans, J., Huggett, J., Kubista, M., et al. (2009). The MIQE guidelines: minimum information for publication of quantitative real-time PCR experiments. *Clin. Chem.* 55, 611–622. doi: 10.1373/clinchem.2008.112797

Callahan, B. J., McMurdie, P. J., Rosen, M. J., Han, A. W., Johnson, A. J. A., and Holmes, S. P. (2016a). DADA2: High-resolution sample inference from Illumina amplicon data. *Nat. Methods* 13, 581–583. doi: 10.1038/nmeth.3869

Callahan, B. J., Sankaran, K., Fukuyama, J. A., McMurdie, P. J., and Holmes, S. P. (2016b). Bioconductor workflow for microbiome data analysis: from raw reads to community analyses. *F1000Research* 5, 1492. doi: 10.12688/f1000research.8986.2

Camacho-Sanchez, M., Herencia, J. F., Arroyo, F. T., and Capote, N. (2023). Soil microbial community responses to different management strategies in almond crop. *J. Fungi* 9, 95. doi: 10.3390/jof9010095

Campos-Herrera, R., Blanco-Pérez, R., Bueno-Pallero, F. Á., Duarte, A., Nolasco, G., Sommer, R. J., et al. (2019). Vegetation drives assemblages of entomopathogenic nematodes and other soil organisms: Evidence from the Algarve, Portugal. *Soil Biol. Biochem.* 128, 150–163. doi: 10.1016/j.soilbio.2018.10.019

Campos-Herrera, R., Palomares-Ruis, J. E., Blanco-Pérez, R., Rodríguez-Martín, J. A., Landa, B. B., and Castillo, P. (2022). Irrigation modulates entomopathogenic nematode community and its soil food web in olive groves under different agricultural managements. *Agricult. Ecosyst. Environ.* 337, 108070. doi: 10.1016/j.agee.2022.108070

Cao, Y., Tian, B., Ji, X., Shang, S., Lu, C., and Zhang, K. (2015). Associated bacteria of different life stages of *Meloidogyne incognita* using pyrosequencing-based analysis. *J. Basic Microbiol.* 55, 950–960. doi: 10.1002/jobm.201400816

Carneiro, R. G., Mazzafera, P., and Ferraz, L. C. C. B. (1999). Carbon partitioning in soybean infected with *Meloidogyne incognita* and *M. javanica*. *J. Nematol.* 31, 348–355.

Castillo, J. D., Vivanco, J. M., and Manter, D. K. (2017). Bacterial microbiome and nematode occurrence in different potato agricultural soils. *Microb. Ecol.* 74, 888–900. doi: 10.1007/s00248-017-0990-2

Chen, Z. X., and Dickson, D. W. (1998). Review of *Pasteuria penetrans*: biology, ecology, and biological control potential. *J. Nematol.* 30, 313–340.

Ciancio, A., Rosso, L. C., Lopez-Cepero, J., and Colagiero, M. (2022). Rhizosphere 16S-ITS metabarcoding profiles in banana crops are affected by nematodes, cultivation, and local climatic variations. *Front. Microbiol.* 13. doi: 10.3389/fmicb.2022.855110

Clavero-Camacho, I., Archidona-Yuste, A., Cantalapiedra-Navarrete, C., Castillo, P., and Palomares-Rius, J. E. (2024). Prevalence and ecological factors affecting the distribution of plant-parasitic nematodes in *Prunus* groves in Spain. *J. Integr. Agric.* 23, 566–589. doi: 10.1016/j.jia.2023.02.033

Clavero-Camacho, I., Cantalapiedra-Navarrete, C., Archidona-Yuste, A., Castillo, P., and Palomares-Rius, J. E. (2022). Distribution, ecological factors, molecular diversity, and specific PCR for major species of pin nematodes (*Paratylenchus* spp.) in *Prunus* plantations in Spain. *Plant Dis.* 106, 2711–2721. doi: 10.1094/pdis-01-22-0188-re

Coolen, W. A. (1979). "Methods for extraction of Meloidogyne spp. and other nematodes from roots and soil," in *Root-knot nematodes (Meloidogyne species). Systematics, biology and control*. Eds. F. Lamberti and C. E. Taylor (Academic Press, New York, USA), 317–329.

Darriba, D., Taboada, G. L., Doallo, R., and Posada, D. (2012). jModelTest 2: more models, new heuristics and parallel computing. *Nat. Methods* 9, 772–772. doi: 10.1038/nmeth.2109

Day, P. R. (1965). "Particle fractionation and particle-size analysis," in *Methods of Soil Analysis*. Ed. C. A. Black (American Society of Agronomy, Madison, Wisconsin), 545–567.

Diehl, H., Goetz, C. A., and Hach, C. C. (1950). The versenate titration for total hardness. *Am. Water Works Assoc.* 42, 40–48. doi: 10.1002/j.1551-8833.1950.tb18799.x

Douglas, G. M., Maffei, V. J., Zaneveld, J. R., Yurgel, S. N., Brown, J. R., Taylor, C. M., et al. (2020). PICRUSt2 for prediction of metagenome functions. *Nat. Biotechnol.* 38, 685–688. doi: 10.1038/s41587-020-0548-6

Du Preez, G., Daneel, M., De Goede, R., Du Toit, M. J., Ferris, H., Fourie, H., et al. (2022). Nematode-based indices in soil ecology: Application, utility, and future directions. *Soil Biol. Biochem.* 169, 108640. doi: 10.1016/j.soilbio.2022.108640

Elhady, A., Adss, S., Hallmann, J., and Heuer, H. (2018). Rhizosphere microbiomes modulated by pre-crops assisted plants in defense against plant-parasitic nematodes. *Front. Microbiol.* 9. doi: 10.3389/fmicb.2018.01133

Engelbrektson, A., Kunin, V., Wrighton, K. C., Zvenigorodsky, N., Chen, F., Ochman, H., et al. (2010). Experimental factors affecting PCR-based estimates of microbial species richness and evenness. *ISME J.* 4, 642–647. doi: 10.1038/ismej.2009.153

Escudero, N., and Lopez-Llorca, L. V. (2012). Effects on plant growth and root-knot nematode infection of an endophytic GFP transformant of the nematophagous fungus *Pochonia chlamydosporia*. *Symbiosis* 57, 33–42. doi: 10.1007/s13199-012-0173-3

Esmenjaud, D., Minot, J. C., Voisin, R., Pinochet, J., Simard, M. H., and Salesses, G. (1997). Differential response to root-knot nematodes in *Prunus* species and correlative genetic implications. *J. Nematol.* 29, 370–380.

Evans, H. C., and Kirk, P. M. (2017). "Systematics of Pochonia," in *Perspectives in sustainable nematode management through Pochonia chlamydosporia applications for root and rhizosphere health*. Eds. R. H. Manzanilla-López and L. V. Lopez-Llorca (Springer International Publishing, Cham, Switzerland), 21–43.

Ewels, P., Magnusson, M., Lundin, S., and Käller, M. (2016). MultiQC: summarize analysis results for multiple tools and samples in a single report. *Bioinformatics* 32, 3047–3048. doi: 10.1093/bioinformatics/btw354

FAOSTAT (2021). *Food and Agricultural Organisation of the United Nations (FAO)*. Available online at: https://www.fao.org/faostat/en/#data/QC (Accessed 22/07/2023).

Furneaux, B., and Song, Z. (2021). *FUNGuildR: Look up guild information for Fungi. R Package Version 0.2.0.9000*.

Gardes, M., and Bruns, T. D. (1993). ITS primers with enhanced specificity for basidiomycetes - application to the identification of mycorrhizae and rusts. *Mol. Ecol.* 2, 113–118. doi: 10.1111/j.1365-294X.1993.tb00005.x

Giné, A., Carrasquilla, M., Martínez-Alonso, M., Gaju, N., and Sorribas, F. J. (2016). Characterization of soil suppressiveness to root-knot nematodes in organic horticulture in plastic greenhouse. *Front. Plant Sci.* 7. doi: 10.3389/fpls.2016.00164

Guindon, S., Dufayard, J.-F., Lefort, V., Anisimova, M., Hordijk, W., and Gascuel, O. (2010). New algorithms and methods to estimate maximum-likelihood phylogenies: Assessing the performance of PhyML 3.0. *System. Biol.* 59, 307–321. doi: 10.1093/sysbio/syq010

Handoo, Z. A., Nyczepir, A. P., Esmenjaud, D., van der Beek, J. G., Castagnone-Sereno, P., Carta, L. K., et al. (2004). Morphological, molecular, and differential-host characterization of *Meloidogyne floridensis* n. sp. (nematoda: Meloidogynidae), a root-knot nematode parasitizing peach in Florida. *J. Nematol.* 36, 20–35.

Herlemann, D. P. R., Labrenz, M., Jürgens, K., Bertilsson, S., Waniek, J. J., and Andersson, A. F. (2011). Transitions in bacterial communities along the 2000 km salinity gradient of the Baltic Sea. *ISME J.* 5, 1571–1579. doi: 10.1038/ismej.2011.41

Hetz, S. A., and Horn, M. A. (2021). *Burkholderiaceae* are key acetate assimilators during complete denitrification in acidic cryoturbated peat circles of the arctic tundra. *Front. Microbiol.* 12. doi: 10.3389/fmicb.2021.628269

Hirschmann, H. (1986). *Meloidogyne hispanica* n. sp. (Nematoda: Meloidogynidae), the 'Seville root-knot nematode'. *J. Nematol.* 18, 520–532.

Hussey, R. S., and Barker, K. R. (1973). A comparison of methods of collecting inocula of *Meloidogyne* spp., including a new technique. *Plant Dis. Rep.* 57, 1025–1028.

Ihrmark, K., Bödeker, I. T., Cruz-Martinez, K., Friberg, H., Kubartova, A., Schenck, J., et al. (2012). New primers to amplify the fungal ITS2 region - evaluation by 454-sequencing of artificial and natural communities. *FEMS Microbiol. Ecol.* 82, 666–677. doi: 10.1111/j.1574-6941.2012.01437.x

Jackson, M. L. (1958). *Soil Chemical Analysis* (Englewood Cliffs, N. J: Prentice-Hall Inc).

Jiménez, S., Pinochet, J., Abadía, A., Moreno, M. Á., and Gogorcena, Y. (2008). Tolerance response to iron chlorosis of *Prunus* selections as rootstocks. *HortScience* 43, 304–309. doi: 10.21273/hortsci.43.2.304

Jones, J. T., Haegeman, A., Danchin, E. G. J., Gaur, H. S., Helder, J., Jones, M. G. K., et al. (2013). Top 10 plant-parasitic nematodes in molecular plant pathology. *Mol. Plant Pathol.* 14, 946–961. doi: 10.1111/mpp.12057

Jorgensen, S. L., Hannisdal, B., Lanzén, A., Baumberger, T., Flesland, K., Fonseca, R., et al. (2012). Correlating microbial community profiles with geochemical data in highly stratified sediments from the Arctic Mid-Ocean Ridge. *Proc. Natl. Acad. Sci.* 109, E2846–E2855. doi: 10.1073/pnas.1207574109

Katoh, K., and Standley, D. M. (2013). MAFFT multiple sequence alignment software version 7: Improvements in performance and usability. *Mol. Biol. Evol.* 30, 772–780. doi: 10.1093/molbev/mst010

Kembel, S. W., Cowan, P. D., Helmus, M. R., Cornwell, W. K., Morlon, H., Ackerly, D. D., et al. (2010). Picante: R tools for integrating phylogenies and ecology. *Bioinformatics* 26, 1463–1464. doi: 10.1093/bioinformatics/btq166

Kerry, B. R. (2000). Rhizosphere interactions and the exploitation of microbial agents for the biological control of plant-parasitic nematodes. *Annu. Rev. Phytopathol.* 38, 423–441. doi: 10.1146/annurev.phyto.38.1.423

Khleborodova, A. (2023). *lefser: R implementation of the LEfSe method for microbiome biomarker discovery. R Package Version 1.10.1*. doi: 10.18129/B9.bioc.lefser

Kiewnick, S., and Sikora, R. A. (2006). Biological control of the root-knot nematode *Meloidogyne incognita* by *Paecilomyces lilacinus* strain 251. *Biol. Control* 38, 179–187. doi: 10.1016/j.biocontrol.2005.12.006

Kiewnick, S., Wolf, S., Willareth, M., and Frey, J.-E. (2013). Identification of the tropical root-knot nematode species *Meloidogyne incognita*, *M. javanica* and *M. arenaria* using a multiplex PCR assay. *Nematology* 15, 891–894. doi: 10.1163/15685411-00002751

Kishimoto, N., Kosako, Y., Wakao, N., Tano, T., and Hiraishi, A. (1995). Transfer of *Acidiphilium facilis* and *Acidiphilium aminolytica* to the genus *Acidocella* gen. nov., and emendation of the genus *Acidiphilium*. *System. Appl. Microbiol.* 18, 85–91. doi: 10.1016/S0723-2020(11)80453-4

Köhl, J., Kolnaar, R., and Ravensberg, W. J. (2019). Mode of action of microbial biological control agents against plant diseases: relevance beyond efficacy. *Front. Plant Sci.* 10. doi: 10.3389/fpls.2019.00845

Kreader, C. A. (1996). Relief of amplification inhibition in PCR with bovine serum albumin or T4 gene 32 protein. *Appl. Environ. Microbiol.* 62, 1102–1106. doi: 10.1128/aem.62.3.1102-1106.1996

Lahti, L., and Shetty, S. (2012-2019). *microbiome R package*. doi: 10.18129/B9.bioc.microbiome

Lamelas, A., Desgarennes, D., López-Lima, D., Villain, L., Alonso-Sánchez, A., Artacho, A., et al. (2020). The bacterial microbiome of *Meloidogyne*-based disease complex in coffee and tomato. *Front. Plant Sci.* 11. doi: 10.3389/fpls.2020.00136

Lu, P., Shi, H., Tao, J., Jin, J., Wang, S., Zheng, Q., et al. (2023). Metagenomic insights into the changes in the rhizosphere microbial community caused by the root-knot nematode *Meloidogyne incognita* in tobacco. *Environ. Res.* 216, 114848. doi: 10.1016/j.envres.2022.114848

MAPA (2022). *Ministery of Agriculture, Fisheries and Food* (Spain: MAPA). Available online at: https://www.mapa.gob.es/es/estadistica/temas/estadisticas-agrarias/agricultura/superficies-producciones-anuales-cultivos/ (Accessed 13/07/2023).

MAPA (2023). *Ministery of Agriculture, Fisheries and Food* (Spain: MAPA). Available online at: https://www.mapa.gob.es/es/agricultura/temas/sanidad-vegetal/productos-fitosanitarios/registro-productos/ (Accessed 26/07/2023).

Martin, M. (2011). Cutadapt removes adapter sequences from high-throughput sequencing reads. *EMBnet.journal* 17, 3. doi: 10.14806/ej.17.1.200

Masson, A.-S., Ho Bich, H., Simonin, M., Nguyen Thi, H., Czernic, P., Moulin, L., et al. (2020). Deep modifications of the microbiome of rice roots infected by the parasitic nematode *Meloidogyne graminicola* in highly infested fields in Vietnam. *FEMS Microbiol. Ecol.* 96, 1–14. doi: 10.1093/femsec/fiaa099

McMurdie, P. J., and Holmes, S. (2013). phyloseq: an R package for reproducible interactive analysis and graphics of microbiome census data. *PloS One* 8, e61217. doi: 10.1371/journal.pone.0061217

Micke, W. C. (1996). *Almond production manual* (University of California, Division of Agriculture and Natural Resources).

Migunova, V. D., and Sasanelli, N. (2021). Bacteria as biocontrol tool against phytoparasitic nematodes. *Plants* 10, 389. doi: 10.3390/plants10020389

Minh, B. Q., Schmidt, H. A., Chernomor, O., Schrempf, D., Woodhams, M. D., von Haeseler, A., et al. (2020). IQ-TREE 2: New models and efficient methods for phylogenetic inference in the genomic era. *Mol. Biol. Evol.* 37, 1530–1534. doi: 10.1093/molbev/msaa015

Moens, M., Perry, R. N., and Starr, J. L. (2009). ""*Meloidogyne* species-a diverse group of novel and important plant parasites,"," in *Root-knot nematodes*. Eds. R. N. Perry, M. Moens and J. L. Starr (CAB International, Wallingford, UK), 1–17.

Neher, D. A. (2001). Role of nematodes in soil health and their use as indicators. *J. Nematol.* 33, 161.

Nguyen, N. H., Song, Z., Bates, S. T., Branco, S., Tedersoo, L., Menke, J., et al. (2016). FUNGuild: An open annotation tool for parsing fungal community datasets by ecological guild. *Fungal Ecol.* 20, 241–248. doi: 10.1016/j.funeco.2015.06.006

Nordbring-Hertz, B., Jansson, H.-B., and Tunlid, A. (2011). "Nematophagous Fungi," in *Encyclopedia of Life Sciences* (John Wiley & Sons, Ltd, Chichester), 1–11.

Nyczepir, A. P. (1991). Nematode management strategies in stone fruits in the United States. *J. Nematol.* 23, 334–341.

Oksanen, J., Kindt, R., Legendre, P., O'Hara, B., Stevens, M. H. H., Oksanen, M. J., et al. (2007). The vegan package. *Community Ecol. Package* 10, 719.

Olsen, S. R. (1954). *Estimation of available phosphorus in soils by extraction with sodium bicarbonate* (Washington, DC, USA: US Department of Agriculture).

Ortega, E., and Dicenta, F. (2003). Inheritance of self-compatibility in almond: breeding strategies to assure self-compatibility in the progeny. *Theor. Appl. Genet.* 106, 904–911. doi: 10.1007/s00122-002-1159-y

Özbolat, O., Sánchez-Navarro, V., Zornoza, R., Egea-Cortines, M., Cuartero, J., Ros, M., et al. (2023). Long-term adoption of reduced tillage and green manure improves soil physicochemical properties and increases the abundance of beneficial bacteria in a Mediterranean rainfed almond orchard. *Geoderma* 429, 116218. doi: 10.1016/j.geoderma.2022.116218

Pathak, E., El-Borai, F. E., Campos-Herrera, R., Johnson, E. G., Stuart, R. J., Graham, J. H., et al. (2012). Use of real-time PCR to discriminate parasitic and saprophagous behaviour by nematophagous fungi. *Fungal Biol.* 116, 563–573. doi: 10.1016/j.funbio.2012.02.005

Pinochet, J., Aglès, M., Dalmau, E., Fernández, C., and Felipe, A. (1996). *Prunus* rootstock evaluation to root-knot and lesion nematodes in Spain. *J. Nematol.* 28, 616–623.

Pocurull, M., Fullana, A. M., Ferro, M., Valero, P., Escudero, N., Saus, E., et al. (2020). Commercial formulates of *Trichoderma* induce systemic plant resistance to *Meloidogyne incognita* in tomato and the effect is additive to that of the *Mi-1.2* resistance gene. *Front. Microbiol.* 10. doi: 10.3389/fmicb.2019.03042

Quast, C., Pruesse, E., Yilmaz, P., Gerken, J., Schweer, T., Yarza, P., et al. (2012). The SILVA ribosomal RNA gene database project: improved data processing and web-based tools. *Nucleic Acids Res.* 41, D590–D596. doi: 10.1093/nar/gks1219

Rammah, A., and Hirschmann, H. (1990). *Meloidogyne morocciensis* n. sp. (Meloidogyninae), a root-knot nematode from Morocco. *J. Nematol.* 22, 279–291.

R Core Team (2023). *R: A language and environment for statistical computing* (Vienna, Austria: R Foundation for Statistical Computing).

Revell, L. J. (2012). phytools: an R package for phylogenetic comparative biology (and other things). *Methods Ecol. Evol.* 3, 217–223. doi: 10.1111/j.2041-210X.2011.00169.x

Richards, L. A. (1954). *Diagnosis and improvement of saline and alkali soils* (Washington D.C: US Government Printing Office).

Rubio-Cabetas, M., Felipe, A., Reighard, G., R. Socias i Company (2017). "Rootstock development," in *Almonds: botany, production and uses*. Ed. T. M. Gradziel (CABI International, Boston, MA, USA), 209–227.

Saeed, M., Mukhtar, T., Ahmed, R., Ahmad, T., and Iqbal, M. A. (2023). Suppression of *Meloidogyne javanica* infection in peach (*Prunus persica* (L.) Batsch) using fungal biocontrol agents. *Sustainability* 15, 13833. doi: 10.3390/su151813833

Samson, R. A. (1974). *Paecilomyces* and some allied hyphomycetes. *Stud. Mycol.* 6, 1–119.

Samuels, G. J. (1996). *Trichoderma*: a review of biology and systematics of the genus. *Mycol. Res.* 100, 923–935. doi: 10.1016/S0953-7562(96)80043-8

Saucet, S. B., Van Ghelder, C., Abad, P., Duval, H., and Esmenjaud, D. (2016). Resistance to root-knot nematodes *Meloidogyne* spp. in woody plants. *New Phytol.* 211, 41–56. doi: 10.1111/nph.13933

Segata, N., Izard, J., Waldron, L., Gevers, D., Miropolsky, L., Garrett, W. S., et al. (2011). Metagenomic biomarker discovery and explanation. *Genome Biol.* 12, 1–18. doi: 10.1186/gb-2011-12-6-r60

Shetty, S., and Lahti, L. (2023). *microbiomeutilities: utilities for microbiome analytics. R package version 1.0.17*.

Sieriebriennikov, B., Ferris, H., and de Goede, R. G. (2014). NINJA: An automated calculation system for nematode-based biological monitoring. *Eur. J. Soil Biol.* 61, 90–93. doi: 10.1016/j.ejsobi.2014.02.004

Singh, K. P., Jaiswal, R. K., Kumar, N., and Kumar, D. (2007). Nematophagous fungi associated with root galls of rice caused by *Meloidogyne graminicola* and its control by *Arthrobotrys dactyloides* and *Dactylaria brochopaga*. *J. Phytopathol.* 155, 193–197. doi: 10.1111/j.1439-0434.2007.01208.x

Six, J., Frey, S. D., Thiet, R. K., and Batten, K. M. (2006). Bacterial and fungal contributions to carbon sequestration in agroecosystems. *Soil Sci. Soc. America J.* 70, 555–569. doi: 10.2136/sssaj2004.0347

Stirling, G. R. (2014). *Biological Control of Plant-parasitic Nematodes: Soil Ecosystem Management in Sustainable Agriculture* (Wallingford, Boston, MA: CABI).

Stirling, G., McKenry, M., and Mankau, R. (1979). Biological control of root-knot nematodes (*Meloidogyne* spp.) on peach. *Phytopathology* 69, 806–809. doi: 10.1094/Phyto-69-806

Tian, B.-Y., Cao, Y., and Zhang, K.-Q. (2015). Metagenomic insights into communities, functions of endophytes and their associates with infection by root-knot nematode, *Meloidogyne incognita*, in tomato roots. *Sci. Rep.* 5, 17087. doi: 10.1038/srep17087

Toju, H., and Tanaka, Y. (2019). Consortia of anti-nematode fungi and bacteria in the rhizosphere of soybean plants attacked by root-knot nematodes. *R. Soc. Open Sci.* 6, 181693. doi: 10.1098/rsos.181693

Trivedi, P., Leach, J. E., Tringe, S. G., Sa, T., and Singh, B. K. (2020). Plant–microbiome interactions: from community assembly to plant health. *Nat. Rev. Microbiol.* 18, 607–621. doi: 10.1038/s41579-020-0412-1

Turenne, C. Y., Sanche, S. E., Hoban, D. J., Karlowsky, J. A., and Kabani, A. M. (1999). Rapid identification of fungi by using the ITS2 genetic region and an automated fluorescent capillary electrophoresis system. *J. Clin. Microbiol.* 37, 1846–1851. doi: 10.1128/jcm.37.6.1846-1851.1999

Turner, S., Pryer, K. M., Miao, v., and Palmer, J. D. (1999). Investigating deep phylogenetic relationships among cyanobacteria and plastids by small subunit rRNA sequence analysis. *J. Eukaryotic Microbiol.* 46, 327–338. doi: 10.1111/j.1550-7408.1999.tb04612.x

Verdejo-Lucas, S., and Talavera, M. (2009). "). "Integrated managemenr of nematodes parasitic on *Prunus* spp,"," in *Integrated management of fruit crops and forest nematodes*. Eds. A. Ciancio and K. Mukerji (Springer, Dordrecht), 177–193.

Vestheim, H., and Jarman, S. N. (2008). Blocking primers to enhance PCR amplification of rare sequences in mixed samples – a case study on prey DNA in Antarctic krill stomachs. *Front. Zool.* 5, 12. doi: 10.1186/1742-9994-5-12

Westphal, A., Maung, Z. T. Z., Doll, D. A., Yaghmour, M. A., Chitambar, J. J., and Subbotin, S. A. (2019). First report of the peach root-knot nematode, *Meloidogyne floridensis* infecting almond on root-knot nematode resistant 'Hansen 536' and 'Bright's Hybrid 5' rootstocks in California, USA. *J. Nematol.* 51, 1–3. doi: 10.21307/jofnem-2019-002

White, T., Bruns, T., Lee, S., and Taylor, J. (1990). "Amplification and direct sequencing of fungal ribosomal RNA genes for phylogenetics," in *PCR Protocols: a guide to methods and applications*. Eds. M. Innis, D. Gelfand, J. Sninsky and T. White (Academic Press, New York), 315–322.

Yang, C., Mai, J., Cao, X., Burberry, A., Cominelli, F., and Zhang, L. (2023). ggpicrust2: an R package for PICRUSt2 predicted functional profile analysis and visualization. *Bioinformatics* 39, 1–5. doi: 10.1093/bioinformatics/btad470

Yeates, G. W., Bongers, T., De Goede, R. G., Freckman, D. W., and Georgieva, S. S. (1993). Feeding habits in soil nematode families and genera-an outline for soil ecologists. *J. Nematol.* 25, 315–331.

Yergaliyev, T. M., Alexander-Shani, R., Dimerets, H., Pivonia, S., Bird, D. M., Rachmilevitch, S., et al. (2020). Bacterial community structure dynamics in *Meloidogyne incognita*-infected roots and its role in worm-microbiome interactions. *mSphere* 5, 1–18. doi: 10.1128/mSphere.00306-20

Zhang, L., Liu, X., Zhu, S., and Chen, S. (2006). Detection of the nematophagous fungus *Hirsutella rhossiliensis* in soil by real-time PCR and parasitism bioassay. *Biol. Control* 36, 316–323. doi: 10.1016/j.biocontrol.2005.08.002

Zhou, D., Feng, H., Schuelke, T., De Santiago, A., Zhang, Q., Zhang, J., et al. (2019). Rhizosphere microbiomes from root knot nematode non-infested plants suppress nematode infection. *Microb. Ecol.* 78, 470–481. doi: 10.1007/s00248-019-01319-5

Zijlstra, C., Donkers-Venne, D. T. H. M., and Fargette, M. (2000).). Identification of *Meloidogyne incognita*, *M. javanica* and *M. arenaria* using sequence characterised amplified region (SCAR) based PCR assays. *Nematology* 2, 847–853. doi: 10.1163/156854100750112798

frontiers | Frontiers in Plant Science

TYPE Original Research
PUBLISHED 23 September 2024
DOI 10.3389/fpls.2024.1458330

OPEN ACCESS

EDITED BY
Andressa Machado,
Agronema, Brazil

REVIEWED BY
Lingan Kong,
Chinese Academy of Agricultural Sciences, China
Admilton Gonçalves de Oliveira,
State University of Londrina, Brazil
Fauzze Jose,
State University of Londrina, Brazil, in collaboration with reviewer AGO

*CORRESPONDENCE
Yumei Xu
ymxu@sxau.edu.cn

RECEIVED 02 July 2024
ACCEPTED 30 August 2024
PUBLISHED 23 September 2024

CITATION
Hu Y, Ma Y, Wang L, Luo Q, Zhao Z, Wang J and Xu Y (2024) Research on the mechanism of *Bacillus velezensis* A-27 in enhancing the resistance of red kidney beans to soybean cyst nematode based on TMT proteomics analysis.
Front. Plant Sci. 15:1458330.
doi: 10.3389/fpls.2024.1458330

Research on the mechanism of *Bacillus velezensis* A-27 in enhancing the resistance of red kidney beans to soybean cyst nematode based on TMT proteomics analysis

Yi Hu[1], Yibing Ma[1], Liyi Wang[1], Qingqing Luo[1], Zengqi Zhao[2], Jianming Wang[1] and Yumei Xu[1,3]*

[1]Laboratory of Nematology, Department of Plant Pathology, College of Plant Protection, Shanxi Agricultural University, Jinzhong, China, [2]Inveterate Group, Systematics, Manaaki Whenua-Landcare Research, Auckland, New Zealand, [3]Shanxi Key Laboratory of Integrated Pest Management in Agriculture, Shanxi Agricultural University, Taiyuan, China

Soybean cyst nematode (SCN) poses a significant challenge to red kidney beans cultivation, resulting in yield losses and quality deterioration. This study investigates the molecular mechanisms using Tandem Mass Tag (TMT) based proteomics technology to explore how the plant growth-promoting rhizobacterium (PGPR) *Bacillus velezensis* A-27 enhances the resistance of red kidney beans against SCN. The results revealed that out of 1,374 differentially expressed proteins (DEPs) in the red kidney beans roots, 734 DEPs were upregulated and 640 DEPs were downregulated in the A-27 + J2 *vs* J2 treatment group. KEGG analysis revealed that 14 DEPs were involved in the α-LeA metabolic pathway, crucial for the biosynthesis of jasmonic acid (JA) in plants. Quantitative real-time PCR (qRT-PCR) confirmed the upregulation of 4 key genes (*PLA1, AOS*, *AOC*, *ACX*) in the JA biosynthesis pathway, while enzyme-linked immunosorbent assay (ELISA) demonstrated a significant increase in JA content in the roots. The study demonstrates that *B. velezensis* A-27 stimulates induced systemic resistance (ISR) in red kidney beans, and induce JA biosynthesis by regulating the expression of key enzymes in the α-LeA metabolic pathway. This enhances the plant's defense against SCN, providing a theoretical foundation for the potential use of *B. velezensis* A-27 as a biocontrol agent for managing SCN in leguminous crops.

KEYWORDS

red kidney bean, SCN, Bacillus velezensis A-27, JA biosynthesis, TMT, induced systemic resistance (ISR)

1 Introduction

Red kidney bean (*Phaseolus vulgaris* L.) is a cultivated variety of common bean, from the legume family, with a dwarf erect plant. Introduced to Lan county, Shanxi Province from Italy in 1992, it has become a extensively cultivated cereal crop in the region (Han et al., 2016). Originally from Mexico and Argentina, this crop is highly popular among consumers locally and globally due to its economic value. By 2018, the planting area in Lan county alone had reached 8,667 hm^2, ranking first nationwide in cultivation and export scale. Apart from Shanxi Province, red kidney beans are also grown in Heilongjiang, Shaanxi, Yunnan, and other regions in China (Hao et al., 2019).

In recent years, the extensive cultivation and field management practices have led to a significant issue with soybean cyst nematode (SCN), which has become a major limiting factor affecting the yield and quality of red kidney beans. SCN infestation can cause yield reductions of 20% to 30% in mild cases and complete crop failure in severe instances. Additionally, the feeding site created by SCN can pave the way for root rot pathogens to invade, resulting in compound infections that severely hinder the development scale and export quality of the red kidney bean industry (Duan et al., 2011).

Plant growth-promoting rhizobacteria (PGPR), such as *Bacillus firmus* (Terefe et al., 2009), have demonstrated potential as biocontrol agents against plant-pathogenic nematodes (PPNs) (TariqJaveed et al., 2021). Studies have shown that *B. firmus* (Seo and Lee, 2004), *Klebsiella pneumoniae* (Kang et al., 2018; Liu et al., 2018), *B. amyloliquefaciens* (Jamal et al., 2017), *B. subtilis* (Cao et al., 2019), *B. atrophaeus* (Ayaz et al., 2021), *B. cereus* (Yin et al., 2021), and *B. altitudinis* (Jiao et al., 2022) can stimulate plants to develop induced systemic resistance (ISR), thereby enhancing their defense against PPNs. *Bacillus velezensis*, as PGPR, dedicates over 9% of its genome to the synthesis of various metabolic intermediates (Adeniji et al., 2019), which include antibiotics, antioxidants, antifungal factors, and growth promoters. The antimicrobial compounds produced by *B. velezensis* consist mainly of bacteriocins, polyketides, and lipopeptides (Jamal et al., 2017; Rabbee et al., 2019; Heo et al., 2022). These compounds not only inhibit the growth of certain bacteria by disrupting their cell walls or membranes but also suppress the growth of pathogenic fungal hyphae and spore germination (Rabbee and Baek, 2020). Flagellin or secondary metabolites from *B. velezensis* can trigger ISR in plants (Tian et al., 2022), enhancing their defensive capabilities against pathogenic microbes and nematodes, thus reducing plant diseases. These compounds can bind to receptor proteins on the cell membrane, initiating primary signals that activate systemic signal transduction pathways (JA, ethylene and SA pathway). This stimulation leads to the production of defense responses in plants such as the secretion of antimicrobial enzymes, reinforcement of cell walls, secretion of plant defense compounds, and activation of the lipoxygenase pathway. These responses help plants in combating pathogen infection (Ayaz et al., 2021; She et al., 2021).

Jasmonates (JAs) are lipid-derived stress hormones synthesized by plants, playing a crucial role in regulating plant responses to biotic stresses, including defense against pathogen infection and herbivore damage (Wasternack and Hause, 2013; Kammerhofer et al., 2015; Wasternack and Strnad, 2016). The biosynthesis of JAs begins with alpha-linolenic acid (α-LeA) through the octadecanoid pathway (Kombrink, 2012). In plastids, α-LeA is initially produced through the coordinated actions of fatty acid desaturase (FAD) and phospholipase A1 (PLA). It is then converted to 13-hydroxy-9,11,15-trienoic acid (13-HPOT) by 13-lipoxygenase (LOX), followed by transformation into 12,13-epoxy-9,11,15-trienoic acid (12, 13-EOT) through the activities of allene oxide synthase (AOS) and hydroperoxide dehydratase (HPL). Subsequently, it is converted to 12-oxo-phytodienoic acid (OPDA) by allene oxide cyclase (AOC). OPDA is then transported to peroxisomes, where it is reduced to 3-oxo-2-(cis-2'-pentenyl)-cyclopentane-1-octanoic acid (OPC-8) by OPDA reductase (OPR). OPC-8 is further activated to OPC-8 CoA by OPC-8 CoA ligase (OPCL) and subsequently transformed into JA through three rounds of β-oxidation catalyzed by various enzymes, including acyl-CoA oxidase (ACX), multifunctional protein (MFP), and 3-ketoacyl-CoA thiolase (KAT) (Wasternack and Hause, 2013; Wasternack and Strnad, 2016).

JA, as a principal plant defense hormone, plays a crucial role in plant resistance against PPNs (Liu et al., 2022). Research has shown that JA signaling is involved in defense mechanisms against root-knot nematodes such as *Meloidogyne incognita* (Huang et al., 2022), *M. chitwoodi* (Vieira dos Santos et al., 2013), and *M. graminicola* (Nahar et al., 2011), as well as the cyst nematode *Heterodera schachtii* (Kammerhofer et al., 2015). Treatment with methyl jasmonate (MeJA) has been found to induce resistance to *M. graminicola* in rice (Nahar et al., 2011; Kumari et al., 2015). The accumulation of JA precursor cis-c-12-oxo-phytodienoic acid (OPDA), along with JA or jasmonoyl isoleucine (JA-IIe), enhances *Arabidopsis* resistance against *M. hapla* (Gleason et al., 2016). Moreover, overexpressing *Arabidopsis* JA biosynthesis genes in soybean plants offers some defense against SCN (Olson-Manning et al., 2015). Conversely, SCN infection can suppress both JA biosynthesis genes and JA signaling response in soybean plants (Ithal et al., 2007).

To investigate the molecular mechanism by which *B. velezensis* enhances the resistance of red kidney beans to SCN disease. Tandem Mass Tag (TMT) proteomic technology was employed to compare and analyze the differentially expressed proteins (DEPs) under different treatments, followed by corresponding bioinformatics analysis. Quantitative real-time PCR (qRT-PCR) was used to analyze the changes in the transcriptional levels of key genes in the JA synthesis pathway, and the content of JA in plant roots was quantified. These experiments and analyses provide theoretical support for the management of SCN through the use of *B. velezensis*.

2 Materials and methods

2.1 Collection of cysts and J2 of SCN

The roots of diseased red kidney beans (*Phaseolus vulgaris* L.) collected from Lan County, Shanxi Province, were gently brushed to remove cysts attached to the root surface and subsequently examined

under a dissecting microscope. The collected cysts were surface-disinfected with a 0.1% NaClO solution for 1 min, followed by three rinses with sterile distilled water. They were then placed in a Baermann funnel and incubated at room temperature (25°C), with J2 being collected from the bottom of the Baermann funnel every 2-3 days.

2.2 Preparation of *Bacillus velezensis* A-27 fermentation broth

A single colony of A-27 grown on a plate was inoculated into 30 mL of liquid LB medium and shaken for 24 hours to prepare a seed solution. This seed solution was then inoculated into LB medium at a ratio of 1:100 and shaken at 28°C and 150 rpm for 72 hours until the OD_{600} value to 1.3.

2.3 Plant material and treatments

The red kidney bean cultivar Pinjinyun no. 4 was chosen as the experimental material. The seeds were surface-disinfected with 0.5% NaClO for 10 min, rinsed with sterile distilled water, air-dried, and then sown directly into plastic pots filled with sterilized soil and vermiculite. Upon reaching the vegetative cotyledon (Vc) stage, the seedlings were allocated into four treatments: (1) irrigation with 5 mL of LB medium only (CK), (2) root irrigation with 5 mL of A-27 fermentation broth (A-27), (3) inoculation with 2000 SCN J2 (J2), and (4) root irrigation with A-27 fermentation broth followed by inoculation with 2000 SCN J2 after 3 days (A-27 + J2). The plants were maintained at a day/night temperature of 25/20°C, with relative humidity between 60-80%, 16 hours of daily light, and were irrigated with a 1/4 strength Hoagland nutrient solution throughout the growth cycle. Root samples from the treated red kidney bean plants were collected for proteomic and transcriptomic analysis at 3, 7, 14, 21, and 28 days after inoculation (DAI). Each collection involved sampling five plants per treatment, with each treatment replicated three times.

2.4 Extraction, TMT labeling, and identification of proteins

Frozen samples were transferred into low protein binding tubes (2 mL Eppendorf), and 500 μL of extraction buffer was added to each sample with steel beads. The samples were ground at 60 Hz for 2 min. Subsequently, additional extraction buffer was added to achieve a final volume of 1 mL. Tris-phenol buffer was added to the mixtures, which were then mixed for 30 min at 4°C. Subsequently, the mixtures were centrifuged at 7,100 rpm for 10 min at 4°C to collect the phenol supernatants. These supernatants were mixed with 5 times their volume of 0.1M cold ammonium acetate-methanol buffer and precipitated overnight at -40°C. After precipitation, the samples were centrifuged at 12,000 rpm for 10 min to collect the precipitate, which was washed with cold methanol and gently mixed. This washing step was repeated once. Subsequently, methanol was replaced with acetone, and the washing step was repeated twice to remove any methanol contamination. The samples were then centrifuged at 12,000 rpm for 10 min at 4°C to collect the precipitate, which was dried at room temperature for 3 min and dissolved in a lysis buffer supplemented with 1 mM PMSF for 3 min. Finally, the samples underwent an additional centrifugation step at 12,000 rpm for 10 min to ensure the complete removal of any remaining precipitate.

The protein concentration was determined using the Bradford assay (Bio-Rad) with bovine serum albumin (BSA) as the standard. The protein samples were then aliquoted and stored at -80°C for further analysis. For TMTpro labeling, the lyophilized samples were resuspended in 100 μL of 100 mM TEAB (pH 8.5) and 40 μL of each sample were transferred into a new tube for labeling. Anhydrous acetonitrile was added to the TMT reagent vial at room temperature. The reagents were centrifuged, dissolved for 5 min, mixed and centrifuged, repeating this step once. Subsequently, 10 μL of the TMTpro label reagent was added to each sample for mixing. The tubes were then incubated at room temperature for 1 hour. Finally, 5 μL of 5% hydroxylamine was added to each sample and incubated for 15 min to quench the reaction.

The labeled peptide solutions were freeze-dried and stored at -80°C. The separation process was conducted using an Agilent 1100 HPLC System equipped with an Agilent Zorbax Extend -C18 column (5 μm, 150 mm × 2.1 mm). A gradient of mobile phases A (2% acetonitrile in HPLC water) and B (90% acetonitrile in HPLC water) were used. The solvent gradient was set as follows: 0-8 min, 98% A; 8-8.01 min, 98%-95% A; 8.01-48 min, 95%-75% A; 48-60 min, 75-60% A; 60-60.01 min, 60-10% A; 60.01-70 min, 10% A; 70-70.01 min, 10-98% A; 70.01-75 min, 98% A. Tryptic peptides were separated at a flow rate of 300 μL/min and monitored at 210 nm. Samples were collected for 8-60 min, with the eluent collected in centrifugal tubes 1-15 every minute in sequence. The peptides were recycled in this order until the end of the gradient. Subsequently, the separated peptides were freeze-dried for mass spectrometry analysis.

2.5 LC-MS/MS analysis and protein annotation

Changes in the proteome of red kidney bean roots from four different treatments were analyzed using TMT-LC/MS-MS technology. All analyses were conducted using a Q-Exactive HF mass spectrometer (Thermo, USA) equipped with a Nanospray Flex source (Thermo, USA). Samples were loaded and separated on a C18 column (25 cm × 75 μm) using an EASY-nLCTM 1200 system (Thermo, USA). The flow rate was 300nL/min with a linear gradient over 240 min (0-160 min, 3%-21% B; 160-220 min, 21%-42% B; 220-230 min, 42%-90% B; 230-240 min, 90% B; where mobile phase A= 0.1% FA in water and B = 0.1% FA in 80% ACN and 19.9% water). Full MS scans were conducted in the mass range of 300-1650 m/z with a resolution of 120000 and an AGC target value of 3e6. The 15 most intense peaks in the MS were fragmented using higher-energy collisional dissociation (HCD) with a collision energy of 30 MS/MS spectra were obtained with a resolution of 30000, an AGC

target of 1e5, and a maximum injection time of 80 ms. The Q Exactive HF dynamic exclusion was set to 30.0 s and the analysis was run in positive mode.

The LC-MS/MS raw data were analyzed in MaxQuant (Version 1.6.17.0) with a global false discovery rate (FDR) of 0.01 and a minimum of 3 peptides for protein group quantification. In order to be identified as substantially differentially expressed, searches were based on quantitative data from the UniProt library with fold change of ≥1.5 or ≤1/1.5, expression levels at $p<0.05$, and a false discovery rate of less than 1%. Gene Ontology (GO) annotations for the *Phaseolus vulgaris* proteome were obtained from the UniProtKB at the Gene Ontology Annotation (GOA) database. Identified protein IDs were converted to UniProt IDs and then annotated to GO IDs. Proteins without UniProt GOA annotations underwent further GO function analysis using the InterPro database through protein sequence alignment. Metabolic pathways were annotated using the Kyoto Encyclopedia of Genes and Genomes (KEGG) database and mapped to the KEGG pathway database using the KEGG mapper online service tool.

2.6 RNA extraction and transcriptional analysis

Total RNA was extracted from red kidney bean roots subjected to four treatments at 3, 7, 14, 21, and 28 DAI with SCN J2. The RNA extraction was performed using the RNA pure Plant Kit (Tiangen, Beijing, China) following the manufacturer's instructions. Transcriptional analysis of differentially expressed genes (DEGs) encoding proteins involved in α-LeA metabolism was conducted using qRT-PCR. Gene-specific primers were designed using SnapGene 4.0 (Table 1). The housekeeping gene *Actin* (GenBank accession: KF033476) from red kidney beans was served as the internal control. The qRT-PCR was carried out with a 20 μL reaction system, including 2 μL cDNA template (100 ng), 0.5 μL (10 mM) forward and reverse primers each, 12 μL 2 × SYBR Premix ExTaq (TaKaRa, Beijing, China), and 5 μL double-distilled H_2O. Cycling conditions for the qRT-PCR reactions were as follows: 95°C for 30 s, followed by 30 cycles of 95°C for 5 s and 60°C for 20 s, 95°C for 60 s, 55°C for 30 s, and 95°C for 30 s. The qRT-PCR data were analyzed using the $2^{-\Delta\Delta Ct}$ relative quantification method. The significant difference between treatments was determined using the Statistical Investigation Data Processing System. Each experiment was conducted with three biological replicates.

TABLE 1 Primers and their sequences used in the qRT-PCR analysis.

Gene	Primer	Sequence (5′-3′)
ACX	*ACX* F	GTGGCGGCGGAGCAGTTG
	ACX R	AGGTGCGGATTGGCGTTGAAG
AOC	*AOC* F	GCTGTTACAGGAGGCTCTGGAATC
	AOC R	AGGTTCAACAGGCTTCCCAAGTAG
PLA1	*PLA1* F	TGGTGAACGCCGAAGGAGGAG
	PLA1 R	ATCCGCAGCATCTCGTACACAAC
AOS	*AOS* F	CCGACGAGGTGAGGGCGATC
	AOS R	GAACTCCATGTCAGCGAGCAGAAG

Letters FandRindicate the forward and reverse primers.

2.7 Measurement of JA contents in red kidney beans roots

Total JA content was extracted from 0.5 g fresh root samples collected under four different treatments using the ELISA method. The roots were immediately frozen in liquid nitrogen, finely ground into a homogenate, and then mixed with 200 μL of PBS (pH 7.4). Following this, the mixture was then centrifuged for 20 min at 2000 rpm, and the supernatant was carefully collected for further analysis. For testing, 10 μL of the sample was mixed with 40 μL of sample diluent in a testing sample well. Subsequently, 100 μL HRP-conjugate reagent was added to each well, covered with an adhesive strip, and incubated for 60 min at 37°C. After incubation, each well was aspirated and washed four times with wash solution (400 μL per wash). Following the washes, chromogen solution A (50 μL) and chromogen solution B (50 μL) were added to each well, gently mixed, and incubated for 15 min at 37°C. Stop solution (50 μL) was then added to each well, resulting in a color change from blue to yellow. The plate was gently tapped to ensure thorough mixing. Optical density (O.D.) was measured at 450 nm using a microtiter plate reader within 15 min. A concentration-OD plot was created in an Excel worksheet, with the concentration of the standard solution on the x-axis and the corresponding OD values on the y-axis. A linear regression curve was calculated for the standard solution, and the concentration values of each sample were determined based on the curve equation.

2.8 Statistical analysis

Statistical analysis was conducted using a two-way ANOVA in GraphPad Prism9. Significant differences between group means were determined using the Tukey's multiple comparisons test at a significance level of $p<0.05$ (Wang et al., 2020).

3 Results

3.1 Protein identification by TMT analysis

Data from three biological replicates were examined using TMT-LC/MS-MS technology, and proteins were identified by querying a *Phaseolus vulgaris* protein database. A total of 87,785 effective spectra (out of 350,121) were detected across the four groups, leading to the identification 8,186 distinct peptides (out of 50,022) through proteomic analysis.

DEPs were selected based on a threshold of more than 1.5-fold change and $p<0.05$. Following these criteria, 299 DEPs were identified in red kidney bean roots, with 112 (49.2%) showing increased abundance and 187 (50.8%) showing decreased

abundance between A-27 *vs* CK treatment. Additionally, 1,374 DEPs were identified in red kidney bean roots between A-27 + J2 *vs* J2 treatment, with 734 (47.6%) showing increased abundance and 640 (52.4%) showing decreased abundance. In the case of A-27 + J2 *vs* CK treatment, 636 DEPs were identified, with 300 up-regulated and 336 down-regulated proteins (Figure 1).

3.2 GO and KEGG annotations of DEPs

GO annotation was conducted all DEPs in A-27 + J2 *vs* J2, resulting in a total of 856 annotated GO terms. These terms encompassed 359 biological processes, 88 molecular functions, and 409 cellular components. Among the top 10 terms identified across the three categories, notable biological processes included response to oxidative stress (30 DEPs), hydrogen peroxide catabolic process (24 DEPs), carbohydrate metabolic process (48 DEPs), and response to heat (10 DEPs). The cellular components with the highest number of annotated proteins were nucleolus (25 DEPs), extracellular region (50 DEPs), and MCM complex (5 DEPs), while the molecular functions enriched with the most proteins were heme binding (60 DEPs), lactoperoxidase activity (25 DEPs), and oxidoreductase activity (52 DEPs) (Figure 2; Supplementary Table S1).

The KEGG analysis identified 118 pathways, focusing on the synthesis and metabolism of various biological substances. Some of these metabolic pathways may be related to plant disease resistance, such as isoflavonoid biosynthesis (pvu00943), arachidonic acid metabolism (pvu00590), phenylpropanoid biosynthesis (pvu00940), glutathione metabolism (pvu00966), pyruvate metabolism (pvu00640), biosynthesis of various plant secondary metabolites (pvu00999), and α-LeA metabolism (pvu00592) (Figure 3; Supplementary Table S2). Further investigations are needed to explore additional metabolic pathways associated with other DEPs.

3.3 Validation of the DEPs in α-LeA metabolism pathway by qRT-PCR at transcriptional level

The study revealed that *Bacillus velezensis* A-27 increased red kidney bean resistance to SCN by enhancing 14 DEPs involved in the α-LeA metabolism pathways. To confirm these results, 4 key genes including PHAVU_008G052100g (*PLA1*), PHAVU_003G111500g (*AOC*), PHAVU_002G254200g (*ACX*), and PHAVU_003G010700g (*AOS*) (Supplementary Table S3), which are involved in the α-LeA metabolism pathway, were selected for qRT-PCR analysis.

At 3 DAI, there was no significant change in the *PLA1* expression level across treatments. However, by 7 DAI, when J2 feeding sites began to form, *PLA1* expression significantly increased

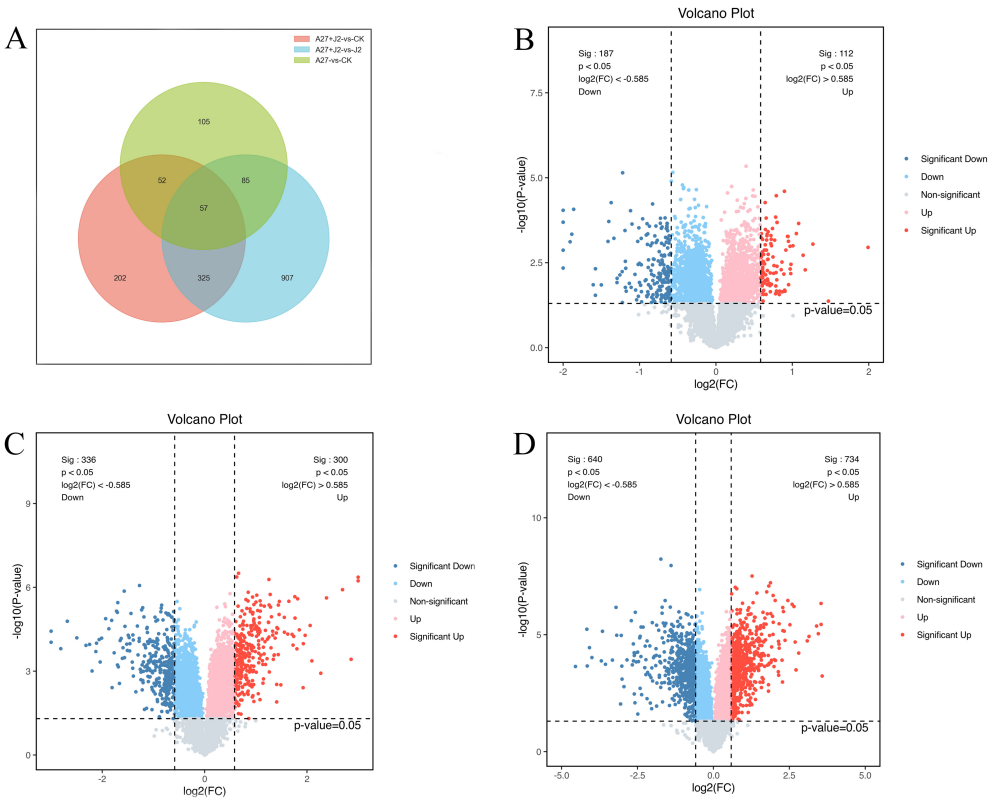

FIGURE 1
Venn diagram of DEPs responsive in A-27 *vs* CK, (A-27 + J2) *vs* CK and (A-27 + J2) *vs* J2 **(A)**; Volcano plot shows DEPs that up and down regulated in A-27 *vs* CK **(B)**, (A-27 + J2) *vs* CK **(C)**, and (A-27+J2) *vs* J2 **(D)**.

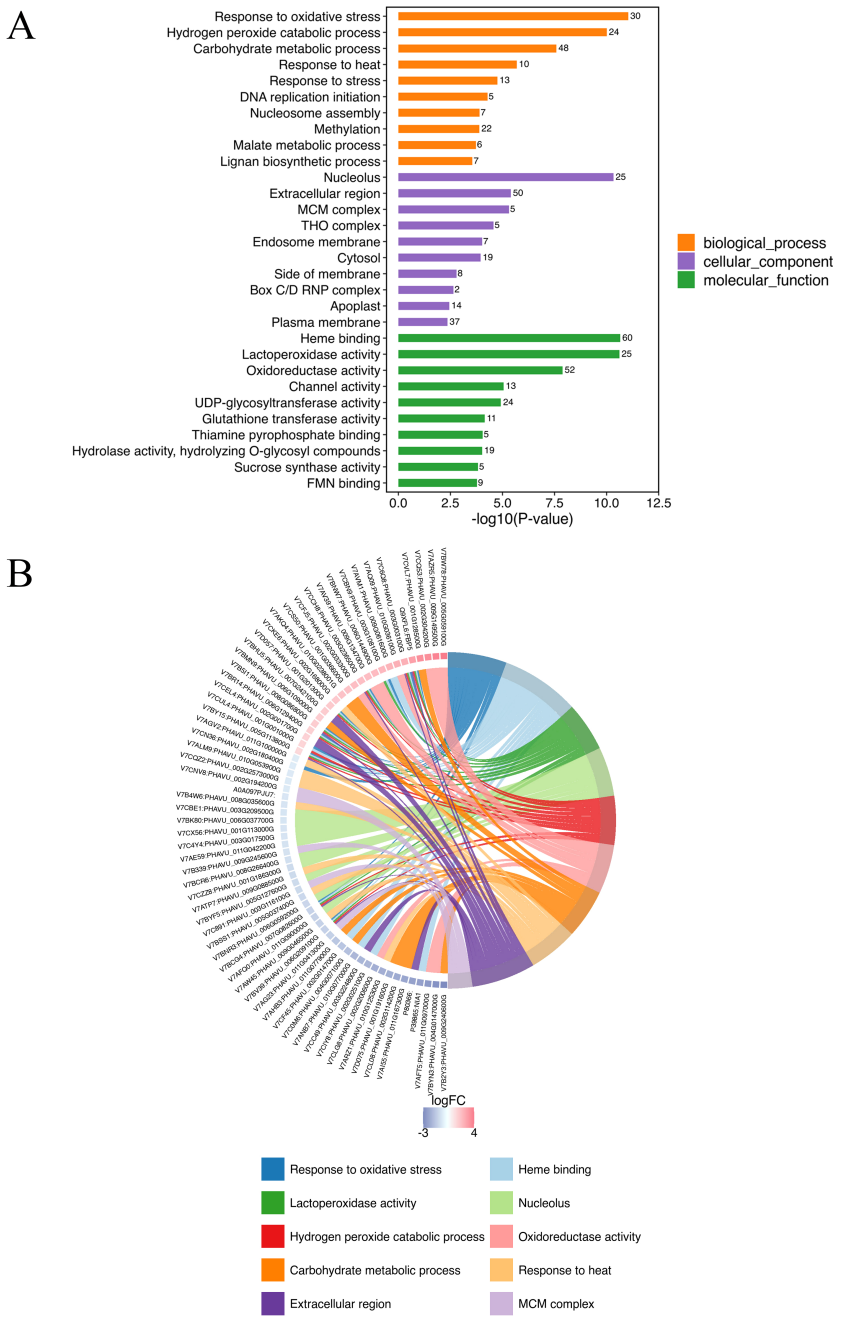

FIGURE 2
Top GO annotations of DEPs in (A-27 + J2) *vs* J2 **(A)** and GO Chord of top 10 GO terms **(B)**.

in the A-27 and A-27 + J2 treatments. By 14 DAI, *PLA1* expression was significantly upregulated in all treatments, with the highest level observed at 7.9-fold higher. Expression levels gradually returned to normal by 21 DAI, with no significant differences by 28 DAI. The *AOC* gene expression showed significant differences among treatments at 3 DAI, with significant downregulation in the A-27 and J2 treatments, while significant upregulation was observed in the A-27 + J2 treatment. This trend continued at 7 DAI, with *AOC* expression in the A-27 + J2 treatment being 4.5-fold higher than the control by 14 DAI. The *HPL* gene was significantly upregulated in the A-27 + J2 treatment at 3 DAI, with expression sharply increasing in the A-27 and A-27 + J2 treatments by 14 DAI, reaching 9.7-fold higher and 9.9-fold higher, respectively. The A-27 + J2 treatment peaked at 12.3-fold higher by 21 DAI. In contrast, the *ACX* expression downstream of the JA synthesis pathway varied significantly across stages. In the A-27 + J2 treatment, *ACX* was significantly upregulated at 3, 7, 14, and 21 DAI, reaching its highest level of 4.9-fold higher at 21 DAI. Similarly, the J2 treatment group showed a peak in *ACX* expression at 5.2-fold higher at 21 DAI (Figure 4).

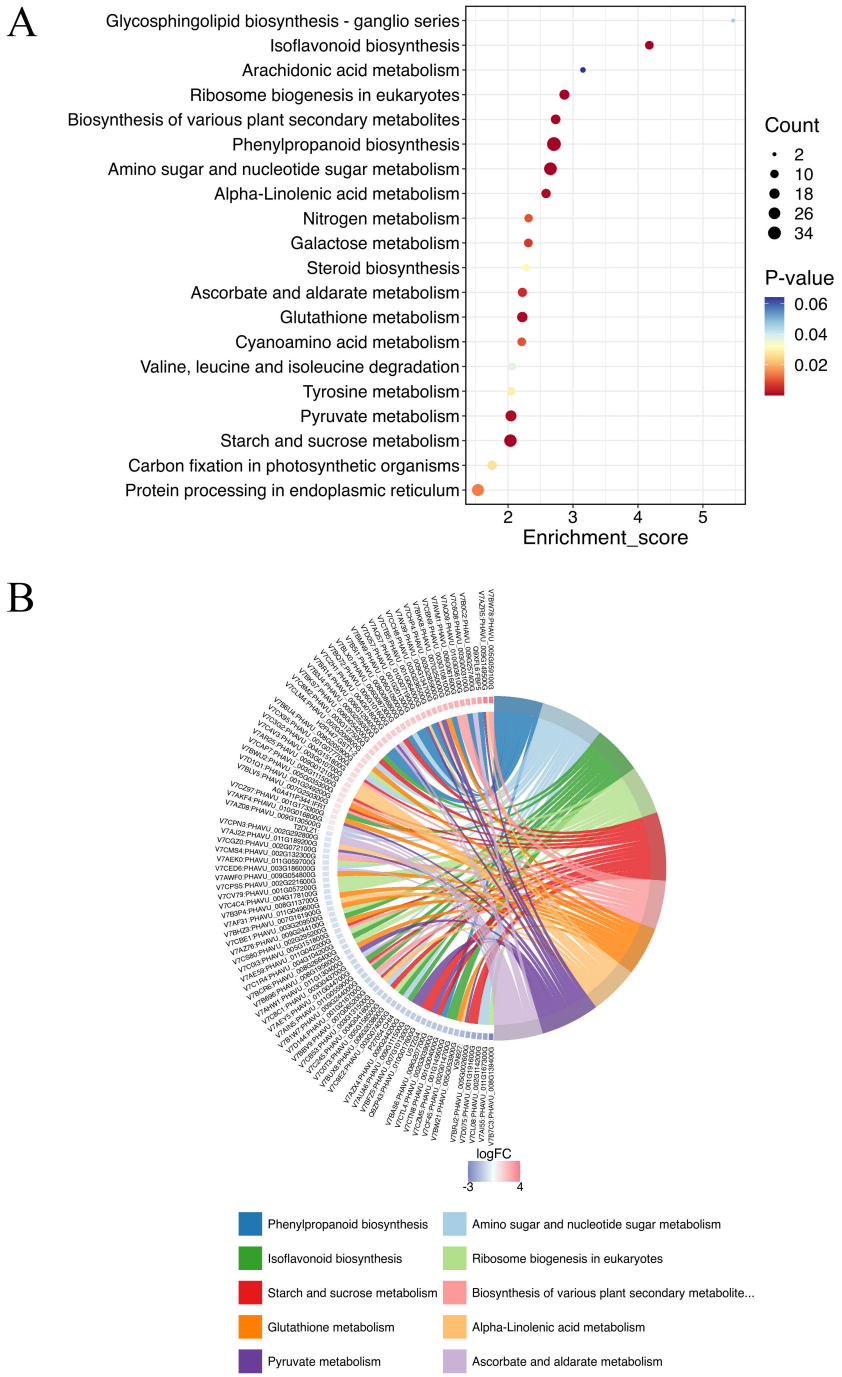

FIGURE 3
Top KEGG enrichment analysis of all DEPs in (A-27 + J2) *vs* J2 **(A)**, and KEGG Chord of top 10 KEGG terms **(B)**.

3.4 Measurement of JA contents in red kindy bean roots

The study investigated the impacts of genetic modifications on genes related to the α-LeA metabolism pathway, specifically examining whether these modifications would result in a substantial change in JA concentrations in red kidney bean roots under four different treatments. JA levels were measured using ELISA, with the results are shown in Figure 5.

Overall, the JA content in red kidney bean roots exhibited a gradual increase over time across all three treatment groups, with significant differences observed from 14 DAI. No significant changes in JA content were detected at 3 DAI and 7 DAI across different treatments. However, by 14 DAI, both the A-27 and A-27 + J2 treatment exhibited a significant increase in JA content, which was consistently maintained until 28 DAI. Furthermore, starting from 21 DAI, the J2 treatment group also demonstrated a significant increase in JA content.

10.3389/fpls.2024.1458330

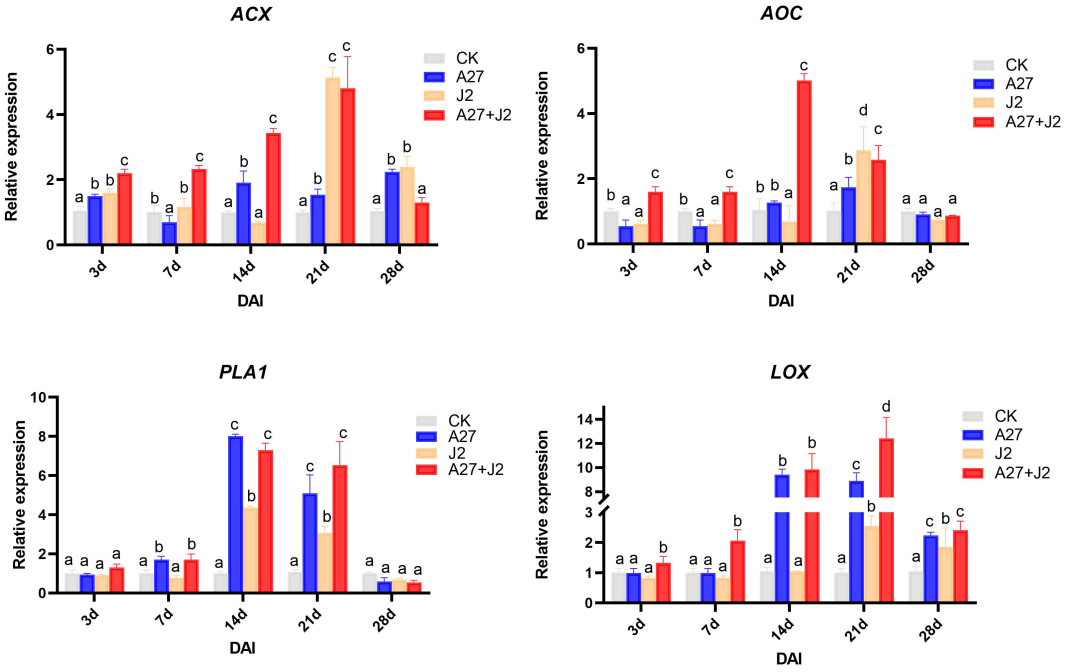

FIGURE 4
Quantitative RT-PCR analysis of 4 key genes involved in the α-LeA metabolism pathway in the root. Gene expression levels were analyzed from four treatments: CK, A-27, J2, and A-27 + J2 at 3, 7, 14, 21, and 28 DAI. Data are represented as mean ± standard deviation (SD) of three biological replicates. Different letters a, b, c, and d indicate the significant difference set at p value < 0.05.

4 Discussion

The severity of SCN disease has progressively worsened due to continuous cultivation in red kidney bean planting areas of Shanxi Province, China. Previous research conducted in our laboratory has classified the SCN population infecting red kidney beans as race 5 (Riggs and Schmitt, 1988). Our results demonstrated that the cultivar Pinjinyun no. 4, when treated with A-27 in combination with SCN J2, exhibited increased fresh plant weight and root weight, along with a reduced number of cysts in the roots compared to CK (Supplementary Figure S1). In this study, we aim to investigate the mechanism by which the PGPR *B. velezensis* A-27 enhances the growth and resistance of red kidney beans to SCN. This research seeks to provide a foundation for the application of *B. velezensis* A-27 in the prevention and management of SCN infestations in various leguminous crops.

TMT technology was used to compare the total proteins in red kidney beans root systems to investigate the induction of resistance to SCN by A-27 in this study. SCN J2 usually takes 3-7 days to locate host root by recognizing root exudate signals and establishing feeding sites (Duan et al., 2011). Consequently, root samples were

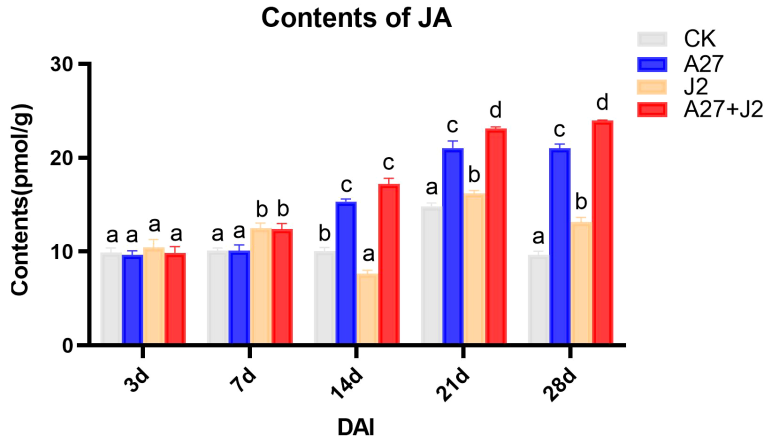

FIGURE 5
Contents of JA in red kindy beans roots at different times intervals. Data are represented as mean ± standard deviation (SD) of three biological replicates. Different letters a, b, c, and d indicate the significant difference set at p value < 0.05.

collected at 7 DAI for TMT proteomics analysis. The results revealed 1,374 DEPs in the A-27 + J2 *vs* J2 treatment, which is significantly higher than the 299 DEPs observed in the A-27 *vs* CK treatment and the 636 DEPs found in the A-27 + J2 *vs* CK treatment. This suggests that the combined infection of A-27 and J2 on plants enhances the complexity of the plant immune response, adding significant value to our research. Interestingly, despite both A-27 + J2 *vs* J2 and A-27 *vs* CK treatments involving A-27 treatment on plant roots, KEGG analysis highlighted the α-LeA metabolism pathway as a key pathway. However, there were 14 DEPs associated with the former and only 3 with the latter, indicating that J2 infection complicates JA biosynthesis in plants.

The focus of this study will be to discuss key DEPs related to the α-LeA biosynthesis pathway. The synthesis of JAs through the α-LeA pathway initiates with the conversion of phosphatidylcholine from chloroplasts or plastid membranes via phospholipases (PLAs) (Abdelkareem et al., 2017). Notably, a *PLA* gene in the red kidney bean roots exhibited significant expression changes, consistent with alterations at the transcriptome level, potentially offering new insights into the role of A-27 as a PGPR that enhances plant resistance by stimulating JA biosynthesis. The LOX pathway, a crucial secondary metabolic pathway in plants, involves the peroxidation of polyunsaturated fatty acids released from glycerides to produce peroxide fatty acids. One pathway involves the oxidation of 13-HPOT by HPL, resulting in the production of short-chain volatile aldehydes, alcohols, or oxygenated acids as defense responses to biotic (bacteria, fungi, or viruses) or abiotic (mechanical damage, high temperature, drought stresses) stressors (Heitz et al., 2019). Another pathway includes the conversion of 13-HPOT to 12-oxo-phytodienoic acid (12-OPDA) by AOS and AOC, followed by the reduction of 12-OPDA to JA and its derivatives by OPR and ACX in the peroxisomes (Browse, 2009; Gfeller et al., 2010; Lahari et al., 2024). Although no significant changes were observed in LOX in the A-27 + J2 *vs* J2 treatment, significant changes were detected in 2 genes encoding AOS, 2 genes encoding AOC, and 1 gene encoding HPL (Figure 6).

This results in an increase in volatile aldehydes and alcohols produced by HPL catalysis without altering the concentration of 13-HPOT, potentially repelling SCN from plant roots and reducing their harmful impact on plants. This finding offers a novel perspective on the enhanced resistance of A-27 to SCN. Furthermore, the production of 12-OPDA, catalyzed by AOS and AOC, has been associated with determining plant susceptibility to PPN (Carty et al., 2023).

Four key genes in the α-LeA biosynthesis pathway (*PAL1, AOS, AOC, ACX*) were regulated at various stages after treatment, leading to the biosynthesis and accumulation of JA in red kidney bean roots. The induction process and abundance of JA varied among the four treatments. Both SCN and *B. velezensis* A-27, whihc are known as parasites of soybean, can induce the plant's resistance response through pattern-triggered immunity (PTI), leading to the production of non-specific defense responses in plants (Sathiyamoorthy et al., 2010). Among the four treatments, we investigated the accumulation of JA and found a more advanced accumulation process in red kidney beans

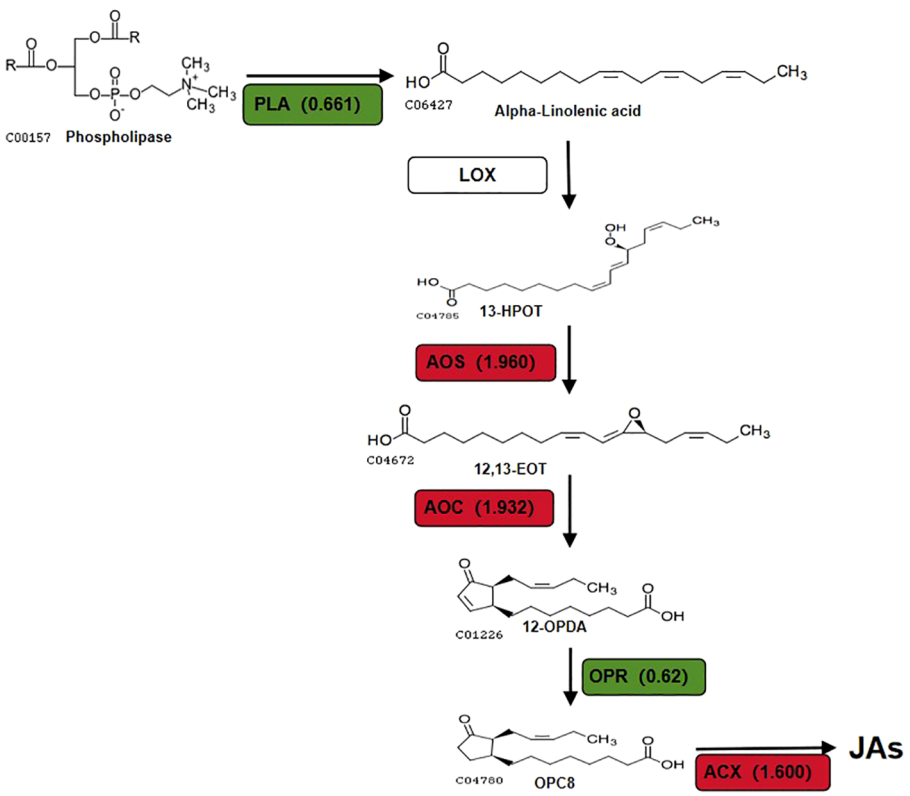

FIGURE 6
DEPs that involved in JAs biosynthesis pathway in (A-27 + J2) vs J2. Different colors and numbers show the fold-changes in protein abundance (Han et al., 2016) based on the TMT data.

treated with A-27 compared to untreated ones. This indicates significant differences in the processes of inoculating A-27 and J2 infection in stimulating plant resistance. Upon successful colonization of red kidney bean roots by A-27, a rapid plant immune response is activated, enhancing the transcription of AOS and AOC, and promoting JA biosynthesis compared to the control and J2 treatments. Interestingly, at 7 DAI, JA accumulation was initially observed in both J2 and A-27 + J2 treatments; however, by 14 DAI, as J2 established feeding sites and successfully invaded, JA content decreased significantly. This decrease may be attributed to effectors released during the successful J2 infection, which possess mechanisms to suppress plant defense responses. In contrast, samples treated with A-27 exhibited a continuous increase in JA content. Previous studies have suggested that, in addition to activating plant defense responses, JA may influence the recognition and infection behavior of nematodes on plants, as well as their developmental processes (Schouteden et al., 2017), potentially hindering continuous J2 infection.

This study presents a novel discovery showing that *B. velezensis* A-27 induces the biosynthesis of JA in red kidney beans, resulting in the activation of ISR. In addition to the significant increase in JA levels, the stimulation of intermediate metabolites, including volatile aldehydes and 12-OPDA along the metabolic pathway, may also contribute to enhancing the plants' defense against nematode infections. Analysis of key enzymes and transcriptomes in the α-LeA metabolic pathway revealed that *B. velezensis* A-27 enhances red kidney bean resistance to SCN by promoting JA biosynthesis. However, further research is needed to fully elucidate the intricate mechanism by which *B. velezensis* A-27 induces systemic acquired resistance (SAR) in leguminous crops, like red kidney beans to improve their resistance against SCN. Overall, *B. velezensis* A-27 demonstrates potential as a biocontrol agent (BCA) for SCN management.

5 Conclusions

This study investigated the molecular mechanisms by which the PGPR *Bacillus velezensis* A-27 enhances the resistance of red kidney beans to SCN by modulating the JA biosynthesis pathway. Through the use of TMT proteomics technology, a total of 1,374 DEPs were identified in the roots of red kidney beans treated with A-27 + J2 compared to those treated with J2 alone. These results highlighted the significant role of the JA biosynthesis pathway in enhancing disease resistance. Validation through qRT-PCR confirmed the upregulation of 4 key genes in the JA biosynthesis pathway, and ELISA demonstrated a significant increase in JA content in the roots. This study reveals that *B. velezensis* A-27 induces ISR in red kidney beans by modulating the JA biosynthesis pathway, thereby enhancing the plant's defense against SCN.

Data availability statement

The original contributions presented in the study are publicly available. This data can be found here: NGDC, accession number PRJCA030088, https://ngdc.cncb.ac.cn/omix/preview/oecEpt3Q.

Ethics statement

The manuscript presents research on animals that do not require ethical approval for their study.

Author contributions

YH: Writing – review & editing, Writing – original draft, Validation, Methodology, Data curation. YM: Writing – review & editing, Methodology. LW: Writing – review & editing, Validation. QL: Writing – review & editing, Software. ZZ: Writing – review & editing, Project administration, Methodology, Data curation. JW: Writing – review & editing, Resources, Methodology, Data curation. YX: Writing – review & editing, Resources, Methodology, Funding acquisition, Data curation, Conceptualization.

Funding

The author(s) declare financial support was received for the research, authorship, and/or publication of this article. This research was funded by Central Project Guide Local Science and Technology for Development of Shanxi Province (YDZJSX2021A033), Scientific Research Cultivation and Innovation Program of Plant Protection College of Shanxi Agricultural University (ZBXY23B-2) and Postgraduate Scientific Research Innovation Project of Shanxi Province (2024KY306).

Conflict of interest

The authors declare that the research was conducted in the absence of any commercial or financial relationships that could be construed as a potential conflict of interest.

Publisher's note

Supplementary material

The Supplementary Material for this article can be found online at: https://www.frontiersin.org/articles/10.3389/fpls.2024.1458330/full#supplementary-material

References

Abdelkareem, A., Thagun, C., Nakayasu, M., Mizutani, M., Hashimoto, T., and Shoji, T. (2017). Jasmonate-induced biosynthesis of steroidal glycoalkaloids depends on *COI1* proteins in tomato. *Biochem. Biophys. Res. Commun.* 489, 206-210. doi: 10.1016/j.bbrc.2017.05.132

Adeniji, A. A., Loots, D. T., and Babalola, O. O. (2019). *Bacillus velezensis*: phylogeny, useful applications and avenues for exploitation. *Appl. Microbiol. Biotechnol.* 103, 3669-3682. doi: 10.1007/s00253-019-09710-5

Ayaz, M., Ali, Q., Farzand, A., Khan, A. R., Ling, H., and Gao, X. (2021). Nematicidal volatiles from *Bacillus atrophaeus* GBSC56 promote growth and stimulate induced systemic resistance in tomato against *Meloidogyne incognita*. *Int. J. Mol. Sci.* 22, 5049. doi: 10.3390/ijms22095049

Browse, J. (2009). Jasmonate passes muster: a receptor and targets for the defense hormone. *Annu. Rev. Plant Biol.* 60, 183-205. doi: 10.1146/annurev.arplant.043008.092007

Cao, H., Jiao, Y., Yin, N., Li, Y., Ling, J., Mao, Z., et al. (2019). Analysis of the activity and biological control efficacy of the *Bacillus subtili* strain Bs-1 against. *Meloidogyne incognita*. *Crop Prot.* 122, 125-135. doi: 10.1016/j.cropro.2019.04.021

Carty, M., Wang, C., Wang, D., and Fu, Z. Q. (2023). Autophagy and jasmonate fight nematode blight. *Trends Parasitol.* 39, 893-895. doi: 10.1016/j.pt.2023.09.008

Duan, Y., Chen, L., Liu, G., Li, H., Wang, X., and Wang, Y. (2011). *Plant pathogenic nematodes the economic importance of plant pathogenic nematodes* (Beijing: Sinece Pres), 1–2.

Gfeller, A., Dubugnon, L., Liechti, R., and Farmer, E. (2010). Jasmonate biochemical pathway. *Sci. Signaling* 3. doi: 10.1126/scisignal.3109cm3

Gleason, C., Leelarasamee, N., Meldau, D., and Feussner, I. (2016). OPDA has key role in regulating plant susceptibility to the root-knot nematode Meloidogyne hapla in *Arabidopsis*. *Front. Plant Sci.* 7, 1565. doi: 10.3389/fpls.2016.01565

Han, J. H., Kong, Y., Wang, X. W., Guan, Y., and Xi, Z. H. (2016). Cultivation techniques of red kidney beans in the Heilongjiang reclamation area. *Modern Agric.* 2016, 25–26.

Hao, X. P., Wang, Y., Zhao, J. D., and Chang, J. W. (2019). Red kidney bean variety 'Pin Jin Yun 3' and its cultivation techniques. *China Seed Industry* 2019, 76–77.

Heitz, T., Smirnova, E., Marquis, V., and Poirier, L. (2019). Metabolic control within the jasmonate biochemical pathway. *Plant Cell Physiol.* 60, 2621-2628. doi: 10.1093/pcp/pcz172

Heo, G., Kong, H., Kim, N., Lee, S., Sul, S., Jeong, D. W., et al. (2022). Antibiotic susceptibility of *Bacillus velezensis*. *FEMS Microbiol. Lett.* 369, fnac017. doi: 10.1093/femsle/fnac017

Huang, H., Zhao, W., Qiao, H., Li, C., Sun, L., Yang, R., et al. (2022). SlWRKY45 interacts with jasmonate-ZIM domain proteins to negatively regulate defense against the root-knot nematode *Meloidogyne incognita* in tomato. *Horticulture Res.* 9, uhac197. doi: 10.1093/hr/uhac197

Ithal, N., Recknor, J., Nettleton, D., Hearne, L., Maier, T., Baum, T. J., et al. (2007). Parallel genome-wide expression profiling of host and pathogen during soybean cyst nematode infection of soybean. *Mol. Plant-Microbe Interact.* 20, 293-305. doi: 10.1094/mpmi-20-3-0293

Jamal, Q., Cho, J. Y., Moon, J. H., Munir, S., Anees, M., and Kim, K. Y. (2017). dentification for the first time of Cyclo(d-Pro-l-Leu) produced by *Bacillus amyloliquefaciens* Y1 as a nematocide for nontrol of *Meloidogyne incognita*. *Molecules* 22, 1839. doi: 10.3390/molecules22111839

Jiao, H., Xu, W., Hu, Y., Tian, R., and Wang, Z. (2022). Citric acid in rice root exudates enhanced the colonization and plant growth-promoting ability of *Bacillus altitudinis* LZP02. *Microbiol. Spectr.* 10, e01002-22. doi: 10.1128/spectrum.01002-22

Kammerhofer, N., Radakovic, Z., Regis, J. M., Dobrev, P., Vankova, R., Grundler, F. M., et al. (2015). Role of stress-related hormones in plant defence during early infection of the cyst nematode Heterodera schachtii in *Arabidopsis*. *New Phytol.* 207, 778-789. doi: 10.1111/nph.13395

Kang, W., Zhu, X., Wang, Y., Chen, L., and Duan, Y. (2018). Transcriptomic and metabolomic analyses reveal that bacteria promote plant defense during infection of soybean cyst nematode in soybean. *Plant Biol.* 18, 1-14. doi: 10.1186/s12870-018-1302-9

Kombrink, E. (2012). Chemical and genetic exploration of jasmonate biosynthesis and signaling paths. *Planta* 236, 1351-1366. doi: 10.1007/s00425-012-1705-z

Kumari, P., Reddy, C. R. K., and Jha, B. (2015). Methyl jasmonate-induced lipidomic and biochemical alterations in the intertidal Macroalga Gracilaria dura (*Gracilariaceae, Rhodophyta*). *Plant Cell Physiol.* 56, 1877-1889. doi: 10.1093/pcp/pcv115

Lahari, Z., van Boerdonk, S., Omoboye, O. O., Reichelt, M., Höfte, M., Gershenzon, J., et al. (2024). Strigolactone deficiency induces jasmonate, sugar and flavonoid phytoalexin accumulation enhancing rice defense against the blast fungus *Pyricularia oryzae*. *New Phytol.* 241, 827-844. doi: 10.1111/nph.19354

Liu, D., Chen, L., Zhu, X., Wang, Y., Xuan, Y., Liu, X., et al. (2018). *Klebsiella pneumoniae* SnebYK mediates resistance against *Heterodera glycines* and promotes soybean growth. *Front. Microbiol.* 9, 1134. doi: 10.3389/fmicb.2018.01134

Liu, R., Wang, Z., Zheng, J., Xu, Z., Tang, X., Huang, Z., et al. (2022). The effects of methyl jasmonate on growth, gene expression and metabolite accumulation in *Isatis indigotica Fort. Ind. Crops Products* 177, 114482. doi: 10.1016/j.indcrop.2021.114482

Nahar, K., Kyndt, T., De Vleesschauwer, D., Höfte, M., and Gheysen, G. (2011). The Jasmonate pathway is a key player in systemically induced defense against root knot nematodes in rice. *Plant Physiol.* 157, 305-306. doi: 10.1104/pp.111.177576

Olson-Manning, C. F., Strock, C. F., and Mitchell-Olds, T. (2015). Flux control in a defense pathway in *Arabidopsis thaliana* is robust to environmental perturbations and controls variation in *Adaptive Traits*. *G3-Genes Genomes Genet.* 5, 2421-2427. doi: 10.1534/g3.115.021816

Rabbee, M. F., Ali, M. S., Choi, J., Hwang, B. S., Jeong, S. C., and Baek, K. H. (2019). *Bacillus velezensis*: A valuable Mmmber of bioactive molecules within plant microbiomes. *Molecules* 24, 1046. doi: 10.3390/molecules24061046

Rabbee, M., and Baek, K. H. (2020). Antimicrobial activities of lipopeptides and polyketides of *Bacillus velezensis* for agricultural applications. *Molecules* 25, 4973. doi: 10.3390/molecules25214973

Riggs, R. D., and Schmitt, D. P. (1988). Complete characterization of the race scheme for Heterodera glycines. *J. Nemat* 20, 39–395.

Sathiyamoorthy, S., In, J. G., Gayathri, S., Kim, Y. J., and Yang, D. C. (2010). Gene ontology study of methyl jasmonate-treated and non-treated hairy roots of *Panax ginseng* to identify genes involved in secondary metabolic pathway. *Russian J. Genet.* 46, 828-835. doi: 10.1134/s1022795410070070

Schouteden, N., Lemmens, E., Stuer, N., Curtis, R., Panis, B., and De Waele, D. (2017). Direct nematicidal effects of methyl jasmonate and acibenzolar-S-methyl against *Meloidogyne incognita*. *Natural Product Res.* 31, 1219-1222. doi: 10.1080/14786419.2016.1230111

Seo, J. H., and Lee, S. P. (2004). Optimization of the production of fibrinolytic enzyme from *Bacillus firmus* NA-1 in fermented soybeans. *Prev. Nutr. Food Sci.* 9, 14–20.

She, W., Yi, L., and Liang, Y. (2021). Isolation and characterization of *Bacillus velezensis* YL1 producing surfactin. *Appl. Biochem. Microbiol.* 57, 743-749. doi: 10.1134/s0003683821060120

TariqJaveed, M., Farooq, T., Al-Hazmi, A. S., Hussain, M. D., and Rehman, A. U. (2021). Role of Trichoderma as a biocontrol agent (BCA) of phytoparasitic nematodes and plant growth inducer. *J. Invertebrate Pathol.* 183, 107626. doi: 10.1016/j.jip.2021.107626

Terefe, M., Tefera, T., and Sakhuja, P. K. (2009). Effect of a formulation of Bacillus firmus on root-knot nematode *Meloidogyne incognita* infestation and the growth of tomato plants in the greenhouse and nursery. *J. Invertebrate Pathol.* 100, 94-99. doi: 10.1016/j.jip.2008.11.004

Tian, X. L., Zhao, X. M., Zhao, S. Y., Zhao, J. L., and Mao, Z. C. (2022). The biocontrol functions of *Bacillus velezensis* strain Bv-25 against *Meloidogyne incognita*. *Front. Microbiol.* 13, 843041. doi: 10.3389/fmicb.2022.843041

Vieira dos Santos, M. C., Curtis, R. H. C., and Abrantes, I. (2013). Effect of plant elicitors on the reproduction of the root-knot nematode Meloidogyne chitwoodi on susceptible hosts. *Eur. J. Plant Pathol.* 136, 193-202. doi: 10.1007/s10658-012-0155-6

Wang, Y., Yang, R., Feng, Y., Sikandar, A., Zhu, X., Fan, H., et al. (2020). iTRAQ-Based proteomic analysis reveals the role of the biological control agent, *Sinorhizobium fredii* strain Sneb183, in enhancing soybean resistance against the soybean cyst nematode. *Front. Plant Sci.* 11, 597819. doi: 10.3389/fpls.2020.597819

Wasternack, C., and Hause, B. (2013). Jasmonates: biosynthesis, perception, signal transduction and action in plant stress response, growth and development. An update to the 2007 review in annals of botany. *Ann. Bot.* 111, 1021-1058. doi: 10.1093/aob/mct067

Wasternack, C., and Strnad, M. (2016). Jasmonate signaling in plant stress responses and development - active and inactive compounds. *New Biotechnol.* 33, 604–613. doi: 10.1016/j.nbt.2015.11.001

Yin, N., Zhao, J. L., Liu, R., Li, Y., Ling, J., Yang, Y. H., et al. (2021). Biocontrol efficacy of Bacillus cereus strain Bc-cm103 against *Meloidogyne incognita*. *Plant Dis.* 105, 2061-2070. doi: 10.1094/pdis-03-20-0648-re

Frontiers in
Plant Science

Cultivates the science of plant biology and its applications

The most cited plant science journal, which advances our understanding of plant biology for sustainable food security, functional ecosystems and human health.

Discover the latest Research Topics

See more →

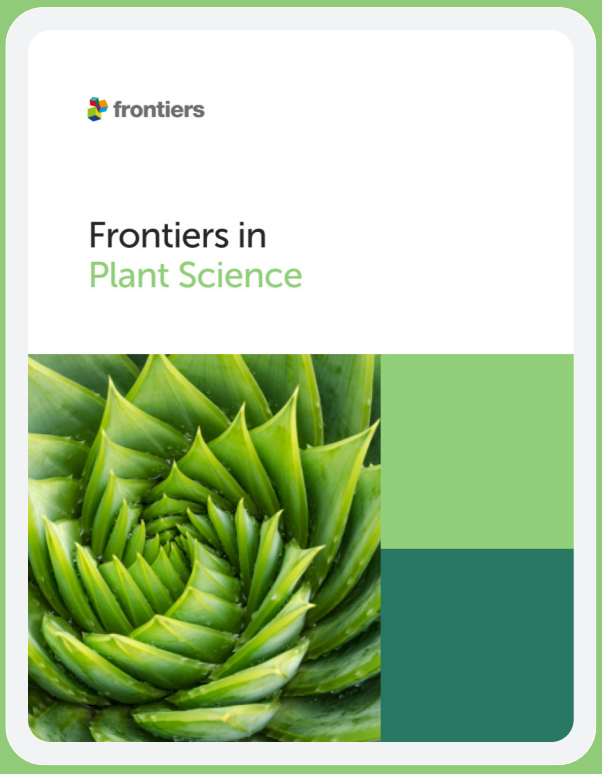

Frontiers

Avenue du Tribunal-Fédéral 34
1005 Lausanne, Switzerland
frontiersin.org

Contact us

+41 (0)21 510 17 00
frontiersin.org/about/contact